The role of species-specific modifications in peptidoglycan biosynthesis

Nicola Frances Galley

A thesis submitted in partial fulfilment
of the requirements for the degree of

Doctor of Philosophy

University of Warwick
School of Life Sciences

September 2015

Contents

Table of Contents

Chapter 5. Enzymology of transglycosylation: the characterisation of *Staphylococcus aureus* transglycosylases and novel inhibitors of their activity..**179**

List of Tables

List of Figures

Acknowledgements

I would like to thank my supervisors Dr. David Roper and Prof. Chris Dowson for their guidance and support during my PhD, in particular Dave for providing me with the opportunity to take this project on 3 years ago, and for his continued patience and trust. I have thoroughly enjoyed the journey.

Particular thanks go to Dr. Adrian Lloyd for his expertise, patience, inspirational advice, thorough proofreading of my thesis, and many a cup of coffee over the years. Not to mention the odd trip to A&E!

I also thank past and current members of C10 for making the lab such a wonderful place to work. In particular Karen, Vita, Julie, Chris and Kyle for their advice, friendship and laughs both in and out of the lab. You are all incredible.

I acknowledge Julie Todd, Anita Catherwood and Smita Chauhan for synthesis of substrates that were the foundation to my project. The support services in the School of Life Sciences, in particular Cerith and Mark in media prep for their advice and help. It is always a pleasure to work with you both, and thank you for saving my bacon on many occasions with last minute requests. Also, Sue Slade for mass spectrometry support.

Thanks to Dr. Krystyna Zielinski-Smith, Brian Taylor, Dr Ian Harvey, and Dr Tonia Schofield for being my inspirations, encouraging me to pursue science, and showing a continued interest in my career.

Special thanks go to my friends and family, especially Kat and Aideen for their friendship and advice. Dean for your understanding and love over the years, and Face for company and entertainment during the writing process. In particular I would like to thank my parents for your love, support and understanding over the years. This thesis is dedicated to you.

Declaration

I hereby declare that I personally have carried out the work submitted in this thesis under the supervision of Dr David Roper and Professor Christopher Dowson at the School of Life Sciences, University of Warwick. Where work has been contributed to by other individuals it is specifically stated in the text.

No part of this work has previously been submitted to be considered for a degree or qualification. All sources of information are specifically acknowledged in the form of references.

Some of the content of this thesis has been published previously, and papers are attached at the end of this thesis:

- Galley, N. F., O'Reilly, A. M., and Roper. D. I., Prospects for novel inhibitors of peptidoglycan transglycosylases. *Bioorganic Chemistry* **2014** 55**:** 16-26.

- Paulin, S, Jamshad, M., Dafforn, T. R., Garcia-Lara, J., Foster, S. J., Galley, N. F., Roper, D. I., Rosado, H., Taylor, P. W., Surfactant-free purification of membrane protein complexes from bacteria: application to the staphylococcal penicillin-binding protein complex PBP2/PBP2a. *Nanotechnology* **2014**, 25, 285101-285108

- Zuegg, J., Muldoon, C., Adamson, G., McKeveney, D., Le Thanh, G., Premraj, R., Becker, B., Cheng, M., Elliot, A. G., Huang, J. X., Butler, M. S., Bajaj, M., Seifert, J., Sing, L., Galley, N. F., Roper, D. I., Lloyd, A. J., Dowson, C. G., Cheng, TJ., Cheng, WC., Demon, D., Meyer, E., Meutermans, W., Cooper, M. A., Carbohydrate scaffolds as glycosyltransferase inhibitors with *in vivo* antibacterial activity. *Nature Communications* **2015** 6, 7719-7730

Abstract

Penicillin binding proteins (PBPs) are responsible for the final extracellular steps (transglycosylation and transpeptidation) in the biosynthesis of peptidoglycan, the essential cell-wall carbohydrate polymer, from its Lipid II precursor. They are excellent targets for antibiotics due to their essentiality for cell viability in most bacteria. Genus- and species-specific variation in the chemical structure of Lipid II can have significant consequences for the formation and metabolism of the peptidoglycan sacculus by the PBPs. Characterisation of these enzymes from Gram-positive bacteria, including the substrate-enzyme interactions involved, is essential in both understanding the mechanisms of peptidoglycan biosynthesis and contributing to the development of new antimicrobials.

The work presented in this thesis focuses primarily on the substrate specificity of the *Streptococcus pneumoniae* bifunctional PBPs; PBP1a and PBP2a; both recombinantly expressed and purified to a high level. The preference, by both enzymes, for amidated Lipid II as a transglycosylase substrate was identified by two complementary assay systems. A novel spectrophotometric assay was used to observe transpeptidation by *S. pneumoniae* PBP1a in a continuous manner; the first time this has been achieved for a Gram-positive PBP, and with potentially far-reaching implications in the future of antibiotic discovery. Attempts were made to synthesise dipeptide branched Lipid II, implicated in β-lactam resistance, as substrates for the bifunctional PBPs. The role of amidation in *Staphylococcus aureus* peptidoglycan biosynthesis was also investigated, and variation in the requirement for this modification between the monofunctional transglycosylase MGT and bifunctional PBP2 identified. Two novel monosaccharide compounds were identified as inhibitors of transglycosylation.

This thesis provides an important basis for understanding the peptidoglycan biosynthesis mechanisms of two globally important pathogens. This insight, and future work leading from it, could contribute to the development of new antibiotics, helping to reduce the global threat of antimicrobial resistance.

Abbreviations

3D	three-dimensional
Å	Angstrom
A_{Xnm}	Absorbance at X nm
ADP	Adenosine 5'-diphosphate
APS	Ammonium persulphate
ATP	Adenosine 5'-triphosphate
AU	Absorbance Unit
BaCWAN	Bacterial Cell Wall Assembly Network
BCA	Bicinchoninic acid
bp	base pair
C_{35}/C_{55} Lipid II	Lipid II (See below) with C35 or C55 lipid carrier
CAZY	Carbohydrate-Active enZYmes
CHAPS	3-[(3-cholamidopropyl)dimethylammonio]-1-propanesulfonate
CHES	N-Cyclohexyl-2-aminoethanesulfonic acid
CH_2Cl_2	Dichloromethane
CMC	Critical Micelle Concentration
C-terminus	Carboxy-terminus
CV	Column volume
D-Ala	D-Alanine
D-Ala-D-Ala	D-Alanyl-D-Alanine
D-Ala-D-Lac	D-Alanyl-D-Lactate
Da	Dalton
DAAO	D-amino acid oxidase
DDM	n-Dodecyl-β-D-maltopyranoside
DEAE	Diethylaminoethyl
Decyl-PEG	Octaethylene glycol monodecyl ether
D-Gln	D-Glutamine
D-Glu	D-Glutamate
DMSO	Dimethyl sulfoxide
DNA	Deoxyribonucleic acid

DNAse	Deoxyribonuclease I, from bovine pancreas
DTT	Dithiothreitol
E_6C_{12}	Hexaethylene glycol dodecyl ether
E. coli	*Escherichia coli*
EDTA	Ethylenediaminetetraacetic acid
EDC	1-ethyl-3-(3-dimethylaminopropyl)-carbodiimide hydrochloride
E. faecalis	*Enterococcus faecalis*
E. faecium	*Enterococcus faecium*
EGS	Ethylene glycol *bis*(succinic acid) N-hydroxysuccinimide ester
eq.	Equivalents
ESI-MS	Electrospray Ionisation Mass Spectrometry
et al.	*et alia*, and others
Fmoc	Fluorenylmethyloxycarbonyl
g	gram
Glc*N*Ac	*N*-acetylglucosamine
Gly_5	Glycyl-Glycyl-Glycyl-Glycyl-Glycine
HCl	Hydrochloric acid
HEPES	N-(2-hydroxyethyl)piperazine-N'-(3-ethanesulfonic acid)
HMW	High molecular weight
HPLC	High Performance Liquid Chromatography
h	hill coefficient
HRP	Horseradish peroxidase
IC_{50}	Half maximal inhibitory concentration
IMAC	Immobilised Metal Affinity Chromatography
IPP	Inorganic pyrophosphatase
IPTG	Isopropyl-β-D-thiogalactopyranoside
iso-Gln	iso-Glutamine
kb	kilobase
k_{cat}	turnover number
KCl	Potassium chloride
kDa	kiloDalton
K_d	dissociation constant

K_m	Michaelis constant
K_{m1}	Michaelis constant at the first subsite of the enzyme
K_{m2}	Michaelis constant at the second subsite of the enzyme
kpsi	kilopound per square inch
L	Litre
L-Ala	L-Alanine
L-Ala-L-Ala	L-Alanyl-L-Alanine (described from C- to N-terminus)
L-Ala-γ-D-Glu/Gln-L-Lys-D-Ala-D-Ala:	L-Alanyl-γ-D-Glutamyl/Glutaminyl-L-Lysyl-D-Alanyl-D-Alanine
LB	Lysogeny broth (Luria-Bertani bacteria growth media)
LC-MS	Liquid chromatography mass spectrometry
LDAO	Lauryldimethylamine oxide
Lipid I	Undecaprenyl pyrophosphoryl-*N*-acetylmuramyl-L-Alanyl-γ-D-Glutamyl-L-Lysyl-D-Alanyl-D-Alanine
Lipid II (X, Y)	Undecaprenyl pyrophosphoryl-*N*-acetylmuramyl-(*N*-acetylglucosaminyl)-L-Alanyl-γ-D-X-L-Lysyl(Y)-D-Alanyl-DAlanine (X is the amino acid at position 2, and Y is appended to the ε amino group of the third position lysine)
Lipid IV	Undecaprenyl pyrophosphoryl-*N*-acetylmuramyl(-*N*-acetylglucosaminyl)-L-Alanyl-γ-D-Glutamyl-L-Lysyl-D-Alanyl-D-Alanine)$_2$
L-Lys	L-Lysine
LMW	Low molecular weight
L-Ser	L-Serine
L-Ser-L-Ala	L-Seryl-L-Alanine (described from C- to N-terminus)
M	Molar (grams per litre)
mA	Milliamps
mAU	milli absorbance unit
MES	2-morpholinoethane sulphonic acid
MESG	7-methyl-6-guanosine
meso-DAP	*meso*-diaminopimelic acid
M. flavus	*Micrococcus flavus*
mg	milligram

MGT	monofunctional glycosyltransferase
MIC	Minimal Inhibitory Concentration
min	minute
mL	millilitre
mm	millimetre
mM	millimolar
MOPS	3-(N-morpholino)propanesulfonic acid
M_r	molecular weight
MPA	Megapascal
mRNA	messenger ribonucleic acid
MRSA	Methicillin-resistant *Staphylococcus aureus*
MST	Microscale thermophoresis
Mur*N*Ac	*N*-acetylmuramic acid
$NaBH_4$	Sodium borohydride
NAD_+	Nicotinamide adenine dinucleotide (oxidised)
NADH	Nicotinamide adenine dinucleotide (reduced)
$NADP_+$	Nicotinamide adenine dinucleotide phosphate (oxidised)
NADPH	Nicotinamide adenine dinucleotide phosphate (reduced)
NBD	7-nitro-2,1,3-benzoxadiazol-4-yl
ng	nanogram
NHS	N-hydroxysuccinimide
nm	nanometre
nM	nanomolar
nmol	nanomole
N-terminus	Amino-terminus
°C	degrees Celsius
OD_{600nm}	optical density at 600 nm
PBP	Penicillin-Binding Protein
PBS	Phosphate Buffered Saline
PCR	Polymerase Chain Reaction
PDB	Protein Data Bank
PEG	Polyethylene glycol
PEP	Phosphoenol pyruvate

pH	$\log_{10}[H+]$
P_i	Inorganic phosphate
pI	Isoelectric point
PNP	Purine Nucleoside Phosphorylase
RFU	Relative fluorescence units
RNA	Ribonucleic acid
rpm	rotations per minute
$S_{0.5}$	Substrate concentration at half maximal rate
SAP	Shrimp alkaline phosphatase
SOC	Super Optimal broth with Catabolite repression
S. pneumoniae	*Streptococcus pneumoniae*
S. aureus	*Staphylococcus aureus*
SDS	Sodium Dodecyl Sulfate
SDS-PAGE	Sodium Dodecyl Sulfate Polyacrylamide Gel Electrophoresis
sec	second
SMALP	Styrene Maleic Acid copolymer Lipid Polymer
Spp.	Species
TAE	Tris Acetate Ethylenediaminetetraacetic acid
Tris	Tris (hydroxymethyl) aminomethane
TEMED	N,N,N',N'-tetramethylethylenediamine
TFA	Trifluoroacetic acid
TLC	Thin layer chromatography
TM	Transmembrane
tRNA	transfer ribonucleic acid
TX-100	Triton X-100
UDP	Uridine 5'-diphosphate
UDP-Glc*N*Ac	Uridine 5'-diphospho-*N*-acetylglucosamine
UDP-Mur*N*Ac	Uridine 5'-diphospho-*N*-acetylmuramic acid
UDP-Mur*N*Ac pentapeptide (X):	Uridine 5'-diphospho-*N*-acetylmuramyl-L-Ala-D-X-L-Lys-D-Ala-D-Ala (Where X is Gln or Glu)
UDP-Mur*N*Ac-hexapeptide (X, Y)	Uridine 5'-diphospho-*N*-acetylmuramyl-L-Ala-D-X-L-Lys(Y)-D-Ala-D-Ala (Where X

is Gln or Glu and Y is Ser or Ala (appended to ε amino group of the third position lysine from C to N-terminus))

UDP-MurNAc-heptapeptide (X, Y)   Uridine 5'-diphospho-*N*-acetylmuramyl-L-Ala-D-X-L-Lys(Y)-D-Ala-D-Ala (Where X is Gln or Glu and Y is SerAla or AlaAla (appended to ε amino group of the third position lysine from C to N-terminus))

µg	microgram
µL	microlitre
µm	micrometer
µM	micromolar
µmol	micromole
VanFL	BODIPY FL conjugate of vancomycin
V_{max}	maximal velocity
VRE	Vancomycin Resistant Enterococci
WHO	World Health Organisation
w/v	weight to volume ratio
V	Volts
v/v	volume to volume ratio
× g	centrifugal force

Other abbreviations are explained in the text where appropriate

Standard three and one amino acid abbreviations are used throughout.

Amino acid	Three letter code	One letter code
Alanine	Ala	A
Arginine	Arg	R
Asparagine	Asn	N
Aspartic acid	Asp	D
Cysteine	Cys	C
Glutamic acid	Glu	E
Glutamine	Gln	Q
Glycine	Gly	G
Histidine	His	H
Isoleucine	Ile	I
Leucine	Leu	L
Lysine	Lys	K
Methionine	Met	M
Phenylalanine	Phe	F
Proline	Pro	P
Serine	Ser	S
Threonine	Thr	T
Tryptophan	Trp	W
Tyrosine	Tyr	Y
Valine	Val	V

Chapter 1. Introduction

1.1 Antimicrobial resistance

The serendipitous discovery of penicillin by Alexander Fleming in 1928 (Fleming, 1929) led to the global introduction of antimicrobials to treat bacterial infections, widely considered one of most significant developments in medical practice (Chopra, 1998). The 'Golden age' of antimicrobial discovery between 1940-1960 (Walsh and Wright, 2005) saw the introduction of a large number of new classes, which were considered sufficient to keep bacterial infections at a low level. As a result, the pharmaceutical industry focused on more profitable areas, leading to a period of nearly 40 years in which no new classes of antimicrobials were introduced (von Nussbaum *et al.*, 2006). This coincided with the gradual and eventually rapid increase in global prevalence of antimicrobial resistance due to overuse of existing drugs.

Antimicrobial Resistance (AMR) is a major threat to both humans and animals, dramatically reducing the effectiveness of drugs that we have come to rely on in common medical practice. Increasing resistance threatens to send us back to the dark ages of medicine, with minor infections becoming untreatable; simple operations could become extremely dangerous, and more complex procedures impossible. The most recent O'Neill report (O'Neill, 2015a) estimates that by 2050, ten million people may die annually, overtaking cancer death rates, at a worldwide economic cost of $100 trillion. It is crucially important that an interdisciplinary, multinational effort is made to exploit existing and identify new targets for antimicrobials.

Note that the term antimicrobial is used to describe compounds active on all microorganisms including bacteria, parasites, viruses and fungi. The focus of this thesis is on bacteria, and therefore the term antibiotic will be used throughout to describe compounds that act specifically on bacteria.

1.2 Antibiotic targets

Effective targets for antibiotic drugs are fundamental for bacterial cell viability but distinct from the equivalent eukaryotic process, enabling selective toxicity towards bacterial cells (Walsh, 2003). Most current antibiotics target one of the three main validated metabolic targets; DNA replication and repair, protein synthesis or bacterial cell wall biosynthesis (Walsh, 2003). The major classes of antibiotics are summarised in Table 1.1.

1.2.1 DNA replication and repair

The DNA double helix must be unwound for the genetic information within it to be accessed, and therefore complementary strands are separated temporarily for transcription, and permanently for replication. Transcription; the production of mRNA from DNA, is performed by RNA polymerase (Cramer, 2002) and is essential for viability. RNA polymerase is the target of the rifamycin class of antimicrobials, which bind close to the RNA polymerase active site and stop initiation of RNA synthesis (Floss and Yu, 2005). DNA topoisomerases are found in both prokaryotic and eukaryotic cells and are responsible for the control of DNA topology and relieving torsional stress during strand separation. DNA gyrase is the prokaryotic specific topoisomerase, responsible for introducing both negative and positive DNA supercoiling and is essential for bacterial viability (Champoux, 2001). The fluoroquinolone class of antibiotics forms a complex with DNA gyrase stopping re-ligation and therefore leading to the accumulation of double-stranded DNA breaks and subsequent cell death (Drlica *et al*., 2008).

1.2.2 Protein synthesis

A range of antibiotic classes target bacterial protein biosynthesis, an attractive target due to its complex nature and machinery that is sufficiently different from its eukaryotic counterpart. Central in protein synthesis is the ribosome, a ribonucleoprotein made of two subunits (30S and 50S), which associate to form a 70S ribosome upon the initiation of protein synthesis (Nissen *et al*., 2000). The large

number of processes involved in initiation, elongation and termination provide ample possibilities for disruption, and examples of existing antimicrobials include streptogramins, macrolides and phenicols, which target the 50S ribosomal subunit, and aminoglycosides and tetracyclines that act on the 30S subunit (Kohanski *et al.,* 2010).

1.2.3 Bacterial cell wall biosynthesis

The bacterial cell wall is essential for viability, predominantly due to its main component, peptidoglycan. This forms a sacculus surrounding the cell providing mechanical strength to withstand the high internal turgor pressure, as well as acting as an anchor for cell wall associated proteins and carbohydrates. The peptidoglycan biosynthetic pathway is highly conserved between species, despite the variations in composition seen, and therefore antibiotic classes are able to inhibit homologous targets (Lazar and Walker, 2002). Peptidoglycan and its biosynthesis is the main focus of this thesis and is covered comprehensively in Sections 1.5 and 1.6.

Class	Example	Target
Quinolones	Ciproflaxin	DNA replication
Rifamycins	Rifampin	Transcription
Sulfonamides	Sulfadimethoxine	Folate synthesis
Tetracyclines	Minocycline	Translation
Aminoglycosides	Streptomycin	Translation
Macrolides	Erythromycin	Translation
Oxazolidinones	Linezolid	Translation
β-lactams	Penicillin	Peptidoglycan biosynthesis
Glycopeptides	Vancomycin	Peptidoglycan biosynthesis
Lipopeptides	Daptomycin	Cell membrane
Cationic peptides	Colistin	Cell membrane

Table 1.1: Major classes of antibiotic. Examples of common antibiotics within the main clinically used classes of antibiotics, and their mode of action. Not intended to be an exhaustive list. Davies and Davies, 2010

1.3 Antibiotic resistance

Resistance to antibiotics is a natural, evolutionary mechanism that all bacteria employ in order to survive (Normark and Normark, 2002). Low-level resistance, which exists for nearly all clinical antibiotics (Levy and Marshall, 2004), only becomes a problem when it increases to the point where widespread therapeutic failure occurs. However, the natural process of resistance development has been hugely accentuated by over 60 years of strong man-made selection pressure due to the underuse, overuse and misuse of antibiotics, and the vast quantities released into the environment (Davies and Davies, 2010).

Resistance to many antibiotics exists before they are introduced to the clinic, such as pneumococcal resistance to optochin in lab animals, observed before it was used to treat infections in the early 1900s (Harwell and Brown, 2000). An entire species can be inherently resistant to large numbers of drugs such as *Pseudomonas aeruginosa,* which has an outer membrane impermeable to most hydrophobic antibiotics and a multidrug efflux pump that removes many that do enter (Lambert, 2002; Normark and Normark, 2002). Mycoplasma do not have a peptidoglycan layer in their cell wall, and therefore are inherently resistant to any antibiotics targeting it (Taylor-Robinson and Bébéar, 1997)

The development of resistance has a very broad time scale; it can be rapid such as the development of sulphonamide resistance, which was observed in the late 1930s following its clinical introduction in 1937, and was subsequently enhanced by gene amplification (Davies and Davies, 2010). It can be much slower in some cases, such as vancomycin resistance, which wasn't detected for nearly 30 years (Johnson *et al.*, 1990). However, it is not always clear whether the antibiotic or resistance came first (Davies and Davies, 2010). The acquisition of resistance is generally through mutations or gene transfer, as a result of persistent selection pressure.

Spontaneous mutations within the genome result in insertions, deletions, point mutations and inversions, and the frequency of these events vary hugely between bacteria. This mechanism is employed by *Mycobacterium tuberculosis*, which cannot

readily undergo genetic exchange (Riska *et al.,* 2000), and has developed resistance to many drugs including rifampicin, streptomycin and macrolides (Ramaswamy and Musser, 1998). The stepwise build up of mutations resulting in high-level resistance is more clinically important than single-step mutations, as identification in the early stages should lead to steps being taken to slow down development. Fluoroquinolone resistance is a well-understood example of step-wise resistance, through mutation of genes causing increased expression of efflux pumps. This has the potential for high level multidrug resistance development as efflux pumps have a range of substrates (Normark and Normark, 2002). Resistance mutations can affect the natural function of the antibiotic target resulting in fitness costs and therefore compensatory mechanisms are required, often involving the target protein, and these prevent future mutational reversion (Normark and Normark, 2002).

Horizontal gene transfer is common between bacteria within a genus, although it can occur in more evolutionary distinct organisms too (Alekshun and Levy, 2007) and is identifiable by the presence of DNA within bacterial genomes originating from different sources (Normark and Normark, 2002). Genetic transfer is either by transformation (uptake of environmental DNA by naturally competent bacteria), transduction (transfer via bacteriophages) or conjugation (direct transfer between bacterial cells) and involves a range of mobile genetic elements such as plasmids, transposons and integrons. Plasmids range in size from 1-100 kb and contain several genes including those encoding antibiotic resistance and those required for self-replication. Transposons have their own transposase enabling them to insert into the host chromosome, and they encode specific resistance to one antibiotic. Integrons are incorporated into genetic elements and can further acquire exogenous gene cassettes which they turn into functional genes (Alekshun and Levy, 2007).

1.3.1 Physiological mechanisms of antibiotic resistance

Both inherent and acquired resistance manifest in three main physiological mechanisms of antibiotic evasion; inactivation of the drug, reduced uptake and accumulation in the cell or alteration of the drug target. Bacteria can use one or more of these mechanisms.

1.3.1.1 Antibiotic inactivation

Inactivation of antibiotics can be by modification or hydrolysis, for both of which there are well-characterised examples. Modification of the ribosome targeting antibiotics chloramphenicol (50S) and aminoglycosides (30S) by the addition of functional groups dramatically reduces their affinity for the target (Blair *et al.,* 2015). These modifications include *O*-phosphorylation, *N*-acetylation and *O*-adenylation catalysed by phosphoryltransferases, acetyltransferases and adenyltransferases respectively (Shaw *et al.,* 1993).

β-lactam antibiotics are inactivated by enzymatic hydrolysis of the β-lactam ring, which removes their functional group. β-lactamases are a large group of enzymes with active site similarity to the antibiotic target (Philippon *et al.,* 1989), which are highly efficient in drug removal by hydrolysing up to 10^3 penicillin molecules/sec (Walsh, 2000). The β-lactamases are grouped into 4 classes; A, C and D comprising an active site serine, and class B which require zinc for activity and catalysis is through direct attack of a hydroxide ion rather than through a covalent intermediate (Palzkill, 2013). Thousands of enzymes exist that can hydrolyse a wide range of antibiotics such as macrolides, aminoglycosides and phenicols (Blair *et al.,* 2015).

1.3.1.2 Reduced uptake and accumulation

Antibiotics must reach sufficient concentrations at the target site in order to be effective and there are several mechanisms by which this can be avoided. Gram-negative bacteria are inherently more resistant to most antibiotics, due to the presence of an outer membrane in their cell wall that excludes both hydrophobic and large molecules. Antibiotics such as quinolones and β-lactams can enter the cell through outer membrane porins, which are required by the cell for nutrient uptake, although reduced absorption efficiency resulting in antibiotic resistance has been observed in a number of bacteria including *P. aeruginosa* and *Escherichia coli* (Fernández and Hancock, 2012).

If antibiotics enter the cell in sufficient quantities, they can be removed by active efflux. Efflux pumps are found in the cytoplasmic or outer membrane of all bacteria and are used for the energy-dependent transport of lipophilic and amphipathic molecules. They are also used as a protective mechanism to remove toxic compounds such as antibiotics (Webber and Piddock, 2003). Mutational removal of transcriptional repressors leads to overexpression and as pumps often exhibit wide substrate specificity this can results in high-level multidrug resistance such as that observed in *P. aeruginosa* (Blair *et al.,* 2015; Fernández and Hancock, 2012)

1.3.1.3 Alteration of the antibiotic target

Alteration of the drug target is another effective mechanism, as observed in resistance to β-lactams and vancomycin. Mutations in *Streptococcus pneumoniae* penicillin-binding protein (PBP) active sites result in low affinity for β-lactam antibiotics but enables the bacterium to continue to build its cell wall effectively. As a main focus of this thesis, this is covered in more detail in Section 1.8. *Staphylococcus aureus* has acquired an additional PBP with low affinity for β-lactams which can compensate for the lost activity of native proteins upon antibiotic treatment (Pinho *et al.,* 2001).

Vancomycin resistance is commonly achieved through target modification. Glycopeptide antibiotics such as vancomycin bind to the terminal D-Ala-D-Ala residues of the peptidoglycan precursor Lipid II (Nieto and Perkins, 1971). Substrate sequestration results in inhibition of peptidoglycan synthesis and consequently cell lysis. Resistant bacteria express the products of the *vanHAX* genes, which are responsible for incorporation of D-Ala-D-Lac instead of D-Ala-D-Ala into Lipid II (Walsh *et al.,* 1996). The resulting loss of a single hydrogen bond in the vancomycin-Lipid II interaction reduces affinity by 1000-fold (McComas *et al.,* 2003).

1.3.2 Overcoming antibiotic resistance

Antibiotic resistance will always exist, as it is a natural evolutionary mechanism. However, a coordinated, multinational and interdisciplinary approach is required to enable us to continue treating bacterial infections and to enable the medical profession to continue breaking boundaries. Efforts need to be focused towards conserving the lifespan and efficacy of existing drugs, and changes in behaviour resulting from this can help to ensure relative longevity of new antibiotics introduced in the future. The recent, and on-going O'Neill Reports highlight the importance of improved diagnostics (O'Neill, 2015), a problem that the longitude research prize hopes to solve (www.longitudeprize.org). The £10 million pound prize fund is offered to the first group to create a cheap, accurate, rapid and easy-to-use point of care test for infections with the aim of reducing the number of inappropriately prescribed antibiotics.

In parallel with changes in behaviour it is important that we further exploit existing antimicrobial targets and identify new drugs. There are a huge number of possible approaches for the discovery of new antibiotics, which will not be covered here. These include, and are by no means restricted to rational and *de novo* drug design, high throughput screening, genomics based approaches as well as screening of compounds from natural sources. Natural products, or their derivatives make up a vast proportion of the antibiotic agents that currently exist (Brown *et al.,* 2014). These are most often identified through screening of soil microorganisms and extraction of antibiotic compounds. However, only 1% of bacteria are culturable in laboratory conditions. A particularly exciting recent development in this area is the development of the Ichip by Nichols *et al.* (2010), which enables the growth of a range of previously unculturable microorganisms. Use of this method has already resulted in the discovery of a new cell wall inhibitor, teixobactin, to which no resistance has been detected (Ling *et al.,* 2015).

This thesis focuses on improved understanding of bacterial cell wall synthesis as a fundamentally interesting biological mechanism, as well as a validated target for antibiotics. Better understanding can help in the design of new drugs, which is just

one way in which we can help to ensure bacterial infections remain only a minor health problem for future generations.

1.4 The bacterial cell wall

Bacteria are classed as Gram-positive or Gram-negative based upon their reaction with the dye-iodine complex of Gram stain (Gram, 1884), which demonstrates the main difference in the cell wall structure of these two classes. The Gram stain reacts with the peptidoglycan polymer found exclusively in almost all eubacteria, with the exception of *Mycoplasma*. In Gram-positive bacteria, the stain interacts with the 20-80 nm thick peptidoglycan layer, which makes up 30-70% of the overall cell wall structure (Bugg, 1999, Schleifer and Kandler, 1972). In contrast, in Gram-negative bacteria the thin 2-3 nm peptidoglycan layer surrounded by an outer membrane cannot interact with the stain (Gram, 1884, Bugg, 1999). The Gram-negative outer membrane is a complex layer made up of phospholipids, lipoproteins, lipopolysaccharides and porins (Bugg, 1999). The main features of the Gram-positive and Gram-negative cell wall structure are illustrated in Figure.1.1.
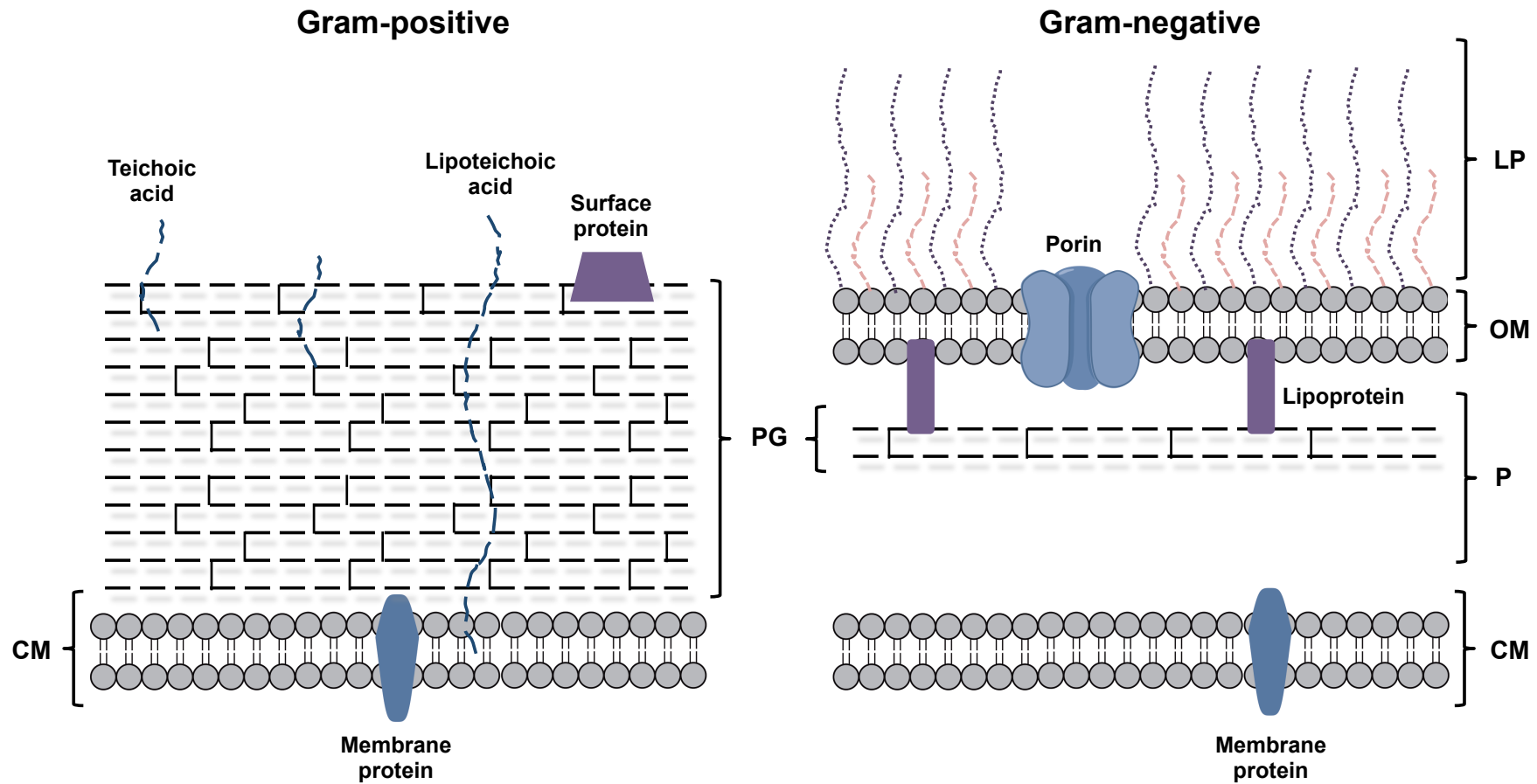
Figure 1.1: The major features of the Gram-positive and Gram-negative cell wall. Major features are illustrated in schematic form**.** CM: cytoplasmic membrane, OM: outer membrane, P: periplasm. LP: Lipopolysaccharide, PG: peptidoglycan. Both cell walls have a peptidoglycan layer which is 10-20 layers thick in Gram-positive and 1-3 layers in Gram-negative. Adapted from Cabeen and Jacobs-Wagner (2005)

1.4.1 The Gram-positive cell wall

The Gram-positive bacteria *Streptococcus pneumoniae* and *Staphylococcus aureus* are the particular focus of this thesis. Both have the structure of a typical Gram-positive organism (Figure 1.1) with a thick layer of peptidoglycan (Section 1.5). Both also have a highly decorated cell surface with wall teichoic acids (WTA) and lipoteichoic acid (LTA), the former is anchored to the peptidoglycan sacculus and the latter to the cytoplasmic membrane. Teichoic acids are anionic glycopolymers consisting of phosphodiester-linked polyol units. WTA makes up approximately 90% of the *S. pneumoniae* cell wall teichoic acids (Vollmer, 2007), and are required for full expression of β-lactam resistance in methicillin resistant *Staphylococcus aureus* (MRSA) (Brown *et al.*, 2013). They are involved in maintaining cell shape, cell division and the susceptibility to antibiotics of many Gram-positive bacteria (Brown *et al.*, 2013).

Pathogens (both Gram-positive and Gram-negative) responsible for invasive diseases often produce an extracellular polysaccharide capsule (CPS)(O'Riordan and Lee, 2004)(not shown in Figure 1.1), which helps to resist phagocytosis and therefore is crucial for virulence. CPS range from linear polymers of two or more monosaccharides to complex branched polysaccharides with additional side chains (Paton and Morona, 2007), and distinct CPS types are used to define the serotype of bacteria. There are 90 known *S. pneumoniae* serotypes to date (Henrichsen, 1995), but relatively few strains of *Staphylococcus aureus* have been recognised as capsule positive (O'Riordan and Lee, 2004). CPS has successfully been targeted in the design of vaccinations against pneumococcal infections (World Health Organisation, 2012), although the full mechanisms of CPS biosynthesis and expression are not fully understood (Paton and Morona, 2007).

1.5 Peptidoglycan

1.5.1 The role of peptidoglycan

Peptidoglycan is essential for bacterial survival and inhibition of its biosynthesis results in cell lysis. The polymer forms a sacculus surrounding the bacterial cell cytoplasmic membrane and its primary role is to withstand cellular turgor pressure (Vollmer *et al.,* 2008), which can be up to 3 MPa in some Gram-positive bacteria (Bugg, 1999), due to its high mechanical strength. It is responsible for maintaining the defined cell shape (Young, 2003) through its close association with cell growth and division (Vollmer *et al*., 2008). Peptidoglycan also has a non-structural role as a scaffold to anchor extracellular structures such as lipoproteins in Gram-negative bacteria and proteins and teichoic acids in Gram-positive. Proteins on the surface of Gram-positive bacteria are involved in adhesion, invasion and resistance to phagocytic killing and therefore are often crucially important in pathogenicity (Navarre and Schneewind, 1999).

1.5.2 Peptidoglycan structure

Peptidoglycan is a polymer of linear glycan strands cross-linked by short peptide stems. This basic structure is conserved but a high level of genus- and species-specific diversity exists in the peptidoglycan sacculus. This variation is important in the interaction and action of cell wall synthesis and modification enzymes, as well as in resistance to antibiotics and sacculus degradation. Interspecies variation is used for the taxonomic classification of bacteria (Schleifer and Kandler, 1972).

This section describes the conserved general structure of peptidoglycan, which is illustrated in Figure 1.2, with subsections detailing the main modifications observed.
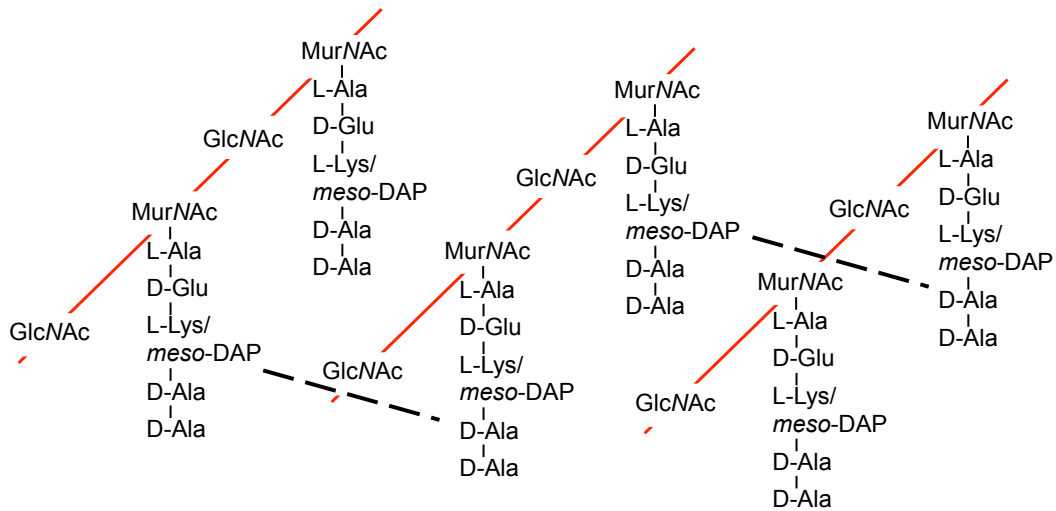
Figure 1.2: Basic structure of peptidoglycan. Glycan chains of alternating *N*-acetylglucosamine (Glc*N*Ac) and *N*-acetylmuramic acid (Mur*N*Ac) linked by β-1,4-glycosidic bonds (red -). Peptide stems generally contain L-Lys in the third position in Gram-positive bacteria and *meso*-DAP in Gram-negative. Cross-links between peptide stems (- - -) normally between position 3 and 4 of adjacent stems and are shown as direct links here. Variation exists in every component as discussed in the text. Adapted from Bugg *et al.,* (1999).

1.5.2.1 The glycan backbone

The glycan chain backbone of peptidoglycan is made up of alternating *N*-acetylglucosamine (Glc*N*Ac) and *N*-acetylmuramic acid (Mur*N*Ac) sugar residues linked by β-1,4-glycosidic bonds. A pentapeptide stem is appended to the lactoyl side chain of the Mur*N*Ac residues (Section 1.5.2.2) (Bugg, 1999; Vollmer, 2008). This β-1,4-linked glycan backbone is found in all bacteria, although no known bacterial species possess an unmodified version (Section 1.5.2.1.1) in their mature peptidoglycan (Vollmer, 2008). Sugar residues are either linked to other cell-wall polymers or directly modified post synthesis.

1.5.2.1.1 Variation in the glycan backbone

The action of glycan strand-cleaving enzymes such as glucosaminidases and muramidases give variation in the terminal sugar residue of the polysaccharide backbone. Gram-positive *Staphylococcus aureus* may possess a Glc*N*Ac residue at the reducing end rather than Mur*N*Ac due to cleavage by *N*-acetylglucosaminidase (Boneca *et al*., 2000), whereas the glycan chain of all Gram-negative bacteria and

some Gram-positive terminate with a 1,6-anhydrous-*N*-acetylmuramic acid (with an intramolecular ring) due to degradation by lytic transglycosylases (Section 1.6.4)(Vollmer, 2008).

Secondary modifications such as *N*-deacetylation, *O*-acetylation and *N*-glycolylation are observed frequently. *N*-deacetylation of Glc*N*Ac and Mur*N*Ac to Glc*N* and Mur*N* is responsible for lysozyme resistance, and are formed by peptidoglycan deacetylases acting on polymerised peptidoglycan (Vollmer, 2008). *O*-acetylation and de-*O*-acetylation of Mur*N*Ac also occurs on newly polymerised peptidoglycan and have a role in resistance to most known muramidases. It is also associated with a range of other functions such as peptidoglycan cross-linking, autolysis and the recognition of peptidoglycan by host factors in infection (Vollmer, 2008). *N*-Glycolylation of the muramic acid 2-amino group to a glycolyl residue is found in most genera with mycolic acid, such as *Rhodococcus*, *Gordonia* and *Mycobacterium* (Azuma *et al.,* 1970; Sutcliffe, 1998), and also in some genera within the *Acinomycetales* (Evtushenko *et al*., 2002; Li *et al*., 2005; Matsumoto*,* 2003). This modification occurs on the final soluble cytoplasmic precursor, UDP-Mur*N*Ac pentapeptide, through the action of monooxygenases, and is believed to play a role in antibiotic and lysozyme resistance (Vollmer, 2008).

The average glycan chain length varies significantly between bacteria, and at different locations within the cell (Wang *et al*., 2008), but surprisingly does not correlate with the thickness of the peptidoglycan layer. Gram-positive *Bacilli* spp. and *Staphylococcus aureus* have thick cell walls and glycan chains ranging in length from 50-250 disaccharides, and approximately 6 units respectively (Boneca *et al.,* 2000; Hughes, 1971). The model Gram-negative organism; *E. coli* has chains of 10-40 disaccharide units (Vollmer, 2008).

1.5.2.2 The pentapeptide stem

A pentapeptide stem is attached to the Mur*N*Ac sugar and has the basic structure of L-Ala-γ-D-Glu-*meso*-DAP(or L-Lys)-D-Ala-D-Ala. The third position amino acid is *meso*-DAP in Gram-negative bacteria and L-Lys in Gram-positive (Schleifer and

Kandler, 1972). Several components of the pentapeptide structure are unusual, such as the γ linked D-Glutamic acid, with the only other documented occurrences in folate derivatives (Kislliuk, 1981) and bacterial exopolymers (Troy, 1973). D-amino acids are formed by racemisation of L-amino acids and are important in resistance to protease digestion of the cell wall (Bugg, 1999). *meso*-DAP is a non-protein amino acid not found in animals, and together with the presence of D-amino acids provide interesting bacterial specific targets for antibiotics (Bugg, 1999). The pentapeptide stem is commonly described as the stem peptide as it is often lacking the terminal D-Ala in mature peptidoglycan, and in some cases the penultimate D-Ala; resulting in tetra- and tripeptides.

1.5.2.2.1 Variation in the stem peptide

A large amount of variation occurs at every position on the stem peptide (Schleifer and Kandler, 1972), introduced through the action of Mur ligases (Section 1.6.1) or by modifications later in peptidoglycan biosynthesis. Most variation is in the cross-linking third position amino acid, incorporated by the MurE ligase, where a wide variety of amino acids exist such as L-Lys, *meso*-DAP, LL-DAP and less commonly residues including L-homoserine, 2,4-diaminobutyric acid, L-ornithine and *meso*-lanthionine (Vollmer *et al.,* 2008). Of particular note is the presence of D-Lac or D-Ser in the fifth position in strains resistant to the vancomycin antibiotic (Healy *et al.,* 2000).

Post synthesis modifications such as hydroxylation, amidation, acetylation and attachment of proteins most commonly occur on position 2 or 3 at the lipid-linked stage of peptidoglycan synthesis, although many of the mechanisms involved are as yet unknown. D-Glu, *meso*-DAP and L-Lys have a hydroxylated hydrocarbon chain in some species, which in the case of D-Glu is dependent on oxygen supply during growth, and the ε-carboxyl of *meso*-DAP and α-carboxyl of glutamic acid are frequently amidated (see Section 1.5.2.2.2). Stem peptides act as a covalent anchor for many cell envelope proteins in both Gram-positive and Gram-negative bacteria (Dramsi *et al*., 2008).

1.5.2.2.2 Amidation of the stem peptide

A particular focus of this thesis is the amidation of D-glutamate at position 2 to D-isoglutamine, by the coordinated action of a glutamine amidotransferase like protein (GatD) and a Mur ligase homologue (MurT). These were first isolated from *Staphylococcus aureus* (Münch *et al*., 2012; Figueiredo *et al*., 2012), and more recently *Streptococcus pneumoniae* (Zapun *et al*., 2013). Amidation is frequently observed in Gram-positive bacteria (Schleifer and Kandler, 1972) and homologous transcriptional units have been identified in many bacteria of this class including *Clostridium perfringens* and *Mycobacterium tuberculosis* (Münch *et al.*, 2012). Loss of amidation in *Staphylococcus aureus* results in a slower growth rate, increased sensitivity to lysozyme and reduced β-lactam resistance (Figueiredo *et al*., 2012), and is believed to play a role in innate immune signalling (Münch *et al*., 2012). Recent work has identified amidated peptidoglycan to be an optimal substrate for the late cell wall synthetic enzymes in *S. pneumoniae* (Zapun *et al*., 2013), and is investigated more fully in this thesis.

A model for amidation by GatD/MurT has been proposed (Münch *et al*., 2012) (Figure 1.3), in which ammonia from glutamine (the primary nitrogen donor) is shuttled from GatD to the MurT synthetase active site, which subsequently amidates Lipid II in an ATP dependent manner. The exact timing of the process in peptidoglycan biosynthesis is not categorically confirmed, particularly with respect to peptide bridge formation (Section 1.5.2.3), but it has been demonstrated to be at the bactoprenol-bound stage.
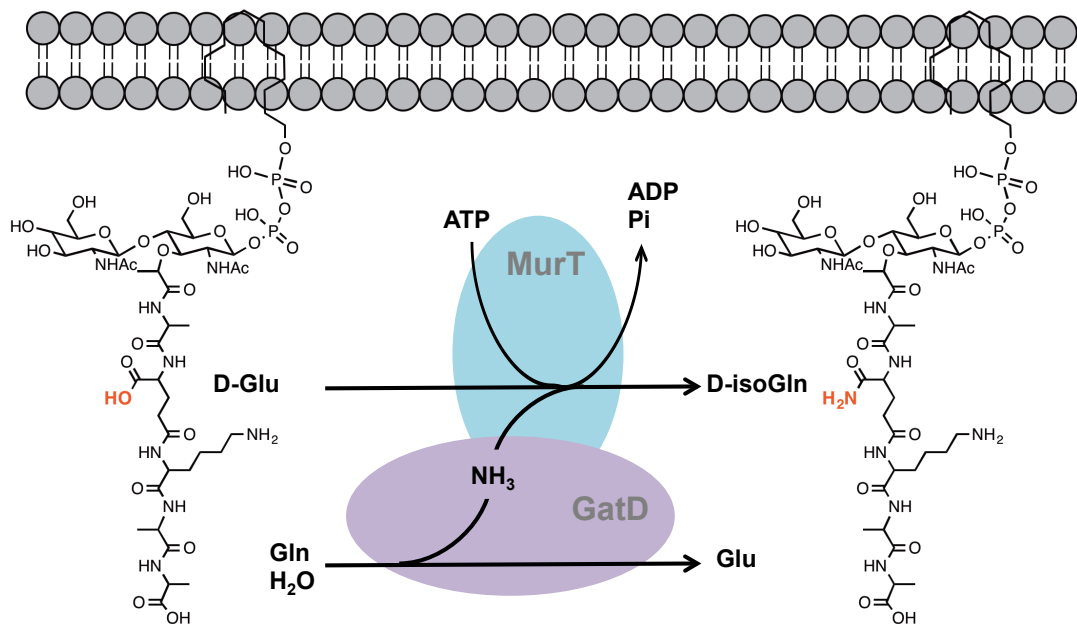
Figure 1.3: Proposed mechanism of D-glutamate amidation by GatD/MurT. Ammonia is shuttled from glutamine by the GatD glutaminase active site. MurT subsequently amidates D-glutamate to D-isoglutamine in an ATP dependent manner. Diagram is a cartoon representation and not to scale. Lipid linker is shown as a representation and is not biologically correct. Adapted from Münch *et al.,* (2012)

1.5.2.3 Stem peptide cross-links

Cross-links between pentapeptide stems are critical for peptidoglycan rigidity, and provide significant structural variation. The extent of cross-linking varies, typically between 25-50% in Gram-negative bacteria, and 70-90% in Gram-positive species (Glauner, 1988). Direct cross-links between the ε-amino group of *meso*-DAP (or L-Lys) and the α-carbonyl of the position 4 D-Alanine in an adjacent peptide stem occur most commonly in Gram-negative bacteria with *meso*-DAP in the third position (but are also found in L-Lys containing stems). Gram-positive bacteria predominantly form indirect cross-links through an interpeptide bridge of 1-5 amino acids (Section 1.5.2.3.1). A peptide bond is formed between the α-amino group of the N-terminal amino acid in the peptide bridge and the α-carbonyl of the position 4 D-Alanine in these cases (Vollmer *et al.,* 2008). Interpeptide bridges exhibit a large amount of variation between bacterial species and are covered in more detail in the following section.

1.5.2.3.1 Variation in stem-peptide cross-links

Intracellular membrane-associated ligases catalyse the addition of interpeptide bridges on the ε-amino group of the third position *meso*-DAP or L-Lys. Assembly is in the opposite direction to that of protein synthesis (Bugg, 1999) and uses aminoacyl-tRNAs as substrates. Bridge assembly occurs mostly at the lipid-linked stage, with the exception of *Lactobacillus viridescens* and *Enterococcus faecalis* (Hegde and Blanchard, 2003). Table 1.2 shows some examples of the peptide bridges formed in a range of bacteria.

Bacterial species	Peptide bridge composition
Streptococcus pneumoniae	L-Ser-L-Ala or L-Ala-L-Ala
Staphylococcus aureus	Gly-Gly-Gly-Gly-Gly
Lactobacillus viridescens	L-Ala-L-Ser or L-Ala-L-Ser-L-Ala
Enterococcus faecium	D-Asp, D-Asn
Enterococcus faecalis	L-Ala-L-Ala
Streptomyces coelicolor	Gly

Table 1.2: Peptide bridge composition in Gram-positive branched peptidoglycan. (Vollmer *et al.,* 2008) Sequence is carboxyl to amino terminal from left to right.

Of particular interest in this project is the peptide bridge of *S. pneumoniae* (and *Staphylococcus aureus* to a lesser extent), both of which are essential in the expression of high level β-lactam resistance. The *S. pneumoniae* L-Ala-L-Ala or L-Ser-L-Ala cross-link is assembled by the MurM and MurN tRNA-dependent ligases, which are non-essential but required for β-lactam resistance (Filipe *et al*., 2000), in which MurM plays a particularly important role (Lloyd *et al*., 2008). MurM is responsible for the addition of the first L-Ser or L-Ala and MurN the second L-Ala (De Pascale *et al*., 2008; Lloyd *et al*., 2008). Pentaglycine bridge formation in *Staphylococcus aureus* is catalysed by the FemX, FemA and FemB ligases, in which FemX adds the first glycine and FemA and FemB subsequently add two each (Rohrer and Berger-Bächi, 2003). FemX is essential (Tschierske *et al*., 1999) and all

three proteins must be present for full expression of β-lactam resistance (Ling and Berger-Bächi, 1998).

Variation is also observed in direct cross-links. Peptide bonds between adjacent meso-DAP residues are important in β-lactam resistance; up to 10% of *E. coli* crosslinks are of this type (Glauner*,* 1988), and are found in high levels in non-replicating *Mycobacterium tuberculosis* (Lavollay *et al.,* 2008). *Micrococcaceae* peptidoglycan cross-linking is between the L-Ala at position one and D-Ala at position four (Ghuysen *et al*., 1968).

1.5.3 Is peptidoglycan biosynthesis a viable antibiotic target?

Peptidoglycan biosynthesis is validated as an antibiotic target as the success of two of the most clinically important classes of antibiotic, β-lactams and glycopeptides, have demonstrated (Bugg, 1999). The biosynthesis of peptidoglycan is a complex and essential process, making it an excellent target for antibiotics. The intracellular, membrane bound and extracellular steps provide a wide range of possible targets, and targeting the extracellular catalytic steps negates the structural difficulties associated with drug penetration of the cytoplasmic membrane.

Understanding the biosynthesis of peptidoglycan is vitally important in the development of new antibiotics, as despite it being the target for key classes of drugs and its essentiality for cell survival, it has been underexploited as a target. Recent developments in structural biology, the *in vitro* synthesis of peptidoglycan biosynthetic intermediates and the development of high throughput screening (HTS) methods now makes detailed biochemical characterisation of the enzymes involved a possibility (Bugg *et al.,* 2011). The insight obtained will progress the understanding of this fundamental process as well as aiding in the development of novel antibiotics to reduce the burden of antimicrobial resistance.

1.6 Peptidoglycan biosynthesis

The biosynthesis of peptidoglycan is a complicated, multi-stage process, involving approximately 20 reactions and is under tight spatial and temporal control (Scheffers and Pinho, 2005). The biosynthetic steps can be split into three distinct stages; cytoplasmic, intracellular membrane bound and extracellular membrane bound. The first two stages are illustrated in Figure 1.4, and the final extracellular in Figure 1.5.

1.6.1 Cytoplasmic steps

The cytoplasmic steps of peptidoglycan synthesis are catalysed in a tightly ordered mechanism by six enzymes, MurA-F and involves the synthesis of UDP-Mur*N*Ac-pentapeptide from UDP-Glc*N*Ac (Figure 1.4). Several additional 'side' reactions are required to synthesise the D-glutamate and D-Ala-D-Ala substrates for MurD and MurF respectively (Barreteau *et al.,* 2008).

MurA forms the UDP-Glc*N*Ac-enolpyruvate substrate for MurB by transfer of an enolpyruvate group to UDP-*N*-acetylglucosamine from PEP (phosphoenolpyruvate). MurB subsequently reduces this to UDP-*N*-acetylmuramic acid (UDP-Mur*N*Ac) in an NADPH dependent manner. ATP dependent amino acid ligases; MurC-F attach the pentapeptide stem to the UDP-Mur*N*Ac lactoyl group using an Mg^{2+} cofactor. Detailed analysis of the biochemical properties of MurC-MurF has shown that they have the same three-dimensional structure, reaction mechanism and six-amino acid ATP binding site. Variation at the N-terminus allows for the different lengths of the stem peptide substrates (Smith, 2006).

1.6.2 Intracellular membrane associated steps

The intracellular membrane associated steps of peptidoglycan biosynthesis are catalysed by MraY and MurG (Figure 1.4). MraY initially transfers the phosphor-Mur*N*Ac-pentapeptide from the product of the cytoplasmic steps onto undecaprenyl phosphate (C_{55}) to form Lipid I (Bouhss *et al.*, 2004; Lloyd *et al.,* 2004). The undecaprenyl phosphate carrier is produced by either dephosphorylation of

undecaprenyl pyrophosphate or kinase mediated phosphorylation of undecaprenol (Manat *et al*., 2014). The MraY catalysed reaction is coupled to MurG, which transfers *N*-acetylglucosamine from UDP-Glc*N*Ac to Lipid I to form Lipid II (undecaprenyl pyrophosphoryl-Mur*N*Ac-(Glc*N*ac)-pentapeptide)(Ha *et al.,* 1999). Many of the amino acid based modifications in peptidoglycan structure (Sections 1.5.2.2 and 1.5.2.3) occur at his point.

1.6.2.1 Linking the intracellular and extracellular steps

Lipid II must be flipped to the extracellular face of the cytoplasmic membrane before it can be incorporated into peptidoglycan by extracellular enzymes. The protein (or proteins) responsible remain a controversial research area, after more than 30 years of research. The main considered candidates have been MurJ, FtsW, RodA and SpoVE. In 2011, Mohammadi *et al*. demonstrated that FtsW could transport Lipid II across both proteoliposomes and membrane vesicles (Mohammadi *et al.,* 2011) and later went on to demonstrate the substrate specificity of FtsW for Lipid II and suggested a mechanism for transport through a size-restricted pore-like structure (Mohammadi *et al,* 2014). This was widely considered to have solved the elusive flippase problem. However, almost coinciding evidence from elegant *in vivo* investigations has suggested that MurJ may actually be responsible for the translocation of Lipid II (Sham *et al*., 2014). The authors went so far as to demonstrate that FtsW does not flip Lipid II *in vivo*, going against the conclusions from previous *in vitro* work (Mohammadi *et al.,* 2011). The real identity of the Lipid II flippase remains to be confirmed, with the possibility of multiple complementary or coordinated partners not discussed in the literature to date, and all work so far concerning *E. coli*, the flippase may in fact be a family of flippases with different roles at different points in the cell cycle.

Page 22: Figure 1.4: The cytoplasmic and intracellular membrane associated steps in peptidoglycan biosynthesis. NAM = Mur*N*Ac, NAG = Glc*N*Ac. UDP-Glc*N*Ac converted to UDP-Mur*N*Ac by MurA and MurB. MurC-MurF sequentially add L-Ala, D-Glu, L-Lys (or meso-DAP) and D-Ala-D-Ala to UDP-Mur*N*Ac. Side reactions required to make novel amino acids also shown. Gram-negative specific steps in green. MraY transfers UDP-Mur*N*Ac-pentapeptide to the undecaprenyl lipid carrier and MurG adds a final Glc*N*Ac to form Lipid II. Lipid II is flipped to the extracellular (periplasmic in Gram-negative) space by FtsW or MurJ.. Figure adapted from unpublished figure by Dr Vita Godec

extracelluar space/
periplasmic space

lipid
carrier

Lipid II

NAM-NAG

cytoplasm

P
P

undecaprenyl
phosphate

MraY

NAM

MurG

NAM-NAG

FtsW/MurJ

UDP-NAG

UDP

UMP

Lipid I

Lipid II

UDP-NAM-L-Ala-D-Glu-(L-Lys/*m*-DAP)-D-Ala-D-Ala

MurF

ATP
D-Ala-D-Ala

DdlB

D-Ala

Alr

L-Ala

UDP-NAM-L-Ala-D-Glu-(L-Lys/*m*-DAP)

MurE

ATP
L-Lys (Gram+) or *m*-DAP (Gram-)

DapF

L,L-DAP

UDP-NAM-L-Ala-D-Glu

MurD

ATP
D-Glu

ATP
L-Ala

NADPH

PEP

UDP-NAM-L-Ala

UDP-NAM

UDP-NAG

MurC

MurB

MurA
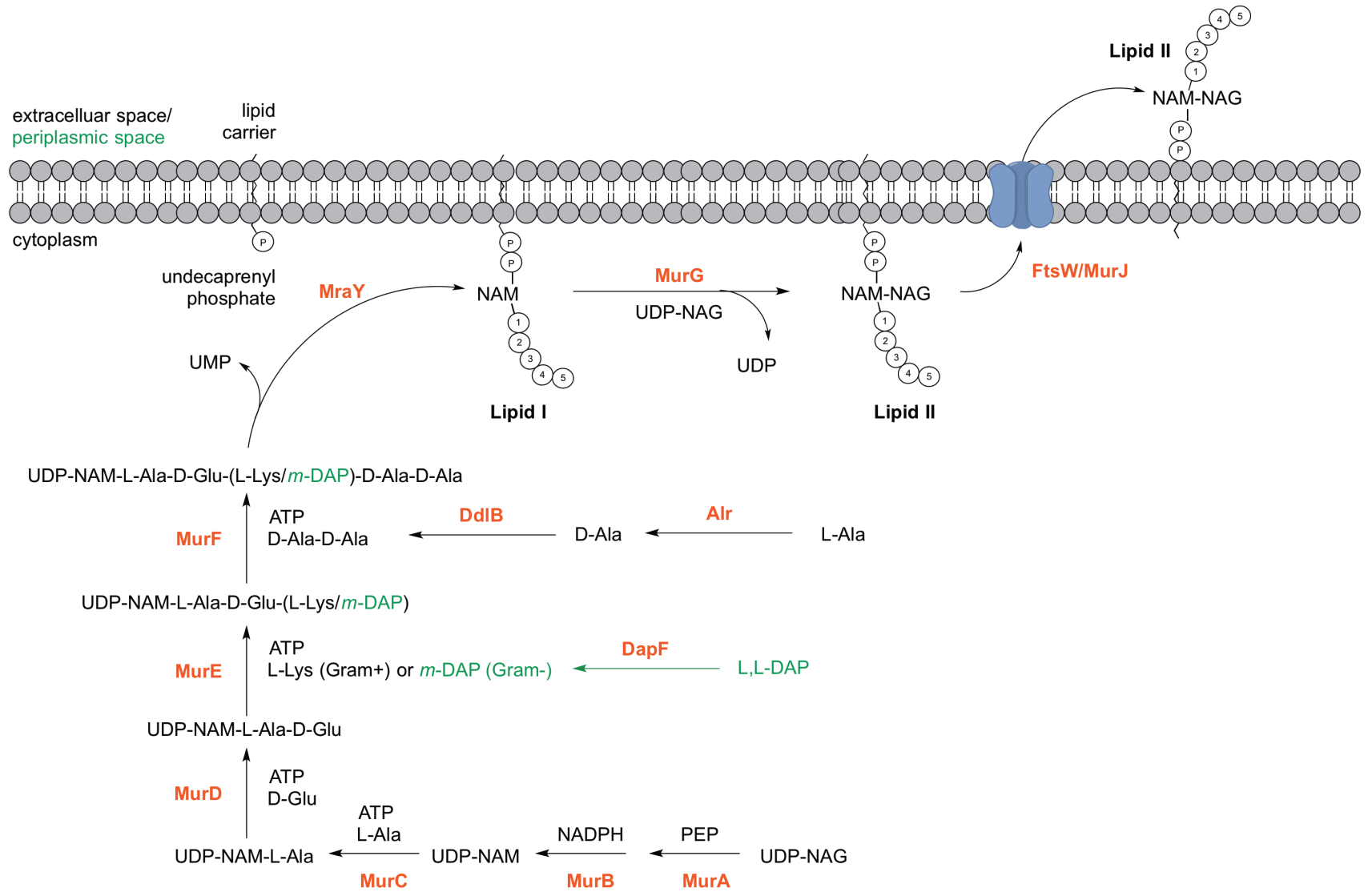
1.6.3 Extracellular membrane associated steps

Lipid II is incorporated into peptidoglycan on the extracellular face of the cytoplasmic membrane by the penicillin-binding proteins (PBPs), which catalyse transglycosylation and transpeptidation (Figure 1.5). The PBPs are the focus of this thesis and are covered in more detail in Section 1.7.

Transglycosylation is the elongation of glycan chains from Lipid II by incorporation of the disaccharide-pentapeptide into a growing polymer. A β-1,4-glycosidic bond is formed between the incoming Glc*N*Ac and terminal Mur*N*Ac of the glycan chain, with the release of undecaprenyl pyrophosphate. The lipid carrier is translocated back across the cytoplasmic membrane either before or after dephosphorylation (Manat *et al.,* 2014), resulting in undecaprenyl phosphate, the substrate for MraY (Section 1.6.2).

The soluble glycan polymers are cross-linked by the transpeptidase activity of PBPs to form an insoluble sacculus, which can withstand the high internal turgor pressure of the cell. Cross-linking consists of direct or indirect peptide bonds between amino acids of adjacent peptide stems as described in Section 1.5.2.3. Both PBP catalysed reactions are covered in more detail in Section 1.7.
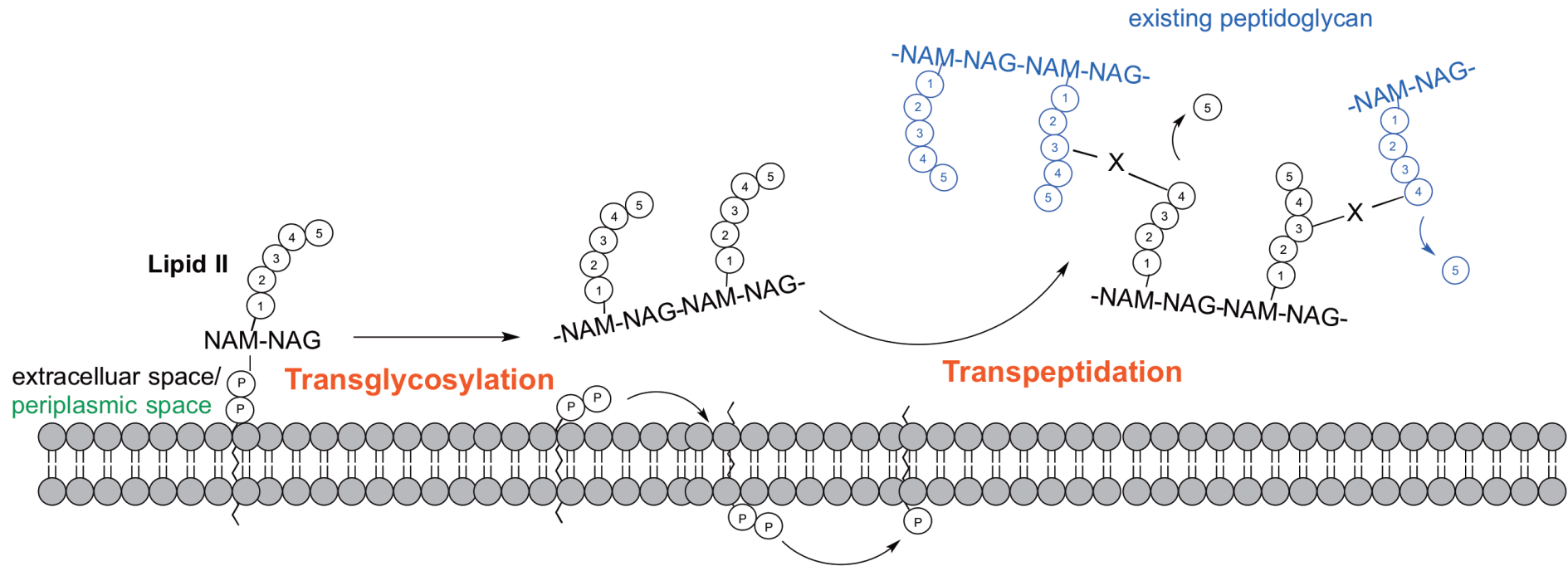
Figure 1.5: Extracellular membrane associated steps of peptidoglycan biosynthesis. NAM = Mur*N*Ac, NAG = Glc*N*Ac. Following the translocation of Lipid II to the extracellular (periplasmic in Gram-negative bacteria) side of the cytoplasmic membrane, the disaccharides are polymerised into glycan chains by transglycosylases. Transpeptidases form cross-links between pentapeptide stems to give structural rigidity. The lipid carrier is translocated back across the cytoplasmic membrane either before or after dephosphorylation. Figure adapted from unpublished figure by Dr Vita Godec

1.6.4 Processing and recycling of peptidoglycan

Peptidoglycan biosynthesis is regulated at multiple levels in order to balance cell wall synthesis with cell growth, and in response to many factors including growth conditions, other bacteria and the cell cycle (Egan *et al.,* 2015). The sacculus must be constantly remodelled and rebuilt in order to allow cell growth, separation of daughter cells and peptidoglycan turnover (Vollmer *et al.*, 2008a). The peptidoglycan synthases are regulated by localisation and spatial regulation, precursor availability, environmental conditions and protein-protein interactions (Egan *et al.,* 2015). In addition, the peptidoglycan hydrolases, made up of glycosidases (glycan strand cleaving) and peptidases (peptide stem cleaving) are responsible for the localised breakdown of the cell wall to allow modification of the sacculus. They have also been extensively used in the study of native peptidoglycan structure for many years (Vollmer *et al.,* 2008a). This expansive class of enzymes possesses a large amount of redundancy, and many enzymes within it have multiple functions making the attribution of roles particularly difficult (Höltje and Tuomanen, 1991; Smith *et al*., 2000). There is a known hydrolase for every bond in peptidoglycan, although only a subset is found in each bacterial species (Vollmer *et al.,* 2008a). Table 1.3 summarises the roles of cell wall hydrolases in *S. pneumoniae*, and Figure 1.6 illustrates their hydrolytic activity on peptidoglycan.

Cell wall hydrolase	Pneumococcal protein	Role
DD-carboxypeptidase	PBP3	Cell wall synthesis regulation
N-acetylglucosaminidase	LytB	Daughter cell separation
N-acetylmuramyl-L-alanine amidase	LytA	Major autolysin
N-acetylmuramidase	LytC	Autolysin
Peptidoglycan Glc*N*Ac deacetylase	PgdA	Lysozyme resistance

Table 1.3: *S. pneumoniae* peptidoglycan hydrolases. Pneumococcal protein responsible for each hydrolytic activity illustrated in Figure 1.6, and cell cycle role of each enzyme (Vollmer, 2007)
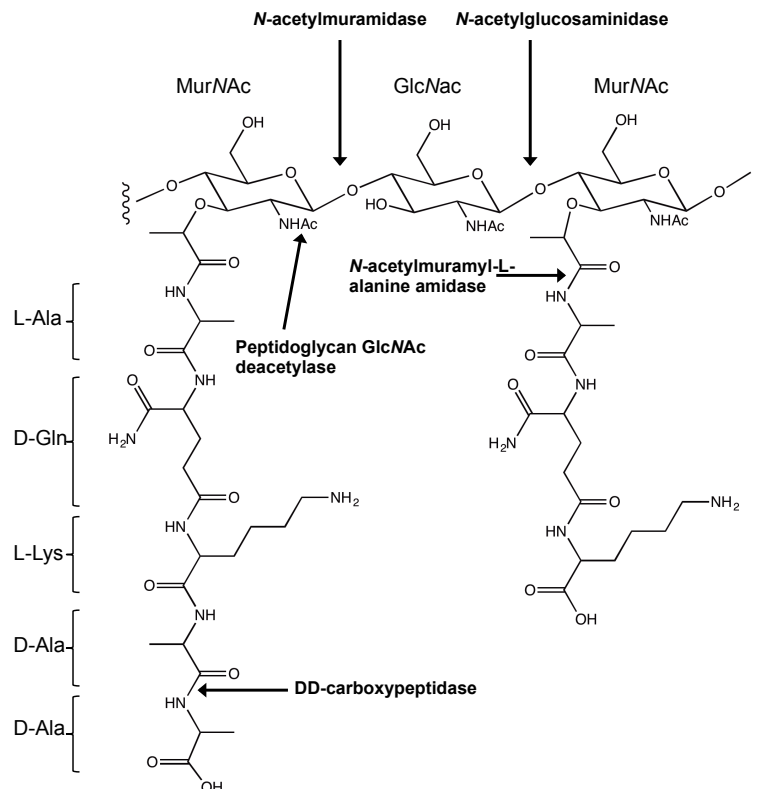
Figure 1.6: *S. pneumoniae* peptidoglycan hydrolases. Arrows mark the point of cleavage of peptidoglycan hydrolases, illustrated with the basic structure of *S. pneumoniae* peptidoglycan. Adapted from Vollmer, 2007.

Peptidoglycan recycling has been documented in Gram-negative but not Gram-positive bacteria to date. A large degree of variation exists in the extent of peptidoglycan turnover between bacterial strains and also within them dependent on growth conditions (Reith and Mayer, 2011). Up to 50% of *E. coli* peptidoglycan is recycled and either used as an energy source, or to synthesise new peptidoglycan (Park and Uehara, 2008). Gram-positive bacteria shed 25-50% of its peptidoglycan per generation through outward expansion and the action of hydrolases, (Reith and Mayer, 2011). Following the identification of orthologs of recycling enzymes, and the massive loss of cell wall material involved, a Gram-positive peptidoglycan recycling system has been speculated but not proven (Reith and Mayer, 2011)

1.7 The penicillin-binding proteins

The work in this thesis focuses on the activity of the penicillin-binding proteins (PBPs), which are responsible for polymerisation of the glycan chains of peptidoglycan (transglycosylation) as well as peptide stem cross-linking (transpeptidation), the final stages in the peptidoglycan biosynthesis pathway. PBPs are essential for cell viability due to their role in peptidoglycan tensile strength, and in addition to their lack of eukaryotic counterparts this makes them excellent antimicrobial targets (Bugg, 1999). Penicillin bears a structural resemblance to the natural PBP substrate: the D-Ala-D-Ala terminus of the stem pentapeptide precursor, thus they are sensitive to penicillin (where resistance is not found). This is the characteristic by which the class of enzymes were discovered, and subsequently named by Tipper and Strominger (1965). The term penicillin-binding proteins is misleading with regards to their function as the catalytic activities they are responsible for are transglycosylation, transpeptidation and carboxypeptidation.

PBPs have been studied since they were first discovered in the 1960s (Tipper and Strominger, 1965), but despite this, relatively little is known about their enzymatic mechanisms and interactions with other cell wall proteins. Progress has been slow predominantly due to the nature of the enzymes and substrates involved. PBPs are integral membrane proteins, which are notoriously difficult to study, but the main barrier has been availability of the structurally complex Lipid II substrate. Recent advances in both areas have made their detailed study possible, and the biochemistry of these critical enzymes is beginning to be revealed.

1.7.1 Nomenclature and classification of PBPs

Most bacterial species express between three and eight different PBPs, which vary in relative abundance and constitute approximately 1% of their membrane protein population (Waxman and Strominger, 1983). *Bacillus subtilis* is unusual in its expression of sixteen distinct PBPs (Sauvage *et al.,* 2008). PBPs are numbered within organisms based on their relative separation by SDS-PAGE (sodium dodecyl sulfate-polyacrylamide gel electrophoresis) due to differences in molecular weight.

The gradual nature of identification means that some PBPs have an additional letter after the number. This nomenclature is confusing as PBPs of similar sizes and properties have different numbers in a range of organisms, making comparisons of function complicated.

PBPs can be divided into two main classes; high molecular weight (HMW) and low molecular weight (LMW)(Waxman and Strominger, 1983) and their characterisation and topology is illustrated in Figure 1.7. HMW PBPs (60-140kDa) are integral membrane proteins consisting of a cytoplasmic tail, transmembrane spanning anchor and two extracellular domains joined by a β-rich linker. HMW PBPs are further sub-classified into class A or class B depending on the characteristics of the N-terminal extracellular domain. In class A it is responsible for transglycosylase activity, and in class B it is thought to interact with cell cycle proteins to affect cell morphogenesis (Macheboeuf *et al.,* 2006; Sauvage *et al.,* 2008). The C-terminal extracellular domain has transpeptidase activity in both classes of HMW PBPs, and class A are known as bifunctional due to their dual transglycosylase and transpeptidase activity. LMW PBPs (40-50kDa) are commonly referred to as class C PBPs and have a single catalytic domain with either D,D-carboxypeptidase or endopeptidase activity (Denome *et al*., 1999), making up some of the peptidoglycan hydrolases covered in Section 1.6.4. Class C PBPs are membrane associated through a transmembrane or amphipathic helix (Macheboeuf *et al*., 2006).

Monofunctional glycosyl transferases (MGTs) are expressed by some bacteria and have a complementary role to the transglycosylase activity of HMW class A PBPs (Di Berardino *et al.,* 1996; Reed *et al.,* 2011; Spratt *et al.,* 1996; Wang *et al.,* 2001). These differ from PBPs in that they have no penicillin-binding domain; however, they are integral membrane proteins with a crucial role in peptidoglycan polymerisation (Macheboeuf *et al*., 2006).
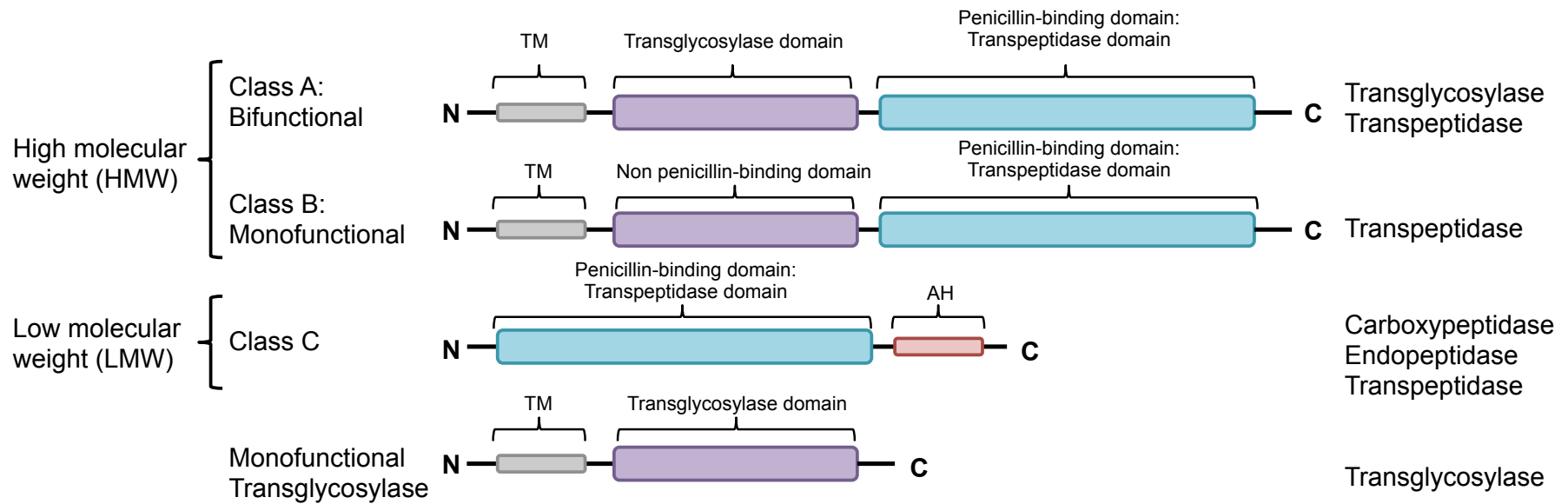
Figure 1.7: Classification of the Penicillin-Binding Proteins: Classification shown on the left. Monofunctional transglycosylases are not PBPs but are shown for completeness due to their complementary role. Domain topology of each class shown where TM: transmembrane region, AH: amphipathic helix. Enzymatic activity of each class shown on the right.

1.7.2 PBPs as part of the cell wall synthesis complex

Some PBPs are unique and essential, whereas others demonstrate a level of functional redundancy within the cell. The interaction of a range of PBPs for localisation as well as functional and regulatory reasons has been shown. Cell wall metabolism during the cell cycle can be generally divided into two stages in rod shaped bacteria and the pneumococci; elongation and division, requiring tight temporal and spatial control of a range of essential proteins (Macheboeuf *et al.,* 2006) and increasingly recognised as involving two separate large multi-subunit complexes (Zapun *et al.,* 2012). Variation exists in the mechanisms due to the different shapes of bacteria (Pinho *et al.,* 2013), and the components of spatially distinct division and elongation complexes are best understood in the Gram-negative model organism *Escherichia coli* (Typas and Sourjik, 2015).

The tightly regulated polymerisation of FtsZ (bacterial tubulin homologue) at the septum forms the Z ring and initiates cell division (Bi and Lutkenhaus, 1991; Errington *et al*., 2003) by recruitment of other members of the septal machinery to the division site, including the septal PBPs. In rod shaped bacteria, the PBPs involved in peripheral peptidoglycan synthesis co-localise with an actin-like cytoskeleton containing MreB in patches that move along the long axis of the cell powered by peptidoglycan synthesis (Domínguez-Escobar *et al.,* 2011; Garner *et al.,* 2011; van Teeffelen *et al.,* 2011). Cocci do not possess an MreB homologue and therefore the mechanism of peripheral cell wall synthesis is unclear (Pinho *et al.,* 2013).

Immunoprecipitation, biochemical, immunofluorescence and genetic experiments in *E. coli, Bacillus subtilis* and *Streptococcus pneumoniae* have shown cell division and elongation to involve at least one Class A and Class B PBP, along with lytic transglycosylases and other cell wall proteins (Massidda *et al.,* 2013; Popham and Young, 2003; Typas and Sourjik, 2015).

This thesis focuses on the Gram-positive pathogens *Staphylococcus aureus* and *S. pneumoniae* and the following sections briefly summarise the current knowledge of

the role of PBPs in the cell wall synthetic machinery of these bacteria. Illustrated in Figure 1.8.

1.7.2.1 *Staphylococcus aureus* cell wall synthesis machinery

Spherical cocci such as *Staphylococcus aureus* build their cell wall using a single basic machinery that can be transient in some cases (Pinho *et al.,* 2013). *Staphylococcus aureus* has an exceptionally minimal mechanism of cell wall synthesis which occurs only at the septum (Kuru *et al.,* 2012; Pinho and Errington, 2003) and requires only four PBPs (and one monofunctional transglycosylase), with an additional acquired transpeptidase in methicillin resistant strains. One each of Class A HMW, Class B HMW and LMW PBPs; PBP2, PBP1 and PBP4 localise at the septum (Pinho and Errington, 2003), and the localisation of the fourth HMW Class B PBP3 is not known to date. PBP1 is recruited to the mid-cell by an as yet unidentified divisome protein (Pereira *et al*., 2007; 2009), and PBP2 is recruited by its Lipid II substrate (Pinho and Errington, 2005). PBP4 as a LMW PBP is unusual in having transpeptidase activity and is responsible for forming highly cross-linked peptidoglycan. It is recruited by an intermediate of the wall teichoic acid (WTA) synthesis (pathway) (Atilano *et al.,* 2010) after the initiation of peptidoglycan synthesis by PBP1 and PBP2.

1.7.2.2 *Streptococcus pneumoniae* cell wall synthesis machinery

The ovoccocal shape of pneumococcal cells suggests that the cell wall is formed by successive elongation and division processes, and therefore is likely to involve a distinct elongasome and divisome similar to that of rod shaped bacteria such as *E. coli.* However, the peripheral machinery in streptococci is adjacent to the septum instead of in the sidewall (Pinho *et al.*, 2013), which may more resemble the recently identified FtsZ dependent preseptal elongation of *E. coli* (Typas *et al*., 2012). The current evidence suggests the presence of one large complex containing both sub-machineries, which assembles at the midcell (reviewed excellently by Massidda *et al.,* 2013). The currently favoured two-state model suggests that the peripheral machinery inserts new peptidoglycan between the septum and equatorial rings,

causing the cell to elongate, and the septal machinery synthesises the cross wall by following the leading edge of the septum (Pinho *et al*., 2013). Recent high-resolution microscopy of live cells following the incorporation of fluorescent probes into the growing cell wall has suggested that the apparatus may separate into two separate machineries in late cell division (Cadby and Lovering, 2014; Tsui *et al.,* 2014), which would support this two state model. It is clear that the mechanisms of cell wall synthesis in ovococci such as *S. pneumoniae* are not fully understood, but new methods of observing live cells (Tsui *et al.,* 2014) show real promise for future work.

The current knowledge of the role of PBPs in the pneumococcal cell wall identifies that the Class B transpeptidases PBP2x and PBP2b are found in the septal and peripheral sub-machinery respectively (Massidda *et al.,* 2013), however PBP2x may play a more exceptional role in an unusual form of septal closure as it locates separately from all other peptidoglycan synthesis proteins in the mid to late stages of cell division (Tsui *et al.,* 2014). This may be mediated through the extracellular C-terminal PASTA domains of PBP2x (Peters *et al.,* 2014). The bifunctional Class A PBP1a has been observed in both the peripheral and septal machinery (Land and Winkler, 2011; Massidda *et al.,* 2013), and it is believed to be important in creating the septum. The Class C carboxypeptidases are located across the entire cell surface (Barendt *et al.,* 2011). The mechanism of PBP localisation is not well understood, but is believed to be substrate dependent (Hasper *et al*., 2006; Pinho *et al.,* 2013) and mediated by the trimming activities of PBP3 restricting the correct substrate to the mid-cell (Morlot *et al.,* 2004). Recent work has identified the importance of the StkP/DivIVA/GpsB triad in fine-tuning septal and peripheral peptidoglycan biosynthesis and therefore maintainance of the oval shape of *S. pneumoniae* (Fleurie *et al.,* 2014). This is in keeping with the theory of a single large complex with sub-machineries.
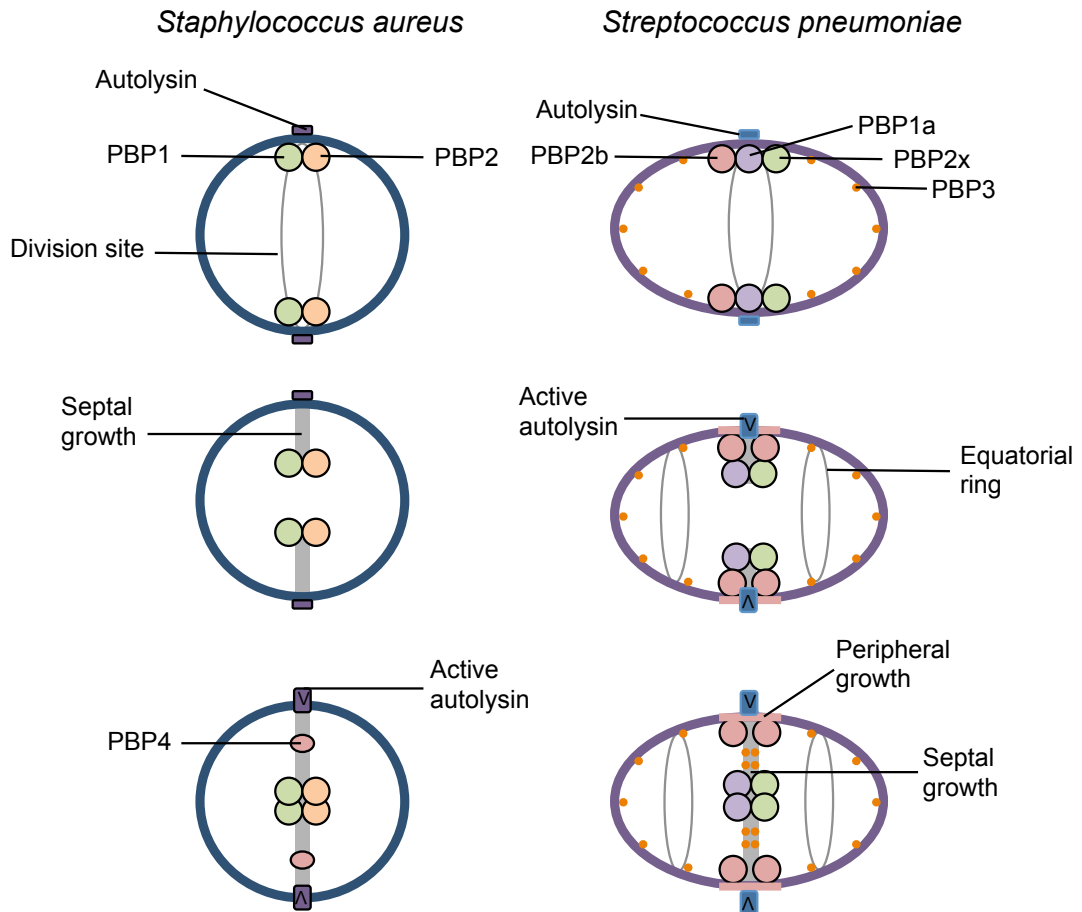
Figure 1.8 Organisation of PBPs in cell wall synthesis of *Staphylococcus aureus* and *S. pneumoniae*. *Staphylococcus aureus*: PBP1 and PBP2 synthesise peptidoglycan at the septum. PBP4 is recruited later and is responsible for high levels of cross-linking. Autolysin (Atl) becomes active in the later stages of the cell cycle and causes septum splitting. *S. pneumoniae*: Septal peptidoglycan synthesis is catalysed by PBP1a and PBP2x. Peripheral insertion of new cell wall is by PBP2a. PBP3 is located throughout the cell and is thought to trim the terminal D-Ala from peptidoglycan stem peptides so that the correct substrate for PBPs is at the mid-cell. Adapted from Pinho *et al.,* (2013).

1.7.3 The transglycosylase domain of PBPs

Monofunctional glycosyltransferases (MGTs) and Class A bifunctional PBPs possess a transglycosylase domain which is responsible for the polymerisation of Lipid II into glycan chains. Peptidoglycan transglycosylases are classified in the glycosyltransfer family 51 (GT_{51}) according to the Carbohydrate-Active enzymes (CAZY) scheme (www.cazy.org). This class is characterised by being membrane bound, using undecaprenyl-based substrates and possessing a novel structural fold (Section 1.7.3.1).

1.7.3.1 Structure of the transglycosylase domain

Crystal structures of peptidoglycan transglycosylases from *Staphylococcus aureus* and *Aquifex aeolicus* (Lovering *et al.,* 2007; Yuan *et al.,* 2007) enabled the first structural identification of the catalytic domain, and further structures published since have confirmed the same common predominantly α-helical topological fold (Heaslet *et al.,* 2009; Huang *et al.,* 2012; Sung *et al*., 2009).

The active site is found in a deep cleft between two lobes: a globular "head" region, which has low homology with λL lysozyme and a small hydrophobic region, termed the 'jaw' domain (Lovering *et al.,* 2007; Yuan *et al.,* 2007). The 'jaw' is thought to interact with Lipid II and the membrane by embedding or closely associating and is rich in hydrophobic residues (Lovering *et al.,* 2007; Yuan *et al.,* 2007). The λL lysozyme and transglycosylase active sites have secondary structure similarities, despite low sequence homology. The globular 'head' domain of both overlay well, with differences in the 'jaw' domain; which is composed mainly of β-sheets in lysozyme and α-helices in the transglycosylases. This structural similarity can be rationalised by the substrate similarity between the two and suggests a possible evolutionary acquisition of the GT_{51} fold by lysozyme (Lovering *et al.,* 2007). The homology extends as far as the active site, with the essential catalytic glutamate of *Staphylococcus aureus* PBP2 and λL lysozyme oriented similarly, as well as the reaction products of lysozyme and reactants of PBP2 (Lovering *et al*., 2012a).

Structures of *E. coli* PBP1b and *Staphylococcus aureus* MGT including the transmembrane (TM) spanning region, show that it is in close contact with the transglycosylase domain, but doesn't affect the active site structure. Both structures show that the TM region maintains proper membrane orientation (Huang *et al.,* 2012; Sung *et al.,* 2009). Binding experiments showed the importance of the TM region in moenomycin interaction for both enzymes, and the transglycosylase activity of MGT (Huang *et al.,* 2012). The overall structure of *E. coli* PBP1b, *Staphylococcus aureus* MGT and *Staphylococcus aureus* PBP2 transglycosylase domains are shown in Figure 1.9, bound to moenomycin as a substrate mimic (Section 1.7.3.2).
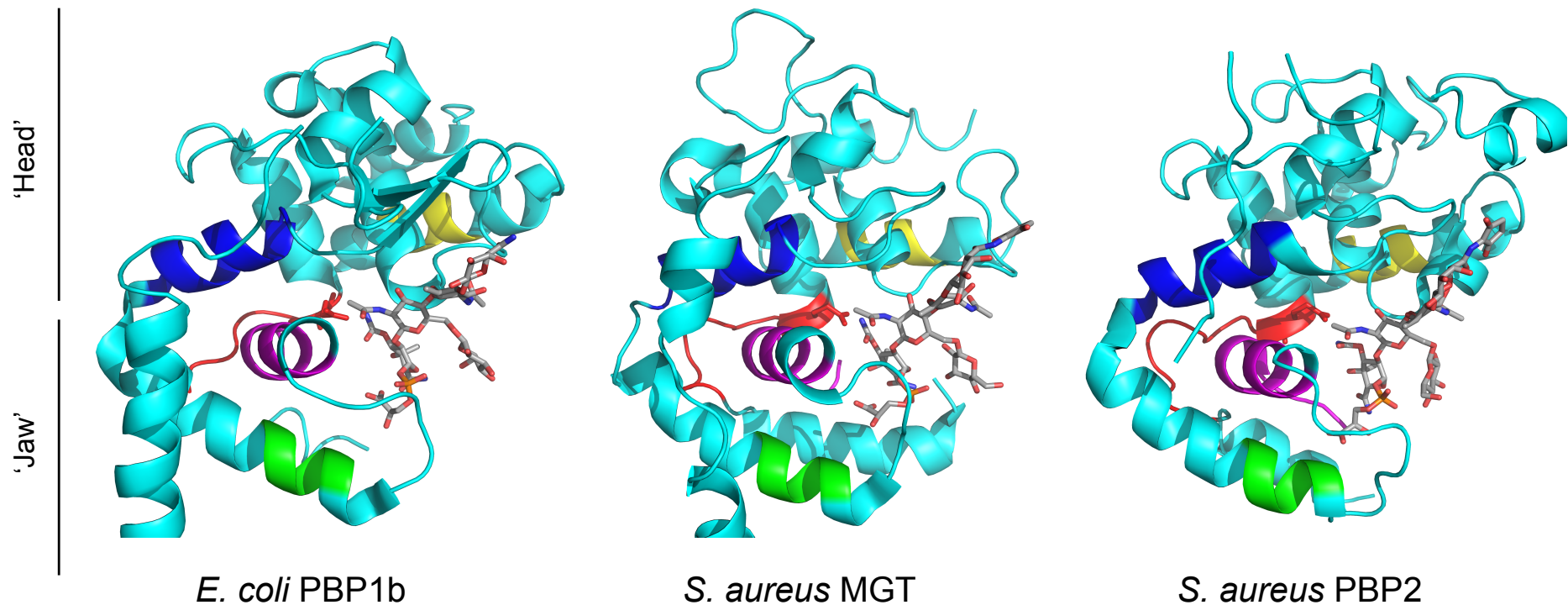
Figure 1.9: Structural comparison of the transglycosylase domains of *E. coli* PBP1b, *Staphylococcus aureus* MGT and *Staphylococcus aureus* PBP2. Comparison of the structures of transglycosylase domains bound to moenomycin in the donor site as a substrate mimic (Section 1.7.3.2) Full domain is shown in ribbon form in cyan. Conserved motifs 1-5 are shown in red, magenta, green, dark blue and yellow respectively (Section 1.7.3.3). Conserved active site glutamate shown in stick form as part of motif 1. Moenomycin in stick form shown bound in the donor site. The globular 'head'domain and flexible 'jaw domain' are labelled on the left of the figure. Structural alignments using moenomycin; *Staphylococcus aureus* PBP2 against *Staphylococcus aureus* MGT; RMSD: 0.856 Å for 71 atoms, *E. coli* PBP1b against *Staphylococcus aureus* MGT; RMSD: 1.14Å for 67 atoms. The transmembrane region of *E. coli* PBP1b and *Staphylococcus aureus* MGT can be seen extending from the bottom of the image. image. The structure of *Staphylococcus aureus* PBP2 was solved without the transmembrane region, and the linker and transpeptidase domain were removed for this image for both *Staphylococcus aureus* PBP2 and *E. coli* PBP1b. Credit: Dr Dean Rea for help in producing this figure. PDB accession codes; *E. coli* PBP1b: 3FWL; *Staphylococcus aureus* MGT: 3VMR; *Staphylococcus aureus* PBP2: 2OLV.

A linker region known as the UB2H domain directly joins the transglycosylase and transpeptidase domains of *E. coli* PBP1b. It consists of five anti-parallel β-sheets and one α-helix, and is known to interact with LpoB, an outer membrane lipoprotein that stimulates transpeptidase activity (Paradis-Bleau *et al.*, 2010; Typas *et al.,* 2010). Linker regions exist in other bifunctional PBPs such as *Staphylococcus aureus* PBP2 (Lovering *et al.,* 2007), although have not been shown to functionally interact to date.

1.7.3.2 Moenomycin: a transglycosylase inhibitor and structural tool

The natural product moenomycin is the best characterised directly binding inhibitor of transglycosylase activity. The moenomycins are a family of glycolipid antibiotics produced by *Streptomyces ghanaensis*, and Moenomycin A is the main antimicrobial component (Ostash and Walker, 2010). Moenomycin A will be referred to as moenomycin throughout this thesis. Moenomycin is highly active against many Gram-positive bacteria, but due to its poor pharmacokinetic properties such as a long half-life and poor absorption, it cannot be developed as an antibiotic and has instead been used extensively in animal feed. The first crystal structure of a PBP bound to moenomycin (Lovering *et al.,* 2007) gave direct evidence that it mimics the growing glycan chain (Lipid IV more specifically) in the donor site, an outcome predicted from its structural similarity (shown in Figure 1.10). This led to the conclusion that the growing glycan chain is the transglycosylase donor and Lipid II is the acceptor. Further crystal structures of transglycosylases bound to moenomycin have supported this (Heaslet *et al.,* 2009; Huang *et al.,* 2012; Sung *et al.,* 2009; Yuan *et al.,* 2008), and Perlstein *et al.* (2007) confirmed the donor and acceptor identities. Figure 1.9 shows the crystal structures of *E. coli* PBP1b, *Staphylococcus aureus* MGT and *Staphylococcus aureus* PBP2 bound to moenomycin in the donor site.
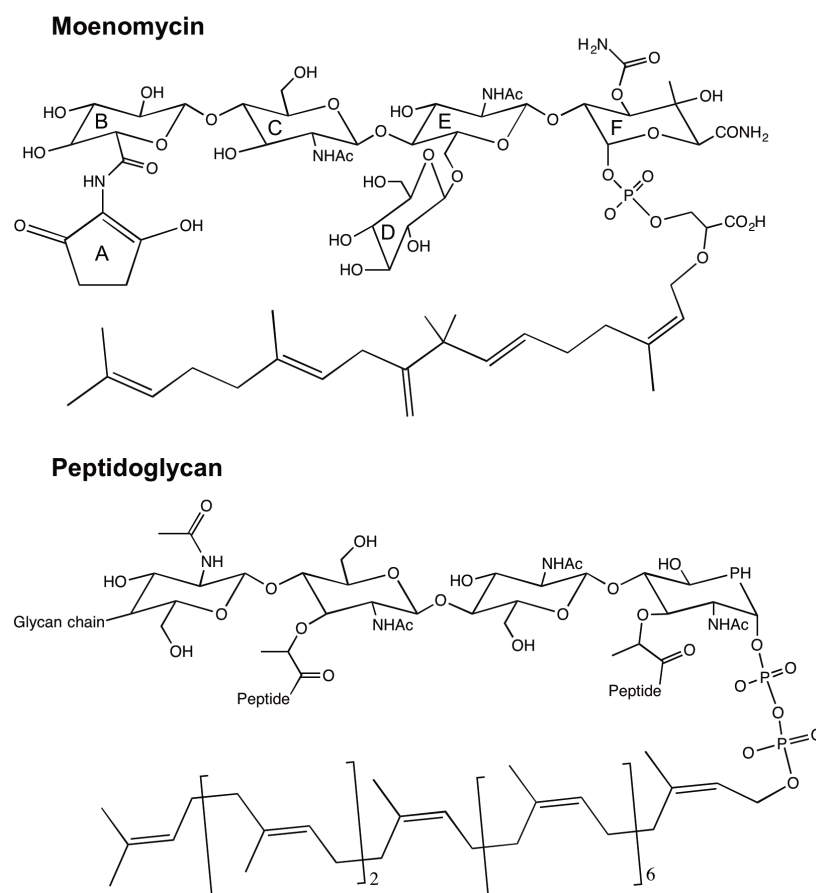
Figure 1.10: Structural comparison of moenomycin and peptidoglycan (Lipid IV). The structure of moenomycin (top) and Lipid IV (2 disaccharides) are shown. The glycan components of both are very similar, as well as the lipid anchor of peptidoglycan and lipid tail of moenomycin. Rings A-F are labelled on the structure. Peptide on the peptidoglycan structure represents the pentapeptide stem appended to the lactoyl group of the Mur*N*Ac sugar.

1.7.3.3 Conserved residues of the transglycosylase domain

The conserved residues of the transglycosylase domain are found in five motifs (Figure 1.9)(Lovering *et al.,* 2008a), which have been shown to be essential in *E. coli* PBP1b, *A. aeolicus* PBP1a and *Staphylococcus aureus* MGT (Barrett *et al*, 2007; Heaslet *et al.*, 2009; Terrak *et al.,* 2008). Motifs 1-3 are central in the catalytic cleft, with motif 2 dividing the two substrate binding pockets; one for the growing glycan chain and the other for the incoming Lipid II. Motif 4 and 5 are proposed to play a more structural role; as motif 4 lines the back of the cleft, and motif 5 is found more peripherally in the globular 'head' domain. (Lovering *et al.*, 2007). Mutational

analyses have confirmed the role of the conserved residues, with motif 2 shown as essential for Lipid II recognition (Di Guilmi *et al.,* 2003), and the catalytic glutamate identified as part of motif 1 (Terrak *et al.,* 1999), with surrounding motif 1 conserved residues important in its positioning (Terrak *et al,* 2008). Positively charged lysine and arginines in motif 2 and 3 are predicted to be involved in substrate positioning (Lovering *et al,* 2007; Terrak *et al.,* 2008).

The first structure of a transglycosylase (*Staphylococcus aureus* MGT) bound to a Lipid II analogue in the acceptor site (Huang *et al.,* 2012) identified the important acceptor interacting residues structurally for the first time (Figure 1.11). An unexpected observation was that the D-lactyl ether of Mur*N*Ac interacts with the transglycosylase domain, a region thought to only be involved in the transpeptidase reaction. This has implications for the role of the pentapeptide stem recognition in transglycosylase activity. Mutation of the proposed Lipid II contacting residues and activity analysis confirmed the crucial residues, in particular showing that K140 and R148 together stabilise the pyrophosphate leaving group, a departure from the previous prediction (Huang *et al.,* 2012).
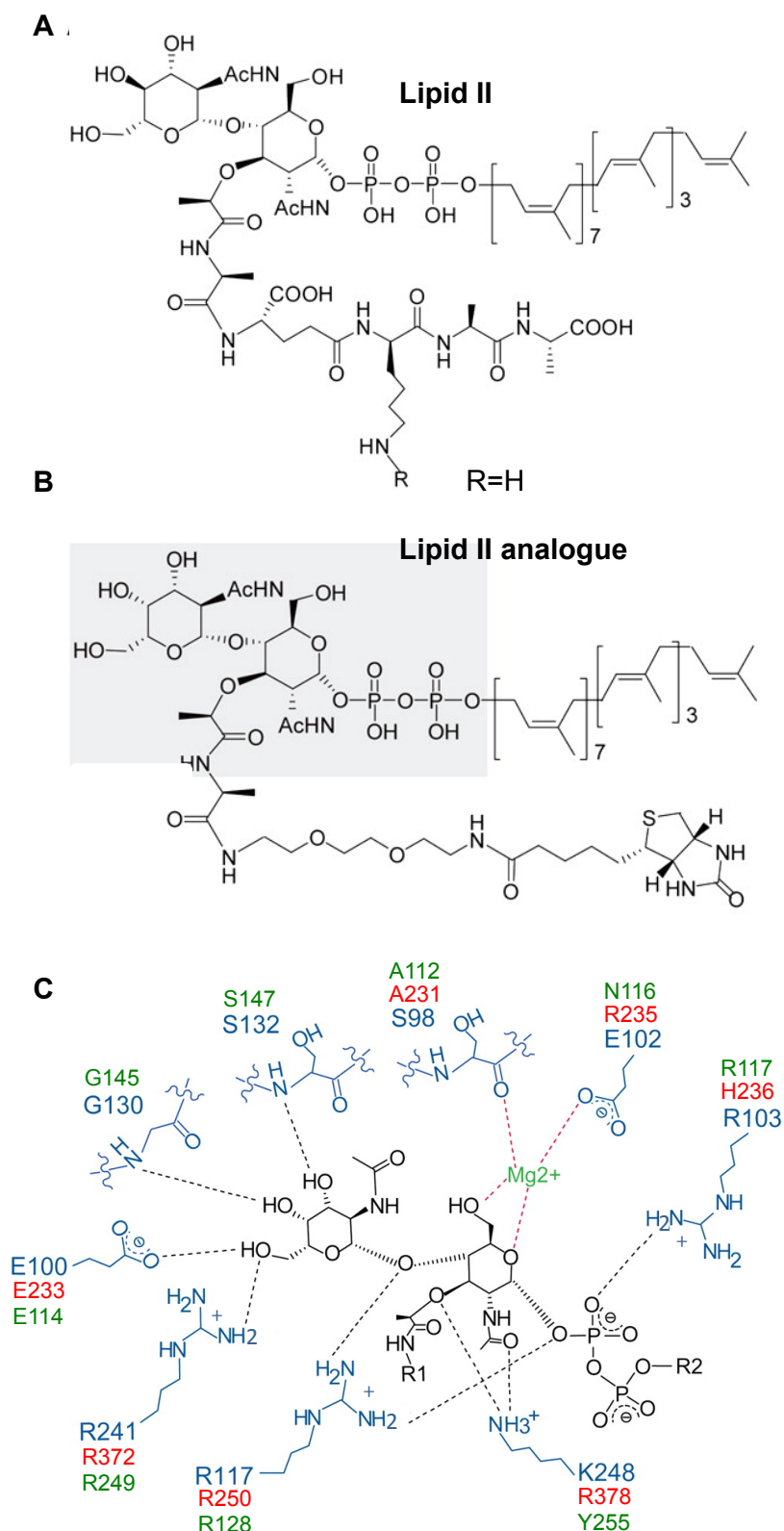
Figure 1.11: The MGT transglycosylase acceptor site. A: Natural substrate for the acceptor site: Lipid II. B: Lipid II analogue used for co-crystallisation with *Staphylococcus aureus* MGT FL by Huang *et al*.,(2012). Grey denotes the area observable on the electron density map. C: Schematic view of the interaction between *Staphylococcus aureus* MGT and Lipid II analogue showing hydrogen-bonding networks (black) and interactions around Mg^{2+} (red) of conserved resides (blue font). Interacting residues from sequence alignment and comparison of crystal structures shown for *E. coli* PBP1b (red) and *Staphylococcus aureus* PBP2 (green). Figure adapted from Huang *et al*., (2012).

1.7.3.4 Mechanistic features of transglycosylation

Transglycosylation involves integration of the disaccharide units of Lipid II onto the reducing terminus of a growing glycan chain (Perlstein *et al*., 2007) as demonstrated by an elegant set of experiments in which the terminal Glc*N*Ac of Lipid II was blocked with [^{14}C]-labelled-galactose, preventing it from acting as a glycosyl acceptor at the non-reducing end. Chain extension by *E. coli* PBP1a, *E. coli* PBP1b, *Staphylococcus aureus* PBP2 and *A. aeolicus* PBP1a with this modified substrate demonstrated that chain extension occurs at the reducing terminus of the diphospholipid.

Transglycosylation is a processive activity (Yuan *et al.,* 2007), in such that the transglycosylase catalyses several rounds of polymerisation before releasing the glycan product. Time-course analysis of glycan products separated by SDS-PAGE identified long chains rather than the accumulation of short chains (Barrett *et al.,* 2007) supporting the model, along with the presence of an active site flap covering the *A. aeolicus* transglycosylase site observed in the crystal structure (Yuan *et al.,* 2007).

Wang *et al.,* (2008) demonstrated by SDS-PAGE separation of transglycosylase products, that PBPs from different organisms (and enzymes within the same organism) produce glycan chains of differing lengths, independent of the substrate: enzyme ratio. This is unsurprising given the variety of shapes and sizes of bacterial cells, and the presence of multiple transglycosylases in many organisms. *E. coli* PBP1a, *E. coli* PBP1b, *E. faecalis* PBP2a and *Staphylococcus aureus* PBP2 were found to produce chain lengths of approximately 30, 50, 15 and 15 disaccharide units respectively and *S. pneumoniae* PBP2a makes glycan chains of 20-30 units (Helassa *et al*., 2012). A mechanism for release of the product at the enzyme specific threshold length has not been elucidated to date.

1.7.3.5 Transglycosylase catalytic mechanism

A catalytic mechanism for transglycosylation has been proposed based on crystal structures and accompanying biochemical analyses. The recent structure of *Staphylococcus aureus* MGT with a Lipid II analogue (Huang *et al.,* 2012) has enabled the most detailed mechanistic insight to date supported by a comprehensive mutagenesis study (Illustrated in Figure 1.12), and has built on previous insight from the structures of *Staphylococcus aureus* PBP2, *E. coli* PBP1b and an earlier *Staphylococcus aureus* MGT structure (Heaslet *et al.,* 2009; Lovering *et al.,* 2007; 2008; Sung *et al.,* 2009). The binding of two Lipid II molecules, one in the donor and one in the acceptor site initiates transglycosylation, involving the interaction with several specific residues (detailed in Figure 1.12). E100 acts as a base to deprotonate the 4-OH of the Glc*N*Ac in the acceptor site, which is stabilised by R241 and subsequently reacts with the C1 of the donor site Lipid II (or growing glycan chain). This results in a β-1,4-glycosidic bond and an inversion of the configuration of the C1 anomeric carbon. The displaced undecaprenyl pyrophosphate leaving group is stabilized by K140 and R148 of the donor site, an alteration from the previous suggestion of E156. The Lipid IV (or longer chain) is shuffled to the donor site, before a new Lipid II binds to the acceptor site in a mechanism proposed to be assisted by the higher affinity of the pyrophosphate-lipid moiety for the donor site (Lovering *et al.,* 2007). The presence of a π-bulge on the edge of the jaw subdomain could allow local unfolding or disorder to allow this transition to occur (Lovering *et al.,* 2008).

Recently, positive cooperativity has been demonstrated between the acceptor and donor sites of the monofunctional transglycosylase (MGT) from *Staphylococcus aureus* (Bury *et al.,* 2015). Binding of Lipid II analogues to the acceptor site causes an allosteric activation of the donor site leading to an increase in affinity for moenomycin. Bury and colleagues propose that Lipid II binds preferentially to the acceptor site causing a conformation change that stabilises the mobile region between motifs 1 and 2, previously implicated to be involved in acceptor binding (Lovering *et al.,* 2008). This conformational change extends to the donor site, thus increasing its affinity for a second Lipid II (or maintaining the interaction with the growing glycan chain). This mechanism is likely to be particularly important in the

initiation of transglycosylation but also in processivity due to increased binding of the elongating chain.
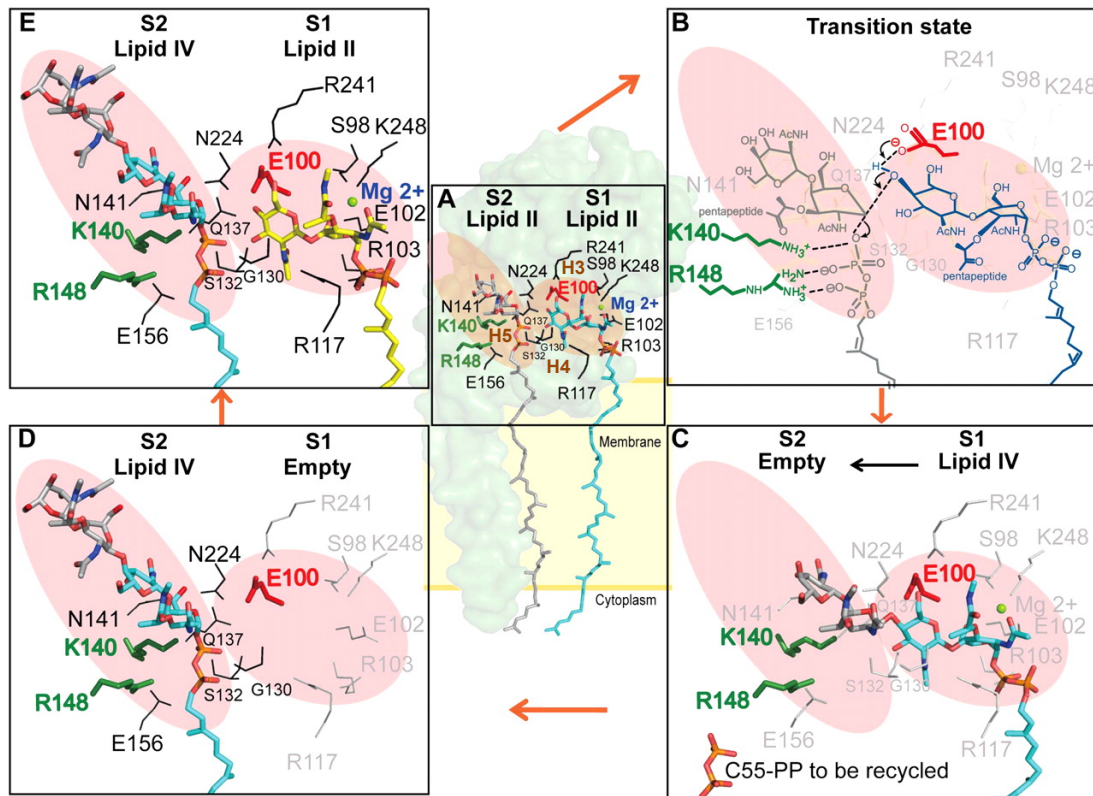
Figure 1.12: Proposed mechanism for transglycosylation by PBPs. Illustrated with *Staphylococcus aureus* MGT. A: Donor (S2) and acceptor (S1) sites shaded in red. Binding of two Lipid II substrates represented by moenomycin (S2 site) and a Lipid II analogue (S1 site). The acceptor site Lipid II is stabilised through Mg^{2+} cations by S98, E102, R103, R117, S132, R241 and K248 and binding to the donor site by G130, Q137, K140, N141, R148 and N224. Helix 3,4 and 5 (labelled H3, H4 and H5 in brown) form the glycosyl acceptor site. B: E100 (red sticks) deprotonates the 4-OH of Lipid II GlcNAc in the S1 site, stabilised by R241 and this simultaneously reacts with the C1 of Lipid II in the S2 site. K140 and R148 (green sticks) stabilise the pyrophosphate leaving group and facilitate its departure. C: Lipid II (or the growing glycan chain) in the donor site (S2) is transferred to the Lipid II in the acceptor site with the formation of a β-1,4-glycosidic bond, and D: the product is shuffled to the S2 donor site. E: A new Lipid II molecule binds to the acceptor site (S1) and the cycle continues. Adapted from Huang *et al.,* (2012).

1.7.4 The penicillin-binding domain

Class A and B high molecular weight (HMW) as well as the low molecular weight (LMW) PBPs, all possess a penicillin-binding domain. These were named following early experiments showing that penicillin blocked the formation of peptide cross-links, leading to morphological differences in *E. coli* cells (Gardner, 1940; Tipper and Strominger, 1965). Tipper and Strominger (1965) proposed that penicillin formed a stable covalent penicilloyl enzyme by binding to the active site due to its

structural similarity with the terminal D-Ala-D-Ala of the natural substrate (Figure 1.16 (A and B)), which was later confirmed by binding of a [^{14}C]-benzylpenicillin to be via a covalent linkage with a serine residue (Frère *et al.,* 1976). The pentapeptide stem of the substrate was later shown to bind to this active site serine as well (Yocum *et al.,* 1979).

The penicillin-binding domain is found in both transpeptidases (HMW) and DD-carboxypeptidases (LMW) (Section 1.7.4.2), the latter of which are less susceptible to β-lactam inhibition by comparison (Waxman and Strominger, 1983). This results in a bias towards hydrolase activity following antibiotic treatment leading to fragile peptidoglycan (Höltje, 1998).

High levels of resistance to β-lactams has developed through several mechanisms, of particular importance in *Staphylococcus aureus* and *Streptococcus pneumoniae,* the latter of which is discussed in more detail in Section 1.8.

1.7.4.1 The penicillin-binding domain active site

Despite low overall sequence homology between the HMW and LMW penicillin-binding domains, they exhibit similar overall structures consisting of two subdomains, as identified from crystal structures in both the apo and liganded state (liganded state of *S. pneumoniae* PBP1a and PBP2a as HMW and LMW PBPs respectively shown in Figure 1.13 bound to β-lactam antibiotics in the active site (Section 1.7.4.2)). A five-stranded β-sheet surrounded by three α-helices make up the first subdomain, and the second is completely α-helical. The active site is found at the bottom of an elongated cleft at the interface of the two subdomains, and inter-domain flexibility is responsible for varied ligand affinity (Sauvage *et al.,* 2008). The active site consists of three conserved sequence motifs (Figure 1.13); SXXK containing the catalytic serine and lysine general base, found in the centre of the catalytic cleft. Motif 2 and 3 lie on opposite sides of the catalytic cavity; motif 2; (S/Y)X(N/C) in a loop between α-helices 4 and 5, and motif 3; (K/H)(S/T)G inside β3 of the five-stranded β-sheet. An additional glycine found in the back of the

catalytic cleft is also highly conserved (Fonzé *et al.,* 1999; Goffin *et al.,* 1998; Macheboeuf *et al.,* 2005).
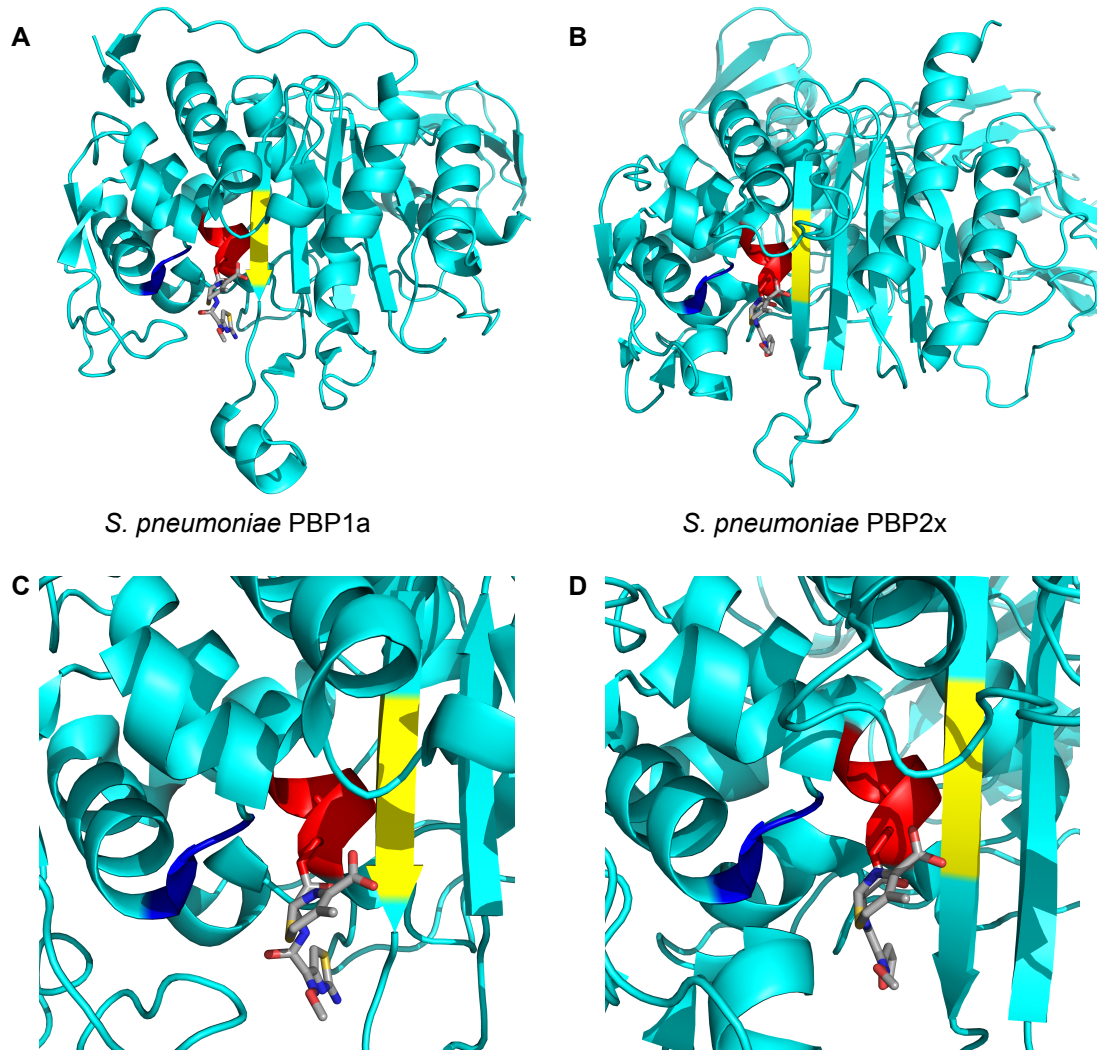
Figure 1.13: Comparison of the transpeptidase domains of *S. pneumoniae* PBP1a (HMW) and *S. pneumoniae* PBP2x (LMW). Ribbon view of the overall transpeptidase domain of PBP1a (A) and PBP2x (B), and zoomed in view of the active site (PBP1a (C), PBP2x (D)). Conserved motifs 1-3 are shown in red, blue and yellow respectively. Active site serine can be seen (red sticks in motif 1) covalently bound to cefotaxime (PBP1a) and cefuroxime (PBP2x) both in grey stick form. Structures aligned through protein molecules. PBP2x aligned to PBP1a; RMSD: 3.3Å from 208 α-carbons. Credit: Dr Dean Rea for help in producing this figure. PDB accession codes; PBP1a: 2C5W; PBP2x: 1QMF.

The analysis of several structures bound to substrate mimics has led to the identification of important regions and residues in substrate binding and catalysis (Sauvage *et al.,* 2008). The amide of the donor stem-peptide terminal D-alanine is found between the second motif asparagine side chain and the β-3 backbone and the carbonyl (or β-lactam ring) hydrogen bonds with an oxyanion hole formed by the catalytic serine and residues following motif 3. The methyl group of the same D-

alanine inserts into a hydrophobic pocket, in which the conserved glycine is found and is important for binding specificity. The motif 3 hydroxyl is oriented towards the terminal D-alanine carboxyl, and the glycine is important for avoiding steric hindrance, and therefore allowing the substrate into the active site. The serine and lysine of motif 1 are important for catalysis; the serine is the catalytic residue, and lysine abstracts a proton and activates the serine as a nucleophile for acylation.

A crystal structure of *S. pneumoniae* PBP1b showed that ligand binding led to a conformational change resulting in an 'open' active site (Macheboeuf *et al.,* 2005), mediated through change from an antiparallel interaction between β-3 and β-4 to a parallel conformation through movement of an intervening loop. Substrate mediated activation was proposed in order to convert from a 'closed' inactivated state to an 'open' active state (Figure 1.14). The same phenomena was discovered in *Staphylococcus aureus* acquired PBP2a, and shown to be due to the presence of an allosteric binding domain 60 Å away from the transpeptidase active site, which could be activated by muramic acid, peptidoglycan or the ceftaroline anti-MRSA antibiotic (Otero *et al.,* 2013). This confirmed a previous prediction of allosteric regulation of PBP2a through activity studies (Fuda *et al.,* 2005), and the Tipper-Strominger substrate mimicry hypothesis was later shown to exist at the allosteric site as well as the active site (Fishovitz *et al.,* 2015). An allosteric site has not been demonstrate to date for other penicillin-binding domains, although the presence of a second cefuroxime molecule remote from the active site in the crystal structure of *S. pneumoniae* PBP2x suggests that they may exist (Gordon *et al.,* 2000).

1.7.4.2 Transpeptidation and DD-carboxypeptidation

The penicillin-binding domain of PBPs is responsible for both transpeptidase and carboxypeptidase activity. The former is catalysed by the HMW-PBPs (PBP1a, PBP1b, PBP2a, PBP2b and PBP2x in *S. pneumoniae*) and results in cross-links between the pentapeptide stems of the glycan polymer (Sauvage *et al.,* 2008). Carboxypeptidation involves the removal of the terminal D-Ala from non- cross-linked stem peptides and is carried out by the LMW-PBPs (PBP3 in *S. pneumoniae*)(Morlot *et al.,* 2005). Both are illustrated in Figure 1.15.
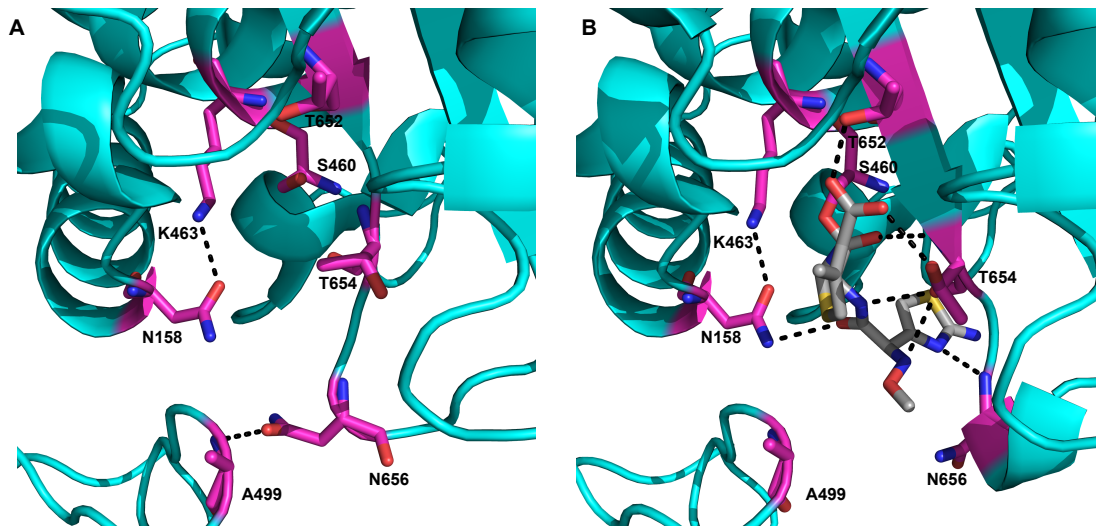
Figure 1.14: Substrate mediated opening of the *S. pneumoniae* PBP1b transpeptidase active site. Zoomed in view of active site shown in ribbon style in cyan. Key interacting residues shown in stick form in magenta and hydrogen bonds in dashed black lines. A: 'Closed' non-liganded active site showing interaction between A499 and N656 blocking entrance to the catalytic cleft. B: 'Open' liganded active site with cefotaxime in stick form covalently bound to the active site serine (S460). Liganded aligned to non-liganded through protein molecules with an RMSD of 0.37 Å for 365 α-carbons, showing no significant overall structural changes upon ligand binding. Credit: Dr Dean Rea for help in producing this figure. PDB accession numbers: "closed": 2BG1; "open": 2BG4

Both transpeptidation and carboxypeptidation proceed via a three-step mechanism, initiated by non-covalent binding of the donor stem peptide substrate to the active site. This is followed by attack of the penultimate D-Ala of the pentapeptide stem by the PBP active site serine, forming a covalent acyl-enzyme intermediate and displacing the terminal D-Ala from the donor pentapeptide stem. The nature of the 'acceptor' determines the outcome of the third step; deacylation. In transpeptidation the primary amine on the third position L-Lys of the 'acceptor' pentapeptide stem (or the terminal amino acid of the branch) nucleophilically attacks the intermediate and forms a peptide bridge. H_2O is the 'acceptor' in carboxypeptidation, which leads to hydrolysis and results in tetrapeptide stems (Figure 1.15) (Sauvage *et al.,* 2008).

Page 47: Figure 1.15: Proposed mechanism for transpeptidation and DD-carboxypeptidation. Only the pentapeptide stem of peptidoglycan is shown for simplicity. In both situations, Lys (motif 1) abstracts a proton from the catalytic Ser, which attacks the penultimate D-Ala in the "donor" stem peptide. An acyl-enzyme intermediate is formed and the terminal D-Ala released. During deacylation the acceptor ε-amino group of the third position L-Lys (or amino of branching amino acid)(transpeptidation) or a water molecule (DD-carboxypeptidation) forms a cross-link with the "donor" stem peptide or hydrolyses the acyl-enzyme intermediate respectively. Both result in regeneration of the active site serine and either cross-linked peptidoglycan or formation of a tetrapeptide stem.

Glycan polymer

D-Ala

D-iGln

L-Lys

D-Ala

D-Ala

Stem peptide 1
"donor"

PBP- Lys—NH₂

PBP- Ser

Acylation

Stem peptide 2
"acceptor"

Stem peptide 1
"donor"

PBP- Ser

Transpeptidation

Cross-linked
peptidoglycan

PBP- Ser

Deacylation

Stem peptide 1
"donor"

H₂O
"acceptor"

PBP- Ser

DD-carboxypeptidation

Stem tetrapeptide

PBP-Ser

47
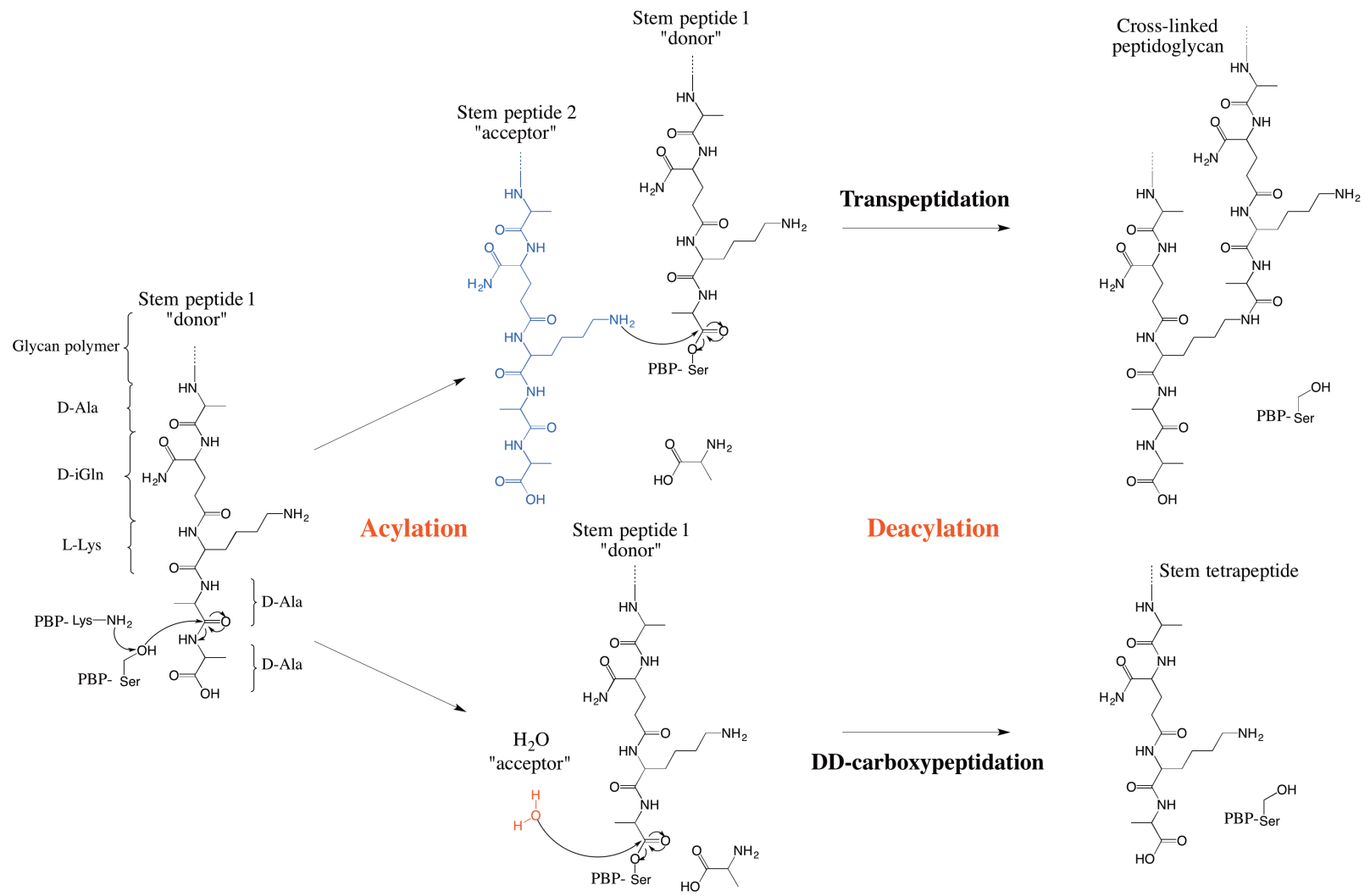
β-lactam antibiotics act as pseudosubstrates for the penicillin-binding domain of PBPs, as the β-lactam ring mimics the terminal D-Ala-D-Ala of the pentapeptide stem (Figure 1.16 A and B). The antibiotic is acylated by the active site serine, thus forming a covalent adduct, which is slow to deacylate and therefore prevents further reactions (Wise and Park, 1965), as illustrated in Figure 1.16 (C).
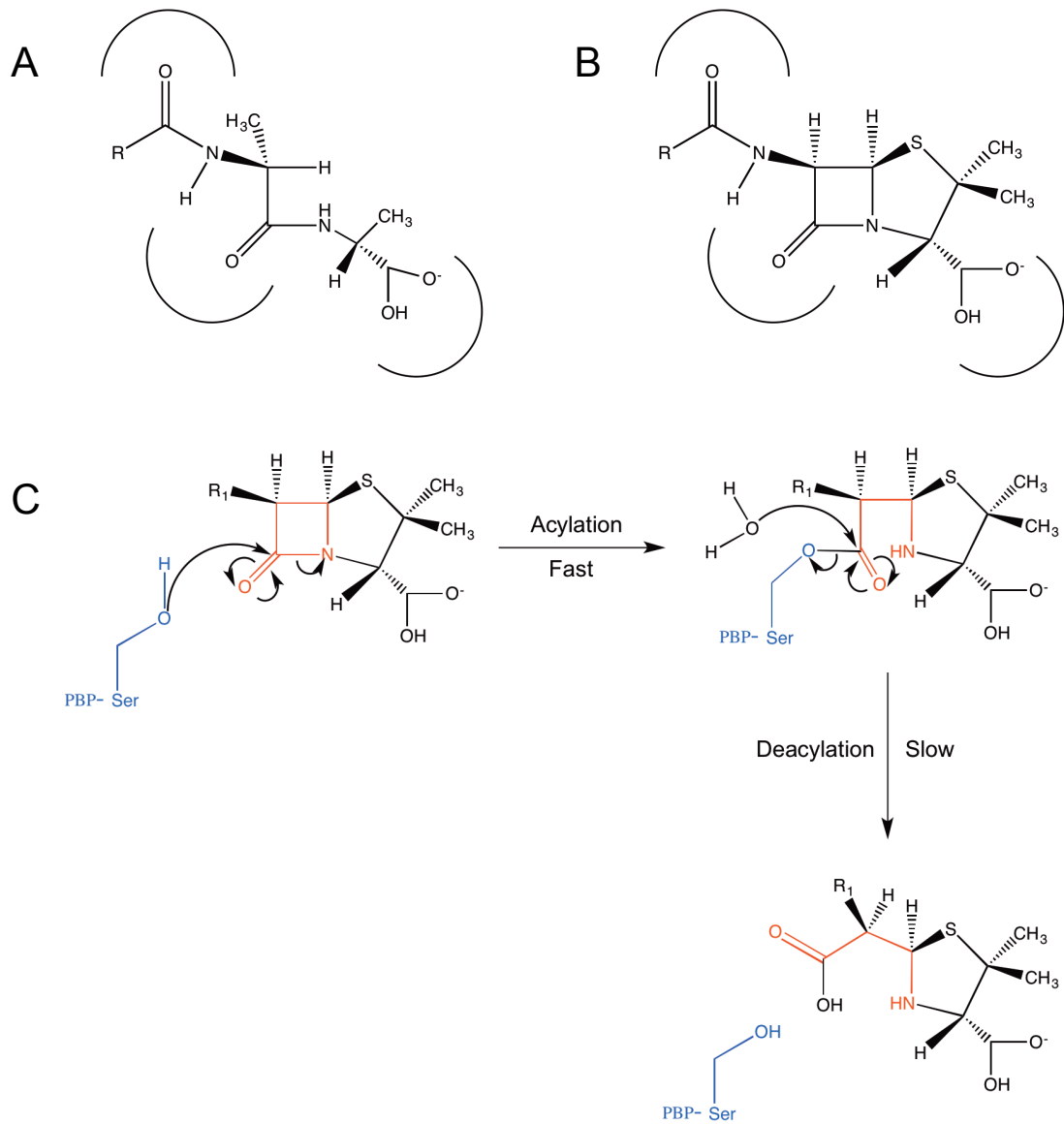
Figure 1.16: Structural comparison between β-lactams and the natural PBP substrate, and the β-lactam mechanism of action. A: D-Ala-D-Ala terminus of the peptidoglycan pentapeptide stem. B: Generic structure of a β-lactam, showing the structural similarity with the natural substrate. The distribution of negative charge is similar in both structures and is shown by curves. C: β-lactams act as a suicide substrate by forming an inactive acyl-enzyme intermediate which has deacylation rate significantly slower than the rate of bacterial division. The PBP active site nucleophilic serine attacks the β-lactam ring carbon atom forming a covalent ester link. Figure adapted from Zapun *et al.,* (2008).

1.8 *Streptococcus pneumoniae*

Two chapters in this thesis (Chapters 4 and 6) focus on the *Streptococcus pneumoniae* PBPs, which play a particularly unusual and important role in antibiotic resistance. This section details the clinical significance of *S. pneumoniae* as a pathogen and its mechanisms of β-lactam antibiotic resistance.

S. pneumoniae is a Gram-positive oval shaped coccus which can be both a commensal and a pathogen. In its carrier state it colonises the nasopharynx and is found in up to 4% of adults and 50% of children (Regev-Yochay *et al*., 2004). Pneumococci cause a range of diseases including otitis media, sinusitis and bronchitis and also pneumonia, meningitis and febrile bacteraemia invasive infections. The introduction of pneumococcal vaccines such as pneumococcal polysaccharide vaccine 23 (PPSV23) and pneumococcal conjugate vaccine 7 (PCV7) over the last 20 years has helped to lower the burden of invasive disease (Bocchini *et al.,* 2010), however it still remains a major worldwide cause of mortality, particularly in developing countries and amongst children, the elderly and those with underlying health problems (World Health Organisation, 2012). WHO have previously estimated that 1.6 million deaths per year are caused by pneumococcal disease (World Health Organisation, 2007), with infants and young children particularly affected. An estimated 10% of global deaths of children under the age of 5 are due to pneumococcal infections (O'Brien *et al*., 2009).

The remaining burden can be largely attributed to increasing levels of antibiotic resistance. *S. pneumoniae* is most commonly resistant to β-lactams such as penicillin, and macrolides, but also in some cases fluoroquinolones which are considered a drug class of last resort with serious side effects. Multidrug resistant strains are an increasing problem (Song *et al*., 2012).

1.8.1 *Streptococcus pneumoniae* β-lactam resistance

β-lactam antibiotics have been particularly successful in the treatment of pneumococcal infections, due to its notable high susceptibility to these compounds (Hakenbeck *et al.,* 2012). However, levels and frequency of penicillin-resistance in strains has increased rapidly worldwide since they were first isolated in the late 1970s, predominantly due to the increasing use of antibiotics (Granizo *et al.,* 2000), and now represent approximately 50% of isolates worldwide (Henriques-Normark, 2007). Resistance to β-lactams in *S. pneumoniae* is not through the typical mechanism of β-lactamase production, but mainly due to modification of the PBPs, through expression of mosaic genes formed by recombination events both within pneumococci, and with other species (Hakenbeck *et al.,* 2012; Zapun *et al.,* 2008). The resulting PBPs in resistant strains have a lower affinity for β-lactams but maintain their natural physiological activity (Job *et al*., 2008). This is a remarkable mechanism given the similarity in structure of the β-lactams to the PBP substrate, and the way in which these PBPs are still able to cross-link peptidoglycan is unknown to date. Penicillin resistance in pneumococci is multifactorial, with several other known, and many more unknown factors playing a role (Hakenbeck *et al*., 2012).

S. pneumoniae peptidoglycan stem peptides are chemically modified by the addition of an L-Ala-L-Ala or L-Ser-L-Ala dipeptide branch (C- to N- terminus) on the ε-amino group of the third position lysine (Filipe and Tomasz 2000; Fiser *et al.,* 2003)(Section 1.5.2.3), added to Lipid II during peptidoglycan biosynthesis by the MurM and MurN tRNA-dependant ligases (De Pascale *et al*., 2008; Lloyd *et al*., 2008). Stem peptide bridges have been associated with β-lactam resistance, as some highly resistant strains have an increased level of branching compared to sensitive strains, due to expression of a mosaic *murM* gene (Garcia-Bustos and Tomasz, 1990; Smith and Klugman, 2001). This has been shown to be required for high-level resistance in clinical strains even in those already possessing low affinity PBPs (Filipe and Tomasz, 2000; Weber *et al*., 2000). Work within our lab has shown this 'resistant' MurM to have a higher catalytic efficiency than its 'susceptible' counterpart, with a preference for incorporation of L-Ala over L-Ser (Lloyd *et al.,*

2008). PBPs can function with either linear or branched peptides in the absence of β-lactams, but in the presence of these antibiotics the *murM* product is essential for expression of resistance (Filipe and Tomasz, 2000; Severin *et al.,* 1996; Weber *et al.,* 2000). It has been suggested that glycan chains with branched pentapeptides might be preferential substrates for the resistant PBPs and outcompete the β-lactam, allowing the cell wall to be synthesised in these resistant strains (Dessen *et al.,* 2001; Pernot *et al.,* 2004). Additionally they may serve as a signal for other cell wall processes involved in resistance (Filipe and Tomasz, 2000)

Clinical isolates with identical MurM and PBP alleles can have significantly different resistance levels (Chesnel *et al.,* 2005), suggesting the involvement of an additional factor or factors in high level β-lactam resistance. Other implicated mechanisms include the serine-threonine kinase StkP (Dias *et al.,* 2009), and variations in enzymes catalysing glycan chain *N*-deacetylation and *O*-acetylation (Crisostomo *et al.,* 2006; Tait-Kamradt *et al*., 2009) amongst others (comprehensively reviewed recently; Hakenbeck *et al.,* 2012). Most recently, the cytoplasmic amino acid ligase, MurE has been implicated in clinical resistance in combination with low affinity PBP2b and PBP2x (Todorova *et al.,* 2015).

Lipid II with isoglutamine at position two in the stem peptide due to the action of the MurT/GatD amidase (Figueiredo *et al.,* 2012; Münch *et al.,* 2012)(Section 1.5.2.2.2) is required for efficient peptidoglycan cross-linking (Zapun *et al.,* 2013). Non-amidated peptides are rare in *S. pneumoniae*, making up 12.6 % of non cross-linked and only 1.8% of cross-linked peptides (Zapun *et al.,* 2013), and resistant strains have a much greater proportion of cross-linked glycan chains (Garcia-Bustos and Tomasz, 1990). Stem peptide amidation is required for full expression of β-lactam resistance in *Staphylococcus aureus,* which may be due to substrate specificity of the PBPs, the FemXAB enzymes responsible for adding the pentaglycine stem or a combination of both (Discussed in Section 5.8.4.3). Therefore the importance of this peptidoglycan modification in the addition of the stem peptide bridge, as well as subsequent cross-linking is of great interest in understanding β-lactam resistance.

1.8.2 *Streptococcus pneumoniae* PBPs; key players in resistance

Peptidoglycan chain polymerisation in *Streptococcus pneumoniae* is catalysed by the high molecular weight (HMW) Class A bifunctional penicillin-binding proteins (PBPs); PBP1a (79.7 kDa), PBP2a (80.7 kDa) and PBP1b (89.4 kDa); which catalyse both polymerisation of the glycan chain (transglycosylation) and cross-linking between them (transpeptidation). Either PBP1a or PBP2a must be functional for viability (Hoskins *et al.,* 1999). *S. pneumoniae* also has two class B monofunctional transpeptidases; PBP2b (74.4 kDa) and PBP2x (82.2 kDa) which are essential for viability (Kell *et al.*, 1993) and one Class C non essential regulatory PBP (PBP3 (41.4 kDa) (Morlot *et al.*, 2005). The general structure and activity of PBPs is covered in detail in Section 1.7.

PBP2x, PBP2b and PBP1a are the main PBPs associated with β-lactam resistance in *S. pneumoniae*, although PBP2a is associated with low affinity in some strains (Hakenbeck *et al.,* 2012). Resistance is mediated through mutations in the transpeptidase domain, although not necessarily the active site, that reduce the affinity for β-lactam antibiotics (Figure 1.17). PBPs in resistant strains have sequence blocks that vary by around 20%, compared to the highly conserved genes found in sensitive strains (Hakenbeck *et al.*, 2012). The identification of mutations involved in resistance is complicated as compensatory mechanisms affecting enzymatic activity may also be present, and the mutations in clinical and laboratory strains differ significantly. Mutations in PBPs of clinically resistant *S. pneumoniae* strains associated with reduced affinity for β-lactams are shown in Figure 1.17.

Low-level resistance is associated with mutations in the transpeptidase domain of PBP2x and PBP2b, which have different selective antibiotics (Hakenbeck *et al.,* 2012). Mutations in PBP1a confer high-level resistance, but only in the presence of low affinity PBP2b and/or PBP2x. The combined effect of PBP2x and PBP1a is particularly interesting in clinical isolates and suggests an interaction between the two *in vivo* (Zerfass *et al.*, 2009). The proposed interactions of PBPs in cell wall synthesis in *S. pneumoniae* are covered in more detail in Section 1.7.2.2.
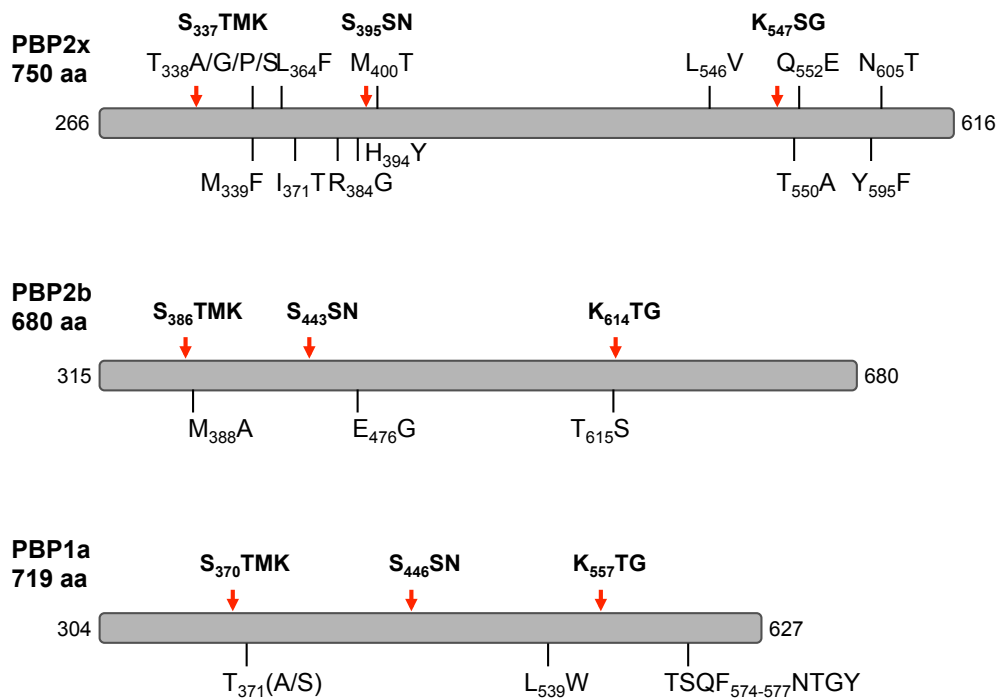
Figure 1.17: *S. pneumoniae* PBP altered affinity for β-lactams. Transpeptidase domain of PBP2x, PBP2b and PBP1a shown in grey with first and last amino acid labelled at each end. Conserved active site motifs indicated by red arrow and bold text. Mutations within the transpeptidase domain associated with reduced β-lactam affinity in clinical strains labelled. Figure adapted from Hakenbeck *et al.,* 2012

1.9 *Staphylococcus aureus*

The PBPs from *Staphylococcus aureus* are the focus of Chapter 5 of this thesis. This section briefly describes the clinical significance of this pathogen with a particular focus on its resistance to antibiotics, highlighting the importance of research that may lead to the development of new compounds.

Gram-positive Staphylococci account for 20% of all healthcare associated infections (Centres for Disease Control and Prevention, 2013). Of particular importance is *Staphylococcus aureus*, an opportunistic pathogen responsible for a range of conditions from minor skin infections to life threatening diseases such as pneumonia, septicaemia and infective endocarditis (Benfield *et al*., 2007; Deurenberg and Stobberingh, 2008). *Staphylococcus aureus* bacteraemia has become a leading cause of bloodstream infections in the world (Rasmussen *et al.,* 2011) and these are becoming increasingly difficult to treat due to the rapid emergence of resistance to methicillin and vancomycin in particular (Rasmussen *et al*., 2011).

1.9.1 *Staphylococcus aureus* antibiotic resistance

Within two decades of the introduction of penicillin, 80% of *Staphylococcus aureus* infections were resistant due to the production of a β-lactamase (Section 1.3.1.1) (Appelbaum, 2007) Soon after the introduction of methicillin to treat these infections, the first methicillin resistant *Staphylococcus aureus* (MRSA) strain was documented (Jevons, 1961), which arose through the acquisition of a non-native PBP with low affinity for β-lactams (Hartman and Tomasz, 1984; Utsui and Yokota, 1985). Incidences of MRSA increased rapidly worldwide, resulting in it becoming one of the main causes of hospital-acquired bacteraemia (Chambers *et al.*, 2001). Community acquired MRSA is more virulent but currently more susceptible to antibiotics than its hospital acquired counterpart (Appelbaum, 2007), and is believed to be mediated in part by a native class C PBP with unexpected transpeptidase activity (Memmi *et al.,* 2008). Interpeptide bridges (Section 1.5.2.3.1) and stem peptide amidation (1.5.2.2.2) are both associated with particularly high levels of β-lactam resistance. Mandatory surveillance, amongst other measures, has led to a greater than 50% reduction in reported cases of MRSA within the UK healthcare system (Johnson *et al.,* 2012). However, increasing cases of vancomycin-resistant *Staphylococcus aureus* (VRSA) (Howden *et al.*, 2010) and insensitivity to antibiotic classes considered "drugs of last resort" such as daptomycin and linezolid (Mangili *et al.,* 2005, Sorlozano *et al.,* 2010), means that research into this globally important pathogen is as important as ever.

1.10 Thesis aims

Antimicrobial Resistance (AMR) poses an already severe and growing threat to modern healthcare. Coordinated, international efforts are required to prolong the clinical life of current and future antibiotics. In addition to this, new drug classes are required, and the design of these requires full characterisation of new and existing drug targets.

The *Staphylococcus aureus* and *S. pneumoniae* penicillin-binding proteins (PBPs) are validated targets for antibiotics, and in the latter are responsible for the mediation

of resistance to β-lactam antibiotics. Chemical modifications to the Lipid II substrates are important in the activity and expression of resistance by these essential proteins, although the mechanisms involved are not well understood

This thesis aims to contribute to current understanding of the enzymatic activity and substrate specificity of PBPs from these two globally significant pathogens, in particular the role of stem peptide amidation in their catalytic activity, and peptide branching in antibiotic resistance. A greater understanding could help to answer some fundamental biochemical questions and enable the future design of novel inhibitors against these excellent targets.

Chapter 2. Materials and Methods

2.1 Buffers and solutions

All chemicals were obtained as analytical grade from the following companies unless otherwise stated: Acros Organics (USA), Bachem (Germany), Calbiochem (USA), Fisher Scientific (USA), Novabiochem (Germany), Sigma (USA).

MilliQ purified water was used to make all buffers. The pH of solutions was measured using a WPA pH meter CD720 from Hanna Instruments with pH 4, pH 7 and pH 10 buffer standards. For chromatography, buffers were filtered prior to use with a 0.2 μm filter.

2.2 Growth and maintenance of *E. coli* strains

2.2.1 Bacterial strains

The following bacterial strains are used throughout this thesis for DNA cloning and protein over-expression.

E. coli strain	Genotype	Reference
TOP 10	F⁻ *mcrA* Δ(*mrr⁻ hsdRMS⁻ mcrBC*) φ80*lacZ*ΔM15 Δ*lacX*74 *deoR recA*1 *araD*139 Δ (*ara⁻leu*)7697 *galU galK rpsL* (Str^R) *endA1 nupG*	Grant *et al.* (1990)
BL21 (DE3)	F⁻*omp*T *hsd*SB(rB⁻, mB⁻) *gal dcm* (DE3)	Studier and Moffatt, (1986)
BL21 (DE3) pRosetta	F⁻*omp*T *hsd*SB(rB⁻, mB⁻) *gal dcm* (DE3) and pRosetta plasmid for rare codon overexpression	Studier and Moffatt, (1986)

Table 2.1 Bacterial strains used for DNA cloning and protein over-expression

2.2.2 Bacterial growth media

The following bacterial growth media and LB-agar plates were used throughout this project.

2.2.2.1 LB-agar plates

LB media with 1.5% (w/v) bacto-agar was sterilised by autoclaving, cooled to 50°C before the addition of appropriate antibiotics and 25 mL poured into sterile Petri dishes. Prepared plates were stored at 4°C.

2.2.2.2 Super Optimal broth with Catabolite repression (SOC) media

2% (v/v) peptone, 0.5% (w/v) yeast extract, 10 mM NaCl, 2.5 mM KCl, 10 mM MgCl$_2$, 10 mM MgSO$_4$, 20 mM glucose.

2.2.2.3 Luria Bertani (LB) broth (Bertani, 1951)

1% (w/v) tryptone, 0.5% (w/v) NaCl, 0.5% (w/v) yeast extract.

2.2.2.4 ZY media (Studier, 2005)

1% (w/v) N-Z amine, 0.5% (w/v) yeast extract.

2.2.2.5 Autoinduction media (Studier, 2005)

ZY media, 1 × NPS (giving final concentrations of 25 mM ammonium sulphate, 50 mM potassium dihydrogen phosphate, 50 mM disodium hydrogen phosphate) and 1 x 5052 (final 0.5% (v/v) glycerol, 0.05% (w/v) glucose, 0.2% (w/v) α-lactose), 1 mM MgSO$_4$ with appropriate antibiotics. 5052 made as 50 x stock and NPS as 20 × stock routinely.

2.2.3 Preparation of competent cells

5 mL sterile Luria-Bertani (LB) broth 10:5:5 (tryptone:yeast extract:NaCl) containing the appropriate antibiotic was inoculated with the required *E. coli* strain from a glycerol stock, and incubated with 180 rpm shaking at 37°C overnight. 250 mL sterile LB broth (plus 20 mM $MgSO_4$ and appropriate antibiotics) was inoculated with 2.5 mL of the overnight culture and incubated at 37°C with shaking at 180 rpm until an optical density (A_{600nm} (OD_{600nm})) of between 0.4 and 0.6 was reached. Centrifugation at 4500 × g for 10 min (Beckman JA-14 rotor) pelleted the cells, and this pellet was gently resuspended in 100 mL ice cold TFB1 buffer (30 mM potassium acetate, 10 mM calcium chloride, 50 mM manganese chloride, 100 mM rubidium chloride, 15% (v/v) glycerol, pH 5.8), incubated on ice for 5 min and then centrifuged at 4500 × g for 5 min (Beckman JA-14 rotor). The pellet was resuspended in 10 mL TFB2 buffer (10 mM MOPS, pH 6.5, 75 mM calcium chloride, 10 mM rubidium chloride, 15% (v/v) glycerol) and incubated on ice for 1 hour. Competent cells were flash frozen in 50 μL aliquots in liquid nitrogen and stored at -80°C.

2.2.4 Transformation of *E. coli* strains

Competent cells (50 μL) were thawed on ice and incubated with 1 μL DNA (25-100 ng) for 30 min on ice. Cells were heat-shocked at 42°C for 30 sec using a water bath and incubated on ice for 2 min. 250 μL of SOC media (Super optimal broth plus glucose)(Section 2.2.2.2) was added and the cells incubated at 37°C for 30-60 min with shaking. 100 μL of the transformed cells were plated using aseptic technique onto LB-agar plates containing the appropriate antibiotic and were incubated at 37°C overnight without shaking.

2.2.5 Preparation of glycerol stocks

5 mL sterile LB broth containing the appropriate antibiotic was inoculated with an *E. coli* colony from a fresh transformation and cultured overnight at 37°C with shaking at 180 rpm. 1 mL of this culture was mixed using aseptic technique with 1

mL sterile 100% (v/v) glycerol in a Corning cryo-vial, frozen in liquid nitrogen and stored at -80°C.

2.3 DNA manipulation and cloning

2.3.1 Oligonucleotides

DNA oligonucleotides for PCR amplification were designed against the target gene and ordered from Integrated DNA Technologies (UK).

2.3.2 Polymerase Chain Reaction (PCR)

Q5® High-Fidelity DNA Polymerase (NEB) was used according to the manufacturer's instructions to carry out DNA amplification. Unless otherwise stated, a 100 μL mix of reagents was made and divided into four 25 μL aliquots. PCR was in an Eppendorf Mastercycler Gradient thermocycler with an annealing temperature optimised according to the primers used (typically between 45-65°C).

2.3.3 Restriction enzyme digestion of DNA

Restriction enzymes (NEB) in the appropriate buffer (stipulated by the manufacturer) were used for restriction digests. 500 ng of plasmid DNA or PCR product was used and unless otherwise stated reactions were incubated at 37°C for 3 hours.

2.3.4 Purification of DNA from PCR and restriction digests

Polymerases and endonucleases were removed from DNA following PCR and restriction digests by purification with a QIAquick® PCR Purification kit (Qiagen) according to the manufacturer's instructions.

2.3.5 Preparation of plasmid DNA

Plasmid DNA was extracted from *E. coli* TOP10 cells following transformation and overnight culture using a Fermentas GeneJet™ miniprep extraction kit according to the manufacturer's instructions.

2.3.6 DNA concentration determination

1.5 μL samples were quantified using a NanoDrop ND-1000 spectrophotometer (Thermo Scientific).

2.3.7 Ligation of DNA fragments with complementary ends

Following restriction digestion of plasmid DNA and PCR-amplified genes to give DNA with complementary sticky ends, ligation was carried out with the NEB Instant Sticky-End Ligase Master Mix (containing T4 DNA ligase) and was used according to the manufacturer's instructions. Ligations were in a final volume of 10 μL, incubated at room temperature for 5 min and 5 μL was used to transform *E. coli* TOP10 cells. The following day colonies were picked and grown overnight in 2 mL sterile LB broth before DNA was extracted using the Fermentas GeneJet™ miniprep extraction kit.

2.3.8 Agarose gel electrophoresis

0.8% (w/v) agarose gels were used to separate DNA fragments. Gels were prepared by dissolving 2 g of agarose (high-melting point agarose (GibcoBRL)) per 250 mL of 1 × Tris-acetate EDTA (TAE, 40 mM Tris acetate, 1 mM EDTA) buffer and heating in a microwave until dissolved. The agarose solution was cooled to hand-heat and 1 μL of 10 mg.mL^{-1} Ethidium Bromide added per 30 mL solution, before pouring into a gel cast and allowing to set. The gel was submerged in a Geneflow gel tank containing 1 × TAE, and DNA samples were loaded into the wells with 1 × DNA loading dye solution (6 x stock: 0.25% (w/v) bromophenol blue, 0.25% (w/v) xylene cyanol FF and 15% (v/v) Ficoll 400) (Fermentas). 5 μL DNA standard 1 kb

ladder (Fermentas) (pre-mixed with loading buffer) was loaded as a size reference. Electrophoresis was at 100 V for 40 min and a Syngene GeneSnap G:Box gel illuminator and analysis system used to visualise the gel under ultraviolet light.

2.3.9 DNA sequencing of plasmid constructs

To confirm insertion of the cloned gene in the correct orientation, reading frame and with no PCR induced mutations; DNA constructs were sequenced. 80-100 ng.μL^{-1} plasmid DNA and 5 pmol.μL^{-1} primer (either specific for the T7 promoter and terminator of the pET vector (Table 2.2) or the primers used for the original PCR amplification of the target gene) were used for each sequencing reaction in a final volume of 10 μL. Reactions were submitted to GATC Biotech (Germany), and resulting sequences were manually checked using ApE plasmid editor, blasted against a database (www.ncbi.nih.gov/BLAST; Altschul *et al.* (1990)) and aligned using ApE.

Primer	Sequence (5'-3')
T7 promoter	TAATACGACTCACTATAGGG
T7 terminator	GCTAGTTATTGCTCAGCGG

Table 2.2 Sequences of T7 promoter and terminator primers used for DNA sequencing

2.3.10 Gene constructs used in this project

Construct	Description	Selection	Affinity Tag	Source
pET21b::*pbp2*	*S. aureus pbp2* (full-length) in pET21b vector	Ampicillin	Non-cleavable N-term 6-His	N. Strynadka (UBC, Canada)
pET41a::*pbp2-Δ59*	*S. aureus pbp2-Δ59* (ΔTM domain) in pET41a vector	Kanamycin	Untagged	N. Strynadka (UBC, Canada)
pET15b::*mgt*	*S. aureus mgt-Δ27* (full-length) in pET15b vector	Ampicillin	Thrombin cleavable N-term 6-His	Cloned for this project
pET46::*mgt-Δ67*	*S. aureus mgt-Δ67* (ΔTM domain) in pET46 vector	Ampicillin	Enterokinase cleavable N-term 6-His	K. Abrahams (Warwick)
pET15b::*pbp2a-Δ22*	*S. aureus* D39 *pbp2a-Δ22* (ΔTM domain) in pET15b vector	Ampicillin	Thrombin cleavable N-term 6-His	N. Strynadka (UBC, Canada)
pET30::*pbp2a*	*S. pneumoniae* D39 *pbp2a* (full-length) in pET 30 vector	Kanamycin	Untagged	A. Zapun (Grenoble)
pGEX-2T::*pbp2a-Δ77*	*S. pneumoniae pbp2a-Δ77* (ΔTM domain) in pGEX-2T vector	Ampicillin	Thrombin cleavable N-term GST	A. Zapun (Grenoble)
pET46::*pbp1a*	*S. pneumoniae* D39 *pbp1a* (full-length) in pET46 vector	Ampicillin	Non-cleavable N-term 12-His	K. Abrahams (Warwick)
pET46::*pbp1a-Δ30*	*S. pneumoniae* D39 *pbp1a-Δ30* (ΔTM domain) in pET46 vector	Ampicillin	Non-cleavable N-term 12-His	K. Abrahams (Warwick)
pET26b::*pbp1a*	*S. pneumoniae* D39 *pbp1a* (full-length) in pET26b vector	Kanamycin	Untagged	Cloned for this project

Table 2.3 Gene constructs used for this project

2.4 Protein Expression and Purification

Most proteins overexpressed and purified within this project were by pre-published methods, and there is a large amount of variation between protocols. References to the relevant literature are included throughout the text in each results chapter. This section covers the general methods for recombinant protein over-expression in *E. coli*, and details of modification from the published protocols for individual proteins are included for clarity, where significant deviations were made.

2.4.1 Recombinant protein over-expression in *E. coli*

A range of *E. coli* strains used for protein expression (Table 2.3) were used to over-express recombinant proteins. Competent cells (Section 2.2.3) were transformed (Section 2.2.4) with an expression plasmid (Table 2.1) and plated onto selective media. Induction was either with IPTG or autoinduction.

2.4.1.1 Isopropyl-β-D-thiogalactopyranoside (IPTG) induction

5 mL LB (including appropriate antibiotic) was inoculated with a single colony from a fresh transformation, and cultured overnight at 37°C with shaking at 180 rpm. 1 L LB (with antibiotic selection) was inoculated with the whole overnight culture and incubated at 37°C with shaking at 180 rpm. At OD_{600nm} of 0.6, cultures were induced with 1 mM IPTG and cultured at 25°C overnight (unless otherwise specified in this thesis or the published protocol). Cells were harvested in a Beckman JLA-8.100 rotor at 10,000 × g and the cell pellet stored at -20°C.

2.4.1.2 Autoinduction

Method adapted from the Studier Autoinduction System (Studier, 2005). 2 mL ZYP-0.8G medium (ZY, 1 mM $MgSO_4$, 0.8% (w/v) glucose, NPS) plus antibiotic selection was inoculated with a single colony from a fresh transformation. After overnight incubation at 37°C with shaking at 180 rpm, 1 mL was used to inoculate 1 L of ZYP-5052 rich medium (ZY, 1 mM $MgSO_4$, 5052, NPS) plus antibiotic

selection. Cells were cultured at 25°C for 22 h with shaking at 180 rpm, before harvesting at 10,000 × g in a Beckman JLA-8.100 rotor. Cell pellets were stored at -20°C.

2.4.2 Preparation of cell lysates

Frozen cell pellets (Section 2.4.1) were thawed on ice, resuspended in 3 mL.g^{-1} cell weight of phosphate buffered saline (PBS) supplemented with 2.5 mg.mL^{-1} hen egg-white lysozyme and 20 µg.mL^{-1} DNAse and incubated with agitation at 4°C for 45 min. Cells were lysed by sonication on ice for four bursts of 30 sec at 70% power using a Bandelin Sonoplus sonicator or passing three times through a continuous cell disruptor (Constant Cell Disruption Systems) at 30 kpsi at 4°C as specified in the text. Cell lysate was centrifuged at 20,000 × g using a Beckman JA-25.50 rotor for 20 min at 4°C to pellet cell debris. Cellular localisation of the protein determines the next step used in the protocol.

2.4.2.1 Soluble protein

Supernatant following 20,000 × g centrifugation (Section 2.4.2) was clarified by further centrifugation at 50,000 × g for 45 min at 4°C (Beckman JA-25.50 rotor). The supernatant was used for purification.

2.4.2.2. Insoluble protein

The pellet from 20,000 × g centrifugation (Section 2.4.2) was resuspended in a buffer containing the detergent required for solubilisation (specified in text), and incubated at 4°C for 1 hour with agitation. Following centrifugation at 50,000 × g for 45 min at 4°C (Beckman JA-25.50 rotor), the supernatant containing detergent-solubilised proteins was used for purification.

2.4.2.3 *E. coli* membranes

Supernatant following 20,000 × g centrifugation was treated as for soluble proteins (Section 2.4.2.1). The resulting supernatant was centrifuged at 150,000 × g for 1 h at 4°C to pellet the membrane fraction in an ultracentrifuge (Beckman Ti45 rotor in Beckman Coulter Optima L-90K). Membranes were resuspended in PBS (10 mL.L^{-1} original cell culture) and stored at -20°C.

2.4.3 Protein purification

Basic methods for the main purification techniques used are covered here. Specific methods are included in the main text.

2.4.3.1 Affinity chromatography

Proteins with a hexa- or dodecahistidine affinity tag were purified by immobilised metal affinity chromatography (IMAC), using either TALON Metal Affinity Resin (Cobalt metal ions (Clontech)) and gravity flow, or a pre-packed column on an AKTA 10/100 system (GE Healthcare) in a cold cabinet at 4°C. Pre-packed columns were either HiTrap TALON crude 5 mL or HisTrap 5 mL (both GE healthcare). 5 mL TALON Metal Affinity Resin was poured into an Econo-Pac® Chromatography column (BioRad) prior to purification and the basic development method employed was the same for all three types of column.

Columns were washed with 10 column volumes (CV) sterile water, and equilibrated with a further 10 CV of purification buffer containing no imidazole. Protein solutions were loaded directly onto the column, and where necessary with TALON Metal Affinity Resin were incubated with agitation to increase binding. Flow-through was collected and columns washed with 10 CV equilibration buffer to remove unbound proteins. Columns were developed by washing with either a gradient (pre-packed columns) or step-wise increases in imidazole concentration (TALON Metal Affinity Resin) over 10 CV. The concentrations used were specific to the protein and its

affinity for the resin. 10 mL fractions were collected and protein elution from pre-packed columns monitored by absorbance at 280 nm on the AKTA 10/100.

Columns were washed with 10 CV of buffer containing 1 M imidazole, 10 CV sterile water, and 10 CV 20% (v/v) ethanol and stored at 4°C.

2.4.3.2 Size exclusion chromatography

2.4.3.2.1 Preparative size exclusion chromatography

Proteins were separated according to size using a Superdex 200 (26/60) or Superose 6 (10/300) size exclusion column (separation of proteins with mass range of 10-600 kDa and 5-5000 kDa respectively) on an AKTA 10/100 purifier system (GE healthcare) in a cold cabinet at 4°C. Columns were equilibrated with 1.5 CV of the required buffer and samples loaded via an injection loop at a volume of <2% of the total column volume to ensure high resolution of separation. Elution was with 1 CV buffer at 1 mL.min^{-1} for Superdex 200 (26/60) and 0.4 mL.min^{-1} for Superose 6 (10/300) with 1 mL and 0.5 mL fractions collected respectively. Protein elution was monitored by absorbance at 280 nm.

2.4.3.2.2 Analytical size exclusion chromatography

Analytical size exclusion chromatography was as described in Section 2.4.3.2.1 using a Superdex 200 Increase 10/300 GL column (GE Healthcare) pre equilibrated with a Gel Filtration HMW Calibration Kit (GE Healthcare) to allow molecular weight estimation. 100 μL pure protein at 8 mg.mL^{-1} was loaded and elution was at 0.3 ml.min^{-1} with the collection of 0.5 mL fractions.

2.4.3.3 Ion exchange chromatography

Anion exchange was carried out using a ResourceQ 6 mL column (GE Healthcare) and cation exchange with a 5 mL HP SP Sepharose column (GE Healthcare) on an AKTA 10/100 purifier system (GE healthcare) in a cold cabinet at 4°C unless otherwise stated. The ResourceQ column contains 15 μm beads of Source 15Q resin, a strong anion exchanger due to its quaternary amine group, and SP Sepharose 34 μm beads of sulfopropyl, a strong cation exchanger. Both maintain their charge over a large pH range. Columns were washed with 10 CV sterile water, 10 CV low salt buffer, 10 CV high salt buffer and finally a further 10 CV low salt buffer until the conductivity was observed at baseline. Protein was loaded in a low salt buffer with a pH selected to ensure a net negative (anion exchange) or positive (cation exchange) charge. Protein was eluted with a salt gradient of 0-1 M NaCl over 10 CV at a flow rate of 6 mL.min^{-1} or 2 mL.min^{-1} for ResourceQ and HP SP Sepharose respectively. Protein elution was monitored by an increase in absorbance at 280 nm and 1 mL fractions were collected.

2.4.3.4 Buffer exchange and concentration

Buffer exchange was either through the use of a PD-10 Desalting column (GE healthcare), used according to the manufacturer's instructions, or with a Vivaspin® centrifugal concentrator (Sartorius) with a molecular weight cut-off of 10, 30 or 100 kDa (specified in text) unless otherwise stated. Concentrators were centrifuged at 3,000 × g in a bench-top centrifuge (Eppendorf Centrifuge 5810R) at 4°C, and if buffer exchange was required; refilled with exchange buffer until a sufficient dilution factor was reached. Protein solutions were concentrated until the required volume was achieved, and subsequently quantified (Section 2.5.1).

2.4.4 Specific protein purification protocols

Where significant deviations are made from the published method for purification, the protocol is detailed here. More minor modifications are included in the text within the relevant chapter sections.

2.4.4.1 *S. pneumoniae* PBP2a-Δ77 (Section 4.3.4)

Expression and purification was according to Di Guilmi *et al*., (1999) with the following modifications. Over-expression was in the BL21 (DE3) *E. coli* cell line but otherwise as described. Gel filtration chromatography was replaced with anion exchange chromatography (Section 2.4.3.3)(6 mL ResourceQ column). Fractions containing PBP2a-Δ77 after glutathione sepharose purification were concentrated to 2.5 mL in a Vivaspin® centrifugal concentrator (10 kDa cut-off) and buffer exchanged into 50 mM HEPES pH 7.5, 10 mM MgCl$_2$, 0.02% (v/v) TX-100 using a PD-10 Desalting column (GE healthcare). A 6 mL ResourceQ column was equilibrated as described in Section 2.4.3.3 with 50 mM HEPES pH 7.5, 10 mM MgCl$_2$, 0.02% (v/v) TX-100 and 50 mM HEPES pH 7.5, 10 mM MgCl$_2$, 0.02% (v/v) TX-100, 1M NaCl. The PBP2a-Δ77 sample was injected onto the column and eluted over a salt gradient as described in Section 2.4.3.3. Fractions were analysed by SDS-PAGE (Section 2.5.2), concentrated (Section 2.4.3.4) and the protein concentration determined (Section 2.5.1).

2.4.4.2 *S. aureus* PBP2a-Δ22 (Section 5.6.1)

Several modifications were made from the original protocol by Lim and Strynadka (2002), and the protocol used is as follows. Harvested cells were resuspended in 25 mL.L^{-1} cells lysis buffer (50 mM K$_2$HPO$_4$ pH 8, 1 mM EDTA) and soluble proteins obtained by sonication (Section 2.4.2 and 2.4.2.1). Lysate was applied to 5 mL DEAE Sepharose Fast Flow resin (GE Healthcare) in a falcon tube pre-equilibrated with Buffer A (50 mM K$_2$HPO$_4$ pH 8) and incubated on rollers at 4°C for 1 hour. Resin was spun at 2000 rpm for 5 min and supernatant taken as flow-through, before washing with 2 x 10 mL Buffer A. Flow-through containing PBP2a-Δ22 was

dialysed against Buffer B (50 mM K_2HPO_4 pH7) overnight and spun at 15,000 rpm for 30 min at 4°C before the supernatant was loaded onto a SP Sepharose (GE Healthcare) column (50 mL bed volume) pre-equilibrated with 10 CV Buffer B. This was washed with a further 10 CV Buffer B before eluting with a gradient over 10 CV of 0-100% Buffer C (50 mM K_2HPO_4 pH7, 1 M NaCl). Identified fractions after SDS-PAGE analysis were concentrated with a Vivaspin® centrifugal concentrator (30 kDa cut-off) to < 5 mL concomitant with buffer exchange before loading onto a Superdex 200 26/60 column pre equilibrated with 1 CV Buffer D (50 mM K_2HPO_4 pH7, 150 mM NaCl). Fractions identified by SDS-PAGE were concentrated (Section 2.4.3.4) and the protein concentration determined (Section 2.5.1) before storing at -80°C.

2.5 Protein analysis and detection

2.5.1 Protein quantification

The concentrations of proteins purified without detergent were determined using the Bio-Rad colorimetric assay at 595 nm. 2 μL protein solution was added to 1 mL diluted Bio-Rad reagent in a plastic semi-micro cuvette, mixed and allowed to stand for 5 min. Absorbance at 595 nm was measured using a Jenway 6306 UV-visible spectrophotometer. Triplicate readings were taken and dilutions made if values were outside of the linear range.

The protein concentration ($\mu g.mL^{-1}$) was calculated using the following formula;

[Protein] ($\mu g.mL^{-1}$) = (A_{595nm}/0.1) × 1.95 × dilution factor × (1000/volume assayed)

The concentration of proteins purified in detergent (most of those within this thesis), were established using the bicinchoninic acid (BCA) assay (Pierce) as this is less affected by detergents. The assay was carried out according to the manufacturer's instructions and absorbance at 562 nm was measured using a Jenway 6306 UV-visible spectrophotometer.

2.5.2 SDS-Polyacrylamide Gel Electrophoresis

Proteins were separated and visualised under denaturing conditions by discontinuous SDS-Polyacrylamide Gel Electrophoresis (SDS-PAGE) with the Tris-glycine buffer system (Laemmli, 1970). A 5 mL resolving gel (375 mM Tris pH 8.8, 0.4% (w/v) SDS, 12% acrylamide:bis-acrylamide (37.5:1)) was cast using the Hoeffer Mighty Small gel kit and polymerised with 100 μL 10% (w/v) APS (ammonium persulfate) and 10 μL *N,N,N',N'*-Tetramethylethylenediamine (TEMED). Prior to setting, the gel was overlaid with 100% (v/v) ethanol to ensure an even set. A 2 mL stacking gel (125 mM Tris pH 6.8, 0.4% (w/v) SDS, 4% acrylamide:bis-acrylamide (37.5:1)) polymerised with 50 μL 10% (w/v) APS and 10 μL TEMED, was poured on top of the polymerised resolving gel after removal of the overlaid ethanol, with the insertion of a plastic comb to form wells.

10 μg protein samples (or a maximum volume of 20 μL if the protein concentration was too low) were mixed with 1 × loading buffer (6 ×; 63.5 mM Tris pH 6.8, 0.4% (w/v) SDS, 5% (v/v) β-mercaptoethanol, 20% (v/v) glycerol, 2.5% (w/v) bromophenol blue) and were heat-denatured at 95°C for 10 min using an Eppendorf Mastercycler Gradient thermocycler. Samples were pipetted into the wells and the gel run in SDS-PAGE running buffer (25 mM Tris pH 8.3, 0.19 M glycine, 0.1% (w/v) SDS) at 180 V until the dye front reached the bottom of the gel.

Proteins separated by SDS-PAGE were stained for 1 hour using Instant Blue stain (Expedeon). Gels were washed in water briefly and imaged using Syngene GeneSnap G:Box Gel Doc and analysis system.

2.5.3 Microscale Thermophoresis (MST)

NT-647 fluorescent label was covalently attached to the required protein using a Monolith™ Protein Labelling Kit RED-NHS (Nanotemper Technologies, Germany) according to the manufacturer's instructions and subsequently diluted to 150 nM. Non-labelled protein at final concentrations ranging from 64.95 μM to 2 nM were mixed in equal volumes with labelled protein to achieve 75 nM final concentration of

the dyed version. Assays were performed in protein storage or reaction buffer (as described in the text) plus 0.005% (v/v) Tween20 to reduce sticking to capillaries. MST analysis was in standard glass capillaries using the Monolith NT.115 (Nanotemper Technologies, Germany) according to the manufacturer's instructions.

2.6 Synthesis of Lipid II intermediates

2.6.1 UDP-Mur*N*Ac-pentapeptide biosynthesis

Method adapted from Lloyd *et al.* (2008). 2 mL reaction volumes were used, containing 50 mM HEPES pH 7.5, 10 mM MgCl$_2$, 200 mM PEP, 50 mM KCl, 10 mM dithiothreitol, 10 mM UDP-Glc*N*Ac, 30 mM L-Ala, 30 mM D-Glu (or 100 mM D-Gln), 30 mM L-Lys, 30 mM D-Alanyl-D-Ala, 200 µM NADPH, 6 mM ATP, 25 mM isocitrate, 40 units isocitrate dehydrogenase (Sigma-Aldrich), 500 units of pyruvate kinase (Sigma-Aldrich), 300 µg MurA, 2000 µg MurB, 750 µg MurC, 1000 µg MurD, 1250 µg MurE and 1500 µg MurF. This was incubated at 37°C overnight, before dilution with 5 mL sterile water, and filtration with a Vivaspin® centrifugal concentrator (10 kDa cut-off) to remove proteins.

2.6.1.1 UDP-Mur*N*Ac-pentapeptide purification

A Source 30Q column (26 x 120 mm) on an AKTApurifier 10 was used to purify the UDP-Mur*N*Ac-pentapeptides by anion exchange chromatography. Prior to use, the column was pre-equilibrated with 6 CV of 10 mM ammonium acetate pH 7.5, 6 CV of 1 M ammonium acetate pH 7.5, and a further 10 CV of 10 mM ammonium acetate pH 7.5 until conductivity was at baseline. Samples (Section 2.6.1) were diluted into 100 mL of 10 mM ammonium acetate pH 7.5 and loaded onto the column. 10 mL fractions were collected during an ammonium acetate gradient from 10 mM to 300 mM over 7 CV at 10 mL.min^{-1}. Presence of the UDP-Mur*N*Ac-pentapeptide was determined by an increase in absorbance at 254 nm and 280 nm and fractions containing the required product were freeze dried 4 times and resuspended in a small volume of sterile water.

2.6.1.2 UDP-MurNAc-pentapeptide further purification

Size exclusion chromatography was used to remove residual ammonium acetate prior to subsequent reactions. A Biogel P2 column (89 cm x 2.6 cm) was equilibrated with 2 CV of H_2O at 1 mL.min^{-1}. UDP-MurNAc-pentapeptide for desalting was injected via the injection loop and the column developed over one CV with H_2O at 1 mL.min^{-1}. 10 mL fractions were collected and absorbance at 254 nm and 280 nm used to identify the UDP-MurNAc-pentapeptide. The product peak was freeze dried, resuspended in 500 mM $NaHCO_3$ pH 10 (or H_2O depending on the next step) and frozen at -20°C.

2.6.1.3 Quantification of UDP-MurNAc-pentapeptide

The concentration of the final product was calculated by absorbance at 260 nm, by virtue of the uracil of UDP-MurNAc-pentapeptide (extinction coefficient of 10,000 $M^{-1}cm^{-1}$). A quartz cuvette in a Jenway 6306 UV-visible spectrophotometer was used.

2.6.1.4 Purity of UDP-MurNAc-pentapeptide

The purity of UDP-MurNAc-pentapeptides was analysed by anion exchange chromatography using a 1 mL MonoQ HR 5/5 column (10 μM beads)(GE Healthcare). The column was pre-equilibrated with 10 CV 10 mM ammonium acetate pH 7.5, 10 CV 1 M ammonium acetate pH 7.5, and a further 10 CV 10 mM ammonium acetate pH 7.5 until conductivity was at baseline. A sample of 2 μL intermediate in a total of 1000 μL 10 mM ammonium acetate pH 7.5 was loaded through an injection loop and eluted over 10 CV at 1 mL.min^{-1} with a gradient of 1-100% 1 M ammonium acetate pH 7.5. Elution was monitored by an increase in absorbance at 254 nm and 280 nm, and integration of the A_{254nm} peak as a percentage of the total area using UNICORN (GE healthcare) software provided percentage purity.

2.6.2 Production of Mur*N*Ac-pentapeptide

Mur*N*Ac-pentapeptide was made from UDP-Mur*N*Ac-pentapeptide by either acid or enzymatic hydrolysis as described.

2.6.2.1 Acid hydrolysis of UDP-Mur*N*Ac-pentapeptide

1 M HCl was added to 10 mg UDP-Mur*N*Ac-pentapeptide in H_2O to give a final concentration of 0.1 M, and additional added dropwise if required until pH 1 was reached. Samples were boiled at 99°C for 30 min and subsequently neutralised to pH 7.5 with 1 M NaOH. Samples were diluted to 5 mL in 10 mM ammonium acetate pH 7.6 and purified as described in Section 2.6.2.3.

2.6.2.2 Enzymatic hydrolysis of UDP-Mur*N*Ac-pentapeptide

10 units of each of Phosphodiesterase from *Crotalus adamanteus* (Sigma-Aldrich) and Shrimp alkaline phosphatase (SAP)(NEB) were added to 10 mg UDP-Mur*N*Ac-pentapeptide in H_2O and Tris.HCl pH 8.5 added to a final concentration of 50 mM. This was incubated at 37°C overnight, before dilution with 5 mL sterile water, and filtration with a Vivaspin® centrifugal concentrator (10 kDa cut-off) to remove proteins. The flow-through was purified as described in Section 2.6.2.3.

2.6.2.3 Purification of Mur*N*Ac-pentapeptide

Purification was as described for UDP-Mur*N*Ac-pentapeptide (Section 2.6.1.1) with the additional monitoring of absorbance at 218nm to detect peptide bonds. Mur*N*Ac-pentapeptide has no overall negative charge at pH 7.6 and therefore elutes in the flow-through. Fractions containing the required product were freeze dried 4 times and resuspended in a small volume of H_2O.

2.6.2.4 Purity of Mur*N*Ac-pentapeptide

The purity of Mur*N*Ac-pentapeptide was analysed by cation exchange chromatography using a 1 mL MonoS HR 5/5 column (10 μM beads)(GE Healthcare). The column was pre-equilibrated with 10 CV 20 mM phosphoric acid 10 mM NaCl pH 4, 10 CV 20 mM phosphoric acid 1 M NaCl pH 4, and a further 10 CV 20 mM phosphoric acid 10 mM NaCl pH 4 until conductivity was at baseline. A sample of 2 μL intermediate in a total of 600 μL 20 mM phosphoric acid 10 mM NaCl pH 4 was loaded through an injection loop and was subsequently washed with 10 CV of the same buffer at 1 mL.min^{-1}. Elution was with a gradient of 1-100% 20 mM phosphoric acid 1 M NaCl pH 4 and was monitored by an increase in absorbance at 218 nm, 254 nm and 280 nm. Integration of the A_{218nm} peak as a percentage of the total area using UNICORN software (GE healthcare) provided percentage purity of the Mur*N*Ac-pentapeptide.

2.6.2.5 Quantification of Mur*N*Ac-pentapeptide

Mur*N*Ac-pentapeptide was quantified by the Amplex Red assay for D-Ala release coupled to *E. coli* DacA (DD-carboxypeptidase to remove the terminal D-Ala). 200 μL reactions in 50 mM HEPES pH 7.6, 5 mM MgCl$_2$ containing 50 μM Amplex Red, 33.51 mM.min^{-1} *Rhodotorula oracalis* DAAO, 7.41 mM.min^{-1} horseradish peroxidase and 1 mg.ml^{-1} *E. coli* DacA were monitored in a quartz cuvette in a Varian Cary 100 spectrophotometer at 37°C, until a stable baseline at A_{555nm} was reached. 2.5 μL of a 1/100 dilution of the Mur*N*Ac-pentapeptide stock was added and overall change in absorbance used to calculate the concentration of Mur*N*Ac-pentapeptide in the cuvette. Note that the catalytic concentration of DAAO and HRP enzyme activity (mM.min^{-1}) was calculated as described in Appendix 2

2.6.3 Dansylation of UDP-Mur*N*Ac-pentapeptide

Dansylation was carried out by Julie Todd or Anita Catherwood of BaCWAN (UK; Clarke *et al.,* 2009; Lloyd *et al.,* 2008), methods are included here for clarity.

Desalted UDP-Mur*N*Ac-pentapeptide (Section 2.6.1.2) in sterile water was mixed with an equal volume of acetone and reacted with a 42 × molar ratio of dansyl chloride (Sigma-Aldrich) in a tin foil covered glass vial. The reaction was allowed to proceed overnight at room temperature in the dark with stirring. A 10 × molar ratio of Tris pH 9 to dansyl chloride (previously added) was added and the reaction transferred to a round bottom flask. Quenching was for 1 hour at room temperature before rotary evaporation to remove solvents. Dried products were resuspended in 1 mL sterile water and purified by size exclusion chromatography on a Superdex peptide 10/300 column (GE Healthcare) pre equilibrated with 1.5 CV   0.1 M ammonium bicarbonate. The sample was loaded via a 1 mL injection loop and elution monitored by absorbance at 254, 280 and 340 nm. Dansylated UDP-Mur*N*Ac-pentapeptide is the first peak to elute with an absorbance at 340 nm. Fractions containing the required product were freeze dried 4 times and resuspended in a small volume of sterile water. Quantification (Section 2.6.1.3) and purity checks (Section 2.6.1.4) were as described previously.

2.6.4 Branched UDP-Mur*N*Ac-pentapeptide derivatives

2.6.4.1 Fmoc-dipeptide synthesis

Synthesis of Fmoc-L-Ala-L-Ser was carried out using two methods (Section 2.6.4.1.1. and 2.6.4.1.2), and Fmoc-L-Ala-L-Ala by one (Setion 2.6.4.1.1).

2.6.4.1.1. Fmoc-OSu and dipeptide coupling

Dipeptide (L-Ala-L-Ala-OH or L-Ala-L-Ser-OH) (620 μmol) was dissolved in 155 mL H_2O and 1550 μmol $NaHCO_3$ added, before cooling to 0°C. A solution of Fmoc-OSu (620 μmol) in 155 mL acetonitrile was made and also cooled to 0°C, before being added drop wise to the dipeptide solution, whilst stirring. This was allowed to warm to room temperature overnight whilst stirring before rotary evaporation to remove acetonitrile. The pH was adjusted to 10 with 5 M NaOH and 100 mL dichloromethane added in a separating funnel. The dichloromethane phase (bottom)

was decanted and stored, whilst the aqueous phase was acidified to pH 5 with concentrated HCl. The aqueous phase was washed with 100 mL ethyl acetate twice in the same way, and the resulting ethyl acetate phase (top) was rotary evaporated, before being dried under high pressure.

2.6.4.1.2 Fmoc-L-Ala and O-*tert*-butyl-L-Ser *tert*-butyl ester

235 mg Fmoc-L-Ala (755 μmol), 215 mg EDC (1375 μmol), 107 mg oxyma pure (750 μmol) and 163 mg O-*tert*-butyl-L-Ser *tert*-butyl ester (750 μmol) were added to 5 mL CH_2Cl_2 and 2.15 mL triethylamine before stirring at room temperature overnight, and subsequently dried by rotary evaporation. The product was resuspended in 10 mL CH_2Cl_2 and 6 mL 5% (v/v) citric acid, the CH_2Cl_2 phase (bottom) decanted off and washed again with 5% (v/v) citric acid. 2 mL saturated $NaHCO_3$ and 2 mL H_2O were added to the remaining organic phase, the aqueous phase decanted off and the process repeated. 2 teaspoons of dried $MgSO_4$ were added to the organic phase and the suspension filtered and dried by rotary evaporation. The product was purified by silica gel chromatography and de-protection of the Ot-butyl groups was carried out with 5 mL TFA and 5 mL dichloromethane (dried) for 5 hours. The final product was dried by rotary evaporation and washed with diethyl ether before being dried under high pressure over night.

2.6.4.2 UDP-Mur*N*Ac-hexa- and heptapeptide synthesis

All reactions (Ser, Ala, Ser-Ala and Ala-Ala branching) were carried out in 2 mL of 80% (v/v) acetonitrile. Added to this was Fmoc-X (24 μmol) where X is a peptide or dipeptide, *N*-hydroxysuccinimide (NHSu) (60 μmol), MES hydrate (10 μmol), 1-ethyl-3-(3-dimethylaminopropyl)-carbodiimide hydrochloride (EDC)(110 μmol), and the pH adjusted to 5.0. This was incubated at room temperature for 20 min (10 min for SerAla or Ser to reduce interaction of EDC with Ser side group) before the addition of UDP-Mur*N*Ac-pentapeptide (2 μmol) in 500 mM $NaHCO_3$ at pH 10. Incubation, with stirring, was carried out for 3 hours before 100 μL ethanolamine was added, and 20 min later, 100 μL 20% (v/v) piperidine for a further 30 min. 2 mL reactions were diluted to 20 mL with sterile H_2O and filtered with a 0.20 μm

nitrocellulose syringe filter. Filtrate was rotary evaporate to remove residual solvent, freeze-dried and stored at -20°C.

2.6.4.3 UDP-Mur*N*Ac-hexa- and heptapeptides purification

Purification was as described in Section 2.6.1.1.

2.6.4.4 UDP-Mur*N*Ac-hexa- and heptapeptides quantification

Quantification was as described in Section 2.6.1.3.

2.6.5 Lipid II preparation

2.6.5.1 Lipid II synthesis

Method adapted from Breukink *et al.* (2003). Synthesis was in a glass vial in 3.5 mL buffer (100 mM Tris.HCl pH 8, 5 mM MgCl$_2$, 1% (v/v) Triton X-100) and contained 10.5 mg *Micrococcus flavus* membranes (Appendix 1) with 48 μmol UDP-Glc*N*Ac (Sigma), 12 μmol UDP-Mur*N*Ac-pentapeptide (or branched/fluorescent derivative) and 4.8 μmol undecaprenyl phosphate, and was incubated at 37°C for 3 hours. Lipid was extracted with 3.5 mL 6 M pyridine-acetate pH 4.2 and 3.5 mL n-butanol. Centrifugation at 4500 × g for 10 min separated the phases and the n-butanol (top) phase was taken and washed with an equal volume of H$_2$O. After a second centrifugation (4500 × g, 10 min), the top phase was collected, rotary evaporated and frozen at -80°C.

2.6.5.2 Lipid II purification

Lipid II purification was by anion exchange using DEAE-Sephacel. 8 mL resin was poured into a sawn-off 20 mL glass pipette with a glass wool fret, and washed with 5 CV of 1 M ammonium acetate, 5 CV H$_2$O and 10 CV of chloroform/methanol/water

(2:3:1) (solvent A). The sample was resuspended in 6 mL solvent A and loaded onto the column by pipette whilst collecting the flow through. The column was washed with 4 CV of solvent A and developed with stepwise increases in concentration of 8 mL chloroform/methanol/1 M ammonium bicarbonate (2:3:1) using steps from 50 mM ammonium bicarbonate to 1 M. Amidated Lipid intermediates required 10 washes at 100 mM ammonium bicarbonate in order to separate the Lipid II from unused undecaprenyl phosphate.

2.6.5.3 Analysis by thin layer chromatography (TLC)

Fractions from anion exchange were analysed by Silica TLC. Dried samples from purification were resuspended in 20 μL solvent A and loaded 2 cm apart and 1.5 cm from the bottom of the plate in 5 μL aliquots with air drying. TLC running buffer (chloroform/methanol/water/0.88 ammonia (88:48:10:1) was poured into the tank at a 1 cm depth and chromatography carried out at room temperature for approximately 4 hours. Iodine vapour in a sealed tank was used to stain the TLC plate. A flat bed scanner was used to image results as iodine staining fades over time.

2.6.5.4 Lipid II quantification

Duplicate Lipid II samples (50 μL) and a chloroform/methanol/water 2:3:1 (v/v) control were dried down under nitrogen flow and resuspended in 50 μL 50 mM HEPES, 10 mM $MgCl_2$, 30 mM KCl, 1.5% (w/v) CHAPS, pH 7.6. 50 μL. 1 M HCl was added to one Lipid II sample and the control, and both boiled for 20 min before centrifuging at 3,000 × g for 5 min. Samples were neutralised to pH 7.6 with 1 M NaOH.

A P_i detection assay was used to quantify the inorganic phosphate released from Lipid II through acid hydrolysis. Purine nucleoside phosphorylase (PNP) converts 7-methyl-6-guanosine (MESG) (strong A_{330nm}) to ribose-1-phosphate and 7-methyl-6-guanine (strong A_{360nm}) in a P_i dependent manner. This increase in absorbance can be followed spectrophotometrically. Including inorganic pyrophosphatase (IPP) releases remaining phosphate from the inorganic pyrophosphate yielded by the acid

hydrolysis. 200 μL assays containing 50 mM HEPES pH 7.6, 10 mM MgCl$_2$, 200 μM MESG (Berry and Associates, USA), 1 unit PNP and 1 unit IPP are monitored for a stable baseline at 360 nm before the addition of 10 μL Lipid II sample. The extinction coefficient for the change in A$_{360nm}$ by 1 M P$_i$ is 10,000 M^{-1}cm^{-1} and is used to quantify the lipid taking into consideration that each Lipid II molecule has two P$_i$.

2.6.6 Mass spectrometry

Samples of UDP-Mur*N*Ac-peptide intermediates and Lipid II were analysed by the Proteomics Facility RTP (School of Life Sciences, University of Warwick) or by Dr Adrian Lloyd (School of Life Science, University of Warwick) unless otherwise stated. Masses were established by negative or positive ion electrospray ionisation mass spectrometry (ESI-MS), and positive ion fragmentation used to verify structures. Data analysis was by the Proteomics Facility RTP or Dr Adrian Lloyd using MassLynx (Waters, USA).

2.7 Assays for transglycosylase activity

Two assay systems were used in this project to analyse the transglycosylase activity of penicillin-binding proteins. These are illustrated diagrammatically for comparison along with alternative assay systems in Figure 2 of Galley *et al.,* (2014) (attached in Appendix 8).

2.7.1 Continuous spectrophotometric assay for transglycosylation

The continuous spectrophotometric assay for transglycosylase activity was carried out as described in Helassa *et al.* (2012), based on the original assay reported by Schwartz *et al.* (2002). Modifications were made to the buffer conditions and additional components as well as Lipid II and enzyme concentrations, and these are detailed throughout the text. In general. 50 μL reactions consisted of 5 μL 100% dansylated Lipid II (Lipid II (Glu, Dans) or Lipid II (Gln, Dans)) from a 10 × stock

and 40 μL of the specified reaction buffer containing any additional components required in a FLUOTRAC^{TM} 600 high binding 96-well plate (Greiner). Lipid stocks were made at 10 × the required Lipid II concentration in 10 × the desired detergent concentration by removal of chloroform/methanol/water (2:3:1) under nitrogen flow and resuspended by vortexing in the detergent buffer. Fluorescence measurements with excitation at 340 nm and emission at 521 nm were made in a Clariostar platereader (BMG Labtech) at the specified temperature until a steady baseline was observed. The reading was paused, plate ejected and 5 μL PBP at 10 × the required concentration, or 5 μL enzyme storage buffer (control) added to initiate the reaction with a multichannel pipette. A ThermalSeal RT^{TM} film was applied to the plate to reduce evaporation. Fluorescence readings were continued for 100 minutes as standard.

Fluorescence values were exported using MARS Data Analysis Software (BMG Labtech), rates were calculated in RFU/second and data plotted in GraphPad Prism (Version 6.0).

2.7.2 SDS-PAGE analysis of transglycosylase products

SDS-PAGE analysis of transglycosylase products was based on the method described by Helassa *et al.* (2012) and Barrett *et al.* (2007). Modifications were made to the buffer conditions, Lipid II and enzyme concentrations for individual experiments, and these are detailed throughout the text. In general, reactions were in a final volume of 15 μL in 0.6 mL low binding eppendorfs to minimise sticking. 1.5 μL 100% dansylated Lipid II (Lipid II (Glu, Dans) or Lipid II (Gln, Dans)) from a 10 × stock was added to 12 μL of the specified reaction buffer. 10 × stocks were made as described in Section 2.7.1. 1.5 μL PBP at 10 × the required concentration, or 1.5 μL enzyme storage buffer (control) were added and reactions incubated in an Eppendorf Mastercycler Gradient thermocycler at a temperature and time specific to the experiment. Reactions were terminated with 0.5 mM moenomycin and 1 × loading buffer was added (6 × stock: 100 mM Tris pH 8.8, 4% (w/v) SDS, 40% (v/v) glycerol).

Polyacrylamide gels were prepared as previously described (Barrett *et al.,* 2007) for the detection of glycan chain. Gels were cast using a Hoeffer Mighty Small gel kit with a 7.5 mL gel recipe of 2.5 mL gel buffer (1.25 M Tris pH 8.45, 0.4% (w/v) SDS), 3.3 mL H_2O, 1.7 mL Acrylamide/Bis-acrylamide 37.5/1 40% and polymerised by the addition of 30 μL 10% (w/v) APS and 15 μL TEMED. Samples were loaded without heat denaturation. In a single lane, reaction buffer plus loading buffer with bromophenol blue was loaded to monitor migration. Gels were run in anode buffer (0.1 M Tris, pH 8.8) and cathode buffer (0.1 M Tris, 0.1 M Tricine, 0.1% (w/v) SDS, pH 8.25) at 100 V and 50 mA for 1 h. Imaging was in a Syngene GeneSnap G:Box Gel Doc under UV (302nm) transillumination with a SW06 filter (516-600 nm) (Syngene).

2.8 Assays for transpeptidase activity

Several methods were used for the detection of transpeptidase activity of PBPs throughout this thesis.

2.8.1 BOCILLIN FL binding

Fluorescently labelled BODIPY penicillin; BOCILLIN FL, was used to identify the correct folding of the penicillin-binding domain. 16 μg PBPs were incubated with 200 μM ampicillin, 200 μM moenomycin or an equivalent volume of sterile water for 30 min at room temperature. A 5:1 molar ratio of BOCILLIN FL to PBP was then incubated at 37°C for 1 hour in the dark before the addition of 1 × loading dye and analysis by SDS-PAGE (Section 2.5.2). Samples were not heat denatured to preserve the interaction between the PBP and BOCILLIN FL. Fluorescence was detected using a Typhoon FLA 9500 laser scanner (GE Healthcare) with a Y520 filter prior to Coomassie-staining of total protein.

2.8.2 SDS-PAGE analysis of transpeptidation products

Polyacrylamide gel analysis of reaction products can detect transpeptidation using a modified version of the method in Section 2.7.2 (for transglycosylation). By use of a 10:1 ratio (50 μM; 5 μM) dansylated to non-dansylated Lipid II, cross-linking is able to occur (dansylated Lipid II cannot be a transpeptidase acceptor), and fluorescence can be detected by the method described previously. Reactions in the presence and absence of 1 mM Penicillin G and 0.5 mM moenomycin were analysed by SDS-PAGE as described in Section 2.7.2.

2.8.3 *N*-acetylmuramidase digestion of SDS-PAGE gel bands for mass spectrometry

The high molecular weight band remaining at the top of the SDS-PAGE gel was visualised by transillumination and removed with a scalpel. A band from the same location in a lane containing only reaction buffer was also removed as a negative control. Both samples were treated identically throughout. 150 μL 100% acetonitrile was added to gel bands in low binding eppendorfs and incubated at 40°C in an Eppendorf Mastercycler Gradient thermocycler for 40 min to dehydrate the acrylamide. Acetonitrile was aspirated and eppendorfs heated at 80°C with the lid open to remove residual solvent. Dehydrated acrylamide was crushed with tweezers and resuspended in 100 μL 50 mM Bis.Tris pH6.2. 10 μL 10 mg.mL^{-1} hen egg-white lysozyme or Mutanolysin from *Streptomyces globisporus* (both *N*-acetylmuramidases) were added and mixtures incubated overnight at 37°C. A further 10 μL *N*-acetylmuramidase was added for 2 hours at 37°C the following morning before centrifugation at 13,000 rpm for 4 min to pellet the acrylamide. The supernatant was carefully removed and the pellet washed in 100 μL 50 mM Bis.Tris pH 6.2 and centrifuged again. The supernatants from both spins were pooled and heated for 10 min at 100°C before centrifugation at 13,000 rpm for 10 min to remove proteins. 150 μL 10 mg.mL^{-1} NaBH$_4$ was added for 30 min at room temperature to reduce the sugar rings following cleavage and finally 17.5 μL 20% (v/v) phosphoric

acid to cleave the lipid linker. Samples were analysed by liquid chromatography mass spectrometry (LC-MS) in positive mode by Dr A. Lloyd.

2.8.4 Amplex Red assay for D-Ala release

The Amplex Red assay for D-Ala release was used for the detection of transpeptidase and/or DD-carboxypeptidase activity. 200 μL reactions were performed in the specific buffer described in the text plus 50 μM Amplex Red, 33.51 mM.min^{-1} *Rhodotorula oracalis* DAAO and 14.82 mM.min^{-1} horseradish peroxidase. The catalytic concentration of DAAO and HRP enzyme activity (mM.min^{-1}) was calculated as described in Appendix 2. In a quartz cuvette; Lipid II or Lipid II storage buffer plus reaction buffer including the above coupling enzymes was monitored for absorbance at 555 nm for 2 min to ensure a stable baseline before the addition of PBP. The reaction was monitored until completion when using a Lipid II capable of being either a donor and an acceptor, or for 6 min before the addition of a transpeptidase acceptor if not. Assays were performed in a Varian Cary 100 spectrophotometer at 30°C.

2.8.5 *N*-acetylmuramidase digestion of cuvette contents for mass spectrometry

Cuvette contents following a positive reaction were digested with Mutanolysin from *Streptomyces globisporus* prior to mass spectrometry in order to identify cross-linked products. 20 μL 2.2 M Bis.Tris pH 6.2 was added to the 200 μL cuvette contents plus 20 μL 10 mg.mL^{-1} Mutanolysin and incubated for 2 h at 37°C. The reaction was incubated for a further 2 h with an additional 20 μL aliquot of Mutanolysin before boiling at 100°C for 10 min and centrifugation at 13,000 rpm for 10 min to remove proteins. 150 μL 10 mg.mL^{-1} NaBH$_4$ was added for 30 min at room temperature to reduce the sugar rings following cleavage and finally 17.5 μL 20% (v/v) phosphoric acid added to cleave the lipid linker. Samples were analysed by liquid chromatography mass spectrometry (LC-MS) in positive mode, and subsequently by collision induced fragmentation by Dr A. Lloyd.

Chapter 3. Synthesis of *Streptococcus pneumoniae* specific Lipid II intermediates

3.1 Introduction

Peptidoglycan has the same basic structure, but is subject to many genus- and species-specific modifications, leading to variations in the chemical structure (covered in detail in Section 1.5.2). In order to study the *in vitro* enzymatic activities and substrate specificities of the Class A PBPs from Gram-positive pathogens (Chapter 4, 5 and 6), a range of substrate variants are required. These include Lipid II with species-specific modifications (Section 3.1.1), as well as fluorescently labelled variants for use in assays of transglycosylase activity (Sections 3.1.2, 4.1.4). Assay development to study the enzymes of the later stages of peptidoglycan biosynthesis has been hampered by lack of availability of the required lipid linked substrates. The extraction of Lipid II from bacteria is difficult as it has a low natural abundance and is structurally complex (Nakagawa *et al.*, 1984; Van Heijenoort, 1992). However, several groups have developed chemical and chemo-enzymatic methods for synthesis of this important substrate, in sufficient yield for the development of assays (Breukink *et al*., 2003; Lloyd *et al.,* 2008; Schwartz *et al.,* 2001; VanNieuwenhze *et al*., 2002).

3.1.1 Peptidoglycan modifications in *Streptococcus pneumoniae*

S. pneumoniae peptidoglycan stem peptides are chemically modified by the addition of an L-Ala or L-Ser followed by L-Ala to form dipeptide branches on the ε-amino group of the third position lysine (Filipe and Tomasz, 2000; Fiser *et al*., 2003). These branches are described from their C-terminus to N-terminus as L-Ala-L-Ala and L-Ser-L-Ala for the remainder of this thesis. The stem peptide is also modified by amidation of the α-carboxyl of D-glutamate at position 2 in the stem peptide to isoglutamine by the amidase MurT/GatD (Zapun *et al.,* 2013). Dipeptide branching and its involvement in *S. pneumoniae* β-lactam resistance is covered in more detail in

Chapter 6, and stem peptide branching more generally in Section 1.5.2.3. Amidation of the second or third position amino acid of the stem peptide is a common modification in Gram-positive bacteria (Vollmer *et al.,* 2008; Section 1.5.2.2.2) and occurs on the second position D-glutamate in both *S. pneumoniae* and *S. aureus*. The role of this modification in both bacteria is studied and discussed in more detail in chapter 4 and 5 respectively.

Glutamate amidation and the appendage of a dipeptide branch to the stem peptide occur at the lipid-linked stage of peptidoglycan biosynthesis, and therefore for further study of PBPs both the amidated and dipeptide branched Lipid II substrates are required. Specifically, these are; Lipid II (Gln), (and Lipid II (Glu)); to enable investigation into the effect of amidation on PBP activity (for both *S. aureus* and *S. pneumoniae*), as well Lipid II with the addition of either L-Ala-L-Ala or L-Ser-L-Ala branches (*S. pneumoniae*) (Figure 3.1 (X_1, X_2, R_3 and R_4). Synthesis of the Lipid II substrate with position 2 isoglutamine and a dipeptide branch has not been described to date, and thus this work is essential for the *in vitro* study of *S. aureus* and *S. pneumoniae* PBPs with their native substrate, and investigation into the role of branched substrates in peptidoglycan synthesis. Note that all Lipid II described in this thesis has lysine at the third position of the stem peptide unless stated otherwise.

3.1.2 Fluorescently labelled Lipid II

Lipid II can be modified to enable detection in assay systems. Historically, this was with radioactive [^{14}C]Glc$N$Ac (Bertsche *et al.,* 2005), but more recently by covalent labelling with a fluorescent molecule, increasing the sensitivity and specificity of detection. A fluorescent group such as dansyl (excitation 340 nm, emission 521 nm; Schwartz *et al*., 2002) or 7-nitro-2,1,3-benzoxadiazol-4-yl (NBD; excitation 466 nm, emission 535 nm; van Dam *et al.,* 2007) can be attached via a sulphonamide linkage to the ε-amino group of the lysine in the third position of the pentapeptide chain, or alternatively incorporated into the lipid chain (Liu *et al.,* 2010). For use in the assay systems in this project (see section 4.1.4 for details), Lipid II with a dansyl group on the third position lysine was required (Figure 3.1 (R_2)), with and without amidation of the second position glutamate α-carboxyl (Figure 3.1 (X_1 and X_2)).
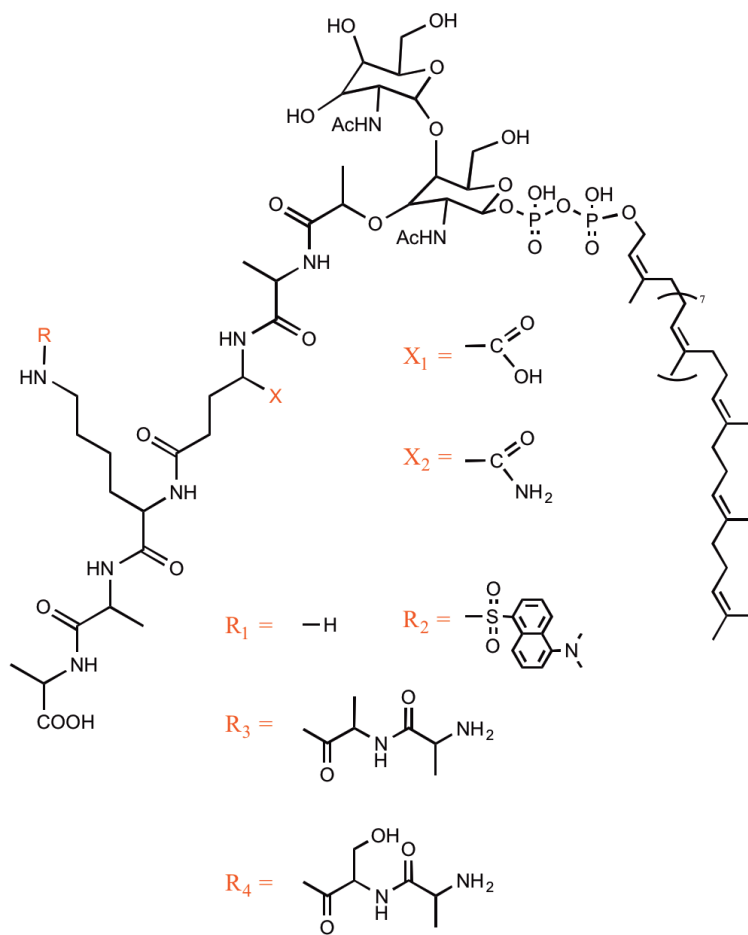
Figure 3.1: Lipid II variants. Structure of the Lipid II variants required for this project. Basic structure of lysine Lipid II is varied at two points (X and R). Lipid II is either X_1: D-glutamate (non-amidated) in the second position or X_2: D-isoglutamine (amidated) in the second position. The third position lysine is unchanged (R_1), fluorescently labelled with a dansyl group (R_2) or with the addition of a dipeptide branch; R_3: L-Ala-L-Ala or R_4: L-Ser-L-Ala.

3.1.3 *In vitro* Lipid II synthesis

The synthesis of peptidoglycan intermediates, including Lipid II is well established within our group (BaCWAN, UK; Clarke *et al*., 2009; Lloyd *et al*., 2008). Lipid II can be made by either a chemical or enzymatic route (Breukink *et al*., 2003; Lloyd *et al*., 2008; Schwartz *et al.,* 2001; VanNieuwenhze *et al.,* 2002), the latter of which is detailed in Figure 3.2 (Illustrated for Lipid II (Glu/Gln)), and is the method used in this chapter (full method details in sections 2.6.1 and 2.6.5). In short, a single one-pot incubation containing the MurA-MurF enzymes mimics the cytoplasmic steps of peptidoglycan biosynthesis and produces UDP-Mur*N*Ac-L-Ala-γ-D-Glu/D-Gln-L-Lys-D-Ala-D-Ala (UDP-Mur*N*Ac-pentapeptide (Glu/Gln)), which is then converted

to Lipid II by addition of undecaprenyl phosphate and UDP-Glc*N*Ac using *Micrococcus flavus* membranes (Breukink *et al.,* 2003).

3.2 Experimental Aims

- To synthesise UDP-Mur*N*Ac-L-Ala-γ-D-Gln-L-Lys-D-Ala-D-Ala (UDP-Mur*N*Ac-pentapeptide (Gln)) and adequately desalt for later reactions.

- To develop a method for the chemical synthesis of UDP-Mur*N*Ac-hexapeptide (Gln, Ala), UDP-Mur*N*Ac-hexapeptide (Gln, Ser), UDP-Mur*N*Ac-heptapeptide (Gln, AlaAla) and UDP-Mur*N*Ac-heptapeptide (Gln, SerAla).

- To convert these branched UDP-Mur*N*Ac-pentapeptide derivatives to Lipid II, with sufficient yield for use in enzymatic studies.

- To obtain Lipid II (Glu), Lipid II (Gln) and their fluorescently labelled derivatives; Lipid II (Glu, Dans) and Lipid II (Gln, Dans) for assays of PBP activity
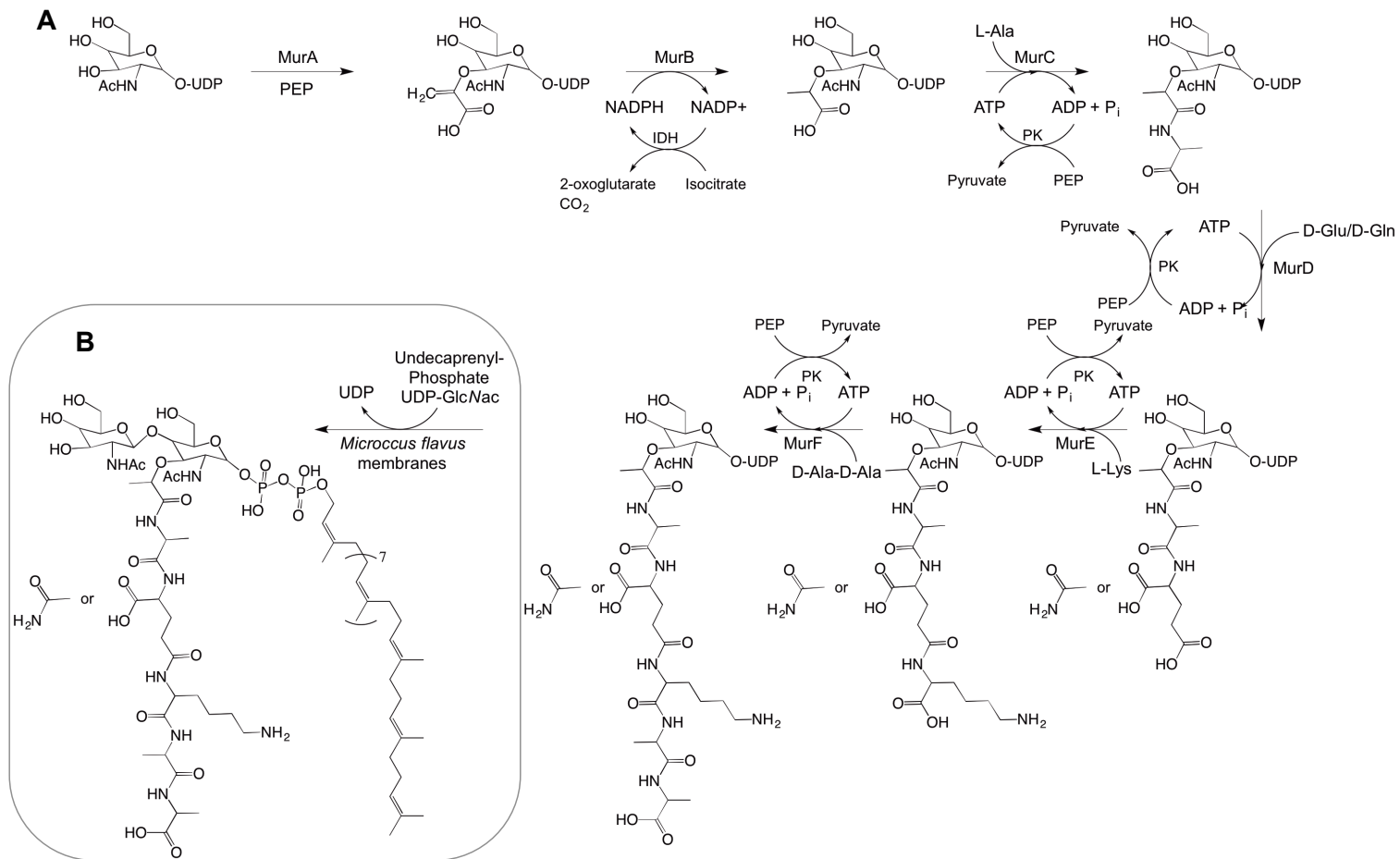
Figure 3.2: Enzymatic synthesis of Lipid II. .A: MurA-MurF one pot synthesis including substrates and cofactors for the Mur enzymes as well as recycling enzymes produces UDP-MurNAc-pentapeptide (Glu/Gln) from UDP-GlcNAc. B: UDP-MurNAc-pentapeptide converted to Lipid II by *Micrococcus flavus* membranes and the addition of UDP-GlcNAc and undecaprenyl phosphate. PK: Pyruvate kinase, IDH: Isocitrate dehydrogenase

3.3 Enzymatic biosynthesis of UDP-MurNAc-pentapeptide

UDP-MurNAc-pentapeptide can be made in one step by enzymes MurA-MurF and their substrates (Section 2.6.1 and 3.1.3). UDP-MurNAc-pentapeptide (Glu) was made according to a published method (Lloyd *et al.,* 2008). Work by Dr A. Lloyd established that MurD incorporates D-isoglutamine into position 2 of the pentapeptide when added in sufficient quantities (3 x excess required over natural D-glutamate substrate). (Dr Adrian Lloyd, Personal communication), giving UDP-MurNAc-pentapeptide (Gln). An alternative strategy is the enzymatic amidation of glutamate containing Lipid II using MurT/GatD in the presence of ATP and L-glutamine (Zapun *et al.,* 2013). However, this would require a purification step by anion exchange, reducing the final yield, as well as using costly Lipid II as a substrate. Additionally there is the possibility of incomplete purification, and thus a mix of final products, which can be avoided by ensuring that only isoglutamine can be incorporated at an early stage in the synthesis. Both UDP-MurNAc-pentapeptide (Glu) and UDP-MurNAc-pentapeptide (Gln) were synthesised by the one pot method (Section 2.6.1), purified by anion exchange (Section 2.6.1.1)(Figure 3.3) and freeze dried four times to remove the ammonium acetate required for elution from the Source30Q column.

Elution of UDP-MurNAc-pentapeptide was monitored by absorbance changes at 254 nm and 280 nm (2.6:1 A_{254nm}:A_{280nm} characteristic of the Uridine ring; Dawson *et al.,* 1986). Figure 3.3 shows a clear peak (A(i)) at the expected conductivity of approximately 13 mS.cm^{-1} (estimated based on previous work by Dr. A. Lloyd) and with clear separation from the ATP (A(ii)) required by MurC-MurF. UDP-MurNAc-pentapeptide (Gln) was eluted at a lower conductivity than the non-amidated version (B(i)) at 12.6 mS.cm^{-1}, due to the loss of a negative charge lowering the affinity for the anion exchange resin. The pentapeptide product was again well separated from ATP (B(ii)). No peaks were observed for contaminating ADP, suggesting proper functioning of the recycling system for ADP.
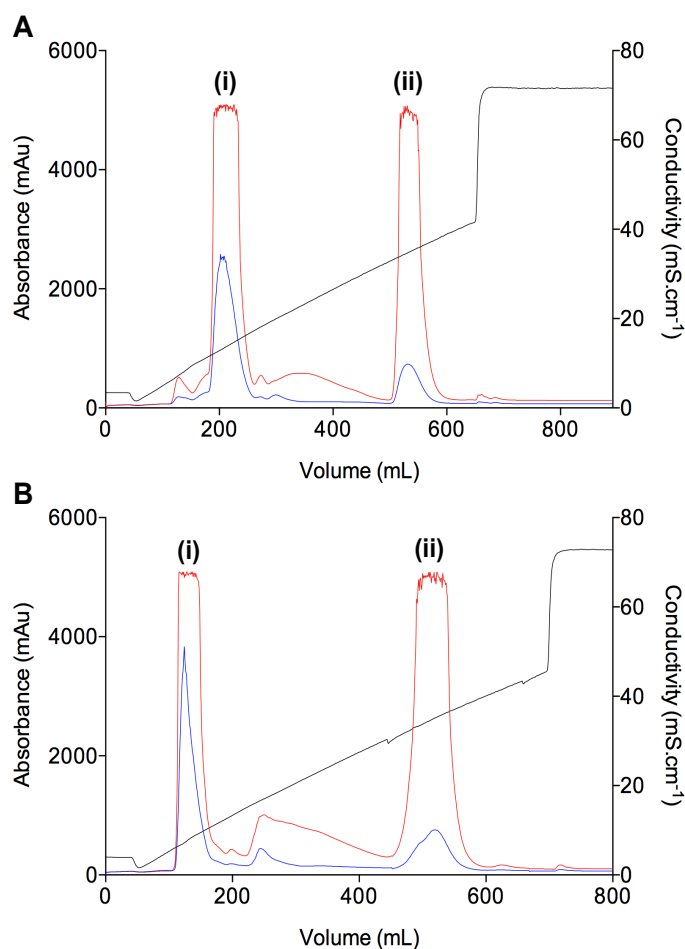
Figure 3.3: Purification of UDP-Mur*N*Ac-pentapeptides (Glu/Gln) by anion exchange chromatography (Source30Q resin). A: The purification of UDP-Mur*N*Ac-L-Ala-γ-D-Glu-L-Lys-D-Ala-D-Ala (i) eluting at a conductivity of 13.3 mS.cm^{-1}. B: The purification of UDP-Mur*N*Ac-L-Ala-γ-D-Gln-L-Lys-D-Ala-D-Ala (i) eluting at a conductivity of 12.6 mS.cm^{-1}. A(ii) and B(ii) ATP (required by MurC-MurF). Red trace is absorbance at 254 nm, blue trace: absorbance at 280 nm and black trace; conductivity.

As residual ammonium acetate salt after Source30Q elution would inhibit subsequent carbodiimide coupling steps (Section 3.5.3), UDP-Mur*N*Ac-pentapeptide was desalted by size exclusion chromatography (Figure 3.4) using Bio-Gel P2 resin and H$_2$0 as described in Section 2.6.1.2.

Despite the use of a large volume (475 mL) column, and elution in upflow, poor separation was observed between the UDP-Mur*N*Ac-pentapeptides and ammonium acetate (Figure 3.4), resulting in a significant loss of yield (discussed in Section 3.7.2.2). Selected fractions containing UDP-Mur*N*Ac-pentapeptide separated from the salt peak were freeze-dried once and resuspended in a minimum volume of 500 mM NaHCO$_3$ pH 10. The product was quantified by absorbance at 260 nm (the

uracil portion of the UDP-MurNAc-pentapeptide has an extinction coefficient of 10,000 M^{-1}cm^{-1}; Dawson *et al.,* 1986). A yield of ~20 mg per synthesis was achieved following both Source30Q and Bio-Gel P2 purification.
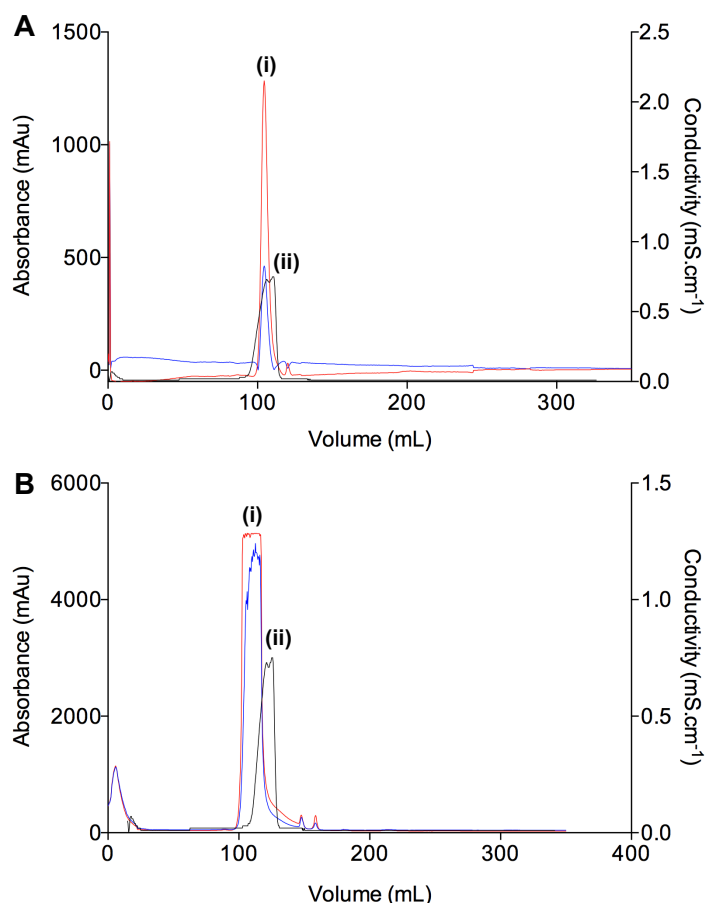
Figure 3.4: Desalting of UDP-MurNAc-pentapeptides (Glu/Gln) by gel filtration chromatography (Bio-Gel P2 resin). A: The desalting of UDP-MurNAc-L-Ala-γ-D-Glu-L-Lys-D-Ala-D-Ala (i) (elution volume:104 mL) from ammonium acetate (ii) (elution volume:114 mL) B: The desalting of UDP-MurNAc-L-Ala-γ-D-Gln-L-Lys-D-Ala-D-Ala (i) (elution volume:108 mL) from ammonium acetate (ii) (elution volume:114 mL). Red trace is absorbance at 254 nm, blue trace: absorbance at 280 nm.

Analytical anion exchange chromatography (MonoQ resin) was used to determine the final purity of UDP-MurNAc-pentapeptide (Glu) and UDP-MurNAc-pentapeptide (Gln) (Section 2.6.1.4 and Figure 3.5). A 1 μL sample of each pentapeptide product variant in 1 mL 10 mM ammonium acetate was loaded onto a 1 mL MonoQ column before elution over a 10 mL gradient from 10 mM to 1 M ammonium acetate. The D-Gln containing UDP-MurNAc-pentapeptide eluted earlier (14.4 mS.cm^{-1}) than the D-Glu containing derivative (23.3 mS.cm^{-1}), consistent with the structure. Integration of required peaks as a percentage of the overall area using

UNICORN software (GE Healthcare) established the purity of UDP-Mur*N*Ac-pentapeptide (Glu) as 98.4%, and UDP-Mur*N*Ac-pentapeptide (Gln) as 91.9%. Purity over 90% was deemed sufficient and taken forward and if purity was below this, the intermediate was re-purified by anion exchange (Source30Q).

The synthesis of UDP-Mur*N*Ac-pentapeptide (Glu) and UDP-Mur*N*Ac-pentapeptide
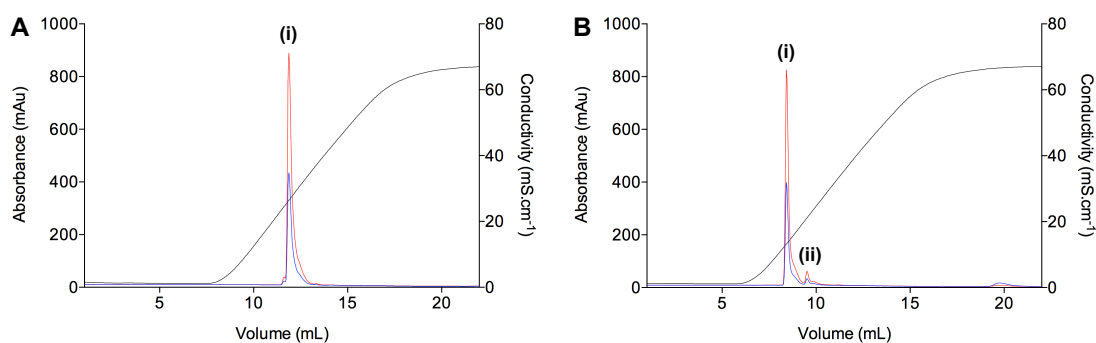
Figure 3.5: Purity checks of UDP-Mur*N*Ac-pentapeptides (Glu/Gln) by anion exchange chromatography (MonoQ resin) A: Purity check of UDP-MurNAc-L-Ala-γ-D-Glu-L-Lys-D-Ala-D-Ala (i) (conductivity 23.3 mS.cm^{-1}). Peak integration established purity as 98.4 %. B: Purity check of UDP-MurNAc-L-Ala-γ-D-Gln-L-Lys-D-Ala-D-Ala (i) (conductivity 14.4 mS.cm^{-1}) from a minor contaminant (ii). Peak integration established as 91.9 %. Red trace is absorbance at 254 nm, blue trace: absorbance at 280 nm.

(Gln) was confirmed by negative ion mass spectrometry (carried out by the University of Warwick Proteomics Facility RTP) (Figure 3.6 and 3.7). Spectra are shown as full page images with embedded isotope profile predictions, which identify both variants to contain only UDP-Mur*N*Ac-pentapeptide (Glu) or UDP-Mur*N*Ac-pentapeptide (Gln) respectively. All subsequent mass spectrometry in this chapter was carried out by the Proteomics Facility RTP unless otherwise stated.
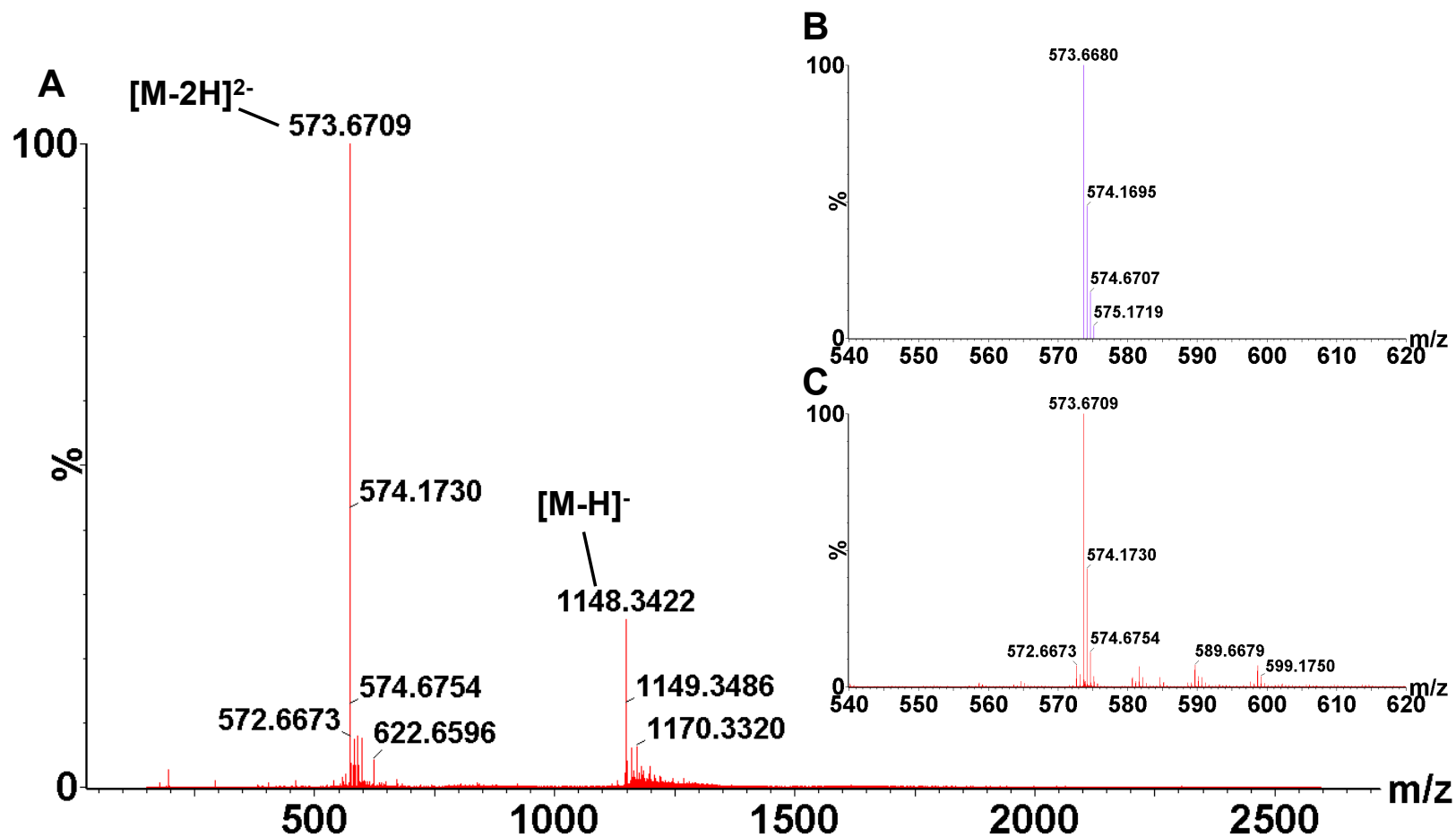
Figure 3.6: Negative ion mass spectra of UDP-Mur*N*Ac-pentapeptide (Glu) A: Mass spectra with $[M-2H]^{2-}$ (observed 573.6709, expected 573.6680), and $[M-H]^-$ (observed 1148.3422, expected 1148.3446) indicated. B: Predicted isotope distribution of $[M-2H]^{2-}$ based on the empirical formula of UDP-Mur*N*Ac-pentapeptide (Glu) (predicted by MassLynx^{TM} software (Waters, USA). C: Observed isotope distribution of $[M-2H]^{2-}$ (zoomed in view of $[M-2H]^{2-}$ peak in A showing exact match with the predicted distribution in B.
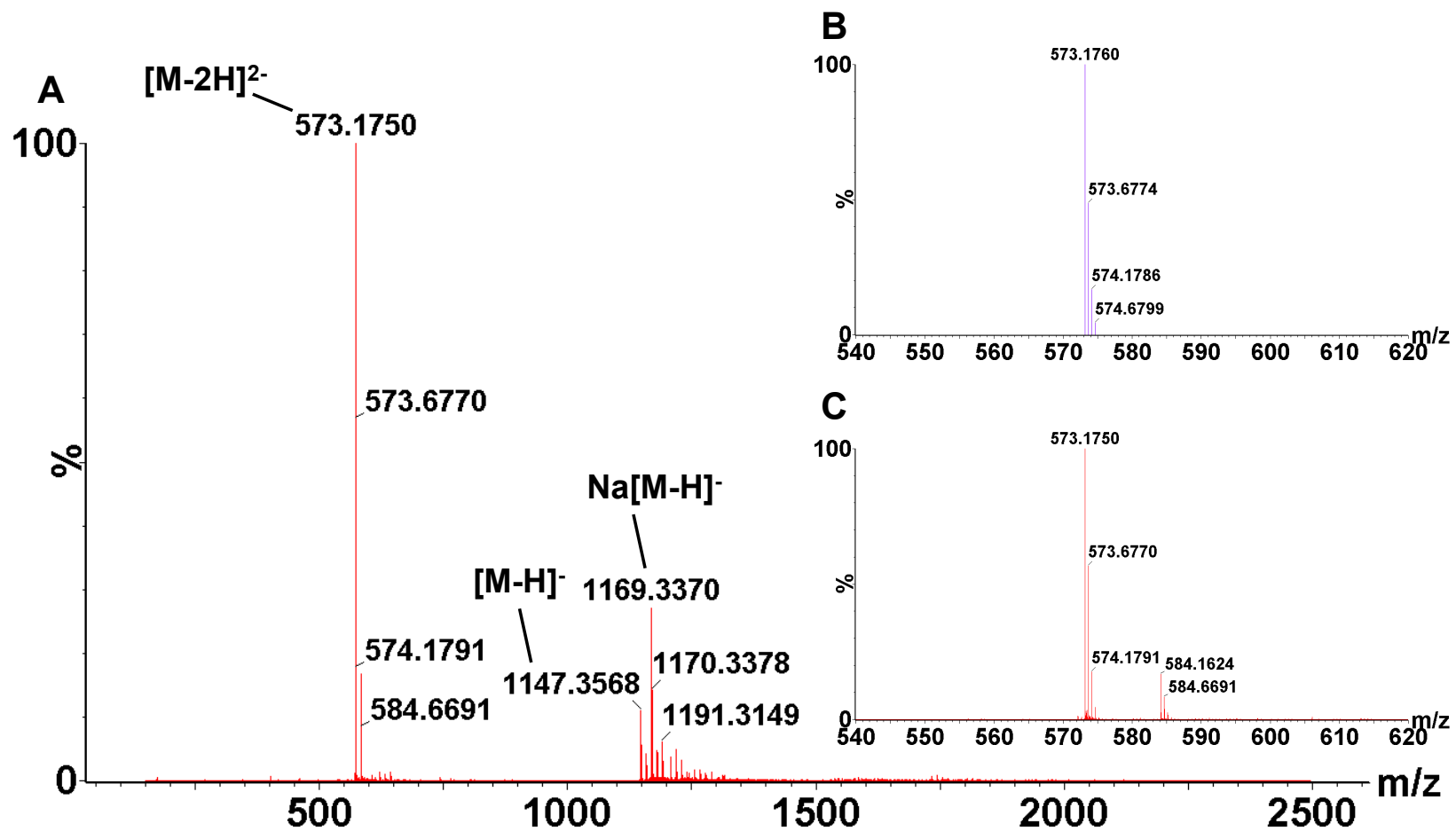
Figure 3.7: Negative ion mass spectra of UDP-Mur*N*Ac-pentapeptide (Gln) A: Mass spectra with $[M-2H]^{2-}$ (observed 573.1750, expected 573.1760),, $[M-H]^-$ (observed 1147.3568, expected 1147.3606) and sodiated $[M-H]^-$ ($Na[M-H]^-$) indicated. B: Predicted isotope distribution of $[M-2H]^{2-}$ based on the empirical formula of UDP-Mur*N*Ac-pentapeptide (Glu) (predicted by MassLynx^{TM} software (Waters, USA). C: Observed isotope distribution of $[M-2H]^{2-}$ (zoomed in view of $[M-2H]^{2-}$ peak in A showing exact match with the predicted distribution in B.

3.4 Synthesis of dansylated UDP-Mur*N*Ac-pentapeptide

In order to obtain the fluorescently labelled Lipid II (Figure 3.1 (R$_2$)) required for transglycosylase assays in later chapters (chapter 4 and 5), a dansyl group was covalently attached to the third position lysine by a sulphonamide linkage, as covered in Section 3.1.2, by Julie Todd or Anita Catherwood of BaCWAN (UK; Clarke *et al.*, 2009; Lloyd *et al.*, 2008), and is briefly covered here for completeness.

Full methodological details are in Section 2.6.3 Briefly, desalted UDP-Mur*N*Ac-pentapeptide (Gln/Glu) was incubated with a 42 × molar ratio of dansyl chloride (Sigma-Aldrich) in acetone overnight in the dark and with stirring. Unincorporated dansyl chloride was quenched with Tris pH 9 for 1 hour and rotary evaporation used to remove solvent. Dansylated UDP-Mur*N*Ac-pentapeptide (Glu/Gln) was purified from starting material by size exclusion chromatography on a Superdex Peptide column (GE Healthcare). Elution of dansylated product was identified by absorbance at 340 nm. Fractions were pooled, freeze dried and resuspended in a small volume of water. Purity was determined by anion exchange as before (Section 2.6.1.4) and negative ion mass spectrometry used to confirm identity. This was also used to confirm the presence of 100% dansylated product (and amidated where required) prior to Lipid II synthesis. Mass spectra are shown in Appendix 3.

3.5 Chemical synthesis of branched UDP-Mur*N*Ac-pentapeptide derivatives

3.5.1 Method choice

A similar protocol to the enzymatic synthesis of the UDP-Mur*N*Ac-pentapeptides was considered for the synthesis of the *S. pneumoniae* branched pentapeptide derivatives. The amino acid ligases MurM and MurN use Lipid II and amino acids esterified to their cognate tRNAs as substrates to add the dipeptide branches in *S. pneumoniae* (Lloyd *et al.,* 2008). This method was decided against due to the large quantities of Lipid II required, particularly at the method optimisation stage, and also

the low resolution of the Lipid II purification method, which is unable to separate branched and non-branched product sufficiently (Lloyd *et al.,* 2008). Additionally due to the substrate specificity of MurM (Lloyd *et al.,* 2008) it would not be trivial to separate the two products with either serine or alanine in the first position of the branch. Instead a chemical method for attachment of the amino acid was used.

3.5.1.1 Chemo-enzymatic method

The presence of the sole amino group present on the UDP-Mur*N*Ac-pentapeptide (Glu/Gln); on the ε-carbon of the third position L-Lys, has been exploited previously with the addition of fluorescent groups such as dansyl by sulphonamide linkage (Section 3.4) which can used to follow incorporation of the labelled Lipid II into non cross-linked peptidoglycan (Helassa *et al*., 2012; Schwartz *et al.,* 2002). This ε-carbon is also the position at which the species-specific branching amino acids are attached (Lloyd *et al.,* 2008). Carbodiimide coupling chemistry was used to attach L-Ala, L-Ser, L-Ala-L-Ala and L-Ser-L-Ala to the lysine of UDP-Mur*N*Ac-pentapeptide (Glu/Gln) as shown in Figure 3.8 illustrated for UDP-Mur*N*Ac-pentapeptide (Glu) and Fmoc-Ala-Ala.

For coupling EDC (1) (1-ethyl-3-(3-dimethylaminopropyl)-carbodiimide) was used to activate the free carboxyl of Fmoc-Ala-Ala (2) to form an O-acylisourea conjugate (3) of the latter. This was then displaced by N-hydroxysuccinimide (NHS) (4) with the displacement of the urea derivative of EDC (5) to yield the NHS ester of Fmoc-Ala-Ala (6). This intermediate was attacked by the nucleophilic ε amino group of UDP-MurNAc-pentapeptide (7) to form a peptide bond between the two species and yield UDP-Mur*N*Ac-Ala-Glu-Lys(AlaAla-Fmoc)-Ala-Ala (8) which was subsequently deprotected with piperidine (9) to produce the final UDP-Mur*N*Ac-Ala-Glu-Lys(AlaAla)-Ala-Ala (10) product, and the piperidine derivative of Fmoc (11). The presence of NHS in the reaction converted the amine-reactive O-acylisourea intermediate into an amine-reactive NHS ester, which made it more stable and has been reported to result in a more efficient coupling reaction (Staros *et al.,* 1986).
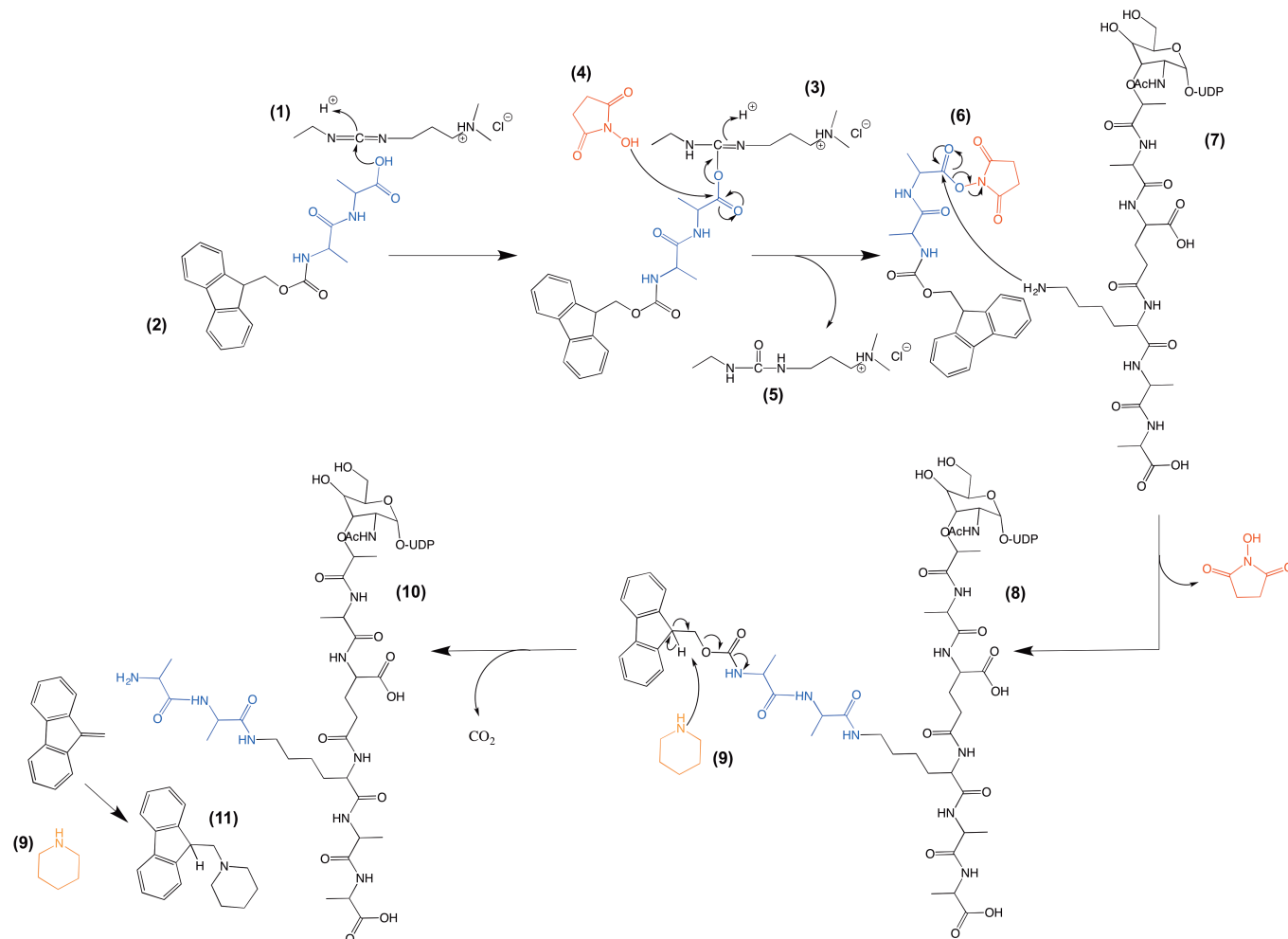
Figure 3.8: Mechanism of coupling of peptides to UDP-Mur*N*Ac-pentapeptide (Glu). Reaction mechanism showing the carbodiimide coupling used to attach branching amino acids. Compounds labelled as described in the text. Illustrated for the coupling of Fmoc-L-Ala-L-Ala to UDP-Mur*N*Ac-pentapeptide (Glu). Mechanism identical for all other peptides.

3.5.2 Peptide and dipeptide branches

For carbodiimide coupling, peptides to be added to the ε-amino group of the lysine must be protected on the primary amine with a group such as fluorenylmethyloxycarbonyl (Fmoc) to prevent side reactions between the amino acids and dipeptides, which would result in polymers (Carpino and Wu, 2000). Many amino acids can be purchased already attached to a Fmoc group, whereas others are prohibitively expensive and therefore it is more cost effective to add the protecting group to purchased peptides. Figure 3.9 illustrates the two methods used to produce Fmoc coupled peptides, as detailed in the remainder of this section.

3.5.2.1 Fmoc-Ala and Fmoc-Ser

Fmoc-Ala-OH and Fmoc-Ser-OH are available commercially and were purchased from Novabiochem (Germany).

3.5.2.2 Fmoc-Ala-Ala

Fmoc-Ala-Ala-OH is not available commercially and the cost of custom synthesis was prohibitively high, thus the protected dipeptide was synthesised as described in section 2.6.4.1.1, with the reaction of Ala-Ala-OH with Fmoc-OSu (Figure 3.9 (A); mechanism illustrated for Fmoc-Ala-Ser), before extraction with ethyl acetate. A 57% yield was achieved; with 136 mg produced in a single reaction. Successful synthesis was confirmed by negative ion mass spectrometry (Figure 3.10 (A); [M-H]$^-$ expected 381.1459, observed 381.1494; dimeric species 2[M-H]$^-$ expected 763.2988, observed 763.3110).
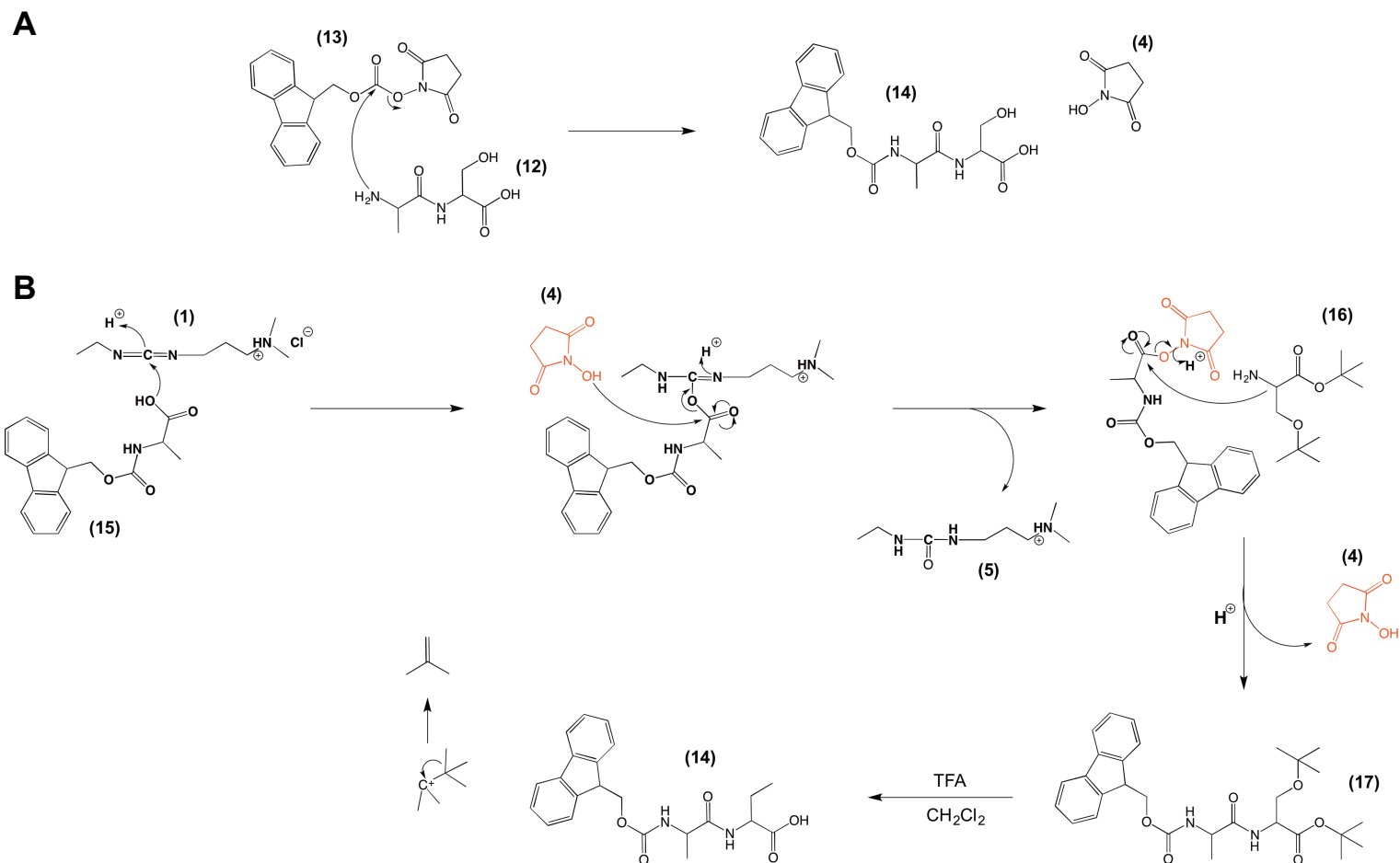
Figure 3.9: Mechanism of dipeptide protection with Fmoc. Illustrated for Fmoc-L-Ala-L-Ser. A: Reaction of L-Ala-L-Ser (12) with Fmoc-OSu (13) to yield Fmoc-L-Ala-L-Ser (14) protected on the N-terminus. This method was also used for Fmoc-L-Ala-L-Ala (2); compound numbering contiguous from Figure 3.8. B: Carbodiimide coupling of Fmoc-L-Ala (15) and O-*tert*-Butyl-L-Ser *tert*-butyl ester (16) to yield Fmoc-L-Ala-L-Ser protected on the N-terminus with Fmoc and C-terminus with t-butyl (17). TFA hydrolysis removes the C-terminal protection to yield Fmoc-L-Ala-L-Ser (14).

3.5.2.3 Fmoc-Ala-Ser

Similarly, the cost of custom synthesis of Fmoc-Ala-Ser-OH was prohibitive. Two methods were attempted and their yields compared. The first method was as illustrated in Figure 3.9 (A)(method Section 2.6.4.1.1), with the reaction of Ala-Ser-OH with Fmoc-OSu. Extraction with ethyl acetate achieved a yield of 53% (126 mg per reaction). For the second, Fmoc-L-Ala was coupled to O-*tert*-Butyl-L-Serine *tert*-butyl ester using carbodiimide chemistry (Figure 3.9 (B))(full method section 2.6.4.1.2); similar to that described for the addition of the branching peptides. The L-Ala is protected on the amine by Fmoc, and the L-Ser on the carboxyl and β-hydroxyl by t-butyl ester to prevent side reactions between the amino acids. EDC (1) and NHS (4) form an O-NHS ester intermediate with the carboxylic acid of the L-Ala (Figure 3.9 (B)), thus activating it for nucleophilic attack by the O-*tert*-Butyl-L-Serine *tert*-butyl ester (16) to form an amide bond. The product was extracted in dichloromethane and purified by silica gel chromatography.

T-butyl removal from the seryl carboxyl was with TFA (trifluoroacetic acid). A 5 hour hydrolysis was required as the standard 2 hour method yielded a mix of unprotected serine and some with 1 O-*tert*-Butyl group remaining. The yield from this method was substantially lower than the previous one, at 3%, most likely due to the large numbers of steps in the process.

This could have been optimised further, but due to the high yield achieved with the first method and its simplicity, this was used to synthesise Fmoc-Ala-Ser for use in coupling. Again successful synthesis was confirmed by negative ion mass spectrometry (Figure 3.10 (B); [M-H]$^-$ expected 397.1408, observed 397.1278; dimeric species 2[M-H]$^-$ expected 795.2886, observed 795.2565).
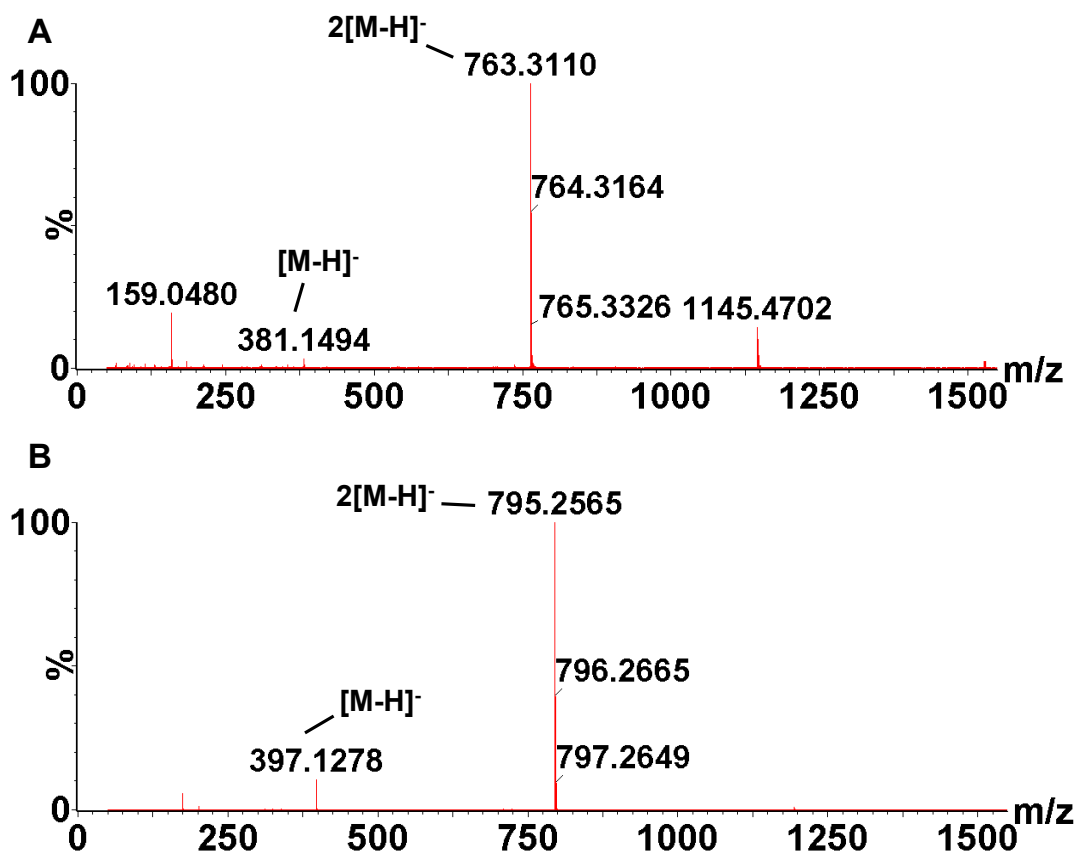
Figure 3.10: Negative ion mass spectrometry of Fmoc-Ala-Ala (A) and Fmoc-Ala-Ser (B). A: Negative ion electrospray time-of-flight mass spectra of Fmoc-Ala-Ala-OH. [M-H]⁻ expected 381.1459, observed 381.1494. Dimeric species 2[M-H]⁻ expected 763.2988, observed 763.3110. B: Negative ion electrospray time-of-flight mass spectra of Fmoc-Ala-Ser-OH. [M-H]⁻ expected 397.1408, observed 397.1278. Dimeric species 2[M-H]⁻ expected 795.2886, observed 795.2565.

3.5.3 Synthesis of branched UDP-Mur*N*Ac-pentapeptide intermediates

Fmoc protected amino acids and dipeptides (Section 3.5.2) were reacted with EDC and NHS at pH 5 and the resulting O-acylisourea intermediates incubated with UDP-Mur*N*Ac-pentapeptide (Glu) or UDP-Mur*N*Ac-pentapeptide (Gln) at pH10. The Fmoc protecting group was removed with piperidine and the products rotary evaporated to remove organic solvent and freeze-dried prior to purification. The reaction scheme is detailed in Figure 3.8 and is described in more detail in section 2.6.4.2. This method was derived from earlier work by Dr Gianfranco De Pascale (De Pascale, 2007), Dr Tom Clarke (Clarke, 2008) as well as De Pascale *et al.,* (2008). Previous optimisation with single amino acid branches and UDP-Mur*N*Ac-pentapeptide (Glu) established pH, incubation times and ratios of reagents; 45 eq. (equivalents) EDC, 30 eq. NHS, 12 eq. amino acid, 1 eq. 5P (De Pascale, 2007), that

enabled the optimum yield. An important point to note with amidated pentapeptides is the presence of the amide group on the isoglutamine, which has the potential to act as a nucleophile in the EDC coupling reaction. Although, the relative lack of nucleophilic character of this amide nitrogen due to delocalisation of electrons with the adjacent carbonyl group makes this unlikely.

Purification of branched intermediates was by anion exchange chromatography using Source30Q resin with a bed volume of 75 mL (Section 2.6.4.3). An ammonium acetate gradient from 10 mM to 300 mM over 7 column volumes was used to separate products, and the presence of UDP-Mur*N*Ac-pentapeptide derivatives were confirmed by absorbance at 254 nm and 280 nm. Fractions were freeze dried 4 times and resuspended in a small volume of H_2O, prior to further analysis and identification of species.

Figures 3.11 and 3.12 show both the purification and confirmation of synthesis by negative ion mass spectrometry of each of UDP-Mur*N*Ac-L-Ala-γ-D-Gln-L-Lys-(L-Ala)-D-Ala-D-Ala (Figure 3.11 (A) and (B)), UDP-Mur*N*Ac-L-Ala-γ-D-Gln-L-Lys-(L-Ser)-D-Ala-D-Ala (Figure 3.11 (C) and (D)), UDP-Mur*N*Ac-L-Ala-γ-D-Gln-L-Lys-(L-Ser-L-Ala)-D-Ala-D-Ala (Figure 3.12 (A) and (B)), UDP-Mur*N*Ac-L-Ala-γ-D-Gln-L-Lys-(L-Ala-L-Ala)-D-Ala-D-Ala (Figure 3.12 (C) and (D)). The addition of branching amino acids to amidated UDP-Mur*N*Ac pentapeptide is novel work, which has not been published to date. Dipeptide branching with non-amidated UDP-Mur*N*Ac pentapeptide (Glu) was also attempted as shown in Table 3.1, but detailed results are not shown here as mass spectrometry confirmation of syntheses was not performed. Note that the mass spectrum shown in Figure 3.12 (B) was obtained on an open source machine for which raw data could not be obtained to produce a high-resolution image. Therefore Figure 3.12 (B) is also reproduced in Appendix 4 as a full-page image for clarity.
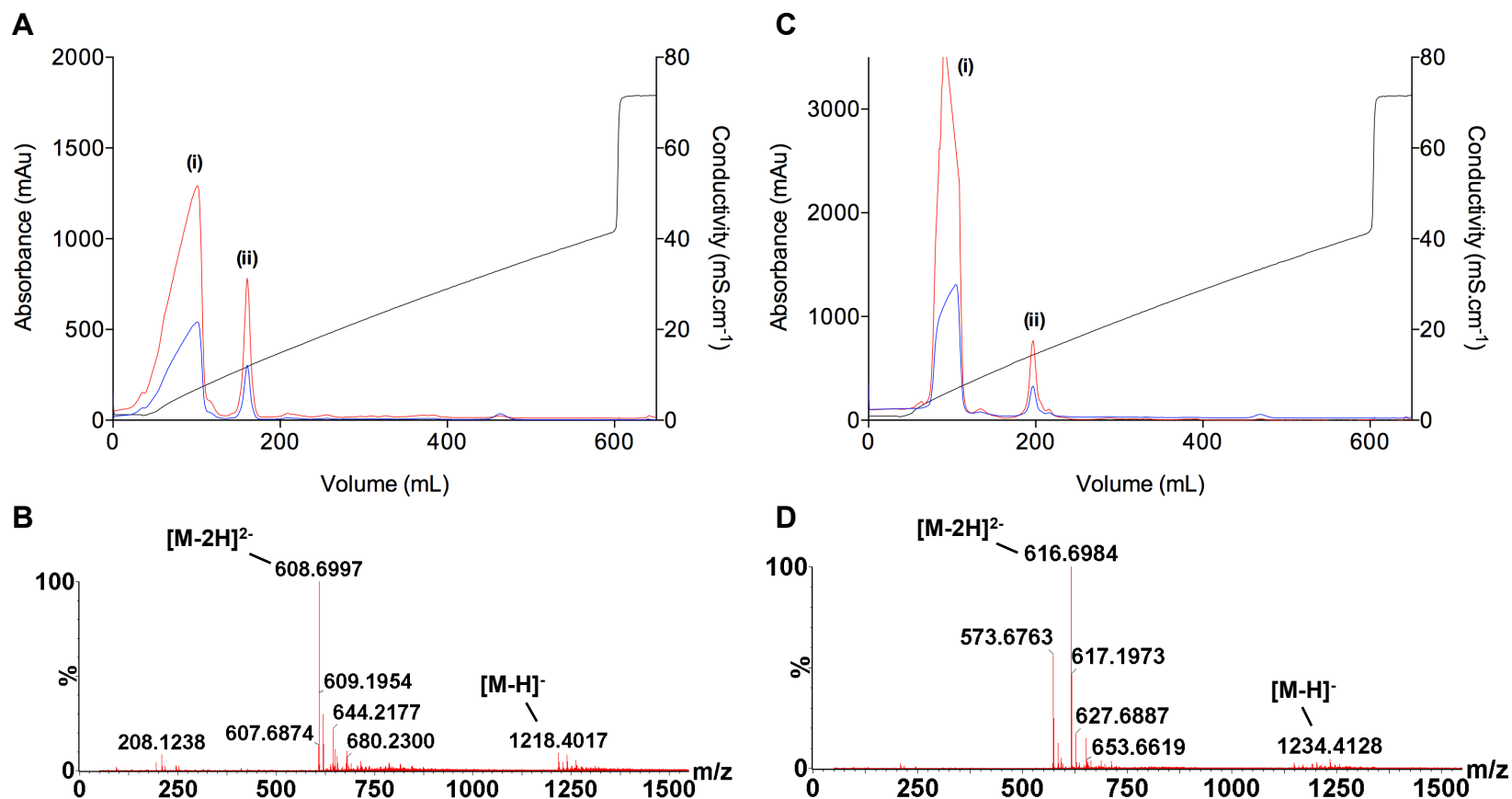
Figure 3.11: Purification and characterisation of UDP-Mur*N*Ac-hexapeptides (Gln, Ala)(A,B) and (Gln, Ser)(C,D) by anion exchange chromatography (Source30Q resin) and negative ion mass spectrometry. A: Purification of UDP-Mur*N*Ac-L-Ala-γ-D-Gln-L-Lys(L-Ala)-D-Ala-D-Ala (elution at 10.9 mS.cm^{-1} (A(ii)). (A(i)) is a peak of organic reagents used in the coupling reaction. Red: A$_{254nm}$; blue: A$_{280nm}$, black: conductivity. B: Negative ion electrospray time-of-flight mass spectra of UDP-Mur*N*Ac-L-Ala-γ-D-Gln-L-Lys(L-Ala)-D-Ala-D-Ala. [M-H]$^-$expected 1218.3977, observed 1218.4017, [M-2H]$^{2-}$ expected 608.6954 observed 608.6997. C: The purification of UDP-Mur*N*Ac-L-Ala-γ-D-Gln-L-Lys(L-Ser)-D-Ala-D-Ala (elution at 13.5 mS.cm^{-1} (C(ii)). (C(i)) is a peak of organic reagents used in the coupling reaction. Red: A$_{254nm}$; blue: A$_{280nm}$, black: conductivity B: Negative ion electrospray time-of-flight mass spectra of UDP-Mur*N*Ac-L-Ala-γ-D-Gln-L-Lys(L-Ser)-D-Ala-D-Ala. m/z: [M-H]$^-$expected 1234.3926 observed 1234.4128, [M-2H]$^{2-}$ expected 616.6928 observed 616.6984.

Figure 3.12: Purification and characterisation of UDP-Mur*N*Ac-heptapeptides (Gln, AlaAla)(A, B) and (Gln, SerAla) (C,D) by anion exchange chromatography (Source30Q resin) and negative ion mass spectrometry. A: Purification of UDP-Mur*N*Ac-L-Ala-γ-D-Gln-L-Lys(L-Ala-L-Ala)-D-Ala-D-Ala (elution at 11.04 mS.cm^{-1}) (A(ii)). (A(i)) is a peak of organic reagents used in the coupling reaction. Red: A$_{254nm}$; blue: A$_{280nm}$, black: conductivity. B: Negative ion electrospray time-of-flight mass spectra of UDP-Mur*N*Ac-L-Ala-γ-D-Gln-L-Lys(L-Ala-L-Ala)-D-Ala-D-Ala. [M-2H]$^{2-}$ expected 644.2139 observed 644.2. This spectra is reproduced as a full page in Appendix 4 due to low quality image. C: Purification of UDP-Mur*N*Ac-L-Ala-γ-D-Gln-L-Lys(L-Ser-L-Ala)-D-Ala-D-Ala (elution at 11.4 mS.cm^{-1})(C(iii)). Unreacted UDP-Mur*N*Ac-L-Ala-γ-D-Gln-L-Lys-D-Ala-D-Ala elutes at 8.5 mS.cm^{-1} (C(ii)) and (C(i)) is a peak of organic reagents used in the coupling reaction. Red: A$_{254nm}$; blue: A$_{280nm}$, black: conductivity. B: Negative ion electrospray time-of-flight mass spectra of UDP-Mur*N*Ac-L-Ala-γ-D-Gln-L-Lys(L-Ser-L-Ala)-D-Ala-D-Ala. [M-2H]$^{2-}$ expected 652.2114 observed 652.2113.

Table 3.1 details the range of intermediates made using this method. Priority was given to the synthesis of the amidated variants (left-hand column) due to these being the *in vitro* synthetic precursor to the native substrate in *S. pneumoniae*, and therefore the more interesting for study (amidated Lipid II substrates are the preferred substrate of the *S. pneumoniae* PBPs (Zapun *et al.,* 2013; and Chapter 4)). However, the overall aim was to produce all 8 variants, in order to provide a full range of substrates for studies now and in future work. Following confirmation of synthesis by negative ion mass spectrometry, the product was quantified by measuring absorbance at 260 nm (as in Section 3.3). Yields are shown in brackets in Table 3.1 where known.

Branch	UDP-Mur*N*Ac-pentapeptide (Gln)	UDP-Mur*N*Ac-pentapeptide (Glu)
Ala	MS confirmed	N/A
Ser	MS confirmed	N/A
Ala-Ala	MS confirmed (14% yield)	Attempted, no MS data
Ser-Ala	MS confirmed (22% yield)	Attempted, no MS data

Table 3.1. Branched UDP-Mur*N*Ac hexa- and heptapeptides synthesised. Branching amino acids described from C- to N-terminus

Negative ion electrospray time-of-flight (TOF) mass spectrometry was used to confirm attachment of peptide and dipeptide branches (Figure 3.11 (B, D), Figure 3.12 (B, D)). In all cases these were successful, although the observed species with a m/z of 573.6763 in Figure 6.11 (D) is consistent with the $[M-2H]^{2-}$ of UDP-Mur*N*Ac-pentapeptide (Glu) (expected 573.6688). This suggests that in addition of the L-Ser branching amino acid, isoglutamine has become deamidated and the addition of the branch failed. This was not the case in any other reaction products analysed by mass spectrometry (discussed Section 3.7.2.1). UDP-Mur*N*Ac-hexapeptide (Gln, Ser) was not used for conversion to Lipid II intermediates.

Positive ion fragmentation was attempted in order to confirm that branching had occurred on the ε-amino of the third position lysine (carried out by Dr. Adrian Lloyd). UDP-Mur*N*Ac-hexapeptide (Gln, Ala), UDP-Mur*N*Ac-hexapeptide (Gln, Ser), UDP-Mur*N*Ac-heptapeptide (Gln, AlaAla) and UDP-Mur*N*Ac-heptapeptide (Gln, SerAla) were subjected to positive ion electrospray time-of-flight mass

spectrometry prior to fragmentation. The spectra of both hexapeptides showed the correct mass for the singly charged cations and were subsequently subjected to collision induced fragmentation (Appendix 5). The singly charged cation consistent with the mass of UDP-Mur*N*Ac-pentapeptide (Glu) ([M+H$^+$] expected 1150.36 observed 1150.36) was also detected in the UDP-Mur*N*Ac-hexapeptide (Gln, Ser) mass spectrum (Figure A5.2(A)) as expected following detection of the doubly charged anion in Figure 3.11(D). However, specific selection of the singly charged cation with a m/z consistent with that of UDP-Mur*N*Ac-hexapeptide (Gln, Ser) ensured that the deamidated product was not fragmented. Species specific to both hexapeptide structures were observed, conclusively showing that the Ser and Ala branching amino acids were attached correctly (Appendix 5). Despite observation of the correct species for UDP-Mur*N*Ac-heptapeptide (Gln, AlaAla) and UDP-Mur*N*Ac-heptapeptide (Gln, SerAla) by negative ion mass spectrometry (Figure 3.12 (B) and (D)), the corresponding singly, doubly or triply charged cations were not observed by analysis in positive mode. Therefore positive ion fragmentation could not be performed (Discussed further in Section 3.7.2.1)

As the single amino acid branches were properly attached, and the correct mass was observed by negative ion TOF, the decision was made to take the prioritised heptapeptides forward for preparation of Lipid II.

3.6 Preparation of Lipid II

UDP-Mur*N*Ac-pentapeptides (and derivatives) can be converted into lipid linked intermediates enzymatically (Section 3.1.3 and Figure 3.2). This section covers the preparation of Lipid II derivatives; amidated, fluorescently labelled and branched (Figure 3.1), required for the study of Gram-positive PBPs throughout the rest of this thesis.

3.6.1 Lipid II synthesis

MraY and MurG are responsible for the conversion of UDP-Mur*N*Ac-pentapeptide into Lipid II (Bouhss *et al.,* 2004; Ha *et al.,* 1999; Lloyd *et al.,* 2004) (Section 1.6.2).

106

These are not trivial to express and purify recombinantly, particularly MraY due to its ten transmembrane spanning helices (Lloyd *et al.,* 2004). Therefore, Lipid II can be prepared from UDP-Mur*N*Ac-peptide precursors *in vitro* with *Micrococcus flavus* membranes supplemented with undecaprenyl phosphate and UDP-Glc*N*Ac (Breukink *et al*., 2003). *M. flavus* membranes are used because they are rich in MraY and MurG. The routine synthesis of radiolabelled, fluorescently labelled and other Lipid II variants within our lab shows this system to be robust and able to accept a range of non-natural substrates. Lipid II variants in the forthcoming section were prepared with *M. flavus* membranes as described in Section 2.6.5, with any deviations from the protocol detailed.

3.6.1.1 Lipid II purification

Following synthesis, Lipid II, along with undecaprenyl phosphate, detergents and phospholipids were separated from proteins by solvent extraction. Lipid II was subsequently purified by anion exchange chromatography on DEAE-sephacel resin, pre-equilibrated with 1M ammonium acetate followed by chloroform/methanol/water (2:3:1) (solvent A). Lipid II was loaded in solvent A before a stepwise elution with increasing proportions of solvent B (chloroform/methanol/1 M ammonium bicarbonate (2:3:1)) was performed. This elution was modified for Lipid II variants with differing affinity for the resin. In particular, amidated versions of Lipid II have lower affinity for the DEAE Sephacel column and therefore required increased low buffer B concentration washes in order to elute undecaprenyl phosphate before the Lipid II and avoid overlap of the two components. This purification method is described in more detail in Section 2.6.5.2. Fractions from anion exchange were analysed by Silica thin layer chromatography (TLC) with the buffer chloroform/methanol/water/0.88 ammonia (88:48:10:1) (Section 2.6.5.3).

3.6.2 Preparation of amidated and fluorescently labelled Lipid II

Lipid II (Glu), Lipid II (Gln), Lipid II (Glu, Dans) and Lipid II (Gln, Dans) were prepared from UDP-Mur*N*Ac-pentapeptide derivatives by the method described in Section 2.6.5 by Julie Todd or Anita Catherwood (BacWAN, UK; Clarke *et al.,*

2009; Lloyd *et al.,* 2008). Purification of both Lipid II (Gln) and Lipid II (Gln, Dans) required additional washes with 100 mM ammonium bicarbonate (10% solvent B) in order to separate the Lipid II from the remaining undecaprenyl phosphate (Section 2.6.5.2).

Negative ion electrospray time-of-flight mass spectrometry was used to confirm the correct species, with particular attention paid to amidation (1 mass difference relative to non-amidated), and the number of dansyl groups present. The latter is important as the amide of isoglutamine could react with dansyl chloride and result in doubly dansylated Lipid II (although the difference in strength of the nucleophile makes it less likely). Detailed analysis of the mass spectra was consistent with 100% yield of the required species in each case (Appendix 6) and quantification was carried out by an assay of phosphate release (Section 2.6.5.4).

3.6.3 Preparation of Lipid II (Gln, SerAla)

Sufficient yield of UDP-Mur*N*Ac-heptapeptide (Gln, SerAla) was achieved in Section 3.5.3 to enable a small scale Lipid II synthesis to be performed. This was exactly the same method as described in Section 3.6.1 and Section 2.6.5, but with reagents reduced to 25% of a full reaction. This method has previously been shown to be scalable with no significant loss of relative yield (Dr A. Lloyd, Personal Communication).

Products of the synthesis were purified by anion exchange chromatography and analysed by Silica TLC (Sections 2.6.5.2, 2.6.5.3 and 3.6.1.1). As described previously, further 100 mM ammonium bicarbonate (10% solvent B) washes were required when purifying amidated Lipid II variants due the lack of a negative charge on isoglutamine compared to glutamate. Figure 3.13 shows the Silica TLC of the purification of this synthesis.

An initial TLC carried out with the routinely used 400 µL of each 4 mL eluted fraction showed no species behaving in a manner typical of Lipid II (not shown). Therefore the TLC in Figure 3.13 was performed with 3 mL of each 4 mL fraction

dessicated, resuspended in chloroform/methanol/water (2:3:1) (solvent A) and loaded. This suggests a very low yield of the possible Lipid species (c) (identified by behavior in this solvent system based on experience with other Lipid II derivatives). Despite additional 100 mM ammonium bicarbonate washes, overlap between the elution of undecaprenyl phosphate (b) and species (c) was seen. This suggests lower affinity for DEAE sephacel of the product of this synthesis than Lipid II (Gln), which could be due the addition of the branching amino acids. These are unlikely to cause significant difference in charge but the increased bulkiness could reduce its ability to bind to the resin. The smaller purification bed volume used in order to reduce losses may also have contributed to the poor separation.
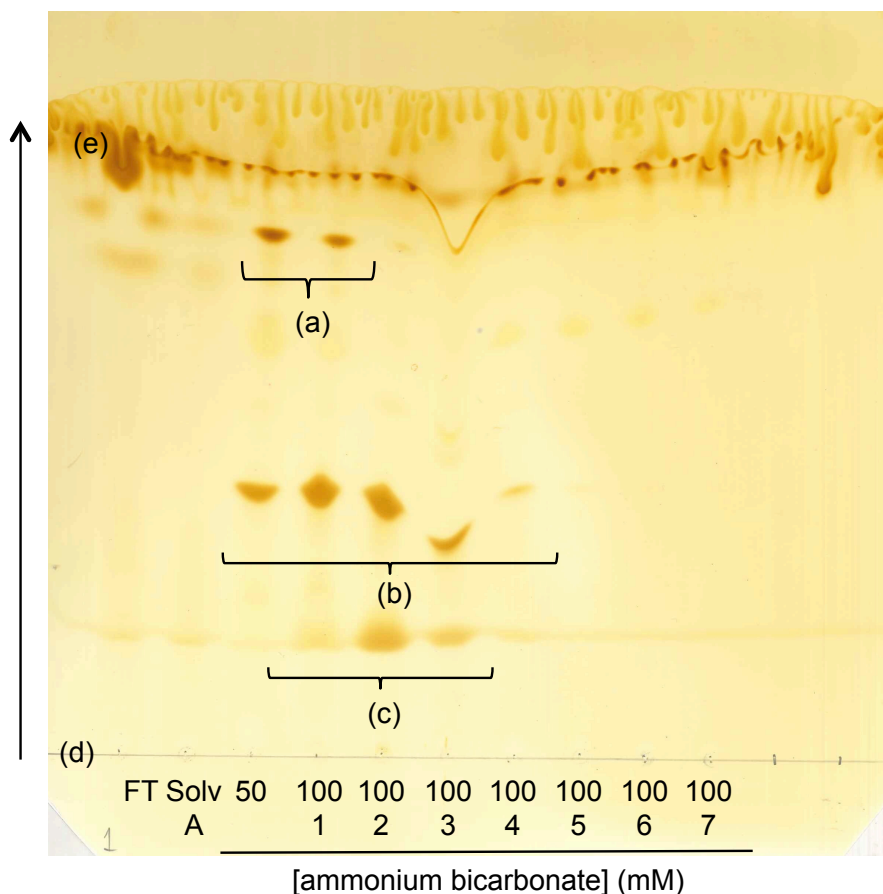
Figure 3.13: Thin-layer chromatography of fractions from initial anion exchange purification of Lipid II (Gln, SerAla). Silica gel TLC plate chromatography with Chloroform/methanol/water/ammonia (88:48:10:1) solvent. TLC plate staining was with iodine vapour. (a) undecaprenyl pyrophosphate, (b) is undecaprenyl phosphate, (c) is suspected Lipid II, (d) is the origin and (e) denotes the solvent front.

3.6.3.1 Re-purification of products of Lipid II (Gln, SerAla) synthesis

In order to separate species (b) and (c) (Figure 3.13), the remainder of the fractions denoted (c) were pooled and re-purified on DEAE sephacel resin with ammonium bicarbonate at pH 9. Typically the pH of ammonium bicarbonate used in solvent B is not monitored but approximately neutral at the concentration used. This increase in pH was intended to increase binding of species (c) to the resin by increasing the number of negative charges due to deprotonation. A further Silica TLC was performed (Figure 3.14)
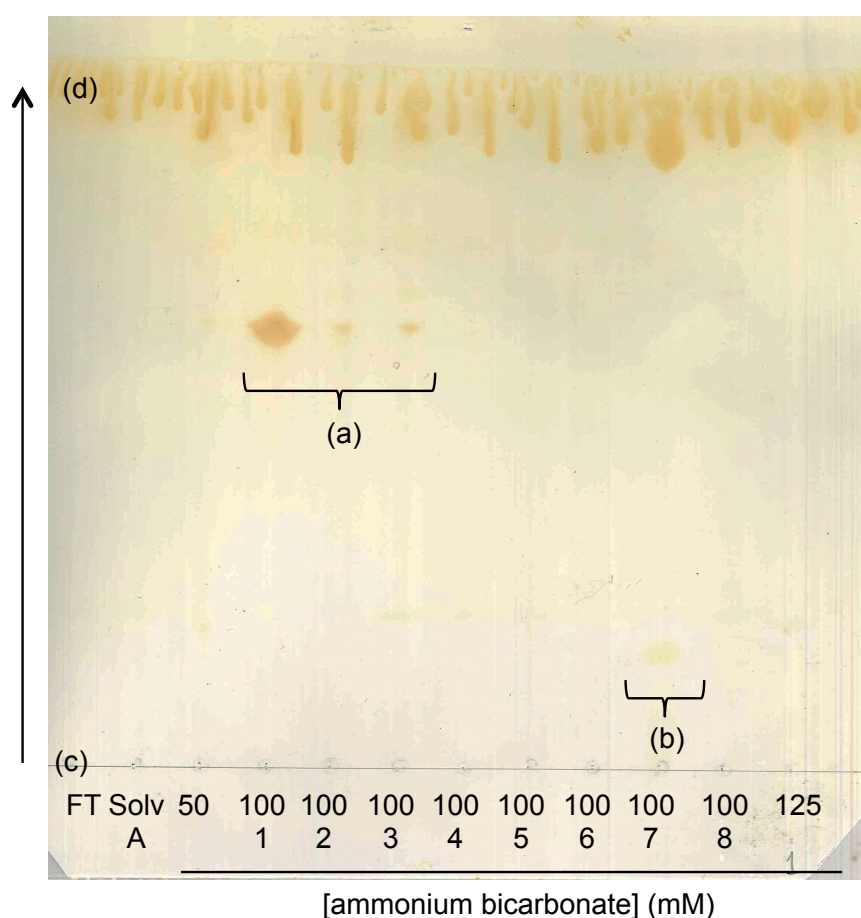
Figure 3.14: Thin-layer chromatography of fractions from anion exchange re-purification at pH 9 of Lipid II (Gln, SerAla). Silica gel TLC plate chromatography with Chloroform/methanol/water/ammonia (88:48:10:1) solvent. TLC plate staining was with iodine vapour. (a) undecaprenyl phosphate, (b) is suspected lipid II, (c) is the origin and (d) denotes the solvent front.

Re-purification separated species (b) and (c) from Figure 3.13 to (a) and (b) on Figure 3.14, however, species (b) in the latter is barely visible. This suggests extremely low yield from re-purification. Fraction (b) (100 mM Ammonium

bicarbonate fraction 7) was freeze-dried three times and submitted to negative ion mass spectrometry. The correct species could not be identified.

It was hypothesised that salt may have remained following freeze-drying, which may prevent the Lipid II from being observed by mass spectrometry. Therefore, samples were re-extracted in organic solvent as used at the beginning of Lipid II purification (Section 2.6.5.2). Any remaining salt would separate into the aqueous phase, and Lipid II into the organic phase. Despite this, the correct species were still not observed.

3.6.3.2 Acid hydrolysis of suspected Lipid II (Gln, SerAla) product

Negative ion time-of-flight mass spectrometry of UDP-Mur*N*Ac-heptapeptide (Gln, SerAla) prior to Lipid II preparation was successful (Figure 3.12 (D)). The behaviour of species (b) (Figure 3.14) suggests that it is a Lipid II derivative, due to its location on the TLC, and further separation from undecaprenyl phosphate at pH 9. Therefore, acid hydrolysis was attempted, as if this hypothesis is correct, the undecaprenyl pyrophosphate would be removed, yielding Mur*N*Ac-heptapeptide (Gln, SerAla), which could be observed by mass spectrometry. Acid hydrolysis was performed as for Lipid II quantification (Section 2.6.5.4), with a parallel non-hydrolysed control. Samples were subsequently desiccated, resuspended in Solvent A (chloroform/methanol/water (2:3:1)) and centrifuged at 13,000 rpm for 1 minute in silicised eppendorfs to remove insoluble material. Both samples were split, with half submitted to negative ion electrospray time-of-flight mass spectrometry and the remainder analysed by TLC (Section 2.6.5.3) (Figure 3.15). Hydrolysis of confirmed Lipid II (Gln, Dans) was used as a positive control.

Species (c) was attributed to Lipid II (Gln, Dans) based on previous TLC and mass spectrometric analysis of the stock the sample came from. Acid hydrolysis of the positive control yielded species (d), which migrates in a manner consistent with undecaprenyl phosphate, the product of acid hydrolysis of Lipid II. No species that migrated in this solvent system was observed in the sample of suspected Lipid II (Gln, SerAla) prior to acid hydrolysis, apart from species (a) which was also found in

the positive control and is likely due to a solvent component. Following acid hydrolysis species (b) was observed suggesting that the suspected Lipid II (Gln, SerAla) species was acid hydrolysed. However, species (b) did not migrate similarly to species (d), the expected product of acid hydrolysis of Lipid II. The results of this acid hydrolysis were inconclusive.
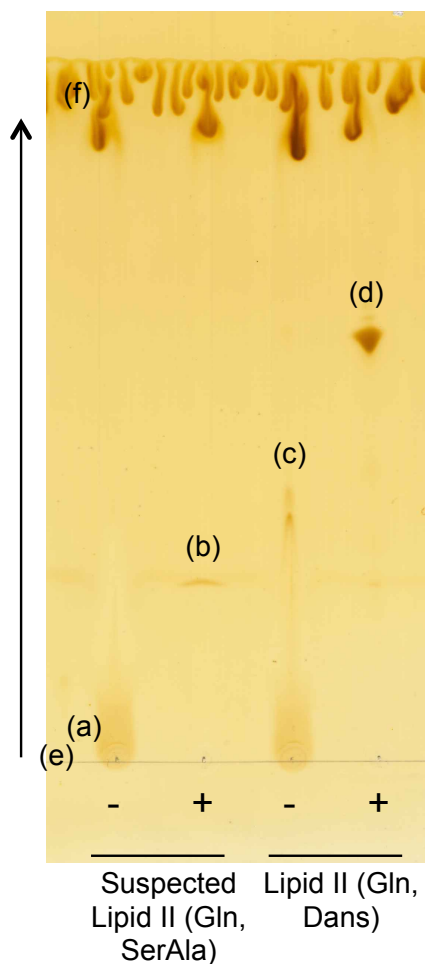
Figure 3.15: Thin-layer chromatography of suspected Lipid II (Gln, SerAla) and Lipid II (Gln, Dans) acid hydrolysis. Silica gel TLC plate chromatography with Chloroform/methanol/water/ammonia (88:48:10:1) solvent. -; non-hydrolysed, +; acid hydrolysed. TLC plate staining was with iodine vapour. (a) suspected solvent contamination b) product of acid hydrolysis of suspected Lipid II (Gln, SerAla), (c) Lipid II (Gln, Dans) , (d) product of acid hydrolysis of (c). (e) is the origin and (f) denotes the solvent front.

Negative ion time-of-flight mass spectrometry was carried out on all samples, and the expected species corresponding to either Mur*N*Ac-pentapeptide derivative or undecaprenyl phosphate were not observed. The lack of success with the positive control suggests that sample preparation may be to blame. Insufficient sample

remained to repeat the analysis and therefore no conclusion could be made regarding the synthesis of Lipid II (Gln, SerAla) following these results (discussed further in Section 3.7.4).

3.6.4 Preparation of Lipid II (Gln, AlaAla)

Sufficient UDP-MurNAc-heptapeptide (Gln, AlaAla) was produced to carry out a Lipid II preparation scaled down to 10% of that described in Section 3.6.1 and 2.6.5. Based on the knowledge acquired in Section 3.6.3.1, the anion exchange purification was carried out at pH 9 initially, in order to avoid the loss of yield associated with re-purification. Despite this, and the subsequent loading of the entire eluted fractions onto a TLC plate, no species suggestive of Lipid II could be observed. This is likely due to very low yield, particularly in a reaction $1/10^{th}$ of the size normally carried out.

3.7 Discussion and further work

The methods used throughout this chapter are discussed in detail in this section, and future work required is detailed.

3.7.1 UDP-MurNAc-pentapeptides

UDP-MurNAc-pentapteptide (Glu) and (Gln) were successfully synthesised enzymatically and purified. The former was made according to a published protocol (Lloyd *et al.,* 2008), and the latter by a modified version. The importance of incorporating only D-isoglutamine at this point (through the activity of MurD) is significant in later comparisons of the substrate specificity of *S. pneumoniae* and *S. aureus* PBPs.

The final yield achieved was significantly affected by poor separation of peaks during gel-filtration chromatography intended to remove ammonium ions from UDP-MurNAc-pentapeptides prior to addition of branching amino acids (Figure 3.4). This

was despite a low loading volume (<1 mL) onto a large (475 mL) column and elution in upflow, all steps taken to improve separation. Due to the significant effect of salt in later coupling stages, any fractions in the region of overlapping peaks were discarded. Re-purification by gel-filtration of these peaks did not achieve sufficient yield to be economical. Therefore to obtain a higher final yield, an alternative method for desalting will be required. Sephadex G-10 resin (GE healthcare) in a 200 mL bed volume, and a Superdex Peptide 10/300 GL column (GE Healthcare) were trialled as alternative size exclusion matrices. Separation of salt from UDP-Mur$N$Ac-pentapeptide was greater with Superdex Peptide than BioGel-P2, however the column size only enables small quantities of material to be loaded at once. Sephadex G-10; a resin specifically optimised for desalting of small biomolecules, showed a slight increase in separation from BioGel-P2 although has a lower loading capacity due to the bed volume, and therefore made negligible difference in resulting yield relative to desalting with BioGel-P2. The multiple runs required did not make this an option in the development of an efficient synthesis method. An alternative strategy of anion exchange could be used, which has been optimised within the group since this work was carried out. Here, the sample is bound to the anion exchange resin Q sepharose (53 mL bed volume) in a small fraction, before being washed in water to remove ammonium ions and subsequently eluted in upflow into a small volume in the buffer required (500 mM NaHCO$_3$ pH 10). This method allows tens of mgs to be loaded and freed from ammonium ions, removing any possibility of contamination with species that could hinder further manipulation of the pentapeptide.

3.7.2 Branched hexa- and heptapeptides

UDP-Mur$N$Ac-heptapeptides (Gln, AlaAla) and (Gln, SerAla) were synthesised for the first time. This is an important step in the aim of producing the *S. pneumoniae* specific Lipid II variants. The main focus of this work was on these as precursors to the PBP substrates, although the UDP-Mur$N$Ac-hexapeptides (Gln, Ala) and (Gln, Ser) are also of interest on conversion to Lipid II species in the study of the substrate specificity of the MurM and MurN amino acid ligases. These are responsible for the *in vivo* addition of dipeptide branches and all work so far has been with non-amidated Lipid II precursors (De Pascale *et al.,* 2008; Lloyd *et al*., 2008). It is to date

unknown whether branching occurs before or after amidation, and therefore these hexapeptides are of use in future work should they be converted into Lipid II species.

3.7.2.1 Limitations of the chemo-enzymatic method for synthesis of branched UDP-Mur*N*Ac-pentapeptide derivatives

The chemo-enzymatic method used for the synthesis of branched UDP-Mur*N*Ac-pentapeptide derivatives was successful for all of the variants attempted and analysed by mass spectrometry, however it was unreliable, with varied and generally low yield, and often no branched product observed. There are many possible explanations for this, some of which are covered in this section.

Fmoc-L-Ala and Fmoc-L-Ser were purchased from Novabiochem (Germany) at 99% purity (assured by rigorous HPLC analysis), ensuring negligible free-amino acid content as well as <0.02% acetic acid, both of which significantly affect coupling reaction yield. Conversely, purity checks were not performed on the Fmoc-L-Ala-L-Ala and Fmoc-L-Ser-L-Ala (Section 3.5.2). Negative ion mass spectrometry identified no other peaks of significance, suggesting (although not categorically proving) the absence of non-protected dipeptides. However, the presence of acetic acid, which will be activated by EDC coupling, cannot be ruled out. Therefore HPLC purification using a C18 reversed-phase column and desalting of the Fmoc protected dipeptides should be carried out in future to optimise the experimental yield.

The optimal reaction volume for branched peptide coupling to UDP-Mur*N*Ac-pentapeptide (Glu) was established previously (De Pascale, 2007) as 2 mL, with scaling up of this volume associated with significant reductions in yield. Therefore the percentage yields quoted in Table 3.1 are misleading in terms of absolute quantities of product made. Approximately 1-1.5 mg of UDP-Mur*N*Ac-pentapeptide (Gln, AlaAla) and (Gln, SerAla) were produced per 2 mL reaction, meaning a large number of syntheses would be required to obtain reasonable quantities for later steps. This is laborious and time consuming, and therefore if this method is to be used in the synthesis of large quantities of branched Lipid II for future enzymatic studies, a

renewed effort is required to scale up this process (discussed further in section 3.7.2.2).

The attachment of branching peptides to the isoglutamine of UDP-Mur*N*Ac-pentapeptide (Gln) could not *a priori* be ruled out. However, the lack of nucleophilic character of the amide nitrogen due to delocalisation of electrons with the adjacent carbonyl group, makes it is unlikely to form a peptide bond. Negative ion mass spectrometry (Figure 3.11 (B,D) and 3.12 (B,D)) would not distinguish between branching on the isoglutamine or lysine, which could only be categorically determined by positive ion fragmentation. However, it could be expected that if the isoglutamine amide were reactive then so would the L-lysine ε-amino group and consequently some double branching would occur, which would be separated in the anion exchange purification (note the clear separation between branched and non-branched in Figure 3.12 (C)). Additionally, the positive ion fragmentation of UDP-Mur*N*Ac-hexapeptide (Gln, Ser) and (Gln, Ala) showed the branching to have occurred on the lysine side chain, which is suggestive of the same situation with the L-Ser-L-Ala and L-Ala-L-Ala branched UDP-Mur*N*Ac-heptapeptides (Gln). These arguments make a compelling case suggesting that the isoglutamine residue of the stem peptide did not undergo peptide coupling to L-Ala, L-Ser or the dipeptides.

It was noted that following the synthesis of UDP-Mur*N*Ac-hexapeptide (Gln, Ser), that some UDP-Mur*N*Ac-pentapeptide (Glu) was observed by both negative and positive ion mass-spectrometry (Section 3.5.3). The pentapeptide used for the coupling reaction was confirmed to be fully amidated before use and therefore this deamidation occurred either during synthesis or in the mass spectrometer. De Pascale *et al.,* (2008) showed that UDP-Mur*N*Ac-hexapeptide (Glu, Ser) was separated from UDP-Mur*N*Ac-pentapeptide (Glu) by anion exchange performed in the same way as it was here. However, amidated pentapeptides elute earlier on a salt gradient as they are less negatively charged than the non-amidated variants. Therefore it is possible that the elution of UDP-Mur*N*Ac-pentapeptide (Glu) and UDP-Mur*N*Ac-hexapeptide (Gln, Ser) overlapped in Figure 3.11 (C) if deamidation had occurred prior to purification. The reason for deamidation in only this case is unknown but shows a potential significant limitation of this method. This issue also highlights the requirement for a higher resolution purification method such as HPLC.

The reason for the failure of positive ion mass spectrometry with UDP-Mur*N*Ac-heptapeptides (Gln, SerAla) and (Gln, AlaAla) is unknown. It is unlikely that the difference in one amino acid between the single and double branch is responsible, but is a possibility. An alternative explanation is a by-product of the synthesis of Fmoc protected dipeptides brought through the coupling and purification, which masks the observed signal (any by-product from the coupling reaction would also be present in the hexapeptides). It was assumed due to the success with fragmentation of the hexapeptides that branching was in the correct position, and therefore these heptapeptides were taken forward to Lipid II synthesis with the intention to repeat the positive ion fragmentation on the final Lipid II product. However, NMR should be considered in the future for detection of the products of coupling reactions as it is both non-destructive and relative proportions of products can be seen.

An important point to note is that chiral conversion during amino acid activation cannot be ruled out with EDC and NHS coupling (Kuefner *et al.,* 1990). This would result in diastereoisomers, and therefore in future work HPLC media such as immobilised vancomycin or teicoplanin, should be used as they can resolve diastereroisomers.

3.7.2.2 Improving the UDP-Mur*N*Ac-hexa- and hepta- peptide yield of the chemo-enzymatic method

The majority of identified limitations of the chemo-enzymatic method could be improved or overcome with an increase in yield of the coupling step. Several suggestions for this were made throughout Section 3.7.2.1 and further proposals are made in this section.

The desalting of UDP-Mur*N*Ac-pentapeptides (Glu) and (Gln) was associated with a significant reduction in final yield due to poor separation from the salt peak. Fractions were selected to ensure no salt was taken forward to the coupling step, however, an improved desalting method as discussed in section 3.7.1 would be more thorough. Additionally, Nessler's reagent (Dipotassium tetraiodomercurate(II) in dilute sodium hydroxide) (Vanselow, 1940) can be used to qualitatively detect the

presence of ammonium compounds. This would form a useful test to ensure complete desalting before EDC coupling, and thus limit the effect on yield.

It was proposed that purification of the amine-reactive NHS ester prior to coupling could improve the yield, as non-activated peptides and other reagents are removed before UDP-Mur*N*Ac-pentapeptide is added. However, Dr Aleš Žula (University of Ljubljana, Slovenia) isolated the activated esters of Fmoc-L-Ala-L-Ser and Fmoc-L-Ala-L-Ala and subsequently reacted them with UDP-Mur*N*Ac-pentapeptide (Glu) in dimethylformamide (DMF). Products were purified by reverse-phase chromatography (mobile phase 99%/1% H_2O/CH_3CN) and the Fmoc group was removed with morpholine before a second reverse-phase step. On arrival at the University of Warwick, further purification by gel filtration chromatography (Superdex Peptide 10/300 (GE Healthcare)) was performed and peaks analysed by negative ion mass spectrometry. Only starting UDP-Mur*N*Ac-pentapeptide (Glu) was observed, showing that coupling was unsuccessful. An improvement of conditions may be required in order for this method to be pursued further,

3.7.3 Confirmation that amidation and dansylation of Lipid II species was complete

Lipid II (Glu), Lipid II (Gln), Lipid II (Glu, Dans) and Lipid II (Gln, Dans) were synthesised by Julie Tod or Anita Catherwood (BacWAN, UK: Clarke *et al.,* 2009; Lloyd *et al.,* 2008) by methods described in the text, purified, quantified and their identity confirmed by negative ion mass spectrometry. Its inclusion was important in this chapter, as many conclusions throughout the remainder of this thesis rely on the assurance that the Lipid II substrate was 100% amidated, 100% dansylated (or both). This was ensured by modification of the UDP-Mur*N*Ac-pentapeptide precursor synthetic scheme prior to purification, confirmation by mass spectrometry and a sensitive purity check. Modification at this stage results in only the required soluble intermediate being put into a Lipid II synthesis, the purification of which would not distinguish different final products so clearly. The identity was again confirmed at this point by negative ion mass spectrometry and this evidence supports many of the conclusions in the following chapters.

3.7.4 Preparation of *S. pneumoniae* specific Lipid II variants

Unsuccessful attempts were made to convert UDP-Mur*N*Ac-heptapeptide (Gln, AlaAla) and (Gln, SerAla) into Lipid II. The availability of *M. flavus* membranes and undecaprenyl phosphate led to the prioritisation of these particular variants, as the native, and therefore more interesting substrates for the PBPs. The failure of the Lipid II (Gln, AlaAla) synthesis (Section 3.6.4) is most likely due to the very small-scale reaction carried out in addition to the poor conversion by *M. flavus* membranes (discussed later in this section). The results for Lipid II (Gln, SerAla) synthesis (Section 3.6.3), and reasons for the lack of success, are discussed in more detail in this section.

Unlike after the synthesis of UDP-Mur*N*Ac-pentapeptide (section 3.3), desalting and purity check by anion exchange were not carried out on the UDP-Mur*N*Ac-heptapeptides. This was due to very low yield, which would be significantly reduced even further by these additional steps. In future experiments, when sufficient yield is achieved, these purification steps should be performed prior to Lipid II synthesis, to ensure no contaminants are present which may affect the subsequent reaction.

It is possible that amidated and branched *S. pneumoniae* specific UDP-Mur*N*Ac-heptapeptides are not transferred to undecaprenyl phosphate efficiently by *M. flavus* MraY. MurG is unlikely to be the limiting factor as it has been shown to use a wide range of substrates including those with large fluorescent groups (Liu *et al*., 2003; van Dam *et al.,* 2007; Dr A. Lloyd, Personal Communication). Additionally, an accumulation of Lipid I would be expected if this was the case, and this was not observed. Fluorescence and radioactivity based assay systems exist for MraY activity (Brandish *et al*.,1996; Solapure *et al.,* 2005), however the former relies on a dansyl group on the third position lysine, and is therefore not suitable for the testing of branched substrates. Therefore, the radiolabel exchange assay could be used to compare the transfer of UDP-Mur*N*Ac-heptapeptides (Gln, SerAla) by *M. flavus* membranes and *E. coli* membranes with overexpression of recombinant *S. pneumoniae* MraY, a method previously successful for *E. coli, P. aeruginosa, S. aureus, M. flavus* and *B. subtilis* MraY using the fluorescence assay (Rodolis *et al.,* 2014).

119

An important observation to note is the result of repurification at pH 9. The resulting spot (b) (Figure 3.14) is not convincing but the separation of the original spots (b) and (c) (Figure 3.13) suggests that purification at pH 9 is a useful strategy for further experiments. The alteration was successful in achieving better separation between undecaprenyl phosphate and Lipid II (Gln) (Rebecca Bolton, Personal Communication) and therefore is an important modification to the method for subsequent experiments.

TLC analysis of the products of UDP-Mur*N*Ac-heptapeptide (Gln, SerAla) incubation with *M. flavus* membranes is suggestive of a successful synthesis. The position of spot (c) in Figure 3.13 and (b) in 3.14 is consistent with the behaviour of other Lipid II variants. However, negative ion mass spectrometry data could not be obtained to confirm this. Due to the high sensitivity of mass spectrometry it is unlikely that the low yield observed was responsible. Attempts to remove any contaminating salt, and the undecaprenyl phosphate did not alleviate the issue. Lipid II (Gln, SerAla) would be expected to fly in negative ion mass spectrometry, as data is routinely obtained for Lipid II (Gln, Dans), predominantly the same structure but with a higher molecular weight due to the dansyl group.

Coupled with this, the behaviour of the suspected Lipid II (Gln, SerAla) upon acid hydrolysis was unusual. TLC analysis suggests that undecaprenyl phosphate was yielded by hydrolysis of Lipid II (Gln, Dans) and an unknown product from Lipid II (Gln, SerAla). The expected products were not observed by negative ion mass spectrometry for either Lipid II (Gln, SerAla) or the Lipid II (Gln, Dans) control. This may have been due to plasticisers in the sample due to use of eppendorfs (albeit silicised) for the removal of insoluble material. This experiment could not be repeated in the time available, as no material remained from the synthesis.

3.7.5 Future direction

Efforts to synthesis the *S. pneumoniae* specific branched Lipid II substrates (Lipid II (Gln, AlaAla) and (Gln, SerAla)) have been unsuccessful to date. This is predominantly due to poor absolute yield of the EDC coupling step to produce UDP-

Mur*N*Ac heptapeptides. Therefore the main priority for further work in the first instance is the optimisation of this protocol to enable scaling up. This is crucial in establishing a viable method to produce sufficient quantities of this valuable substrate. Previous attempts were unsuccessful (Clarke, 2008; De Pascale, 2007), however, alterations in the ratios of reaction components may be essential in achieving this, as chemical syntheses of this type are not always directly scalable (Dr Vita Godec, Personal Communication). Additionally, ensuring adequate desalting of both UDP-Mur*N*Ac-pentapeptide (Gln) and purification of Fmoc protected dipeptides will limit side reactions and thus improve the yield.

Once sufficient quantities of UDP-Mur*N*Ac-heptapeptide have been synthesised, detailed optimisation of Lipid II conversion can be carried out. As mentioned previously (Section 3.7.4), confirmation that MraY is able to transfer the amidated and branched substrates to the lipid carrier should be carried out. Several strategies could be employed to overcome a low turnover by MraY if required. For example, addition of a larger excess of membranes or a longer incubation period.

If the yield by this method cannot be increased to adequate levels, the alternative enzymatic method could be employed (Section 3.5.1). This has been successful for the enzymatic addition of the *S. aureus* pentaglycine interpeptide bridge to non-amidated (Schneider *et al.,* 2004) and amidated Lipid II (Rebecca Bolton, Personal Communication) using the FemXAB peptidyltransferases. The presence of either L-Ser or L-Ala on the first position of the *S. pneumoniae* branch makes this more complicated than for the pentaglycine stem. The addition of a L-Ala-L-Ala branch could in theory be performed in one pot with Lipid II, alanyl-tRNA^{Ala}, L-alanine and both MurM and MurN followed by purification. However, in order to achieve an L-Ser-L-Ala branch, seryl-tRNA^{Ser}, L-Serine and MurM from the Pn16 penicillin sensitive strain (MurM$_{PN16}$), shown to preferentially alanylates the Lipid II (Lloyd *et al.,* 2008) would need to be incubated with Lipid II first. Purification would be required before the addition of alanyl-tRNA^{Ala}, L-alanine and MurN. This method requires large quantities of Lipid II for optimisation and HPLC purification may be essential to ensure that the final product has the branching required. However, if insufficient yield is achieved by the chemical method then this may be a suitable strategy. Alternatively, the L-Ser and L-Ala single amino acid branches could be

added chemically to UDP-Mur*N*Ac-pentapeptide as was previously performed by De Pascale *et al.,* (2008) for the non-amidated version and in this chapter for the amidated. The product of this could be incubated with *M. flavus* membranes followed by MurN, alanyl-tRNA^{Ala} and L-alanine to add the second amino acid to the branch.

Of particular note is that for the study of transpeptidase activity of the *S. pneumoniae* PBPs, Mur*N*Ac-pentapeptide should be able to act as an acceptor (see chapter 6 for more details). This is made by acid or enzymatic hydrolysis of UDP-Mur*N*Ac-pentapeptide (Section 6.4.2). Therefore, the role of substrate branching in transpeptidation can be studied to a certain extent without the requirement for Lipid II conversion, should this continue to be unsuccessful.

3.8 Conclusion

The dipeptide branched, amidated UDP-Mur*N*Ac-heptapeptides (Gln, AlaAla) and (Gln, SerAla) have been synthesised chemo-enzymatically for the first time. These are important precursors to the Lipid II substrates that will enable detailed enzymatic study of *S. pneumoniae* PBP substrate specificity, and analysis of the role of Lipid II branching in β-lactam resistance. Steps were taken to convert these to Lipid II, which have been unsuccessful to date, but further work informed by the data within this chapter, holds promise for the future availability of these substrates. The synthesis of amidated and fluorescently labelled Lipid II (Dans) was covered briefly, and confirmed to be 100% the required Lipid II variant, crucially important in the experiments throughout Chapters 4, 5 and 6.

Chapter 4. Enzymology of transglycosylation: the effect of Lipid II amidation on the transglycosylation activity of *Streptococcus pneumoniae* Class A PBPs

4.1 Introduction

Streptococcus pneumoniae is responsible for a range of diseases from bronchitis to endocarditis and meningitis (Section 1.8 for more detail). The spread of multi-drug resistant strains is making treatment increasingly difficult, highlighting the requirement for new lines of intervention. Instrumental in this is a greater understanding of the biochemistry of the pneumococcal cell wall.

4.1.1 *S. pneumoniae* penicillin-binding proteins

Peptidoglycan chain polymerisation in *Streptococcus pneumoniae* is catalysed by the high molecular weight (HMW) Class A bifunctional penicillin-binding proteins (PBPs); PBP1a, PBP2a and PBP1b (Hoskins *et al.,* 1999); which catalyse both polymerisation of the glycan chain (transglycosylation) and cross-linking between them (transpeptidation). PBPs generally, and specifically to *S. pneumoniae* are reviewed comprehensively in Section 1.7 and 1.8.2 respectively.

Efforts to study the enzymatic activity of the PBPs have focused predominantly on their transpeptidase function, and in particular the development of resistance to the β-lactam family of antibiotics (See Section 1.8 and Chapter 6 for more detail). Relatively little focus has been placed on the transglycosylase function, which is necessary to provide the polymerised substrate for the cross-linking reaction, although the hydrophobic transmembrane region of PBP2a was previously shown to be important (Helassa *et al.,* 2012). In order to understand the mechanisms of peptidoglycan synthesis more fully and aid future development of novel antibiotics,

the study of transglycosylation is essential. The transglycosylase domain, its enzymatic activity and proposed catalytic mechanism are covered in Section 1.7.3.

4.1.2 Assays for transglycosylation

Transglycosylase assay development has been slow due to the requirement for the complex Lipid II substrate, which has previously been difficult to synthesise. Additionally, PBPs are mainly integral membrane proteins, interacting with a lipid-linked substrate, making them particularly difficult to study *in vitro*. However, due to advances in membrane protein isolation in recent years and progress at the University of Warwick and elsewhere in the production of the complex substrate intermediates (Breukink *et al.,* 2003; Lloyd *et al.,* 2008; Schwartz *et al.*, 2001; VanNieuwenhze *et al.,* 2002), assays with these substrates are now possible.

The main assay methods for transglycosylase activity have recently been comprehensively reviewed (Galley *et al.,* 2014) (attached in Appendix 8). Two complementary assay systems were selected for this project.

The SDS-PAGE assay system is unique in allowing the processivity of a transglycosylase to be studied by providing qualitative data on chain length although calibration of gels is problematic given the lack of suitable standards. Glycan products of *in vitro* reactions have a net negative charge and can be separated by Tris-Tricine SDS-PAGE (Barrett *et al.,* 2007; Lesse *et al.,* 1990; Schägger *et al.,* 1987). Initial studies with this technique used radiolabelled substrates (Barrett *et al.,* 2007), and more recently, Lipid II substrate with a fluorescent dansyl group (Lipid II (Dans)) linked via a sulphonamide linkage to the ε-amino group of the stem peptide lysine side chain (Section 3.1.2)(Helassa *et al.,* 2012). This substrate serves two purposes in the study of transglycosylase activity. Firstly, a GeneSnap Gel Doc transilluminator with a blue light convertor and short-pass filter enables the dansyl fluorescence at 521 nm to be detected to visualise the products, more rapidly than imaging by autoradiography required with radiolabelled substrate. Secondly, due to the location of the fluorescence group, the use of 100% dansylated Lipid II prevents transpeptidation as the third position lysine on the donor stem is blocked. Previous

studies have suggested that transglycosylase kinetic parameters are only marginally affected by the addition of fluorescence side groups (Schwartz *et al.,* 2002; Zhang *et al.,* 2007).

Unlike the SDS-PAGE assay, an assay for transglycosylase activity coupled to *N*-acetylmuramidase digestion with dansylated Lipid II provides complementary quantitative initial rate data (Schwartz *et al.,* 2002), and optimisation for a 96-well plate format (Offant *et al.,* 2010) enables the rapid screening of conditions. Lipid II is presented in detergent micelles, and upon polymerisation by PBPs and subsequent digestion by *N*-acetylmuramidase, aqueous soluble monomers are produced, accompanied by a reduction in the quantum yield of fluorescence of the dansyl fluorophore due to the change in environment from a lipid bilayer to an aqueous solution. This fluorescence decrease is used to follow transglycosylation. To date, full incorporation of Lipid II into glycan chains over the assay time-course has been assumed, and kinetic values established from the initial rate of fluorescence decrease (Helassa *et al.,* 2012; Offant *et al.,* 2010; Schwartz *et al.,* 2002). This is discussed further in Section 4.6.2.2

4.1.3 Amidation of Lipid II in *S. pneumoniae*

S. pneumoniae peptidoglycan stem peptides are chemically modified by the addition of a L-Ala-L-Ala or L-Ser-L-Ala dipeptide branch on the ε-amino group of the stem peptide lysine (Filipe and Tomasz, 2000; Fiser *et al.,* 2003) and by amidation of glutamate at position 2 to isoglutamine by the amidase MurT/GatD (Zapun *et al.,* 2013) (Sections 1.5.2.3 and 1.5.2.2 for more details). Dipeptide branching is covered in more detail in Chapters 3 and 6. Amidated peptidoglycan makes up > 90% of the *S. pneumoniae* cell wall; (Bui *et al*., 2012) and is likely to be essential for *S. pneumoniae* PBP2a and optimal for *S. pneumoniae* PBP1a transpeptidase activity (Zapun *et al.,* 2013; Chapter 6). However, the effect of this modification on the crucial preceding transglycosylase activity has not been studied to date.

This chapter focuses on the effect of the amidation of Lipid II on the transglycosylase activity of *S. pneumoniae* bifunctional Class A PBPs; PBP1a and

PBP2a. These two class A PBPs are of particular interest as at least one of them must be active for viable cells. PBPs were recombinantly expressed from the D39 penicillin-susceptible strain, the progenitor of the commonly used avirulent, unencapsulated R6 lab strain (Williams *et al.,* 2007). There are no nucleotide level differences between the *pbp* genes in D39 and R6 (Job *et al.,* 2008).

Understanding the substrate-enzyme interactions involved in transglycosylation is important since it has significant consequences in the formation and metabolism of the peptidoglycan sacculus of this important pathogen and may be crucial in the design of novel antibacterial compounds targeting transglycosylation.

4.2 Experimental Aims

- To express and purify PBP1a and PBP2a from *S. pneumoniae* with and without the transmembrane spanning domain.
- To study the effect of stem peptide amidation on transglycosylation activity of *S. pneumoniae* PBP1a and PBP2a by SDS-PAGE separation of the products and continuous fluorescence assay.
- To examine the role of the transmembrane region in processivity of *S. pneumoniae* PBP1a and PBP2a transglycosylation.

4.3 Expression and purification of *S. pneumoniae* D39 PBP1a and PBP2a

In order to investigate the transglycosylation activity of PBP1a and PBP2a, they were expressed and purified as both the full-length protein and devoid of the transmembrane spanning domain from the penicillin-susceptible D39 strain. The constructs for expression of PBP1a were obtained from Dr K. Abrahams, and for PBP2a from Dr A. Zapun (IBS, Grenoble) (Table 4.1). Expression and purification are described in this section.

Construct	Selection	Source
pET46::*pbp1a*	Ampicillin	Dr K. Abrahams (University of Warwick)
pET46::*pbp1aΔ30*	Ampicillin	Dr K. Abrahams (University of Warwick)
pET30b::*pbp2a*	Kanamycin	Dr A. Zapun (IBS, Grenoble)
pGEX-2T::*pbp2aΔ77*	Ampicillin	Dr A. Zapun (IBS, Grenoble)

Table 4.1: Gene constructs provided for expression and purification of *S. pneumoniae* D39 Class A PBPs

4.3.1 Expression and purification of *S. pneumoniae* D39 PBP1a FL

Full-length PBP1a was expressed and purified as described previously (Abrahams, 2011). Briefly, pET46::*pbp1a* was expressed in BL21 Star (DE3) pRosetta cells and grown under autoinduction at 25°C, solubilised in 1% (w/v) sodium deoxycholate and purified by IMAC (Section 2.4.3.1) in 0.1% (w/v) DDM. DDM is a mild, non-denaturing detergent, often used for membrane protein purification (Privé, 2007), which has been demonstrated to maintain PBP1a in an active state (Abrahams, 2011). IMAC fractions were analysed by SDS-PAGE (Figure 4.1(a)). PBP1a that eluted at 250 mM imidazole was concentrated using a 100 kDa cut-off centrifugal concentrator before further purification by injection onto an analytical Superose 6 10/300 GL gel filtration column pre-equilibrated and eluted in 20 mM Tris pH 7.5, 150 mM NaCl, 0.03% (w/v) DDM in order to separate aggregated and non-aggregated protein (Figure 4.1(b)). Lowering the detergent concentration to slightly above the CMC reduces excessive micelle formation, which could interfere with

future structural and activity studies. Final selected fractions were concentrated in a 100 kDa cut-off centrifugal concentrator before storage in 20 mM Tris pH 7.5, 150 mM NaCl, 0.03% (w/v) DDM, 50% (v/v) glycerol at -20 °C (previously determined to be optimal (Abrahams, 2011).
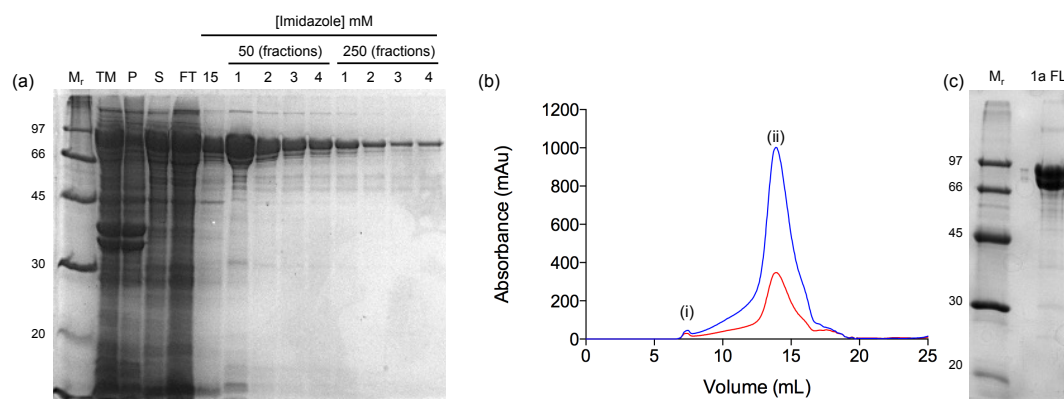
Figure 4.1: Purification of *S. pneumoniae* D39 PBP1a FL by IMAC and size exclusion chromatography. (a) 12% SDS-PAGE Coomassie-stained gel showing the isolation of membranes, solubilisation in 1% (w/v) sodium deoxycholate and subsequent IMAC purification of PBP1a FL. M_r, molecular weight markers (kDa); TM, total membrane fraction; P, ultracentrifugation pellet following sodium deoxycholate solubilisation; S, ultracentrifugation supernatant containing soluble protein; FT, unbound protein following 3 h incubation of supernatant with cobalt-chelated sepharose resin; 15, wash with buffer containing 15 mM imidazole; 50 (fractions) 1-4, elution with buffer containing 50 mM imidazole; 250 (fractions) 1-4, elution with buffer containing 250 mM imidazole. (b) Size exclusion chromatogram using the Superose 6 10/300 GL column. Red: absorbance at 254nm, Blue: absorbance at 280 nm (i) shows the elution of aggregated material in the column void volume and (ii) the elution of PBP1a FL. (c) 12% SDS-PAGE Coomassie-stained gel of the final purity of PBP1a FL. M_r, molecular weight markers (kDa); 1a FL, purity of PBP1a FL following both purification steps.

4.3.2 Expression and purification of *S. pneumoniae* D39 PBP1a-Δ30

PBP1a-Δ30 was expressed and purified from pET46::*pbp1a-Δ30* as described in (Abrahams, 2011), and in an identical manner to PBP1a FL (Section 4.3.1). Despite the protein lacking the transmembrane spanning region, detergent is required for solubilisation due to the presence of a membrane interaction site in the transglycosylase domain of bifunctional PBPs (Di Guilmi *et al.,* 1999; Lovering *et al.,* 2007; Sung *et al.,* 2009). Figure 4.2 shows the purification and final purity of PBP1a-Δ30. The yield of purified protein was substantially lower than that for the full-length PBP1a, due to a significantly lower expression level, as observed previously (Abrahams, 2011)
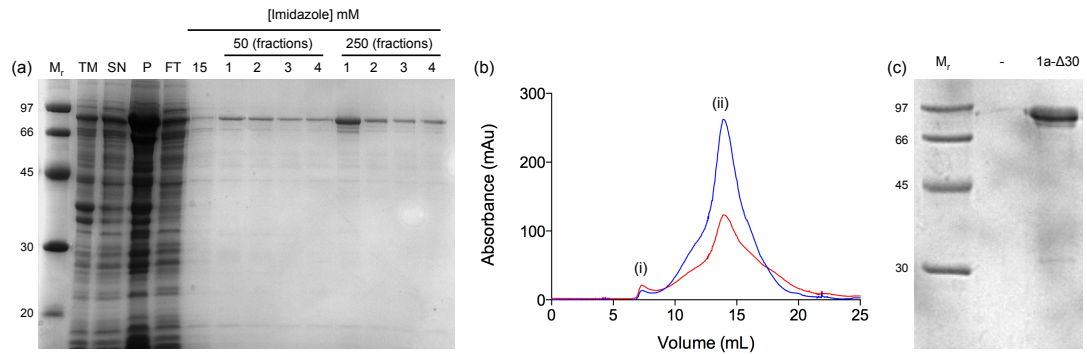
Figure 4.2: Purification of *S. pneumoniae* D39 PBP1a-Δ30 by IMAC and size exclusion chromatography. (a) 12% SDS-PAGE Coomassie-stained gel showing the isolation of membranes, solubilisation in 1% (w/v) sodium deoxycholate and subsequent IMAC purification of PBP1a-Δ30. M_r, molecular weight markers (kDa); TM, total membrane fraction; SN, ultracentrifugation supernatant containing soluble protein; P, ultracentrifugation pellet following sodium deoxycholate solubilisation; FT, unbound protein following 3 h incubation of supernatant with cobalt-chelated sepharose resin; 15, wash with buffer containing 15 mM imidazole; 50 (fractions) 1-4, elution with buffer containing 50 mM imidazole; 250 (fractions) 1-4, elution with buffer containing 250 mM imidazole. (b) Size exclusion chromatogram using the Superose 6 10/300 GL column. Red: absorbance at 254nm, Blue: absorbance at 280 nm (i) Elution of aggregated material in the column void volume and (ii) Elution of PBP1a-Δ30 (c) 12% SDS-PAGE Coomassie-stained gel of the final purity of PBP1a-Δ30. M_r, molecular weight markers (kDa); -, empty lane; 1a-Δ30, purity of PBP1a-Δ30 following both purification steps.

4.3.3 Expression and purification of *S. pneumoniae* PBP2a FL

Expression and purification of pET30b::*pbp2a* was as described in Helassa *et al*., (2012) with the addition of a 50,000 × g centrifuge spin prior to the first affinity purification to remove insoluble material, and is shown in Figure 4.3. PBP2a is purified without an affinity tag by successive anion and cation exchange steps by exploitation of the differing predicted isoelectric points (pI) of the cytoplasmic and extracellular regions of the protein (Helassa *et al.,* 2012). A high level of purity was achieved by this method (Figure 4.3 (c)).
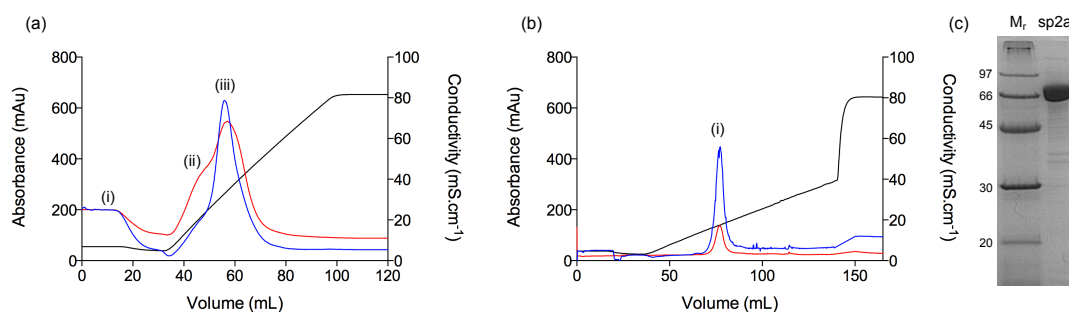
Figure 4.3: Purification of *S. pneumoniae* D39 PBP2a FL by successive cation and anion exchange chromatography. (a) Cation exchange chromatogram of the elution from a 5 mL HP SP Sepharose column. Red: absorbance at 254nm, Blue: absorbance at 280 nm (i) Peak of unbound material eluted in no salt wash following column loading (ii) Shoulder of main peak consisting of PBP2a FL and a large number of other proteins (iii) Main peak elution of PBP2a FL taken forward to anion exchange chromatography (b) Anion exchange chromatogram showing the elution from a 6 mL ResourceQ column. Red: absorbance at 254nm, Blue: absorbance at 280 nm (i) The single peak of pure PBP2a FL eluted (c) 12% SDS-PAGE Coomassie-stained gel of the final purity of PBP2a FL. M_r, molecular weight markers (kDa); sp2a, PBP2a FL following successive cation and anion exchange steps.

4.3.4 Expression and purification of *S. pneumoniae* PBP2a-Δ77

Expression and purification of PBP2a-Δ77 was as described in Di Guilmi *et al.,* (1999) with the addition of an anion exchange step on a 6 mL ResourceQ column and full methodological details are in Section 2.4.4.1 . Briefly, the PBP2a-Δ77 GST fusion protein was overexpressed and purified on a glutathione Sepharose column followed by cleavage of the GST tag by thrombin digestion. Eluted protein was analysed by SDS-PAGE (Figure 4.4 (a)). Remaining bound GST was eluted with 10 mM reduced L-glutathione, and the presence of three bands in this lane indicates that thrombin cleavage proceeded almost to completion, with little GSTPBP2a-Δ77 eluted and a large band of GST. All fractions containing PBP2a-Δ77 were buffer exchanged and purified by anion exchange chromatography (ResourceQ) (Figure 4.4 (b)).

A good level of purity was achieved for PBP2a-Δ77 (Figure 4.4 (c)), with a single lower molecular weight contaminant not removed by the two purification steps. This is likely an interacting protein, or proteolytically cleaved PBP2a and is too close in molecular weight to remove by the addition of an additional size exclusion chromatography step.
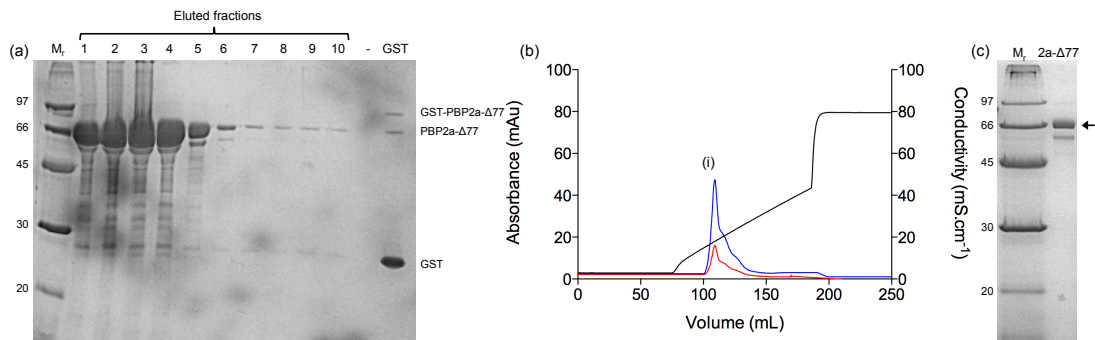
Figure 4.4: Purification of *S. pneumoniae* D39 PBP2a-Δ77 by Glutathione Sepharose and anion exchange chromatography (a) 12% SDS-PAGE Coomassie-stained gel of the elution of PBP2a-Δ77 following thrombin cleavage on a 5 mL glutathione sepharose column. M_r, molecular weight markers (kDa); Eluted fractions 1-10, 1 mL fractions eluted from column; -, empty lane; GST, Elution of cleaved GST from column with reduced L-glutathione. Location of GST-PBP2a-Δ77, PBP2a-Δ77 and GST indicated on the gel. .(b) Anion exchange chromatogram showing the elution from a 6 mL ResourceQ column. Red: absorbance at 254nm, Blue: absorbance at 280 nm (i) The single peak of pure PBP2a FL eluted (shoulder excluded from selected fractions) (c) 12% SDS-PAGE Coomassie-stained gel of the final purity of PBP2a-Δ77. M_r, molecular weight markers (kDa); 2a-Δ77, purity of PBP2a-Δ77 following both purification steps. Small arrow indicated location of PBP2a-Δ77 on the gel.

4.3.5 Final purity of *S. pneumoniae* D39 PBP1a and PBP2a

S. pneumoniae PBP1a FL, PBP1a-Δ30, PBP2a FL and PBP2a-Δ77 were expressed and purified by previously determined methods with modifications where required. The final purity of each of the variants is shown in Figure 4.5.
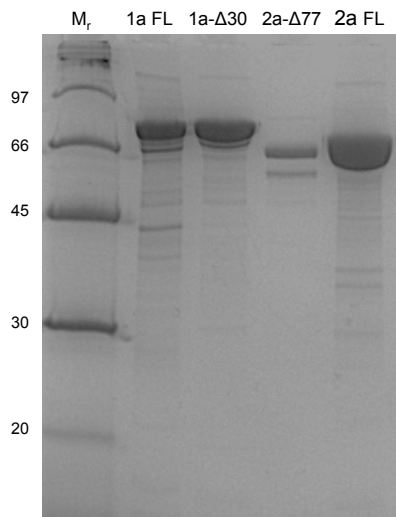
Figure 4.5: 12% Coomassie–stained gel of the final purity of the *S. pneumoniae* Class A PBPs to be studied. M_r, Molecular weight markers (kDa). Lanes are labelled with the PBP

131

4.4 Analysis of transglycosylase products by SDS-PAGE

Tris-tricine SDS-PAGE can be used to separate the products of glycan chain polymerisation with fluorescently labelled dansylated Lipid II substrate (Sections 4.1.2 and 2.7.2), providing valuable insight into the processivity of the transglycosylase domain of PBPs. This section describes the study of peptidoglycan chain synthesis by *S. pneumoniae* PBP1a and PBP2a, in particular focusing on the specificity for the amidated stem peptide variant of the Lipid II substrate (Section 4.1.3).

4.4.1 Conditions for observation of transglycosylase activity of *S. pneumoniae* PBP1a and PBP2a by SDS-PAGE

In vitro transglycosylase activity is critically affected by buffer conditions including divalent cations, detergent and dimethylsulfoxide (DMSO) concentration (Barrett *et al.,* 2007; Offant *et al.,* 2010; Schwartz *et al*., 2002). Transglycosylation by PBP1a and PBP2a has previously been observed by the SDS-PAGE technique with the non-amidated Lipid II variant, and non-dansylated in the case of PBP1a (Abrahams, 2011; Helassa *et al*., 2012; Zapun *et al.,* 2013) and thus optimised conditions amenable to *in vitro* activity are known.

The method used for SDS-PAGE is detailed in Section 2.7.2, and specific buffer requirements, temperatures and incubation times are indicated in the following sections. Dansylated Lipid II, both amidated and non-amidated (Lipid II (Glu, Dans) and Lipid II (Gln, Dans)) were synthesised by the BaCWAN facility (University of Warwick, Coventry, UK), and confirmed by mass spectrometry to be 100% fluorescently labelled (and 100% amidated where required)(Section 3.6.2 and Appendix 6). Lipid II substrate was stored in 3:2:1 chloroform:methanol:water and required evaporation under nitrogen flow before resuspension by vigorous vortexing in the required buffer. Consequently, pipetting of small volumes and evaporation of the organic solvent affected the accuracy with which solutions of known concentration could be prepared. Therefore larger stocks of Lipid II at 500 μM in 0.1% (v/v) TX-100 were made routinely and diluted to the concentration of Lipid II

and detergent required for assays. Where higher TX-100 concentrations were required, or alternative detergents, a master stock with a suitable detergent concentration was made. Lipid II solutions in TX-100 are stable on storage at -80°C for at least 6 months (Dr Adrian Lloyd, Personal Communication).

It should be noted for this assay format that a true replicate is represented by the use of different enzyme preparations and separate reactions run on a different gel. Exact replicates were not always performed but comparisons made with comparable reactions performed for different experiments where possible. Where exact replicates were performed the number of repeats are indicated in the figure legend.

4.4.2 Comparison of transglycosylation products of *S. pneumoniae* PBP1a and PBP2a with Lipid II (Glu, Dans) and Lipid II (Gln, Dans)

As described in Section 4.1.3, the amidation of Lipid II is necessary for PBP2a and optimal for PBP1a in order to observe high molecular weight material attributed to cross-linking (Zapun *et al.,* 2013). However, this study did not directly analyse the effect of the stem peptide chemical modification on transglycosylase activity. Therefore single time point reactions were carried out to compare the substrate specificity of PBP1a FL and PBP2a FL. 10 μM Lipid II (Lipid II (Glu, Dans) or Lipid II (Gln, Dans)) in either 50 mM HEPES pH 7.5, 10 mM MgCl$_2$, 150 mM NaCl, 25% (v/v) DMSO, 0.02% (v/v) Triton X-100 (PBP1a) or 50 mM HEPES pH 7.5, 25 mM MgCl$_2$, 200 mM NaCl, 25% (v/v) DMSO, 0.02% (v/v) Triton X-100 (PBP2a) was incubated with 1 μM PBP1a FL, 1 μM PBP2a FL or an equivalent volume of enzyme storage buffer at 30°C overnight. Overnight incubations were used to ensure reactions proceeded to completion. Reaction products were analysed by SDS-PAGE as described in Section 2.7.2 (Figure 4.6). Reaction buffers described here are used for the rest of this chapter unless specified.
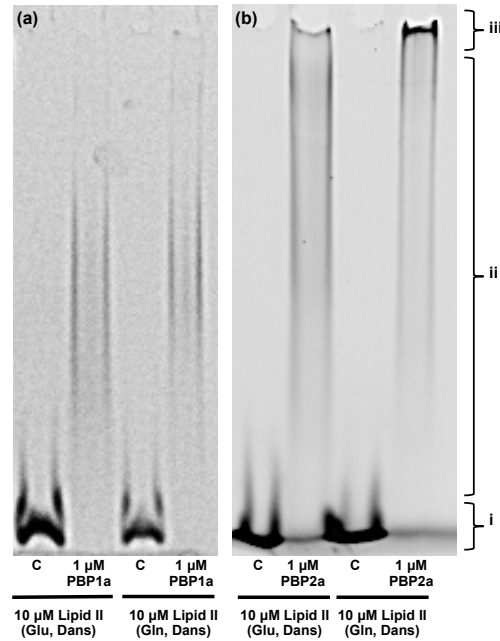
Figure 4.6: Comparison of the effect of Lipid II amidation on the transglycosylase products of *S. pneumoniae* PBP1a (a) and PBP2a (b). Products of transglycosylation separated on a 8.5% T/2.7% C SDS-PAGE gel. Representative of n=2. Dansyl fluorescence at 521 nm was detected using a blue light converter and short pass filter on a GeneSnap Gel Doc. All reactions contained 10 μM total Lipid II (either Lipid II (Glu, Dans) or Lipid II (Gln, Dans)) as labelled below the gel and 1 μM PBP1a or 1 μM PBP2a where indicated. C, –enzyme: 10 μM Lipid II with enzyme replaced with an equal volume of enzyme storage buffer. Reactions in a final volume of 15 μL were incubated at 30°C overnight. (i) denotes unpolymerised Lipid II; (ii) glycan chains of varying lengths and (iii) the location of very high molecular weight material if present, which does not enter the gel.

Under the conditions used it is evident due to the presence of dansylated material higher up the gel, that with both Lipid II (Glu, Dans) and Lipid II (Gln, Dans), PBP2a FL produces larger products than PBP1a FL. This suggests that PBP2a FL is more processive than PBP1a FL. Amidation of Lipid II does not appear to have an effect on the length of glycan products of PBP1a FL as material is seen at equivalent positions in the lanes containing Lipid II (Glu, Dans) and Lipid II (Gln, Dans). However, the distribution of product lengths of PBP2a FL with Lipid II (Gln, Dans) are higher up the gel than that with Lipid II (Glu, Dans), and more material is not able to enter the gel (as seen by the band of material indicated by (iii)). This shows that PBP2a produces longer glycan chains with amidated substrate, and therefore that amidation has an effect on the processivity of the enzyme.

4.4.3 The effect of Triton X-100 concentration on processivity of *S. pneumoniae* PBP1a and PBP2a transglycosylation

The presence of detergent (TX-100 in the case of PBP1a and PBP2a) in the assay buffer is important for the solubility of the Lipid II substrate, and the full-length PBP possessing a hydrophobic transmembrane region. Previous studies have identified a combined effect of detergent and DMSO, where increasing DMSO concentration rescues transglycosylase activity at high detergent concentrations, which would otherwise be inhibitory (Helassa *et al.,* 2012, Offant *et al.,* 2010, Schwartz *et al.,* 2002). This effect has been attributed to DMSO mediated increase in solubility of the lipid substrate and more rapid exchange between detergent micelles, allowing Lipid II and PBP to come into contact (Schwartz *et al.,* 2002). The effect of TX-100 concentration on PBP1a FL and PBP2a FL transglycosylase activity was analysed by SDS-PAGE whilst maintaining DMSO at a set concentration.

10 µM Lipid II (Lipid II (Glu, Dans) or Lipid II (Gln, Dans)) was incubated with 1 µM PBP1a FL, 1 µM PBP2a FL or an equivalent volume of enzyme storage buffer in either 50 mM HEPES pH 7.5, 10 mM $MgCl_2$, 150 mM NaCl, 25% (v/v) DMSO (PBP1a) or 50 mM HEPES pH 7.5, 25 mM $MgCl_2$, 200 mM NaCl, 25% (v/v) DMSO (PBP2a) both with a range of TX-100 concentrations ranging from $0.2 \times$ CMC to $10.7 \times$ CMC (CMC = 0.015% (v/v)). 15 µL reactions were incubated at 30°C overnight before analysis by SDS-PAGE (Section 2.7.2) (Figure 4.7)

PBP1a exhibited transglycosylase activity until $2.7 \times$ CMC (0.04% (v/v)) with both Lipid II substrates, with little effect on processivity. Above $2.7 \times$ CMC, activity is severely inhibited, showing that the DMSO concentration used is not able to rescue this inhibition. Below the TX-100 CMC, a faint band of unpolymerised Lipid II was observed after overnight incubation indicating poor transglycosylase activity.
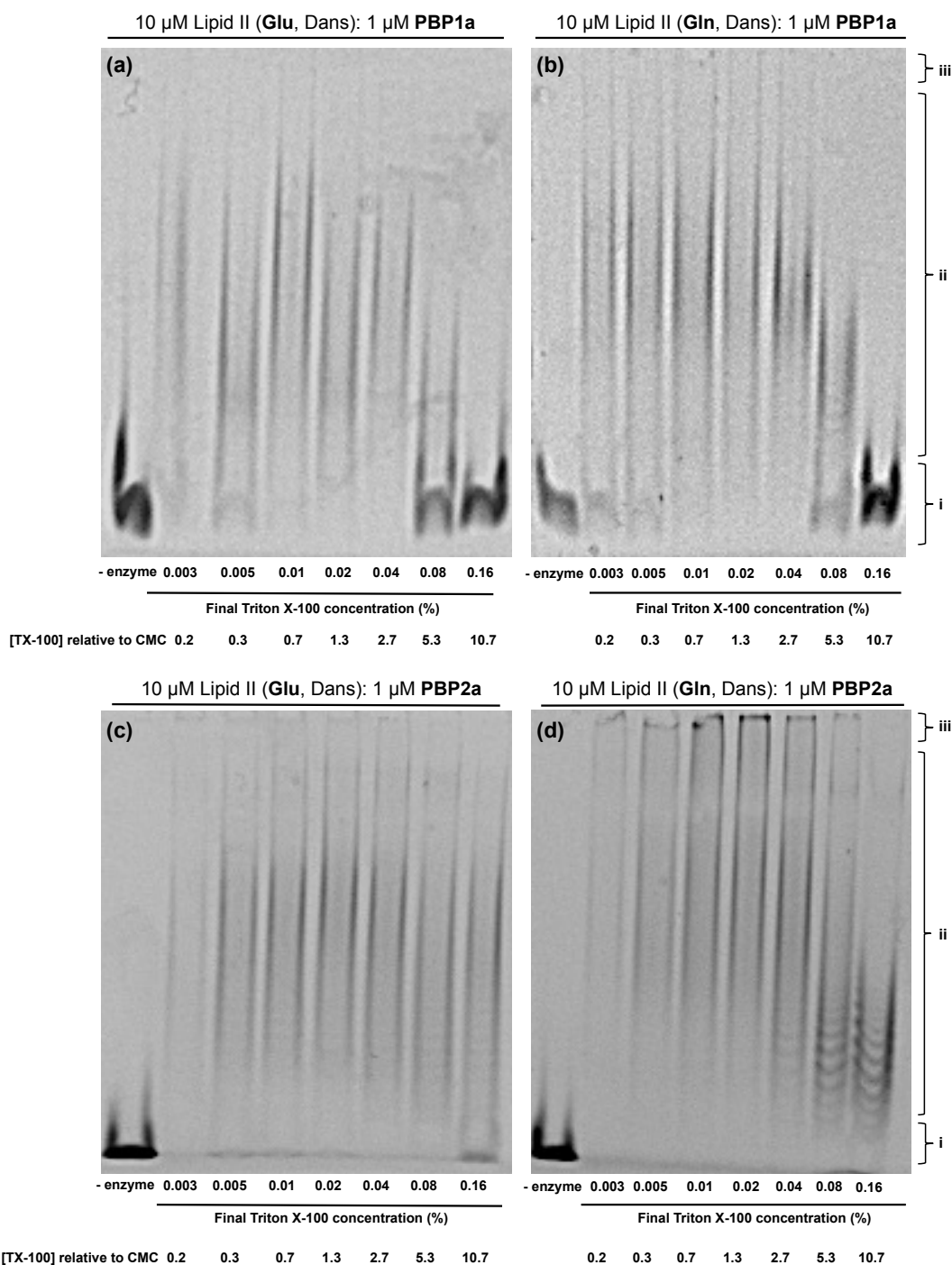
Figure 4.7: Effect of Triton X-100 concentration on the processivity of *S. pneumoniae* PBP1a ((a) and (b)) and PBP2a transglycosylase activity ((c) and (d)). Products of transglycosylation separated on a 8.5% T/2.7% C SDS-PAGE gel. Dansyl fluorescence at 521 nm detected using a blue light converter and short pass filter on a GeneSnap Gel Doc. All reactions contain 10 μM total Lipid II (either Lipid II (Glu, Dans)((a),(c)) or Lipid II (Gln, Dans)((b),(d)) as labelled above the gel and 1 μM PBP1a ((a), (b)) or 1 μM PBP2a ((c),(d)) where indicated. –enzyme: 10 μM Lipid II with enzyme replaced with an equal volume of enzyme storage buffer. Control reactions at 0.02% (v/v) TX-100). Reactions in a final volume of 15 μL were incubated at 30°C overnight. (i) denotes unpolymerised Lipid II; (ii) glycan chains of varying lengths and (iii) the very high molecular weight material, if present, which does not enter the gel.

PBP2a FL is less affected by TX-100 concentration than PBP1a FL, as activity observed at all concentrations used. The polymerisation of Lipid II (Glu, Dans) was mainly unaffected by varying the TX-100, with only minor inhibition at 10.7 × CMC. However, with Lipid II (Gln, Dans), 2.7 × CMC (0.04% (v/v)) TX-100 causes a shortening in the glycan chain length; observed by a reduction in the band at the top of the gel (iii), and a shortening of the chain lengths towards the bottom of the gel. At TX-100 concentrations above this, short chains are observed but not full inhibition as was seen with PBP1a.

4.4.4 Time-course studies of the transglycosylase activity of *S. pneumoniae* PBP1a and PBP2a

Whilst the SDS-PAGE method is predominantly useful for obtaining qualitative information on the processivity of PBP transglycosylase activity, it can also indicate relative rates between enzymes and conditions through time-course studies. This approach was used to investigate differences in substrate preference between Lipid II (Glu, Dans) and Lipid II (Gln, Dans) of PBP1a and PBP2a. 0.02% (v/v) TX-100 was used, as good activity was observed in all cases previously at this concentration (Section 4.4.3), and it is above the CMC (0.015% (v/v)).

10 μM Lipid II (Lipid II (Glu, Dans) or Lipid II (Gln, Dans)) in 120 μL reaction buffer (PBP1 or PBP2a (Section 4.4.2) containing 0.02% (v/v) TX-100) was incubated with 1 μM PBP1a FL or PBP2a FL at 30°C. 15 μL samples were removed after 0, 1, 2, 4, 7 and 24 hours (PBP1a)(Figure 4.8) or 0, 1, 2, 4 and 8 hours (PBP2a)(Figure 4.9) and the reaction stopped with 0.5 mM moenomycin (transglycosylase inhibitor). Products were analysed by SDS-PAGE (Section 2.7.2).

As observed in Figure 4.6, amidation of Lipid II does not affect PBP1a processivity. Figure 4.8 indicates that Lipid II (Gln, Dans) is polymerised more rapidly than Lipid II (Glu, Dans), although the difference in fluorescence intensity suggests more Lipid II (Glu, Dans) is present. However, all Lipid II (Gln, Dans) visible by eye is used within the first hour of reaction, whereas an appreciable amount of Lipid II (Glu, Dans) remains after 7 hours.
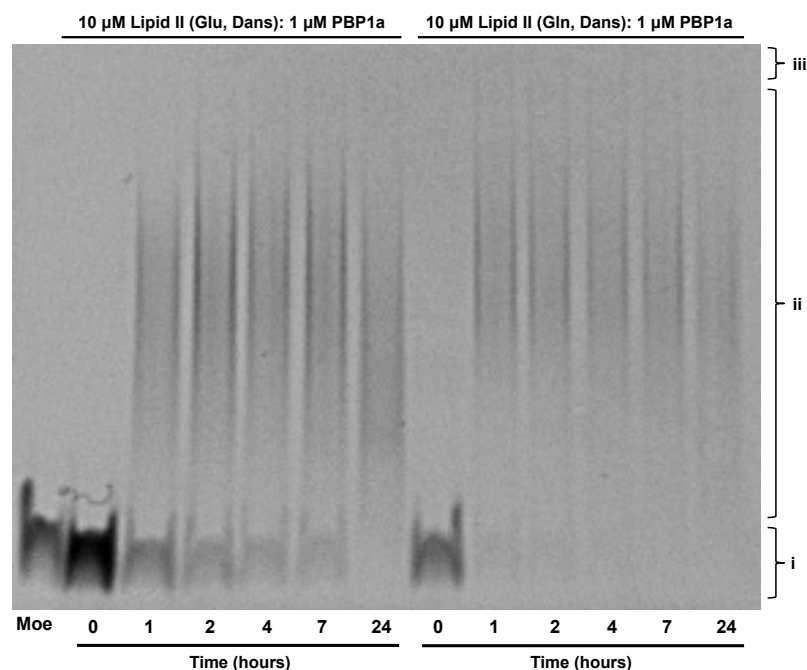
Figure 4.8: A time-course comparison of Lipid II (Glu, Dans) and Lipid II (Gln, Dans) as substrates for *S. pneumoniae* PBP1a. Products of transglycosylation separated on a 8.5% T/2.7% C SDS-PAGE gel. Representative of n=2. Dansyl fluorescence at 521 nm detected using a blue light converter and short pass filter on a GeneSnap Gel Doc. Parallel reactions containing 10 μM Lipid II (Glu, Dans) or 10 μM Lipid II (Gln, Dans) (as indicated above gel) were incubated at 30°C. 15 μL aliquots removed at time points shown, and reaction stopped with 0.5 mM moenomycin. Moe, control reaction of 10 μM Lipid II (Gln, Dans), 1 μM PBP1a FL and 0.5 mM moenomcyin incubated at 30°C for 24 hours (i) denotes unpolymerised Lipid II; (ii) glycan chains of varying lengths and (iii) the location of very high molecular weight material if it were present, which does not enter the gel.

Amidation of Lipid II increases the processivity of *S. pneumoniae* PBP2a transglycosylation (Figure 4.6). Figure 4.9 demonstrates that Lipid II (Gln, Dans) is also polymerised more rapidly than Lipid II (Glu, Dans) by PBP2a, with all visible amidated Lipid II used within the first hour. This also shows that PBP2a is more able to use Lipid II (Glu, Dans) than PBP1a as all substrate is polymerised within 4 hours, compared to over 7 hours by PBP1a.

24 hour and 8 hour controls in Figures 4.8 and 4.9 respectively were included with the addition of 0.5 mM moenomycin. This demonstrates that the activity observed is inhibited by the specific transglycosylase inhibitor, and confirms the rationale for stopping each time point aliquot with 0.5 mM moenomycin.
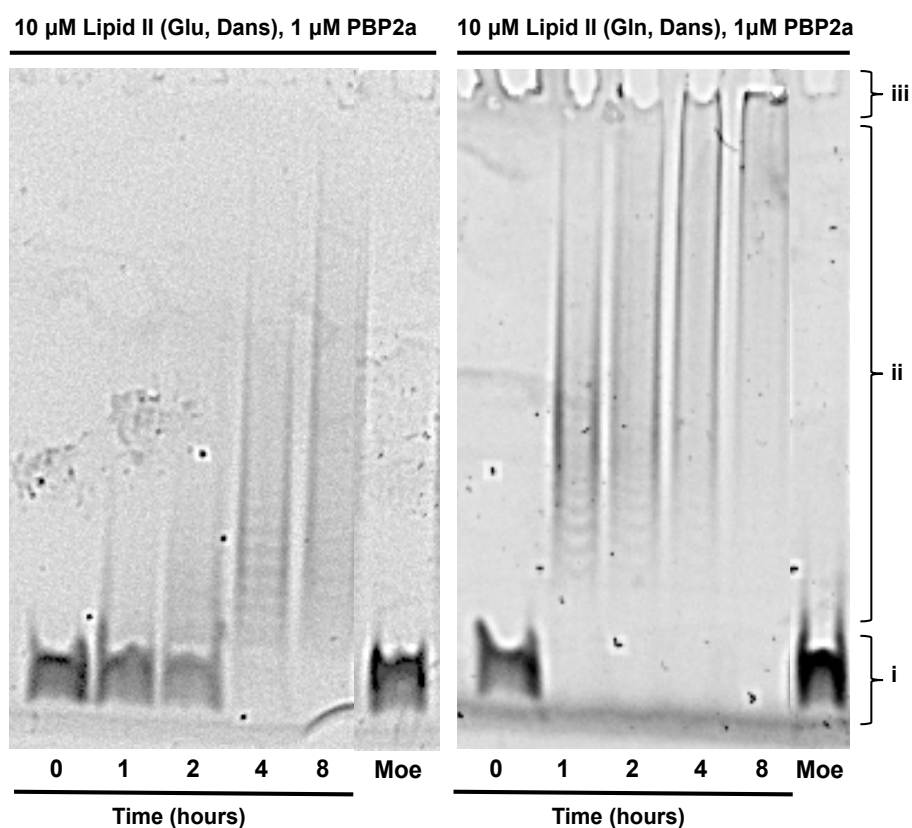
Figure 4.9: A time-course comparison of Lipid II (Glu, Dans) and Lipid II (Gln, Dans) as substrates for *S. pneumoniae* PBP2a-FL. Products of transglycosylation separated on a 8.5% T/2.7% C SDS-PAGE gel. Dansyl fluorescence at 521 nm was detected using a blue light converter and short pass filter on a GeneSnap Gel Doc. Parallel reactions containing 10 μM Lipid II (Glu, Dans) or 10 μM Lipid II (Gln, Dans) and 1 μM PBP2a FL were incubated at 30°C, aliquots were removed at time points shown, and reaction stopped with 0.5 mM moenomycin. Moe, control reaction of 10 μM Lipid II (Lipid II (Glu, Dans) or Lipid II (Gln, Dans) as indicated), 1 μM PBP2a FL and 0.5 mM moenomycin were incubated at 30°C for 24 hours (i) denotes unpolymerised Lipid II; (ii) glycan chains of varying lengths and (iii) the very high molecular weight material, which does not enter the gel.

4.4.5 The role of the *S. pneumoniae* PBP2a transmembrane region in transglycosylase activity

Helassa *et al.,* (2012) identified that the transmembrane spanning (TM) region of PBP2a has a significant influence on the length of glycan polymers produced, with its removal resulting in a 4-fold decrease in chain length. Chemical cross-linking experiments suggested an involvement of the TM region in dimerisation of PBP2a and the increased processivity was attributed to either this or a more direct interaction between the Lipid II substrate and the PBP transmembrane helix. The TM region of *E. coli* PBP1b is crucial in its affinity for moenomycin, and this has led to

139

the suggestion that it is important in binding of Lipid II and moenomycin (Cheng *et al.,* 2008; Sung *et al.,* 2009). Additionally these effects could be due to differences in interaction of enzyme and substrate due to the presence of a detergent micelle surrounding the hydrophobic TM region (Helassa *et al*., 2012).

Helassa and co-workers conducted their experiments at a TX-100 concentration of 0.04% (v/v) with non-amidated dansylated Lipid II, therefore an obvious comparison to make is the effect of removal of the TM helix (Δ77) on the processivity of PBP2a with Lipid II (Gln, Dans), compared to that displayed by the complete protein. This experiment was conducted at the lower TX-100 concentration of 0.02% (v/v), to keep the concentration sufficiently below that observed to be inhibitory in Figure 4.7 (D).

10 μM Lipid II (Lipid II (Glu, Dans) or Lipid II (Gln, Dans)) was incubated with 1 μM PBP2a FL or 1 μM PBP2a-Δ77 in PBP2a reaction buffer at 30°C overnight before analysis by SDS-PAGE (Section 2.7.2)(Figure 4.10). A parallel set of reactions were identical but with the addition of 1 mM moenomycin.
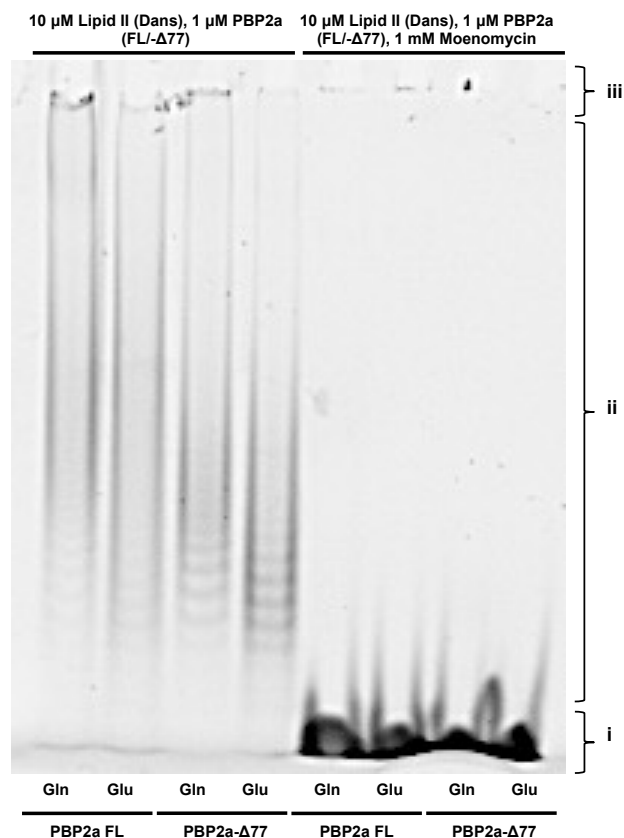
Figure 4.10: Comparison of PBP2a FL and PBP2a-Δ77 processivity with Lipid II (Glu, Dans) and Lipid II (Gln, Dans). All reactions contain 10 μM total Lipid II (either Lipid II (Glu, Dans) indicated by Glu below the gel or Lipid II (Gln, Dans) indicated by Gln) and 1 μM PBP2a FL or 1 μM PBP2a-Δ77 where indicated. Control reactions on the right of the gel containing an additional 1 mM moenomycin are labelled. Reactions in a final volume of 15 μL were incubated at at 30°C overnight and products of transglycosylation separated on a 8.5% T/2.7% C SDS-PAGE gel. Representative of n=2. Dansyl fluorescence at 521 nm detected using a blue light converter and short pass filter on a GeneSnap Gel Doc. (i) denotes unpolymerised Lipid II; (ii) glycan chains of varying lengths and (iii) the very high molecular weight material, which does not enter the gel.

Figure 4.10 shows a reduction in chain lengths from Lipid II (Gln, Dans) to Lipid II (Glu, Dans) for both the full-length and -Δ77 enzyme, further demonstrating the role of Lipid II amidation on PBP2a processivity (see Figure 4.6 and 4.9). Processivity is also reduced with both substrates following removal of the TM region as observed by Helassa *et al.,* (2012) with Lipid II (Glu, Dans).

In order to test the possibility that the processivity effect between full-length and truncated enzyme could be due to differences in the detergent micelle surrounding the hydrophobic TM region, the effect of TX-100 concentration on PBP2a-Δ77 transglycosylase activity was investigated as in Section 4.4.3 for PBP2a FL. As before, 10 μM Lipid II (Lipid II (Glu, Dans) or Lipid II (Gln, Dans)) was incubated with 1 μM PBP2a-Δ77 or an equivalent volume of enzyme storage buffer in PBP2a reaction buffer with a range of TX-100 concentrations from 0.2 × CMC to 10.7 × CMC. 15 μL reactions were incubated at 30°C overnight before analysis by SDS-PAGE (Section 2.7.2)(Figure 4.11).
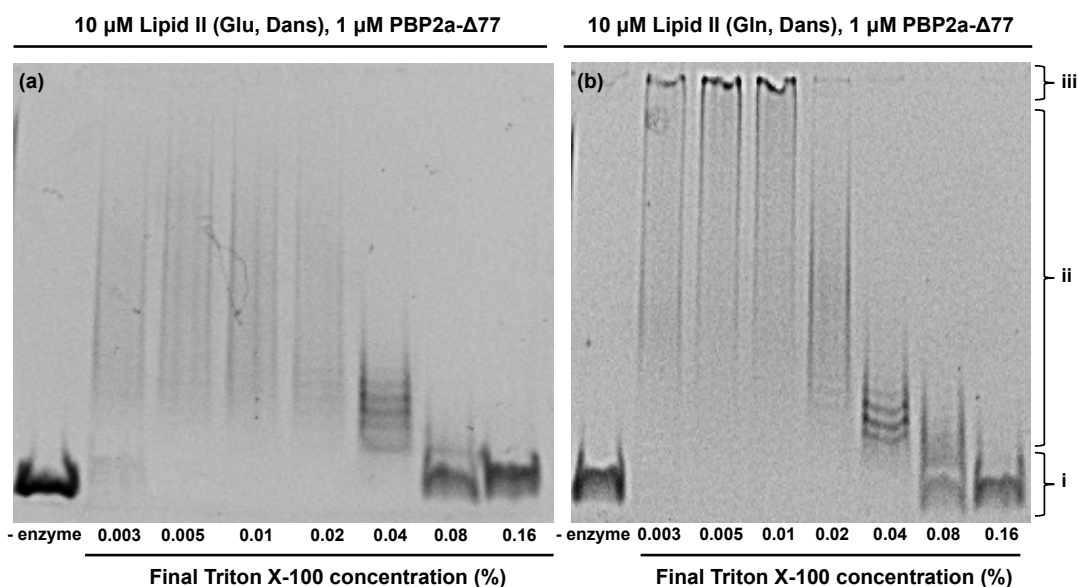
Figure 4.11: Effect of Triton X-100 concentration on the processivity of *S. pneumoniae* PBP2a-Δ77. All reactions contain 10 μM total Lipid II (either Lipid II (Glu, Dans)(a) or Lipid II (Gln, Dans)(b)) as labelled above the gel and 1 μM PBP2a-Δ77 PBP2a reaction buffer with various TX-100 concentrations. –enzyme: 10 μM Lipid II with enzyme replaced with an equal volume of enzyme storage buffer. (Control reactions at 0.02% (v/v) TX-100). Reactions in a final volume of 15 μL were incubated at 30 °C overnight and products of transglycosylation separated on a 8.5% T/2.7% C SDS-PAGE gel. Dansyl fluorescence at 521 nm detected using a blue light converter and short pass filter on a GeneSnap Gel Doc. (i) denotes unpolymerised Lipid II; (ii) glycan chains of varying lengths and (iii) the very high molecular weight material, which does not enter the gel.

A more significant effect on processivity was observed with truncated PBP2a (Figure 4.11) at increasing TX-100 concentrations than for the full-length enzyme (Figure 4.7). Inhibition was first observed at just above the CMC (0.02% (v/v) TX-100) for both Lipid II (Glu, Dans) and Lipid II (Gln, Dans), with severe inhibition at 2.7 × CMC (0.04% (v/v)) and above (Figure 4.11). Activity was observed with PBP2a FL at all TX-100 concentrations tested with both substrates. A possible explanation for

this is a difference in detergent-micelle interaction between the two protein variants, reducing the likelihood of PBP and Lipid II interactions with the truncated version at increasing TX-100 concentrations. PBP2a possesses a membrane association site within the transglycosylase domain between Lys 78 and Ser 156 (Di Guilmi *et al.,* 1999) and therefore this hydrophobic region is likely to interact with TX-100, and this could affect vital protein-substrate interactions.

An interesting point arising from these observations is that the study on glycan chain length conducted by Helassa *et al.,* (2012) was with TX-100 at 0.04% (v/v), and in Figure 4.10 at 0.02% (v/v). The comparison of Figures 4.7 and 4.11 shows that at the detergent concentrations used previously (in both cases), which are both above the CMC (0.015% (v/v)), the chain lengths produced by PBP2a-Δ77 are shorter than at 0.01% (v/v)(Figure 4.11). The effect is more significant at 0.04% (v/v) TX-100. Conversely, full-length PBP2a is not as affected by these TX-100 concentrations (Figure 4.7 (c) and (d)). Therefore the shortening of chains observed with PBP2a-Δ77 is a result of the TX-100 concentrations used.

A time-course analysis was conducted for PBP2a-Δ77 transglycosylase activity at two TX-100 concentrations, to identify any further effects of the detergent concentration on enzyme activity. 0.01% (v/v) and 0.04% (v/v) were selected due to the significant difference seen between enzyme activities at these concentrations in Figure 4.11.

10 μM Lipid II (Lipid II (Glu, Dans) or Lipid II (Gln, Dans)) in 120 μL PBP2a reaction buffer, with either 0.01% (v/v)(a) or 0.04% (v/v)(b) TX-100 was incubated with 1 μM PBP2a-Δ77 at 30°C. 15 μL samples were removed after, 0, 1, 2, 4, 7 and 24 hours and reactions stopped with 0.5 mM moenomycin. Products were analysed by SDS-PAGE (Section 2.7.2)(Figure 4.12).
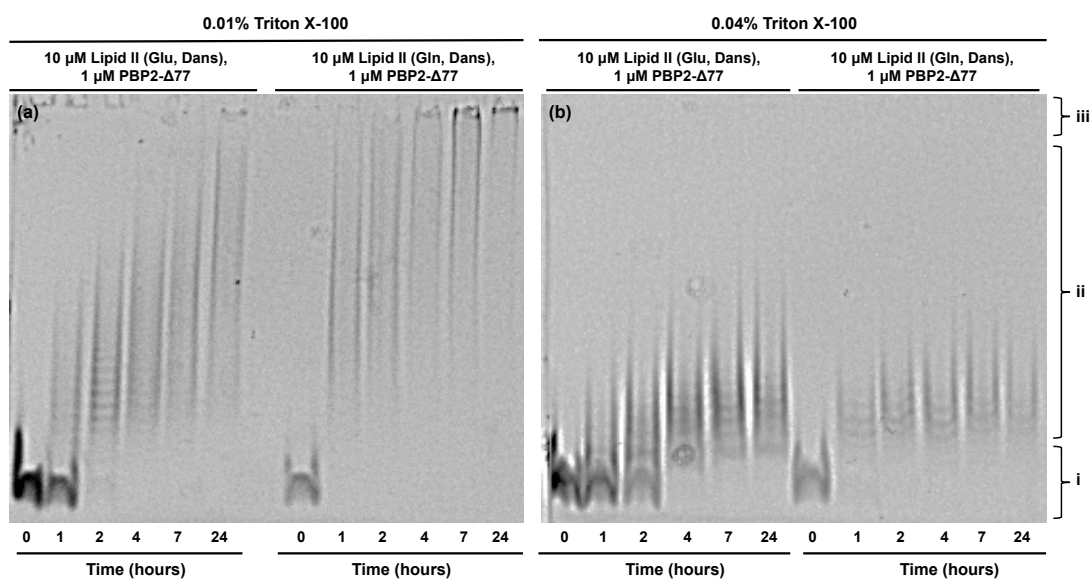
Figure 4.12: A time-course comparison of Lipid II (Glu, Dans) and Lipid II (Gln, Dans) as substrates for *S. pneumoniae* PBP2a-Δ77 and the effect of TX-100 concentration. Parallel 120 uL reactions containing 10 μM Lipid II (Glu, Dans) or 10 μM Lipid II (Gln, Dans) (as indicated above gel) in PBP2a reaction buffer containing 0.01% (v/v) TX100 (a) or 0.04% (v/v) TX-100 (b) and 1 μM PBP2a-Δ77 were incubated at 30°C. 15 μL aliquots were removed at time points shown, and reaction stopped with 0.5 mM moenomycin. Products of transglycosylation were separated on a 8.5% T/2.7% C SDS-PAGE gel. Representative of n=2. Dansyl fluorescence at 521 nm detected using a blue light converter and short pass filter on a GeneSnap Gel Doc. (i) denotes unpolymerised Lipid II; (ii) glycan chains of varying lengths and (iii) the very high molecular weight material, which does not enter the gel.

Lipid II (Gln, Dans) was polymerised more rapidly by PBP2a-Δ77 at both TX-100 concentrations than Lipid II (Glu, Dans), as was seen previously with PBP2a FL (Figure 4.9). The main difference identified was a slowing of the rate of transglycosylation of Lipid II (Glu, Dans) with a TX-100 concentration of 0.04% (v/v) compared to that at 0.01% (v/v).

4.4.6 Requirement for the TM region in PBP2a oligomerisation

In vitro cross-linking experiments with EGS (ethylene glycol *bis*(succinic acid) N-hydroxysuccinimide ester) by Helassa *et al.,* (2012) identified apparent dimerisation of full-length PBP2a, but not PBP2a-Δ77. Several experiments were performed to confirm this.

Firstly, Microscale thermophoresis (MST) was used to investigate the dimerisation of PBP2a. Changes in molecule size are identified by movement in a temperature

gradient (thermophoresis) with the titration of non-fluorescent molecules against a constant concentration of fluorescent molecule (for detection). Changes in thermophoresis can be used to monitor binding (Jerabek-Willemsen *et al*., 2011; Seidel *et al*., 2013; Wienken *et al.,* 2010).

Experiments were performed by Dr James Wilkinson as part of a demonstration from NanoTemper Technologies (Germany) GmbH (methodological detail Section 2.5.3). NT-647 fluorescent label was covalently attached to primary amines on PBP2a-FL and PBP2a-Δ77 and non-labelled proteins subsequently titrated (64.95 μM to 2 nM) against a constant concentration of 75 nM labelled PBP. Assays were performed in PBP2a-FL and PBP2a-Δ77 storage buffers (Section 4.3.3 and 4.3.4 respectively) at 30°C plus 0.005% (v/v) Tween20 to reduce sticking to capillaries. MST analysis was in standard glass capillaries using the Monolith NT.115 (NanoTemper GmbH). Data analysis performed by Dr James Wilkinson established a K_d of 500 nM for PBP2a FL and no indication of binding for PBP2a-Δ77.

Experiments were subsequently repeated in PBP2a assay buffer for both PBP2a-FL and PBP2a-Δ77 but data was not obtained due to protein aggregation affecting the fluorescence signal. This has important implications in the discussion of assay conditions used to observe transglycosylase activity (Discussed section 4.6.2).

Dimerisation of PBP2a-FL was further probed by analytical size exclusion chromatography (Section 2.4.3.2.2). 100 μL of pure protein (Section 4.3.3) at 8 mg.ml^{-1} was loaded onto a Superdex 200 Increase 10/300 GL (GE Healthcare) column and eluted with 1 column volume (CV) of PBP2a storage buffer at 0.3 ml.min^{-1} (Figure 4.13(a)). SDS-PAGE analysis of the two peaks identified them to contain only PBP2a-FL (Figure 4.13(b)), suggesting two oligomerisation states. Pre-equilibration of the column with a Gel Filtration HMW Calibration Kit (GE Healthcare) enables a rough estimation of molecular weight. This is not very accurate due to the presence of large TX-100 detergent micelles, and the assumption of globular protein required for this calculation. However, the estimate suggested peak (i) to be 280 kDa and (ii) 141 kDa in size. The molecular weight of PBP2a-FL at 80 kDa and TX-100 at approximately 90 kDa suggests that peak (ii) may be a

monomer and at (i) a dimer of PBP2a-FL. An interesting observation is the intensity of peak (ii) in correspondence with the amount of protein present (Figure 4.13(b). The higher intensity of absorbance signal at 280 nm and 254 nm of the less abundant protein may suggest interaction with a molecule with absorbance at this wavelength (such as tightly bound TX-100), or a reduction in absorbance observed due to dimerisation.
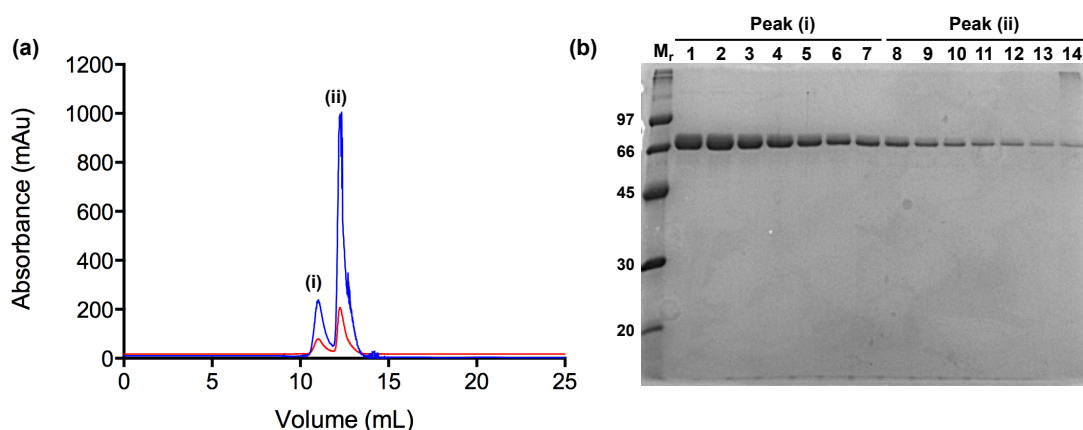
Figure 4.13: Gel filtration analysis of oligomeric state of _S. pneumoniae_ PBP2a-FL. (a) Superdex 200 Increase 10/300 FL chromatogram showing the elution of 2 peaks of PBP2a-FL at (i) 11.0 mL and (ii) 12.3 mL. Red: absorbance at 254nm, Blue: absorbance at 280 nm (b) 12% SDS-PAGE Coomassie-stained gel showing the analysis of these peaks and showing they both contain pure PBP2a-FL with no contaminants or break-down products. M_r, molecular weight markers (kDa); Peak (i) 1-7 Samples from fractions in peak (i); Peak (ii) 8-14 Fractions in peak (ii). All samples 10 μL from 500 μL fractions.

Re-injection of peak (i) onto the Superdex 200 Increase column resulted in a chromatogram of the same peaks and relative intensities of that observed in Figure 4.13. This suggests an equilibrium state between monomeric and dimeric PBP2a-FL.

4.4.7 Role of the _S. pneumoniae_ PBP1a transmembrane region in transglycosylase activity

The effect of TM helix removal on PBP1a activity was also investigated. A comparable experiment to that shown in Figure 4.10 was performed. Here, 10 μM Lipid II (Lipid II (Glu, Dans) or Lipid II (Gln, Dans)) was incubated with 1 μM PBP1a FL or 1 μM PBP1a-Δ30 in PBP1a reaction buffer at 30°C overnight before analysis by SDS-PAGE (Section 2.7.2)(Figure 4.14)(control reactions also included 1 mM moenomycin).

146
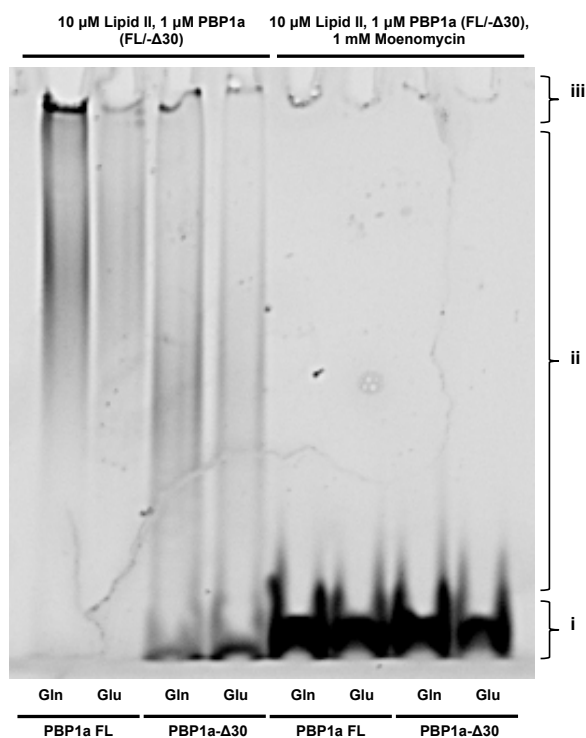
Figure 4.14: Comparison of PBP1a FL and PBP1a-Δ30 processivity with Lipid II (Glu, Dans) and Lipid II (Gln, Dans). All reactions contained 10 μM total Lipid II (either Lipid II (Glu, Dans) indicated by Glu below the gel or Lipid II (Gln, Dans) indicated by Gln) and 1 μM PBP1a FL or 1 μM PBP1a-Δ30 where indicated. Control reactions on the right of the gel containing an additional 1 mM moenomycin are labelled. Reactions in a final volume of 15 μL were incubated at 30°C overnight and products of transglycosylation separated on a 8.5% T/2.7% C SDS-PAGE gel. Dansyl fluorescence at 521 nm was detected using a blue light converter and short pass filter on a GeneSnap Gel Doc. (i) denotes unpolymerised Lipid II; (ii) glycan chains of varying lengths and (iii) the very high molecular weight material, which does not enter the gel.

Figure 4.14 suggests there may be a reduction in glycan chain lengths between Lipid II (Glu, Dans) and Lipid II (Gln, Dans) for both full-length and truncated enzymes, which contradicts the previous observation (Figures 4.6 and 4.8) that PBP1a-FL processivity is unaffected by Lipid II amidation. However, it is clear that less Lipid II (Glu, Dans) is present, and therefore strong conclusions cannot be drawn. The comparison between Figures 4.6, 4.8 and 4.14 also highlights an issue with reproducibility between gels (Discussed Section 4.6.2.1). It is clear that removal of the TM region affects PBP1a transglycosylase activity, as with both substrates unpolymerised Lipid II substrate remains after an overnight incubation.

MST experiments as in Section 4.4.6 were performed for PBP1a-FL and PBP1a-Δ30 in reaction buffer, but aggregation prevented data analysis.

4.5 Continuous coupled fluorescence assay for transglycosylase activity

As described in Section 4.1.2, the polymerisation of fluorescent Lipid II (Dans) can be coupled to digestion by *N*-acetylmuramidase to obtain quantitative data on transglycosylation. In Section 4.4, it was established by SDS-PAGE analysis that amidated Lipid II (Lipid II (Gln, Dans)) is an optimal substrate for *S. pneumoniae* PBP1a and PBP2a transglycosylation, and time-course studies suggest that it is polymerised more rapidly by both enzymes than the non-amidated variant (Lipid II (Glu, Dans)). This section details the study of the effect of amidation of Lipid II on the rate of transglycosylation in a quantitative manner by the continuous transglycosylation assay in a 96-well plate assay format (Helassa *et al.,* 2012; Offant *et al.,* 2010). The standard methodology for this assay is detailed in Section 2.7.1.

4.5.1 Optimisation of conditions for PBP1a and PBP2a transglycosylase activity

As described in Section 4.4.1, optimal buffer conditions are known for PBP1a and PBP2a (Abrahams, 2011; Helassa *et al.,* 2012). As for the gel assays, larger, more concentrated stocks of Lipid II were made to improved accuracy. In initial experiments a gradual reduction in fluorescence over the experimental time-course was observed in all reactions including controls. This was attributed to evaporation over time leading to a change in buffer conditions and was overcome by the use of optically transparent ThermalSeal RT^{TM} film to seal the plate upon reaction initiation. A reduction in dansyl fluorescence yield of ~8%, but no effect on the fluorescent properties was observed (Figure 4.15). This was acceptable as the reduction in fluorescence due to evaporation was more significant.

Reaction buffers used in this section were, PBP1a: 50 mM HEPES pH 7.5, 10 mM MgCl$_2$, 150 mM NaCl, 25% (v/v) DMSO, 0.02% (v/v) TX-100 and PBP2a: 50 mM HEPES pH 7.5, 25 mM MgCl$_2$, 200 mM NaCl, 25% (v/v) DMSO, 0.02% (v/v) TX-100 unless stated otherwise.

4.5.1.1 Fluorescent properties of Lipid II (Dans)

The published optimal excitation and emission wavelengths of the dansyl fluorophore appended to Lipid II are 340 nm and 521 nm respectively (Schwartz *et al.,* 2002). In order to ensure the highest signal, any effect of the assay buffer system on the dansyl fluorescent properties was investigated (Figure 4.15). 10 μM Lipid II (Glu, Dans) or Lipid II (Gln, Dans) in 50 μL PBP1a or PBP2a reaction buffer plus 0.1 mg.ml^{-1} *N*-acetylmuramidase (mutanolysin from *Streptomyces globisporus*), in a Greiner FLUOTRAC^{TM} 600 96-well plate was scanned for wavelength maxima in a CLARIOstar® platereader (BMG Labtech). Emission from 400-600 nm was measured after excitation at 340 nm and emission at 521 nm with excitation over the 320-400 nm range. All measurements were performed with and without a seal, and with buffer only controls, in duplicate. No difference was observed between the two buffer systems or between Lipid II (Glu, Dans) and Lipid II (Gln, Dans), therefore Figure 4.15 demonstrates the effect of the seal and shows buffer only controls, with Lipid II (Gln, Dans) in PBP1a buffer for simplicity.

The emission maxima observed with excitation at 340 nm was 521 nm, and the intensity was reduced slightly by the inclusion of a seal. An increase in emission at lower wavelengths was observed due to the seal, but not in the region that may affect the monitored wavelengths. Similarly, a reduction in intensity was seen when emission was measured at 521 nm. The optimal excitation wavelength was 359 nm, higher than that expected. In both cases, the buffer control confirms that the fluorescence observed is due to the presence of the Lipid II (Dans). A test reaction was performed with excitation at 359 nm and emission at 521 nm, with more noise observed than the usual parameters of 340 nm and 521 nm. Therefore, the published conditions of excitation at 340 nm and emission at 521 nm were taken forward with the use of a plate seal to prevent evaporation.
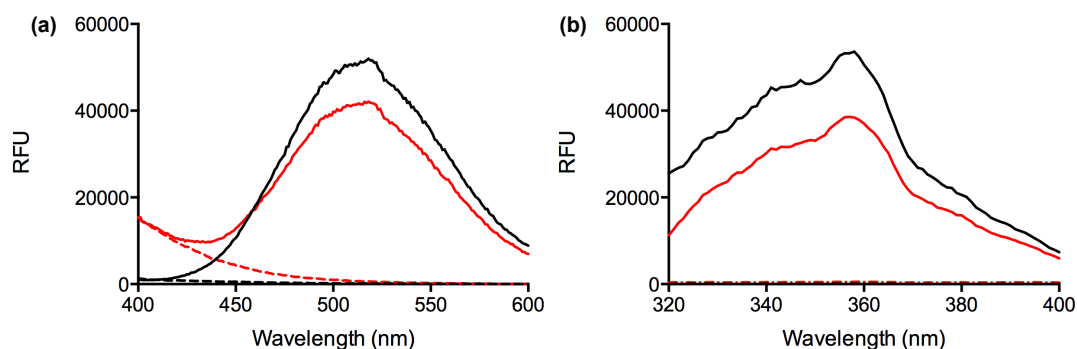
Figure 4.15: Optimal emission and excitation wavelengths of Lipid II (Dans). 10 μM Lipid II (Gln, Dans) in 50 μL 50 mM HEPES pH 7.5, 10 mM MgCl$_2$, 150 mM NaCl, 25% (v/v) DMSO, 0.02% (v/v) TX-100 in a Greiner FLUOTRAC[TM] 600 96-well plate. a) Excitation at 340 nm, emission measured at 400 nm-600 nm. Black solid, Lipid II; Red solid; Lipid II + seal, Black dashed; Buffer control, Red dashed; Buffer control + seal. Emission maxima observed at 521 nm. b) Excitation at 320 nm – 400 nm, emission at 521 nm. Black solid, Lipid II; Red solid; Lipid II + seal, Black dashed; Buffer control, Red dashed; Buffer control + seal. Excitation maxima observed at 359 nm.

An additional control, with the removal of Lipid II, but the inclusion of 1 μM PBP1a or PBP2a in their respective reaction buffer plus 0.1 mg.ml^{-1} mutanolysin showed no signal at 521 nm following excitation at 340 nm, which rules out a fluorescence effect due to the protein (data not shown).

All assays hereafter were carried out in the reaction buffers stated above (Section 4.5.1) in a CLARIOstar® platereader (BMG Labtech) with Greiner FLUOTRAC[TM] 600 black 96-well plates, at 30°C with excitation at 340 nm, emission at 521 nm and with a ThermalSeal RT[TM] film unless specified otherwise. Basic experimental methods for the assay system are detailed in Section 2.7.1.

4.5.1.2 Lysozyme as an alternative *N*-acetylmuramidase coupling enzyme

N-acetylmuramidases are responsible for cleavage of the β-1,4-linkage between Mur*N*Ac and Glc*N*Ac of the peptidoglycan polysaccharide backbone. Mutanolysin from *Streptomyces globisporus* has been used in all published work to date using this fluorescence assay (including Helassa *et al.,* 2012; Offant *et al.,* 2010; Schwartz *et al.,* 2002). It was hypothesised that the cheaper, more readily available, Lysozyme from hen egg-white could replace mutanolysin as this catalyses the same reaction and is also active against Gram-positive peptidoglycan (Nakimbugwe *et al.,* 2006). A

search of the literature revealed no information on the minimum length of glycan chain required by mutanolysin as a substrate, and that the minimum requirement for optimal activity of lysozyme is 6 saccharides (Vocadlo *et al.,* 2001). Parallel assays were carried out with 0.1 mg.ml^{-1} lysozyme and mutanolysin to test the hypothesis. Both Lipid II (Glu, Dans) and Lipid II (Gln, Dans) were tested to ensure no difference in *N*-acetylmuramidase specificity was observed between the two (Figure 4.16).
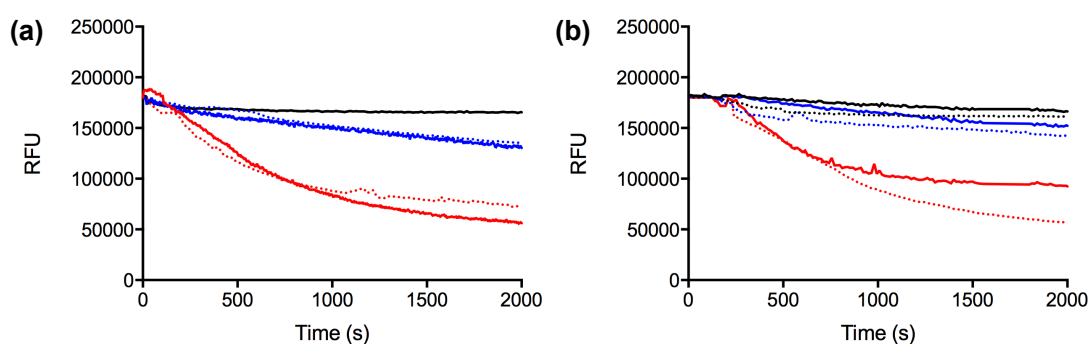
Figure 4.16: Comparison of lysozyme and mutanolysin as coupling enzymes in the continuous fluorescence assay for *S. pneumoniae* PBP1a (a) and PBP2a (b) transglycosylase activity 10 μM Lipid II ((Lipid II (Glu, Dans) (Blue lines) or Lipid II (Gln, Dans)(Red lines)) a) In 50 mM HEPES pH 7.5, 10 mM MgCl$_2$, 150 mM NaCl, 25% (v/v) DMSO, 0.02% (v/v) TX-100 with 0.1 mg.ml^{-1} lysozyme (dashed lines) or 0.1 mg.ml^{-1} mutanolysin (solid lines) plus 1 μM PBP1a. b) In 50 mM HEPES pH 7.5, 25 mM MgCl$_2$, 200 mM NaCl, 25% (v/v) DMSO, 0.02% (v/v) TX-100 with 0.1 mg.ml^{-1} lysozyme (dashed lines) or 0.1 mg.ml^{-1} mutanolysin (solid lines) plus 1 μM PBP2a. Controls in both a) and b) solid black lines, 10 μM Lipid II (Gln, Dans) in mutanolysin containing reaction buffers as before with PBP storage buffer replacing PBP. Dashed black lines, 10 μM Lipid II (Gln, Dans) in lysozyme containing reaction buffers as before with PBP storage buffer replacing PBP. Reaction volume ; 50 μL in a Greiner FLUOTRAC^{TM} 600 96-well plate. Excitation at 340 nm, emission at 521 nm. Readings at 30 second intervals. Plotted lines are averages of 3 repeats.

Emission at 521 nm following excitation at 340 nm was followed for 2000 seconds with measurements at 30 second intervals. Reactions consisted of 10 μM Lipid II (Lipid II (Glu, Dans) or Lipid II (Gln, Dans)) and 1 μM PBP1a or PBP2a in the enzyme specific reaction buffer. Parallel reactions contained either 0.1 mg.ml^{-1} mutanolysin from *Streptomyces globisporus* or 0.1 mg.ml^{-1} hen egg-white lysozyme and were initiated with the addition of enzyme. Relative fluorescence measurements were plotted against time. Initial rates were not calculated at this point as the raw data is shown for direct comparison to ensure linearity of response, and full analysis of the effect of enzyme and substrate concentrations is carried out in Section 4.5.2.

151

This initial comparison of Lipid II (Glu, Dans) and Lipid II (Gln, Dans) by continuous assay agrees with previous results by SDS-PAGE analysis, showing that the amidated substrate is preferred. For PBP1a, no difference was observed between mutanolysin and lysozyme, and for PBP2a lysozyme performed better. A greater fluorescence drop was observed over the time-course, suggesting that the glycan chains were digested more fully. In both cases a linear response was observed between fluorescence change and time showing that the coupling enzyme is not limiting. The difference between PBP1a and PBP2a may be due to the greater processivity of the latter, as observed in Section 4.4, and the differences in substrate specificity of the two *N*-acetylmuramidases. However it could be due to the mutanolysin stock used.

The rationale for using lysozyme as a coupling enzyme in the assay system has been demonstrated here, and therefore 0.1 mg.ml^{-1} lysozyme was used hereafter for continuous fluorescence transglycosylase assays of PBP1a and PBP2a, unless stated otherwise.

4.5.2 Do *S. pneumoniae* PBP1a and PBP2a polymerise Lipid II (Gln, Dans) more rapidly than Lipid II (Glu, Dans)?

A simple comparison between the two substrates with 10 μM Lipid II and 1 μM enzyme suggested that both PBP1a and PBP2a polymerise Lipid II (Gln, Dans) more rapidly than Lipid II (Glu, Dans)(Figure 4.16). This section describes a more thorough investigation of this difference.

4.5.2.1 Continuous fluorescence assay for transglycosylation of Lipid II (Gln, Dans)

Due to substrate availability, initial experiments were performed with Lipid II (Gln, Dans). A range of enzyme concentrations was tested against a single substrate concentration in order to establish direct proportionality between the amount of enzyme assayed and the rate measured. 1 μM Lipid II was chosen, as sufficient signal was observed and by significantly reducing the amount of Lipid II per

reaction, a greater number of experiments could be performed with the stock available. This is pertinent as the Lipid II substrates are costly to produce.

50 µL reactions containing 1 µM Lipid II (Gln, Dans) in either PBP1a or PBP2a reaction buffer plus 0.1 mg.ml^{-1} hen egg-white lysozyme were initiated with the addition of 0, 0.02, 0.06, 0.1, 0.2, 0.4, 0.8 or 1 µM enzyme in triplicate. The reaction was monitored for 100 min and the rate in fluorescence change per second of the initial linear portion calculated (with the background rate of the control reaction without PBP subtracted). This was plotted against enzyme concentration to establish the relationship between enzyme concentration and transglycosylation rate (Figure 4.17 black data points).

A linear increase in rate was observed with increasing concentrations of PBP1a and PBP2a, to 0.2 µM PBP1a and 0.1 µM PBP2a (Figure 4.17 (b) and (d)). The relationship becomes non-linear at this point, dropping for PBP1a and more significantly with increasing PBP2a concentrations. To test whether this was due to lysozyme insufficiency, the same reaction was repeated in an identical manner, with an increase in lysozyme concentration to 0.5 mg.ml^{-1} (Figure 4.17 red data points).

Increasing the lysozyme concentration had no significant effect on the relationship observed between enzyme concentration and reaction rate with 1 µM Lipid II (Gln, Dans) for either enzyme, thus demonstrating that the coupling enzyme was not the limiting factor at higher enzyme concentrations.
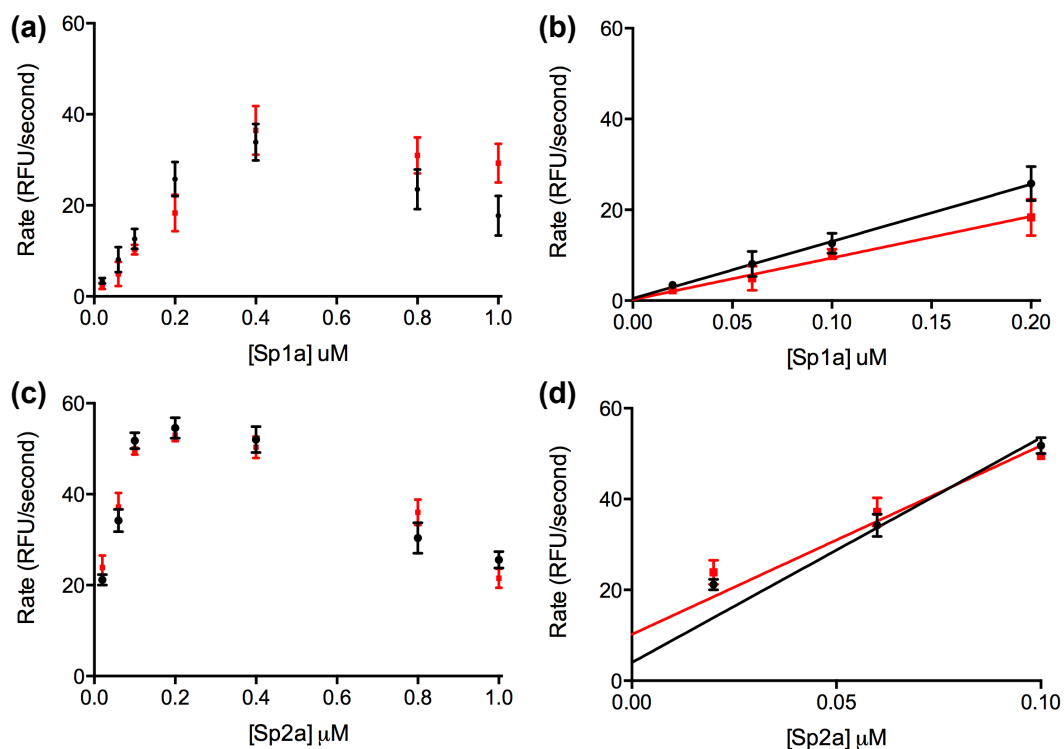
Figure 4.17: Rate of Lipid II (Gln, Dans) transglycosylation by *S. pneumoniae* PBP1a (a), (b) and PBP2a (c), (d) 1 μM Lipid II Lipid II (Gln, Dans) a) In 50 mM HEPES pH 7.5, 10 mM MgCl$_2$, 150 mM NaCl, 25% (v/v) DMSO, 0.02% (v/v) TX-100 with 0.1 mg.ml^{-1} lysozyme (black) or 0.5 mg.ml^{-1} lysozyme (red) plus 0, 0.02, 0.06, 0.1, 0.2, 0.4, 0.8 or 1 μM PBP1a. b) In 50 mM HEPES pH 7.5, 25 mM MgCl$_2$, 200 mM NaCl, 25% (v/v) DMSO, 0.02% (v/v) TX-100 with 0.1 mg.ml^{-1} lysozyme (black) or 0.5 mg.ml^{-1} lysozyme (red) plus 0, 0.02, 0.06, 0.1, 0.2, 0.4, 0.8 or 1 μM PBP2a. Reaction volume; 50 μL in a Greiner FLUOTRAC^{TM} 600 96-well plate. Excitation at 340 nm, emission at 521 nm with readings at 30 second intervals. RFU (relative fluorescence unit) change per second calculated from initial linear portion of time-course. Values represent mean ± standard deviation of triplicate reactions. Linear regression fitted to region with linear relationship (b) PBP1a: Black, 0.1 mg.ml^{-1} lysozyme Slope 125.8 ± 9.556, R^2: 0.9612 ; Red, 0.5 mg.ml^{-1} lysozyme Slope 91.7 ± 9.531, R^2: 0.9297 (d) PBP2a: Black, 0.1 mg.ml^{-1} lysozyme Slope 495.2 ± 42.36, R^2: 0.9513 ; Red, 0.5 mg.ml^{-1} lysozyme Slope 415.7 ± 64.35, R^2: 0.8925

4.5.2.2 Comparison between transglycosylation rates with Lipid II (Glu, Dans) and Lipid II (Gln, Dans)

Once sufficient Lipid II (Glu, Dans) was obtained, the same enzyme dependency experiments could be repeated. Reactions were exactly as previously described for the 0.1 mg.ml^{-1} lysozyme experiments in Section 4.5.2.1 but with a substrate concentration of 2 μM for both Lipid II (Glu, Dans) and Lipid II (Gln, Dans). This increased substrate concentration allows a greater range of enzyme concentrations (0, 0.02, 0.06, 0.1, 0.2, 0.4, 0.8, 1, 1.5 and 2 μM) to be tested, and to observe whether the phenomenon observed in Section 4.5.2.1 applies at the higher substrate

concentration. Reactions with both substrates were performed in the same 96-well plate to ensure comparable starting fluorescence values were measured, and therefore Lipid II concentrations. Two replicates were performed in each of two plates. Rate in RFU change per second of the initial linear portion of the reaction were calculated. This was plotted against enzyme concentration in μM (Figure 4.18).
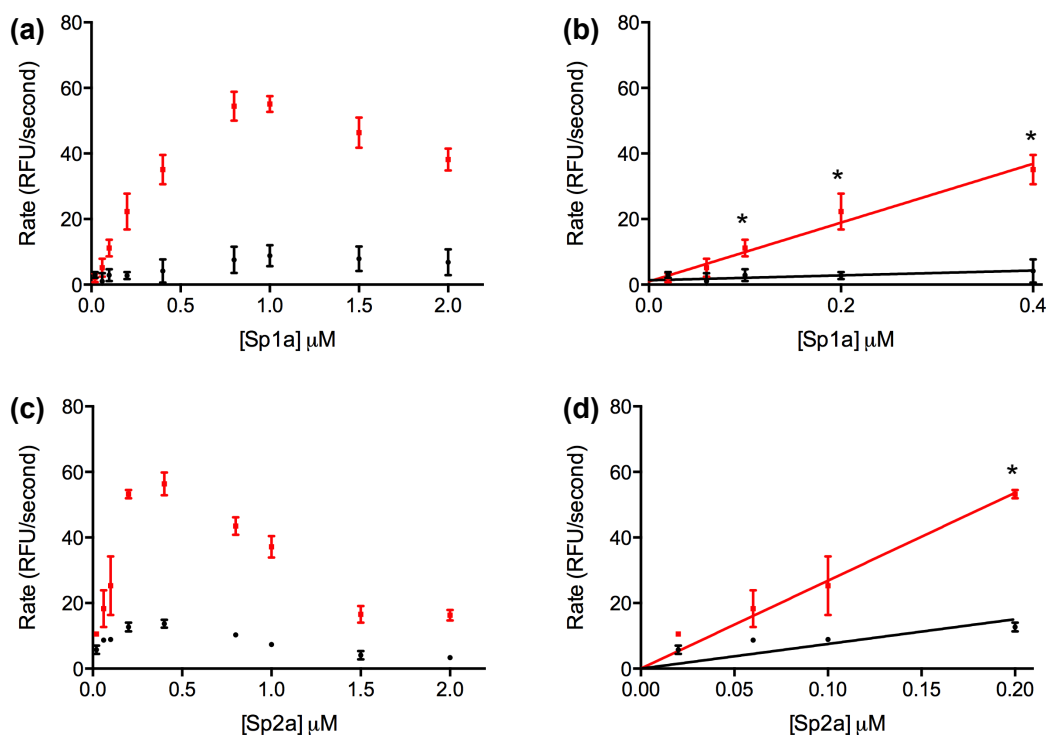
Figure 4.18: Dependency of Lipid II (Glu, Dans) and Lipid II (Gln, Dans) transglycosylation on *S. pneumoniae* PBP1a ((a)and(b)) and PBP2a ((c)and(d)) concentration 2 μM Lipid II (Lipid II (Glu, Dans)(black) or Lipid II (Gln, Dans)(red)) (a) In 50 mM HEPES pH 7.5, 10 mM MgCl$_2$, 150 mM NaCl, 25 % (v/v) DMSO, 0.02 % (v/v) TX-100 with 0.1 mg.ml^{-1} lysozyme plus 0, 0.02, 0.06, 0.1, 0.2, 0.4, 0.8, 1, 1.5 or 2 μM PBP1a. (b) In 50 mM HEPES pH 7.5, 25 mM MgCl$_2$, 200 mM NaCl, 25 % (v/v) DMSO, 0.02 % (v/v) TX-100 with 0.1 mg.ml^{-1} lysozyme plus 0, 0.02, 0.06, 0.1, 0.2, 0.4, 0.8, 1, 1.5 or 2 μM PBP2a. Reaction volume; 50 μL in a Greiner FLUOTRAC^{TM} 600 96-well plate. Excitation at 340 nm, emission at 521 nm with readings at 30 second intervals. RFU change per second calculated from initial linear portion of time-course. Values represent mean ± standard deviation of 4 reactions. Initial linear portion of reaction fitted by linear regression (b) PBP1a: Black, Lipid II (Glu, Dans) Slope 7.418 ±3.077, R^2: 0.8090 ; Red, Lipid II (Gln, Dans) Slope 89.79 ± 5.243, R^2: 0.9302 (d) PBP2a: Black, Lipid II (Glu, Dans) Slope 75.33 ± 9.672, R^2: 0.7654 ; Red, Lipid II (Gln, Dans) Slope 268.3 ± 13.69, R^2: 0.9532. Students' two-tailed t-test performed on (b) and (d) to determine statistical significance. * indicates a *p* value below 0.001.

The same relationship between rate and enzyme concentration was observed as previously (Figure 4.17), with both Lipid II (Glu, Dans) and Lipid II (Gln, Dans) (Figure 4.18 (a) and (c)). An initial linear relationship was observed with increasing concentrations of PBP1a and PBP2a, to 0.4 μM PBP1a and 0.2 μM PBP2a (Figure 4.18 (b) and (d)), double that observed with 1 μM Lipid II, thus implicating an

importance of enzyme:substrate ratio in this phenomenon (below 5:1 Lipid II:PBP1a and 10:1 Lipid II:PBP2a). With PBP1a and PBP2a enzymes, and both substrates, a reduction in rate was observed at higher enzyme concentrations (below 2:1 Lipid II:PBP1a and 5:1 Lipid II:PBP2a). These results are discussed further in Section 4.6.3.1.1.

4.5.3 Moenomycin inhibition of *S. pneumoniae* PBP1a and PBP2a

Inhibition with the specific transglycosylase inhibitor, moenomycin, was confirmed for both PBP1a and PBP2a under the conditions for which the maximum rates were obtained in Section 4.5.2.2. 1 μM PBP1a or 400 nM PBP2a was added to initiate a reaction with 2 μM Lipid II (Lipid II (Glu, Dans) or Lipid II (Gln, Dans)) in the relevant enzyme reaction buffer including 0.1 mg.ml^{-1} lysozyme and increasing concentrations of moenomycin (0, 0.2, 0.4, 0.5, 0.8, 5, 10 or 50 μM) in triplicate. Initial rates as RFU/second were calculated and percentage inhibition compared to the no moenomycin control determined. The data were fitted to a simple saturation model of inhibitor binding to a single site (Equation 1), which enabled IC$_{50}$ values to be extracted (Figure 4.19)

Equation 1: $$\%Inhibition = \frac{100.[I]}{IC_{50}+[I]}$$

The IC$_{50}$ values (Table 4.2) obtained are consistent with tight binding nature of moenomycin as an inhibitor. Perfect results would establish the IC$_{50}$ as 50% of the enzyme concentration, which is close to the values seen for PBP1a. IC$_{50}$ values for PBP2a were also within a range consistent with moenomycin as a tight inhibitor. No difference was observed between inhibition of Lipid II (Glu, Dans) and Lipid II (Gln, Dans). The difference in PBP2a is likely due to experimental error.
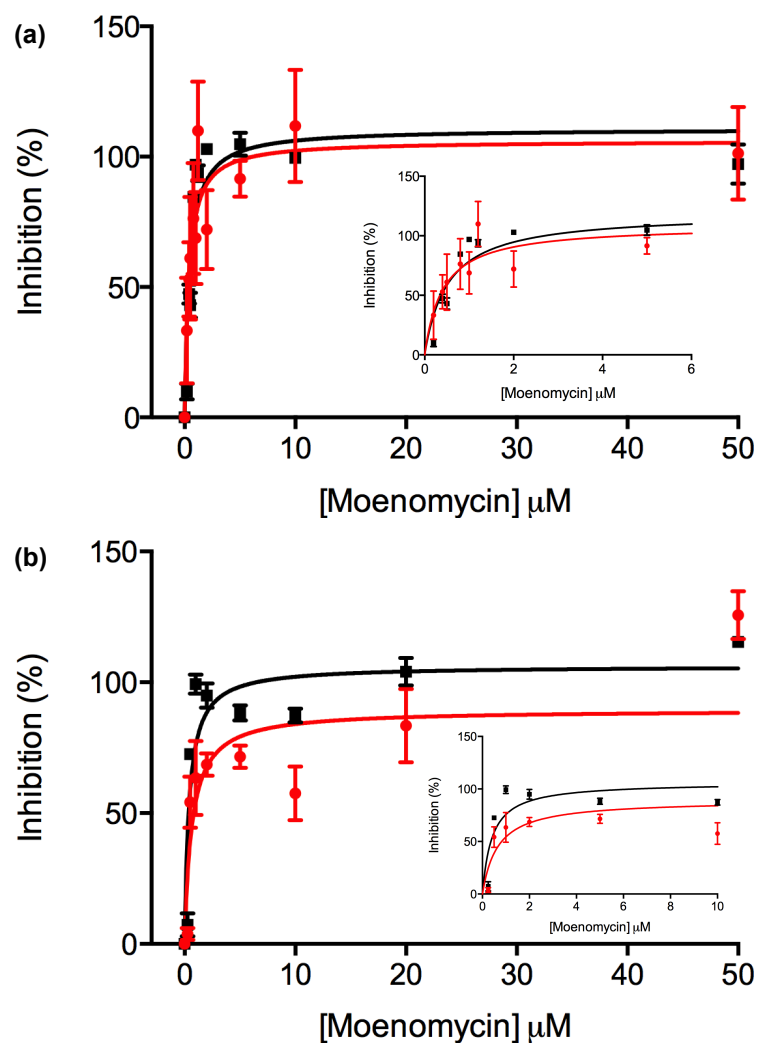
Figure 4.19: Inhibition of *S. pneumoniae* PBP1a (a) and PBP2a (b) activity by moenomycin. 2 μM Lipid II (Lipid II (Glu, Dans)(red) or Lipid II (Gln, Dans)(black)) (a) In 50 mM HEPES pH 7.5, 10 mM MgCl$_2$, 150 mM NaCl, 25% (v/v) DMSO, 0.02 % (v/v) TX-100 with 0.1 mg.ml^{-1} lysozyme plus 0, 0.2, 0.4, 0.5, 0.8, 1, 1.5, 2, 5, 10 or 50 μM moenomycin and 1 μM PBP1a. (b) In 50 mM HEPES pH 7.5, 25 mM MgCl$_2$, 200 mM NaCl, 25% (v/v) DMSO, 0.02% (v/v) TX-100 with 0.1 mg.ml^{-1} lysozyme plus 0, 0.2, 0.4, 0.5, 0.8, 1, 1.5, 2, 5, 10 or 50 μM moenomycin and 400 nM PBP2a. Reaction volume; 50 μL in a Greiner FLUOTRAC^{TM} 600 96-well plate. Excitation was at 340 nm, emission was at 521 nm with readings at 30 second intervals. Inhibition was calculated as a percentage relative to rate without inhibitor and plotted against moenomycin concentration in μM. Values represent mean ± standard deviation of 3 reactions. R^2 values of regression fit: a) Lipid II (Glu, Dans)(red): 0.8841, Lipid II (Gln, Dans)(black): 0.7873. b) Lipid II (Glu, Dans): 0.7274, Lipid II (Gln, Dans): 0.8211

Substrate	IC$_{50}$ (μM)	
	PBP1a	**PBP2a**
Lipid II (Glu, Dans)	0.373 ± 0.107	0.644 ± 0.242
Lipid II (Gln, Dans)	0.431 ± 0.092	0.117 ± 0.117

Table 4.2 IC$_{50}$ values for moenomycin inhibition of *S. pneumoniae* PBP1a and PBP2a transglycosylation

157

4.5.4 Establishing kinetic parameters for Lipid II (Glu, Dans) and Lipid II (Gln, Dans) polymerisation by *S. pneumoniae* PBP1a and PBP2a

In section 4.5.2 it was clearly established that amidated Lipid II is a preferable transglycosylase substrate for *S. pneumoniae* PBP1a and PBP2a. In order to investigate this further, the dependency on substrate concentration was investigated. Enzyme concentrations at which an appreciable rate (although not necessarily maximal) was detected in Figure 4.18 were chosen. A substrate ((Lipid II (Glu, Dans) or Lipid II (Gln, Dans)) concentration range from 1/2 to at least 20 times the enzyme concentration was tested where possible.

Reactions were exactly as previously described for the 0.1 mg.ml^{-1} lysozyme experiments in Section 4.5.2, but with a range of substrate concentrations (made from larger stocks for accuracy)(methods Section 2.7.1). Initial rates of the linear portion of the time-course were calculated in RFU/sec/μg protein and plotted against substrate concentration (Figures 4.20 (PBP1a) and 4.21 (PBP2a)). Data were initially fitted to the Michaelis-Menten equation (Equation 2) using GraphPad Prism. Vmax and K_m could be extracted from this. Note that K_{cat} could not be established by this method as the fluorescence change could not be accurately correlated with an amount of substrate used (Discussed in Section 4.6.2.2).

Equation 2: $$V_o = \frac{V_{max}[S]}{K_m + [S]}$$

A sigmoidal relationship between substrate concentration and rate was noted in all but the PBP1a reaction with Lipid II (Glu, Dans). This may be because one catalytic cycle involves the consumption of two substrates, or indicate some cooperativity in activity. Therefore, the data were also fitted to two variations of the Michaelis-Menten equation using GraphPad prism; one considering the binding and turnover of two substrates per reaction (Equation 3)(Zawadzke *et al.,* 1991) and one taking into account cooperativity in activity (Equation 4)(Copeland, 2000). Although two K_m values for the consumption of 2 molecules of substrate per catalytic turnover could be extracted (Equation 3), only $S_{0.5}$ values could be quoted for the cooperative

equation (4) because the true meaning of this parameter is more obscure. The R^2 value for the equation fit to the data was used to determine the best fit.

Equation 3:
$$V_O = \frac{V_{max}[S]^2}{K_{m(1)}(K_{m(2)}+[S])+[S]^2}$$

Equation 4:
$$V_O = \frac{V_{max}[S]^h}{S_{0.5}+[S]^h}$$

In Figure 4.20 and 4.21, where data are best fitted to Equation 2 the curve is in black, Equation 3 in blue, and Equation 4 in red. Kinetic parameters extracted are detailed in Tables 4.3 and 4.4. The kinetic profiles for each enzyme are shown on the same Y-axis scale in Figure 4.22 for ease of comparison.
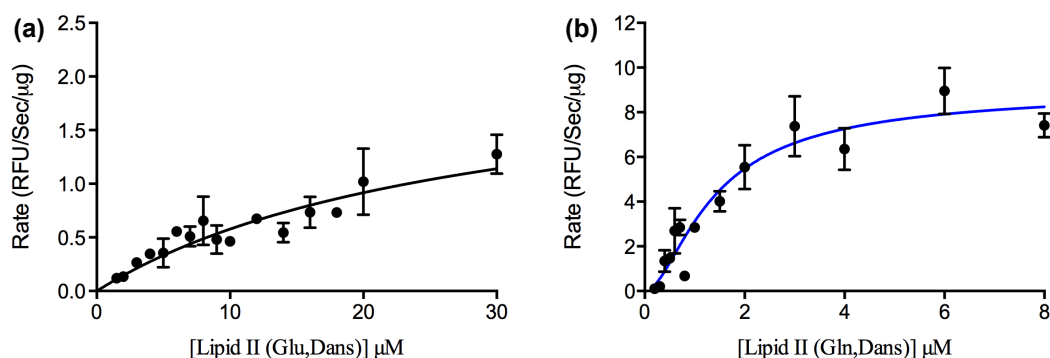
Figure 4.20: Dependency of PBP1a transglycosylation on Lipid II (Glu, Dans)(a) and Lipid II (Gln, Dans)(b) concentrations. Reactions in 50 mM HEPES pH 7.5, 10 mM MgCl$_2$, 150 mM NaCl, 25% (v/v) DMSO, 0.02% (v/v) TX-100 with 0.1 mg.ml^{-1} lysozyme. Excitation at 340 nm, emission at 521 nm with readings at 30 second intervals. RFU change per second per μg PBP1a calculated from initial linear portion of time-course. Values represent mean ± standard deviation of 3 reactions. Data best fitted to either Equation 2 (a) or Equation 3 (b). (a) 1.5 μM – 30 μM Lipid II (Glu, Dans) and 1 μM *S. pneumoniae* PBP1a. Fitted to equation 2. R$_2$ = 0.784. (b) 0.1 μM – 8 μM Lipid II (Gln, Dans) and 0.1 μM *S. pneumoniae* PBP1a. Fitted to equation 3. R$_2$ = 0.898. Note the different X and Y axis scales

The data could not be accurately fitted for 1 μM PBP1a with Lipid II (Glu, Dans) (Figure 4.20 (a)) as the substrate concentration tested were not high enough to allow the rate to plateau. However, it was fitted to equation 2 with an R^2 value of 0.784 indicating poor fit. Rates obtained with Lipid II (Gln, Dans) (Figure 4.20 (b)) were fitted to all three equations. Comparison within GraphPad Prism rejected the null hypothesis that Equation 2 was a better fit than Equation 3, however the null hypothesis that Equation 4 was a better fit than Equation 3 was neither accepted or

rejected. Therefore it can be concluded that the data does not fit standard Michaelis-Menten kinetics but there is no strong evidence for cooperativity. Values for V_{max} and $S_{0.5}$ extracted from Figure 4.20 are shown in Table 4.3.

The data obtained with PBP2a were analysed in the same way (Figure 4.21). For both Lipid II (Glu, Dans) (a) and Lipid II (Gln, Dans) (b) a sufficient range of substrate concentrations were tested to observe a plateau in rate. In both cases a clear sigmoidal relationship was observed between substrate concentration and initial rate. Neither set of data would fit to equation 3 but both fitted to Equation 4 with high R^2 values. This is consistent with cooperativity in the dependency of PBP2a activity on Lipid II. The kinetic values extracted are shown in Table 4.4.
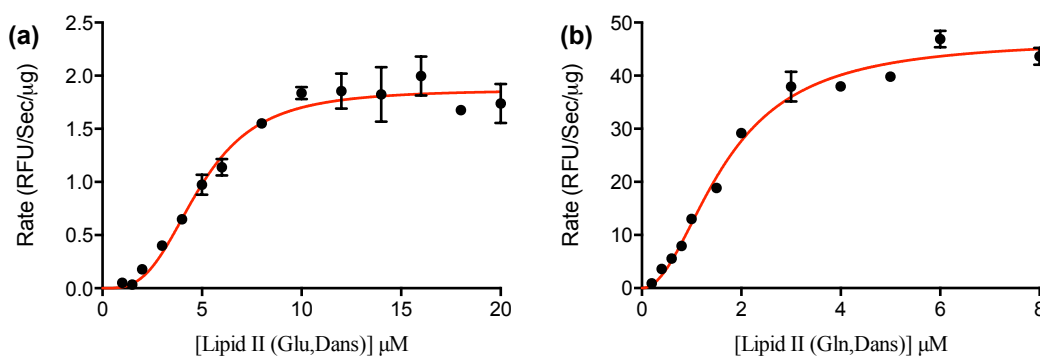
Figure 4.21: Dependency of PBP2a transglycosylation on Lipid II (Glu, Dans)(a) and Lipid II (Gln, Dans)(b) concentrations. Reactions in 50 mM HEPES pH 7.5, 10 mM MgCl₂, 150 mM NaCl, 25% (v/v) DMSO, 0.02% (v/v) TX-100 with 0.1 mg.ml⁻¹ lysozyme. Excitation at 340 nm, emission at 521 nm with readings at 30 second intervals. RFU change per second per μg PBP2a calculated from initial linear portion of time-course. Values represent mean ± standard deviation of 3 reactions. Data fitted to either Equation 4. (a) 1 μM – 20 μM Lipid II (Glu, Dans) and 1 μM *S. pneumoniae* PBP2a. $R_2 = 0.962$. (b) 0.1 μM – 8 μM Lipid II (Gln, Dans) and 0.06 μM *S. pneumoniae* PBP2a.. $R_2 = 0.984$. Note the different X and Y axis scales.

Kinetic parameters for all four enzyme and substrate combinations are shown in Tables 4.3 and 4.4. Data for PBP1a with Lipid II (Glu, Dans) substrate is poor and therefore it cannot be used with much certainty. However, given that a maximal rate has not been reached at 30 μM, the K_m will be at least 15 μM.

Lipid II	V_{max} (RFU/sec/µg)	K_m (µM)	Vmax/K_m	R^2 of fit
Glu, Dans*	*2.22 ± 0.50*	*31.91 ± 11.70*	*0.07± 0.03*	*0.784*
Gln, Dans	9.18 ± 0.42	1: 0.76 ± 0.70 2: 1.55 ± 1.96	5.92 ± 7.49^	0.898

Table 4.3: Kinetic parameters for PBP1a transglycosylase activity. Values for Vmax and K_m extracted from the fits shown in Figure 4.20 and Vmax/K_m calculated as a measure of catalytic efficiency. R^2 of fit shown. * fit is poor and therefore the values are not very accurate for this row.^ value calculated using K_{m2}

Lipid II	V_{max} (RFU/sec/µg)	$S_{0.5}$ (µM)	Vmax/$S_{0.5}$	Hill coefficient	R^2 of fit
Glu, Dans	1.89 ± 0.05	4.85 ± 0.20	0.39 ± 0.02	3.20 ± 0.42	0.962
Gln, Dans	46.85 ± 1.50	1.67 ± 0.17	28.05± 2.99	2.04 ± 0.17	0.984

Table 4.4: Kinetic parameters for PBP2a transglycosylase activity. Values for Vmax, $K_{0.5}$ and the hill coefficient for cooperativity (h) extracted from the fits shown in Figure 4.21 and Vmax/$K_{0.5}$ calculated as a measure of catalytic efficiency. R^2 of fit shown.

Note that K_{m2} for PBP1a with amidated Lipid II is used for subsequent comparisons, as binding of the second substrate molecule is required for formation of the active enzyme complex. A lower $S_{0.5}$(PBP2a) or K_{m2}(PBP1a) for Lipid II (Gln, Dans) compared to Lipid II (Glu, Dans) was calculated showing that both have a higher affinity for the amidated substrate. The $S_{0.5}$ (PBP2a) and K_{m2} (PBP1a) values for Lipid II (Gln, Dans) show comparable affinity and Vmax values identify the transglycosylation rate to be higher for both PBP1a and PBP2a with amidated Lipid II (notably so for PBP2a). The difference in rates can be seen clearly in Figure 4.22 with both substrates plotted on the same Y axis scale. K_{cat}/K_m cannot be calculated without confirmation of the amount of Lipid II consumed in the time-course (discussed in Section 4.6.2.2), however Vmax/K_m and Vmax/$S_{0.5}$ were calculated as measures of catalytic efficiency, and are 85 and 72 fold greater with amidated substrate relative to the non-amidated substrate for PBP1a and PBP2a respectively.
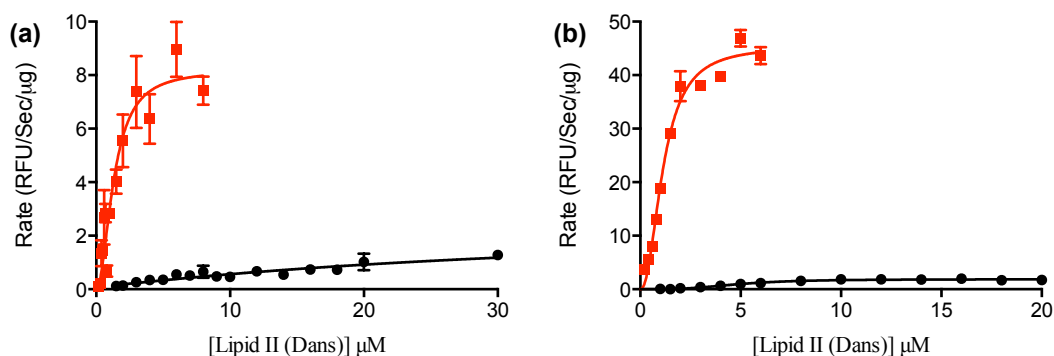
Figure 4.22: Comparison of transglycosylation rates of Lipid II (Glu, Dans) and Lipid II (Gln, Dans). Data from Figure 4.20 and 4.21 plotted on the same Y-axis scale for each enzyme: (a) PBP1a (b) PBP2a. Lipid II (Gln, Dans) shown in red and Lipid II (Glu, Dans) in black

The Hill coefficient (h) is used as a measure of cooperativity. When the value of h is greater than 1 this indicates positive cooperativity, where the binding of one molecule of substrate increases the affinity of another site for further binding (Segel, 1993). The data were fitted to Equation 4 for PBP2a which gave a positive value for the hill coefficient irrespective of substrate amidation. There is uncertainty regarding cooperativity of PBP1a towards Lipid II (Gln, Dans) binding as the data fitted equally well to Equation 3. Equation 4 accounts for cooperativity between molecules of enzyme (discussed in Section 4.6.3.1.2).

4.6 Discussion and future work

This chapter has demonstrated the clear preference for amidated Lipid II by the bifunctional Class A PBPs from *S. pneumoniae*. The importance of the transmembrane spanning domain and dimerisation in this activity were also investigated. This section discusses the data in the context of its biological implications, and highlights the required future work leading from the findings.

4.6.1 Expression and purification of *S. pneumoniae* PBP1a and PBP2a

PBP1a and PBP2a from *S. pneumoniae* D39 were both expressed and purified successfully according to previously established protocols with minimal modifications as described in Section 4.3. The final purity was shown in Figure 4.5. The use of existing protocols gave confidence in the activity of proteins due to earlier experiments.

4.6.2 Limitations of the assay systems used

Before the results are discussed it is important to consider the limitations of the assay systems used. The methodological limitations of these assay systems were covered in a recent review (Galley *et al.,* 2014; attached in Appendix 8). They apply here and are briefly mentioned throughout this section. However, further limitations were identified in the course of this investigation:

Firstly, the use of a fluorescently labelled substrate variant may affect the observed results. It has previously been established that the use of substrates with modifications of the third position amino acid does not significantly affect the kinetic parameters measured (Schwartz *et al.,* 2002; Zhang *et al*., 2007). However, given the findings here that modification to the second position amino acid has a significant effect on transglycosylase activity, and a recent crystal structure of *Staphylococcus aureus* MGT showing that the lactoyl group of the Mur*N*Ac sugar interacts with active site residues (Huang *et al.,* 2012), a large dansyl fluorescence group on the third position may have more of an effect than first thought. The effect of this on the

results is mitigated slightly by the use of 100% dansylated Lipid II in all experiments. This allows relative comparisons between the amidated and non-amidated substrates as the fluorescence group is present in both cases.

An important observation was made during the MST experiment, with respect to stability of enzymes in the buffer conditions used for both assay types. The MST assays of PBP2a were successful in enzyme storage buffer, but protein aggregation was detected by this sensitive technique in the buffers used for transglycosylase assays. This could have been due to use of different enzyme preparations than for previous experiments, although aggregation was observed for both PBP1a and PBP2a, which makes this explanation less likely. The high DMSO concentration used in assays is the most probably reason for protein aggregation, although this is necessary for the observation of activity by the continuous assay (Section 6.4.4). Further work should test whether the DMSO concentration can be reduced for the SDS-PAGE assay to see if this is the case.

The following sections detail the assay specific limitations identified.

4.6.2.1 SDS-PAGE analysis of transglycosylase products

This assay system is unique as it allows visualisation of complete reaction products and comparisons between enzymes and conditions, providing vital information regarding transglycosylase processivity. This quantitative data is very useful and has been used in many studies, including a comprehensive analysis of the chain lengths made by different transglycosylases (Wang *et al.,* 2008). However, the method does have a number of limitations, which should be considered when interpreting results.

- Samples are loaded with no colour dye as bromophenol blue affects the mobility of products. However, loading clear samples into clear wells can lead to loading errors, which cannot be seen. Using combs that make wider wells can help to overcome this, however it limits the number of samples possible on one gel.

- Reproducibility between gels can be problematic. This is particularly an issue with longer glycan chains that may not be able to enter the gel. Additionally, the distinct separation of short glycan chains is highly dependent on the voltage the gel is run at. Despite this, meaningful comparisons can still be made between samples on the same gel.

- No standards for glycan chain length are available to date. Therefore quantification of polymer lengths is an estimate based on known values with the use of controls, unless very short chains are observed and distinguishable.

- The resolution of longer chains is not possible with a standard gel system, in the same way that it is for the shorter chains. A smear is typically seen towards the top of the gel, and distinct chain lengths cannot be observed. This may be overcome using larger SDS-PAGE gels, or gradient gels.

- Finally, quantitative data on reaction rates are not possible, apart from observations of relative rates using a time-course experiment, with low temporal resolution

Despite these limitations the qualitative data available are incredibly useful, and have been used for many studies. Recent advancements at Warwick, with the availability of Dansylated Lipid II substrate (Section 3.6.2) and the installation of a more specific wavelength filter to the Syngene GeneSnap G-Box Gel Doc system, allows the detection of significantly lower quantities of polymerised product than previously possible (Abrahams, 2011). This has significantly reduced the Lipid II concentration required in assays with a subsequent reduction in enzyme, thus enabling more efficient use of the costly substrate.

4.6.2.2 Continuous fluorescence assay

Several assumptions must be made for the use of the continuous assay to follow transglycosylation.

Using this assay for the study of processive enzymes adds a level of complication and uncertainty to the analysis. Lysozyme recognises heptasaccharide units as preferential substrates (ie. Lipid VI) and cleaves off two disaccharides (Vocadlo *et*

al., 2001). However, it is not known how the muramidase interacts with the extending chain whilst it is being polymerised. It is likely that the glycan chains are extended to a certain length out of the catalytic site of the PBP before the muramidase begins to cleave, which complicates analysis. However, the initial linear rate is measured to try to overcome this. A reduction in fluorescence is observed in assays if the muramidase is omitted (not shown) which could be due to the increased distance between dansyl groups and the lipid linker surrounded by a detergent micelle. It may also be as a result of quenching of dansyl groups on adjacent pentapeptide stems. The buffer conditions, particularly the presence of DMSO may have an effect on the fluorescence as well (Section 4.6.2).

The full conversion of Lipid II to soluble disaccharide pentapeptide was not assumed, and therefore K_{cat} (and subsequently K_{cat}/K_m) could not be extracted from the data. Initial publication of this method (Schwartz *et al.,* 2002), optimised with *E. coli* PBP1b was accompanied with a parallel HPLC analysis of products showing full conversion of Lipid II. However, subsequent studies (Helassa *et al.,* 2012; Offant *et al.,* 2010) have assumed full conversion based upon this, despite using different conditions. This assumption should be confirmed by HPLC methods for each enzyme tested. Particularly with the use of TX-100 as a detergent, both in this study and work by Helassa *et al.,* (2012), as some Lipid II may be located inside the large detergent micelle and therefore is not available for polymerisation. An attempt was made to analyse the starting and end products of reactions by TLC (not shown), which could simply and sensitively determine if all Lipid II has been used. However the presence of detergent (DDM) affected the mobility of species and no conclusions could be made. In order for K_{cat} to be calculated by this method, the full conversion of Lipid II should be confirmed by HPLC analysis. $S_{0.5}$ or K_m and V_{max} values were calculated as ratios for comparison of substrates, but K_{cat}/K_m would be a preferential comparison.

4.6.3 Characterisation of *S. pneumoniae* PBP1a and PBP2a transglycosylase activity

4.6.3.1 The effect of Lipid II amidation on PBP1a and PBP2a activity

Lipid II amidation has previously been shown to be important for *S. pneumoniae* PBP1a and PBP2a transpeptidase activity (Zapun *et al.,* 2013). This study focused on the transpeptidase activity of the enzyme and did not separate the two enzyme activities of the bifunctional PBPs. The generally accepted theory is that ongoing transglycosylase activity is required for transpeptidation (Zapun *et al*., 2013) and therefore understanding the crucial first reaction is important in understanding the full assembly of peptidoglycan. The study reported in this chapter aimed to assay solely the transglycosylase activity of PBP1a and PBP2a to investigate substrate specificity.

4.6.3.1.1 Amidated Lipid II is a preferential substrate for PBP1a and PBP2a transglycosylation

Both assay systems showed a clear substrate specificity for amidated Lipid II as a transglycosylase substrate for PBP1a and PBP2a. Amidated Lipid II was polymerised more rapidly by both enzymes as demonstrated by both SDS-PAGE analysis and the continuous fluorescence assay (Figures 4.8, 4.9, 4.12, 4.17, 4.18, 4.21, 4.22 and 4.23). The processivity of PBP1a catalysed transglycosylation was not affected as demonstrated by SDS-PAGE analysis of reaction products (Figure 4.6, 4.7 and 4.8). PBP2a exhibited greater processivity with the preferred substrate, as demonstrated by SDS-PAGE analysis of reaction products (Figures 4.6, 4.7, 4.9, 4.10 and 4.11). The faster rate observed could suggest that the increased processivity may be partly due to the speed of polymerisation.

A linear relationship was observed between rate and PBP1a concentration up to a 5:1 Lipid II:PBP ratio and up to 10:1 Lipid II:PBP for PBP2a (Figures 4.17 and 4.18). At ratios below this, the linear relationship was lost which may be because the transglycosylation reaction requires 2 substrates for every enzyme molecule. This

mechanism suggests several possible explanations for the relationship observed. Firstly, with high enzyme concentrations, a large proportion (approaching all) of the substrate will be bound to enzyme, which could result in quenching of the dansyl group. Alternatively, and perhaps additionally, the binding of 1 molecule of Lipid II to each enzyme molecule as the ratio approaches 1:1 would result in the insufficient formation of an active enzyme complex which requires 2:1 Lipid II: enzyme, and thus an inhibition of rate would be observed. The coupling system is unlikely to explain the reduction in rate seen at higher enzyme concentrations as a sigmoidal relationship between fluorescence and time was not observed, which would suggest that it is limiting, and increasing the lysozyme concentration in Figure 4.17 had no effect.

There is evidence to suggest that PBP2a oligomerises above 500 nM (Section 4.4.6), in which case two enzyme molecules with a donor and an acceptor site each could bind up to 4 molecules of Lipid II at once to form an active complex. This may explain the reduction in rate as the Lipid II:PBP2a ratio approaches 4:1 (Figure 4.18 (c). It may also explain the reduction in rate observed above 500 nM PBP2a generally, as a higher substrate concentration may be required to maintain sufficient levels of activity. The data presented in Figure 4.17 (c) support this hypothesis. This could be studied further by repeating the same experiment presented in Figure 4.18 ((c) and (d)) with a number of substrate concentrations.

4.6.3.1.2 Extraction of kinetic parameter for PBP1a and PBP2a transglycosylase activity

Analysis of the relationship between rate and substrate concentration enabled kinetic parameters to be extracted for both PBP1a and PBP2a (Figures 4.20, 4.21, 4.22 and Tables 4.3 and 4.4). An insufficient range of substrate concentrations was tested for PBP1a with Lipid II (Glu, Dans), which restricted the ability to fit the data to the Michaelis-Menten equation with high accuracy (Table 4.3). The K_m value extracted of 31.91 μM, is much higher than that of 0.76 and 1.55 μM for the binding of the first and second substrate with amidated Lipid II, showing that PBP1a has a much higher affinity for the amidated substrate. The Vmax increase and catalytic efficiency

(measured by Vmax/K_m) increase of approximately 5-fold and 85-fold respectively confirm Lipid II (Gln, Dans) to be a preferential substrate. The Lipid II (Glu, Dans) data could be fitted to standard Michaelis-Menten kinetics (Equation 2), but the binding and turnover of two substrates or cooperativity could not be distinguished between for Lipid II (Gln, Dans)(Equation 3 or 4). No published K_m value of PBP1a transglycosylase activity exists for either substrate for comparison. The data presented for PBP1a with both substrates (Figures 4.20 and 4.22), has a reasonably high level of variation in it, possibly due to the errors associated with calculating rates of slow reactions in particular. This in addition to the need for higher substrate concentrations for Lipid II (Glu, Dans) means that kinetic parameters cannot be confidently extracted and compared for PBP1a. The experiments should be repeated, with higher enzyme concentrations if necessary, to confirm the findings.

The data for PBP2a activity were fitted to a modified Michaelis-Menten equation taking into account cooperativity of substrate binding (Equation 4). The data fit to this very well, as opposed to the standard Michaelis-Menten equation (Equation 2) or a modified version taking into account each kinetic cycle involves consumption of two substrates (Equation 3). The inability to fit the data to Equation 3 may be due to cooperativity in activity, although sigmoidal data may also be observed because the substrate is not pure and the enzyme exhibits distinct catalytic efficiencies with different components within the substrate preparation. The method of synthesis of amidated and dansylated Lipid II, plus confirmation of the products be mass spectrometry (Appendix 6) suggest this is not the case. Additionally, a sigmoidal relationship was seen with 100% non-amidated Lipid II. The data fitted very well to the equation assuming cooperativity, as determined by the R^2 values (Table 4.4). The Hill coefficient (h) of both were calculated as >1 showing positive cooperativity. This coefficient can also be used to estimate the number of binding sites involved in cooperativity (Segel, 1993). Interestingly, PBP2a at 1 μM was used for the Lipid II (Glu, Dans) test (h=3.20 ± 0.42) and at 60 nM for the Lipid II (Gln, Dans) study (h=2.04 ± 0.17). This could suggest the involvement of two sites in cooperativity at concentrations below the proposed K_d and 3 or 4 above it, although the error associated with the data should lead to caution with this theory. A fuller test of enzyme concentrations either side of the K_d for both Lipid II (Glu, Dans) and Lipid II

(Gln, Dans) transglycosylation could be carried out to investigate whether dimerisation affects cooperativity, or vice versa.

The $S_{0.5}$ values extracted show the amidated Lipid II substrate to have a higher affinity for PBP2a, and the V_{max} demonstrates the much higher rate observed (almost 25-fold faster with Lipid II (Gln, Dans)). Vmax/K_m as a measure of catalytic efficiency was 72-fold higher for amidated Lipid II. This clearly demonstrates how preferential amidated Lipid II is as a substrate. Only K_{cat} values are available in the literature for PBP2a and therefore direct comparisons cannot be made. These values were also obtained by assuming full consumption of Lipid II, which affects their reliability (Di Guilmi *et al.,* 2003; Helassa *et al.,* 2012) (discussed in Section 4.6.2.2).

An interesting area of further work in relation to this data is the modelling of Lipid II concentrations within the pneumococcal cell and correlation with the exponential region of the graphs, where transglycosylase rate is increasing rapidly with respect to substrate concentration. This could elucidate methods of PBP regulation through substrate availability. However, analysis would not be trivial as Lipid II concentration is likely to vary between the inner and outer leaflet of the inner membrane and throughout the cell generally. Detailed modelling alongside microscopy to identify the location of Lipid II may enable this study to be performed.

4.6.3.2 Role of the transmembrane region in PBP1a and PBP2a transglycosylase activity

A previous study by Helassa *et al*., (2012) showed that removal of the transmembrane (TM) region of PBP2a gave a 4-fold decrease in glycan chain length produced with non-amidated Lipid II. This was replicated, and additionally shown to be the case with amidated Lipid II (Figure 4.10). However, both results were subsequently shown to be at least in part a result of the TX-100 concentrations used (Section 4.4.5). This could be explained by the presence of a membrane interacting region within the PBP2a transglycosylase domain (Di Guilmi *et al*., 1999), which

was shown to be hydrophobic and is therefore likely to be the part of the protein to interact with TX-100 detergent micelles following removal of the TM region. Therefore, the TX-100 micelle will surround the TM region in full-length PBP2a and the hydrophobic part of the transglycosylase domain in PBP2a-Δ77. This second interaction may affect the Lipid II-PBP2a interactions required for activity, and appears to lead to early release of product.

The role of the PBP1a transmembrane spanning region (TM region) in transglycosylase activity was briefly investigated by SDS-PAGE analysis of reaction products (Figure 4.14). This has not been investigated to date, although the TM region has previously been demonstrated to be important for substrate interaction in *Staphylococcus aureus* MGT and *E. coli* PBP1b transglycosylase activity (Huang *et al.*, 2012; Sung *et al.,* 2009), and possibly *S. pneumoniae* PBP2a as discussed above. Removal of the TM region of PBP1a resulted in poor transglycosylase activity as identified by incomplete use of substrate in an overnight incubation. This was the case for both Lipid II (Glu, Dans) and Lipid II (Gln, Dans), despite the observed difference in the amount of substrate present (Section 4.4.7). This suggests that the TM region is important for PBP1a transglycosylase activity. Although a change in the interaction of the TX-100 detergent micelle with the ΔTM protein compared to full-length cannot be ruled out as for PBP2a above. The presence of a hydrophobic membrane interacting domain has not been demonstrated for PBP1a as for PBP2a and other bifunctional PBPs (Di Guilmi *et al.,* 1999; Lovering *et al.,* 2007; Sung *et al.,* 2009). Further investigation is required to elucidate the importance of the TM region in PBP1a substrate interaction and transglycosylase activity.

Since TX-100 is a mixture of molecular species and thus heterogeneous in nature, future studies of PBP1a and PBP2a may benefit from a more defined detergent-protein *in vitro* system where the direct effects of the detergent relative to the enzyme activity may be investigated.

4.6.3.3 Oligomerisation of PBP2a

In vitro cross-linking experiments and limited proteolysis suggest a self-association of PBP2a dependent on the TM spanning region, which stabilises the transglycosylase domain (Helassa *et al.,* 2012). PBP2a oligomerisation was probed by a further two methods in this chapter (Section 4.4.6). A K_d of 500 nM was established by MST for full-length protein, and a value could not be obtained for PBP2a-Δ77 despite testing up to 64.95 μM. The K_d value is comparable to that of ~100 nM measured for the Class A bifunctional *E. coli* PBP1b (Bertsche *et al.,* 2005), for which dimerisation has been shown by SPR to stimulate transglycosylase activity. Dimerisation has also been observed for *E. coli* PBP1a (Charpentier *et al*., 2002). In this study, size exclusion chromatography was also performed for PBP2a FL and this identified a dynamic equilibrium between two species, estimated to be a dimer and a monomer. No peak was observed in the column flow-through showing that no higher order oligomers or aggregation products were present.

The effect of dimerisation on PBP2a activity was not studied. This would be an interesting experiment in further work, particularly given the stimulated *E. coli* PBP1b transglycosylase activity upon dimerisation (Bertsche *et al.,* 2005), and the possible cooperativity of the dependence of PBP2a on its Lipid II substrate (Section 4.5.4.

4.6.4 Comparison of PBP1a and PBP2a transglycosylase activity

Differences were observed between the transglycosylase activities of PBP1a and PBP2a, and the effect of substrate modifications on each.

SDS-PAGE analysis showed that PBP2a is a more processive transglycosylase under the conditions used. It produces longer glycan chains with both substrate variants than PBP1a and is further stimulated with the use of Lipid II (Gln, Dans) as a substrate.

Similarly the continuous fluorescence assay data (Section 4.5) shows that PBP2a transglycosylation is more efficient than PBP1a. Figure 4.18 shows that at a fixed substrate concentration of 2 μM, a similar maximal initial rate was measured for PBP2a and PBP1a, but at a much lower concentration of PBP2a (400 nM compared to 1 μM). Over double the amount of PBP1a is required to an equivalent rate with the same amount of substrate. PBP2a initial rates are severely affected at high enzyme concentrations with a fixed substrate concentration (Figure 4.18), whereas PBP1a rates are similarly affected but to a much lesser extent. This could be because PBP2a dimerises at higher concentrations and substrate binding leads to increased quenching or depletion of substrate required for the second substrate binding event required for catalysis (Section 4.6.3.1.1).

Both enzymes have a higher affinity for Lipid II (Gln, Dans) than Lipid II (Glu, Dans), reflecting the situation *in vivo* where amidation is known to be essential (Zapun *et al.,* 2013), and both PBP1a and PBP2a have a similar affinity for the amidated substrate. However, the increase in observed V_{max} was much greater for PBP2a with Lipid II (Gln, Dans) than PBP1a, and the reduction in K_m more significant for PBP1a.

The relationship between substrate concentration and rate (Figures 4.20, 4.21 and 4.22) gives evidence of cooperativity in PBP2a transglycosylase activity. Cooperativity of the donor and acceptor sites with respect to substrate binding has recently been observed for a monofunctional transglycosylase from *Staphylococcus aureus* (Bury *et al.,* 2014), and dimerisation has been seen to stimulate *E. coli* PBP1b transglycosylase activity (Bertsche *et al*., 2005) although the recent crystal structure of *E. coli* PBP1b (Sung *et al.,* 2009) shows the protein in a monomer form without the possibility for dimer formation within the crystal packing (Dr D. Roper, Personal Communication). There is no evidence of cooperativity of PBP1a activity with either Lipid II substrate. The possibility of dimerisation was not studied for PBP1a, and would be an interesting investigation for further work.

4.6.5 Biological implications

The results discussed in Sections 4.6.3 and 4.6.4 show that the preference for amidated substrate by the *S. pneumoniae* Class A PBPs extends to their transglycosylase activity. 90% of the peptidoglycan in the pneumococcal cell wall is amidated (Bui *et al.*, 2012) and the lipid II amidase is essential (Zapun *et al.,* 2013), therefore this is clearly a physically small but highly significant chemical modification. Amidation has been shown to be essential for efficient peptidoglycan synthesis *in vitro* (Zapun *et al.,* 2013) and also *in vivo* as non-amidated peptides were only found in monomeric muropeptides (Bui *et al.*, 2012).

The data in this chapter show that the recognition of amidated pentapeptides is important at the transglycosylation stage, and this increased catalytic rate may also have a subsequent effect on transpeptidation. Cross-linking enzymes may preferentially recognise amidated stem peptides, and this would be unsurprising given the proximity of the cross-linking reaction to the second position amino acid. However, the increased rate of glycan chain polymerisation (and processivity in the case of PBP2a) may also help to increase transpeptidation efficiency. An assessment of the influence on transpeptidase activity will be possible following the development of suitable transpeptidase assay technology.

Differences were observed between PBP1a and PBP2a activity both generally, and in their response to amidated substrates (Sections 4.6.3 and 4.6.4). Current evidence suggests that PBP2a is the transglycosylase responsible for peripheral insertion of Lipid II into peptidoglycan and PBP1a for creation of the septum, although it has also been found peripherally (Massidda *et al.,* 2013; Morlot *et al.,* 2003). The greater processivity of PBP2a suggests it continuously inserts Lipid II into the sacculus to grow the cell. PBP2a was also a faster transglycosylase than PBP1a in this study, and this may suggest that a faster rate of peripheral insertion is required to elongate the cell sufficiently before the septum is formed. However, the presence of a histidine tag on the N-terminus of PBP1a should lead to care in making this comparison. The third non-essential transglycosylase in *S. pneumoniae*, PBP1b, has been shown to catalyse transglycosylation *in vitro* (Liu *et al.,* 2006) but its location within the cell has not been identified. It would be of interest to see whether it functionally interacts

with PBP1a, PBP2a or both and whether each produces its own chains or extends those made by one of the other transglycosylases as seen for MGT and PBP2 in *Staphylococcus aureus* (Rebets *et al.,* 2014).

The recent identification of cooperativity between substrate binding in the donor and acceptor site in *Staphylococcus aureus* MGT (Bury *et al.*, 2014) is of great interest and was suggested to be particularly important in initiation of transglycosylation and processivity. The identification of cooperativity in PBP2a suggests interaction between molecules in an oligomer. Both *Staphylococcus aureus* MGT (Chapter 5) and *S. pneumoniae* PBP2a make particularly long glycan chains *in vitro*, so a more detailed study into PBP1a cooperativity would help to identify if this is a mechanism used by more processive enzymes to maintain interaction with the growing chain, or for transglycosylation generally.

4.6.6 Further work

Despite the limitations of the methods used, interesting comparisons and conclusions with regards to *S. pneumoniae* transglycosylation could be made in the context of the current literature. However, it is clear that a better assay system that does not rely on fluorescence is required in parallel to confirm the findings. Previous attempts have coupled the release of undecaprenyl pyrophosphate during transglycosylation to a specific phosphatase PgpB (Touze *et al.,* 2008) with subsequent detection of phosphate release (Abrahams, 2011). However, this was only possible in a stopped assay format due to the limiting activity of the phosphatase. Optimisation of conditions for PgpB activity may enable this to be developed into a continuous assay. Detection of the undecaprenyl pyrophosphate product of transglycosylation is a promising option for a continuous assay without the requirement for a fluorescently labelled substrate. One strategy could be through the use of compounds that bind to undecaprenyl pyrophosphate such as bacitracin (Manat *et al.,* 2014). Modification of bacitracin with a fluorophore reporter could allow indirect monitoring of transglycosylation by binding to the released product. Alternatively, the undecaprenyl lipid linker could be modified, to directly follow release. Modifications to this part of the substrate have less of an effect on substrate recognition than those

on the pentapeptide (Liu *et al.,* 2010). Although significant modifications to the lipid substrate, such as the replacement of undecaprenyl-pyrophosphate with *para*-Nitrophenyl phosphate (*p*-NPP) (Liu *et al.,* 2006), result in a complete loss of activity.

Several lines of further work have been proposed throughout this section. The priority is to complete the analysis of PBP1a by the continuous fluorescence assay by extension of the substrate concentrations used, to enable full comparisons between the PBP1a and PBP2a activities. Testing the relationship between rate and substrate concentration at a range of enzyme concentrations above and below the K_d will allow the effect of PBP2a dimerisation on cooperativity to be elucidated. Using comparable enzyme concentrations for both enzymes and substrates will identify whether cooperativity is substrate or enzyme specific, or a general property of transglycosylases. So far, cooperativity in substrate binding for a monofunctional transglycosylase has been shown (Bury *et al.,* 2014), but it has not been observed in kinetic studies. A repeat of this experiment for PBP2a could allow cooperativity within and between molecules to be distinguished.

By confirming the level of conversion of Lipid II to soluble disaccharide, a full range of kinetic parameters could be obtained enabling differentiation between the effect of amidation on substrate interaction and turnover. Linked to this it would be interesting to structurally characterise the enzyme-substrate interactions involved. The crystal structure of *Staphylococcus aureus* MGT (Huang *et al.,* 2012) shows the lactoyl group of the Mur*N*Ac sugar to interact with the active site, but no more is known about the interaction of the stem peptide given the limitations of the density for the lipid II substrate mimetic in the active site. This could be modelled computationally to identify possible interacting residues, which could be subsequently mutated to test their role. Additionally, the creation of a substrate analogue with at least the first two amino acids in the stem peptide could enable co-crystallisation with *S. pneumoniae* PBPs to identify important residues or regions.

Further investigation into the role of the TM region on oligomerisation and enzyme activity is important. The evidence from this thesis and previous work by Helassa *et al.,* (2012) suggests that PBP2a forms a dimer but the same investigation was not

performed for PBP1a. A study of the oligomeric state of PBP1a and the effect of both on transglycosylation (and subsequent transpeptidation) will be of great interest. It should be remembered that PBPs do not work in isolation and are likely to interact with a number of other cell division proteins, which may modulate their activity (Noirclerc-Savoye *et al.*, 2013; Phillipe *et al.*, 2014)

Several lines of evidence implicate interactions between various PBPs (Section 1.7.2.2) *in vivo*, and it is likely that the TM region as well as other parts of the protein, are involved in these interactions. An ultimate aim is the *in vitro* reconstitution of the cell wall synthetic complexes in *S. pneumoniae*. A crucial first step in this is investigation of the combined activities of PBPs and other cell wall proteins in peptidoglycan synthesis. For example, the effect of PBP2x activity on PBP1a transglycosylase activity could be investigated, as these have been shown to co-localise at points in the cell cycle. The combined functional role of *Staphylococcus aureus* transglycosylases has been identified (Rebets *et al.*, 2014). Although evidence suggests PBP1a and PBP2a localise separately in the pneumococcal cell (Morlot *et al.*, 2003), this investigation only looked at a snapshot in the cell division cycle, and recent studies have suggested that the cell wall complex is more mobile (Tsui *et al.*, 2014). There are likely a plethora of coordinated interactions both spatially and temporally regulated throughout the cell cycle.

Although K_{cat} values could not be calculated for the enzymes in this study, previous work has shown the *in vitro* activity of PBPs to be far below that required to support life. For example, *E. coli* PBP1b catalyses 0.8 transglycosylase reactions/minute/molecule *in vitro*, whereas 300 would be required to support growth and division (Vollmer and Höltje, 2004). Whilst this is not surprising given the removal of the enzyme from its usual interacting partners, many of which are not known (Section 7.1.4), a movement towards a more biologically relevant assay system is paramount. Several methods could be attempted to achieve this;

The inclusion of the *S. pneumoniae* cytoplasmic membrane phospholipids; cardiolipin and phosphatidyl glycerol (Brundish *et al.*, 1967) into assays could help to stimulate PBP activity by providing a more biologically relevant system. This

method has been successful for *E. coli* PgpB (Abrahams, 2011) and *S. pneumoniae* tRNA-dependent ligase MurM (Dr A. Lloyd, Unpublished work) previously.

Purification of PBPs using the novel Styrene Maleic Acid copolymer Lipid Polymer (SMALP) technique could help to stimulate their activity by removing the requirement for detergent extraction for study. SMALP under the correct conditions can form discoidal nanostructures and encapsulate the protein from the membrane, a more biologically relevant system than detergent micelles. This has been used to purify active proteins from liposomes (Jamshad *et al.*, 2011; Knowles *et al.*, 2009; Orwick-Rydmark *et al.*, 2012), overexpressed eukaryotic and prokaryotic proteins, as well as functional complexes from intact drug resistant staphylococcal cells (Paulin *et al.*, 2014 (Appendix 8)). This could be used to isolate complexes of PBPs with the rest of the associated cell wall synthetic machinery following overexpression in *E. coli* strains, or from pneumococcal strains. Proteins purified in this way could then be reconstituted into defined vesicles with known and controlled lipid components, mimicking the *in vivo* environment.

4.6.7 Conclusions

The results shown in this chapter add significantly to the knowledge of transglycosylation by the *S. pneumoniae* Class A PBPs. Either PBP1a or PBP2a must be present in pneumococcal cells for viability, and are proposed to have different roles in cell growth and division. This study has shown for the first time that the activity of Gram positive Class A transglycosylase activity is affected by amidation of the position two stem peptide amino acid and that PBP2a is both more processive and more efficient under the conditions used. Amidation of the stem peptide glutamate has more of an effect on transglycosylase processivity and rate of PBP2a , but a greater impact on the K_m of PBP1a which further supports the theory of their varied roles. The relatively minor modification of glutamate to glutamine in the stem peptide has a very significant role in PBP activity.

Chapter 5. Enzymology of transglycosylation: the characterisation of *Staphylococcus aureus* transglycosylases and novel inhibitors of their activity

5.1 Introduction

Staphylococcus aureus is a globally important opportunistic pathogen (Section 1.9). A greater understanding of the mechanisms by which this bacterium builds its cell wall is of fundamental interest, and could aid in the development of new antibiotics in the future.

5.1.1 Peptidoglycan modifications in *Staphylococcus aureus*

Three main chemical modifications have been identified in mature peptidoglycan of *Staphylococcus aureus*;

- *O*-acetylation of glycan chain muramyl sugar ring C_6 hydroxyl groups by the *oatA* gene product (Bera *et al*., 2005),
- Addition of a pentaglycine interpeptide bridge by the FemXAB peptidyltransferases (Ling and Berger-Bächi, 2003; Rohrer and Berger-Bächi, 2003; Schneider *et al*., 2004; Strandén *et al.,* 1997; Tschierske *et al.,* 1999),
- Stem peptide modification (amidation) of D-glutamate at position 2 to D-isoglutamine by the MurT/GatD complex (Figueiredo *et al.,* 2012; Münch *et al.,* 2012).

Both amidation and the interpeptide bridge are essential for full expression of methicillin resistance in MRSA (Münch *et al*., 2012; Rohrer and Berger-Bächi, 2003). Depletion of amidation, from the normally almost completely isoglutamine containing state (Schleifer and Kandler, 1972) reduces growth rate and increases susceptibility to both β-lactams and lysozyme in MRSA strains (Figueiredo *et al.,*

2012). This relatively minor chemical modification has hugely significant effects on *Staphylococcus aureus* viability and antibiotic resistance.

5.1.2 *Staphylococcus aureus* penicillin-binding proteins

β-lactam sensitive strains of *Staphylococcus aureus* possess 4 PBPs; one class A bifunctional (PBP2), two class B monofunctional transpeptidases (PBP1, PBP3)(Pereira *et al.,* 2007; Pinho *et al.,* 2000; Sauvage *et al*., 2008) and one low molecular weight type 5 PBP (PBP4), which is unusual in displaying transpeptidase activity (Kozarich and Strominger, 1978; Qiao *et al.*, 2014; Wyke *et al.,* 1981). This is important for maintenance of the high level of cross-linking (up to 95%) observed in *Staphylococcus aureus* peptidoglycan (Gally and Archibold, 1993) and is suggested to be the mechanism by which PBP4 contributes to β-lactam resistance in community acquired MRSA infections (Kozarich and Strominger, 1978; Memmi *et al.,* 2008). Methicillin resistant strains have an additional acquired Class B transpeptidase, PBP2a, the expression of which is induced in the presence of β-lactams and it subsequently forms peptidoglycan in a cooperative manner with PBP2 (Pinho *et al.,* 2001). This interaction is important for the enzymatic activities of both proteins as demonstrated by the dramatically reduced MIC for methicillin upon inhibition of PBP2 transglycosylase activity (Pinho *et al.,* 2001).

The single bifunctional penicillin-binding protein; PBP2 along with two additional monofunctional transglycosylases; MGT and SgtA catalyse polymerisation of Lipid II into the glycan chains of peptidoglycan (Reed *et al.,* 2011; Wang *et al.,* 2001). PBP2 is essential for viability in susceptible strains and in resistant strains upon β-lactam treatment (Pinho *et al.,* 2001). MGT and SgtA have been shown to be nonessential in methicillin susceptible *Staphylococcus aureus* (MSSA). However, MGT becomes essential for viability in the absence of PBP2 transglycosylase activity where SgtA remains nonessential (Reed *et al.,* 2011). This may be due to the inability of SgtA to compensate for MGT or PBP2 activity due to differential expression in the cell cycle.

The current catalytic model for transglycosylation by PBPs (Section 1.7.3) is that the formation of long carbohydrate polymers of β-1,4-linked *N*-acetylglucosamine (Glc*N*Ac) and *N*-acetylmuramic acid (Mur*N*Ac) involves an initiation phase (two Lipid II molecules bind to the donor and acceptor active sites) and an elongation phase (the addition of further Lipid II monomers). The processivity demonstrated by the transglycosylases appears to be tightly regulated between different enzymes and species, by a yet unknown mechanism. The interactions of *Staphylococcus. aureus* PBP2, MGT and SgtA, along with other cell wall synthetic enzymes (PBP1 and PBP2a) has been demonstrated (Reed *et al.,* 2011). These have recently been shown to include interactions with wall teichoic acid (WTA) (Farha *et al.,* 2013) providing further evidence for the existence of a large complex responsible for the highly coordinated process cell wall synthesis *in vivo* (Leski and Tomasz, 2005).

5.1.3 Studying the *Staphylococcus aureus* PBPs

The importance of Lipid II amidation in *Staphylococcus aureus* cell wall viability is clear (Figueiredo *et al.,* 2012; Münch *et al.,* 2012), and therefore delineation of the interaction between cell wall biosynthetic enzymes and amidated Lipid II is imperative for an understanding of staphylococcal peptidoglycan synthesis. Now, particularly given the identification of the crucial role of amidation in the transglycosylase activity of *S. pneumoniae* PBPs, the parallel investigation in *Staphylococcus aureus* is of great interest.

5.1.4 Transglycosylase inhibitors

Several comprehensive reviews of transglycosylase inhibitors have been published to date, including Halliday *et al.* (2006), Ostash and Walker (2005) and recently Galley *et al.* (2014), all highlighting these enzymes as promising targets for future antimicrobial discovery. Inhibition of the extracellular steps in cell wall synthesis has been a successful strategy historically, with the well-known β-lactam class of antibiotics targeting transpeptidation. Transglycosylases can be inhibited by direct targeting of the enzyme, or through limiting the availability of the Lipid II substrate (Figure 5.1). Several classes of antibiotics bind to the peptidoglycan precursor, Lipid

II, inhibiting cell wall synthesis, such as glycopeptides, ramoplanin, type B lantibiotics, mannopeptimycins and recently identified, teixobactin (Breukink *et al.,* 2003; Chatterjee *et al.,* 2005; Ling *et al.,* 2015; Kahne *et al*., 2005; Ruzin *et al.,* 2004; Walker *et al.,* 2005).
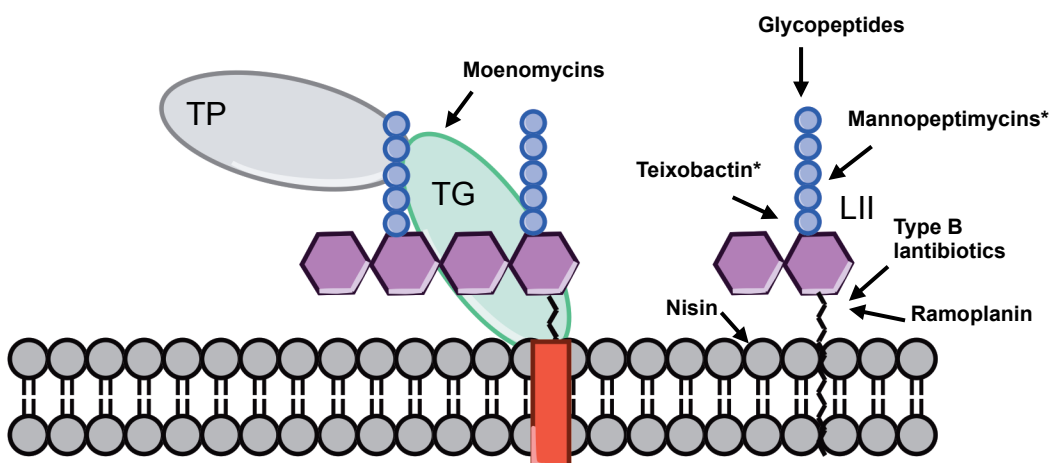
Figure 5.1: Inhibitors of transglycosylation. Known inhibitors of bacterial transglycosylases illustrated for a bifunctional penicillin-binding protein. TG; transglycosylase domain. TP; transpeptidase domain. LII: Lipid II. Arrow indicates presumed stage of intervention where known. * indicates unknown position of intervention

No compounds that directly bind to transglycosylases have been developed for human use to date, although the natural product inhibitor moenomycin strongly validates the classification of these enzymes as antibiotic targets (Figure 5.1). Moenomycin, is a glycolipid antibiotic produced by various *Streptomyces* species. It is active against a large number of Gram-positive bacteria (Welzel, 2005) and recently identified as active against the Gram-negative multidrug resistant *Helicobacter pylori* (Tseng *et al.,* 2014). Moenomycin mimics the structure of the product of a transglycosylation reaction between two molecules of lipid II (referred to as Lipid IV) and blocks the donor site of the transglycosylase. However, its poor pharmacokinetic properties including a long half-life and poor absorption have prevented clinical development for use in humans. The use of moenomycin in animal feed as a growth promoter, has not resulted in development of resistance to the drug in contrast to the use of other antimicrobials which has commonly resulted in rapid resistance development. *In vitro* selection of moenomycin resistance has been shown to occur at only very low frequency (Rebets *et al.,* 2014) and even then, without horizontal gene transfer between organisms (Butaye *et al.,* 2003). The structure of

182

moenomycin along with its biosynthesis and chemical properties has recently been extensively reviewed (Ostash and Walker, 2010).

The lack of natural resistance to moenomycin, plus the theory that antibiotics targeting the transglycosylase step of peptidoglycan synthesis may be less prone to the development of resistance as the polysaccharide backbone is not altered between wild-type and antibiotic resistant strains (Ritter and Wong, 2001), suggest transglycosylases to be good antibiotic targets. Additionally the 5 motifs of the transglycosylase domain are highly conserved (Huang *et al.,* 2012). These reasons make the transglycosylases very promising leads for drug development, as shown recently by Zuegg *et al.* (2015) (Section 5.7)

A better understanding of the mechanisms by which *Staphylococcus aureus* synthesises the carbohydrate polymer of its cell wall by transglycosylation will enable the future design of novel inhibitors against this promising target. This chapter details efforts to understand the substrate specificity of the *Staphylococcus aureus* transglycosylases PBP2 and MGT, and identifies two new inhibitors of MGT glycan chain polymerisation.

5.2 Experimental Aims

- To express and purify MGT and PBP2 from *Staphylococcus aureus* Mu50.
- To establish optimal conditions for the study of MGT and PBP2 transglycosylase activity by SDS-PAGE separation.
- To examine the role of Lipid II amidation on transglycosylase activity of MGT and PBP2.
- To establish conditions for observation of transglycosylase activity of MGT by a continuous fluorescence assay.
- To characterise novel carbohydrate based putative transglycosylase inhibitors *in vitro*

5.3 Expression and purification of the *Staphylococcus aureus* Mu50 transglycosylases; MGT and PBP2

In order to study the enzymatic activity of the *Staphylococcus aureus* transglycosylases, the extracellular domains of MGT and PBP2 from the methicillin- and vancomycin intermediate (VISA) resistant Mu50 strain (Hiramatsu *et al*., 1997) were expressed and purified. Constructs for expression were obtained from Dr K. Abraham (University of Warwick) and Dr N. Strynadka (UBC, Canada), and are detailed in Table 5.1.

Construct	Selection	Source
pET46::*mgt-Δ67*	Ampicillin	Dr K. Abrahams (University of Warwick)
pET41a::*pbp2-Δ59*	Kanamycin	Dr N. Strynadka (UBC, Canada)

Table 5.1 Gene constructs provided for expression and purification of *Staphylococcus aureus* Mu50 transglycosylases

5.3.1 Expression and purification of *Staphylococcus aureus* MGT-Δ67

Expression and purification of MGT-Δ67 was as described in (Abrahams, 2011), with a single modification. Here, IMAC (Section 2.4.3.1) was on a 5 mL HiTrap TALON® crude column (GE Healthcare) on an ÄKTApurifier 100 (GE Healthcare) pre-equilibrated and washed with PBS + 150 mM NaCl before elution with a linear gradient of 0 – 300 mM imidazole in the same buffer. A high level of purity was achieved as shown in Figure 5.4.

5.3.2 Expression and purification of *Staphylococcus aureus* PBP2-Δ59

Expression and purification of PBP2-Δ59 was as previously described in Lovering *et al.,* (2007) with the following alterations: a second Superdex 200 gel filtration purification was carried out by pooling fractions from the first fractionation on this column, concentrating them to a small volume and reapplying to the column. Following buffer exchange to remove salt using a PD-10 desalting column (Section 2.4.3.4), a 1 mL ResourceQ column (GE Healthcare) was used as a replacement for 1

mL MonoQ anion exchange and run in an identical manner, with a salt gradient from 0-600 mM NaCl. Despite the modification of the protocol to include the addition of cOmplete™ EDTA-free Protease Inhibitor Cocktail (Roche), and all steps being carried out at 4°C, a high level of protein degradation was observed (Figure 5.2). A large amount of PBP2-Δ59 did not bind to the ResourceQ column, which may suggest it is incorrectly folded, as this method of purification has been used previously for this protein.
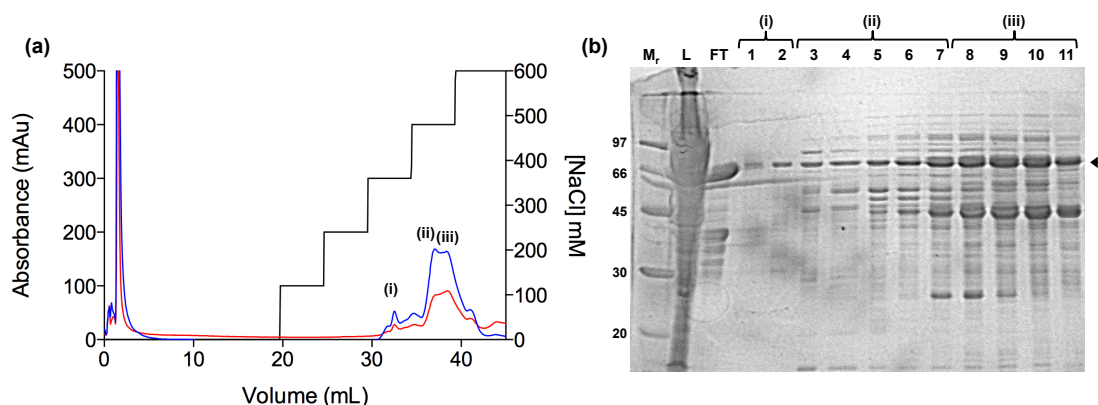
Figure 5.2: Purification of *Staphylococcus aureus* Mu50 PBP2-Δ59 with a final anion exchange step. (a) Anion exchange chromatogram using a ResourceQ column with a stepwise elution up to 600 mM NaCl. 3 main peaks were identified by (i), (ii) and (iii). The blue and red traces refer to absorbance at 280 and 254 nm respectively.b) 12% SDS-PAGE Coomassie-stained gel showing the three main peaks from anion exchange. M_r, molecular weight markers (kDa); L, protein loaded onto column following IMAC, and 2 rounds of gel filtration; FT, protein which did not bind to the ResourceQ column; (i) 1,2, peak (i) from (a); (ii) 3-7, peak (ii) from (a); (iii) 8-11, peak (iii) from (a). Location of PBP2-Δ59 indicated by arrow on the gel.

Due to these issues, and as PBP2-Δ59 was required for activity assays rather than structural analysis, the gel filtration and anion exchange steps were excluded, and protein purified by a single IMAC step (Section 2.4.3.1) in order to minimise handling, shortening the overall time period of purification that may have contributed to the protein degradation observed. IMAC was conducted on a 5 mL HiTrap column (GE Healthcare) at 4°C as described by Lovering *et al.,* (2007) with a stepwise elution at 20 mM, 50 mM and 100 mM imidazole (Figure 5.3). The second eluted peak (ii) was selected as the first did not bind as strongly to the resin, and the third peak contained very little PBP2-Δ59. Peak (ii) was buffer exchanged by PD-10 Desalting column (GE Healthcare) to remove imidazole. The final protein in 10 mM Tris pH 8, 0.2 M NaCl and 0.28 mM LDAO was flash frozen in liquid nitrogen and stored at -80°C.
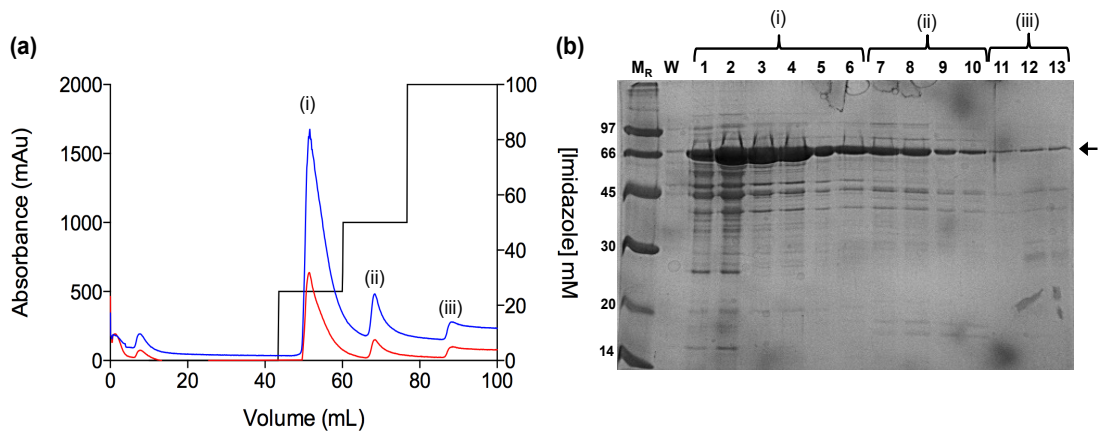
Figure 5.3: Purification of *Staphylococcus aureus* Mu50 PBP2-Δ59 by a single IMAC step. (a) IMAC chromatogram using a 5 mL HiTrap column with a stepwise elution with 20 mM (i), 50 mM (ii) and 100 mM (iii) imidazole. The blue and red traces refer to absorbance at 280 and 254 nm respectively. b) 12% SDS-PAGE Coomassie-stained gel showing the three main peaks from IMAC purification. M_r, molecular weight markers (kDa); W, elution from extensive buffer exchange washing step; (i) 1-6, fractions from peak (i) at 20 mM imidazole; (ii) 7-10, fractions from peak (ii) at 50 mM imidazole; (iii) 11-13, fractions from peak (iii) at 100 mM imidazole. Location of PBP2-Δ59 indicated by arrow on the gel.

5.3.3 Final purity of *Staphylococcus aureus* Mu50 MGT-Δ67 and PBP2-Δ59

Staphylococcus aureus MGT-Δ67 and PBP2-Δ59 were expressed as above. The final purity of both recombinant proteins is shown in Figure 5.4.
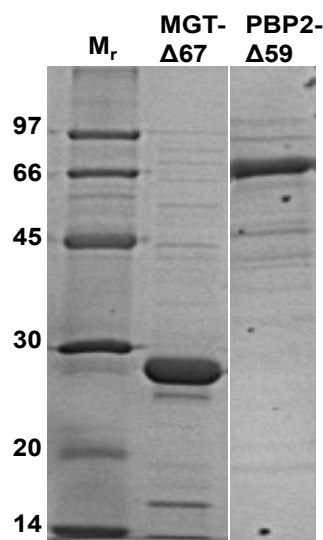
Figure 5.4: 12% Coomassie–stained gel of the final purity of *Staphylococcus aureus* transglycosylases to be studied. M_r, Molecular weight markers (kDa). Lanes are labelled with the relevant PBP.

5.4 Analysis of *Staphylococcus aureus* MGT-Δ67 transglycosylase products by SDS-PAGE and continuous fluorescence assay

Observation of MGT-Δ67 transglycosylase activity was documented previously (Abrahams, 2011; Terrak and Nguyen-Distèche, 2006) and as a result, conditions were available as a starting point for this study. MGT-Δ67 was expressed and purified in the same manner as before (Abrahams, 2011) and therefore it was expected that transglycosylation would be observed under the same conditions.

The conditions used previously for transglycosylase assays (Abrahams, 2011; Terrak and Nguyen-Distèche, 2006), and initially here were 20 mM Tris pH 8.0, 10 mM MgCl$_2$, 0.1% (w/v) DDM, 20% (v/v) DMSO, 0.05% (v/v) decyl PEG. Enzyme and Lipid II were incubated at 20°C for 1 hour followed by 60°C for ten minutes at which point samples were centrifuged at 13,000 rpm to remove protein.

5.4.1 SDS-PAGE separation of MGT-Δ67 transglycosylase products

The products of Lipid II polymerisation were initially analysed by SDS-PAGE separation. Previous work was conducted with [^{14}C]-Lipid II, with detection by tritium phosphor screen (Abrahams, 2011). The use of dansylated Lipid II (Section 3.6.2) as in Chapter 4, enabled more rapid observation of results, and the use of a short-pass filter and blue light convertor within a Syngene GeneSnap G-Box Gel Doc system allowed small quantities of Lipid II to be used. Previous experiments required the use of 4.4 mM Lipid II to enable a signal to be observed following autoradiography. Initial fluorescence assays were carried out with Lipid II (Glu, Dans) at a concentration of 130 μM.

5.4.1.1 Dansylated Lipid II as a substrate for *Staphylococcus aureus* MGT-Δ67

Previous work has demonstrated the ability of the *S. pneumoniae* transglycosylases to polymerise Lipid II (Glu, Dans) (Chapter 4 and references therein). Therefore it was initially surprising that preliminary assays with MGT-Δ67 demonstrated no

transglycosylase activity with the same substrate. An assay was subsequently conducted using varying ratios of labelled and non-labelled Lipid II in order to identify whether the lack of activity was enzyme or substrate specific. Reactions containing 130 μM total Lipid II in 30 μL reaction buffer including 45 μM MGT-Δ67 were incubated as described above. Lipid II was either 100% Lipid II (Glu, Dans), 50:50 Lipid II (Glu, Dans):Lipid II (Glu), 20:80 Lipid II (Glu, Dans):Lipid II (Glu), 10:90 Lipid II (Glu, Dans):Lipid II (Glu), or 100% Lipid II(Glu). The dansyl group enabled the fluorescent lipid II to be detected, and a fluorescent analogue of vancomycin (which binds to the terminal D-Ala-D-Ala of the pentapeptide stem (Nieto and Perkins, 1971)): VanFL (BODIPY FL conjugate of vancomycin) was used post reaction to detect the non-labelled Lipid II in polymers. This was shown previously to be sufficiently sensitive for detection of glycan polymers of MGT-Δ67 (Abrahams, 2011).
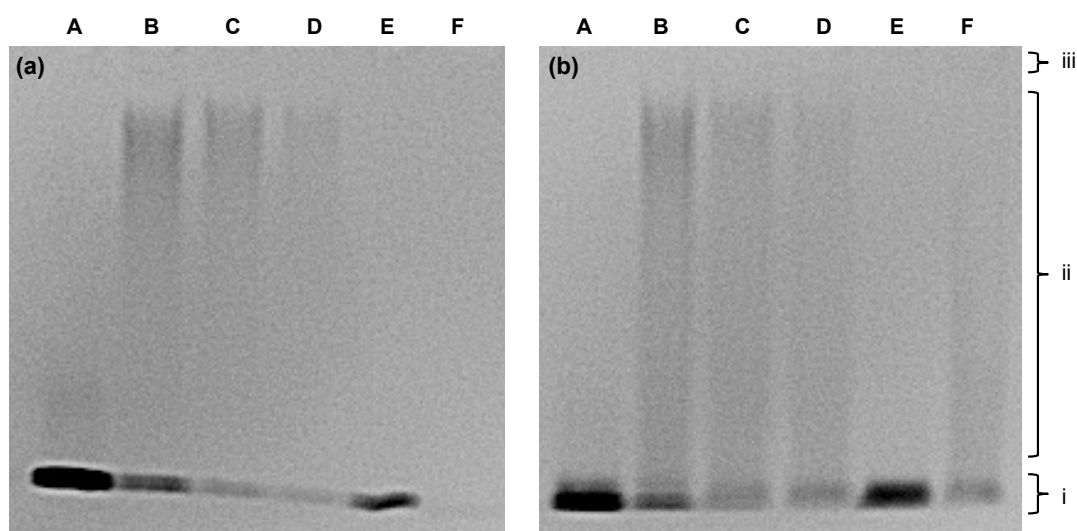
Figure 5.5: Lipid II (Glu, Dans) as a substrate for MGT-Δ67 transglycosylation. 130 μM total Lipid II was polymerised with 45 μM MGT-Δ67: A, 100% Lipid II (Glu, Dans); B, 50:50 Lipid II (Glu, Dans):Lipid II (Glu); C, 20:80 Lipid II (Glu, Dans):Lipid II (Glu); D, 10:90 Lipid II (Glu, Dans):Lipid II (Glu); E, 10:90 Lipid II (Glu, Dans):Lipid II (Glu) no enzyme control; F, 100% Lipid II(Glu). Reactions were split and products of transglycosylation were separated on a 8.5% T/2.7% C SDS-PAGE gel with (b) or without (a) treatment with 24 μM VanFL. Dansyl fluorescence at 521 nm, and VanFL at 512 nm was detected using a blue light converter and short pass filter on a GeneSnap Gel Doc. (i) denotes unpolymerised Lipid II; (ii) glycan chains of varying lengths (iii) denotes where high molecular weight material, unable to enter the gel would be found.

Reactions were split into two 15 μL aliquots, and half treated with 24 μM VanFL for 5 min at room temperature in the dark. The VanFL treated and un-treated samples were analysed by SDS-PAGE and fluorescence of both dansyl and VanFL detected by blue light converter and short-pass filter for fluorescence at 521 and 512 nm respectively.

188

Figure 5.5 demonstrates that MGT-Δ67 will not use 100% dansyl labelled Lipid II as a substrate (Figure 5.5(a) A and (b) A), but will polymerise it when mixed with non-labelled Lipid II (Lane B, C, D). Lane F shows that MGT will polymerise the more native non-fluorescent Lipid II. *S. pneumoniae* bifunctional Class A PBPs; PBP1a and PBP2a (with and without the transmembrane spanning region) will polymerise 100% labelled Lipid II, and this suggests that the larger two domain PBPs are able to accommodate the dansyl fluorescence group more easily. Previous work demonstrating that fluorescently labelled Lipid II does not significantly affect transglycosylation kinetic parameters was only with bifunctional PBPs (Schwartz *et al.,* 2002; Zhang *et al.,* 2007), which makes this an important observation for the use of fluorescently labelled substrates.

The detection of both dansyl and VanFL fluorescence in Figure 5.5 (b) (as wavelengths for detection are close so both would be detected) and detection of only a proportion of all material through dansyl fluorescence in Figure 5.5 (a) does not allow direct comparisons between amounts of Lipid II polymerised to be made between all of the conditions. However, it is clearly demonstrated that 100% Lipid II (Glu, Dans) was not polymerised into glycan chains by MGT-Δ67.

5.4.1.2 Requirement of MGT-Δ67 for DDM in transglycosylase assay buffer

The use of different detergents for Lipid II and enzyme will lead to mixed micelles which may result in mixing effects such as those observed in Section 6.4.4, which could affect future continuous fluorescence assays. Therefore, the requirement for 0.1% (w/v) DDM in the assay buffer in addition to 0.05% (v/v) decyl PEG was tested in 15 μL assays performed as in Section 5.4.1.1 with a 50:50 mix of Lipid II (Glu, Dans): Lipid II (Glu). Reaction buffers were as before (Section 5.4) with and without 0.1% (w/v) DDM and control reactions without the addition of 45 μM MGT were included (Figure 5.6). Gel imaging was by detection of dansyl fluorescence.

DDM was found to have little difference on the extent of polymerisation (Figure 5.6). Slightly more starting material was present in the absence of DDM, however, the smear of product towards the top of the gel is more intense also, suggesting an

inaccuracy in gel loading. Consequently, DDM was omitted from reaction buffers as its removal did not impact upon transglycosylase activity and removed the unknown potential for complication of the results by the formation of mixed micelles which could have significant effects on assay read-outs.
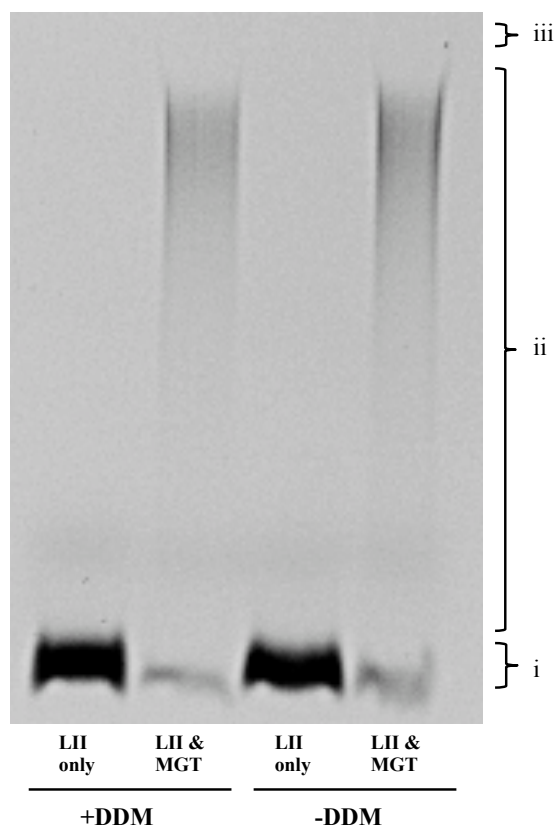
Figure 5.6: Requirement of DDM for MGT-Δ67 transglycosylation. 130 μM total Lipid II (50:50 Lipid II (Glu,Dans): Lipid II (Glu)) was polymerised with 45 μM MGT-Δ67 with or without 0.1% (w/v) DDM as indicated below the gel. LII only: 130 μM Lipid II mix plus enzyme storage buffer. LII & MGT; 130 μM Lipid II mix plus 45 μM MGT-Δ67. Products of transglycosylation were separated on a 8.5% T/2.7% C SDS-PAGE gel. Dansyl fluorescence at 521 nm was detected using a blue light converter and short pass filter on a GeneSnap Gel Doc. (i) denotes unpolymerised Lipid II and (ii) glycan chains of varying lengths . (iii) denotes where high molecular weight material, unable to enter the gel would be found.

5.4.1.3 Cloning and expression of *Staphylococcus aureus* Mu50 MGT-Δ28

Following unsuccessful attempts to polymerise neat Lipid II (Glu, Dans) with MGT-Δ67 (Section 5.4.1.1), and the discovery that a construct containing the amino-terminal membrane spanning region of MGT starting at residue 28 has catalytic activity ten times faster than the -Δ67 version (Huang *et al.*, 2012), a "full-length" MGT construct was cloned, expressed and purified. The sequence encoding residues

190

Q28-R269 from *Staphylococcus aureus* Mu50 *mgt* was cloned into the pET15b vector as described in Section 2.3 and by Huang *et al.* (2012). Successful cloning was confirmed by sequencing. Residues 1-27 were not included as the full-length protein was easily degraded. pET15b::*mgt-Q28-R269* will be referred to as pET15b::*mgt* for the remainder of this thesis. Expression and purification was as described by Huang *et al*., (2012) with a Superose 6 10/300 GL (GE Healthcare) column used instead of Superdex 200 10/300 GL (GE Healthcare) and yielded highly pure MGT(-Δ28) (Figure 5.7).
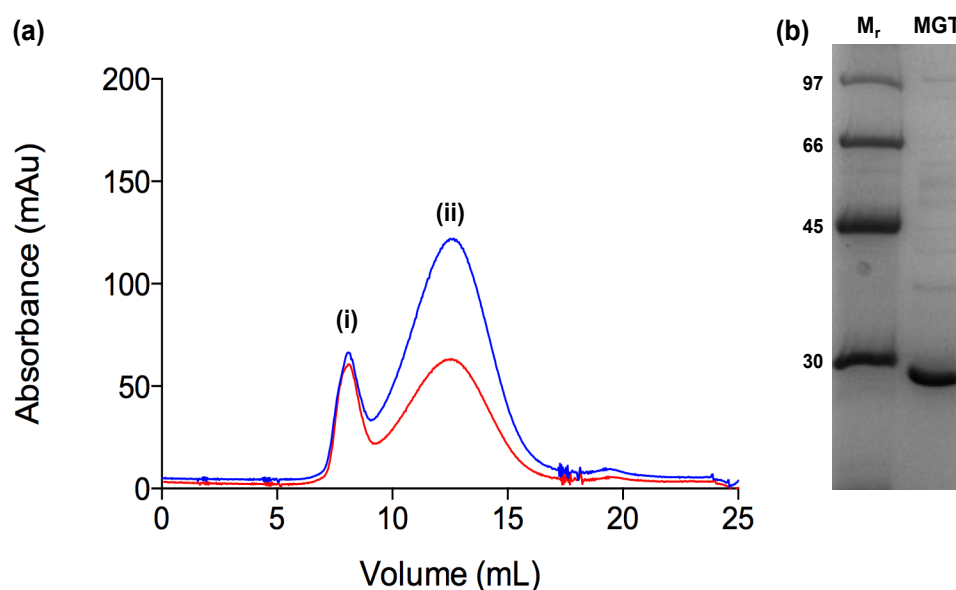
Figure 5.7: Purification of *Staphylococcus aureus* Mu50 MGT-Δ28(FL) by size exclusion chromatography and final purity. (a) Size exclusion chromatogram using the Superose 6 10/300 GL column. (i) shows the elution of aggregated material in the column void volume and (ii) the elution of MGT FL. The blue and red traces refer to absorbance at 280 and 254 nm respectively. (b) 12% SDS-PAGE Coomassie-stained gel showing the final purity of MGT FL following IMAC and size exclusion chromatography. M_r, molecular weight markers (kDa);; MGT, 10 μg MGT FL.

5.4.1.4 Demonstration of full-length *Staphylococcus aureus* MGT(-Δ28) transglycosylase activity by SDS-PAGE

The transglycosylase activity of MGT-Δ28(FL) was compared to that of MGT-Δ67 (Section 5.4.1.2). Huang *et al*., (2012) observed MGT-Δ28(FL) activity by HPLC, and their assay conditions were amended for SDS-PAGE analysis, by the removal of 14% (v/v) MeOH necessary for HPLC and addition of 20% (v/v) DMSO as required by MGT-Δ67. Conditions used were 50 mM Tris.HCl pH 8, 10 mM $MnCl_2$, 0.08%

(v/v) decyl PEG, 20% (v/v) DMSO. Reactions were incubated at 20°C for 1 hour before removal of protein (Section 5.4).

15 μL assays were performed as in Section 5.4.1.2 with a 50:50 mix of Lipid II (Glu, Dans):Lipid II (Glu). Reaction buffers were as described in this section for MGT-Δ28(FL) and Section 5.4.1.2 (without DDM) for MGT-Δ67. The total Lipid II concentration was halved to 65 μM to reduce the quantity of costly substrate required, given that sufficient signal was observed under transillumination previously (Figure 5.6), and the 50:50 ratio of labelled to non-labelled Lipid II was maintained. The Lipid II:enzyme ratio was also preserved by reducing the enzyme concentration to 22.5 μM. Reaction products were separated by SDS-PAGE and detected by dansyl fluorescence at 521 nm (Figure 5.8).
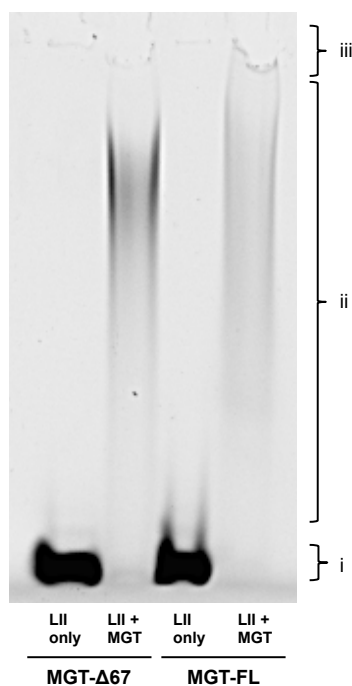
Figure 5.8: SDS-PAGE separation of MGT-Δ67 and MGT-Δ28(FL) transglycosylase products 65 μM total Lipid II (as 32.5 μM Lipid II (Glu, Dans) and 32.5 μM Lipid II (Glu)) were polymerised with 22.5 μM MGT-Δ67 or MGT-Δ28(FL) (MGT-FL) as indicated below the gel. LII only, 65 μM Lipid II mix in reaction buffer plus enzyme storage buffer in replacement of enzyme; LII + MGT, 65 μM Lipid II mix plus 22.5 μM MGT-Δ67 or MGT-Δ28(FL) (MGT-FL) as indicated. Products of transglycosylation were separated on an 8.5% T/2.7% C SDS-PAGE gel. Dansyl fluorescence at 521 nm was detected using a blue light converter and short pass filter on a GeneSnap Gel Doc. (i) denotes unpolymerised Lipid II and (ii) glycan chains of varying lengths, (iii) denotes where high molecular weight material, unable to enter the gel would be found.

Figure 5.8 demonstrates that MGT-Δ28(FL) was active as a transglycosylase under the conditions used and with a 50:50 mix of fluorescently labelled:non-labelled Lipid II (Glu). The glycan chain lengths observed were more variable in length with MGT-Δ28(FL) than MGT-Δ67. The lower intensity of fluorescence observed for MGT-Δ28(FL) products may be due to a greater distribution of glycan chain lengths being produced, leading to the fluorescence detected being more dispersed. Despite this, it has been clearly shown that MGT-Δ28(FL) demonstrates transglycosylase activity under these conditions.

5.4.1.5 Role of Lipid II amidation in *Staphylococcus aureus* MGT transglycosylase activity

It was hypothesised that if amidated Lipid II was a preferential substrate for MGT as for all other Gram-positive PBPs tested so far in this study, and with MGT-Δ28(FL) shown to be 10 times more active than MGT-Δ67 (Huang *et al.*, 2012), then the -Δ28 enzyme may polymerise 100% dansylated Lipid II. This was tested with 10 μM Lipid II (Glu, Dans) or Lipid II (Gln, Dans), as sufficient fluorescent signal was observed at this concentration previously (Section 4.4.2). Lipid II in reaction buffer was incubated with 1 μM MGT-Δ67 or MGT-Δ28(FL) at 20°C for 1 hour, at which point, protein was removed and products were analysed by SDS-PAGE (Figure 5.9).

An apparent error in loading of the Lipid II (Gln, Dans), MGT-Δ28(FL) reaction, means that conclusions could not easily be made from this result. Although MGT-Δ28(FL)(MGT-FL) was able to polymerise Lipid II (Glu, Dans), showing it can use fully labelled substrate. It was unexpected that MGT-Δ67 was able to use Lipid II (Gln, Dans) as well. It is interesting to note that MGT-Δ28(FL) is capable of polymerising 100% Lipid II (Glu, Dans) whereas MGT-Δ67 does not appear to exhibit this activity. This is discussed further in Section 5.8.1.2.1.
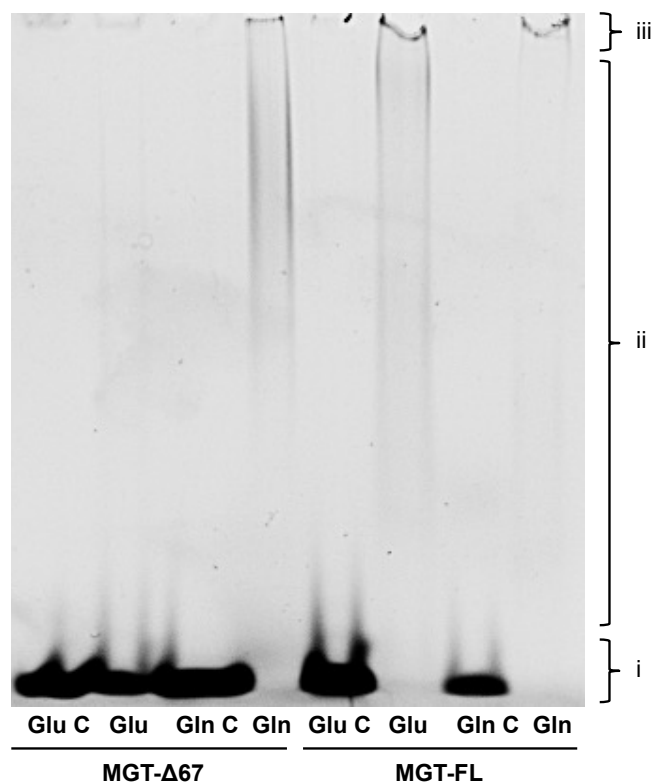
Figure 5.9: Comparison of the effect of Lipid II amidation on the transglycosylase products of *Staphylococcus aureus* MGT-Δ67 and MGT-Δ28(FL): Products of transglycosylation were separated on a 8.5% T/2.7% C SDS-PAGE gel. Dansyl fluorescence at 521 nm was detected using a blue light converter and short pass filter on a GeneSnap Gel Doc. All reactions contained 10 μM total Lipid II (either Lipid II (Glu, Dans) or Lipid II (Gln, Dans)) labelled as Glu and Gln below the gel respectively, and 1 μM MGT-Δ67 or 1 μM MGT-Δ28(FL)(MGT-FL) where indicated. Glu C, –enzyme: 10 μM Lipid II (Glu, Dans) with enzyme replaced by enzyme storage buffer. Gln C, –enzyme: 10 μM Lipid II (Gln, Dans) with enzyme replaced by enzyme storage buffer. (i) denotes unpolymerised Lipid II; (ii) glycan chains of varying lengths and (iii) the very high molecular weight material, which does not enter the gel.

5.4.2 Continuous fluorescence assay of *Staphylococcus aureus* MGT transglycosylation

Following the observation of transglycosylation by MGT-Δ28(FL) with 100% fluorescently labelled Lipid II, the same experiment was performed by the continuous assay system described in Section 4.1.2 (Methods Section 2.7.1). Reaction buffer was as described in Section 5.4.1; 50 mM Tris. HCl pH 8, 10 mM MnCl$_2$, 0.08% (v/v) decyl PEG, 20% (v/v) DMSO with the addition of 0.1 mg.ml^{-1} hen egg-white lysozyme for initial comparisons. This concentration of lysozyme was determined sufficient for the coupled assay of *S. pneumoniae* PBP1a and PBP2a (Section 4.5.1.2), and is discussed further in Section 5.7.1.3.

1 μM, 0.5 μM or 0.25 μM MGT-Δ28(FL) was added to initiate reactions with 2.5 μM, 5 μM or 10 μM Lipid II (Lipid II (Glu, Dans) or Lipid II (Gln, Dans)). Reactions were monitored for 100 min at 25°C. Rates in RFU change per second of the initial linear portion of the reaction were calculated. The observed initial rate increased proportionally with enzyme concentration for both substrates, however, no significant difference was established between rates with Lipid II (Glu, Dans) and Lipid II (Gln, Dans) as demonstrated for 5 μM Lipid II (Figure 5.10).

Unlike the bifunctional PBPs studied in Chapter 4, no difference was observed between the MGT-Δ28(FL) transglycosylation rate with Lipid II (Glu, Dans) and the rate with Lipid II (Gln, Dans).. This may suggest a different substrate specificity of MGT or the *Staphylococcus aureus* transglycosylases more generally. The lowest enzyme concentration used was 0.25 μM and previous HPLC assays (Huang *et al.,* 2012) used enzyme concentrations of 60 nM, so a more detailed study of the effect of enzyme concentration and other *Staphylococcus aureus* transglycosylases is required to further investigate this.
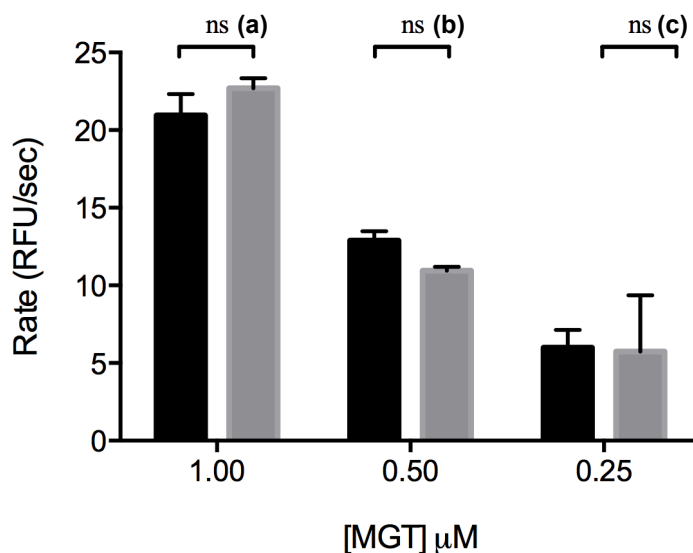
Figure 5.10: Comparison of MGT-Δ28(FL) transglycosylation rates by continuous fluorescence assay with Lipid II (Glu, Dans) and Lipid II (Gln, Dans). 5 µM Lipid II (Glu, Dans)(Black) or Lipid II (Gln, Dans)(Grey) and 1 µM, 0.5 µM or 0.25 µM MGT-Δ28(FL) as labelled on x-axis.. Excitation was at 340 nm, emission was at 521 nm with readings at 30 second intervals. RFU change per second was calculated from initial linear portion of time-course. Values represent the mean ± standard deviation of triplicate reactions. Student's two-tailed t-test was performed to test for statistical significance. *p*-values: (a) 0.225, (b) 0.054, (c) 0.937 where *p*->0.05 was considered not significant.

5.5 Analysis of *Staphylococcus aureus* PBP2-Δ59 transglycosylase products by SDS-PAGE

The data in Section 5.4, indicated that amidation of the lipid substrate made no difference to the transglycosylation rate of MGT-Δ28(FL). Therefore, the bifunctional PBP2 was also investigated.

5.5.1 Demonstration of PBP-Δ59 transglycosylase activity by SDS-PAGE

Due to substrate availability, initial assays of PBP2-Δ59 transglycosylase activity were with Lipid II (Gln, Dans). *Staphylococcus aureus* PBP2 activity had previously been demonstrated (Barrett *et al.,* 2005) by HPLC with [^{14}C]-Lipid II (C$_{35}$). The buffer system ('HPLC assay buffer') used in this assay; 50 mM acetic acid, 50 mM MES, 10 mM CaCl$_2$, 20% (v/v) DMSO at pH 5, was compared to a detergent-omitted *S. pneumoniae* PBP2a reaction buffer (Section 4.4): 50 mM HEPES pH 7.5,

200 mM NaCl, 25 mM MgCl$_2$, 25% (v/v) DMSO. 10 µM Lipid II (Gln, Dans) was incubated with or without 1 µM PBP2-Δ59 at 30°C overnight in these buffers, to ensure the reaction proceeded to completion. Reaction products were analysed by SDS-PAGE (Section 2.7.2) (Figure 5.11).
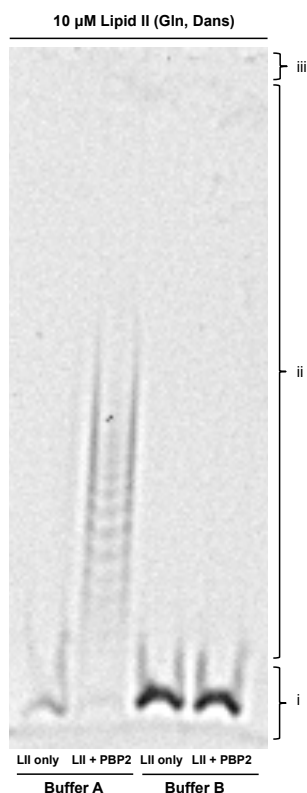
Figure 5.11: SDS-PAGE separation of PBP2-Δ59 transglycosylase products. LII only, 10 µM Lipid II (Gln, Dans) plus PBP2-Δ59 storage buffer; LII+PBP2, 10 µM Lipid II (Gln, Dans) and 1 µM PBP2-Δ59. Buffer A, 50 mM HEPES pH 7.5, 200 mM NaCl, 25 mM MgCl$_2$, 25% (v/v) DMSO; Buffer B, 50 mM acetic acid, 50 mM MES, 10 mM CaCl$_2$, 20% (v/v) DMSO pH 5. Products of transglycosylation were separated on a 8.5% T/2.7% C SDS-PAGE gel. Dansyl fluorescence at 521 nm was detected using a blue light converter and short pass filter on a GeneSnap Gel Doc. (i) denotes unpolymerised Lipid II; (ii) glycan chains of varying lengths (iii) denotes where high molecular weight material, unable to enter the gel would be found.

No activity was observed in the HPLC assay buffer (Barrett *et al.,* 2005), and short glycan chains were produced after overnight incubation in the pneumococcal PBP2a reaction buffer. Detergent was not present in the reaction buffer used by Barrett *et al.,* (2005), and its omission is likely to have not affected transglycosylase activity given the presence of 20% (v/v) DMSO to enhance solubility of the lipid substrate. Significantly, the Lipid II substrate previously (Barrett *et al.*, 2005) also did not have a dansyl fluorescence group, which may be more important in observation of transglycosylase activity than previously thought (Section 5.4). C$_{35}$ Lipid II has

previously been shown to be a more optimal substrate *in vitro* than the C_{55} variant (Ye *et al.,* 2001), however, C_{35} Lipid II was not available for this study. Another way to manipulate the availability of the Lipid II for transglycosylation, distinct from lipid prenyl chain length was to vary the TX-100 concentrations added to the reaction buffer to determine any effect on the enzyme activity, given the use of C_{55} Lipid II. The reaction was exactly as for Figure 5.11 (buffer A) with the addition of 1/3 – 10 x CMC TX-100 (CMC = 0.015% (v/v)). Products were analysed by SDS-PAGE (Figure 5.12).
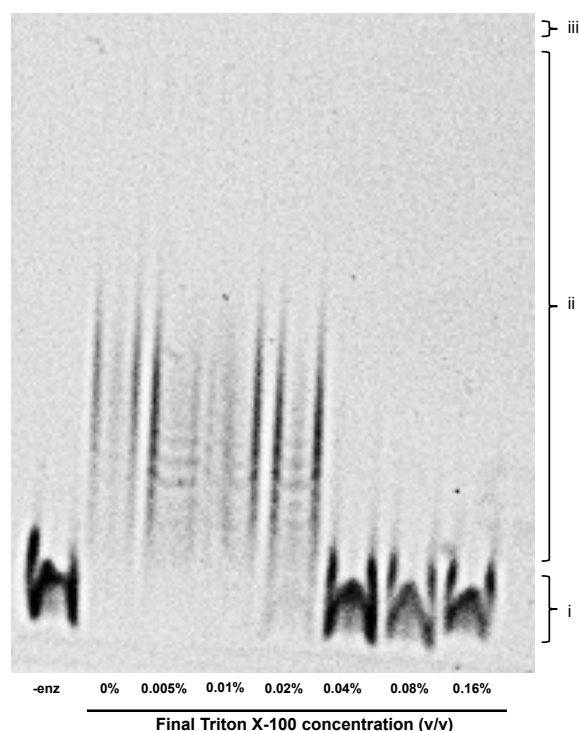
Figure 5.12: Effect of TX-100 concentration on PBP2-Δ59 transglycosylase processivity. –enz, 10 μM Lipid II (Gln, Dans) plus PBP2-Δ59 storage buffer in reaction buffer with 0% TX-100. Remaining lanes, 10 μM Lipid II (Gln, Dans) and 1 μM PBP2-Δ59. Buffer; 50 mM HEPES pH 7.5, 200 mM NaCl, 25 mM MgCl$_2$, 25% (v/v) DMSO with increasing TX-100 concentrations as labelled. Products of transglycosylation were separated on a 8.5% T/2.7% C SDS-PAGE gel. Dansyl fluorescence at 521 nm was detected using a blue light converter and short pass filter on a GeneSnap Gel Doc. (i) denotes unpolymerised Lipid II and (ii) glycan chains of varying lengths. (iii) denotes where high molecular weight material, unable to enter the gel would be found.

No difference in processivity was observed with the addition of increasing TX-100 concentrations, suggesting that the 25% (v/v) DMSO present is sufficient for PBP2-Δ59 activity. Activity was observed up to a TX-100 concentration just above CMC (0.015% (v/v)), but above this full inhibition occurred. Mis-orientation of PBP2 in the detergent micelle due to the absence of the hydrophobic transmembrane domain

of the PBP may have been responsible for this, as seen with *S. pneumoniae* PBP2a (Section 4.4.5). This result shows that TX-100 is not required for PBP2-Δ59 activity in the presence of 25% (v/v) DMSO.

5.5.2 Effect of Lipid II amidation on PBP2-Δ59 transglycosylase activity

The transglycosylase activity of PBP2-Δ59 with amidated and non-amidated substrate was compared by separation of the reaction products by SDS-PAGE. 10 μM Lipid II (Lipid II (Glu, Dans) or Lipid II (Gln, Dans)) was incubated with 1 μM PBP2-Δ59 or an equivalent volume of enzyme storage buffer in 50 mM HEPES pH 7.5, 25 mM MgCl$_2$, 200 mM NaCl, 25% (v/v) DMSO at 30°C overnight. Glycan products were analysed by SDS-PAGE (Figure 5.13)
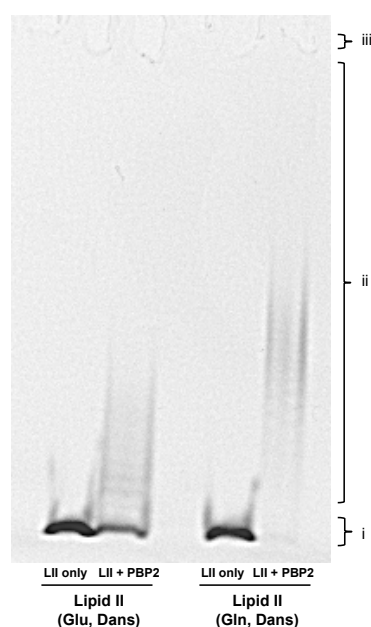
Figure 5.13: Effect of Lipid II amidation on the transglycosylase products of *Staphylococcus aureus* PBP2-Δ59. Products of transglycosylation separated on a 8.5% T/2.7% C SDS-PAGE gel. Dansyl fluorescence at 521 nm was detected by using a blue light converter and short pass filter on a GeneSnap Gel Doc. Reactions contained 10 μM total Lipid II (either Lipid II (Glu, Dans) or Lipid II (Gln, Dans)) as labelled below the gel. LII only, plus enzyme storage buffer; LII +PBP2, plus 1 μM PBP2-Δ59. (i) denotes unpolymerised Lipid II and (ii) glycan chains of varying lengths.. (iii) denotes where high molecular weight material, unable to enter the gel would be found.

Figure 5.13 shows a clear difference between the activity of PBP2-Δ59 with amidated and non-amidated Lipid II. After overnight incubation, unpolymerised Lipid II (Glu, Dans) was observed at the base of the gel, demonstrating a distinct preference for the amidated Lipid II substrate by PBP2-Δ59, as identified previously

for the *S. pneumoniae* bifunctional PBPs (Section 4.4.2). This phenomenon was not observed for the *Staphylococcus aureus* monofunctional transglycosylase MGT (Section 5.4.1.5 and 5.4.2).

5.5.3 Continuous fluorescence assay of PBP2-Δ59 transglycosylase activity

In order to kinetically characterise and accurately quantitate the changes in activity of PBP2-Δ59 in response to modifications of its assay conditions or substrate, the enzyme was assayed with 10 μM Lipid II (Gln, Dans) by the continuous fluorescence assay system (Section 2.7.1). The buffer for observation of activity by SDS-PAGE was used; 50 mM HEPES pH 7.5, 25 mM MgCl$_2$, 200 mM NaCl, 25% (v/v) DMSO with the addition of 0.1 mg.ml^{-1} lysozyme as a coupling enzyme (Section 4.5.1.2), and the assay performed at 30°C for 150 min as described in Section 2.7.1.

No activity was observed by this assay system (data not shown). Transglycosylase activity previously observed by overnight incubation and SDS-PAGE may have been too slow to identify activity within the continuous assay timeframe.

5.5.4 Expression and purification of full-length *Staphylococcus aureus* PBP2

S. pneumoniae bifunctional PBP2a was shown to be less processive after the removal of the TM region (Section 4.4.5), and *Staphylococcus aureus* MGT was able to polymerise 100% Lipid II (Glu, Dans) only in the presence of its TM region (Section 5.4.1.5). Both of these findings, and extensive literature (Section 5.8.1.2), suggested a critical role of the TM region in substrate interaction. This, together with the inability to follow PBP2-Δ59 activity continuously in a kinetic assay prompted attempts to express and purify full-length PBP2, in order to elucidate the importance of the TM region on PBP2 processivity and to allow more detailed characterisation of its enzymology.

The pET21b::*pbp2* plasmid expressing the full-length PBP2 gene was obtained from Dr N. Strynadka (UBC, Canada) and expression and purification was attempted as described by Barrett *et al.,* (2005). Very poor yield was achieved following solubilisation of the post lysis pellet with 0.5% (w/v) Sarkosyl for 1 hour. Several adjustments to the protocol were made, including the addition of cOmplete™ EDTA-free Protease Inhibitor Cocktail (Roche) and an additional ultracentrifugation step of the soluble fraction at 150,000 × g to specifically pellet membranes (Section 2.4.2.3). Both the low speed and high speed pellets were solubilised for longer (3 hours) with 0.5% (w/v) Sarkosyl, resulting in a detectable quantity of protein; mainly in the 50,000 × g pellet (as used in Barrett *et al.,* 2005) rather than the 150,000 × g pellet. Loose Ni^{2+} bound chelating Metal Affinity Resin (Section 2.4.3.1) was used rather than a pre-packed 5 mL HisTrap HP (GE Healthcare) column in order to achieve higher binding, and soluble protein was allowed to incubate with the resin, stirring for 3 hours at 4°C. Despite this, a significant quantity of PBP2 was present in the column flow through from the solubilised 50,000 × g pellet, suggesting mis-folded protein. A stepwise elution from 10 mM to 500 mM imidazole was carried out to develop gravity flow columns. PBP2 containing fractions were concentrated in a 10 kDa cut-off centrifugal concentrator with subsequent buffer exchange to remove imidazole. Protein concentration was not detectable by Bio-Rad assay (Section 2.5.1) for protein solubilised from the ultracentrifuge pellet. A very poor yield of 0.04 mg.L^{-1} was achieved from the low speed pellet, and included a high amount of contaminating protein (Figure 5.14).

PBP2-FL purity was compared to PBP2-Δ59 by SDS-PAGE analysis of the same quantity of loaded protein. Insufficient yield and purity was achieved for PBP2-FL despite alterations to the published protocol.
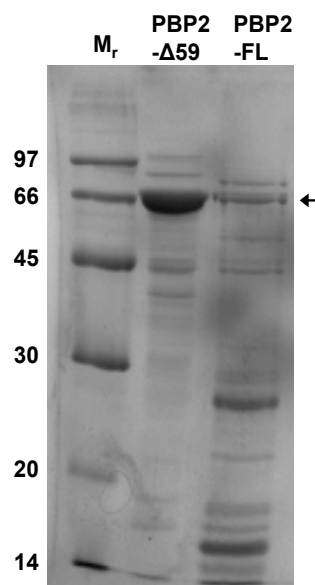
Figure 5.14: 12% SDS-PAGE Coomassie–stained gel to analyse the final purity of *Staphylococcus aureus* PBP2-Δ59 and PBP2-FL. M$_r$, Molecular weight markers (kDa). Lanes are labelled with the relevant PBP. Position of PBP2-Δ59 on the gel indicated by arrow.

5.6 Analysis of *Staphylococcus aureus* PBP2-PBP2a Interactions

5.6.1 Expression and purification of *Staphylococcus aureus* Class B PBP2a

Increasing evidence has accumulated to support that PBPs function within larger complexes containing other PBPs as well as other proteins responsible for the growth, maintenance and turnover of the cell wall (Section 5.8.4.2). One mechanism of methicillin resistance in *Staphylococcus aureus* is due to the acquisition of the monofunctional Class B PBP2a with low affinity for β-lactams, which compensates for the lost transpeptidase activity of the methicillin susceptible PBP2 (Pinho *et al.,* 2001). Therefore, it was hypothesised that PBP2 and PBP2a may form a complex *in vivo*, which may stimulate the transglycosylase activity of PBP2.

To test this hypothesis, *Staphylococcus aureus* PBP2a was expressed and purified from the pET15b::*pbp2a-Δ22* plasmid (obtained from Dr N. Strynadka (UBC, Canada)). Expression of the full-length PBP2a including the TM region has previously been unsuccessful despite extensive efforts within our group (Dr David Roper, Personal Communication). Expression of the -Δ22 PBP2a was as described in Lim and Strynadka, (2002) and purification followed the same basic scheme with modifications, with all steps at 4°C (Section 2.4.4.2). The final high level of purity of PBP2a-Δ22 is shown in Figure 5.15 and a yield of 7 mg.L^{-1} was achieved.
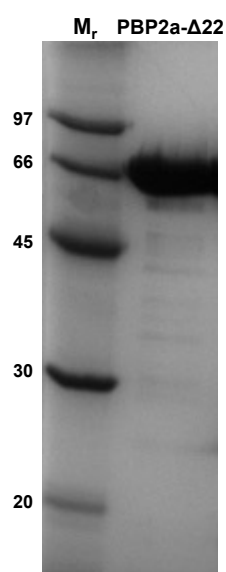
Figure 5.15: 12% SDS-PAGE Coomassie-stained gel showing the final purity of PBP2a-Δ22. M$_r$, molecular weight markers (kDa); TM, total membrane fraction; PBP2a-Δ22, 10 μg PBP2a-Δ22.

A sample of very pure PBP2a-Δ22 was then sent to Professor Simon Foster (University of Sheffield) for anti-PBP2a antibody production in mice, which was subsequently used by Dr Sarah Paulin (UCL, London) to show the co-purification of PBP2/PBP2a as a complex from intact *Staphylococcus aureus* cells (Paulin *et al.,* 2014 (appended to the end of this thesis; Appendix 8)). This further supports the hypothesis for a multi-PBP complex *in vivo*.

5.6.2 Can PBP2-Δ59 processivity be stimulated by other *Staphylococcus aureus* PBPs?

Staphylococcus aureus PBP2a compensates for the loss of methicillin susceptible PBP2 transpeptidase activity during β-lactam treatment (Pinho *et al*., 2001). It was hypothesised that the complex of PBP2 and PBP2a formed may also stimulate PBP2 transglycosylase activity. *E. coli* Class A PBP1a transglycosylase activity has been shown to be stimulated by monofunctional *E. coli* Class B transpeptidase PBP2 (Banzhaf *et al.,* 2012). The ability of PBP2a-Δ22 to stimulate the transglycosylase activity of PBP2-Δ59 was tested. It was anticipated that utility of Lipid II (Gln, Dans) and the solely transpeptidase nature of PBP2a would eliminate any contribution of PBP2a catalysis to the results of this experiment because the third position of the stem peptide was (i) dansylated and therefore blocked for transpeptidase activity and (ii) not appended to a branched stem, which PBP2a requires (Strandén *et al.* 1997). Therefore, overnight incubation of 10 μM Lipid II (Gln, Dans) in PBP2 reaction buffer (Section 5.5.2) at 30°C with 1 μM of each enzyme to be tested was performed. The subsequent reaction products were analysed by SDS-PAGE (Figure 5.16).

PBP2a-Δ22 was shown to not affect the mobility of Lipid II (Gln, Dans) through the gel. However, no increase in processivity of PBP2-Δ59 transglycosylase activity was observed with the addition of PBP2a-Δ22 (Figure 5.16). Any alteration in rate of glycan chain polymerisation cannot be determined in this experiment, as a single overnight time point was conducted. A time-course experiment or continuous fluorescence assay would allow this to be studied.
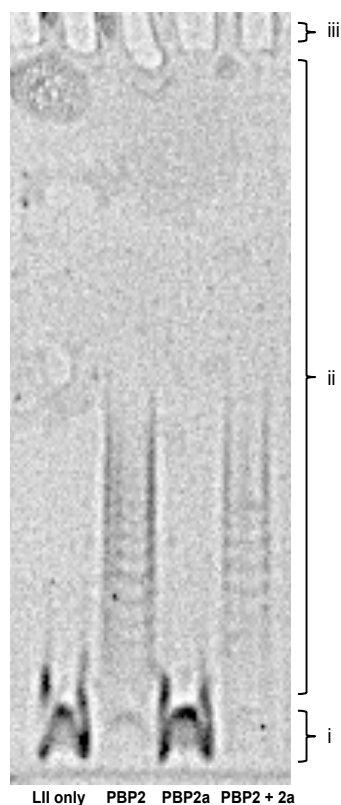
Figure 5.16: Transglycosylase activity of *Staphylococcus aureus* PBP2-Δ59 in the presence or absence of PBP2a-Δ22. 10 μM Lipid II (Gln, Dans) in PBP2 reaction buffer was present in all assays. LII only, plus enzyme storage buffer; PBP2, plus 1 μM PBP2-Δ59**.** PBP2a, plus 1 μM PBP2a-Δ22; PBP2 + 2a, plus 1 μM PBP2-Δ59 and 1 μM PBP2a-Δ22. Products of transglycosylation were separated on a 8.5% T/2.7% C SDS-PAGE gel. Dansyl fluorescence at 521 nm was detected using a blue light converter and short pass filter on a GeneSnap Gel Doc. (i) denotes unpolymerised Lipid II and (ii) glycan chains of varying lengths (iii) denotes where high molecular weight material, unable to enter the gel would be found.

This result suggests that the interaction of PBP2 and PBP2a does not increase the processivity of the transglycosylation observed, although there are many caveats to this. For example, the transmembrane spanning region of one, or both enzymes may be crucial for interaction and/or processivity, as might the pentaglycine moiety appended to the third position of the stem peptide of the native staphylococcal lipid II substrate of these enzymes.

5.7 Characterisation of novel carbohydrate based transglycosylase inhibitors

The need for novel inhibitors of the transglycosylase activity of PBPs was discussed in Section 5.1.4. To address this urgent clinical requirement, the groups of Professor

Matthew Cooper (University of Queensland, Australia) and Dr Wim Meutermans (Alchemia, Australia) synthesised a 500 compound library based on the structure of moenomycin (Zuegg *et al.,* 2015). All 500 compounds were tested against methicillin-sensitive (MSSA) and methicillin-resistant (MRSA) *Staphylococcus aureus*, three enterococcal strains and *E. coli.*

Non-haemolytic compounds demonstrating activity against Gram-positive strains were tested and two of these (Figure 5.17). displayed activity against a broad range of drug resistant *Staphylococcus aureus* strains as well as multi-drug resistant *S. pneumoniae* (Table 1 in Zuegg *et al.,* 2015; attached in Appendix 8) One of these, ACL202015 showed a spontaneous mutation frequency of less than 2.5×10^{-10} at $4 \times$ MIC against *Staphylococcus aureus* (ATCC 13709).
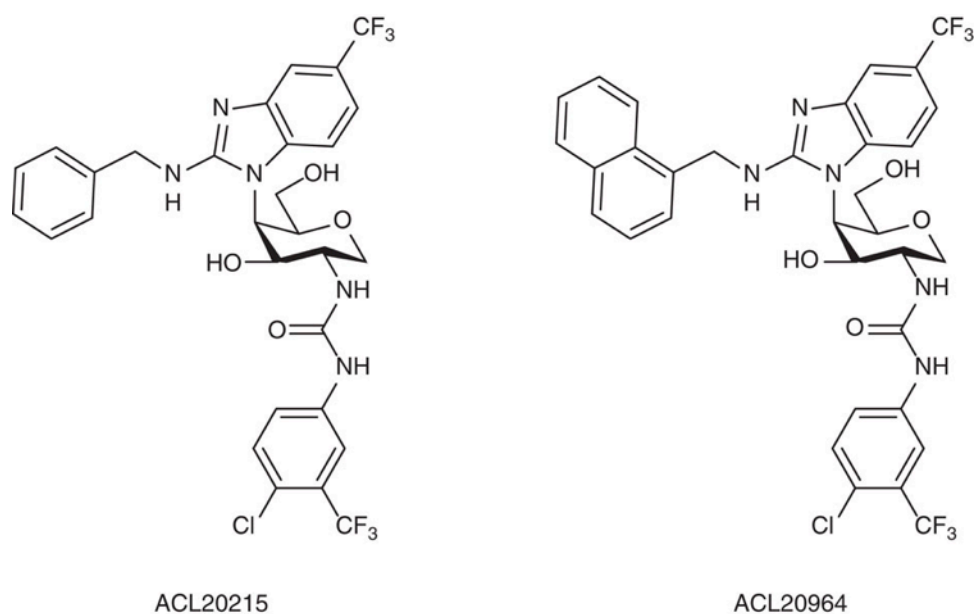
ACL20215   ACL20964

Figure 5.17: Novel carbohydrate based transglycosylase inhibitors.: Structures of two most active inhibitors taken forward; ACL20215 and ACL20964. Adapted from Zuegg *et al.,* (2015).

As the compounds were based originally on the structure of moenomycin and are carbohydrate based, it was predicted that their mode of action is inhibition of transglycosylase activity. This section details the investigation of these inhibitors as transglycosylase inhibitors of *Staphylococcus aureus* MGT-Δ28(FL). Part of this section (Figure 5.21) has been published in Zuegg *et al.,* (2015) (attached at the end of this thesis; Appendix 8)).

5.7.1 A continuous fluorescence assay for MGT-Δ28(FL) transglycosylase activity and inhibition.

MGT-Δ28(FL) transglycosylase activity was previously analysed by the continuous fluorescence assay system (Section 2.7.1 and Section 5.4.2), where no significant difference was observed between the rate of polymerisation of Lipid II (Glu, Dans) and Lipid II (Gln, Dans). Due to this and substrate availability, Lipid II (Glu, Dans) was used as a substrate for the remainder of this chapter. Initial conditions for the assay were as in Section 5.4.2; 50 mM Tris. HCl pH 8, 10 mM MnCl$_2$, 0.08% (v/v) decyl PEG, 20% (v/v) DMSO, 0.1 mg.ml^{-1} hen egg-white lysozyme, at 25°C and the assay was performed as in Section 2.7.1.

5.7.1.1 Fluorescent properties of Lipid II (Dans)

The effect of the MGT-Δ28(FL) assay buffer system on the fluorescent properties of Lipid II (Glu, Dans) was investigated as it was for the *S. pneumoniae* PBPs in Section 4.5.1.1. 10 μM Lipid II (Glu, Dans) in 50 μL MGT-Δ28(FL) reaction buffer in a Greiner FLUOTRAC^{TM} 600 96-well plate was scanned for wavelength excitation and emission optima in a CLARIOstar® platereader (BMG Labtech). Emission from 400-600 nm was measured after excitation at 340 nm and emission at 521 nm with excitation over the 320-400 nm range. All measurements were performed with and without ThermalSeal RT^{TM} film (Section 4.5.1), and with buffer only controls.

As seen previously (Figure 4.16) the emission maxima was observed at 521 nm after excitation at 340 nm (Figure 5.18 (a)). The optimal excitation wavelength for emission at 521 nm was again 359 nm (Figure 5.18 (b)), higher than the published value of 340 nm, and both maxima were reduced marginally by the inclusion of a seal. Other seal induced spectral changes were outside of the range used to follow the assay. Excitation at 359 nm and emission at 521 nm resulted in a high level of noise (seen previously in Section 4.5.1.1), and therefore assays were performed with excitation at 340 nm and emission at 521 nm to achieve the optimal fluorescence signal, with a ThermalSeal RT^{TM} seal to stop evaporation.
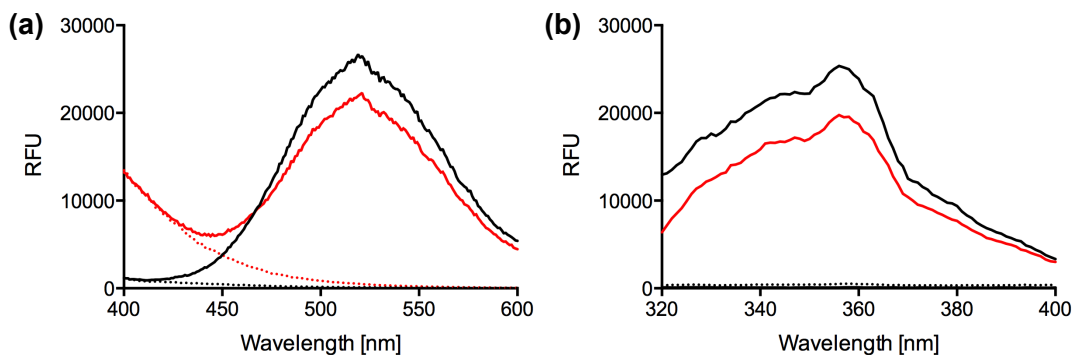
Figure 5.18: Optimal emission and excitation wavelengths of Lipid II (Glu, Dans) in MGT-Δ28(FL) reaction buffer. 10 μM Lipid II (Glu, Dans) in 50 μL 50 mM Tris. HCl, 10 mM MnCl$_2$, 0.08% (v/v) decyl PEG, 20% (v/v) DMSO, 0.1 mg.ml^{-1} hen egg-white lysozyme in a Greiner FLUOTRAC^{TM} 600 96-well plate. a) Excitation was at 340 nm, emission was measured at 400 nm- 600 nm. Black solid line, Lipid II; Red solid line; Lipid II + seal, Black dashed line; Buffer control, Red dashed line; Buffer control + seal. Emission maximum was observed at 521 nm. b) Excitation at 320 nm – 400 nm, emission at 521 nm. Black solid line, Lipid II; Red solid line; Lipid II + seal, Black dashed line; Buffer control, Red dashed line; Buffer control + seal. Excitation maximum was observed at 359 nm.

5.7.1.2 Optimisation of conditions for the continuous fluorescence assay of MGT-Δ28(FL) transglycosylation.

Initiation of the continuous fluorescence assay by addition of substrate rather than enzyme was investigated. Parallel reactions of 10 μM Lipid II (Glu, Dans) and 1 μM MGT-Δ28(FL) were initiated by addition of either enzyme or substrate. No effect on reaction rate was observed, however a lag period of approximately 1 minute was observed before fluorescence decrease began when Lipid II was added last, presumed to be due to mixing of Lipid II containing micelles with decyl PEG micelles. Therefore, reactions were initiated by the addition of enzyme.

Greiner FLUOTRAC^{TM} 600 96-well black plates have been used for all assays in this report. These are treated to make them hydrophilic and therefore have a higher binding capacity for polar molecules. FLUOTRAC^{TM} 200 96-well black plates are more hydrophobic and may mimic the membrane environment more closely. (Greiner website). A standard assay of 10 μM Lipid II (Glu, Dans) and 1 μM MGT-Δ28(FL) was carried out in both plate types and initial rate of transglycosylase activity determined in RFU change per second. A higher rate was observed in the hydrophilic plate (14.36 RFU/second) compared to the hydrophobic plate (9.13

RFU/second). It is likely that the hydrophobic surfaces of the FLUOTRAC™ 200 plates bound, and removed from the bulk solution of the assay, lipid II, detergent and/or MGT-Δ28(FL).

The effect of pH on MGT-Δ28(FL) transglycosylation rate was investigated. 10 μM Lipid II (Glu, Dans) and 1 μM MGT-Δ28(FL) were assayed in 10 mM MnCl$_2$, 0.08% (v/v) decyl PEG, 20% (v/v) DMSO, 0.1 mg.ml^{-1} hen egg-white lysozyme, with the replacement of 50 mM Tris.HCl pH 8.0, by 50 mM HEPES at pH values spanning the full range of the HEPES buffering capacity (pKa = 7.6; pH 6.8-8.2) (Dawson *et al.* 1986). Assays were monitored by the standard method (Section 2.7.1) and the initial rate of transglycosylase activity determined at each pH. (Table 5.2).

pH	Rate (RFU/second)
6.8	5.56
7	9.27
7.5	7.90
8	14.19

Table 5.2. Effect of pH on MGT-Δ28(FL) transglycosylase activity

Within the pH range tested, the optimal pH for activity was pH 8, with a 2-fold faster initial rate than any of the other pH conditions tested. The rate observed with HEPES pH 8, was comparable to that with Tris.HCl buffer at the same pH, used so far for MGT-Δ28(FL) assays. (eg. 14.36 RFU/second in hydrophilic plate test earlier in this section)

Efforts to further improve the transglycosylase rate observed by the methods in this section and 5.7.1.1 were unsuccessful. Based on results in this, and the previous section, assays were subsequently performed in 50 mM Tris.HCl pH 8.0, 10 mM MnCl$_2$, 0.08% (v/v) decyl PEG, 20% (v/v) DMSO, 0.1 mg.ml^{-1} hen egg-white lysozyme in Greiner FLUOTRAC™ 600 96-well black plates at 25°C. Reactions were initiated by the addition of enzyme and dansyl fluorescence monitored by excitation at 340 nm and emission at 521 nm.

5.7.1.3 Lysozyme as the *N*-acetylmuramidase coupling enzyme in the continuous fluorescence assay for transglycosylase activity

0.1 mg.ml^{-1} hen egg-white lysozyme was shown to be sufficient and non-limiting as the *N*-acetylmuramidase coupling enzyme in the continuous fluorescence assay of *S. pneumoniae* Class A PBP transglycosylase activity (Section 4.5.1.2). This was assumed in Section 5.4.2, and is tested more fully in this section. 0.01, 0.05 and 0.1 mg.ml^{-1} hen egg-white lysozyme were tested with 1 μM, 0.5 μM or 0.3 μM MGT-Δ28(FL) and 10 μM Lipid II (Glu, Dans) under the optimised assay conditions for MGT-Δ28(FL). At all lysozyme concentrations, reactions containing 0.5 μM and 0.3 μM MGT-Δ28(FL) did not reach a plateau in 100 min. The fluorescence decrease over time with 1 μM MGT-Δ28(FL) was sigmoidal with both 0.01 and 0.05 mg.ml^{-1} lysozyme, suggesting that the coupling enzyme is limiting at these concentrations. An initial linear phase followed by a plateau was observed with 1 μM MGT-Δ28(FL), 0.1 mg.ml^{-1} and 10 μM Lipid II (Glu, Dans), allowing calculation of initial rate (not shown).

The results described here support the rationale for using 1 μM MGT-Δ28(FL) and 0.1 mg.ml^{-1} in assays with 10 μM Lipid II (Glu, Dans).

5.7.2 Determination of kinetic parameters for MGT-Δ28(FL) transglycosylase activity

In order to investigate the impact of ACL20215 and ACL20964 on the activity of MGT-Δ28(FL), the relationship between Lipid II (Glu, Dans) concentration and MGT-Δ28(FL) transglycosylation rate was first investigated. 1-10 μM Lipid II (Glu, Dans) was assayed with 1 μM MGT-Δ28(FL) in 50 mM Tris.HCl pH 8.0, 10 mM MnCl$_2$, 0.08% (v/v) decyl PEG, 20% (v/v) DMSO, 0.1 mg.ml^{-1} hen egg-white lysozyme. Triplicate reactions were performed, and the initial rate was plotted against substrate concentration (Figure 5.19).

For the substrate range used the relationship between rate and substrate concentration did not plateau. The data best fit to a modified Michaelis-Menten equation considering cooperativity (Equation 4 in Section 4.5.4), and allowed extraction of Vmax: 92.88 ± 14.86 µM, $S_{0.5}$: 6.64 ± 1.25 µM with a hill coefficient of 1.91 ± 0.27. The R^2 of the fit was 0.9911. Although care should be taken extracting kinetic parameters as the data rate did not plateau.
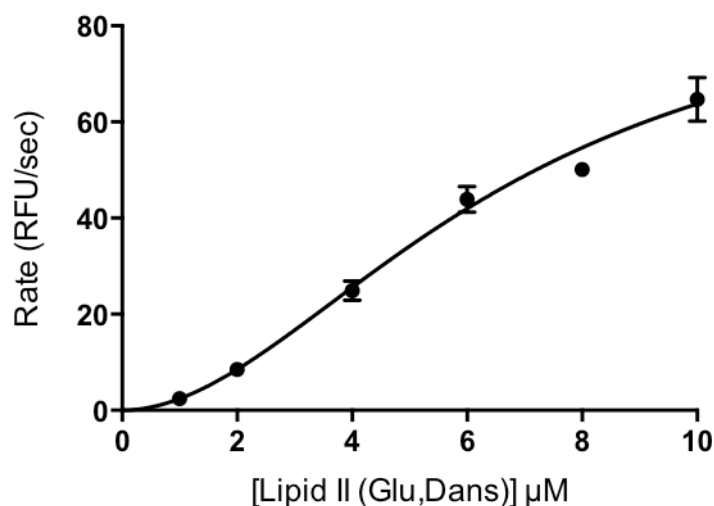
Figure 5.19: Dependence of *Staphylococcus aureus* MGT-Δ28(FL) transglycosylase rate on Lipid II (Glu, Dans) concentration. Initial rate in RFU/second (based on three data sets) plotted against [Lipid II (Glu, Dans)]. Error bars represent standard deviation of triplicate measurements. Data fitted to modified Michaelis-Menten considering cooperativity with an R^2 value of 0.9911.

As substrate availability did not allow higher concentrations to be tested, the published K_m value for MGT-Δ28(FL) of 9.6 ± 0.76 µM (Huang *et al.*, 2012) was used to calculate the concentration of substrate for subsequent inhibitor assays. This fits closely to the $S_{0.5}$ value calculated here as well. A Lipid II (Glu, Dans) concentration at approximately 1/6 K_m (1.45 µM) was used to test for inhibition. This low concentration was selected in order to make the assay more sensitive to inhibition competitive with respect to lipid II..

5.7.3 Inhibition of MGT-Δ28(FL) transglycosylase activity by moenomycin

To validate the MGT-Δ28(FL) assay for detection of inhibitors, the specific inhibitor of transglycosylase activity, moenomycin, was used as a positive control for

inhibition. The moenomycin IC$_{50}$ (the inhibitor concentration at which half maximal inhibition occurs) for MGT-Δ28(FL) inhibition was determined in the presence of 1 μM MGT-Δ28(FL) and 1.45 μM Lipid II (Glu, Dans (Sections 5.7.2 and 2.7.1), between 1 μM and 50 μM moenomycin. Initial rates were used to compute percentage inhibition relative to the no inhibitor control. The data were fitted to a simple saturation model of inhibitor binding (Equation 1) which enabled IC$_{50}$ values to be extracted. Maximum inhibition was fixed at 100% for fitting of the non-linear regression (Figure 5.20).

Equation 1:

$$\% \, Inhibition = \frac{100.[I]}{IC_{50} + [I]}$$
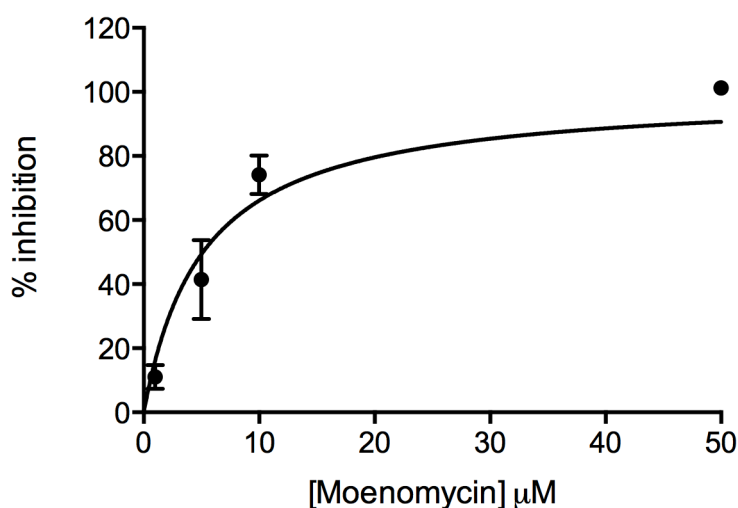
Figure 5.20: Inhibition of *Staphylococcus aureus* MGT-Δ28(FL) transglycosylase activity by moenomycin. Assays of 1.45 μM Lipid II (Glu, Dans) and 1 μM MGT-Δ28(FL) with increasing [moenomycin] from 1 − 50 μM. Excitation was at 340 nm, emission was at 521 nm with readings at 30 second intervals.. Values represent mean ± standard deviation of 4 reactions. R^2 value of regression fit: 0.929

The calculated IC$_{50}$ for moenomycin inhibition of MGT-Δ28(FL) was 5.1 ± 0.729 μM. This is higher than expected given the tight binding nature of moenomycin, although the lack of a full TM region may reduce the affinity of MGT for moenomycin as observed for Class A PBPs (Cheng *et al.,* 2008) However, it demonstrated clear inhibition of MGT-Δ28(FL) transglycosylase activity and was therefore a positive control for testing of inhibition by ACL20215 and ACL20964.

5.7.4 *in vitro* study of transglycosylase inhibition by ACL20215 and ACL20964

ACL202015 and ACL20964 exhibited poor solubility, which could be overcome by reduced pH or the addition of DMSO (Dr Wim Meutermans, Personal communication). pH was previously shown to have a significant effect on MGT-Δ28(FL) transglycosylase activity (Section 5.7.1.2) and therefore the compounds were resuspended at stock concentrations in 100% (v/v) DMSO. The DMSO concentration contributed by the addition of inhibitors to the assay was accounted for in the total concentration of 20% (v/v) in the assay.

The use of a fluorescence assay to test for inhibition requires the screening of inhibitors as a control, to identify any intrinsic fluorescence in the region monitored in the assay. ACL202015 and ACL20964 at 20, 100 and 400 μM in MGT-Δ28(FL) reaction buffer, plus buffer controls were scanned for fluorescence at the wavelengths monitored in the continuous fluorescence assay. No signal was observed above that from buffer alone with either compound (not shown).

1 – 300 μM ACL202015 and ACL20964 were tested for inhibition of MGT-Δ28(FL) in an identical manner to moenomycin in Section 5.7.3. Percentage inhibition data were again fitted to a simple saturation model of inhibitor binding to a single site (Equation 1) with maximum inhibition fixed as 100% (Figure 5.21).
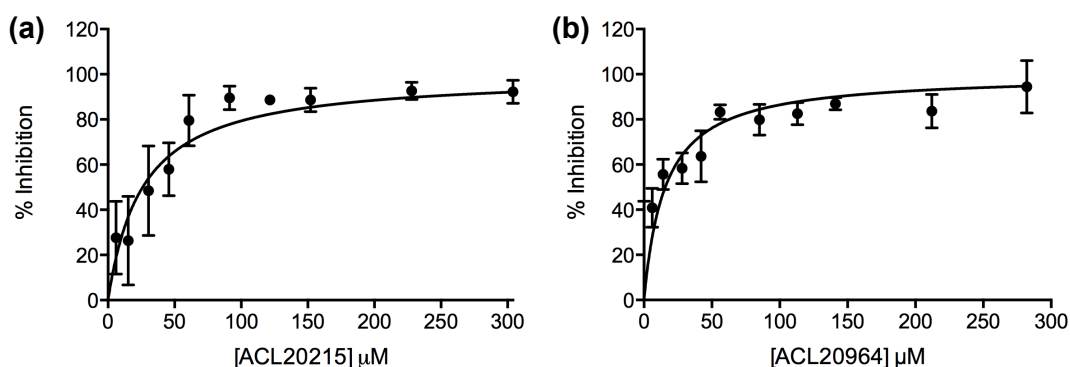
Figure 5.21: Inhibition of *Staphylococcus aureus* MGT-Δ28(FL) transglycosylase activity by ACL20215 (a) and ACL20964 (b). Assays of 1 μM MGT-Δ28(FL) in the presence of 1.45 μM Lipid II (Glu, Dans) with increasing [ACL20215] or [ACL20964] from 1 – 300 μM. Reaction volume was 50 μL. Excitation was at 340 nm, emission was at 521 nm with readings at 30 second intervals. Inhibition was calculated as a percentage relative to rate without inhibitor and plotted against inhibitor concentration in μM. Values represent mean ± standard deviation of 4 reactions. R^2 value of non-linear regression fits were: (a) 0.804 (b) 0.705.

IC$_{50}$ values of 26.1 ± 2.7 μM and 15.6 ± 2.0 μM were calculated for ACL202015 and ACL20964 respectively (compared to 5.1 ± 0.729 μM for moenomycin seen previously). These correspond to 17 and 11 μg.ml^{-1} respectively (8 μg.ml^{-1} for moenomycin). This data identifies these compounds as inhibitors of transglycosylase activity. The impact of these inhibitors on lysozyme activity was discounted as no sigmoidal relationship was observed suggestive of coupling enzyme limitations (Section 5.8.2.1).

5.8 Discussion and future work

This chapter has provided a good basis for understanding of the substrate specificity of the *Staphylococcus aureus* transglycosylases. Additionally, the characterisation of novel inhibitors of transglycosylase activity is pertinent in the discovery of new antimicrobials. This section discusses the data presented and its biological implications and details future work leading from the findings described. For discussion of the limitations of the SDS-PAGE and continuous fluorescence assay for transglycosylase activity, see Section 4.6.2.

5.8.1 Characterisation of *Staphylococcus aureus* MGT transglycosylase activity

5.8.1.1. Role of the transmembrane domain in MGT transglycosylation

In agreement with Huang *et al.* (2012), the importance of the hydrophobic TM region of MGT in transglycosylation was demonstrated. The inability of MGT-Δ67 to use non-amidated fully dansylated lipid II as a substrate (Figure 5.9) suggests that some of the additional 39 residues in the MGT-Δ28 protein are crucially important in substrate interaction, made more obvious in the presence of a sizeable dansyl group on the pentapeptide. The role of the TM region in the interaction of *Staphylococcus aureus* MGT and *E. coli* PBP1b with moenomycin has previously been documented (Cheng *et al.*, 2008; Huang *et al.,* 2012), and its importance in substrate interaction observed in *S. pneumoniae* PBP2a and *E. coli* PBP1b (Cheng *et al.*, 2008; Helassa *et al.,* 2012; Sung *et al.,* 2009). The results presented here led to the hypothesis that

increased affinity of MGT for amidated Lipid II overcame the loss of substrate affinity due to removal of a crucial interacting domain in the MGT-Δ67 protein, thus enabling it to polymerise 100% Lipid II (Gln, Dans) (Figure 5.9). This could be confirmed by isothermal calorimetry experiments comparing amidated and non-amidated Lipid II binding to MGT with and without the TM region, although this would require removal of detergent micelles, which would complicate analysis. A modified MGT or Lipid II substrate would be required for this experiment to ensure the substrate isn't polymerised. With this in mind, current focus in the laboratory is directed towards synthesis of lipid II analogues where the pyrophosphate bridge between the undecaprenyl and Mur*N*Ac moieties has been replaced by non-hydrolysable pyrophosphate mimetics.

An additional explanation for the inability of MGT-Δ67 to use 100% dansylated non-amidated Lipid II is incorrect orientation of the enzyme in detergent micelles due to the truncation of the protein. This has been inferred from the X-ray crystal structures of *Staphylococcus aureus* MGT and *E. coli* PBP1b (Huang *et al.,* 2012; Sung *et al*., 2009). Alternatively, the oligomeric state of MGT-Δ67 and MGT-Δ28(FL) may differ, and this could have implications for substrate access to the active site. Both MGT-Δ67 and MGT-Δ28(FL) have been identified as oligomers of uncertain multiplicity (Reed *et al.,* 2011; Wang *et al*., 2001). Both of these suggestions are only possible if amidation leads to a sufficiently large increase in affinity to allow the substrate to enter the active site and offset the poor orientation of the truncated protein relative to its substrate.

The detection of dansyl containing glycan chains with a mixture of labelled and non-labelled Lipid II Glu substrate (Figure 5.5) suggests that MGT-Δ67 is incorporating some of the fluorescent Lipid II presented, despite being unable to polymerise it alone (Section 5.4.1.1). This observation may be due to differential binding of labelled and non-labelled lipid II in the donor and/or acceptor sites of the transglycosylase. With neither the isoglutamine in the pentapeptide or TM region to aid affinity for the substrate, the presence of two dansyl groups within the active site may be too unfavourable for the formation of a catalytically competent donor/acceptor/ transglycosylase complex. Occlusion of the active site by detergent

or incorrect orientation of Lipid II binding may have the same outcome. The presence of the TM region or amidation is apparently sufficient to overcome this as in both cases the enzyme can use 100% dansylated Lipid II.

The results seen here suggest that if most enzyme molecules bind one labelled and one non-labelled substrate then an active complex is formed. This finding is unique to MGT so far, and has not been described for any bifunctional PBPs studied by the same method (Helassa et al., 2012; Offant et al., 2010; Schwartz et al., 2002; Chapter 4). Despite the fact that dansylation and other modifications of Lipid II do not affect the PBP kinetic parameters (Schwartz *et al.,* 2002; Zhang *et al.,* 2007) the findings presented here have implications in the use of these labelled substrates. A full investigation using amidated and non-amidated Lipid II with fluorescent tags at different positions or with radioactive labelling could enable this to be investigated.

The effect of the TM region on transglycosylation rates was not investigated. Following the observation that MGT-Δ67 can polymerise 100% Lipid II (Gln, Dans), a continuous assay could be carried out comparing the relative rates of transglycosylation of this amidated substrate by MGT-Δ67 and MGT-Δ28(FL). Considering the work by Huang and colleagues (2012) as well as complementary studies on *E. coli* PBP1b (Barrett *et al.,* 2004; Terrak *et al.,* 1999) it is expected that a higher transglycosylation rate would be observed with the full-length protein.

This is the first analysis of MGT processivity towards Lipid II polymerization *in vitro* and the role of the TM region on this process. The lack of suitable standards means that the length of glycan chains produced cannot be accurately calculated but comparison with *S. pneumoniae* PBP2a (Chapter 4) known to produce polymers of 20-30 disaccharide units in length, suggests that the disaccharide polymers generated by MGT are in excess of 20-25 units in length. However, this is likely to be an underestimate: More polymerised material is found in a band at the top of the gel in MGT-Δ28(FL) reactions (Figure 5.9), identifying material too large to enter the acrylamide and suggesting that MGT-Δ28(FL) is more processive than its truncated Δ67 counterpart. This is consistent with literature demonstrating the involvement of the TM region in transglycosylase processivity (Helassa *et al.,* 2012). However, this conclusion should be made with care as interaction of the detergent micelle with the

different MGT variants may also have an effect on the substrate usage discussed in this section (see Section 4.6.3.2, regarding the impact of detergent in *S. pneumoniae* PBP2a processivity).

5.8.1.2 Effect of Lipid II amidation on MGT transglycosylation

The experiments described in this chapter suggest differential effects of amidated substrate on the transglycosylase activity of monofunctional and bifunctional transglycosylase enzymes (discussed further in Section 7.1.1). This chapter detailed the first investigation of the effect of amidation on a monofunctional transglycosylase to date.

Non-amidated Lipid II was clearly shown to be a less optimal substrate than in its amidated form for MGT-Δ67 by SDS-PAGE analysis, and comparisons of transglycosylation rates could not be made as 100% non-amidated dansylated Lipid II, required for the continuous assay, was not a viable substrate. A mixture of labelled and non-labelled Lipid II could be used as an alternative, however due to the unknown specificity of the donor and acceptor sites for the dansylated substrate (Section 5.8.1.1), data analysis would be complicated by the productive or inhibitory interactions of mixtures of dansylated and non-dansylated substrates at either binding site.

No impact of Lipid II amidation in either processivity or rate was observed with the Δ28(FL) enzyme. This could suggest that the transmembrane domain has an important role in substrate interaction, and has a greater effect than the presence of isoglutamine in the second position. MGT-Δ28(FL) is a significantly more active transglycosylase than MGT-Δ67 (Huang *et al.,* 2012). Therefore the rates of transglycosylation with both amidated and non-amidated substrates may have been too high to observe any difference. Therefore, continuous fluorescence assays with a much greater range of enzyme concentrations could be performed to test this hypothesis.

The only literature to date covering the substrate specificity of PBPs for amidated Lipid II concerns the bifunctional enzymes from *S. pneumoniae* (Zapun *et al.,* 2013), in which the requirement for amidated substrate for the formation of a cross-linked peptidoglycan species (but not specifically the transglycosylase activity) was studied.

5.8.2 Characterisation of *Staphylococcus aureus* PBP2 transglycosylase activity

The effect of Lipid II amidation on the transglycosylase activity of the bifunctional *Staphylococcus aureus* PBP2 was also investigated by SDS-PAGE analysis of reaction products.

5.8.2.1 PBP2 purification

PBP2 was successfully purified in the absence of its hydrophobic transmembrane spanning domain (Section 5.3.2), however purification of full-length PBP2 was less successful (Section 5.5.4) where a poor yield of impure protein was achieved. This was mainly due to inefficient solubilisation of protein with detergent. This observation suggests that a screen of alternative detergents might enable more efficient solubilisation of this protein. Furthermore, whether or not the expressed protein was correctly folded was unknown. This point could be addressed by analysing Bocillin FL binding of the expressed protein to establish the integrity of the transpeptidase active site and binding of the protein to immobilised moenomycin (Bury *et al*., 2015; Stembera *et al.,* 2002).

5.8.2.2 PBP2-Δ59 activity

The transglycosylase activity of PBP2 observed previously (Barrett *et al.,* 2005; Wang *et al.,* 2008) could not be repeated under the same conditions. There are several possible reasons for this: Firstly, Barrett and colleagues conducted their experiments with full-length PBP2, which may be more active than the ΔTM version. This theory is supported by both the literature (Helassa *et al.,* 2012; Huang *et al.,* 2012; Sung *et al.,* 2009, Wang *et al.,* 2001) and previous work in this chapter

(Section 5.8.1.1). Significantly, the previous assays (Barrett *et al.,* 2005) with PBP2-FL use a heptaprenyl (C_{35}) Lipid II variant rather than the native undecaprenyl (C_{55}) version. This had been identified to be a more amenable substrate for *in vitro* study (Ye *et al.,* 2001) but may interact with the enzyme differently to natural C_{55} Lipid II.

The Lipid II used previously by Barrett and colleagues was ^{14}C labelled unlike the dansylated substrate used here, and this may account for the lack of activity under the conditions. The buffer system in which activity was observed was as used for *S. pneumoniae* PBP2a in Chapter 4, and may require further optimisation for this particular protein. Additionally, C_{35} dansylated Lipid II could be synthesised and tested to identify the role of this shorter lipid chain on the observed activity differences.

It is likely that efforts to observe PBP2-Δ59 transglycosylase activity by the continuous fluorescence assay were unsuccessful due to a poor rate undetectable by the time-course used for the SDS-PAGE assay. This may be due to the enzyme truncation, presence of the dansyl group on the substrate, or the buffer conditions used. Therefore successful purification of PBP2-FL and an extensive optimisation of the buffer system are important steps in the understanding of PBP2 transglycosylase activity, and are a priority for further work.

5.8.2.3 Effect of Lipid II amidation on PBP2 transglycosylation

PBP2-Δ59 demonstrates a clear preference for amidated Lipid II as a transglycosylase substrate. This was observed by SDS-PAGE analysis of glycan products, as efforts to observe activity by a continuous fluorescence assay were unsuccessful (Section 5.5.3). Lipid II amidation appears to affect processivity of PBP2-Δ59 polymerisation, however, a firm conclusion cannot be drawn as the reaction with Lipid II (Glu, Dans) did not go to completion overnight. This clearly identifies non-amidated Lipid II to be a poor substrate.

The processivity of *Staphylococcus aureus* PBP2 transglycosylase activity has previously been studied (Rebets *et al.,* 2014; Wang *et al.,* 2008) with C_{35} non-

amidated Lipid II substrate and full-length enzyme where glycan chains of ~15 disaccharide units were observed. Based on previous gels and knowledge of chain length, an estimate of an average of 10 disaccharide units in length can be approximated for PBP2-Δ59 with amidated Lipid II, and much shorter (3-4 disaccharides) with non-amidated Lipid II. A comparable study with full-length PBP2 is of great interest to identify any TM region mediated increase in processivity, as suggested for *S. pneumoniae* PBP2a (Helassa *et al.,* 2012). Although the effect of detergent on this difference should be considered as discussed in Section 4.6.3.2. Interestingly, the average length of *Staphylococcus aureus* glycan chains *in vivo* is 6 disaccharides, with a range from 3-10 (Boneca *et al.,* 2000), which correlates well with the experimental data in this chapter.

The work presented here testifies to the catalytic inefficiency of this enzyme with lipid II irrespective of amidation. It is clear however, that this PBP functions in wild type *Staphylococcus aureus* not with lipid II but with lipid II carrying a pentaglycine branch on the ε-amino group of the stem peptide of this precursor. It is probable that PBP2 has a requirement for this branched precursor in order to catalyse transglycosylation fast enough to support cellular viability. This scenario is consistent with the observed essentiality of indirect cross-links in staphylococcal peptidoglycan (Rohrer and Berger-Bächi*,* 2003).

5.8.3 Combined transglycosylase activity of *Staphylococcus aureus* PBPs

The Class B monofunctional transpeptidase PBP2a did not stimulate the processivity of *Staphylococcus aureus* PBP2-Δ59 activity (Figure 5.16), despite evidence for their functional interaction (Paulin *et al.,* 2014; Pinho *et al.,* 2001; Reed *et al.,* 2011). However, both enzymes were truncated at the N-terminus to remove the transmembrane spanning domain. All evidence for the interaction of these proteins is with full-length versions and therefore the TM region may be important. It has been shown to be important in dimerisation of PBPs (Helassa *et al.,* 2012 and Chapter 4) so likely also between proteins in complexes. Reed *et al.,* (2011) identified other PBPs (SgtA, MGT and PBP1) involved in interactions and the experiments by Paulin *et al.,* (2014) implicate the cell division protein FtsZ as well.

Therefore, it is likely that additional PBPs, cell division proteins and other interactions in the proposed cell wall synthesis complex (Section 5.8.4.2) are involved in functional interactions with PBP2. These may be able to stimulate the activity of PBP2; and an extensive range of experiments could be designed to test the many combinations. Consistent with this, MGT has recently been shown to extend glycan products of PBP2 (Rebets *et al.,* 2014) and to have an optimal substrate of Lipid IV (Braddick *et al.,* 2014), and therefore it would be of interest to identify if either PBP stimulates the activity of the other, along with working together to produce longer glycan chains (Rebets *et al.,* 2014).

Despite no observable effect on the processivity of PBP2, the rate of transglycosylase activity could not be studied due to issues in observing activity by the continuous fluorescence assay (Section 5.8.2.2).

5.8.4 Biological implications

5.8.4.1 The requirement for multiple transglycosylases

Clear differences in the substrate specificity and processivity of *Staphylococcus aureus* MGT and PBP2 have been observed; with MGT producing longer glycan chains than PBP2 but being less affected by Lipid II amidation. Distinct requirements for observation of activity of the two enzymes have been seen previously (Abrahams, 2011; Barrett *et al.,* 2005; Terrak *et al.,* 2006). These make up two of the three transglycosylases in *Staphylococcus aureus*, with an additional nonessential monofunctional transglycosylase; SgtA (Reed *et al.,* 2011). Multiple peptidoglycan transglycosylases are present in most bacteria, proposed to act at different stages of cell growth and division (Scheffers and Pinho, 2005). Indeed, PBP2 has been shown to localise to the septum during cell division in a substrate dependent manner (Pinho and Errington*,* 2005). The cellular localisation of MGT is as yet unknown. It has also been suggested that the structure of peptidoglycan varies at different locations in the cell, giving a requirement for different lengths of polymer (Wang *et al*., 2008). It was recently identified that glycan chain length plays a crucial role in determining *Staphylococcus aureus* morphology (Rebets *et al.,* 2014) and that

the long chain lengths produced by MGT may be protective in cell wall stress, as gene expression of this monofunctional transglycosylases is upregulated (Balibar *et al.*, 2010; Steidl *et al.,* 2008).

MGT transglycosylase activity becomes essential in the absence of an active PBP2, and whilst it is able to maintain cell viability, it cannot preserve β-lactam resistance in an MRSA background (Reed *et al.,* 2011). This suggests that the long glycan chains produced by MGT are sufficient for correct growth and division but may not be a substrate for *Staphylococcus aureus* PBP2a transpeptidase activity, whereas those produced by PBP2 are a substrate for PBP2a, allowing coordinated synthesis of peptidoglycan in the presence of β-lactams. MGT and PBP2a have been shown to interact (Reed *et al.,* 2011) but functionality of the complex has not been demonstrated to date and may be an artefact of the yeast two-hybrid system used.

5.8.4.2 A cell-wall synthesis complex

The cooperative function of *Staphylococcus aureus* PBPs in peptidoglycan synthesis is well documented (Leski and Tomasz, 2005; Pinho *et al.,* 2001; Reed *et al.,* 2011) and these are predicted to form part of a larger cell division complex (Steele *et al.,* 2011; Touhami *et al.*, 2004). This is an increasingly disseminated hypothesis for many bacteria (see Section 1.7.2). MGT, SgtA, PBP1, PBP2 and PBP2a from *Staphylococcus aureus* have all been shown to interact (Reed *et al*., 2011). The monofunctional transglycosylase enzymes of *Staphylococcus aureus* have been shown to be non-essential in the presence of a functional PBP2 but it has been suggested that MGT and SgtA interact with PBP2 and other enzymes involved in cell wall synthesis as part of a larger, as-yet-uncharacterized cell wall-synthetic complex (Reed *et al.,* 2011).

It was recently observed that *Staphylococcus aureus* membrane particulates formed longer glycan chains when all transglycosylases were active than by MGT alone (Rebets *et al.,* 2014), suggesting a combined effect of PBP2 and MGT mentioned in Section 5.8.4.1 and also the possibility of the involvement of the final transglycosylase (SgtA) or indirectly other cell-wall enzymes in increased

processivity. The combined effect of MGT and PBP2 was not studied here, but could be tested in further work.

Additional evidence for the requirement of a peptidoglycan synthesis complex comes from the recent identification that formation of Lipid IV is rate limiting and more significantly so in *Staphylococcus aureus* MGT than any other enzyme tested (Wang *et al.,* 2011). Combined with evidence for Lipid IV as the optimal substrate for MGT (Braddick *et al.,* 2014) and that it can extend the polymers produced by PBP2 (Rebets *et al.,* 2014), a clear combined but ultimately non-essential (Reed *et al.,* 2011) role of at least these two transglycosylases at one or all stages of the cell cycle is suggested.

5.8.4.3 Role of Lipid II amidation in *Staphylococcus aureus*

Several explanations for the role of Lipid II amidation in *Staphylococcus aureus* viability have been suggested, including the requirement by peptidoglycan synthesis enzymes such as PBP2 and MGT (Figueiredo *et al.,* 2012). Amidation has been shown to significantly affect growth rate, and resulting cells are of normal size but with fewer complete septa. Point mutations in the PBP2 active site cleft (in the extending polymer binding site) results in shorter glycan chains and septal abnormalities due to incorrect cell division regulation (Rebets *et al.,* 2014). The morphology observed in mutants with depleted amidation of peptidoglycan intermediates could be explained by the ability of MGT to produce long chains with non-amidated Lipid II, and the presumed requirement for amidation for PBP2 activity as demonstrated in this chapter. Experiments with PBP2-Δ59 suggest that stem peptide amidation affects PBP2 more significantly than MGT. If full-length PBP2 were to be less processive with non-amidated than amidated substrate, as the experiments with PBP2-Δ59 suggest, this may explain the septal abnormalities observed. Further work is required to confirm this as all of the literature to date concerns the non-amidated substrate, and full-length PBP2 was not studied here.

The substrate for the MurT/GatD amidation complex has been identified as either Lipid II or Lipid II Gly$_5$ (Münch *et al.,* 2012). Recent work in our lab has shown that

FemX, FemA and FemB will append a pentaglycine branch to amidated Lipid II (Rebecca Bolton, personal communication). If FemXAB is shown to act preferentially on amidated Lipid II, then this could suggest that Lipid II amidation occurs before the addition of the pentaglycine branch. It would suggest an importance for amidation in Lipid II branching, and help to explain the requirement of both isoglutamine containing pentapeptides and Gly_5 branch for full expression of methicillin resistance (Münch *et al*., 2012; Rohrer and Berger-Bächi*,* 2003).

This may also help to explain the decrease in β-lactam resistance observed on depletion of amidation (De Lencastre *et al.,* 1999). Alternatively it has been suggested that structurally abnormal cell wall peptides are poor substrates for PBP2a (Figueiredo *et al.,* 2012; Strandén *et al*., 1997). This may be directly, or due to poorer utilisation of the non-amidated Lipid II by PBP2 to produce the polymerised substrate for cross-linking.

At least one of the two peptidoglycan stem peptides must be amidated for cross-linking to occur (Nakel *et al.,* 1971), and very high cross-linking (> 95%) is required for *Staphylococcus aureus* survival. A reduction in cross-linking results in aberrant septum formation and deformed cells (Gally and Archibold 1993). The role of amidation in this could be; directly, through amidated Lipid II being a better substrate for PBP2a, PBP2 or PBP4 or through the increased branching of amidated Lipid II by FemXAB producing an optimal substrate for cross-linking by these enzymes.

It is clear that many factors are involved in the observed phenotypes (reduced growth rate and increased susceptibility to lysozyme and methicillin) on depletion of amidation, and the results shown here support the evidence that the essentiality is at least in part due to the substrate specificity of the *Staphylococcus aureus* transglycosylases.

5.8.5 The characterisation of novel carbohydrate based transglycosylase inhibitors

Two carbohydrate-based compounds were tested against *Staphylococcus aureus* MGT-Δ28(FL) as putative transglycosylase inhibitors. IC_{50} values of 26.1 μM ± 2.7 (17 μg.ml^{-1}) and 15.6 μM ± 2.0 (11 μg.ml^{-1}) were established for ACL202015 and ACL20964 respectively, compared to 5.1 μM ± 0.729 (8 μg.ml^{-1}) for moenomycin. These results suggest that ACL202015 and ACL20964 do not bind as strongly to the active site (binding site predicted by docking (Zuegg *et al.,* 2015)) as moenomycin. Notably, the IC_{50} value obtained for moenomycin by this assay was higher than expected given its tight binding nature. Despite this, the results (in concert with others within the paper) clearly identify these compounds as inhibitors of transglycosylase activity.

5.8.5.1 Limitations of the assay used

The assumption of 100% turnover of Lipid II in the continuous assay was not made, as there was insufficient evidence to justify it (see section 4.6.2.2 for discussion). Therefore, in order to establish a K_m for Lipid II (Glu, Dans) polymerisation by MGT-Δ28(FL) the initial rate in RFU/second was plotted against substrate concentration. This method allows comparison of the initial rates of fluorescence decrease due to incorporation of substrate into glycan chains, but does not enable rates as a factor of μM quantities of Lipid II per unit time to be established. However, the range of substrate concentrations tested did not allow the rate to plateau with respect to substrate concentration. Notably, the fit to Equation 4 (Section 5.7.4) suggests cooperativity in activity with respect to substrate concentration, as was seen for *S. pneumoniae* PBP2a (Section 4.5.4). The recent identification of cooperativity in substrate binding to the donor and acceptor transglycosylase sites of *S. aureus* MGT (Bury *et al*., 2015), and the suggestion of cooperativity seen in this chapter highlights the need for further work in this respect. Due to substrate limitations, a published value was used to calculate substrate concentrations for inhibitor testing.

This calculation resulted in a 1.45:1 ratio of substrate:enzyme in subsequent assays which initially does not seem realistic given the requirement for two molecules of substrate for each molecule of enzyme. However, the initiation step of transglycosylation has been shown to be limiting in MGT (Wang *et al.,* 2011) and long polymers were observed even at a 1:1 enzyme to substrate ratio, accounted for by slow initiation resulting in only a small amount of the available enzyme producing polymers with the available substrate. Therefore, the ratio of Lipid II:enzyme used here should enable polymer formation for digestion by *N*-acetylmuramidase, but does mean that the active enzyme concentration is likely to be overestimated. This also has implications for any conclusions surrounding the tightness of binding of inhibitors, such as moenomycin, as the inhibitor will be binding to enzyme molecules that would otherwise not be actively polymerising.

The structural similarity between the lysozyme and transglycosylase active site (Lovering *et al.,* 2007; Yuan *et al.,* 2007) raises an important point in the usefulness of this continuous assay for the identification of novel inhibitors of transglycosylase activity. The interaction of moenomycin with lysozyme is not reported in the literature. However, the presence of a large excess of lysozyme as a coupling enzyme in the assay would require its potent inhibition by moenomycin or the novel inhibitors observed tested here. Additionally, a sigmoidal relationship with respect to fluorescence decrease over time would be expected as active lysozyme concentration is reduced below that able to support a linear rate, but this was not observed. Finally, both ACL202015 and ACL20964 were shown to inhibit transglycosylation by an orthogonal assay without the need for a coupling enzyme (Zuegg *et al.,* 2015) supporting the conclusions drawn from the fluorescence data reported here.

Non-amidated Lipid II was used in this investigation due to substrate availability and previous experiments identifying no difference in rate of the continuous assay of MGT-Δ28(FL) (Section 5.8.1.2). The previous experiments did not establish kinetic parameters for the two substrates, which may differ. Therefore a full analysis of MGT-Δ28(FL) activity with a range of Lipid II and enzyme concentrations would establish this. If a difference is observed, then a variation in the effect of the inhibitors may also be observed and should be tested.

5.8.5.2 Implications of the results

Zuegg *et al.,* 2015 (attached at the end of this thesis; Appendix 8) showed via a series of membrane based transglycosylase assays and membrane-disruption experiments that ACL202015 and ACL20964 were able to inhibit transglycosylase activity without disrupting the cell membrane. Both compounds showed good *in vitro* antibacterial activity against a range of Gram-positive bacteria, including drug resistant MRSA, GISA and VanA enterococci as well as good *in vivo* efficacy with no toxicity. Fluorescent NBD-Lipid II incorporation assays showed these compounds to inhibit *Staphylococcus aureu*s MGT, and the dose response assays described here support and extend from this, providing IC$_{50}$ data in a comparable range to that of moenomycin. The data reported here was consistent with virtual docking experiments showing that in comparison to moenomycin, both compounds partly occluded both the donor and acceptor binding site. Consequently the data reported here suggests that these molecules may be considered to be lead compounds in further transglycosylase directed antimicrobial drug discovery.

5.8.5.3 Further work

The discussion of the data covered in this section leads to the suggestion of a number of aspects of further work in the study of these inhibitors.

Confirmation of the IC$_{50}$ values by an alternative assay system such as the recently published Förster resonance energy transfer (FRET) method (Huang *et al.,* 2013) could be used to confirm the results. This would be an essential step in adding weight to these findings, and could enable a kinetic analysis of the mode of inhibition (competitive, un-competitive (unlikely) or non-competitive) by ACL202015 and ACL20964 that could confirm their mode of action as inhibitors suggested by the virtual docking experiments. The inhibitors should also be tested with other transglycosylases, in particular bifunctional PBPs from pathogens of current clinical concern.

Co-crystallisation of MGT and other Gram-positive transglycosylases with the compounds would allow the predicted binding site to be confirmed. This knowledge could aid the design of future novel inhibitors and antibiotics.

5.9 Conclusion

Differences in processivity and substrate specificity of the *Staphylococcus aureus* transglycosylases have been identified, contributing to a new understanding of the role of Lipid II amidation in bacterial cell wall biosynthesis. Two novel carbohydrate based compounds were shown to be inhibitors of transglycosylase activity, aiding the hunt for new antimicrobials.

Chapter 6. Enzymology of transpeptidation: towards kinetic characterisation of the peptidoglycan cross-linking activity of *Streptococcus pneumoniae* PBPs

6.1 Introduction

The final step in the biosynthesis of peptidoglycan is the formation of a peptide bond between the third and fourth position amino acids of adjacent pentapeptide stems (Ghuysen, 1991). These crosslinks may be direct or indirect via a peptide branch, and are critical for structural rigidity of the final glycan sacculus (Vollmer *et al,* 2008). Formation of the peptide bond is catalysed by the transpeptidase activity of HMW bifunctional and monofunctional transpeptidase PBPs (Section 1.7.4)). The transpeptidase (penicillin-binding) domain of PBPs is the target for β-lactam antibiotics (Ghuysen, 1991), to which high levels of resistance have developed through several mechanisms in *S. pneumoniae* (Section 1.8.1). Investigating the peptidoglycan cross-linking activity of the PBPs is crucial in understanding the mechanisms of cell wall synthesis, as well aiding in the discovery of novel antibiotic agents.

6.1.1 *Streptococcus pneumoniae* β-lactam resistance

A primary factor in pneumococcal β-lactam resistance is the presence of low affinity PBPs. In addition, the presence of an L-Ala-L-Ala or L-Ser-L-Ala bridge on the third position lysine is associated with high level resistance and these strains exhibit elevated levels of inter-peptide branching (Garcia-Bustos and Tomasz, 1990) (Section 1.8.1). It has long been hypothesised that glycan chains with branched pentapeptides might be preferential substrates for the resistant PBPs, allowing them to maintain their cell wall synthetic activity and produce the high levels of branched cross-links observed whilst having a low affinity for the substrate mimic β-lactam ring (Filipe and Tomasz 2000). Mutations conferring resistance to β-lactams have

been associated with alterations in transpeptidase active site shape and charge. Greater flexibility is observed in the active site of PBP1a, PBP2b and PBP2x in resistant strains, through alterations in β3 and β4 of the β-sheet (Contreras-Martel *et al.,* 2006; 2009; Job *et al.,* 2008; Pernot *et al.,* 2004). Crystal structures have shown the monofunctional transpeptidases (PBP2b and PBP2x) from some resistant pneumococcal strains to have more open active sites as a result of mutations (Contreras-Martel *et al.,* 2009; Dessen *et al.,* 2001; Pernot *et al.,* 2004), with larger changes in the PBP2b active site associated with higher levels of resistance (Contreras-Martel *et al.,* 2009). The biochemical characterisation of substrate specificity of these enzymes will enable the importance of the aforementioned active site changes to be investigated.

6.1.2 Assays for transpeptidase activity

The penicillin-binding domain of PBPs is responsible for both transpeptidase and carboxypeptidase activity, both of which result in the release of D-alanine (Section 1.7.4.2). Most existing assay methods for studying the penicillin-binding domain do not distinguish between transpeptidase and DD-carboxypeptidase activity, and those that do are discontinuous in their nature. A sensitive, continuous assay of transpeptidase activity is required to enable detailed insight into the kinetic properties of this critical role of PBPs.

6.1.2.1 Assay systems using substrate analogues

Prior to the availability of physiologically relevant lipid-linked substrates, a thiol-ester analogue of the stem peptide (S2d) was used as a donor along with amino acid acceptors in order to identify transpeptidation (Adam *et al.,* 1991; Jamin *et al.,* 1993; Wilkin *et al.,* 1993). Analogue hydrolysis through thioesterase activity of PBPs is monitored spectrophotometrically. Additionally, substrate analogues or inhibitors can be used to determine the acylation and deacylation rates of PBPs by measuring the quenching of intrinsic protein fluorescence upon binding (Jamin *et al.,* 1993; Josephine *et al.,* 2006) and deacetylation alone was studied with [^{3}H]-benzylpenicillin labelling of PBPs, by monitoring the reduction in protein

radioactivity over time (Pagliero *et al.,* 2004). A high throughput assay for binding to immobilised PBPs followed by treatment with biotin-ampicillin has been established (Stefanova *et al.*, 2010). Subsequent addition of streptavidin-horseradish peroxidase (HRP) and a fluorogenic HRP substrate enables quantification of binding. These latter techniques are not able to distinguish between transpeptidase and DD-carboxypeptidase activities, and all use non-canonical substrates.

6.1.2.2 Assay systems using native substrates

Recent advances in synthesis of the native Lipid II substrates for PBPs (Breukink *et al.*, 2003; Lloyd *et al.*, 2008; VanNieuwenhze *et al.*, 2002; Schwartz *et al.,* 2001), has made direct assays of transpeptidase activity possible. Detection of cross-linked material is either directly through chromatographic separation of reaction products, or indirectly through the detection of released D-Ala as described in the following section.

6.1.2.2.1 Chromatographic methods

The products of peptidoglycan synthesis can be separated by HPLC or SDS-PAGE, with the former enabling quantitative analysis. Vinatier *et al.,* (2009) separated peptidoglycan products by HPLC following incubation of *E. coli* membranes with D-Cys containing UDP-Mur*N*Ac-pentapeptides. Products were labelled with fluorescein maleimide prior to digestion, HPLC separation, and mass spectrometry to confirm the presence of cross-linked peptide stems. More recently, radiolabelled products of peptidoglycan biosynthesis by *E. coli* PBP1a (Born *et al.,* 2006) and PBP1b (Bertsche *et al.,* 2005) were separated by HPLC. This enabled the investigation of acceptor strand specificity for transpeptidation. Biboy *et al.,* (2013) give a detailed account of this technique. Analysis of the chromatogram and mass spectrometry of products allows identification of muropeptides, their relative abundance and the extent of cross-linking. Liquid-chromatography mass spectrometry (LC-MS) enables rapid identification of PBP products using completely native substrates (Lebar *et al.*, 2013).

SDS-PAGE analysis of glycan chains has been used as an assay for transglycosylase activity previously (covered in more detail in Section 4.1.2). Through the use of either radiolabelled or a mix of 10% fluorescently labelled (90% non-labelled) Lipid II and a penicillin G control, cross-linking can occur and transpeptidase activity can be probed (Barrett *et al*., 2007; Helassa *et al*., 2012; Zapun *et al.,* 2013). However, unlike the HPLC method, cross-links cannot be proven, as high molecular weight material is excluded from the gel regardless of whether it is long glycan chains or cross-linked peptidoglycan.

6.1.2.2.2 Spectrophotometric assays

Both transpeptidation and D,D-carboxypeptidation result in the release of the terminal D-Ala from the pentapeptide stem (Section 1.7.4.2), and therefore detection of D-Ala can be used to indirectly follow these enzymatic activities. The first use of this method was by Mirelman *et al.,* (1972) through the incorporation of UDP-Mur*N*Ac-L-Ala-D-Glu-L-Lys-D-Ala-[^{14}C]-D-Ala into *Micrococcus luteus* membranes. The release of [^{14}C]-D-Ala due to PBP activity was used to measure the composite transpeptidase and carboxypeptidase activities. Chromogenic assays are now available to follow D-Ala release in a continuous manner and could be used to follow transpeptidation, as described later in this chapter. (Section 6.4)

6.1.2.2.3 D-amino acid exchange

E. coli PBP1b will incorporate D-amino acids into the stem peptide in place of the terminal D-Ala *in vitro*, a phenomena which also occurs *in vivo,* and is thought to have a role in signalling (Lupoli *et al.,* 2011). Lupoli *et al.,* (2014) established an assay to monitor [^{14}C]-D-Ala incorporation as method to study transpeptidation.

6.1.3 Studying *S. pneumoniae* transpeptidase activity

The assays described here have been used in attempts to study the mechanism of transpeptidation. However many fail to distinguish between this and D,D-

carboxypeptidase activity, use a non-native substrate as a proxy or are discontinuous in their nature. Consequently, much more is known about the interaction of the penicillin-binding domain with β-lactams than kinetic parameters with native substrates (Lupoli *et al.,* 2011).

Progress has been slow, with the vast majority of published literature to date concerning only Gram-negative PBPs, in particular those from *E. coli*. Transpeptidase activity of these enzymes was identified *in vitro* by several methods (Bertsche *et al*., 2005, Born *et al.,* 2006) and only very recently significant advances have been made in understanding the substrate specificity and kinetic parameters associated with it (Lebar *et al*., 2013, Banzhaf *et al.,* 2012). Discovery of the role of the outer membrane lipoproteins LpoA and LpoB in *E. coli* PBP1a and PBP1b peptidoglycan assembly respectively (Lupoli *et al.,* 2014) has in part helped to explain the reasons for difficulties encountered with *in vitro* reconstitution. LpoA was shown to stimulate PBP1a catalysed cross-linking by 4.5 fold *in vitro*. Additionally double knock-outs of PBP1a-LpoB and PBP1b-LpoA were lethal which demonstrates the critical role of these lipoproteins *in vivo* (Typas *et al.,* 2010).

Cross-linked peptidoglycan was observed in early work using both isolated membranes and purified PBPs from *Bacillus megaterium* and *Bacillus stearothermophilus* (Jackson and Strominger, 1984; Linnett and Strominger, 1974; Schrader *et al*., 1974; Wickus and Strominger, 1972), however reconstitution of peptidoglycan assembly in other Gram-positive bacteria has historically been problematic. Only very recently, the first *in vitro* observation of transpeptidase activity from *S. pneumoniae* was made (Zapun *et al.,* 2013), and shown to be critically dependent on amidation of the stem-peptide. This discovery should facilitate the development of assays to study cross-linking in Gram-positive bacteria in more detail.

6.1.4 Aims of this chapter

Of the five synthetic PBPs in *S. pneumoniae*; PBP1a, PBP2a, PBP1b, PBP2b and PBP2x (Section 1.8.2), PBP2b and PBP2x are essential (Kell *et al.,* 1993), and one of

either PBP2a or PBP1a must be functional for cell viability (Hoskins *et al.,* 1999). Variants of all four are involved in β-lactam resistance, although mutations in PBP2a have only been described occasionally (Hakenbeck *et al.,* 2012; Zapun *et al.,* 2008).

This chapter focuses on the *in vitro* detection of bifunctional PBP1a and PBP2a transpeptidase activity, concentrating particularly on PBP1a due to its more significant role in β-lactam resistance (Section 1.8.2; Barcus *et al.,* 1995; Hakenbeck *et al.,* 2012). The predominant objective was to observe cross-linking using a continuous assay for the first time, with the eventual aim of studying the substrate specificity of PBP1a from resistant and susceptible strains with the dipeptide branched substrates, in order to test the long standing hypothesis described in Section 6.1.1.

6.2 Experimental aims

- To detect transpeptidase activities of *S. pneumoniae* PBP1a and PBP2a by SDS-PAGE analysis.
- To observe *S. pneumoniae* PBP1a and PBP2a transpeptidase activity by a continuous spectrophotometric assay.
- To investigate substrate specificity of the transpeptidase activity by PBPs from β-lactam susceptible and resistant *S. pneumoniae* strains.

6.3 Detection of transpeptidase activity by SDS-PAGE

Zapun *et al.,* (2013) first made observations consistent with *in vitro* transpeptidase activity of *S. pneumoniae* PBP1a and PBP2a by SDS-PAGE and mass-spectrometry. Full-length (including the transmembrane domain) variants of these enzymes were purified as described in Section 4.3.1 and 4.3.3 respectively, according to the protocol employed by Zapun *et al*., and therefore transpeptidase activity under the same conditions was expected. Tris-Tricine SDS-PAGE analysis of overnight reaction products was performed as described in Section 6.1.2.2.1 in order to confirm this.

6.3.1 Demonstration of PBP1a and PBP2a *in vitro* peptidoglycan assembly

A mix of 50 μM non-dansylated and 5 μM dansylated Lipid II (either Lipid II (Glu) or Lipid II (Gln)) was incubated with 1 μM PBP1a or PBP2a at 30°C overnight. Reactions were in the presence and absence of moenomycin (0.5 mM) or penicillin G (1 mM) as inhibitors of transglycosylation and transpeptidation respectively. Reaction buffers were, PBP1a; 50 mM HEPES pH 7.5, 10 mM $MgCl_2$, 150 mM NaCl, 25% (v/v) DMSO, 0.02% (v/v) Triton X-100, and PBP2a; 50 mM HEPES pH 7.5, 25 mM $MgCl_2$, 200 mM NaCl, 25% (v/v) DMSO, 0.02% (v/v) Triton X-100 and products were analysed by SDS-PAGE (Section 2.8.2) (Figure 6.1).
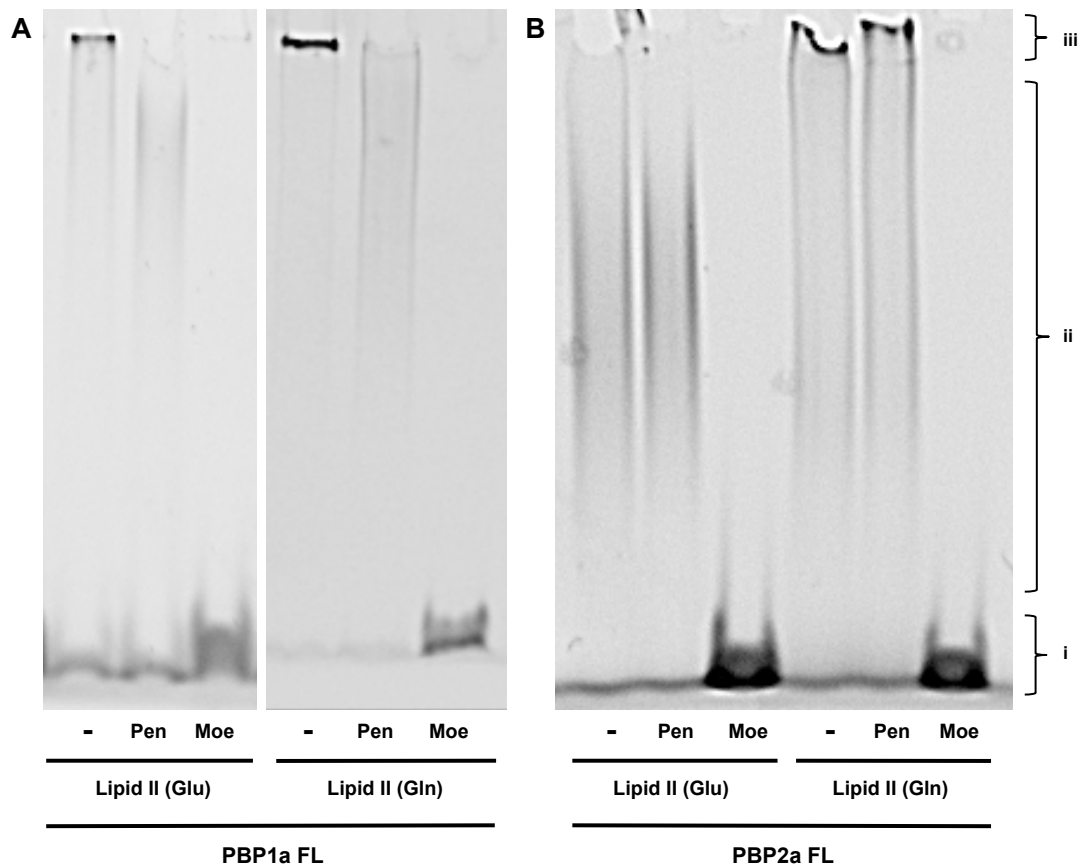
Figure 6.1 Assembly of peptidoglycan by *S. pneumoniae* PBP1a (A) and PBP2a (B) Mixture of 50 μM Lipid II (Lipid II (Glu) or Lipid II (Gln)) and 5 μM dansylated Lipid II (Lipid II (Glu, Dans) or Lipid II (Gln, Dans) as labelled below the gel and 1 μM PBP1a or 1 μM PBP2a where indicated. -,no inhibitor; Pen, 1 mM penicillin G; Moe, 0.5 mM moenomycin. Products of reaction separated on a 8.5% T/2.7% C Tris-Tricine SDS-PAGE gel. Dansyl fluorescence at 521 nm detected using a blue light converter and short pass filter on a GeneSnap Gel Doc. (i) denotes unpolymerised Lipid II; (ii) glycan chains of varying lengths and (iii) the very high molecular weight material, which does not enter the gel.

Figure 6.1 demonstrates the same high molecular weight band observed by Zapun *et al.*, (2013) with PBP1a, which is not detected in the presence of penicillin G. As previously described by Zapun and colleagues, this band is more significant in the presence of amidated Lipid II, consistent with the hypothesis that amidation was required for efficient peptidoglycan assembly. The same band was observed with incubation of amidated Lipid II and PBP2a, and not detected with non-amidated Lipid II. However, unlike in the earlier study, this high molecular weight band was not removed by the addition of penicillin G. Figure 4.6 also identified this species in an assay of transglycosylase activity with the same enzyme, thus demonstrating the clear limitation of this assay system for the differentiation between long polymers and cross-linked glycan chains, both of which are unable to enter the polyacrylamide gel matrix.

6.3.2 Time dependency of peptidoglycan assembly

With the main aim of observing peptidoglycan cross-linking in a continuous assay format, the experiment in Section 6.3.1 was repeated with incubation for 1 hour, a reasonable time-course over which activity could be monitored in a spectrophotometric assay. Due to the clear preference for amidated substrate observed by Zapun *et al.,* (2013), as well as in Chapter 4 of this thesis and Figure 6.1, only this substrate was tested.

A mix of 50 μM Lipid II (Gln) and 5 μM Lipid II (Gln, Dans) was incubated with 1 μM PBP1a or PBP2a at 30°C for 1 hour in the presence and absence of moenomycin (0.5 mM) or penicillin G (1 mM). Reaction buffers were as described in Section 6.3.1. Reaction products were analysed by SDS-PAGE (Section 2.8.2) (Figure 6.2).

The band previously attributed to cross-linked peptidoglycan was observed following a 1 hour incubation with both PBP1a and PBP2a, and not in the presence of Penicillin G demonstrating that in principle, cross-linking could be monitored in a continuous assay format in a reasonable time frame.

PBP1a is more biologically relevant than PBP2a in the context of antibiotic resistance (Barcus *et al.,* 1995; Hakenbeck *et al.,* 2012), and therefore was prioritised for further work in the first instance. Additionally Figure 6.2 shows that with amidated Lipid II, a single clean band is observed which does not enter the gel, as opposed to the smear seen with PBP2a, consistent with a mix of cross-linked and non-cross-linked material. This could complicate analysis, and supports the decision to carry out initial optimisation with PBP1a.
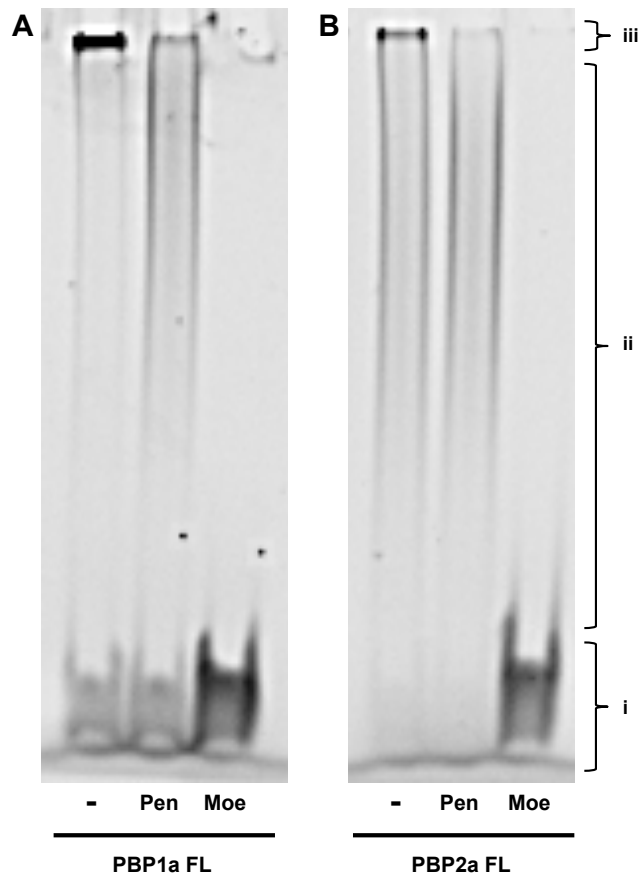
Figure 6.2 Time dependency of peptidoglycan assembly by _S. pneumoniae_ PBP1a (A) and PBP2a (B) Mixture of 50 μM Lipid II (Gln) and 5 μM dansylated Lipid II (Gln, Dans) incubated with 1 μM PBP1a or 1 μM PBP2a where indicated for 1 hour. -,no inhibitor; Pen, 1 mM penicillin G; Moe, 0.5 mM moenomycin. Products of reaction separated on a 8.5% T/2.7% C SDS-PAGE gel. Dansyl fluorescence at 521 nm detected using a blue light converter and short pass filter on a GeneSnap Gel Doc. (i) denotes unpolymerised Lipid II; (ii) glycan chains of varying lengths and (iii) the very high molecular weight material, which does not enter the gel.

6.3.3 Characterisation of the high molecular weight species

One significant limitation of the method used by Zapun _et al_., (2013), and the conclusions that could be drawn from by it, is that the band of product unable to enter the gel matrix was not characterised. The controls used allow an interpretation that it consists of cross-linked peptidoglycan, however, the same band has been observed within this thesis in assays of transglycosylase activity, where cross-linking cannot occur, such as with the _Staphylococcus aureus_ monofunctional transglycosylase (MGT) and _Streptococcus pneumoniae_ PBP2a (Chapter 4 and 5).

Zapun and colleagues carried out mass spectrometric identification of cross-linked product, however all reaction products were analysed, rather than the band from the gel. Additionally, the mass observed could represent a dimer of disaccharide-pentapeptide and disaccharide-tetrapeptide cross-linked through the pentapeptide stem, or through a β-1,4-linkage between sugars (Figure 6.16). Furthermore the masses were inconsistent with the presence of a dansyl group, further reducing the support they give that the high molecular-weight fluorescent material unable to migrate on SDS-PAGE was cross-linked peptidoglycan. Positive ion fragmentation is required to differentiate the two. Therefore, two attempts were made to analyse the high molecular weight band from Figure 6.2 (A) by positive ion mass spectrometry in order to identify its composition. The method used is detailed in Section 2.8.3.

The band was cut from the gel under UV illumination, the acrylamide dehydrated and *N*-acetylmuramidase digestion performed in gel (similar to that for tryptic digest of proteins for mass spectrometry). Initially, digestion was overnight with hen egg-white lysozyme before removal of protein and acrylamide by heating and centrifugation. Lysozyme was chosen as its smaller molecular weight (14.3 kDa) compared to mutanolysin (27 kDa) was thought better for entering the acrylamide matrix and therefore accessing the peptidoglycan polymers. The supernatant was analysed by positive ion mass spectrometry, however no species identifiable to either polymeric glycan chains, or cross-linked peptidoglycan were observed. A repeat experiment using mutanolysin for digestion, and with removal of the undecaprenyl phosphate lipid linker by phosphoric acid hydrolysis was also unsuccessful. In both cases no species characteristic of either polymerised or cross-linked glycan chains were observed.

The identity of the high molecular weight band observed could not be categorically proven, however the controls used both here and some of those executed by Zapun *et al.,* (2013) are consistent with the presence of cross-linked peptidoglycan produced by the *S. pneumoniae* bifunctional PBPs; PBP1a and PBP2a.

6.4 Towards a continuous assay of *S. pneumoniae* PBP transpeptidase activity

The Amplex Red assay for D-Ala release (Figure 6.3 (B)) can be used to follow both transpeptidase and DD-carboxypeptidase activity. Dr Adrian Lloyd (University of Warwick) has established this to be specific for the former through detailed work on *E. coli* PBP1b with the use of (transpeptidase) donor only and acceptor only substrates as well as appropriate controls. By incubation of a donor only Lipid II with PBP initially, any DD-carboxypeptidase activity can be accounted for before the addition of an acceptor that allows subsequent transpeptidase activity to be followed. Controls lacking Lipid II enable any background rate to be taken into consideration. Standard methods for the assay system are detailed in Section 2.8.4.

Many of the experimental decisions detailed within this section are informed by on-going unpublished data and personal communications with Dr A. Lloyd. As mentioned in Section 6.3.2, *S. pneumoniae* PBP1a was prioritised for initial work, due to its importance in β-lactam resistance. This section details the steps taken to observe PBP1a transpeptidase activity by the Amplex Red assay, the scheme for which is illustrated in Figure 6.3.
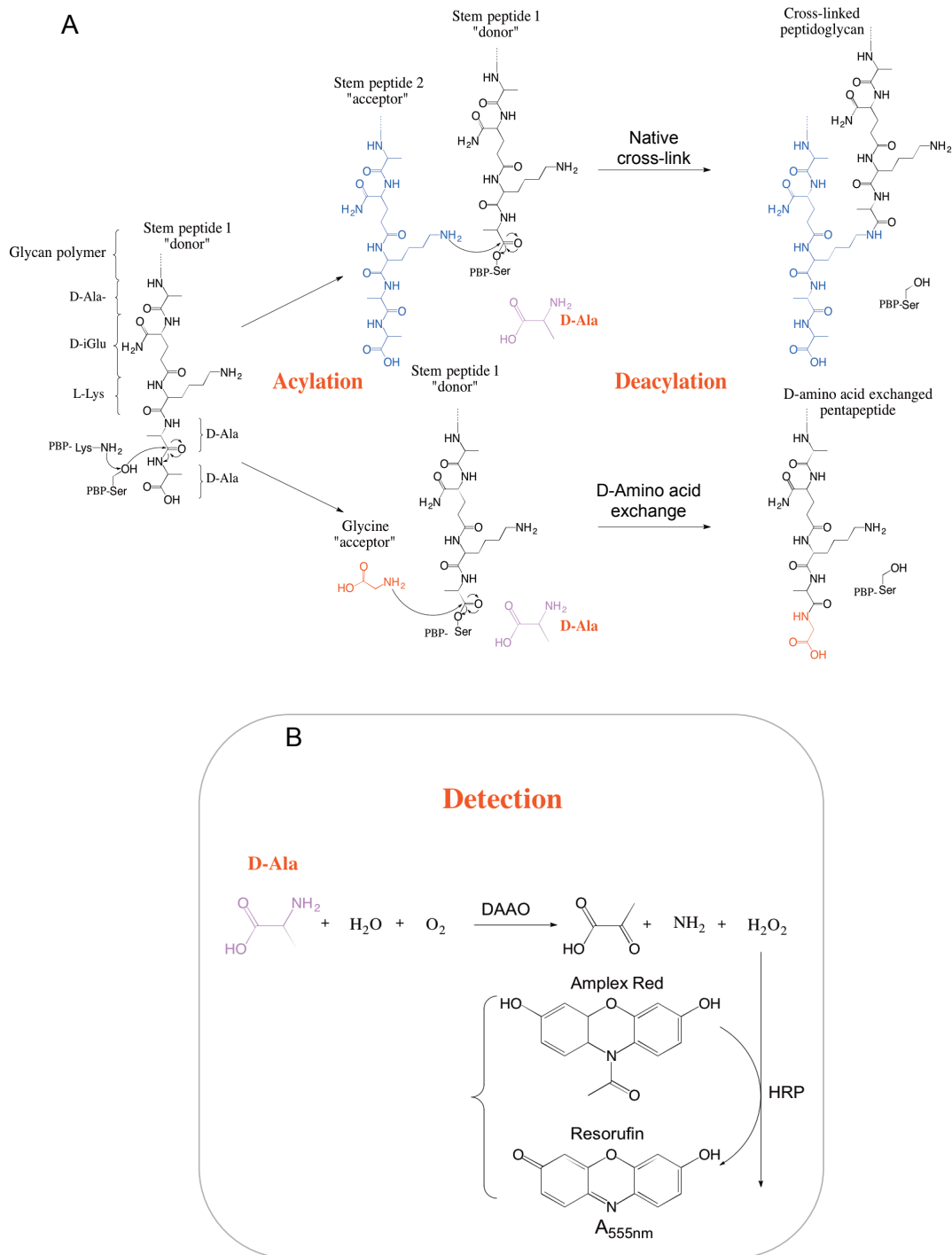
Figure 6.3 Amplex Red assay for D-Ala release as an assay for transpeptidase activity A:Schematic showing PBP catalysed transpeptidation between two stem peptides and incorporation of a simple glycine acceptor, both of which result in release of D-Ala. Use of a donor only substrate as Stem peptide 1 (not shown as not synthetically available at this point) allows D-Ala release due to transpeptidation and D,D-carboxypeptidation to be differentiated. B: Amplex Red assay for D-Ala release. D-amino acid oxidase (DAAO) catalyses the oxidation of D-Ala to pyruvate, with the release of hydrogen peroxide. Horseradish peroxidase (HRP) uses hydrogen peroxide to convert Amplex Red to resorufin, which absorbs strongly at 555 nm.

6.4.1 Initial attempts to detect transpeptidase activity

E. coli PBP1b will incorporate D-amino acids into the stem peptide in place of the terminal D-Ala in a process known as D-amino acid exchange (Lupoli *et al.,* 2011), and therefore the Amplex Red assay was optimised to use simple acceptors such as D-Lac and Glycine (Dr A Lloyd, Personal Communication). Combined with a Lipid II substrate that can only be a donor, and accounting for background D,D-carboxypeptidase activity. Initial attempts to observe *S. pneumoniae* PBP1a transpeptidase activity were under the conditions used for SDS-PAGE analysis (Section 6.3.1). A donor only Lipid II substrate was not available and given the preference for amidated Lipid II for PBP1a transglycosylase (Chapter 4) and transpeptidase activity (Figure 6.2 and Zapun *et al.*, 2013), Lipid II (Gln) was used as a substrate initially. This removes the ability to distinguish transpeptidation and carboxypeptidation as Lipid II (Gln) can be both a donor and an acceptor, but the identification of any rate at all was initially desired. L-Lys or L-Ala were added as additional acceptors in high excess, which was hoped to favour their incorporation. L-amino acids were chosen as the true acceptors *in vivo* are the ε-amino group of L-Lys or the α-amino group of L-Ala rather than *meso*-DAP in *E. coli*. PBP1a was tested at 1, 5 and 10 μM with 20 μM Lipid II (Gln) and 0.1 M L-Lys or L-Ala. The experimental procedure was as described in Section 2.8.4.

No change in absorbance at 555 nm was observed under any of the conditions attempted. The coupling enzyme system was tested with the addition of 5 μM D-Ala, which confirmed that the lack of observable activity was not due to the inability of the assay system to detect D-Ala release.

6.4.2 Alternative substrates

Previous (Abrahams, 2011; Helassa *et al.,* 2012; Zapun *et al.*, 2013) attempts to monitor PBP1a transpeptidase activity have shown a clear requirement for stem peptide amidation. However, the use of amidated Lipid II was unsuccessful in producing detectable activity in the Amplex Red assay with simple acceptors, as described in Section 6.4.1.

Dr A. Lloyd identified MurNAc-pentapeptide to be an efficient acceptor in the *E. coli* PBP1b assay system. MurNAc-pentapeptide is routinely made from UDP-MurNAc-pentapeptide by acid hydrolysis, with approximately a 50% yield (Julie Todd, Personal Communication). In order to test this alternative acceptor, amidated UDP-MurNAc-pentapeptide (Gln)(Section 3.3) was hydrolysed by the standard acid method (Section 2.6.2.1), and an alternative enzymatic method (Section 2.6.2.2) investigated in an attempt to obtain a greater yield.

6.4.2.1 Acid hydrolysis of UDP-MurNAc-pentapeptide

10 mg UDP-MurNAc-pentapeptide (Gln) was hydrolysed with 0.1 M HCl and purified by anion exchange (Full details in Section 2.6.2.3). Figure 6.4 (A) shows the anion exchange chromatogram, identifying the MurNAc-pentapeptide (Gln) peak detected by its absorbance only at 218 nm (peptide bonds)(Figure 6.4 (A)(i)). MurNAc-pentapeptide absorbs at 218nm but not 254 nm or 280 nm due to the loss of the uridine ring. Peak (ii) is known to be UMP and (iii) UDP (Dr A. Lloyd, Personal Communication). Peak (i) was selected, freeze dried three times and resuspended in a small volume of H_2O. Negative ion mass spectrometry (Figure 6.4 (B)) confirmed the presence of MurNAc-pentapeptide (Gln) (observed/expected m/z $[m-H]^-$ 761.3578/761.3759)
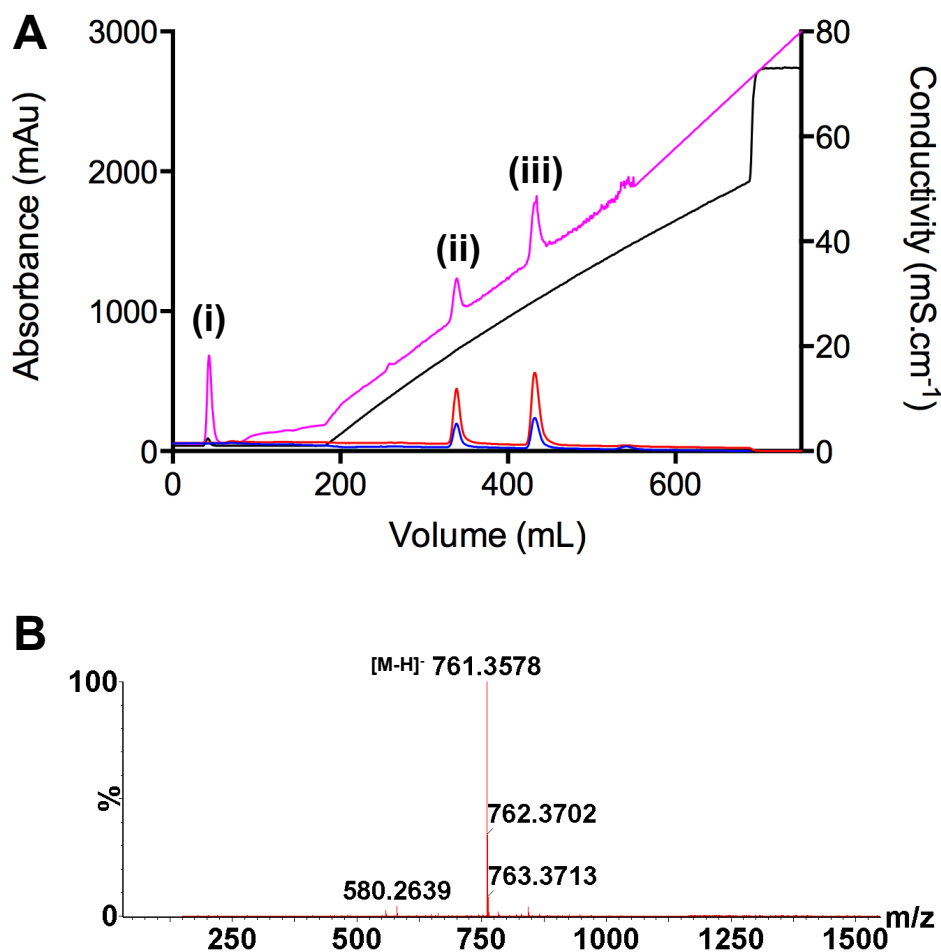
Figure 6.4 Acid hydrolysis of UDP-Mur*N*Ac-pentapeptide (Gln). A. Anion exchange chromatography of acid hydrolysed UDP-Mur*N*Ac-pentapeptide. Blue; absorbance at 280 nm (mAu), Red; absorbance at 254 nm (mAu), Pink; absorbance at 218 nm (mAu), Black; conductivity (mS.cm^{-1}). (i) Mur*N*Ac-pentapeptide (2.20 mS.cm^{-1}), (ii) UMP (19.24 mS.cm^{-1}), (iii) UDP (28.69 mS.cm^{-1}). B: Negative ion time-of-flight spectra of peak (i). Expected m/z [m-H]$^-$=761.3759, observed [m-H]$^-$ 761.3578

6.4.2.2 Enzymatic hydrolysis of UDP-Mur*N*Ac-pentapeptide

The acid hydrolysis method typically yields approximately 50%, and therefore an alternative enzymatic method was investigated in parallel, in an attempt to improve this. 10 units each of Phosphodiesterase from *Crotalus adamanteus* (Sigma-Aldrich; to cleave the phosphodiester linkage), and Shrimp alkaline phosphatase (SAP; NEB) (to remove the remaining phosphate) were used, based on their quoted specific activity, and a Tris.HCl buffer at pH 8.5 chosen as it is within the optimal pH range of both enzymes. Full methods are detailed in Section 2.6.2.2. Despite the poor separation by anion exchange (Figure 6.5 (A)), peak (i) was identified as Mur*N*Ac-

244

pentapeptide (Gln) by negative ion mass spectrometry (observed/expected m/z [m-H]$^-$ 761.3756/761.3759) Peak (iii) was identified as Mur*N*Ac-pentapeptide monophosphate by negative ion mass spectrometry (not shown), remaining due to the inefficient activity of SAP. Peak (ii) was not analysed by mass spectrometry, but was assume to be either uridine or uracil due to its lack of negative charge and absorbance at all three wavelengths.
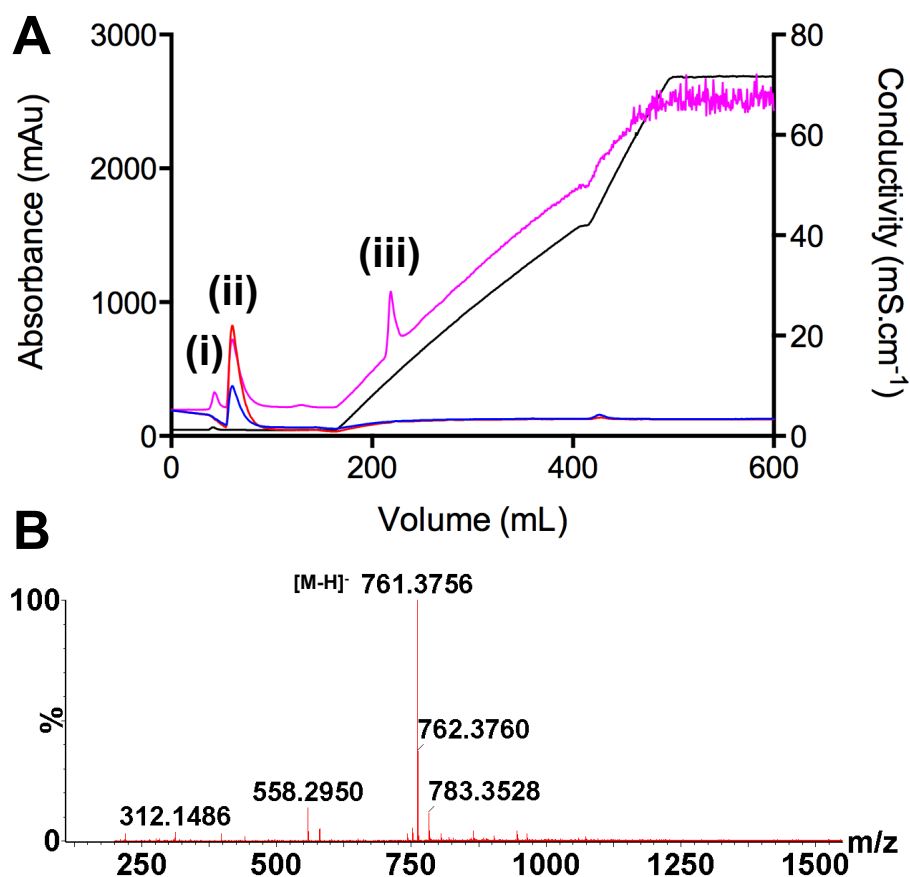
Figure 6.5 Enzymatic hydrolysis of UDP-Mur*N*Ac-pentapeptide (Gln). A. Anion exchange chromatography of UDP-Mur*N*Ac-pentapeptide hydrolysed with 10 units phosphodiesterase and 10 units shrimp alkaline phosphatase. Blue; absorbance at 280 nm (mAu), Red; absorbance at 254 nm (mAu), Pink; absorbance at 218 nm (mAu), Black; conductivity (mS.cm^{-1}). (i) Mur*N*Ac-pentapeptide (1.60 mS.cm^{-1}), (ii) uridine (1.21 mS.cm^{-1}), (iii) MurNAc-pentapeptide monophosphate (11.46 mS.cm^{-1}). B: Negative ion time-of-flight spectra of peak (i). Expected m/z [M-H]$^-$=761.3759, observed m/z [M-H]$^-$=761.3756

245

6.4.2.3 Method choice

Mur*N*Ac-pentapeptide was produced by both methods, as confirmed by negative ion mass spectrometry (Figure 6.4 (B) and 6.5 (B)). Removal of the uridine ring means that quantification by absorbance at 260 nm is no longer possible. Instead, the Amplex Red assay for D-Ala release was used coupled with *E. coli* DacB (Class C D,D-carboxypeptidase) to remove the terminal D-Ala from the Mur*N*Ac-pentapeptide for detection (Section 2.6.2.5). 53% and 18% yields were achieved for the acid and enzymatic methods respectively. Notably, a 47% yield of Mur*N*Ac-pentapeptide monophosphate was obtained from enzymatic hydrolysis, suggesting that optimisation of SAP activity has the potential to significantly improve yield.

Purity of Mur*N*Ac-pentapeptide from both methods was established using a modified version of that for UDP-Mur*N*Ac-pentapeptides in Section 3.3 (Method details Section 2.6.2.4) (Figure 6.6). The lack of negative charge on Mur*N*Ac-pentapeptide required purity checking by cation exchange chromatography (MonoS) (rather than anion exchange) with a phosphoric acid buffer at pH 4 to promote a positive charge on contaminating species, therefore improving separation. Integration of the A_{218nm} peaks established a purity of 95% and 59% for acid and enzymatic hydrolysis respectively. The low purity following enzymatic hydrolysis is due to the elution of two peaks that were unbound to the Source 30Q resin (Figure 6.5 (A (i) and (ii))). This might be alleviated in future through purification by cation exchange at a low pH (as the two peaks were separated in the MonoS purity check (Figure 6.6 (B) (i) and (ii)). Peak (i) was confirmed as Mur*N*Ac-pentapeptide (Gln) by negative ion mass-spectrometry.
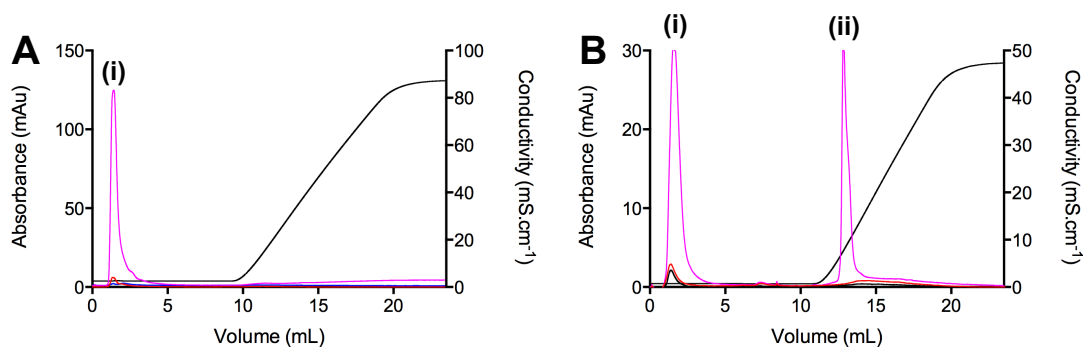
Figure 6.6: Purity checks of Mur*N*Ac-pentapeptide (Gln). Purity check by cation exchange chromatography on MonoS resin. A: Mur*N*Ac-pentapeptide from acid hydrolysis showing single peak (i) (eluting at a conductivity of 2.59 mS.cm^{-1}). Blue; absorbance at 280 nm (mAu), Red; absorbance at 254 nm (mAu), Pink; absorbance at 218 nm (mAu). Peak integration identified purity as 95%. B: Mur*N*Ac-pentapeptide from enzymatic hydrolysis showing two peaks (i) eluting at a conductivity of 0.72 mS.cm^{-1} and (ii) at 8.39 mS.cm^{-1}. Peak integration of (i) identified purity as 59%.

The higher purity and yield of acid hydrolysis mean that this method was used to produce pure Mur*N*Ac-pentapeptide as a potential acceptor for the Amplex Red transpeptidase assay (see Section 6.4.5).

6.4.3 Effect of purification detergent on PBP activity

The detergent in which *E. coli* PBP1b is purified has significant consequences for its observed transpeptidase activity (Dr A Lloyd, Personal Communication). pET46::*pbp1a* with dodecahistidine tag was expressed and purified as before (Section 4.3.1) in DDM, as well as TX-100 and CHAPS in parallel. TX-100 was chosen as Lipid II is routinely presented in this detergent for both transglycosylase (Chapter 4) and transpeptidase (Zapun *et al*., 2013) assays. CHAPS has an extremely high CMC of 0.45% (w/v), and is therefore easily diluted below this to allow assays to be carried out in a different detergent if required, by eliminating the effect of detergent brought to the assay with the enzyme.

6.4.3.1 Parallel purification of PBP1a FL in DDM, TX-100 and CHAPS

PBP1a FL was expressed and solubilised from *E. coli* membranes in 1% (w/v) sodium deoxycholate as described in Section 4.3.1. Purification by IMAC was also as described with buffers containing 0.1% (w/v) DDM, 0.2% (v/v) TX-100 or 0.5% (w/v) CHAPS. The TX-100 concentration was at 10 × CMC, the same as that

routinely used for DDM. However, the CHAPS concentration was just above the CMC due to the large quantities required to achieve 10 × CMC. CHAPS at this concentration has previously been successful for the purification of *E. coli* PBP1b (Dr A. Lloyd, Personal Communication). For gel filtration using a Superose 6 10/300 column (Section 4.3.1), the DDM and TX-100 concentrations were reduced to 0.03% (w/v) and 0.02% (v/v) respectively, just above their CMC in order to reduce the numbers of micelles devoid of protein as much as possible. The CHAPS concentration was maintained at 0.5% (w/v).

The purification of PBP1a in DDM was as described in Section 4.3.1, and final purity achieved is shown in Figure 4.2. For purification in TX-100, the 250 mM imidazole fractions from IMAC (Figure 6.7 (A)) were further purified by size exclusion chromatography (Figure 6.7 (B)), where two peaks but no aggregated material was observed. This was identified due to both peaks eluting outside of the void volume (9 mL) from the Superose 6 column. Peak (ii) was selected, as for the DDM purification (Figure 4.2) and the final purity is shown in Figure 6.7 (C).
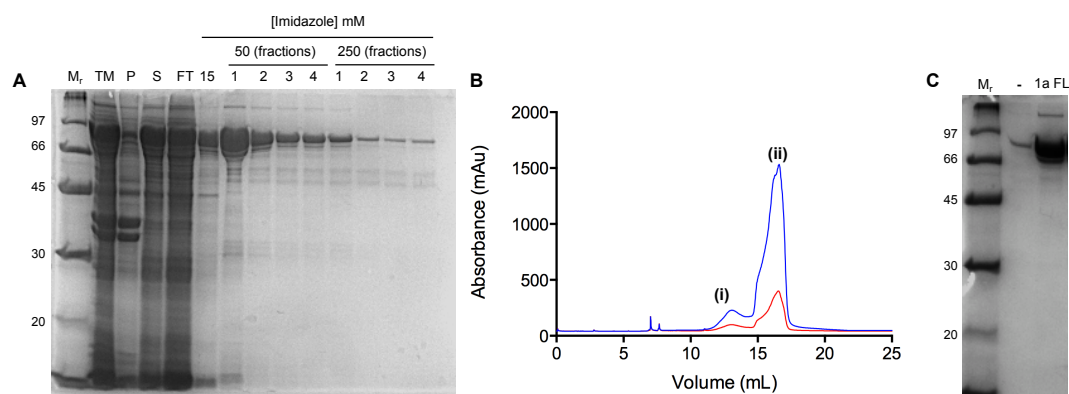
Figure 6.7: Purification of *S. pneumoniae* D39 PBP1a FL by IMAC and size exclusion chromatography in TX-100 detergent. A 12% SDS-PAGE Coomassie-stained gel showing the isolation of membranes, solubilisation in 1 % (w/v) sodium deoxycholate and subsequent IMAC purification of PBP1a FL in TX-100. M_r, molecular weight markers (kDa); TM, total membrane fraction; P, ultracentrifugation pellet following sodium deoxycholate solubilisation; S, ultracentrifugation supernatant containing soluble protein; FT, unbound protein following 3 h incubation of supernatant with cobalt-chelated sepharose resin; 15, wash with buffer containing 15 mM Imidazole; 50 (fractions) 1-4, elution with buffer containing 50 mM imidazole; 250 (fractions) 1-4, elution with buffer containing 250 mM imidazole. (b) Size exclusion chromatogram using the Superose 6 10/300 GL column. Blue; absorbance at 280 nm (mAu), Red; absorbance at 254 nm (mAu) (i) shows the elution of a peak of higher molecular weight protein and (ii) the elution of lower molecular weight protein. (c) 12% SDS-PAGE Coomassie-stained gel of the final purity of PBP1a FL. M_r, molecular weight markers (kDa); -, empty lane; 1a FL, purity of PBP1a FL following both purification steps.

A large amount of protein precipitation occurred in the CHAPS sample following IMAC purification. This was removed by centrifugation at 3,000 × g in a bench-top centrifuge (Eppendorf Centrifuge 5810R) and the supernatant concentrated in a Vivaspin® centrifugal concentrator (10 kDa cut-off) before quantification of the remaining protein by BCA assay (Section 2.5.1). The yield was below detectable levels, and therefore purification in 0.5% (w/v) CHAPS was unsuccessful (discussed Section 6.5.2). Buffer exchange was attempted in order to obtain PBP1a in CHAPS for testing in the transpeptidation assay. 4 mg of pure PBP1a FL in 0.03% (w/v) DDM buffer (Figure 4.2 (c)) was bound to 2 mL TALON Metal Affinity Resin pre-equilibrated in DDM buffer. The resin was washed with 5 × 20 mL 20 mM Tris pH 7.5, 150 mM NaCl, 0.5% (w/v) CHAPS in order to obtain a 50 fold dilution of the 0.03% (w/v) starting DDM concentration. PBP1a FL was eluted in 20 mL 20 mM Tris pH 7.5, 150 mM NaCl, 0.5% (w/v) CHAPS, 250 mM imidazole before concentration using a 10 kDa cut-off centrifugal concentrator and buffer exchange on a PD-10 Desalting column (GE Healthcare) to remove the imidazole (Figure 6.8).

A negligible amount of DDM may remain following this method, however following a 50 fold dilution the amount remaining will be so low that it is unlikely to have an affect. Pure PBP1a in 0.5% (w/v) CHAPS buffer was obtained by this method.
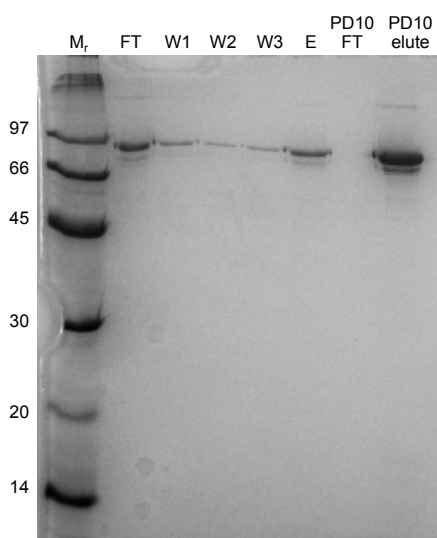
Figure 6.8: Buffer exchange of *S. pneumoniae* D39 PBP1a FL by IMAC. 12% SDS-PAGE Coomassie-stained gel showing the buffer exchange of PBP1a FL from DDM to CHAPS by binding to IMAC resin, M_r, molecular weight markers (kDa); FT, Protein not bound to resin; W1, CHAPS buffer wash 1; W2, CHAPS buffer wash 2; W3, CHAPS buffer wash 3; E, Elution of PBP1a FL in CHAPS buffer plus 250 mM imidazole; PD10 FT, Flow through from loading on PD-10 Desalting column; PD10 elution from PD-10 column.

6.4.3.2 The effect of detergent on PBP1a activity

The relative activity of PBP1a purified in DDM, CHAPS and TX-100 was evaluated using three established methods. Firstly the native conformation of the penicillin-binding domain was investigated with binding of BOCILLIN FL; a fluorescently labelled penicillin. This is acylated by the active site serine, forming a covalent complex, which can be observed by fluorescence detection following SDS-PAGE analysis. PBPs in the three detergents were incubated at a 5:1 BOCILLIN: PBP ratio for 1 hour (in the dark to protect the fluorescent label) at 37°C (Section 2.8.1). Ampicillin will form a covalent complex with the active site and prevent BOCILLIN from binding if pre-incubated with the PBP, and was used as a control. DacB (*E. coli* PBP4) was used as a positive control. Samples were analysed by SDS-PAGE, BOCILLIN binding detected using a Typhoon FLA 9500 laser scanner (GE Healthcare) with Y520 filter and the gel was subsequently Coomassie-stained to detect all protein. Figure 6.9 shows both gels.

The dominant BOCILLIN FL fluorescent bands on the SDS-PAGE gel (Figure 6.9 (A)), correspond in size with the Coomassie-stained PBP1a FL (Figure 6.9 (B)), and are both indicated by an arrow. Samples were not heat denatured prior to SDS-PAGE analysis in order to maintain the interaction with BOCILLIN FL, and therefore several bands are observed above that of the indicated PBP1a FL upon Coomassie staining (Figure 6.9 (B)), suggestive of oligomerisation. The PBP1a FL band also runs slightly differently on the gel than that seen previously, likely due to the same reason. The contaminating protein observed just below PBP1a FL also binds to BOCILLIN, suggesting the presence of an *E. coli* PBP (discussed in Section 6.5.3). The intensity of BOCILLIN binding to PBP1a FL in CHAPS is less than that in DDM or TX-100, implying that its conformation may be affected and reducing the ability of BOCILLIN FL to access the active site serine. However, this could also be due to variation in protein quantification and therefore loading onto the gel. This result suggests that PBP1a FL in all three detergents should be active as a transpeptidase.
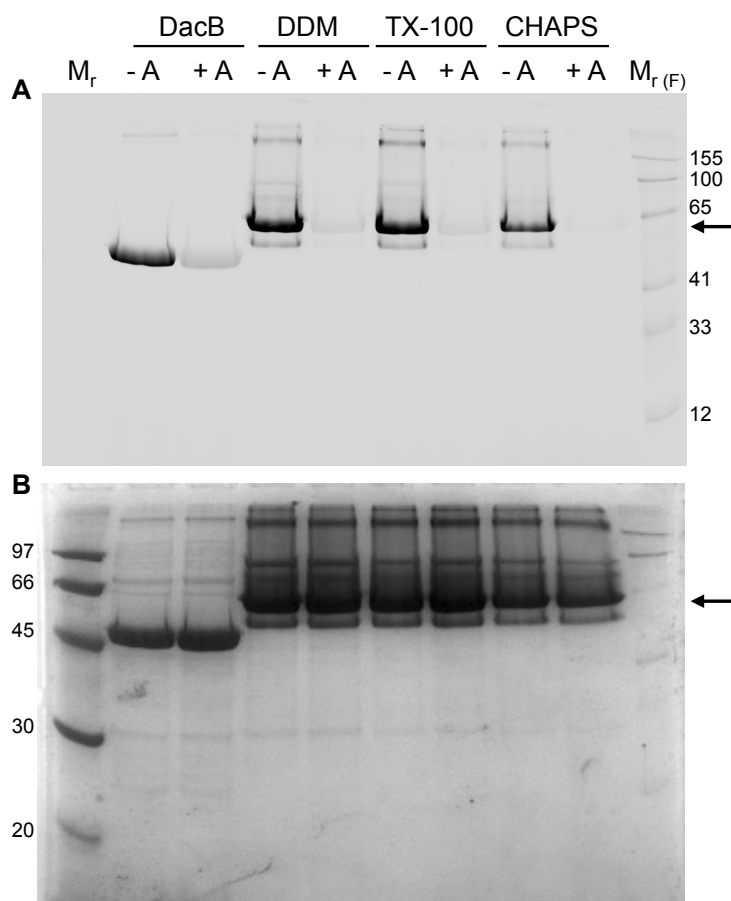
Figure 6.9: BOCILLIN FL labelling of PBP1a FL. Labelling of PBP1a FL in DDM, TX-100 and CHAPS with fluorescent penicillin. A. BOCILLIN FL fluorescence of PBPs (PBP1a FL indicated by arrow). B:12% SDS-PAGE Coomassie-stained gel of PBPs stained with BOCILLIN FL (PBP1a FL indicated by arrow). Proteins labelled as DacB (control) or DDM (PBP1a FL in DDM), TX-100 (PBP1a FL in TX-100) and CHAPS (PBP1a FL in CHAPS). Inclusion of ampicillin as a control indicated as –A, no ampicillin; or +A; plus ampicillin. M_r, molecular weight markers (kDa), M_r (F), fluorescent molecular weight markers. Fluorescence detected using Typhoon FLA 9500 laser scanner (GE Healthcare) with Y510 filter.

Additionally the transglycosylase and transpeptidase activity of all three were determined by a continuous fluorescence assay and SDS-PAGE analysis respectively. Transglycosylase activity was investigated by the continuous fluorescence assay used in Section 4.5 (Section 2.7.1). 1 µM of each enzyme was reacted with 10 µM Lipid II (Gln, Dans) and the initial rate of transglycosylase activity determined by calculating RFU change per second of dansyl fluorescence (Figure 6.10)(A)). Additionally, the transpeptidase activity of the three enzymes was probed by the SDS-PAGE system described in Section 6.3.2 (Section 2.8.2). The assay was exactly as described previously for PBP1a FL in each of the detergents (Figure 6.10 (B)).

251
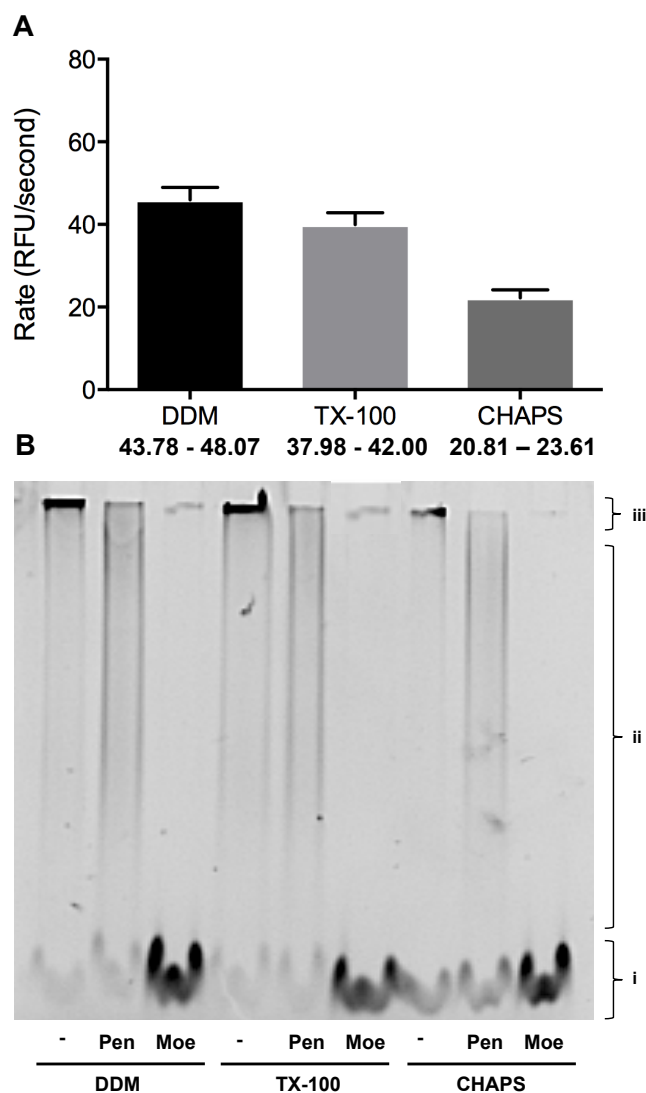
Figure 6.10: Effect of detergent on PBP1a FL activity. A. Transglycosylation rates of PBP1a FL purified in DDM, TX-100 and CHAPS (as indicated on X axis) Rates are average of two replicates and the error bar shows the range of values (range additionally stated in bold below X axis). Rates calculated from continuous fluorescence assay of 1 μM PBP1a FL and 10 μM Lipid II (Gln, Dans). B. Transpeptidase activity determined by SDS-PAGE analysis of reaction products. PBP1a FL purification detergent indicated below the gel. Mixture of 50 μM Lipid II (Gln) and 5 μM dansylated Lipid II (Gln, Dans) incubated with 1 μM PBP1a for 1 hour. -,no inhibitor; Pen, 1 mM penicillin G; Moe, 0.5 mM moenomycin. Products of reaction separated on a 8.5% T/2.7% C SDS-PAGE gel. Dansyl fluorescence at 521 nm detected using a blue light converter and short pass filter on a GeneSnap Gel Doc. (i) denotes unpolymerised Lipid II; (ii) glycan chains of varying lengths and (iii) the very high molecular weight material, which does not enter the gel.

PBP1a FL in CHAPS was less active in both the transglycosylase and transpeptidase assays, although the impact of buffer exchange on this is unknown (discussed Section 6.5.2), and results may be affected by variation in protein concentration determination. PBP1a in CHAPS was not used for further experiments in this chapter.

6.4.4 Optimisation of assay conditions

The acute sensitivity of *in vitro* transglycosylase activity to the buffer conditions has been well documented (Barrett *et al.*, 2004; Offant *et al.*, 2010; Schwartz *et al.*, 2002). Given that the transpeptidation substrate is polymerised peptidoglycan (Born et al., 2006; Lupoli *et al.*, 2011; Zapun *et al.*, 2013) and on-going transglycosylation is required for *S. pneumoniae* transpeptidase activity (Lupoli et al., 2014; Zapun *et al.*, 2013), a thorough analysis of the conditions required to observe transglycosylase activity was needed in order to present the best chance of observing the subsequent cross-linking reaction. This was explored using the continuous fluorescence assay for transglycosylase activity (Section 2.7.1) as 8 fold less Lipid II is required per 50 μL reaction than for each 200 μL Amplex Red assay. The intention was to obtain the best conditions for transglycosylation as a starting point for optimisation in the transpeptidation assay.

The buffer conditions used for *S. pneumoniae* PBP1a FL transglycosylase assays are 50 mM HEPES pH 7.5, 10 mM MgCl$_2$, 150 mM NaCl, 25% (v/v) DMSO, 0.02% (v/v) TX-100 as described in Chapter 4. Salt, detergent and DMSO concentration were varied and their effect on transglycosylase rate determined, following the observation of their significant effect on *E. coli* PBP1b transpeptidase activity (Dr A. Lloyd, Personal Communication). Assays were exactly as described in Section 4.5 (details Section 2.7.1) with 1 μM PBP1a FL and 10 μM Lipid II (Gln, Dans).

The effect of reducing the concentration of NaCl was investigated with DDM purified PBP1a FL (to allow continuity from previous assays in Chapter 4). The rate of transglycosylation fell as salt concentration was reduced (Figure 6.11 (A)). Following this, the concentration of NaCl was maintained at 150 mM, and the effect of detergent type and concentration studied. The reaction buffer and Lipid II were presented in a total of 0.02% (v/v) TX-100 as before, and enzyme in either DDM or TX-100 was added to give an additional final concentration of 1 × CMC or 0.1 × CMC. This was intended to investigate the necessity for enzyme detergent to be maintained above the CMC. CHAPS was not studied due to its poor activity observed in Figure 6.9. A significant bias was observed for both DDM and TX-100

purified enzyme, in favour of maintaining the concentration of detergent brought with the protein above the CMC in the assay (1 × CMC) (Figure 6.11(B)). No obvious difference was observed between 0.1 × CMC for DDM and TX-100 or 1 × CMC for DDM and TX-100, however, a lag phase was seen when enzyme was brought to the reaction in DDM, likely due to the presence of two different detergents in the assay. Enzyme purified in TX-100 was chosen for further optimisation for this reason.

Finally, the DMSO concentration was varied from 0-25% (v/v), with PBP1a FL added to the assay in a final TX-100 concentration (including TX-100 from the Lipid II and reaction buffer (as before)) of 0.02% (v/v) (just above 1 × CMC) and 0.035% (v/v) (2.3 × CMC). At both detergent concentrations, DMSO concentration played a significant role in transglycosylation rate (Figure 6.11 (C) and (D)), with 10% (v/v) and lower resulting in very little activity. At 0.02% (v/v) final TX-100, optimal activity was observed at 20% (v/v) DMSO, whereas 25% (v/v) DMSO was required in the presence of 2.3 × CMC TX-100 in order to observe a reasonable level of activity. This could be because more DMSO is required to increase the rate of exchange between micelles at a higher detergent concentration, enabling Lipid II and enzyme to come into contact. The optimal buffer conditions taken forward following this investigation were 50 mM HEPES pH 7.5, 10 mM $MgCl_2$, 150 mM NaCl, 20% (v/v) DMSO, 0.02% (v/v) TX-100.

It should be noted that the rate observed here with dansylated Lipid II may not represent that with the non-labelled substrate in the Amplex Red assay (discussed further in Section 6.5.3). However, these conditions give a reasonable starting point for analysis of transpeptidase activity.
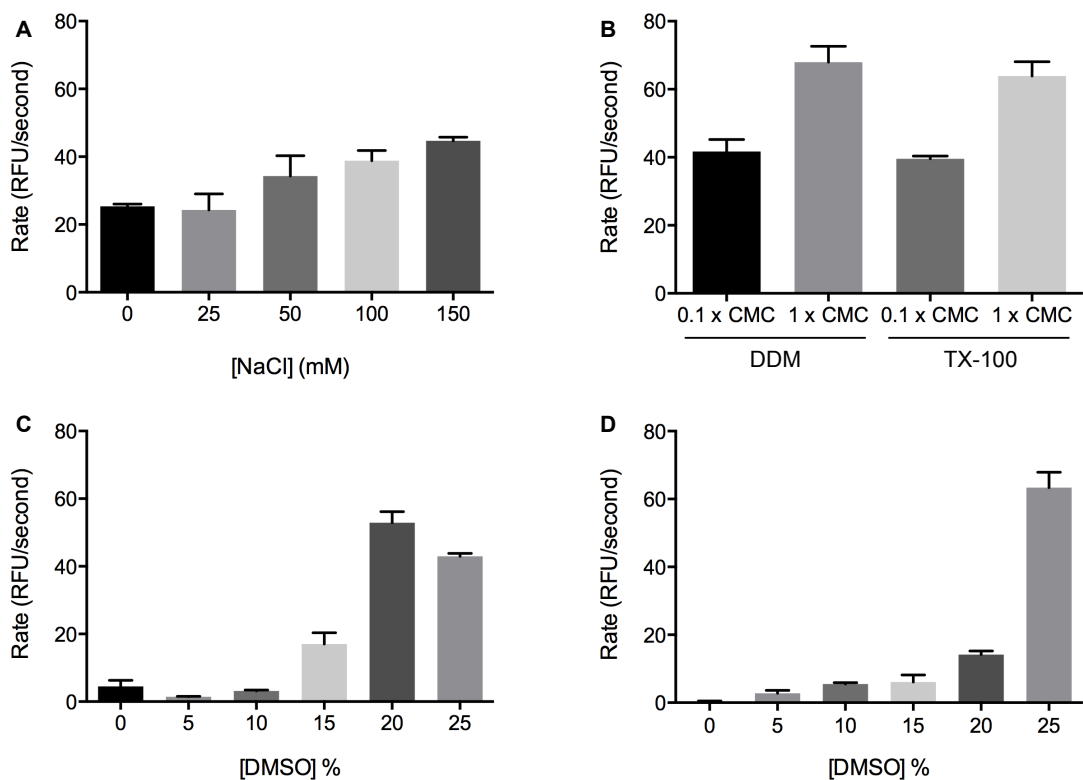
Figure 6.11: Effect of buffer conditions on PBP1a FL transglycosylase activity. 10 μM Lipid II (Gln, Dans) and 1 μM PBP1a FL in all cases in a continuous fluorescence assay for transglycosylase activity. Initial rate calculated as RFU change per second and means of duplicate reactions (error bar = range) plotted against the condition. .A: PBP1a FL purified in DDM with NaCl concentrations from 0-150 mM. B: PBP1a FL purified in either DDM or TX-100, and brought to the reaction with a final concentration of 0.1 × CMC or 1 × CMC (indicated below the figure), in addition to 0.02% (v/v) TX-100 already in the assay. C: PBP1a FL purified in TX-100 and added to the assay in 0.1 × CMC, giving a final concentration of 0.02% (v/v) TX-100 in the assay. DMSO concentration varied from 0-25% (v/v). D: PBP1a FL purified in TX-100 and added to the assay in 1 × CMC, giving a final concentration of 0.035% (v/v) TX-100 in the assay. DMSO concentration varied from 0-25% (v/v). All graph shown on the same scale for comparison.

6.4.5 Detection of *S. pneumoniae* D39 PBP1a transpeptidase activity by the Amplex Red assay

Following the optimisation carried out within this chapter, an Amplex Red assay was performed (Section 2.8.4) in 50 mM HEPES pH 7.5, 10 mM MgCl$_2$, 150 mM NaCl, 20% (v/v) DMSO, 0.02% (v/v) TX-100 final concentrations with 20 μM Lipid II (Gln) and 2 μM PBP1a FL purified in TX-100 (brought to the assay in 0.1 × CMC). The conditions were chosen to minimise the DMSO concentration used as this may affect the coupling enzymes. Lipid II (Gln) will act as both a transpeptidation donor and acceptor, meaning that any rate observed in the first instance cannot necessarily

255

be attributed to transpeptidase over DD-carboxypeptidase activity. However the initial aim was to observe any rate, and with the lack of a donor only substrate, Lipid II (Gln) was the best option. No rate was observed over the no Lipid II control, including after the addition of 20 μM Mur$N$Ac-pentapeptide (Gln)(Section 6.4.2) as an additional acceptor. The coupling enzyme system was tested with the addition of 5 μM D-Ala, yielding an instantaneous increase in A_{555nm} of 0.25 absorbance units, confirming that it was functional under the conditions used.

The length of detergent ethylene glycol moieties has been observed to have a hugely significant effect on *E. coli* PBP1b transpeptidase activity (Dr A. Lloyd, Personal Communication). Triton X-100 contains a range of lengths from 5-20 ethylene glycol units, resulting in a mixture of positive and negative effects on enzyme activity. Therefore, based on this work, hexaethylene glycol dodecyl ether (E_6C_{12})(CMC: 0.0039% (v/v)) was trialled. In order to obtain the entire reaction as exclusively as possible in this detergent, DDM purified PBP1a FL (initial transglycosylase activity tests showed it to be similar to TX-100 purified enzyme (Figure 6.11 (B)) was used due to its significantly higher concentration. This allowed dilution into a buffer containing 10 x CMC E_6C_{12}, reducing the DDM concentration below its CMC. 20 μM Lipid II (Gln) (in E_6C_{12}) and 2 μM PBP1a FL final concentrations in the cuvette were used as before, this time in 50 mM HEPES pH 7.5, 10 mM MgCl$_2$, 150 mM NaCl, 20% (v/v) DMSO, 12 $\times$ CMC E_6C_{12} (final) and also in 50 mM HEPES pH 7.5, 10 mM MgCl$_2$, 12 $\times$ CMC E_6C_{12} (final). The decision was made in this parallel reaction to remove salt and DMSO despite the previous optimisation (Section 6.4.4). This was based upon work by Dr A. Lloyd showing the severe effect of these two components on *E. coli* PBP1b activity. The assay was performed as detailed in Section 2.8.4.

This proved to be a pivotal decision as a significant rate was observed in the Amplex Red assay without DMSO and NaCl (Figure 6.12 (red)). A very slow rate was seen in their presence (not shown).

A steady baseline was established by monitoring A_{555nm} of a cuvette containing 20 μM Lipid II (Gln) in 50 mM HEPES pH 7.5, 10 mM MgCl$_2$, 12 $\times$ CMC E_6C_{12}

(plus Amplex Red coupling reagents (Section 2.8.4)), and rate observed following the addition of 2 μM PBP1a FL. The release of D-Ala was shown to be both Lipid II and enzyme dependent by the replacement of each with E_6C_{12} Lipid II buffer, and enzyme storage buffer respectively (Figure 6.12 (red dashed and black solid respectively)). No reaction occurred in the presence of Lipid II (Glu)(not shown), showing a dependency on the stem peptide composition previously identified as important for PBP1a transpeptidase activity (Zapun *et al.*, 2013, and Figure 6.2). Significantly, the observed reaction could be inhibited completely with 50 μM moenomycin, showing that it is dependent on the preceding transglycosylase activity (Figure 6.12 (blue solid)). Insufficient substrate was available to carry out a penicillin control within the time available.
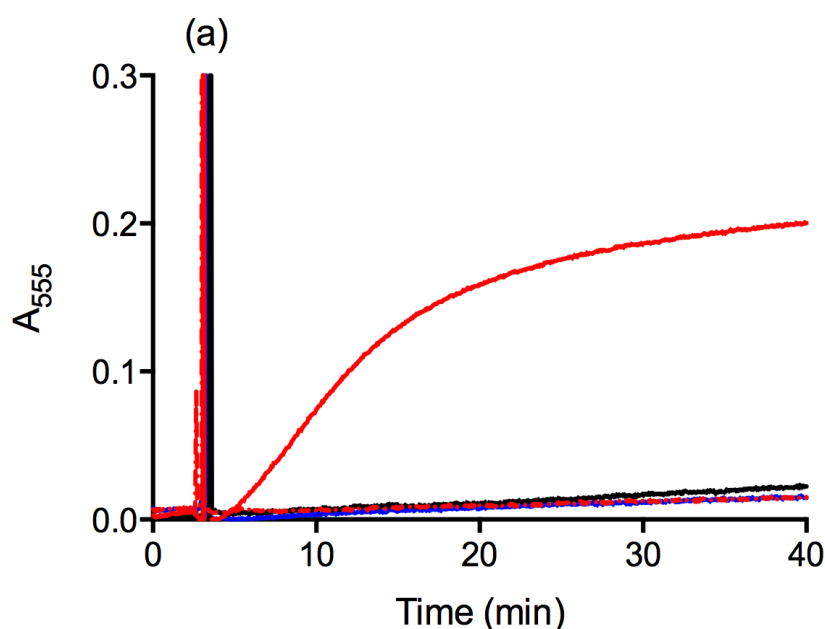
Figure 6.12. *S. pneumoniae* **PBP1a D-Ala release.** Amplex Red assay for D-Ala release by PBP1a, identified by an increase in A_{555nm} due to Resorufin accumulation. 50 mM HEPES pH 7.5, 10 mM $MgCl_2$, 12 × CMC E_6C_{12} with or without 20 μM Lipid II (Gln) allowed to reach a stable baseline. (a) addition of 2 μM PBP1a or equivalent volume of enzyme storage buffer. Black solid, 20 μM Lipid II and no PBP1a; Red solid, 20 μM Lipid II and 2 μM PBP1a, Red dashed; No Lipid II plus 2 μM PBP1a; Blue solid; 20 μM Lipid II, 2 μM PBP1a and 50 μM moenomycin.

Moenomycin does not affect the Amplex Red coupling reagents at the concentration used (Dr A. Lloyd, Personal communication), and was shown not to inhibit binding of BOCILLIN FL to the penicillin-binding domain (Figure 6.13 (A)) of PBP1a FL or DacB. The BOCILLIN FL assay was as described in Section 6.4.4 (method Section 2.8.1) with an additional 200 μM moenomycin control. The fact that DacB

BOCILLIN binding is unaffected, supports that moenomycin does not inhibit DD-carboxypeptidase activity, and therefore supports that the rate observed is at least in part due to transpeptidation (following transglycosylation). The possibility of a contaminating transpeptidase from the purification was accounted for by the inability of *E. coli* PBP1b to use Lipid II (Gln)(Figure 6.13(B)), showing that *E. coli* transpeptidase activity has specificity for the stem peptide.

D-Ala release by *S. pneumoniae* PBP1a at a rate of 0.246 μM/min was calculated with a turnover number of 0.123 min^{-1}. These values are a composite of transpeptidase and carboxypeptidase activity. This is the first quantification of D-Ala release by a pneumococcal PBP using a native substrate, and is consistent with values required to observe microbial growth (0.05 min^{-1} required as a minimum based on a 20 minute doubling time). These values and the exciting plethora of further work now possible are discussed in more detail in Section 6.5.

Notably, a continuous fluorescence assay for transglycosylase activity of PBP1a was conducted under the successful conditions for D-Ala release, and no rate was observed. This has important implications for the assay system used to study transglycosylation, as clearly PBP1a is capable of producing peptidoglycan under these conditions, as demonstrated by the moenomycin control (discussed further in Section 6.5.3).
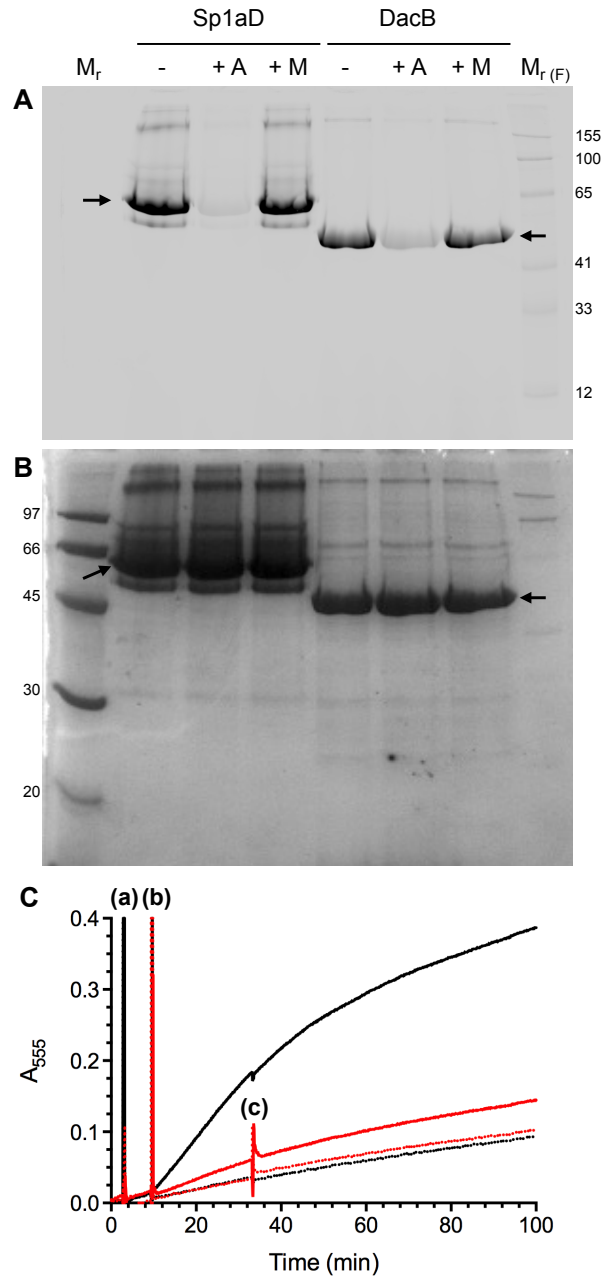
Figure 6.13. Confirmation of *S. pneumoniae* PBP1a transpeptidase activity. A series of controls confirming D-Ala release is due to transpeptidation by PBP1a. A: BOCILLIN FL fluorescence of PBP1a and DacB (control)(indicated by arrows) inhibited by ampicillin but not moenomycin. B: 12% SDS-PAGE Coomassie-stained gel of PBP1a and DacB labelled with BOCILLIN FL (indicated by arrows). Proteins labelled as DacB (E. coli PBP4 control) or Sp1aD (PBP1a FL purified in DDM). +A: plus 200 μM ampicillin, +M: plus 200 μM moenomycin. M_r, molecular weight markers (kDa), M_r (F), fluorescent molecular weight markers. Fluorescence detected using Typhoon FLA 9500 laser scanner (GE Healthcare) with Y510 filter.C: Amplex Red assay of E. coli PBP1b transpeptidase activity with amidated and non amidated lysine containing Lipid II. Assays in 50 mM BisTris propane pH 8.5, 2 mM $MgCl_2$, 1.96 μM LpoB, 4.4 nM E. coli PBP1b (plus Amplex Red coupling reagents), 20 μM Lipid II Lys (black solid), 20 μM amidated Lipid II lys (red solid), or 20 μL 0.1 % TX-100 (black and red dashed lines corresponding with amidated or non-amidated Lipid II) with 20 μM MurNAc-*L*-alanyl-γ-*D*-glutamyl-*meso*-diaminopimelyl-*D*-alanyl-*D*-alanine (acceptor) at 30°C. Absorbance of Lipid II in reaction buffer monitored, until PBP addition (a) followed by acceptor (b). A further 4.4 nM PBP1b was added at (c) to the plus or minus amidated Lipid II reactions.

6.4.6 Confirmation of transpeptidation by mass spectrometry

The controls used in Section 6.4.5 strongly suggested that the D-Ala release detected is due to transpeptidation. Insufficient substrate was available to conduct a full range of controls and therefore Liquid Chromatography positive ion mass spectrometry (LC-MS) was performed on the contents of the cuvettes used to generate Figure 6.12 to categorically confirm the presence of the cross-linked product. LC-MS is a mass spectrometry technique in line with liquid chromatography. Compounds are separated by liquid chromatography and positive ion (in this instance) mass spectrometry performed on each of the eluted peaks. This is useful for the detection of species with particular masses in the presence of other compounds.

2.2 M Bis.Tris pH 6.2 was added to the cuvette contents from a successful reaction, plus a negative control and 1 mg.ml^{-1} Mutanolysin from *Streptomyces globisporus* added for 2 hours at 37°C to digest glycan chains. A further aliquot of Mutanolysin was added for 2 hours to ensure full digestion before the removal of protein by boiling. Products were incubated with 5.8 mg.ml^{-1} NaBH$_4$ to reduce the sugar rings following cleavage and the undecaprenyl pyrophosphate linker removed with 2% (v/v) phosphoric acid. Samples were analysed by LC-MS in positive mode by Dr A. Lloyd. The total ion count (TIC), and detection of two peaks containing ions with a m/z value consistent with the anomeric structure of the cross-linked product are shown in Appendix 7 (Figures A7.1 and A7.2). Anomeric structures were observed, as the NaBH$_4$ treatment was unsuccessful. Figures 6.14 and 6.15 show the mass spectra of the two eluted peaks (elution at 15.2 min and 15.5 min respectively; Figure A7.1) containing species with the expected mass of the unreduced cross-linked product, which is observed in the presence of Lipid II and not in the negative control. Masses consistent with the D,D-carboxypeptidase product and disaccharide-pentapeptide from either Lipid II or its transglycosylation product were also identified in the Lipid II reaction and are shown in Appendix 7.
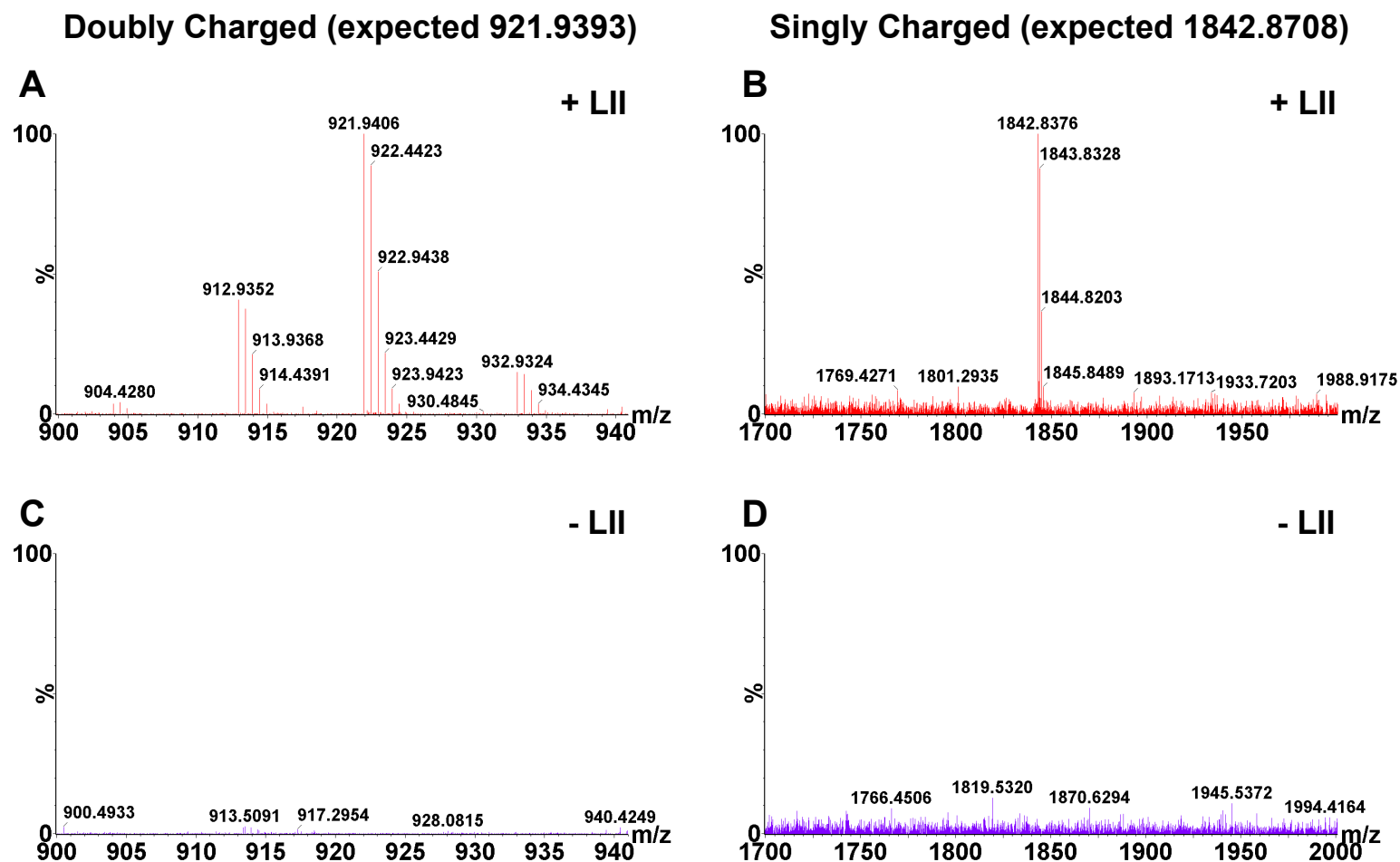
Figure 6.14: Positive ion mass spectra of peak eluting at 15.2 min on liquid chromatography of Amplex Red cuvette contents. Expected m/z of cross-linked disaccharide-pentapeptide-disaccharide-tetrapeptide: $[M-Z]^-$ 1842.8708, $[M-2H]^{2-}$ 921.9393. A, B: Spectra from analysis of cuvette contents with positive Amplex Red response including Lipid II (Gln) (+ LII Lys) showing mass of doubly charged (A) and singly charged (B) species. C, D: Spectra from analysis of negative control cuvette contents showing absence of the same species.
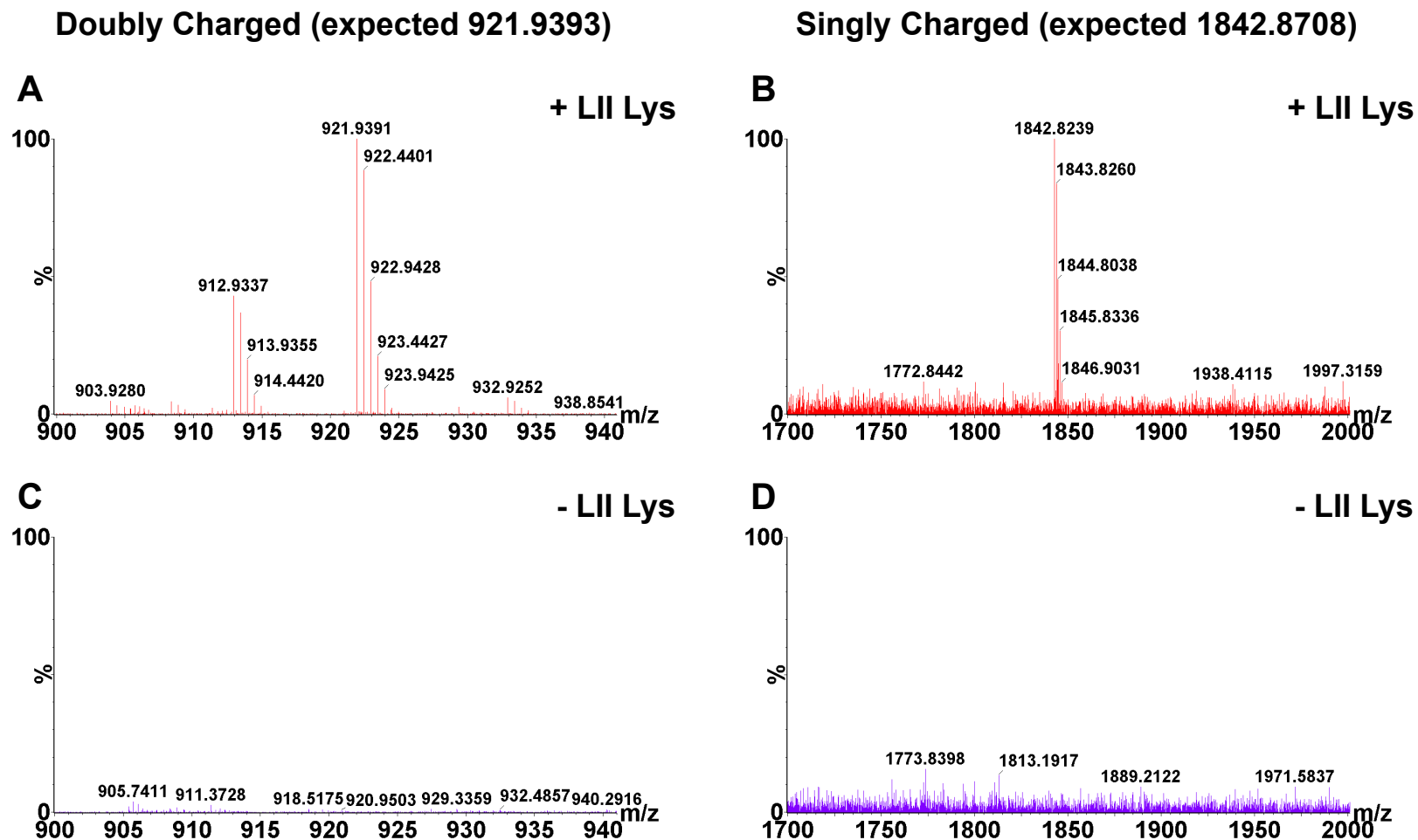
Figure 6.15: Positive ion mass spectra of peak eluting at 15.5 min on liquid chromatography of Amplex Red cuvette contents. Expected m/z of cross-linked disaccharide-pentapeptide-disaccharide-tetrapeptide: $[M-Z]^-$ 1842.8708, $[M-2H]^{2-}$ 921.9393. A, B: Spectra from analysis of cuvette contents with positive Amplex Red response including Lipid II (Gln) (+ LII Lys) showing mass of doubly charged (A) and singly charged (B) species. C, D: Spectra from analysis of negative control cuvette contents showing absence of the same species.

The masses observed in Figures 6.14 and 6.15, along with the controls used strongly suggests the presence of cross-linked species in the positive reaction from Figure 6.12. However, the mass observed could be due to incomplete Mutanolysin digestion of glycan chains resulting in tetrasaccharide with a pentapeptide and tetrapeptide on each of the two MurNAc sugars. It could also be disaccharide-pentapeptide cross-linked to disaccharide-tetrapeptide through the peptide stem. These two possibilities are shown in Figure 6.16.
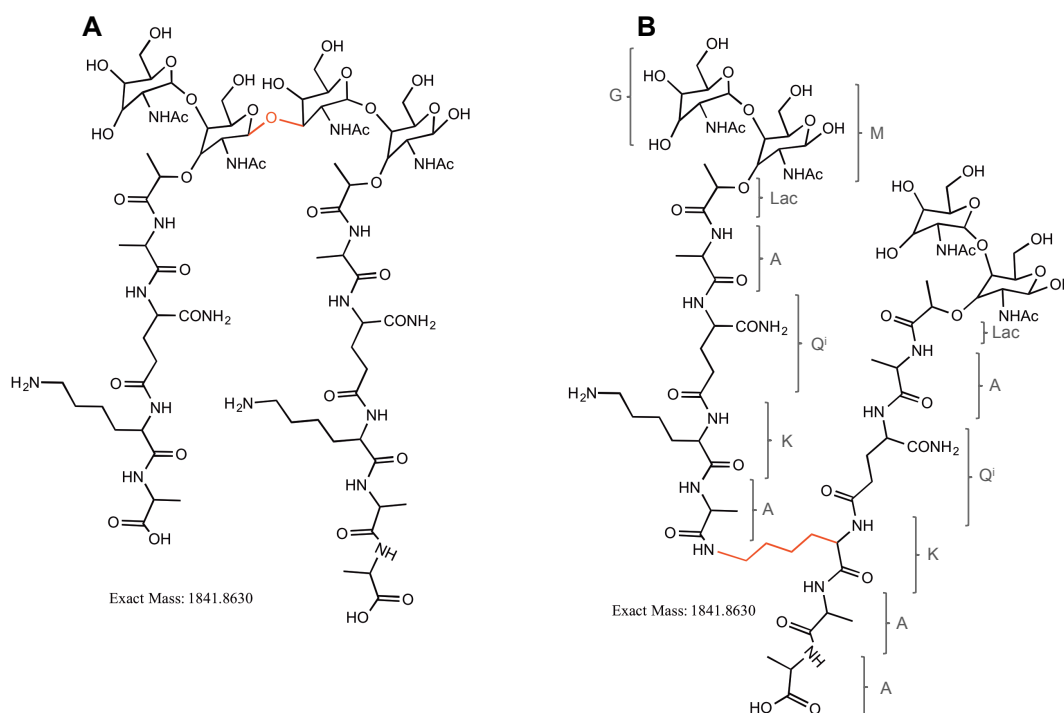
Figure 6.16: Possible structures associated with observed mass by positive ion mass spectrometry. Two possible structures corresponding to exact mass of 1841.8630, and therefore not distinguishable by mass spectrometry. A: dimer of disaccharide-pentapeptide and disaccharide tetrapeptide as a result of transglycosylation and D,D-carboxypeptidation. B: cross-linked product of transpeptidation.

In order to confirm cross-linking, the samples were analysed by LC-MS in positive mode with subsequent isolation and collision induced fragmentation of the species with a mass consistent with the doubly charged cation of the product (Figure 6.17; TIC Appendix 7, 15.2 min peak isolated for fragmentation; carried out by Dr. A. Lloyd). Species were fragmented by increased voltage and collision-induced dissociation with argon. The results of this unambiguously show the *in vitro* detection of transpeptidation by a pneumococcal PBP for the first time, due to the presence of 10 species (indicated by * on Figure 6.17), which can only be reasonably explained by transpeptidation.
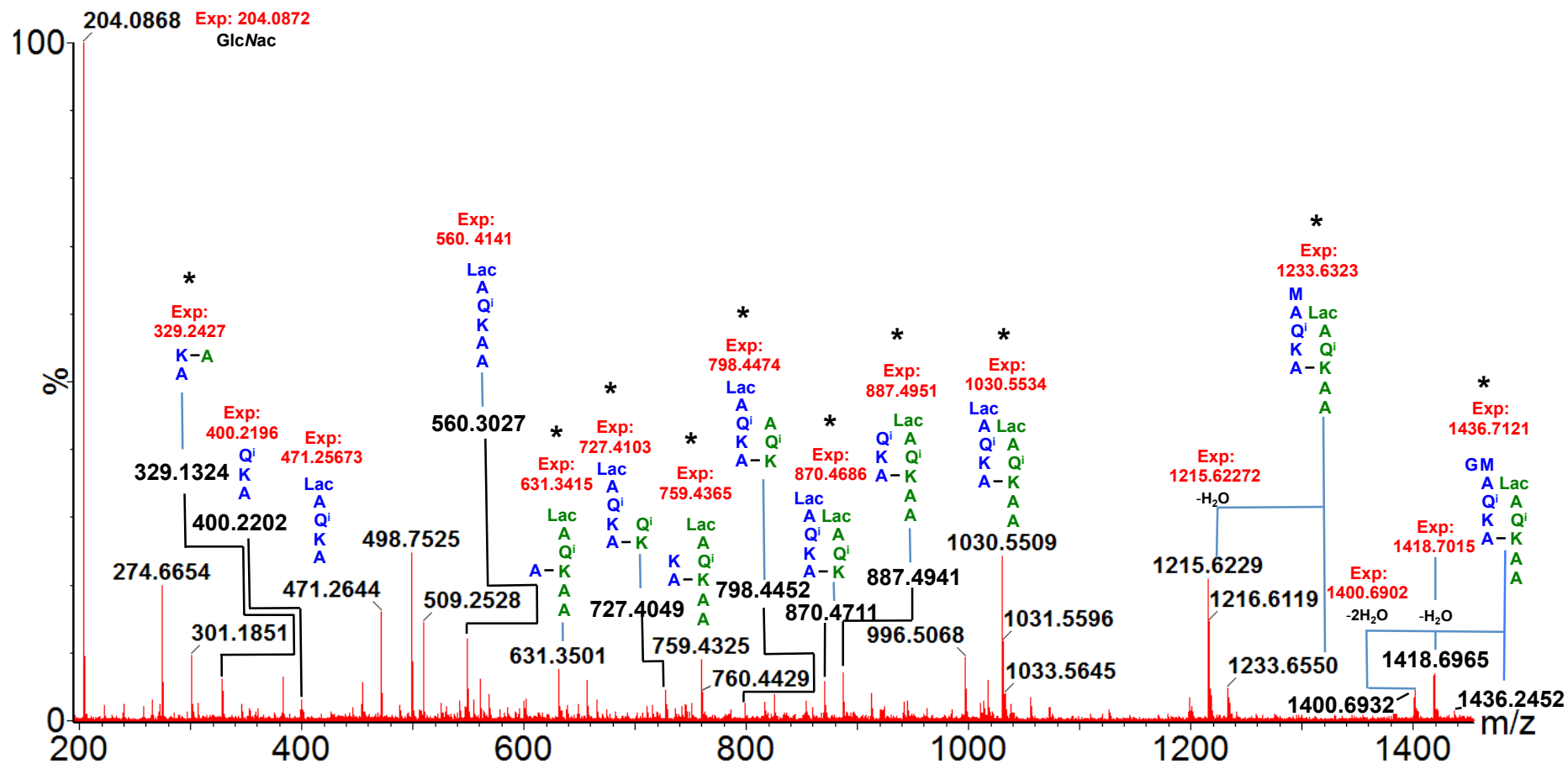
Figure 6.17: Positive ion fragmentation spectra of cross-linked species. Corresponding structure with donor stem in blue and acceptor stem in green shown along with expected mass in red above the corresponding ion in the spectra. * indicated the 10 key species used to identify the species as a product of transpeptidation. Single letter code used to describe fragment corresponds to single letter labels in Figure 6.16 (B) for identification. Fragmentation pattern analysed and figure made by Dr A. Lloyd.

6.5 Discussion and future work

This chapter has detailed the first conclusive evidence of *in vitro* transpeptidase activity by a pneumococcal PBP. This provides the foundation for future work aimed at answering long standing fundamental questions surround *S. pneumoniae* cell wall synthesis. This section discusses the presented work, and highlights particularly interesting areas of further work now possible.

6.5.1 The need for a robust and conclusive transpeptidase assay

The cross-linking of peptidoglycan is crucially important for structural integrity of the bacterial cell wall. The penicillin-binding domain of PBPs catalyses transpeptidation, and is a validated drug target as demonstrated by the success of the β-lactam class of antibiotics. However, high levels of resistance has developed to these agents, notably in *S. pneumoniae* through the modification of the PBP active site to give reduced β-lactam affinity. Understanding how these enzymes are able to continue cross-linking peptide stems despite losing affinity for the pseudosubstrate inhibitor is a long-standing and highly interesting biochemical question. A greater understanding of this current target, and the potential identification of new and related targets gives hope for the future of antibiotic discovery. This requires a robust assay that is specific for transpeptidation.

The *in vitro* observation of cross-linking by Gram-positive PBPs has been historically difficult, and very little progress has been made since the pioneering work of Professor Jack Strominger in the 1970s (Section 6.1.3). Only very recently identification of the important role of stem peptide chemistry was identified, and this led to the first *in vitro* demonstration of transpeptidation by *S. pneumoniae* PBPs (Zapun *et al.,* 2013).

The work by Zapun and colleagues represented a significant step in the right direction, although is not without its flaws. The use of Penicillin G as a specific transpeptidase inhibitor, and active site mutants strongly suggests the products seen

by SDS-PAGE are as a result of peptidoglycan cross-linking. However, overnight incubations were required prior to SDS-PAGE separation of products to observe the high molecular weight species. In addition, as described in Section 6.4.6, the species identified by MALDI-TOF mass spectrometry could be interpreted in two ways in the absence of confirmation by positive ion fragmentation. The masses observed were characteristic of non-dansylated products, so their position on the SDS-PAGE gel (detected by dansyl fluorescence) could not be correlated. Donor stems can in principle be dansylated and cross-linked, and therefore this mass should have been present. Attempts were made to repeat the mass spectrometry analysis (Section 6.3.3) by removal of the high molecular-weight band from the gel, but these were not successful.

This chapter aimed to develop the work published by Zapun and colleagues, providing mass spectrometric evidence for cross-linking as well as detection of cross-linking in a continuous format to enable higher throughput analysis.

6.5.2 Efforts towards a continuous assay for transpeptidation

Initial attempts to observe D-Ala release by the Amplex Red assay were unsuccessful, and several strategies were employed in an attempt to improve both the transpeptidase, and preceding transglycosylase activity. The decisions made were informed by on-going work by Dr A. Lloyd on *E. coli* PBP1b.

Mur*N*Ac-pentapeptide (Gln) was made in reasonable yields and to high purity by acid hydrolysis as an alternative acceptor for transpeptidation. The lack of donor only substrate means that this was added as an additional acceptor in assays but will be of more use in future work as an acceptor only substrate (Section 6.5.4). Enzymatic hydrolysis was also attempted as an alternative method, which was hoped to increase yield. A significantly lower yield and purity was obtained by this method but increasing the amount of SAP added to the reaction, and purification by cation exchange has the potential to improve this. In the interest of time, acid hydrolysis was used, and the correct product was identified by mass spectrometry.

It was hypothesised that the N-terminal dodecahistidine tag on PBP1a may affect the ability of the protein to fold correctly, as well as its activity. Helassa *et al.,* (2012) identified that *S. pneumoniae* PBP2a was inactive as a transglycosylase with a range of affinity tags on either the N- or C-terminus. Given that PBP1a and PBP2a are both bifunctional PBPs, and that on-going transglycosylation is required for transpeptidation (Zapun *et al.,* 2013), the effect of removal of the N-terminal dodecahistidine tag on *S. pneumoniae* D39 PBP1a activity was investigated by two methods (not shown). PBP1a FL was cloned into the pET26b vector without an affinity tag, and calculation of the predicted isoelectric point (p*I*) of the cytoplasmic and extracellular domains suggested that purification by successive anion and cation exchange could be possible as for *S. pneumoniae* PBP2a (Helassa *et al.,* 2012, and Section 4.3.3). Expression and purification by this method was successful, although the level of purity was poor. Subsequent gel filtration chromatography identified the protein to be aggregated as it eluted in the void volume. Cloning into a pProEX Hta vector with a TEV cleavable hexahistidine tag was attempted as affinity chromatography should result in greater purity. However, due to vector and *E. coli* cloning strain contamination this was not achieved in the time available.

Based upon observation of the importance of detergent in *E. coli* PBP1b activity by Dr A. Lloyd, PBP1a was purified in DDM, TX-100 and CHAPS. Purification in DDM and TX-100 were successful but most of the protein precipitated between IMAC and gel filtration chromatography in CHAPS, probably due to the detergent concentration which was just above CMC. A higher concentration was not used because of the significant quantities required to make buffers for both stages of purification, and the concentration used has previously been successful for purification of active *E. coli* PBP1b. Detergent exchange from DDM to CHAPS was subsequently performed for activity testing, although remaining trace amounts of DDM cannot be ruled out. PBP1a purified in DDM and TX-100 had comparable transglycosylase and transpeptidase β-lactam binding (determined by SDS-PAGE and BOCILLIN FL binding) activity. CHAPS purified protein was not as active. This could be affected by variation in the protein concentrations between the three enzyme preparations, but due to this and the precipitation observed, CHAPS purified protein was not used for further analysis.

Given the requirement for transglycosylase activity for the function of the transpeptidase active site and the requirement of amidation for transglycosylase activity (Chapter 4), optimisation of assay conditions were made for transglycosylase activity (Section 6.4.4). Salt, DMSO and detergent concentration were shown to have a substantial effect on the observed rate, and conditions were chosen to optimise this and limit the DMSO concentration used.

6.5.3 The first conclusive demonstration of *in vitro* pneumococcal cross-linking

Despite the attempts to improve activity discussed in Section 6.5.2, a combination of decisions based on parallel work by Dr A Lloyd, and an element of serendipity resulted in a positive Amplex Red result (Figure 6.11). The use of hexaethylene glycol dodecyl ether (E_6C_{12}) detergent and omission of DMSO and NaCl from the reaction proved to be a successful combination. The controls used showed this activity to be substrate dependent, enzyme dependent, require transglycosylase activity and to occur only in the presence of amidated substrate. LC-MS positive ion fragmentation (tandem LC-MSMS) gave conclusive evidence for the presence of cross-linked product, and therefore transpeptidase activity, for the first time.

The Amplex Red coupling reagents had a linear response up to an absorbance change of 0.1 units per minute (Dr A. Lloyd, Personal Communication), and therefore it was clear that they were not limiting under the conditions used. Evidence of the requirement for on-going transglycosylase activity for at least part of the detected D-Ala release came from moenomycin inhibition of the observed rate. The Amplex Red assay coupling system was not inhibited by moenomycin up to a concentration of 1mM (Dr A. Lloyd, Personal Communication) and moenomycin binding was shown to not affect BOCILLIN FL interaction with the transpeptidase domain of PBP1a. Therefore the slight pause observed prior to acceleration of rate in Figure 6.12 was not due to limitations of the coupling system and was likely a result of the requirement for transglycosylation to produce glycan chains of sufficient length.

The Amplex Red response corresponded to a D-Ala release of 0.246 μM/min and a turnover number of 0.123 min^{-1}, which is a composite of transpeptidase and

carboxypeptidase mediated D-Ala release. In order to differentiate between the contributions of each enzymatic activity, a donor only transpeptidase substrate would be required. By incubating this with the PBP and observing A_{555}, the background D,D-carboxypeptidase activity could be measured. The composite rate of transpeptidation and D,D-carboxypeptidation could then be measured on subsequent addition of acceptor (eg. see Figure 6.13) This would also remove the pause seen after addition of enzyme, as glycan chain polymerisation will occur during this period. Donor only substrates are produced by removing the ability of the ε-amino group of the lysine side chain to act as a nucleophile. This could be achieved through acetylation of the amine (Lupoli *et al.,* 2014). Given the clear requirement for isoglutamine containing pentapeptide stems for transglycosylation by pneumococcal PBPs, amidation at this position must be present. Therefore it may be necessary to incorporate pre-acetylated lysine into the pentapeptide stem rather than carrying out chemical modification on the regular peptide stem, to avoid cross-reaction with the second position isoglutamine. *S. pneumoniae* MurE has been observed to incorporate a range of lysine analogues into the stem peptide in the place of lysine (Dr A. Lloyd and Anna York, Personal Communication). The isoglutamine amide is relatively stable and therefore less likely to react, but this should still be considered as a possibility. Alternatively DAP could be incorporated in the third position as the ε-D-amino acid should not be a donor for *S. pneumoniae* PBPs. Whichever substrate is used must be checked as a transglycosylase substrate first to ensure sufficient rate can be achieved to support subsequent cross-linking.

BOCILLIN FL binding to *S. pneumoniae* PBP1a (Figure 6.8) shows a contaminating lower molecular weight protein with a penicillin-binding domain. This could be due to degradation of PBP1a or a contaminating *E. coli* PBP. *E. coli* PBP1b exhibited neither transglycosylase or transpeptidase activity with Lipid II (Gln) when tested, which suggests that the contaminating protein does not contribute to the transpeptidase activity observed. Any D,D-carboxypeptidase activity from the contaminating protein will be accounted for in future experiments using donor only controls, as previously described.

Notably, activity could not be observed by the continuous fluorescence assay for transglycosylation under the conditions used for the successful Amplex Red assay.

Given that D-Ala release was inhibited by moenomycin, and on-going transglycosylation is required for transpeptidation, it is clear that glycan polymerisation can occur under these conditions. This suggests that the high salt and DMSO are required for PBP1a to be able to use dansylated Lipid II as a substrate, for lysozyme activity, or the conditions produce a fluorescence effect. This has important implications for the use of the fluorescence assay system, which is discussed in more detail in Section 4.6.2.2.

6.5.4 Further work

The work presented in this chapter provides the foundation for the future detailed study of transpeptidation by pneumococcal and potentially other Gram-positive PBPs. This section details some of the future work possible leading on from this.

6.5.4.1 Optimisation of the observed rates

Due to substrate and time limitations, a full optimisation of conditions was not carried out. Several strategies could be employed to investigate the effect of a variety of factors on rate.

The buffer conditions used were significantly different to those optimised for transglycosylase activity (see Section 6.4.4) and contained neither salt or DMSO. A range of pH values, NaCl and metal ion types and concentration should be tested in order to identify any effect on the rate observed. All three conditions had a significant effect on *E. coli* PBP1b activity (Dr. A. Lloyd, Personal Communication).

Work by Dr A. Lloyd identified a very strict dependency of *E. coli* PBP1b transpeptidase activity on detergent ethylene glycol polymeric state and chain length. This may be linked to the thickness of the cytoplasmic membrane in the native PBP environment. *S. pneumoniae* PBP1a was only tested with hexaethylene glycol dodecyl ether, the optimal detergent of this type for *E. coli* PBP1b, as substrate limitations meant no further experiments could be performed. The *E. coli* and *S. pneumoniae* cytoplasmic membranes have different compositions, which are

spatially, and temporally regulated throughout the cell and cell cycle (Barák and Muchová, 2013; Epand and Epand, 2009), so testing of a range of detergents will enable the identification of optimal conditions. It will be interesting to compare the *in vitro* detergent preferences of *E. coli* PBP1b and *S. pneumoniae* PBP1a. In future work, testing the specificity for detergent lengths between different PBPs from *S. pneumoniae* may help to identify differences in membrane composition and PBP localisation.

The addition of cardiolipin and phosphatidylglycerol, the main components of the pneumococcal cytoplasmic membrane (Brundish *et al.*, 1967) to the assay as well as the detergent used could improve enzyme activity due to an environment that is closer to that *in vivo.*

A further attempt to obtain PBP1a without an affinity tag, which was previously unsuccessful (Section 6.5.2) could be attempted as this may result in a more active protein.

6.5.4.2 Prospects for the Amplex Red assay system

Following the investigation of conditions to ensure optimal transpeptidase activity (Section 6.5.4.1), and identification of the contribution of carboxypeptidase activity to the observed D-Ala release (Section 6.5.3), several interesting biochemical questions could be answered. Firstly, once the assay is optimised for PBP1a, the four other pneumococcal transpeptidases could be tested. For those that exhibit activity by this method, the first enzymological characterisation with their native substrate can be performed. PBP2a is bifunctional and previous work has suggested that it has both transglycosylase and transpeptidase activity *in vitro* (Zapun *et al.,* 2013). However, monofunctional PBP2b and PBP2x will require glycan chains from another source. Both enzymes were reported to cross-link glycan chains formed concomitantly by a transpeptidase mutant of PBP2a (Zapun *et al.*, 2013). Testing PBP2b and PBP2x with a combination of transpeptidase mutants of PBP1a, PBP1b or PBP2a may help in convincingly identifying the natural functional partners in the cell, as the glycan product of one may be the preferential substrate. PBP1a-PBP2x and PBP2a-PBP2b

interactions have previously been suggested but a high level of uncertainty still surrounds this theory, and very little is known about the activity and localisation of PBP1b (Liu *et al.,* 2006). The requirement for stem peptide amidation of all four *S. pneumoniae* transpeptidases has previously been interpreted from SDS-PAGE experiments (Zapun *et al.*, 2013), therefore with this substrate and the improved detergent, salt and DMSO conditions, which proved successful for PBP1a, there is hope for observation of activity in this system, to finally characterise the transpeptidase activity of the *S. pneumoniae* high molecular weight transpeptidases.

As mentioned previously, no direct evidence exists for functional interactions of the *S. pneumoniae* PBPs with other PBPs or cell division proteins. However, several proteins have been assigned to either the septal or peripheral cell wall synthetic machineries (Massidda *et al.,* 2013). Recent studies have isolated complexes of recombinantly expressed septal (Noirclerc-Savoye *et al.*, 2013) and peripheral (Philippe *et al.,* 2014) machinery proteins. Noirclerc-Savoye *et al.,* (2013) purified several complexes containing DivIC, DivIB, FtsL, FtsW and PBP2x, and did not observe any increase in the transpeptidase activity of PBP2x by hydrolysis of the S2d thioester substrate analogue as part of the complex. This may be due to missing factors or non-functional interactions, or may have been masked by the intrinsic instability of this thiol ester substrate. MreC, MreD and PBP2b, RodA complexes were purified by Philippe *et al.*, (2014) but larger complexes could not be obtained and the activity of PBP2b was not tested. It should be noted that functional interactions between proteins in these complexes may be transient in nature and at different points in the cell cycle. Therefore, although these complexes will co-purify following overexpression, they may not be representative of *in vivo* interactions. No transglycosylases were investigated in these experiments; PBP2a has been suggested to be part of the peripheral machinery and PBP1a both the septal and peripheral, however the localisation of PBP1b has not been investigated. Therefore the interaction of these bifunctional PBPs is of interest in the study of cell wall synthesis.

Bertsche *et al.,* (2006) successfully identified the interaction between the bifunctional PBP1b and monofunctional transpeptidase PBP3 from *E. coli* by immobilisation of PBP3 and affinity chromatography. The interaction was confirmed by surface plasmon resonance (SPR), bacterial two-hybrid and cross-linking/co-

immunoprecipitation. However this study did not investigate the effect of this interaction on catalytic activity. Immobilisation of *S. pneumoniae* bifunctional PBPs, affinity chromatography using pneumococcal membrane preparations and subsequent SDS-PAGE could help to identify the range of proteins interacting with each PBP. Proteomic analysis of the co-eluted proteins will enable identification, and lead to experiments to confirm interactions both physically and functionally.

6.6 Conclusion

This chapter has shown the first unequivocal evidence for *in vitro* cross-linking by a pneumococcal PBP. The potential for the use of a continuous coupled assay for D-Ala release as an assay for transpeptidation was demonstrated. This discovery sets strong foundations for the future enzymological characterisation of pneumococcal PBP transpeptidase activity, and greater understanding of the mechanisms of β-lactam resistance (Discussed Section 7.2.2) in this important Gram-positive pathogen.

Chapter 7. General discussion and conclusions

The current threat from highly- and multi-drug-resistant bacteria is significant and the long-term effects on modern healthcare could prove catastrophic. Therefore, in addition to improvements in diagnosis, prescription practices and education, it is vital that new antibiotics are developed and made available in the clinic. Antibiotic resistance is essentially natural selection and is therefore inevitable to some extent, but it is important that we do a much better job of producing and prescribing these drugs in the future in order to slow the process and protect this vital resource upon which the treatment of many acute illnesses and surgical procedures is entirely dependent.

In addition to assisting drug discovery, a better understanding of bacterial biochemistry and physiology is interesting from the perspective of fundamental research. This thesis has focused on biosynthesis of the bacterial cell wall, which has for a long time been considered an Achilles heel and prime site for pharmacological intervention due to its importance for cellular viability and unique molecular composition. Key to this process are the penicillin-binding proteins (PBPs) that are responsible for synthesis of the sacculus surrounding the cell. As the site of action for penicillins and other β-lactams, PBPs are validated antibiotic targets. Amidation of the Lipid II stem peptide glutamate to isoglutamine is essential in several Gram-positive bacteria including *Staphylococcus aureus* and *S. pneumoniae*, and this is predicted to be at least in part due to the substrate specificity of PBPs.

The main aim of this thesis was to investigate the enzymology of peptidoglycan assembly, with a particular focus on the influence of stem peptide amidation on the activity of Gram-positive PBPs. This approach should further our knowledge of the fundamental science underlying this important physiological process, and may aid in the future development of novel PBP inhibitors.

7.1 Transglycosylase activity of Gram-positive Class A PBPs

Two bifunctional Class A PBPs from *S. pneumoniae* (PBP1a and PBP2a), and another from *Staphylococcus aureus* (PBP2) were studied alongside the *Staphylococcus aureus* monofunctional transglycosylase MGT (Chapters 4 and 5).

7.1.1 Effect of amidation on the transglycosylase activity of Gram-positive PBPs

Almost all *in vitro* enzymological characterisation of Gram-positive PBPs reported to date has involved the use of non-physiological non-amidated Lipid II substrates, with the exception of one recent study that confirmed the importance of amidation in pneumococcal peptidoglycan assembly (Zapun *et al.,* 2013). In this thesis, the activities of four transglycosylases from two Gram-positive bacteria were studied by two complementary assay systems.

S. pneumoniae PBP1a, PBP2a and *Staphylococcus aureus* PBP2 all displayed a clear preference for amidated Lipid II, as demonstrated by kinetic data for the *S. pneumoniae* enzymes (Chapter 4) that revealed a higher affinity (lower $K_m/S_{0.5}$) and increased catalytic efficiency with amidated Lipid II. Although both enzymes displayed a preference for amidated substrate, the effect on PBP2a and PBP1a was different as a more marked decrease in K_m was observed for PBP1a and a more significant increase in Vmax for PBP2a, resulting in an overall similar increase in catalytic efficiency for the two enzymes. Interestingly, cooperativity was also identified for *S. pneumoniae* PBP2a transglycosylase activity (Section 7.1.2), and to my knowledge this has not been previously reported through kinetic data for this enzyme class. Notably, possible cooperativity in MGT activity was identified in Chapter 5, although further work is required to confirm this. In addition, PBP2a acted in a more processive manner with the amidated substrate compared with the non-amidated substrate, although the SDS-PAGE assay system does not allow quantification in its current format. The sole bifunctional Class A PBP from *Staphylococcus aureus* (PBP2) also showed a clear preference for amidated Lipid II, although kinetic values were not established as the continuous fluorescence assay was unsuccessful. SDS-PAGE demonstrated an increase in both substrate usage and

processivity of PBP2. Notably, this preference for amidation was not observed for the full-length monofunctional transglycosylase MGT, although it became more important following removal of the TM region (Section 7.1.3), indicating a more subtle effect than that observed with the bifunctional PBPs. This is the first study to investigate the role of amidation on the activity of a monofunctional transglycosylase, and it will be of great interest in the future to determine if this is a general property of this enzyme class. These results, together with the requirement for on-going transglycosylation during transpeptidation (Zapun *et al.,* 2013), the importance of amidation in transglycosylase activity, and the discovery that amidated stem peptides in *S. pneumoniae* are found mainly in cross-linked peptidoglycan (Bui *et al.,* 2012), suggest that amidation of Lipid II may be more important for bifunctional PBPs than monofunctional transglycosylases to allow them to perform efficient peptidoglycan assembly.

These results show the effect of amidation on transglycosylase activity for the first time and that this simple chemical modification has a large effect on PBP activity. Identifying the molecular mechanisms underlying the observed increase in affinity and catalytic efficiency with amidated Lipid II should be the focus of future work, and may be achieved through determination of crystal structures, molecular modelling, or a combination of these approaches together with further functional analysis.

7.1.2 Cooperativity in transglycosylase activity

Of particular note was the identification of positive cooperativity in the transglycosylase activity of *S. pneumoniae* PBP2a with respect to Lipid II (Section 4.5.4), and possible positive cooperativity of *Staphylococcus aureus* MGT (Section 5.7.2). Cooperativity in substrate binding between the donor and acceptor sites in the active site of *Staphylococcus aureus* monofunctional transglycosylase (MGT) has been shown previously (Bury *et al.,* 2015), but to my knowledge cooperativity between molecules in an oligomeric state, and the effect on catalytic activity has not been described. In contrast, PBP1a data did not suggest cooperativity, and similar experiments with *Staphylococcus aureus* PBP2 were not performed. Therefore this

study should be expanded to include other PBPs, and the work of Bury and colleagues should be repeated to determine if cooperativity between donor and acceptor sites is a factor of bifunctional PBPs as well as the monofunctional *Staphylococcus aureus* MGT.

7.1.3 Importance of the transmembrane region in transglycosylase activity

The hydrophobic TM region of *S. pneumoniae* PBP1a, PBP2a and *Staphylococcus aureus* MGT was shown to be important for transglycosylase activity. However, care must be taken here, as the results presented in this thesis show that previous conclusions by Helassa *et al.,* (2012) on the importance of the TM region in *S. pneumoniae* PBP2a processivity are an artefact of the detergent concentration used, likely due to interaction with the hydrophobic membrane-interacting region (Di Guilmi *et al.,* 1999). The role of the TM helix of MGT is of particular note because when it was absent (in the Δ67 enzyme variant), either amidated or a mixture of labelled and non-labelled Lipid II were required in order to observe any enzyme activity. It may therefore be important for interaction with hydrophobic regions of the substrate and/or in mediating access to the active site, which may be particularly crucial for the smaller monofunctional enzyme. This is also consistent with the important role of the pentapeptide stem in transglycosylase activity suggested in structural studies by Huang *et al.,* (2012), and future structural and functional studies should be performed.

The TM region was found to be essential for oligomerisation (presumably dimerisation) of PBP2a, and this enabled the first reported determination of the dissociation constant (K_d) of a Class A PBP from *S. pneumoniae*. Analytical ultracentrifugation (AUC) experiments could provide further confirmation of the oligomeric state. The observed cooperativity of PBP2a (Section 7.1.2) suggests that oligomerisation is important for enzymatic activity. With amidated Lipid II as a substrate, positive cooperativity was observed at an enzyme concentration significantly below the calculated K_d, suggesting substrate binding may contribute to cooperativity by encouraging and/or stabilising dimerisation. Whether this is a factor of the enzyme or substrate was not established, and a higher Hill coefficient was

observed when the enzyme concentration was double the K_d (in the presence of non-amidated substrate), which may imply that oligomerisation is important for substrate binding. Further work should aim to distinguish the role of enzyme concentration, substrate specificity and the cooperativity between donor and acceptor sites, and has the potential to determine important mechanistic details involved in transglycosylase activity.

7.1.4 PBPs as part of a larger cell wall synthesis complex

Both *Staphylococcus aureus* and *S. pneumoniae* PBPs are believed to act as part of a large, as-yet not fully characterised cell wall synthesis complex (Sections 1.7.2, 4.6.5 and 5.8.4.2), and this should always be remembered when studying isolated enzymes *in vitro*. The activity of *E. coli* PBPs are stimulated *in vivo* and *in vitro* by the outer membrane lipoproteins LpoA and LpoB (Lupoli *et al.,* 2014; Paradis-Bleau *et al.,* 2010; Typas *et al.,* 2010; 2012), and although direct equivalents cannot exist in Gram-positive bacteria due to the absence of an outer membrane, it is highly likely that important extracellular or membrane-associated interacting partners are present *in vivo*. Future work should focus on identifying potential interacting partners using yeast two-hybrid screening and 'fishing' experiments involving protein immobilisation as have proved successful for *E. coli* (Bertsche *et al.,* 2006).

It is important that the results of *in vitro* studies are correlated with *in vivo* approaches such as live cell imaging with fluorescent probes (Tsui *et al.,* 2014). The bacterial cell wall and the machinery involved in its biosynthesis are highly complex, and both *in vitro* analysis and *in vivo* methods will be needed to fully understand the processes involved.

7.1.5 Characterisation of novel carbohydrate-based transglycosylase inhibitors

The potential for targeting transglycosylation with antibiotics has long been discussed (Galley *et al.,* 2014; Halliday *et al.,* 2006; Ostash and Walker, 2005), and two novel carbohydrate-based inhibitors were tested against *Staphylococcus aureus* MGT (Section 5.7), and this work was published recently (Zuegg *et al.,* 2015) and is

attached at the end of this thesis (Appendix 8). The IC_{50} values determined were comparable to the highly potent transglycosylase inhibitor moenomycin, highlighting the potential for using the moenomycin pharmacophore as a starting point for the design of new, direct-binding transglycosylase inhibitors.

7.1.6 The requirement for new assays for transglycosylase activity

Both assay systems used in this thesis together provided valuable information on the catalytic rate and processivity of PBP transglycosylase activity, however both have clear limitations associated with them, as discussed in Sections 4.6.2 (and published recently in Galley *et al*., 2014, attached at the end of this thesis (Appendix 8)). There is a clear requirement for a complementary assay system using native, unmodified, non-fluorescent Lipid II that does not utilise an *N*-acetylmuramidase coupling enzyme (discussed in Sections 4.6.2.2 and 5.8.5.1). This will be important in the future study of transglycosylases and characterisation of novel inhibitors.

7.2 Transpeptidase activity of *S. pneumoniae* PBP1a

7.2.1 The first unequivocal evidence for *in vitro* transpeptidase activity of a *S. pneumoniae* PBP

Chapter 6 described the observation of transpeptidase activity of a Gram-positive PBP by a continuous assay format for the first time, and the first unequivocal evidence for cross-linking by a *S. pneumoniae* PBP. This is a very significant development in the study of Gram-positive PBPs, as it will allow the kinetic characterisation of transpeptidase activity of Gram-positive HMW PBPs with their native substrates. However before the true potential of this development can be realised, it will be necessary to discriminate the contribution made to D-Ala release from carboxypeptidase compared to transpeptidase crosslinking activities (discussed in Section 6.5.3).

7.2.2 Branched substrates

This important development, combined with progress made in the synthesis of native branched Lipid II substrates (described in Chapter 3), paves the way for investigation of a fundamental and long-standing question regarding β-lactam resistance mediated by pneumococcal PBPs. Several crystal structures have suggested that mutations in the transpeptidase domain of *S. pneumoniae* PBPs affect access to the active site (Sections 1.8 and 6.1.1), and this, along with the requirement for MurM and the elevated levels of interpeptide branching present in resistant strains, has led to the theory that branched Lipid II is the preferential substrate for PBPs from penicillin-resistant strains. PBP1a, PBP2a, PBP2b and PBP2x from *S. pneumoniae* 5204 have now all been successfully expressed and purified in our lab. The 5204 strain isolated from sputum in Grenoble in 1999 is highly resistant to β-lactam antibiotics such as Penicillin G and cefotaxime (Chesnel *et al.,* 2003; 2005). Progress on the synthesis of branched Lipid II substrates in this thesis (Chapter 3) and in other work on *Staphylococcus aureus* substrates (Rebecca Bolton, Personal Communication), along with the ability to detect cross-linking by PBP1a in a continuous assay format (Chapter 6) means that the investigation of substrate specificity of PBPs from penicillin susceptible and resistant strains will soon be possible.

7.3 Conclusion

The work presented in this thesis has made a significant contribution to understanding of the enzymology of Gram-positive PBPs from two important global pathogens. Future work that is now possible will enable the investigation of long-standing fundamental questions surrounding bacterial cell wall synthesis and antibiotic resistance, and may assist the future development of much-needed antibiotics.

Bibliography

Abrahams, K. (2011). The Enzymology of *Streptococcus pneumoniae* Peptidoglycan Polymerisation. Unpublished Ph. D, University of Warwick

Adam, M., Damblon, C., Jamin, M., Zorzi, W., Dusart, V., Galleni, M., El Kharroubi, A., Piras, G., Spratt, B. G., and Keck, W. (1991). Acyltransferase Activities of the High-Molecular-Mass Essential Penicillin-Binding Proteins. *Biochemistry Journal* **279**: 601–604.

Alekshun, M. N., and Levy, S. B., (2007). Molecular Mechanisms of Antibacterial Multidrug Resistance. *Cell* **128** (6): 1037–50.

Altschul, S. F., Gish, W., Miller, W., Myers, E.W., and Lipman. D.J., (1990). Basic Local Alignment Search Tool. *Journal of Molecular Biology* **215**: 403–410.

Appelbaum, P. C., (2007). Microbiology of Antibiotic Resistance in *Staphylococcus aureus*." *Clinical Infectious Diseases* **45** Suppl 3 (Supplement 3): S165–170.

Atilano, M. L., Pereira, P. M., Yates, J., Reed, P., Veiga, H., Pinho, M. G., and Filipe, S. R., (2010). Teichoic Acids Are Temporal and Spatial Regulators of Peptidoglycan Cross-Linking in *Staphylococcus aureus*. *Proc Natl Acad Sci USA* **107** (44): 18991–18996.

Azuma, I, D., Thomas, W., Adam, A., Ghuysen, J-M., Petit, J. F., and Lederer, E., (1970) Occurrence of *N*-Glycolylmuramic Acid in Bacterial Cell Walls. *Biochimica Et Biophysica Acta* **208**: 444–451.

Balibar, C. J., Shen, X., McGuire, D., Yu, D., McKenney, D., and Tao, J., (2010). *cwrA*, A Gene That Specifically Responds to Cell Wall Damage in *Staphylococcus aureus*. *Microbiology* **156** (5): 1372–1383.

Banzhaf, M., van den Berg van Saparoea, B., Terrak, M., Fraipont, C., Egan, A., Philippe, J., Zapun, A., Breukink, E., Nguyen-Distéche, M., den Blaauwen, T., and Vollmer, W. (2012). Cooperativity of Peptidoglycan Synthases Active in Bacterial Cell Elongation. *Molecular Microbiology* **85** (1): 179–194.

Barák, I., and Muchová, K., (2013). The Role of Lipid Domains in Bacterial Cell Processes. *International Journal of Molecular Sciences* **14** (2): 4050–4065.

Barcus, V. A., Ghanekar, K., Yeo, M., Coffey, T. J., and Dowson, C. G. (1995). Genetics of High Level Penicillin Resistance in Clinical Isolates of *Streptococcus Pneumoniae*. *FEMS Microbiology Letters* **126**: 299–304.

Barendt, S. M., Sham, L. T., and Winkler, M. E., (2011). Characterization of Mutants Deficient in the L,D-Carboxypeptidase (DacB) and WalRK (VicRK) Regulon, Involved in Peptidoglycan Maturation of *Streptococcus Pneumoniae* Serotype 2 Strain D39. *Journal of Bacteriology* **193** (9): 2290–2300.

Barreteau, H., Kovač, A., Boniface, A., Sova, M., Gobec, S., and Blanot, D., (2008). Cytoplasmic Steps of Peptidoglycan Biosynthesis. *FEMS Microbiology Reviews* **32** (2): 168–207.

Barrett, D., Leimkuhler, C., Chen, L., Walker, D., Kahne, D., and Walker, S., (2005). Kinetic Characterization of the Glycosyltransferase Module of *Staphylococcus aureus* Pbp2. *Journal of Bacteriology* **187** (6): 2215–2217.

Barrett, D., Wang, T-S. A., Yuan, Y., Zhang, Y., Kahne, D., and Walker, S., (2007). Analysis of Glycan Polymers Produced by Peptidoglycan Glycosyltransferases. *The Journal of Biological Chemistry* **282** (44): 31964–31971.

Barrett, D., Chen, L., Litterman, N. K., and Walker, S., (2004). Expression and Characterization of the Isolated Glycosyltransferase Module of *Escherichia coli* PBP1b. *Biochemistry* **43** (38): 12375–12381.

Benfield, T., Espersen, F., Frimodt-Møller, N., Jensen, A. G., Larsen, A. R., Pallesen, L. V., Skov, R., Westh, H., and Skinhøj, P., (2007). Increasing Incidence but Decreasing in-Hospital Mortality of Adult *Staphylococcus aureus* Bacteraemia Between 1981 and 2000. *Clinical Microbiology and Infection* **13** (3): 257–263.

Bera, A., Herbert, S., Jakob, A., Vollmer, W., and Götz, F., (2005). Why Are Pathogenic Staphylococci So Lysozyme Resistant? the Peptidoglycan *O*-Acetyltransferase OatA Is the Major Determinant for Lysozyme Resistance of *Staphylococcus aureus*. *Molecular Microbiology* **55** (3): 778–787.

Bertani, G., (1951). Studies on Lysogenesis. I. the Mode of Phage Liberation by Lysogenic *Escherichia coli*. *Journal of Bacteriology* **62**: 293–300.

Bertsche, U., Breukink, E., Kast, T., and Vollmer, W., (2005). *In Vitro* Murein (Peptidoglycan) Synthesis by Dimers of the Bifunctional Transglycosylase-Transpeptidase PBP1B From *Escherichia coli*. *Journal of Biological Chemistry* **280** (45): 38096–38101.

Bertsche, U., Kast, T., Wolf, B., Fraipont, C., Aarsman, M. E. G., Kannenberg, K., von Rechenberg, M., Nguyen-Distéche, M., den Blaauwen, T., Hötlje, J. V., and Vollmer, W., (2006). Interaction Between Two Murein (Peptidoglycan) Synthases, PBP3 and PBP1B, in *Escherichia coli*. *Molecular Microbiology* **61** (3): 675–690.

Bi, E., and Lutkenhaus, J., (1991). FtsZ Ring Structure Associated with Division in *Escherichia coli*. *Nature* **354**: 161–65.

Biboy, J., Bui, N. K., and Vollmer, W., (2013). *In Vitro* Peptidoglycan Synthesis Assay with Lipid II Substrate. In *Bacterial Cell Surfaces*, **966**:273–288. Methods in Molecular Biology. Totowa, NJ: Humana Press.

Blair, J. M. A., Webber, M. A., Baylay, A. J., Ogbolu, D. O., and Piddock, L. J. V., (2015). Molecular Mechanisms of Antibiotic Resistance. *Nature Reviews Microbiology* **13** (1): 42–51.

Bocchini, J. A., Bradley, J. S., Brady, M. T., Berstein, H. H., Byington, C. L., Fisher, M. C., Glode, M. P., Jackson, M. A., Keyserling, H. L., Kimberlin, D. W., Orenstein, W. A., Schtze, G. E. and Willoughby, R. E. (2010). Recommendations for the Prevention of *Streptococcus pneumoniae* Infections in Infants and Children: Use of 13-Valent Pneumococcal Conjugate Vaccine (PCV13) and Pneumococcal Polysaccharide Vaccine (PPSV23). *Pediatrics* **126** (1): 186–190.

Boneca, I. G., Huang, Z-H., Gage, D. A., and Tomasz, A., (2000). Characterization of *Staphylococcus aureus* Cell Wall Glycan Strands, Evidence for a New β-*N*-Acetylglucosaminidase Activity. *The Journal of Biological Chemistry* **275** (14): 9910–9918.

Born, P., Breukink, E., and Vollmer, W., (2006). *In Vitro* Synthesis of Cross-Linked Murein and Its Attachment to Sacculi by PBP1A From *Escherichia coli*. *The Journal of Biological Chemistry* **281** (37): 26985–26993.

Bouhss, A., Crouvoisier, M., Blanot, D., and Mengin-Lecreulx, D., (2004). Purification and Characterization of the Bacterial MraY Translocase Catalyzing the First Membrane Step of Peptidoglycan Biosynthesis. *The Journal of Biological Chemistry* **279** (29): 29974–29980.

Braddick, D., Sandhu, S., Roper, D. I., Chappell, M. J., and Bugg, T. D. H. (2014). Observation of the Time-Course for Peptidoglycan Lipid Intermediate II Polymerization by *Staphylococcus aureus* Monofunctional Transglycosylase. *Microbiology* **160:** 1628-1636.

Brandish, P. E., Burnham, M. K., Lonsdale, J. T., Southgate, R., Inukai, M., and Bugg, T. D. H. (1996). Slow Binding Inhibition of Phospho-N-Acetylmuramyl-Pentapeptide-Translocase (*Escherichia coli*) By Mureidomycin A. *The Journal of Biological Chemistry* **271**: 7609–7614.

Breukink, E., van Heusden, H. E., Vollmerhaus, P. J., Swiezewska, E., Brunner, L., Walker, S., Heck, A. J. R., and de Kruijff, B., (2003). Lipid II Is an Intrinsic Component of the Pore Induced by Nisin in Bacterial Membranes. *The Journal of Biological Chemistry* **278** (22): 19898–18903.

Brown, D. G., Lister, T., and May-Dracka, T. L., (2014). New Natural Products as New Leads for Antibacterial Drug Discovery. *Bioorganic & Medicinal Chemistry Letters* **24** (2). 413–418.

Brown, S., Santa Maria Jr. J. P., and Walker, S., (2013). Wall Teichoic Acids of Gram-Positive Bacteria. *Annual Review of Microbiology* **67** (1): 313–336.

Brundish, D. E., Shaw, N., and Baddiley, J., (1967). The Phospholipids of *Pneumococcus* I-192r, A.T.C.C. 12213. *Biochemistry Journal* **104**: 205–212.

Bugg, T. D. H., (1999). Bacterial Peptidoglycan Biosynthesis and Its Inhibition. In *Comprehensive Natural Products Chemistry*, 1st edn, vol 3, pp. 241-294. Edited by M G Pinho, Oxford: Elsevier Science Ltd.

Bugg, T. D. H., Braddick, D., Dowson,, C. G., and Roper, D. I., (2011). Bacterial Cell Wall Assembly: Still an Attractive Antibacterial Target. *Trends in Biotechnology* **29** (4): 167–173.

Bui, N. K., Eberhardt, A., Vollmer, D., Kern, T., Bougault, C., Tomasz, A., Simorre, J-P., and Vollmer, W., (2012). Isolation and analysis of cell wall components from *Streptococcus pneumoniae*. *Analytical Biochemistry* **421** (2): 657–666.

Bury, D., Dahmane, I., Derouaux, A., Dumbre, S., Herdewijn, P., Matagne, A., Breukink, E., Mueller-Seitz, E., Petz, M., and Terrak, M., (2015). Positive Cooperativity Between Acceptor and Donor Sites of the Peptidoglycan Glycosyltransferase. *Biochemical Pharmacology* **93** (2): 141–150.

Butaye, P, Devriese, L. A., and Haesebrouck. F., (2003). Antimicrobial Growth Promoters Used in Animal Feed: Effects of Less Well Known Antibiotics on Gram-Positive Bacteria. *Clinical Microbiology Reviews* **16** (2): 175–188.

Cabeen, M. T., and Jacobs-Wagner, C., (2005). Bacterial Cell Shape. *Nature Reviews Microbiology* **3** (8): 601–610.

Cadby, I. T., and Lovering, A. L., (2014). Molecular Surveillance of the Subtle Septum: Discovering a New Mode of Peptidoglycan Synthesis in Streptococci. *Molecular Microbiology* **94** (1): 1–4

Carpino, L. A., and Wu, A. C., (2000). Solubilizing Influence of 2,7-Bis(Trimethylsilyl) Substitution on the Fmoc Residue *The Journal of Organic Chemistry* **65** (26): 9238–9240.

Chambers, H. F., (2001). The Changing Epidemiology of *Staphylococcus aureus*?. *Emerging Infectious Diseases* **7** (2): 178–182.

Champoux, J. J., (2001). DNA Topoisomerases: Structure, Function, and Mechanism. *Annu. Rev. Biochem.* **70**: 369–413.

Charpentier, X., Chalut, C., Rémy, M. H., and Masson, J. M., (2002). Penicillin-Binding Proteins 1a and 1b Form Independent Dimers in *Escherichia coli. Journal of Bacteriology* **184** (13): 3749–3752.

Chatterjee, C., Paul, M., Xie, L., and van der Donk, W F., (2005). Biosynthesis and Mode of Action of Lantibiotics. *Chemical Reviews* **105** (2): 633–684.

Cheng, T-J. R., Sung, M-T., Liao, H-Y., Chang, Y-F., Chen, C-W., Huang, C-Y., Chou, L-Y., Wu, Y. D., Chen, Y. H., Cheng, Y. S., Wong, C. H., Ma, C., Cheng, W. C., (2008). Domain Requirements of Moenomycin Binding to Bifunctional Transglycosylases and Development of High-Throughput Discovery of Antibiotics. *Proc Natl Acad Sci USA* **105** (2): 431–436.

Chesnel, L., Pernot, L., Lemaire, D., Champelovier, D., Croizé, J., Dideberg, O., Vernet, T., and Zapun, A., (2003). The Structural Modifications Induced by the M339F Substitution in PBP2x From *Streptococcus pneumoniae* Further Decreases the Susceptibility to β-Lactams of Resistant Strains. *The Journal of Biological Chemistry* **278** (45): 44448–44456.

Chesnel, L., Carapito, R., Croizé, J., Dideberg, O., Vernet, T., and Zapun, A., (2005). Identical Penicillin-Binding Domains in Penicillin-Binding Proteins of *Streptococcus pneumoniae* Clinical Isolates with Different Levels of β-Lactam Resistance. *Antimicrobial Agents and Chemotherapy* **49** (7): 2895–2902.

Chopra, I., (1998). Research and Development of Antibacterial Agents. *Current Opinion in Microbiology* **1**: 495–501.

Clarke, T. B. (2008). The Biochemistry of the Latter Stages of Peptidoglycan Biosynthesis and Modification. Unpublished Ph. D, University of Warwick

Clarke, T. B., Kawai, F., Park, S-Y., Tame, J. R. H., Dowson, C. G., and Roper, D. I., (2009). Mutational Analysis of the Substrate Specificity of *Escherichia coli* Penicillin Binding Protein 4 . *Biochemistry* 48 (12): 2675–2683.

Contreras-Martel, C., Dahout-Gonzalez, C., Dos Santos Martins, A., Kotnik, M., and Dessen. A., (2009). PBP Active Site Flexibility as the Key Mechanism for β-Lactam Resistance in Pneumococci. *Journal of Molecular Biology* **387** (4). 899–909.

Contreras-Martel, C., Job, V., Di Guilmi, A. M., Vernet, T., Dideberg, O., and Dessen, A., (2006). Crystal Structure of Penicillin-Binding Protein 1a (PBP1a) Reveals a Mutational Hotspot Implicated in β-Lactam Resistance in *Streptococcus pneumoniae. Journal of Molecular Biology* **355** (4): 684–696.

Centres for Disease Control and Prevention.U.S. Department of Health and Human Services: (2013). Antibiotic Resistance Threats in the United States, 2013. 1–114.

Copeland, R. A., (2000). *Enzymes*. 2nd ed. Wiley-VCH.

Cramer, P., (2002). Multisubunit RNA Polymerases. *Current Opinion in Structural Biology* **12**: 89–97.

Crisostomo, M. I., Vollmer, W., Kharat, A. R., Inhulsen, S., Gehre, F., Buckenmaier, S., and Tomasz, A., (2006). Attenuation of Penicillin Resistance in a Peptidoglycan *O*-Acetyl Transferase Mutant of *Streptococcus pneumoniae*. *Molecular Microbiology* **61** (6): 1497–1509.

Davies, J., and Davies, D., (2010). Origins and Evolution of Antibiotic Resistance. *Microbiology and Molecular Biology Reviews* **74** (3): 417–433.

Dawson, R. M. C., Elliot, D. C., Elliot, W. C., and Jones, K. M., (1986). *Data for Biochemical Research*. 3rd ed. Clarendon Press, Oxford.

De Lencastre, H., Wu, S. W., Pinho, M. G., Ludovice, A. M., Filipe, S. R., Gardete, S., Sobral, S., Gill, S., Chung, M., and Tomasz, A., (1999). Antibiotic Resistance as a Stress Response: Complete Sequencing of a Large Number of Chromosomal Loci in *Staphylococcus aureus* Strain COL That Impact on the Expression of Resistance to Methicillin." *Microbial Drug Resistance* **5** (3): 163–75.

De Pascale, G. (2007). Molecular Studies on tRNA-Dependent Ligase MurN From Penicillin-Resistant *S. Pneumoniae*. Unpublished Ph. D, University of Warwick

De Pascale, G., Lloyd, A. J., Schouten, J. A., Gilbey, A. M., Roper, D. I., Dowson, C. G., and Bugg, T. D. H., (2008). Kinetic Characterization of Lipid II-Ala:Alanyl-tRNA Ligase (MurN) From *Streptococcus pneumoniae* Using Semisynthetic Aminoacyl-Lipid II Substrates. *Journal of Biological Chemistry* **283** (50): 34571–34579.

Denome, S. A., Elf, P. K., Henderson, T. A., Nelson, D. E., and Young, K. D., (1999). *Escherichia coli* Mutants Lacking All Possible Combinations of Eight Penicillin Binding Proteins: Viability, Characteristics, and Implications for Peptidoglycan Synthesis. *Journal of Bacteriology* **181** (13): 3981–93.

Dessen, A., Mouz, N., Gordon, E., Hopkins, J., and Dideberg, O., (2001). Crystal Structure of PBP2x From a Highly Penicillin-Resistant *Streptococcus pneumoniae* Clinical Isolate. *Journal of Biological Chemistry* **276** (48): 45106–45112.

Deurenberg, R. H., and Stobberingh, E. E., (2008). The Evolution of *Staphylococcus aureus*. *Infection, Genetics and Evolution* **8** (6): 747–763.

Di Guilmi, A. M., Dessen, A., Dideberg, O., and Vernet, T., (2003). Functional Characterization of Penicillin-Binding Protein 1b From *Streptococcus pneumoniae*. *Journal of Bacteriology* **185** (5): 1650–58.

Di Guilmi, A. M., Mouz, N., Martin, L., Hoskins, J., Jaskunas, S. R., Dideberg, O., and Vernet, T., (1999). Glycosyltransferase Domain of Penicillin-Binding Protein 2a

From *Streptococcus pneumoniae* Is Membrane Associated. *Journal of Bacteriology* **181** (9): 2773–2781.

Dias, R., Félix, D., Caniça, M., and Trombe, M-C., (2009). The Highly Conserved Serine Threonine Kinase *StkP* of *Streptococcus pneumoniae* Contributes to Penicillin Susceptibility Independently From Genes Encoding Penicillin-Binding Proteins. *BMC Microbiology* **9** (1): 121–129.

Di Berardino, M., Dijkstra, A., Stuber, D., Keck, W., and Gubler, M., (1996). The Monofunctional Glycosyltransferase of *Escherichia coli* Is a Member of a New Class of Peptidoglycan-Synthesising Enzymes. *FEBS Letters* **392**: 184–188.

Domínguez-Escobar, J., Chastanet, A., Crevenna, A., Fromion, V., Wedlich-Söldner, R., and Carballido-López, R., (2011). Processive Movement of MreB-Associated Cell Wall Biosynthetic Complexes in Bacteria. *Science* **333**: 225–229.

Dramsi, S., Magnet, S., Davison, S., and Arthur, M., (2008). Covalent Attachment of Proteins to Peptidoglycan. *FEMS Microbiology Reviews* **32** (2): 307–320.

Drlica, K., Malik, M., Kerns, R. J., and Zhao, X., (2008). Quinolone-Mediated Bacterial Death. *Antimicrobial Agents and Chemotherapy* **52** (2): 385–392.

Egan, A. J. F., Biboy, J., van't Veer, I., Breukink, E., Vollmer, W., (2015). Activities and regulation of peptidoglycan synthases. *Phil. Trans. R. Soc*. **370:** 20150031

Epand, R. M., and Epand. R. F., (2009). Lipid Domains in Bacterial Membranes and the Action of Antimicrobial Agents. *BBA - Biomembranes* **1788** (1): 289–294.

Errington, J, R., Daniel, A., and Scheffers, D. J., (2003). Cytokinesis in Bacteria. *Microbiology and Molecular Biology Reviews* **67** (1): 52–65.

Evtushenko, L. I., Dorofeeva, L. V., Krausova, V. I., Gavrish, E. Y., Yashina, S. G., and Takeuchi, M., (2002). *Okibacterium Fritillariae* Gen. Nov., Sp. Nov., a Novel Genus of the Family *Microbacteriaceae*. *Internation Journal of Systematic and Evolutionary Microbiology* **52** (3): 987–993.

Farha, M. A., Leung, A., Sewell, E. W., D'Elia, M. A., Allison, S. E., Ejim, L., Pereira, P. M., Pinho, M. G., Wright, G. D., and Brown, E. D., (2013). Inhibition of WTA Synthesis Blocks the Cooperative Action of PBPs and Sensitizes MRSA to β-Lactams. *ACS Chemical Biology* **8** (1): 226–233.

Fernández, L., and Hancock, R. E. W., (2012). Adaptive and Mutational Resistance: Role of Porins and Efflux Pumps in Drug Resistance. *Clinical Microbiology Reviews* **25** (4): 661–681.

Figueiredo, T. A., Sobral, R. G., Ludovice, A. M., Feio de Almeida, J. M., Bui, N. K., Vollmer, W., De Lencastre, H., and Tomasz, A., (2012). Identification of Genetic

Determinants and Enzymes Involved with the Amidation of Glutamic Acid Residues in the Peptidoglycan of *Staphylococcus aureus*. *PLoS Pathogens* **8** (1): 1–13.

Filipe, S. R., Pinho, M. G., and Tomasz, A., (2000). Characterization of the *murMN* Operon Involved in the Synthesis of Branched Peptidoglycan Peptides in *Streptococcus pneumoniae*. *Journal of Biological Chemistry* **275** (36): 27768–27774.

Filipe, S. R.,, and Tomasz, A., (2000). Inhibition of the Expression of Penicillin Resistance in *Streptococcus pneumoniae* By Inactivation of Cell Wall Muropeptide Branching Genes. *Proc Natl Acad Sci USA* **97** (9): 4891–4896.

Fiser, A., Filipe, S. R., and Tomasz, A., (2003). Cell Wall Branches, Penicillin Resistance and the Secrets of the MurM Protein. *Trends in Microbiology* **11** (12): 547–53.

Fishovitz, J., Taghizadeh, N., Fisher, J. F., Chang, M., and Mobashery. S., (2015). The Tipper–Strominger Hypothesis and Triggering of Allostery in Penicillin-Binding Protein 2a of Methicillin-Resistant *Staphylococcus aureus* (Mrsa). *Journal of the American Chemical Society* **137** (20): 6500–6505.

Fleming, A., (1929). On the Antibacterial Action of Cultures of a Penicillium with Special Reference to Their Use in the Isolation of *B. influenzae*. *The British Journal of Experimental Pathology* **10**: 226–236.

Fleurie, A., Manuse, S., Zhao, C., Campo, N., Cluzel, C., Lavergne, J-P., Freton, C., Combet, C., Guiral, S., Soufi, B., Macek, B., Kuru, E., VanNieuwenhze, M. S., Brun, Y. V. Di Guilmi, A-M., Claverys, J-P., Galinier, A., Grangeasse, C., (2014) Interplay of the Serine/Threonine-Kinase StkP and the Paralogs DivIVA and GpsB in Pneumococcal Cell Elongation and Division. *PLoS Genetics*. **10**: e1004274

Floss, H. G., and Yu, T-W., (2005). Rifamycin-Mode of Action, Resistance, and Biosynthesis. *Chemical Reviews* **105** (2): 621–632.

Fonzé, E., Vermeire, M., Nguyen-Distèche, M., Brasseur, R., and Charlier, P., (1999). The Crystal Structure of a Penicilloyl-Serine Transferase of Intermediate Penicillin Sensitivity. *The Journal of Biological Chemistry* **274** (31): 21853–21860.

Frère, J-M , Duez, C., and Ghuysen, J-M., (1976). Occurrence of a Serine Residue in the Penicillin-Binding Site of the Exocellular DD-Carboxy-Peptidase-Transpeptidase From *Streptomyces* R61. *FEBS Letters* **70** (1): 257–261.

Fuda, C., Hesek, D., Lee, M., Morio, K-I., Nowak, T., and Mobashery, S., (2005). Activation for Catalysis of Penicillin-Binding Protein 2a From Methicillin-Resistant *Staphylococcus aureus* By Bacterial Cell Wall. *Journal of the American Chemical Society* **127** (7): 2056–5207.

Galley, N. F., O'Reilly, A. M., and Roper. D. I., (2014). Prospects for novel inhibitors of peptidoglycan transglycosylases. *Bioorganic Chemistry* **55:** 16-26.

Gally, D., and Archibald, A. R., (1993). Cell Wall Assembly in *Staphylococcus aureus*: Proposed Absence of Secondary Crosslinking Reactions. *Journal of General Microbiology* **139**:1907–1913.

Gampe, C. M., Tsukamoto, H., Doud, E. H., Walker, S., and Kahne, D., (2013). Tuning the Moenomycin Pharmacophore to Enable Discovery of Bacterial Cell Wall Synthesis Inhibitors. *Journal of the American Chemical Society* **135** (10): 3776–3779.

Garcia-Bustos, J., and Tomasz, A., (1990). A Biological Price of Antibiotic Resistance: Major Changes in the Peptidoglycan Structure of Penicillin-Resistant Pneumococci. *Proc Natl Acad Sci USA* **87**: 5415–5419.

Gardner, A. D., (1940). Morphological Effects of Penicillin on Bacteria. *Nature* **146**: 837–838.

Garner, E. C., Bernard, R., Wang, W., Zhuang, X., Rudner, D., and Mitchison, T., (2011). Coupled, Circumferential Motions of the Cell Wall Synthesis Machinery and MreB Filaments in *B. subtilis*. *Science* **333**: 222–226.

Ghuysen, J-M., (1991). Serine β-Lactamases and Penicillin-Binding Proteins. *Annual Review of Microbiology* **45**: 37–67.

Ghuysen, J-M, Bricas, E., Lache, M., and Leyh-Bouille, M., (1968). Structure of the Cell Walls of *Micrococcus lysodeikticus*. *Biochemistry* **1445** (5): 1450–1460.

Glauner, B., (1988). Separation and Quantification of Muropeptides with High-Performance Liquid Chromatography. *Analytical Biochemistry* **172**: 451–464.

Goffin, C., and Ghuysen. J-M., (1998). Multimodular Penicillin-Binding Proteins: an Enigmatic Family of Orthologs and Paralogs. *Microbiology and Molecular Biology Reviews* **62** (4): 1079–1095.

Gordon, E., Mouz, N., Duée, E., Dideberg, O., (2000). The crystal structure of the penicillin-binding protein 2x from *Streptococcus pneumoniae* and its acyl-enzyme form: implication in drug resistance. *J. Mol Biol.* **299**: 477-485

Gram, H., (1884). Über Die Isolierte Färbung Der Schizomyceten in Schnitt- Nd Trockenpräparaten. *Fortschritte Der Medizin* **2**: 185–189.

Granizo, J. J., Aguilar, L., Casal, J., García-Rey, C., Dal-Ré, R., and Baquero, F., (2000). *Streptococcus pneumoniae* Resistance to Erythromycin and Penicillin in Relation to Macrolide and β-Lactam Consumption in Spain (1979-1997). *Journal of Antimicrobial Chemotherapy* **46**: 767–773.

Grant, S.G., Jessee, J., Bloom, F. R., and Hanahan, D., (1990). Differential Plasmid Rescue From Transgenic Mouse DNAs Into *Escherichia coli* Methylation-Restriction Mutants. *Proc Natl Acad Sci USA* **87**: 4645–4469.

Grebe, T., and Hakenbeck, R., (1996). Penicillin-Binding Proteins 2b and 2x of *Streptococcus pneumoniae* Are Primary Resistance Determinants for Different Classes of β-Lactam Antibiotics. *Antimicrobial Agents and Chemotherapy* **40** (4): 829–834.

Ha, S., Chang, E., Lo, M-C., Men, H., Park, P., Ge, M., and Walker, S., (1999). The Kinetic Characterization of *Escherichia coli* MurG Using Synthetic Substrate Analogues. *Journal of the American Chemical Society* **121** (37): 8415–8426.

Hakenbeck, R., Brückner, R., Denapaite, D., and Maurer, P., (2012). Molecular Mechanisms of β-Lactam Resistance in *Streptococcus pneumoniae. Future Microbiology* **7** (3): 395–410.

Halliday, J., McKeveney, D., Muldoon, C., Rajaratnam, P., and Meutermans, W., (2006). Targeting the Forgotten Transglycosylases. *Biochemical Pharmacology* **71** (7): 957–967.

Hartman, B. J., and Tomasz, A., (1984). Low-Affinity Penicillin-Binding Proteins Associated with β-Lactam Resistance in *Staphylococcus aureus. Journal of Bacteriology* **158** (2): 513–516.

Harwell, J. I, and Brown, R. B., (2000). The Drug-Resistant Pneumococcus. *Chest* **117** (2): 530–541.

Hasper, H. E., Kramer, N. E., Smith, J. L., Hillman, J. D., Zachariah, C., Kuipers, O. P., de Kruijff, B., and Breukink, E., (2006). An Alternative Bacteriocidal Mechanism of Action for Lantibiotic Peptides That Target Lipid II. *Science* **313** (5793): 1632–1636.

Healy, V. L., Lessard, I. A. D., Roper, D. I., Knox, J., and Walsh, C., (2000). Vancomycin Resistance in Enterococci: Reprogramming of the D-Ala-D-Ala Ligases in Bacterial Peptidoglycan Biosynthesis. *Chemistry & Biology* **7** (5): 109–119.

Heaslet, H., Shaw, B., Mistry, A., and Miller, A. A., (2009). Characterization of the Active Site of *S. aureus* Monofunctional Glycosyltransferase (Mtg) by Site-Directed Mutation and Structural Analysis of the Protein Complexed with Moenomycin. *Journal of Structural Biology* **167** (2): 129–135.

Hegde, S. S., and Blanchard, J. S., (2003). Kinetic and Mechanistic Characterization of Recombinant *Lactobacillus viridescens* FemX (UDP-*N*-Acetylmuramoyl Pentapeptide-Lysine N^6-Alanyltransferase) *The Journal of Biological Chemistry* **278** (25): 22861–22867.

Helassa, N., Vollmer, W., Breukink, E., Vernet, T., and Zapun, A., (2012). The Membrane Anchor of Penicillin-Binding Protein PBP2a From *Streptococcus pneumoniae* Influences Peptidoglycan Chain Length. *FEBS Journal* **279** (11): 2071–2081.

Henrichsen, J., (1995). Six Newly Recognized Types of *Streptococcus pneumoniae. European Journal of Clinical Microbiology & Infectious Diseases* **33** (10): 2759–2762.

Henriques-Normark, B., (2007). Molecular Epidemiology and Mechanisms for Antibiotic Resistance in *Streptococcus pneumoniae* In *Molecular Biology of Streptococci*, 1st Edn, pp:269-290, Edited by Hakenbeck, R., and Chhatwal, S.

Hiramatsu, K., Hanaki, H., Ino, T., Yabuta, K., Oguri, T., and Tenover, F. C., (1997). Methicillin-Resistant *Staphylococcus aureus* Clinical Strain with Reduced Vancomycin Susceptibility. *Journal of Antimicrobial Chemotherapy* **40**: 135–146.

Hoskins, JA., Matsushima, P., Mullen, D. L., Tang, J., Zhao, G., Meier, T. I., Nicas, T. I., and Jaskunas, R. S., (1999). Gene Disruption Studies of Penicillin-Binding Proteins 1a, 1b, and 2a in *Streptococcus pneumoniae. Journal of Bacteriology* **181** (20): 6552–6555.

Howden, B. P., Davies, J. K., Johnson, P. D. R., Stinear, T. P., and Grayson, M. L., (2010). Reduced Vancomycin Susceptibility in *Staphylococcus aureus*, Including Vancomycin-Intermediate and Heterogeneous Vancomycin-Intermediate Strains: Resistance Mechanisms, Laboratory Detection, and Clinical Implications. *Clinical Microbiology Reviews* **23** (1): 99–139.

Höltje, J-V., (1998). Growth of the Stress-Bearing and Shape-Maintaining Murein Sacculus of *Escherichia coli. Microbiology and Molecular Biology Reviews* **62** (1): 181–205.

Höltje, J-V, and Tuomanen. E., (1991). The Murein Hydrolases of *Escherichia coli*: Properties, Functions and Impact on the Course of Infections *In Vivo. Journal of General Microbiology* **137**: 441–454.

Huang, C-Y., Shih, H-W., Lin, L-Y., Tien, Y-W., Cheng, T-J. R., Cheng, W-C., Wong, C-H., and Ma, Che., (2012). Crystal Structure of *Staphylococcus aureus* Transglycosylase in Complex with a Lipid II Analog and Elucidation of Peptidoglycan Synthesis Mechanism. *Proc Natl Acad Sci USA* **109** (17): 6496–6501.

Hughes, R. C., (1971). Autolysis of *Bacillus cereus* Cell Walls and Isolation of Structural Components. *Biochemistry Journal* **121**: 791–802.

Jackson, M. A., and Strominger, J., (1984). Synthesis of Peptidoglycan by High Molecular Weight Penicillin-Binding Proteins of *Bacillus subtilis* And *Bacillus stearothermophilus. The Journal of Biological Chemistry* **259**: 1483–1490.

Jamin, M., Damblon, C., Millier, S., Hakenbeck, R., and Frère, J. M., (1993). Penicillin-Binding Protein 2x of *Streptococcus pneumoniae*: Enzymic Activities and Interactions with β-Lactams. *Biochemistry Journal* **292**: 735–741.

Jamshad, M., Lin, Y-P, Knowles, T. J., Parslow, R. A., Harris, C., Wheatley, M., Poyner, D. R., Bill, R. M., Thomas, O. R., Overduin, M., Dafforn, T. R., (2011). Surfactant-Free Purification of Membrane Proteins with Intact Native Membrane Environment. *Biochemical Soc Trans* **39** (3): 813–818.

Jerabek-Willemsen, M., Wienken, C. J., Braun, D., Baaske, P., and Duhr, S., (2011). Molecular Interaction Studies Using Microscale Thermophoresis. *Assay Drug Development Technology* **9**: 342–343.

Jevons, M. P., (1961). 'Celbenin'-Resistant Staphylococci. *British Medical Journal* **1**: 124–125.

Job, V., Carapito, R., Vernet, T., Dessen, A., and Zapun, A., (2008). Common Alterations in PBP1a From Resistant *Streptococcus pneumoniae* Decrease Its Reactivity Toward Beta-Lactams: Structural Insights.. *The Journal of Biological Chemistry* **283** (8): 4886–4894.

Johnson, A. P., Davies, J., Guy, R., Abernethy, J., Sheridan, E., Pearson, A., and Duckworth, G., (2012). Mandatory Surveillance of Methicillin-Resistant *Staphylococcus aureus* (MRSA) Bacteraemia in England: the First 10 Years. *Journal of Antimicrobial Chemotherapy* **67** (4): 802–809.

Johnson, A. P., Uttley, A. H. C., Woodford, N., and George, R. C., (1990). Resistance to Vancomycin and Teicoplanin: an Emerging Clinical Problem. *Clinical Microbiology Reviews* **3** (3): 280–291.

Josephine, H. R., Charlier, P., Davies, C., Nicholas, R. A., and Pratt, R. F., (2006). Reactivity of Penicillin-Binding Proteins with Peptidoglycan-Mimetic β-Lactams: What's Wrong with These Enzymes? *Biochemistry* **45** (51): 15873–15883.

Kahne, D., Leimkuhler, C., Lu, W., and Walsh, C., (2005). Glycopeptide and Lipoglycopeptide Antibiotics. *Chemical Reviews* **105** (2): 425–448.

Kell, C. M., Sharma, U. K., Dowson, C. G., Town, C., Balganesh, T. S., and Spratt, B. G., (1993). Deletion Analysis of the Essentiality of Penicillin-Binding Proteins 1A, 2B and 2X of *Streptococcus pneumoniae*. *FEMS Microbiology Letters* **106**: 171–176.

Kislliuk, R. L., (1981). Pteroylpolyglutamates. *Molecular and Cellular Biochemistry* **39** (1): 331–345.

Knowles, T. J., Finka, R., Smith, C., Lin, Y-P., Dafforn, T. R., and Overduin, M., (2009). Membrane Proteins Solubilized Intact in Lipid Containing Nanoparticles Bounded by Styrene Maleic Acid Copolymer. *Journal of the American Chemical Society*

131 (22): 7484–7485.

Kohanski, M. A., Dwyer, D. J., and Collins, J. C., (2010). How Antibiotics Kill Bacteria: From Targets to Networks. *Nature Reviews Microbiology* **8** (6): 423–435.

Kozarich, J.W., Strominger, J,L., (1978) A membrane enzyme from *Staphylococcus aureus* which catalyzes transpeptidase, carboxypeptidase, and penicillinase activities. *J Biol Chem.* **253** (4):1272-1280

Kuefner, U., Esswein, A., Lohrmann, U., Montejano, Y., Vitols, K. S., and Huennekens, F. M., (1990). Occurrence and Significance of Diastereomers of Methotrexate A-Peptides. *Biochemistry* **29**: 10540–10545.

Kuru, E., Hughes, H. V., Brown, P. J., Hall, E., Tekkam, S., Cava, F., de Pedro, M. A., Brun, Y. V., and VanNieuwenhze, M. S., (2012). In Situ Probing of Newly Synthesized Peptidoglycan in Live Bacteria with Fluorescent D-Amino Acids. *Angew. Chem. Int. Ed.* **51** (50): 12519–12523.

Laemmli, U. K., (1970). Cleavage of Structural Proteins During the Assembly of the Head of Bacteriophage T4. *Nature* **227**: 680–685.

Lambert, P. A., (2002). Mechanisms of Antibiotic Resistance in *Pseudomonas aeruginosa. Journal of the Royal Society of Medicine* **95**: 22–26.

Land, A. D., and Winkler, M. E., (2011). The Requirement for Pneumococcal MreC and MreD Is Relieved by Inactivation of the Gene Encoding PBP1a. *Journal of Bacteriology* **193** (16): 4166–4179.

Lavollay, M., Arthur, M., Fourgeaud, M., Dubost, L., Marie, A., Veziris, N., Blanot, D., Gutmann, L., and Mainardi, J-L., (2008). The Peptidoglycan of Stationary-Phase *Mycobacterium tuberculosis* Predominantly Contains Cross-Links Generated by L,D-Transpeptidation. *Journal of Bacteriology* **190** (12): 4360–4366.

Lazar, K., and Walker, S., (2002). Substrate Analogues to Study Cell-Wall Biosynthesis and Its Inhibition. *Current Opinion in Chemical Biology* **6**: 786–793.

Lebar, M. D., Lupoli, T. J., Tsukamoto, H., May, J. M., Walker, S., and Kahne, D., (2013). Forming Cross-Linked Peptidoglycan From Synthetic Gram-Negative Lipid II. *Journal of the American Chemical Society* **135** (12): 4632–4635.

Leski, T. A., and Tomasz, A., (2005). Role of Penicillin-Binding Protein 2 (PBP2) in the Antibiotic Susceptibility and Cell Wall Cross-Linking of *Staphylococcus aureus*: Evidence for the Cooperative Functioning of PBP2, PBP4, and PBP2A. *Journal of Bacteriology* **187** (5): 1815–1824.

Lesse, A. J., Campagnari, A. A., Bittner, W., and Apicella, M., (1990). Increased Resolution of Lipopolysaccharides and Lipooligosaccharides Utilizing Tricine-Sodium

Dodecyl Sulfate-Polyacrylamide Gel Electrophoresis. *Journal of Immunological Methods* **126**: 109–117.

Levy, S. B., and Marshall, B., (2004). Antibacterial Resistance Worldwide: Causes, Challenges and Responses. *Nature Medicine* **10** (12s): S122–129.

Li, W. J., Chen, H-H., Kim, C-J., Park, D-J., Tang, S-K., Lee, J-C., Xu, L., and Jiang, C-L., (2005). *Microbacterium halotolerans* Sp. Nov., Isolated From a Saline Soil in the West of China. *Internation Journal of Systematic and Evolutionary Microbiology* **55** (1): 67–70.

Lim, D., and Strynadka, N., (2002). Structural basis for the β-lactam resistance of PBP2a from methicillin-resistant *Staphylococcus aureus*. Nature Structural Biology **9**: 870-876

Ling, B., and Berger-Bächi, B., (1998). Increased Overall Antibiotic Susceptibility in *Staphylococcus aureus femAB* Null Mutants. *Antimicrobial Agents and Chemotherapy* **42**: 936–938.

Ling, L. L., Schneider, T., Peoples, A. J., Spoering, A. L., Engels, I., Conlon, B. P., Mueller, A., *et al.*, (2015). A New Antibiotic Kills Pathogens Without Detectable Resistance. *Nature* **517**: 455–474.

Linnett, P. E., and Strominger, J., (1974). Amidation and Cross-Linking of the Enzymatically Synthesized Peptidoglycan of *Bacillus stearothermophilus*. *The Journal of Biological Chemistry* **249** (8): 2489–2496.

Liu, C-Y., Guo, C-W., Chang, Y-F., Wang, J-T., Shih, H-W., Hsu, Y. F., Chen, W., Chen, S-H., Wang, Y-C., Cheng, T-J., Ma, C., Wong, C-H., Fang, J-M., Cheng, W C., (2010). Synthesis and Evaluation of a New Fluorescent Transglycosylase Substrate: Lipid II-Based Molecule Possessing a Dansyl-C20 Polyprenyl Moiety. *Organic Letters* **12** (7): 1608–1611.

Liu, H., Ritter, T. K., Sadamoto, R., Sears, P. S., Wu, M., and Wong., C-H., (2003). Acceptor Specificity and Inhibition of the Bacterial Cell-Wall Glycosyltransferase MurG. *ChemBioChem* **4** (7): 603–609.

Liu, H., and Wong, C-H., (2006). Characterization of a Transglycosylase Domain of *Streptococcus pneumoniae* PBP1b." *Bioorganic & Medicinal Chemistry* **14** (21): 7187–7195.

Lloyd, A. J., Brandish, P. E., Gilbey, A. M., and Bugg, T. D. H., (2004). Phospho-*N*-Acetyl-Muramyl-Pentapeptide Translocase From *Escherichia coli:* Catalytic Role of Conserved Aspartic Acid Residues. *Journal of Bacteriology* **186** (6): 1747–1757.

Lloyd, A. J., Gilbey, A. M., Blewett, A. M., De Pascale, G., El Zoeiby, A., Levesque, R. C., Catherwood, A. C., Tomasz, A., Bugg, T. D. H., Roper, D. I., Dowson, C. G.,

(2008). Characterization of tRNA-Dependent Peptide Bond Formation by MurM in the Synthesis of *Streptococcus pneumoniae* Peptidoglycan. *The Journal of Biological Chemistry* **283** (10): 6402–6417.

Lovering, A. L., de Castro, L. H., Lim, D., and Strynadka, N. C. J., (2007). Structural Insight Into the Transglycosylation Step of Bacterial Cell-Wall Biosynthesis. *Science* **315** (5817): 1402–1405.

Lovering, A. L., Gretes, M. C., Safadi, S. S., Danel, F., de Castro, L., Page, M. G. P., and Strynadka, N. C. J., (2012). Structural Insights Into the Anti-Methicillin-Resistant *Staphylococcus aureus* (MRSA) Activity of Ceftobiprole. *The Journal of Biological Chemistry* **287** (38): 32096–32102.

Lovering, A. L., De Castro, L., and Strynadka, N. C. J., (2008). Identification of Dynamic Structural Motifs Involved in Peptidoglycan Glycosyltransfer. *Journal of Molecular Biology* **383** (1): 167–177.

Lovering, A. L., Gretes, M., and Strynadka, N. C. J., (2008a). Structural Details of the Glycosyltransferase Step of Peptidoglycan Assembly. *Current Opinion in Structural Biology* **18** (5): 534–543.

Lovering, A. L., Safadi, S. S., and Strynadka, N. C. J., (2012a). Structural Perspective of Peptidoglycan Biosynthesis and Assembly. *Annu. Rev. Biochem.* **81** (1): 451–478.

Lupoli, T. J., Tsukamoto, H., Doud, E. H., Wang, T-S. A., Walker, S., and Kahne, D., (2011). Transpeptidase-Mediated Incorporation of D-Amino Acids Into Bacterial Peptidoglycan. *Journal of the American Chemical Society* **133** (28): 10748–10751.

Lupoli, T. J., Lebar, M. D., Markovski, M., Bernhardt, T., Kahne, D., and Walker, S., (2014). Lipoprotein Activators Stimulate *Escherichia coli* Penicillin-Binding Proteins by Different Mechanisms. *Journal of the American Chemical Society* **136** (1): 52–55.

Lupoli, T. J., Taniguchi, T., Wang, T-S., Perlstein, D. L., Walker, S., and Kahne, D. E., (2009). Studying a Cell Division Amidase Using Defined Peptidoglycan Substrates. *Journal of the American Chemical Society* **131** (51): 18230–18231.

Macheboeuf, P., Di Guilmi, A. M., Job, V., Vernet, T., Dideberg, O., and Dessen, A., (2005). Active Site Restructuring Regulates Ligand Recognition in Class A Penicillin-Binding Proteins. *Proc. Natl. Acad. Sci. USA* **102** (3): 577–582.

Macheboeuf, P., Contreras-Martel, C., Job, V., Dideberg, O., and Dessen, A., (2006). Penicillin Binding Proteins: Key Players in Bacterial Cell Cycle and Drug Resistance Processes. *FEMS Microbiology Reviews* **30** (5): 673–691.

Manat, G., Roure, S., Auger, R., Bouhss, A., Barreteau, H., Mengin-Lecreulx, D., and Touzé, T., (2014). Deciphering the Metabolism of Undecaprenyl-Phosphate: the Bacterial Cell-Wall Unit Carrier at the Membrane Frontier. *Microbial Drug Resistance*

20 (3): 199–214.

Mangili, A., Bica, I., Snydman, D. R., and Hamer, D. R., (2005). Daptomycin-Resistant, Methicillin- Resistant *Staphylococcus aureus* Bacteremia. *Clinical Infectious Diseases* **40**: 1058–1060.

Massidda, O., Nováková, L., and Vollmer, W., (2013). From Models to Pathogens: How Much Have We Learned About *Streptococcus pneumoniae* cell Division? *Environmental Microbiology*, **15** (12): 3133-3157.

Matsumoto, A., (2003). *Longispora albida* Gen. Nov., Sp. Nov., a Novel Genus of the Family *Micromonosporaceae*. *International Journal of Systematic and Evolutionary Microbiology* **53** (5): 1553–1559.

McComas, C. C., Crowley, B. M., and Boger, D. L., (2003). Partitioning the Loss in Vancomycin Binding Affinity for D-Ala-D-Lac Into Lost H-Bond and Repulsive Lone Pair Contributions. *Journal of the American Chemical Society* **125** (31): 9314–9315.

Memmi, G., Filipe, S. R., Pinho, M. G., Fu, Z., and Cheung, A. (2008). *Staphylococcus aureus* PBP4 Is Essential for β-Lactam Resistance in Community-Acquired Methicillin-Resistant Strains. *Antimicrobial Agents and Chemotherapy* **52** (11): 3955–3966.

Mirelman, D., Bracha, R., and Sharon, N., (1972). Role of the Penicillin-Sensitive Transpeptidation Reaction in Attachment of Newly Synthesized Peptidoglycan to Cell Walls of *Micrococcus luteus*. *Proc Natl Acad Sci USA* **69** (11): 3355–3359.

Mohammadi, T., Sijbrandi, R., Lutters, M., Verheul, J., Martin, N. I., den Blaauwen, T., de Kruijff, B., and Breukink, E. (2014). Specificity of the Transport of Lipid II by FtsW in *Escherichia coli*. *The Journal of Biological Chemistry* **289** (21): 14707–14718.

Mohammadi, T., van Dam, V., Sijbrandi, R., Vernet, T., Zapun, A., Bouhss, A., de Bruin, M. D., Nguyen-Distèche, M., de Kruijff, B., and Breukink, E., (2011). Identification of FtsW as a Transporter of Lipid-Linked Cell Wall Precursors Across the Membrane. *The EMBO Journal* 30: 1425–1432.

Morlot, C., Pernot, l., Le Gouellec, A., Di Guilmi, A. M., Vernet, T., Dideberg, O., and Dessen, A., (2005). Crystal Structure of a Peptidoglycan Synthesis Regulatory Factor (PBP3) From *Streptococcus pneumoniae. The Journal of Biological Chemistry* **280** (16):15984–15991.

Morlot, C., Noirclerc-Savoye, M., Zapun, A., Dideberg, O., and Vernet, T., (2004). The D,D-Carboxypeptidase PBP3 Organizes the Division Process of *Streptococcus pneumoniae*. *Molecular Microbiology* **51** (6): 1641–1648.

Morlot, C., Zapun, A., Dideberg., Vernet, T., (2003) Growth and division of *Streptococcus pneumoniae*: localization of the high molecular weight penicillin-binding proteins during the cell cycle. *Molecular Microbiology* **50** (3): 845-855

Münch, D., Roemer, T., Lee, S. H., Engeser, M., Sahl, H-G., and Schneider, T., (2012). Identification and *In Vitro* Analysis of the GatD/MurT Enzyme-Complex Catalyzing Lipid II Amidation in *Staphylococcus aureus*. *PLoS Pathogens* **8** (1): 1–11.

Nakagawa, J-I., Tamaki, S., Tomioka, S., and Matsuhashi, M., (1984). Functional Biosynthesis of Cell Wall Peptidoglycan by Polymorphic Bifunctional Polypeptides. *The Journal of Biological Chemistry* **259**: 13937–13946.

Nakel, M., Ghuysen, J-M., and Kandler, O., (1971). Wall Peptidoglycan in *Aerococcus viridans* Strains 201 Evans and ATCC 11563 and in *Gaffkya homari* Strain ATCC 10400. *Biochemistry* **10** (11): 2170–2176.

Nakimbugwe, D., Masschalck, B., Deckers, D., Callewaert, L., Aertsen, A., and Michiels, C. W., (2006). Cell Wall Substrate Specificity of Six Different Lysozymes and Lysozyme Inhibitory Activity of Bacterial Extracts. *FEMS Microbiology Letters* **259** (1): 41–46.

Navarre, W. W., and Schneewind, O., (1999). Surface Proteins of Gram-Positive Bacteria and Mechanisms of Their Targeting to the Cell Wall Envelope. *Microbiology and Molecular Biology Reviews* **63** (1): 174–229.

Nichols, D., Cahoon, N., Trakhtenberg, E. M., Pham, L., Mehta, A., Belanger, A., Kanigan, T., Lewis, K., and Epstein, S. S., (2010). Use of Ichip for High-Throughput *In Situ* Cultivation of 'Uncultivable' Microbial Species. *Applied and Environmental Microbiology* **76** (8): 2445–2450.

Nieto, M., and Perkins, H. R., (1971). Modifications of Acyl-D-Alanyl-D-Alanine Terminus Affecting Complex-Formation with Vancomycin. *Biochemistry Journal* **123**: 789–803.

Nissen, P., Hansen, J., Ban, N., Moore, P. B., and Steitz, T. A., (2000). The Structural Basis of Ribosome Activity in Peptide Bond Synthesis. *Science* **289**: 920–930.

Noirclerc-Savoye, M., Lantez, V., Signor, L., Philippe, J., Vernet, T., and Zapun, A., (2013). Reconstitution of Membrane Protein Complexes Involved in Pneumococcal Septal Cell Wall Assembly. *PLoS ONE* **8** (9): e75522–12.

Normark, B., and Normark, S., (2002). Evolution and Spread of Antibiotic Resistance. *Journal of Internal Medicine* **252**: 91–106.

O'Neill, J. (2015). Tackling a Global Health Crisis: Initial Steps. *Review on Antimicrobial Resistance*

O'Neill, J. (2015a). "Securing New Drugs for Future Generations: the Pipeline of Antibiotics." *Review on Antimicrobial Resistance*.

O'Riordan, K., and Lee, J. C., (2004). *Staphylococcus aureus* Capsular Polysaccharides. *Clinical Microbiology Reviews* **17** (1): 218–34.

O'Brien, K. L., Wolfson, L. J., Watt, J. P., Henkle, E., Deloria-Knoll, M., McCall, N., Lee, E., Mulholland, K., Levine, O., and Cherian, T., (2009). Burden of Disease Caused by *Streptococcus pneumoniae* in Children Younger Than 5 Years: Global Estimates. *The Lancet Infectious Diseases* **374** (9693): 893–902.

Offant, J., Terrak, M., Derouaux, A., Breukink, E., Nguyen-Distèche, M., Zapun, A., and Vernet, T., (2010). Optimization of Conditions for the Glycosyltransferase Activity of Penicillin-Binding Protein 1a From *Thermotoga maritima*. *FEBS Journal* **277** (20): 4290–4298.

Qiao, Y., Lebar, M.D., Schirner, K., Schaefer, K., Tsukamot, H., Kahne, D., Walker, S., (2014) Detection of lipid-linked peptidoglycan precursors by exploiting an unexpected transpeptidase reaction. *J Am Chem Soc* **136** (42):14678-14681.

Orwick-Rydmark, M., Lovett, J. E., Graziadei, A., Lindholm, L., Hicks, M. R., and Watts, A., (2012). Detergent-Free Incorporation of a Seven-Transmembrane Receptor Protein Into Nanosized Bilayer Lipodisq Particle for Functional and Biophysical Studies. *Nano Letters* **12** (9): 468–492.

Ostash, B., and Walker, S., (2005). Bacterial Transglycosylase Inhibitors. *Current Opinion in Chemical Biology* **9** (5): 459–466.

Ostash, B., and Walker, S., (2010). Moenomycin Family Antibiotics: Chemical Synthesis, Biosynthesis, and Biological Activity. *Natural Product Reports* **27** (11): 1594–1624.

Otero, L. H., Rojas-Altuve, A., Llarrull, L. I., Carrasco-Lopez, C., Kumarasiri, M., Lastochkin, E., Fishovitz, J., Dawley, M., Hesek, D., Johnson, J. W., Fisher, J. F., Chang, M., Mobashery, S., Hermoso, J. A., (2013). How Allosteric Control of *Staphylococcus aureus* Penicillin Binding Protein 2a Enables Methicillin Resistance and Physiological Function. *Proc Natl Acad Sci USA* **110** (42): 16808–16813.

Pagliero, E., Chesnel, L., Hopkins, J., Croizé, J., Dideberg, O., Vernet, T., and Di Guilmi, A. M., (2004). Biochemical Characterization of *Streptococcus pneumoniae* Penicillin-Binding Protein 2b and Its Implication in β-Lactam Resistance." *Antimicrobial Agents and Chemotherapy* **48** (5): 1848–1855.

Palzkill, T., (2013). Metallo-β-lactamase structure and function. *Ann. N. Y. Acad. Sci.* **1277**: 91-104

Paradis-Bleau, C., Markovski, M., Uehara, T., Lupoli, T. J., Walker, S., Kahne, D. E., and Bernhardt, T. G., (2010). Lipoprotein Cofactors Located in the Outer Membrane Activate Bacterial Cell Wall Polymerases. *Cell* **143** (7): 1110–1120.

Park, J. T., and Uehara, T., (2008). How Bacteria Consume Their Own Exoskeletons (Turnover and Recycling of Cell Wall Peptidoglycan). *Microbiology and Molecular Biology Reviews* **72** (2): 211–227.

Paton, J. C., and Morona, J. K., (2007). Pneumococcal Capsular Polysaccharides: Biosynthesis and Regulation. In *Molecular Biology of Streptococci*, 1st Edn, pp:119-140, Edited by Hakenbeck, R., and Chhatwal, S..

Paulin, S., Jamshad, M., Dafforn, T. R., Garcia-Lara, J., Foster, S. J., Galley, N. F., Roper, D. I., Rosado, H., and Taylor, P. W., (2014). Surfactant-Free Purification of Membrane Protein Complexes From Bacteria: Application to the Staphylococcal Penicillin-Binding Protein Complex PBP2/PBP2a, *Nanotechnology* **25**: 285101–285108

Pereira, S. F. F., Henriques, A. O., Pinho, M. G., de Lencastre, H., and Tomasz, A., (2007). Role of PBP1 in Cell Division of *Staphylococcus aureus*. *Journal of Bacteriology* **189** (9): 3525–3231.

Pereira, S. F. F., Henriques, A. O., Pinho, M. G., De Lencastre, H., and Tomasz, A., (2009) Evidence for a Dual Role of PBP1 in the Cell Division and Cell Separation of *Staphylococcus aureus*. *Molecular Microbiology* **72** (4): 895–904.

Perlstein, D. L., Zhang, X., Wang, T-S., Kahne, D. E., and Walker, S., (2007). The Direction of Glycan Chain Elongation by Peptidoglycan Glycosyltransferases. *Journal of the American Chemical Society* **129** (42): 12674–12675.

Pernot, L., Chesnel, L., Le Gouellec, A., Croizé, J., Vernet, T., Dideberg, O., and Dessen, A., (2004). A PBP2x From a Clinical Isolate of *Streptococcus pneumoniae* Exhibits an Alternative Mechanism for Reduction of Susceptibility to β-Lactam Antibiotics. *The Journal of Biological Chemistry* **279** (16): 16463–16470.

Peters, K., Schweizer, I., Beilharz, K., Stahlmann, C., Veening, J-W., Hakenbeck, R., and Denapaite, D., (2014). *Streptococcus pneumoniae* PBP2x Mid-Cell Localization Requires the C-Terminal PASTA Domains and Is Essential for Cell Shape Maintenance. *Molecular Microbiology* **92** (4): 733–755.

Philippe, J., Vernet, T., and Zapun, A., (2014). The Elongation of Ovococci. *Microbial Drug Resistance* **20** (3): 215–221.

Philippon, A., Labia, R., and Jacoby, G., (1989). Extended-Spectrum β-Lactamases. *Antimicrobial Agents and Chemotherapy* **33** (8): 1131–1136.

Pinho, M. G., Filipe, S. R., de Lencastre, H., and Tomasz, A., (2001). Complementation of the Essential Peptidoglycan Transpeptidase Function of Penicillin-

Binding Protein 2 (PBP2) by the Drug Resistance Protein PBP2A in *Staphylococcus aureus*. *Journal of Bacteriology* **183** (22): 6525–6531.

Pinho, M. G., and Errington, J., (2003). Dispersed Mode of *Staphylococcus aureus* Cell Wall Synthesis in the Absence of the Division Machinery. *Molecular Microbiology* **50** (3): 871–881.

Pinho, M. G., and Errington, J., (2005). Recruitment of Penicillin-Binding Protein PBP2 to the Division Site of *Staphylococcus aureus* Is Dependent on Its Transpeptidation Substrates. *Molecular Microbiology* **55** (3): 799–807.

Pinho, M. G., De Lencastre, H., and Tomasz, A., (2000). Cloning, Characterization, and Inactivation of the Gene *pbpC*, Encoding Penicillin-Binding Protein 3 of *Staphylococcus aureus*. *Journal of Bacteriology* **182** (4): 1074–1079.

Pinho, M. G., Kjos, M., and Veening, J-W., (2013). How to Get (a)Round: Mechanisms Controlling Growth and Division of Coccoid Bacteria. *Nature Reviews Microbiology* **11** (9): 601–614.

Popham, D. L., and Young, K. D., (2003). Role of Penicillin-Binding Proteins in Bacterial Cell Morphogenesis. *Current Opinion in Microbiology* **6** (6): 594–599.

Privé, G. G., (2007). Detergents for the Stabilization and Crystallization of Membrane Proteins. *Methods* **41** (4): 388–397.

Ramaswamy, S., and Musser, J. M., (1998). Molecular Genetic Basis of Antimicrobial Agent Resistance in *Mycobacterium Tuberculosis*:1998 Update. *Tubercle and Lung Disease* **79** (1): 3–29.

Rasmussen, R. V., Fowler Jr, V. G., Skov, R., and Bruun, N. E., (2011). Future Challenges and Treatment of *Staphylococcus aureus* Bacteremia with Emphasis on MRSA." *Future Microbiology* **6** (1): 43–56.

Rebets, Y., Lupoli, T., Qiao, Y., Schirner, K., Villet, R., Hooper, D., Kahne, D., and Walker, S., (2014). Moenomycin Resistance Mutations in *Staphylococcus aureus* Reduce Peptidoglycan Chain Length and Cause Aberrant Cell Division. *ACS Chemical Biology* **9** (2): 459–467.

Reed, P., Veiga, H., Jorge, A. M., Terrak, M., and Pinho, M. G., (2011). Monofunctional Transglycosylases Are Not Essential for *Staphylococcus aureus* Cell Wall Synthesis. *Journal of Bacteriology* **193** (10): 2549–2556.

Regev-Yochay, G., Raz, M., Dagan, R., Porat, N., Shainberg, B., Pinco, E., Keller, N., and Rubinstein, E., (2004). Nasopharyngeal Carriage of *Streptococcus pneumoniae* By Adults and Children in Community and Family Settings. *Clinical Infectious Diseases* **38** (5): 632–639.

Reith, J., and Mayer, C., (2011). Peptidoglycan Turnover and Recycling in Gram-Positive Bacteria. *Applied Microbiology and Biotechnology* **92** (1): 1–11.

Riska, P. F., Jacobs, W. R., and Alland, D., (2000). Molecular Determinants of Drug Resistance in Tuberculosis. *International Journal of Tubercle and Lung Disease* **4** (2): 4–10.

Ritter, T. K., and Wong, C-H., (2001). Carbohydrate-Based Antibiotics: a New Approach to Tackling the Problem of Resistance. *Angew. Chem. Int. Ed.* **40**: 3508–3533.

Rodolis, M. T., Mihalyi, A., O'Reilly, A., Slikas, J., Roper, D. I., Hancock, R. E. W., and Bugg, T. D. H., (2014). Identification of a Novel Inhibition Site in Translocase MraY Based Upon the Site of Interaction with Lysis Protein E From Bacteriophage ϕX174. *ChemBioChem* **15** (9): 1300–1308.

Rohrer, S., and Berger-Bächi, B., (2003). FemABX Peptidyl Transferases: a Link Between Branched-Chain Cell Wall Peptide Formation and β-Lactam Resistance in Gram-Positive Cocci. *Antimicrobial Agents and Chemotherapy* **47** (3): 837–846.

Ruzin, A., Singh, G., Severin, A., Yang, Y., Dushin, R. G., Sutherland, A. G., Minnick, A., Greenstein, M., May, M. K., Shlaes, D. M., Bradford, P. A., (2004). Mechanism of Action of the Mannopeptimycins, a Novel Class of Glycopeptide Antibiotics Active Against Vancomycin-Resistant Gram-Positive Bacteria. *Antimicrobial Agents and Chemotherapy* **48** (3): 728–738.

Sauvage, E., Kerff, F., Terrak, M., Ayala, J. A., and Charlier. P., (2008). The Penicillin-Binding Proteins: Structure and Role in Peptidoglycan Biosynthesis. *FEMS Microbiology Reviews* **32** (2): 234–258.

Schägger, H., and von Jagow, G., (1987). Tricine-Sodium Dodecyl Sulfate-Polyacrylamide Gel Electrophoresis for the Separation of Proteins in the Range From 1 to 100kDa. *Analytical Biochemistry* **166**: 368–379.

Scheffers, D. J., and Pinho, M. G., (2005). Bacterial Cell Wall Synthesis: New Insights From Localization Studies. *Microbiology and Molecular Biology Reviews* **69** (4): 585–607.

Schleifer, K. H., and Kandler, O., (1972). Peptidoglycan Types of Bacterial Cell Walls and Their Taxonomic Implications. *Bacteriological Reviews* **36** (4): 407–477.

Schneider, T., Senn, M. M., Berger-Bächi, B., Tossi, A., Sahl, H-G., and Wiedemann, I., (2004). *In Vitro* Assembly of a Complete, Pentaglycine Interpeptide Bridge Containing Cell Wall Precursor (Lipid II-Gly$_5$) Of *Staphylococcus aureus*. *Molecular Microbiology* **53** (2): 675–685.

Schrader, W. P., Beckman, B. E., Beckman, M. M., Anderson, J. S., and Fan, D. P., (1974). Biosynthesis of Peptidoglycan in the One Million Molecular Weight Range by

Membrane Preparations From *Bacillus megaterium*. *The Journal of Biological Chemistry* **249** (15): 4807–4814.

Schwartz, B. J., Markwalder, A., and Wang, Y., (2001). Lipid II: Total Synthesis of the Bacterial Cell Wall Precursor and Utilization as a Substrate for Glycosyltransfer and Transpeptidation by Penicillin Binding Protein (PBP) 1b of *Eschericia coli*. *Journal of the American Chemical Society* **123** (47): 11638–11643.

Schwartz, B. J., Markwalder, A., Seitz, S. P., Wang, Y., and Stein, R. L., (2002). A Kinetic Characterization of the Glycosyltransferase Activity of *Eschericia coli* PBP1b and Development of a Continuous Fluorescence Assay. *Biochemistry* **41**: 12552–12561.

Segel, I. H., (1993). *Enzyme Kinetics*. 2nd edn. Edited by Segel, I. John Wiley & Sons.

Seidel, S. A., Dijkman, P.M., Lea, W. A., van den Bogaart, G., and Jerabek-Willemsen, M., (2013). Label-Free Microscale Thermophoresis Discriminates Sites and Affinity of Protein-Ligand Binding. *Methods* **59**: 301–315.

Severin, A., Figueiredo, A. M., and Tomasz, A., (1996). Separation of Abnormal Cell Wall Composition From Penicillin Resistance Through Genetic Transformation of *Streptococcus pneumoniae*. *Journal of Bacteriology* **178** (7): 1788–1794.

Sham, L. T., Butler, E. K., Lebar, M. D., Kahne, D., Bernhardt, T. G., and Ruiz, N., (2014). MurJ Is the Flippase of Lipid-Linked Precursors for Peptidoglycan Biogenesis. *Science* **345** (6193): 220–222.

Shaw, K. J., Rather, P. N., Hare, R. S., and Miller, G. H., (1993). Molecular Genetics of Aminoglycoside Resistance Genes and Familial Relationships of the Aminoglycoside-Modifying Enzymes. *Microbiological Reviews* **57** (1): 138–163.

Smith, A. M., and Klugman, K. P., (2001). Alterations in MurM, a Cell Wall Muropeptide Branching Enzyme, Increase High-Level Penicillin and Cephalosporin Resistance in *Streptococcus pneumoniae*. *Antimicrobial Agents and Chemotherapy* **45** (8): 2393–2396.

Smith, C. A., (2006). Structure, Function and Dynamics in the Mur Family of Bacterial Cell Wall Ligases. *Journal of Molecular Biology* **362** (4): 640–655.

Smith, T. J., Blackman, S. A., and Foster, S. J., (2000). Autolysins of *Bacillus subtilis*: Multiple Enzymes with Multiple Functions. *Microbiology* **146**: 249–262.

Solapure, S. M., Raphael, P., Gayathri, C. N., Barde, S. P., Chandrakala, B., Das, K. S., and DeSousa, S. M., (2005). Development of a Microplate-Based Scintillation Proximity Assay for MraY Using a Modified Substrate.. *Journal of Biomolecular Screening* **10** (2). SAGE Publications: 149–156.

Song, J-H., Dagan, R., Klugman, K. P., and Fritzell, B., (2012). The Relationship Between Pneumococcal Serotypes and Antibiotic Resistance. *Vaccine* **30** (17): 2728–2737.

Sorlozano, A., Gutierrez, J., Martinez, T., Yuste, M. E., Perez-Lopez, J. A.,Vindel, A., Guillen, J., and Boquete, T., (2010). Detection of New Mutations Conferring Resistance to Linezolid in Glycopeptide-Intermediate Susceptibility *Staphylococcus hominis* Subspecies *hominis* Circulating in an Intensive Care Unit. *European Journal of Clinical Microbiology & Infectious Diseases* **29** (1): 73–80.

Spratt, B. G., Zhou J. J., Taylor M., and Merrick, M. J., (1996). Monofunctional Biosynthetic Peptidoglycan Transglycosylases. *Molecular Microbiology* **19**: 639–647.

Staros, J. V., Wright, R. W., and Swingle. D. M., (1986). Enhancement of N-Hydroxysulfosuccinimide of Water-Soluble Carbodiimide-Mediated Coupling Reagents. *Analytical Biochemistry* **156**: 220–222.

Steele, V. R., Bottomley, A. L., Garcia-Lara, J., Kasturiarachchi, J., and Foster, S. J., (2011). Multiple Essential Roles for EzrA in Cell Division of *Staphylococcus aureus*. *Molecular Microbiology* **80** (2): 542–555.

Stefanova, M., Bobba, S., and Gutheil, W. G., (2010). A Microtiter Plate-Based β-Lactam Binding Assay for Inhibitors of High-Molecular-Mass Penicillin-Binding Proteins. *Analytical Biochemistry* **396** (1): 164–166.

Steidl, R., Pearson, S., Stephenson, R. E., Ledala, N., Sitthisak, S.,Wilkinson, B. J., and Jayaswal, R. K., (2008). *Staphylococcus aureus* Cell Wall Stress Stimulon Gene-*lacZ* Fusion Strains: Potential for Use in Screening for Cell Wall-Active Antimicrobials. *Antimicrobial Agents and Chemotherapy* **52** (8): 2923–2925.

Stembera, K., Buchynskyy, A., Vogel, S., Knoll, D., Osman, A, A., Ayala, J, A., Welzel, P. (2002) Moenomycin-mediated affinity purification of penicillin-binding protein 1b. *Chembiochem* **3** :332-340

Strandén, A. M., Ehlert, K., Labischinski, H., and Berger-Bächi, B., (1997). Cell Wall Monoglycine Cross-Bridges and Methicillin Hypersusceptibility in a *femAB* Null Mutant of Methicillin-Resistant *Staphylococcus aureus*. *Journal of Bacteriology* **179** (1): 9–16.

Studier, F. W., (2005). Protein Production by Auto-Induction in High-Density Shaking Cultures. *Protein Expression and Purification* **41** (1): 207–234.

Studier, F. W., and Moffat, B. A., (1986). Use of Bacteriophage T7 RNA Polymerase to Direct Selective High-Level Expression of Cloned Genes. *Journal of Molecular Biology* **189**: 113–130.

Sung, M-T., Lai, Y-T., Huang, C-Y., Chou, L-Y., Shih, H-W., Cheng, W-C., Wong, C-H., and Ma, C., (2009). Crystal Structure of the Membrane-Bound Bifunctional Transglycosylase PBP1b From *Escherichia coli*. *Proc Natl Acad Sci USA* **106** (22): 8824–8829.

Sutcliffe, I. C., (1998). Cell Envelope Composition and Organisation in the Genus Rhodococcus. *Antonie Van Leeuwenhoek* **74**: 49–58.

Tait-Kamradt, A. G., Cronan, M., and Dougherty, T. J., (2009). Comparative Genome Analysis of High-Level Penicillin Resistance in *Streptococcus pneumoniae*. *Microbial Drug Resistance* **15** (2): 69-75

Taylor-Robinson, D., and Bébéar, C., (1997). Antibiotic Susceptibilities of Mycoplasmas and Treatment of Mycoplasmal Infections. *Journal of Antimicrobial Chemotherapy* **40**: 622–630.

Terrak, M., and Nguyen-Distèche, M., (2006). Kinetic Characterization of the Monofunctional Glycosyltransferase From *Staphylococcus aureus*. *Journal of Bacteriology* **188** (7): 2528–2532.

Terrak, M., Sauvage, E., Derouaux, A., Dehareng, D., Bouhss, A., Breukink, E., Jeanjean, S., and Nguyen-Dystèche, M., (2008). Importance of the Conserved Residues in the Peptidoglycan Glycosyltransferase Module of the Class a Penicillin-Binding Protein 1b of *Escherichia coli*. *The Journal of Biological Chemistry* **283** (42): 28464–28470.

Terrak, M., Ghosh, T., van Heijenoort, J., Van Beeumen, J., Lampilas, M., Aszodi, J., Ayala, J., Ghuysen, J-M and Nguyen-Distèche, M., (1999). The Catalytic, Glycosyl Transferase and Acyl Transferase Modules of the Cell Wall Peptidoglycan-Polymerizing Penicillin-Binding Protein 1b of *Escherichia coli*. *Molecular Microbiology* **34** (2): 350–364.

Tipper, D., and Strominger, J., (1965). Mechanism of Action of Penicillins: a Proposal Based on Their Structural Similarity to Acyl-D-Alanyl-D-Alanyl. *Proc Natl Acad Sci USA* **54**: 1133–1141.

Todorova, K., Maurer, P., Rieger, M., Becker, T., Khai, N., Bui, Gray, J., Vollmer, W., and Hakenbeck, R., (2015). Transfer of Penicillin Resistance From *Streptococcus oralis* To *Streptococcus pneumoniae* Identifies murE as Resistance Determinant. *Molecular Microbiology*. **97** (5): 866-880

Tomasz, A., (2000). *Streptococcus pneumoniae*: Functional Anatomy." In *Streptococcus Pneumoniae: Molecular Biology and Mechanisms of Disease*, 1st edn. Pp. 9-24. Edited by Tomasz, A., Mary Ann Liebert

Touhami, A., Jericho, M. H., and Beveridge, T., J., (2004). Atomic Force Microscopy of Cell Growth and Division in *Staphylococcus aureus*. *Journal of Bacteriology* **186**

(11): 3286–3295.

Touzé, T., Blanot., D., Mengin-Lecreulz, D., (2008). Substrate specificity and membrane topology of the *Escherichia coli* PgpB, and undecaprenyl pyrophosphate phosphatase. *J. Biol. Chem*. **283** (2): 16573-16583

Troy, F., (1973). Chemistry and Biosynthesis of Poly(γ-D-Glutamyl) Capsule in *Bacillus licheniformis*. *The Journal of Biological Chemistry* **248** (1): 305–315.

Tschierske, M., Mori, C., Rohrer, S., Ehlert, K., Shaw, K. J., and Berger-Bächi, B., (1999). Identification of Three Additional *femAB*-Like Open Reading Frames in *Staphylococcus aureus*. *FEMS Microbiology Letters* **171**: 97–102.

Tseng, Y-Y., Liou, J-M., Hsu, T-L., Cheng, W-C., Wu, M-S., and Wong, C-H., (2014). Development of Bacterial Transglycosylase Inhibitors as New Antibiotics: Moenomycin a Treatment for Drug-Resistant *Helicobacter pylori*. *Bioorganic & Medicinal Chemistry Letters* **24** (11): 2412–2414.

Tsui, H-C. T., Boersma, M. J., Vella, S. A., Kocaoglu, O., Kuru, E., Peceny, J. K., Carlson, E. E., VanNieuwenhze, M. S., Brun, Y. V., Shaw, S. L., Winkler, M. E., (2014). Pbp2x Localizes Separately From Pbp2b and Other Peptidoglycan Synthesis Proteins During Later Stages of Cell Division of *Streptococcus pneumoniae* D39. *Molecular Microbiology* **94** (1): 21–40.

Typas, A., and Sourjik, V., (2015). Bacterial Protein Networks: Properties and Functions. *Nature Reviews Microbiology* **13** (9): 559–572.

Typas, A., Banzhaf, M., van den Berg van Saparoea, B., Verheul, J., Biboy, J., Nichols, R. J., Zietek, M., Beilharz, K., Kannenberg, K., von Rechenberg, M., Breukink, E., den Blaauwen, T., Gross, C. A., Vollmer, W., (2010). Regulation of Peptidoglycan Synthesis by Outer-Membrane Proteins. *Cell* **143** (7): 1097–1109.

Typas, A., Banzhaf, M., Gross, C. A., and Vollmer, W., (2012). From the Regulation of Peptidoglycan Synthesis to Bacterial Growth and Morphology. *Nature Reviews Microbiology* **10** (2): 123–36.

Utsui, Y., and Yokota, T., (1985). Role of an Altered Penicillin-Binding Protein in Methicillin- and Cephem-Resistant *Staphylococcus aureus*. *Antimicrobial Agents and Chemotherapy* **28** (3): 397–403.

van Dam, V., Sijbrandi, R., Kol, M., Swiezewska, E., de Kruijff, B., and Breukink, E., (2007). Transmembrane Transport of Peptidoglycan Precursors Across Model and Bacterial Membranes. *Molecular Microbiology* **64** (4): 1105–1114.

van Heijenoort, Y., Gómez, M., Derrien, M., Ayala, J., and van Heijenoort. J., (1992). Membrane Intermediates in the Peptidoglycan Metabolism of *Escherichia coli*: Possible Roles of PBP 1b and PBP 3. *Journal of Bacteriology* **174** (11): 3549–3559.

van Teeffelen, S., Wang, S., Furchtgott, L., Huang, K. C., Wingreen, N. S., Shaevitz, J. W., and Gitai, Z., (2011). The Bacterial Actin MreB Rotates, and Rotation Depends on Cell-Wall Assembly. *Proc Natl Acad Sci USA* **108** (38): 15822–15827.

VanNieuwenhze, M. S., Mauldin, S. C., Zia-Ebrahimi, M., Winger, B. E., Hornback, W. J., Saha, S. L., Aikins, J. A., and Blaszczak, L. C., (2002). The First Total Synthesis of Lipid II: the Final Monomeric Intermediate in Bacterial Cell Wall Biosynthesis. *Journal of the American Chemical Society* **124** (14): 3656–3660.

Vaneslow, A. P., (1940). Preparation of Nessler's Reagent. *Ind. Eng. Chem. Anal. Ed.* **12** (9): 516–517.

Vinatier, V., Blakey, C. B., Braddick, D., Johnson, B. R. G., Evans, S. D., and Bugg, T. D. H., (2009). *In Vitro* Biosynthesis of Bacterial Peptidoglycan Using D-Cys-Containing Precursors: Fluorescent Detection of Transglycosylation and Transpeptidation. *Chemical Communications*, **27**: 4037–4039.

Vocaldo, D. J., Davies, G. J., Laine, R., and Withers, S. G., (2001). Catalysis by Hen Egg-White Lysozyme Proceeds via a Covalent Intermediate. *Nature* **412**: 835–838.

Vollmer, W., and Höltje, J. V., (2004). The Architecture of the Murein (Peptidoglycan) in Gram-Negative Bacteria: Vertical Scaffold or Horizontal Layer(S)? *Journal of Bacteriology* **186** (18): 5978–5987.

Vollmer, W., (2007). Structure and Biosynthesis of the Pneumococcal Cell Wall. In *Molecular Biology of Streptococci*. Horizon Bioscience. 1st Edn, pp:83-118, Edited by Hakenbeck, R., and Chhatwal, S.

Vollmer, W., (2008). Structural Variation in the Glycan Strands of Bacterial Peptidoglycan. *FEMS Microbiology Reviews* **32** (2): 287–306.

Vollmer, W., Blanot, D., and de Pedro, M. A., (2008). Peptidoglycan Structure and Architecture. *FEMS Microbiology Reviews* **32** (2): 149–167

Vollmer, W., Joris, B., Charlier, P., and Foster, S., (2008a). Bacterial Peptidoglycan (Murein) Hydrolases. *FEMS Microbiology Reviews* **32** (2): 259–286.

von Nussbaum, F., Brands, M., Hinzen, B., Weigand, S., and Häbich. D., (2006). Antibacterial Natural Products in Medicinal Chemistry-Exodus or Revival? *Angew. Chem. Int. Ed.* **45** (31): 5072–5129.

Walker, S., Chen, L., Hu, Y., Rew, Y., Shin, D., and Boger, D. L., (2005). Chemistry and Biology of Ramoplanin: a Lipoglycodepsipeptide with Potent Antibiotic Activity. *Chemical Reviews* **105** (2): 449–476.

Walsh, C. T., and Wright, G., (2005). Introduction: Antibiotic Resistance. *Chemical Reviews* **105** (2): 391–394.

Walsh, C. T., (2000). Molecular Mechanisms That Confer Antibacterial Drug Resistance. *Nature* **406**: 775–782.

Walsh, C. T., (2003). *Antibiotics; Actions, Origins, Resistance*. ASM Press. Washington, DC.

Walsh, C. T., Fisher, S. L., Park, I-S., Prahalad, M., and Wu, Z., (1996). Bacterial Resistance to Vancomycin: Five Genes and One Missing Hydrogen Bond Tell the Story. *Chemistry & Biology* **3**: 21–28.

Wang, T-S. A., Lupoli, T. J., Sumida, Y., Tsukamoto, H., Wu, Y., Rebets, Y., Kahne, D. E., and Walker, S., (2011). Primer Preactivation of Peptidoglycan Polymerases. *Journal of the American Chemical Society* **133** (22): 8528–8530.

Wang, Q. M., Peery, R. B., Johnson, R. B., Alborn, W. E., Yeh, W. K., and Skatrud, P. L., (2001). Identification and Characterization of a Monofunctional Glycosyltransferase From *Staphylococcus aureus*. *Journal of Bacteriology* **183** (16): 4779–4785.

Wang, T-S. A., Manning, S. A., Walker, S., and Kahne, D., (2008). Isolated Peptidoglycan Glycosyltransferases From Different Organisms Produce Different Glycan Chain Lengths. *Journal of the American Chemical Society* **130** (43): 14068–14069.

Ward, B., (1973). The Chain Length of the Glycans in Bacterial Cell Walls. *Biochemistry Journal* **133**: 395–398.

Waxman, D. J., and Strominger, J., (1983). Penicillin Binding Proteins and the Mechanism of Action of β-Lactam Antibiotics. *Annu. Rev. Biochem.* **52**: 825–869.

Webber, M. A., and Piddock, L. J. V., (2003). "The Importance of Efflux Pumps in Bacterial Antibiotic Resistance. *Journal of Antimicrobial Chemotherapy* **51** (1): 9–11.

Weber, B., Ehlert, K., Diehl, A., Reichmann, P., Labischinski, H., and Hakenbeck, R., (2000). The Fib Locus in *Streptococcus pneumoniae* Is Required for Peptidoglycan Crosslinking and PBP-Mediated β-Lactam Resistance. *FEMS Microbiology Letters* **188**: 81–85.

Welzel, P., (2005). Syntheses Around the Transglycosylation Step in Peptidoglycan Biosynthesis. *Chemical Reviews* **105** (12): 4610–4660.

Wickus, G. G., and Strominger, J., (1972). Penicillin-Sensitive Transpeptidation During Peptidoglycan Biosynthesis in Cell-Free Preparations From *Bacillus*

megaterium. The Journal of Biological Chemistry **247** (17): 5307–5311.

Wienken, C. J., Baaske, P., Rothbauer, U., Braun, D., and Duhr S., (2010). Protein-Binding Assays in Biological Liquids Using Microscale Thermophoresis. *Nature Communications* **1**: 100.

Wilkin, J-M., Jamin, M., Damblon, C., Zhao, G-H., Joris, B., Duez, C., and Frère, J. M., (1993). The Mechanism of Action of DD-Peptidases: the Role of Turosine-159 in the *Streptomyces* R61 DD-Peptidase **291**: 537–544.

Williams, S. P., Tait-Kamradt, A. G., Norton, J. E., Albert, T. J., and Dougherty, T. J., (2007). Nucleotide Sequence Changes Between *Streptococcus pneumoniae* R6 and D39 Strains Determined by an Oligonucleotide Hybridization DNA Sequencing Technology. *Journal of Microbiological Methods* **70** (1): 65–74.

Wise, E. M., and Park, J. T., (1965). Penicillin: Its Basic Site of Action as an Inhibitor of a Peptide Cross-Linking Reaction in Cell Wall Mucopeptide Synthesis. *Proc Natl Acad Sci USA* **54**: 75–81.

World Health Organisation. (2007). Pneumococcal Conjugate Vaccine for Childhood Immunization--WHO Position Paper. *Weekly Epidemiology Record* **82** (12): 93–104.

World Health Organisation. (2012). Pneumococcal Vaccines--WHO Position Paper." *Weekly Epidemiology Record* **87** (14): 129–144.

Wyke, A. W., Ward, J. B., Hayes, M. V., and Curtis, N. A. C., (1981). A Role *In Vivo* For Penicillin-Binding Protein-4 of *Staphylococcus aureus*. *European Journal of Biochemistry* **119**: 389–393.

Ye, X-Y., Lo, M-C., Brunner, L., Walker, D., Kahne, D., and Walker, S., (2001). Better Substrates for Bacterial Transglycosylases. *Journal of the American Chemical Society* **123** (13): 3155–3156.

Yocum, R. R., Waxman, D. J., Rasmussen, J., and Strominger, J., (1979). Mechanism of Penicillin Action: Penicillin and Substrate Bind Covalently to the Same Active Site Serine in Two Bacterial D-Alanine Carboxypeptidases. *Proc Natl Acad Sci USA* **76** (6): 2730–2734.

Young, K. D., (2003). Bacterial Shape. *Molecular Microbiology* **49** (3): 571–580.

Yuan, Y., Fuse, S., Ostash, B., Sliz, P., Kahne, D., and Walker, S., (2008). Structural Analysis of the Contacts Anchoring Moenomycin to Peptidoglycan Glycosyltransferases and Implications for Antibiotic Design. *ACS Chemical Biology* **3** (7): 429–436.

Yuan, Y., Barrett, D., Zhang, Y., Kahne, D. E., Sliz, P., and Walker, S., (2007). Crystal Structure of a Peptidoglycan Glycosyltransferase Suggests a Model for

Processive Glycan Chain Synthesis. *Proc. Natl. Acad. Sci. USA* **104** (13): 5348–5353.

Zapun, A., Contreras-Martel, C., and Vernet, T., (2008). Penicillin-Binding Proteins and β-Lactam Resistance. *FEMS Microbiology Reviews* **32** (2): 361–385.

Zapun, A., Philippe, J., Abrahams, K. A., Signor, L., Roper, D. I., Breukink, E., and Vernet, T., (2013). *In Vitro* Reconstitution of Peptidoglycan Assembly From the Gram-Positive Pathogen *Streptococcus pneumoniae*. *ACS Chemical Biology* **8** (12): 2688–2696.

Zapun, A., Noirclerc-Savoye, M., Helassa, N., and Vernet, T., (2012). Peptidoglycan Assembly Machines: the Biochemical Evidence. *Microbial Drug Resistance* **18** (3): 256–260.

Zawadzke, L. E., Bugg, T. D., Walsh, C. T., (1991). Existence of two D-alanine:D-alanine ligases in *Escherichia coli*: cloning and sequencing of the ddlA gene and purification and characterization of the DdlA and DdlB enzymes. *Biochemistry* **30** (6): 1673-1892

Zerfass, I., Hakenbeck, R., and Denapaite, D., (2009). An Important Site in PBP2x of Penicillin-Resistant Clinical Isolates of *Streptococcus pneumoniae*: Mutational Analysis of Thr338. *Antimicrobial Agents and Chemotherapy* **53** (3): 1107–1115.

Zhang, Y., Fechter, E. J., Wang, T-S. A., Barrett, D., Walker, S., and Kahne, D. E., (2007). Synthesis of Heptaprenyl−Lipid IV to Analyze Peptidoglycan Glycosyltransferases. *Journal of the American Chemical Society* **129** (11): 3080–3081.

Zuegg, J., Muldoon, C., Adamson, G., McKeveney, D., Thanh, G. L., Premraj, R., Becker, B., Cheng, M., Elliott, A. G., Huang, J. X., Butler, M. S., Bajaj, M., Seifert, J., Singh, L., Galley, N. F., Roper, D. I., Lloyd, A. J., Dowson, C. G., Cheng, T-J., Cheng, W-C., Demon, D., Meyer, E., Meutermans, W., Cooper, M. A., (2015). Carbohydrate Scaffolds as Glycosyltransferase Inhibitors with *In Vivo* Antibacterial Activity. *Nature Communications* **6**: 1–11.

Appendix 1

Preparation of *Micrococcus flavus* membranes

M. flavus membranes for Lipid II synthesis were prepared by Julie Tod or Anita Catherwood (BaCWAN, UK) from frozen glycerol stocks. 100 mL of tryptone soya broth (TSB) was inoculated from a glycerol stock and cultured overnight at 37°C with 180 rpm agitation. Each of 8 × 650 mL TSB culture were inoculated with 10 mL overnight culture and incubated at 37°C with agitation at 180 rpm until OD_{600nm} reached 4.0 (mid-exponential phase). Cells were harvested by centrifugation at 10,000 × g for 10 min using a Beckman JLA-8.100 rotor.

Cell pellets were washed once in ice-cold membrane buffer (20 mM Tris, 1 mM $MgCl_2$ and 2 mM β-mercaptoethanol, pH 7.5) and resuspended in 3 mL/g^{-1} of the same buffer plus 2.5 $mg.mL^{-1}$ hen egg-white lysozyme in incubated for 15 min on ice. Cells were disrupted using a continuous cell disruptor (Constant Cell Disruption Systems) at 30 kpsi and centrifuged at 10,000 × g for 1 h at 4°C to remove cellular debris. The pellet was resuspended in three times the volume of membrane buffer and centrifuged at 50,000 × g for 1 h at 4°C. The pellet from this, containing the *M. flavus* membranes was resuspended in 3 mL membrane buffer and the protein concentration determined by the Bio-Rad assay (Section 2.5.1). Membranes were stored at -80°C until use.

Appendix 2

Calculation of DAAO and Horseradish peroxidase catalytic concentrations

Dr Adrian Lloyd calculated the catalytic concentration of DAAO and Horseradish peroxidase for use in the Amplex Red assay.

DAAO: DAAO was diluted to 54.13 nM in 50 mM Tris, 50 mM lactitol, 10% (v/v) glycerol and 5 mM EDTA, pH 7.5. To a 0.2 ml cuvette was added (final concentration): 50 mM Bis.Tris propane pH 8.5, 0.1% (v/v) Triton X-100, 20 mM MgCl$_2$, 5.8 units pyruvate kinase/lactate dehydrogenase mix, 0.3 mM NADH and 1.35 nM DAAO. The A$_{340}$ was monitored at 30°C for 5 minutes, before 1mM D-alanine was added to initiate the assay. The DAAO initial rate was obtained from the difference between rates in the presence and absence of D-alanine ($\varepsilon_{1cm, \, 340 \, nm} =$ 6,220 M^{-1}.cm^{-1}).

Horsradish peroxidase: HRP was diluted 1 in 400,000 into 50 mM Bis.Tris propane pH 8.5. To a 0.2 ml cuvette was added (final concentration): 158 μl water, 20 μl 0.5 M BisTris propane pH 8.5 (50 mM), 2 μl 2 M MgCl$_2$ (20mM), 1 μl 10 mM Amplex Red (50 mM) and 5 μl diluted HRP (18.5 pM). The absorbance of any residual resorufin at 555 nm was zeroed, and the A$_{555}$ was monitored at 30°C for five minutes, before the addition of 4 μl 1 mM hydrogen peroxide (20 mM) to initiate the assay. The HRP initial rate was obtained from the difference between rates in the presence and absence of hydrogen peroxide ($\varepsilon_{1cm, \, 555 \, nm} = 55,000$ M^{-1}.cm^{-1}).

In both cases rates were calculated under these defined conditions as mMoles substrate consumed or product produced/ml enzyme/min which results in units of mM.min-1. This parameter (the catalytic concentration of enzyme activity) was then used to determine the exact enzymatic concentration of both DAAO and HRP coupling enzymes in Amplex Red assays of *S. pneumoniae* PBP1a, and other PBPs.

Appendix 3

Negative ion mass spectrometry of UDP-Mur*N*Ac-pentapeptide (Glu, Dans) and UDP-Mur*N*Ac-pentapeptide (Gln, Dans)

UDP-Mur*N*Ac-pentapeptide (Glu, Dans) and UDP-Mur*N*Ac-pentapeptide (Gln, Dans) were synthesised by Julie Tod or Anita Catherwood of BaCWAN (UK; Clarke *et al.,* 2009; Lloyd *et al*., 2008). Negative ion mass spectrometry was used to confirm the synthesis of dansylated intermediates (and amidated where required), and to ensure that no non-dansylated product was present. Mass spectrometry was performed by Warwick Proteomics Facility RTP.

Figures A3.1 and A3.2 show the negative ion mass spectra for UDP-Mur*N*Ac-pentapeptide (Glu, Dans) and UDP-Mur*N*Ac-pentapeptide (Gln, Dans) respectively, with inset images showing the predicted and observed isotope profiles of the [M-H]⁻ species. The correlation between these, in addition to the m/z values observed allowed confirmation of synthesis of the required species.

Note that the spectra shown in Figure A3.1 were acquired using an Orbitap Fusion mass spectrometer (Thermo Scientific) rather than the Synapt G2 HDMS (Waters, USA) used for all other spectra. This data cannot be opened in the same software, and this is the reason for the different formatting of figures A3.1 A and C. Isotope profile prediction (Figure A3.1 (B)) was in MassLynx^{TM} (Waters, USA) as for all others.
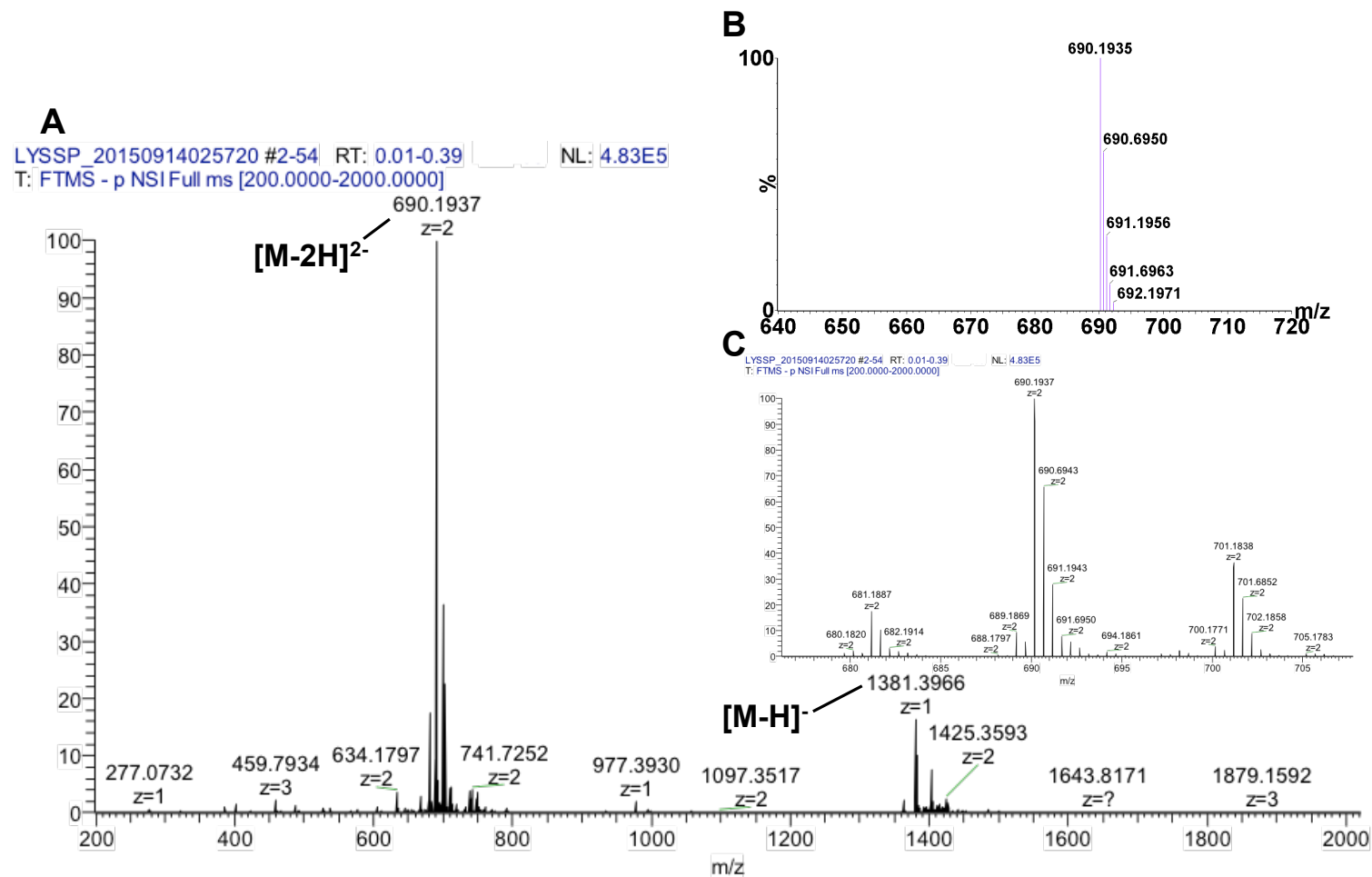
Figure A3.1: Negative ion mass spectra of UDP-Mur*N*Ac-pentapeptide (Glu, Dans) A: Mass spectra with [M-2H]$^{2-}$ (observed 690.1937, expected 690.1943), and [M-H]$^-$ (observed 1381.3966, expected 1381.3956) indicated. B: Predicted isotope distribution of [M-2H]$^{2-}$ based on the empirical formula of UDP-Mur*N*Ac-pentapeptide (Glu, Dans) (predicted by MassLynx^{TM} software (Waters, USA). C: Observed isotope distribution of [M-2H]$^{2-}$ (zoomed in view of [M-2H]$^{2-}$ peak in A showing exact match with the predicted distribution in B.
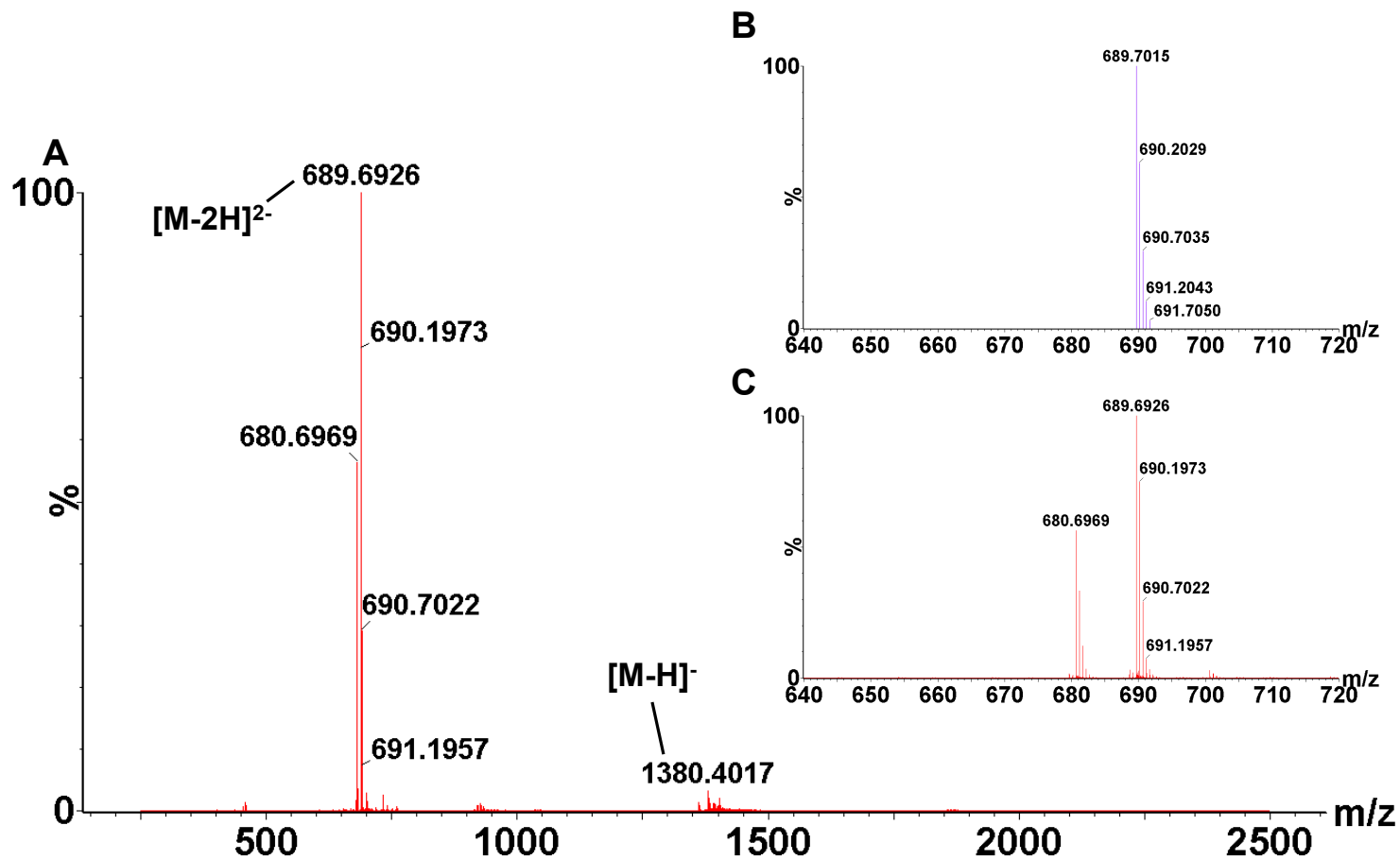
Figure A3.2: Negative ion mass spectra of UDP-Mur*N*Ac-pentapeptide (Gln, Dans) A: Mass spectra with [M-2H]$^{2-}$ (observed 689.6926, expected 689.7203), and [M-H]$^{-}$ (observed 1380.4017, expected 1380.4116) indicated. B: Predicted isotope distribution of [M-2H]$^{2-}$ based on the empirical formula of UDP-Mur*N*Ac-pentapeptide (Gln, Dans) (predicted by MassLynx^{TM} software (Waters, USA). C: Observed isotope distribution of [M-2H]$^{2-}$ (zoomed in view of [M-2H]$^{2-}$ peak in A showing exact match with the predicted distribution in B.

314

Appendix 4

Negative ion mass spectra of UDP-Mur*N*Ac-heptapeptide (Gln, AlaAla)

Negative ion mass spectra from Figure 3.12 (B) is reproduced as a full page figure (Figure A4.1) due to low resolution of the original file. This is due to use of an open source mass spectrometer for which raw data is not available.
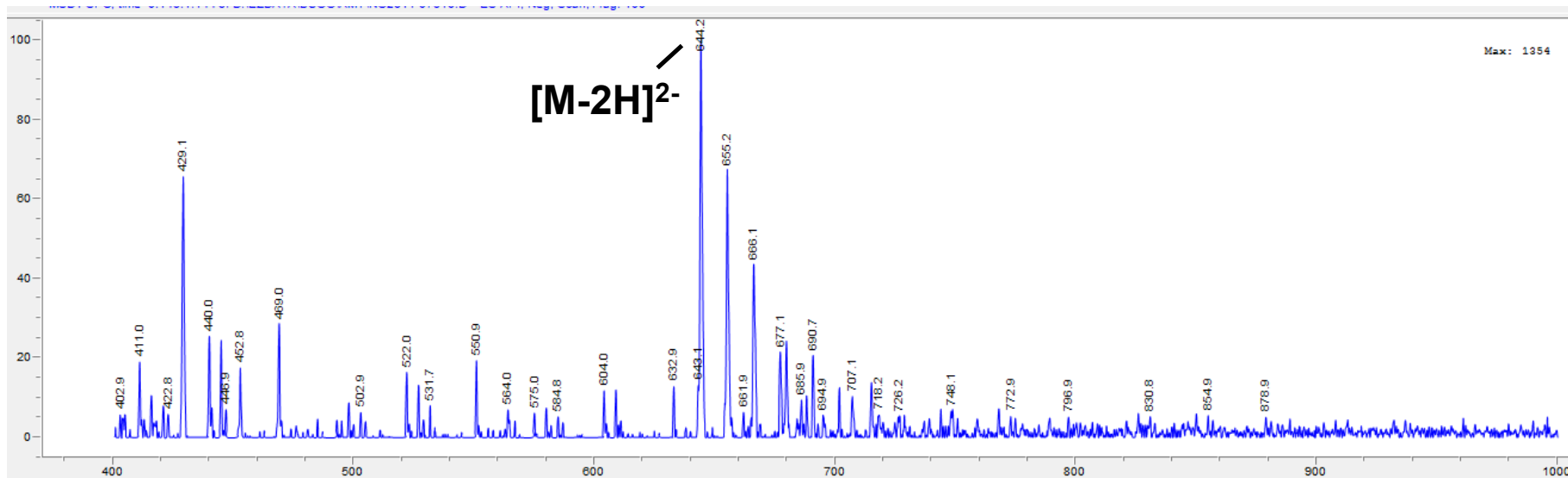
Figure A4.1: Negative ion electrospray time-of-flight mass spectra of UDP-Mur*N*Ac-heptapeptide (Gln, AlaAla). [M-2H]$^{2-}$ expected 644.2139 observed 644.2.

Appendix 5

Collision induced fragmentation of UDP-Mur*N*Ac-hexapeptide (Gln, Ala) and UDP-Mur*N*Ac-hexapeptide (Gln, Ser)

In order to confirm the location of seryl and alanyl amino acid branching on the amidated UDP-Mur*N*Ac-pentapeptide stem, collision-induced fragmentation by positive mode electrospray mass spectrometry (ES-MS) was performed by Dr A. Lloyd.

Figure A5.1 and A5.2 show the positive ion mass spectrum, isolation of the singly charged cation and fragmentation (with argon and a collision energy of 60 eV) for UDP-Mur*N*Ac-hexapeptide (Gln, Ala) and UDP-Mur*N*Ac-hexapeptide (Gln, Ser) respectively. A range of peaks were obtained for both which could be assigned to fragmentation of the UDP-Mur*N*Ac-hexapeptide (Gln, Ala) (Figure A5.3(A)) and UDP-Mur*N*Ac-hexapeptide (Gln, Ser) (Figure A5.3 (B)) specifically. Figure A5.3 shows the annotation of the main peaks and fragment identities are detailed in the figure legend. The fragmentation patterns confirmed the addition of the seryl and alanyl groups onto the ε-amino group of the stem peptide lysine.

It should be noted that the peaks attributed to having seryl amino acid branching in Figure A5.3 (B) have a mass 16 greater than the corresponding peak in Figure A5.3 (A) for alanyl, consistent with the presence of an additional hydroxyl.
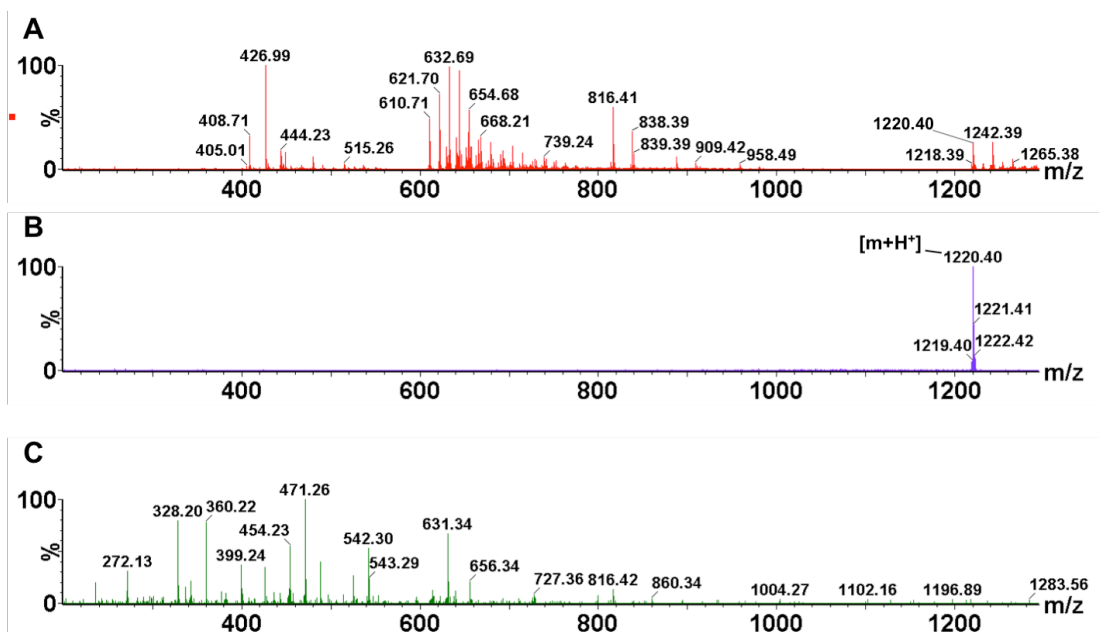
Figure A5.1: Positive ion mass spectra of UDP-Mur*N*Ac-hexapeptide (Gln, Ala). A: Positive ion mass spectrum showing the full range of peaks. B: Isolation of the positively charged cation (expected [m+H$^+$] 1220.40; observed [m+H$^+$] 1220.40). C: Positive ion mass spectrum of collision induced fragmentation at 60 eV with argon of the positively charged cation in B. C is annotated in Figure A5.3(A). Figure generated by Dr A. Lloyd.
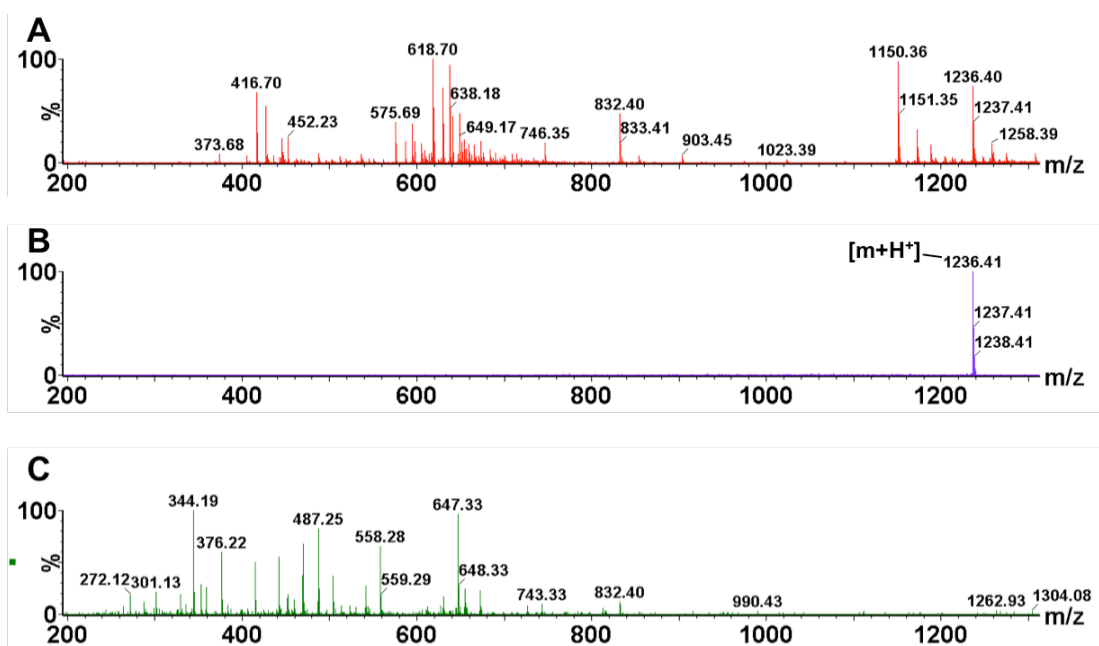

Figure A5.2: Positive ion mass spectra of UDP-Mur*N*Ac-hexapeptide (Gln, Ser). A: Positive ion mass spectrum showing the full range of peaks. B: Isolation of the positively charged cation (expected [m+H$^+$] 1236.41; observed [m+H$^+$] 1236.41). C: Positive ion mass spectrum of collision induced fragmentation at 60 eV with argon of the positively charged cation in B. C is annotated in Figure A5.3(B). Figure generated by Dr A. Lloyd.
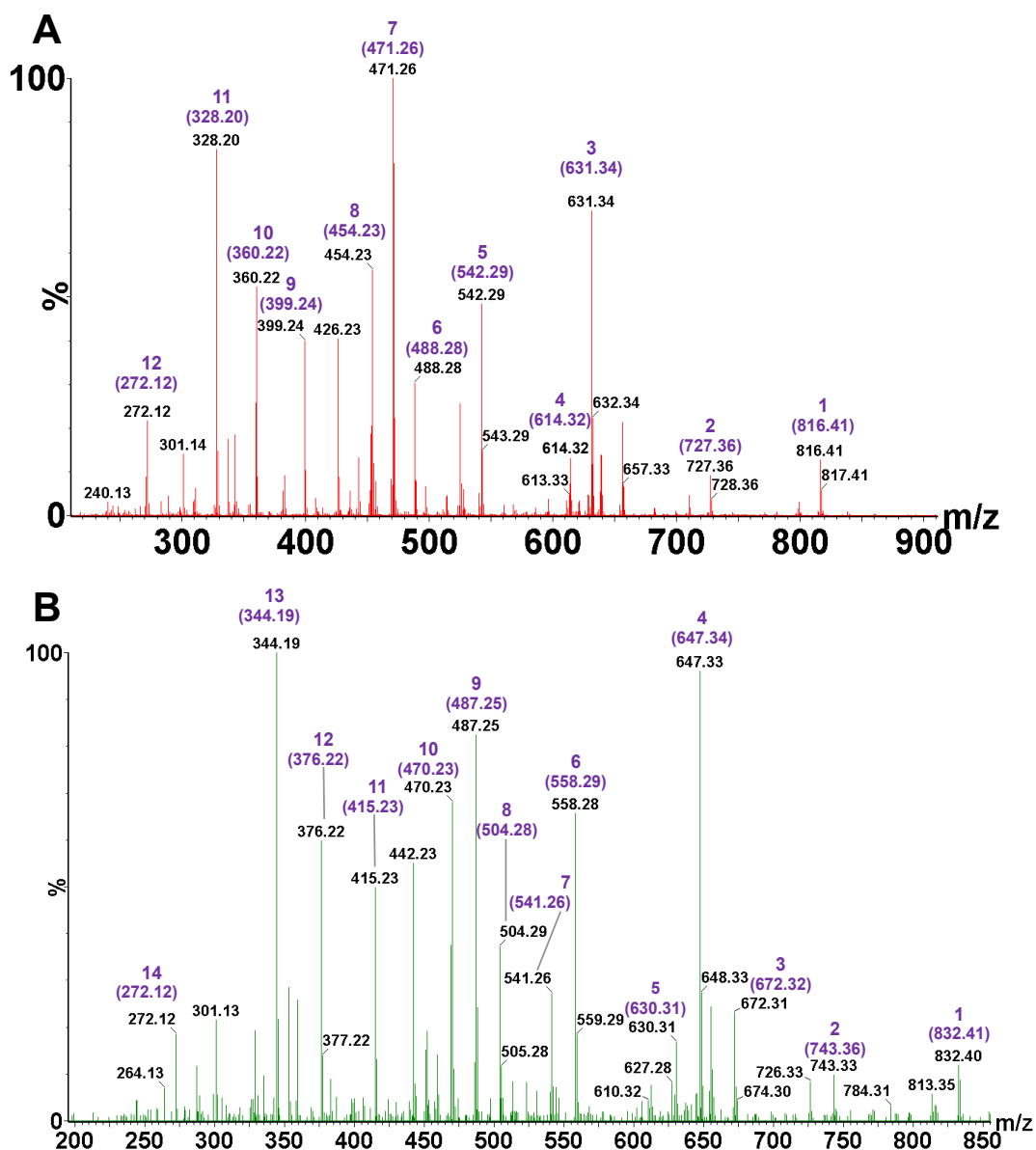
Figure A5.3: Collision induced fragmentation of UDP-Mur*N*Ac-hexapeptide (Gln, Ala) (A) and UDP-Mur*N*Ac-hexapeptide (Gln, Ser) (B). A: UDP-Mur*N*Ac-hexapeptide (Gln, Ala): the singly protonated parent cation ([m+H$^+$]; 1220.40 observed, 1220.40 expected) was fragmented. The expected mass of each observed mass is indicated in brackets and labelled with a number identifying each species. The observed fragments are assigned as follows where (A) denotes an alanyl group appended to the ε-amino group of the third position stem peptide lysine; 1: Mur*N*Ac-AQK(A)AA; 2: Mur*N*Ac-AQA(A)A; 3: lactyl-AQK(A)AA; 4: lactyl-AQK(A)AA-NH$_2$; 5: lactyl-AQA(A)A; 6: QK(A)AA; 7: lactyl-AQK(A); 8: lactyl-AQK(A)-NH$_2$; 9: QK(A)A; 10: K(A)AA; 11: QK(A); 12: lactyl-AQ. **B**: UDP-Mur*N*Ac-hexapeptide (Gln, Ser): the singly protonated parent cation ([m+H$^+$]; 1236.41 observed, 1236.41 expected) was fragmented. The expected mass of each observed mass is indicated in brackets and labelled with a number identifying each species. The observed fragments are assigned as follows where (S) denotes an seryl group appended to the ε-amino group of the third position stem peptide lysine; 1: Mur*N*Ac-AQK(S)AA; 2: Mur*N*Ac-AQK(S)A; 3: Mur*N*Ac-AQK(S); 4: lactyl-AQK(S)AA; 5: lactyl-AQK(S)AA; 6: lactyl-AQK(S)A; 7: lactyl-AQK(S)A-NH$_2$; 8: QK(S)AA; 9: lactyl-AQK(S); 10: lactyl-AQK(S)-NH$_2$; 11: QK(S)A/AQK(S); 12: K(S)AA; 13: QK(S); 14: lactyl-AQ. Peak assignments and figure generation by Dr A. Lloyd.

Appendix 6

Negative ion mass spectrometry of Lipid II (Glu), Lipid II (Gln), Lipid II (Glu, Dans) and Lipid II (Gln, Dans)

Lipid II (Glu), Lipid II (Gln), Lipid II (Glu, Dans) and Lipid II (Gln, Dans) were prepared by Julie Tod, Anita Catherwood or Smita Chauhan of BaCWAN (UK; Clarke *et al.,* 2009; Lloyd *et al.,* 2008) as described in Chapter 3. Purity was confirmed by thin layer chromatography (TLC).

The identity of Lipid II species were confirmed by negative ion electrospray mass spectrometry (ES-MS) performed by the Proteomics Facility RTP (School of Life Sciences, University of Warwick). Figures A6.1-A6.4 show the mass spectra obtained for Lipid II (Glu) ($[M-2H]^{2-}$ expected 936.52, observed 936.51), Lipid II (Gln) ($[M-2H]^{2-}$ expected 936.03, observed 936.02), Lipid II (Glu, Dans) (($[M-2H]^{2-}$ expected 1053.05, observed 1053.06) and Lipid II (Gln, Dans) ($[M-2H]^{2-}$ expected 1052.56, observed 1052.54) respectively. Zoomed in views of the $[M-2H]^{2-}$ species are shown as an inset on each image (red) showing the isotope distribution observed. A second inset figure (blue) shows the predicted isotope distribution (predicted by MassLynx^{TM} (Waters, USA) based on the empirical formula) for comparison. In all cases these match, enabling the species to be positively identified.
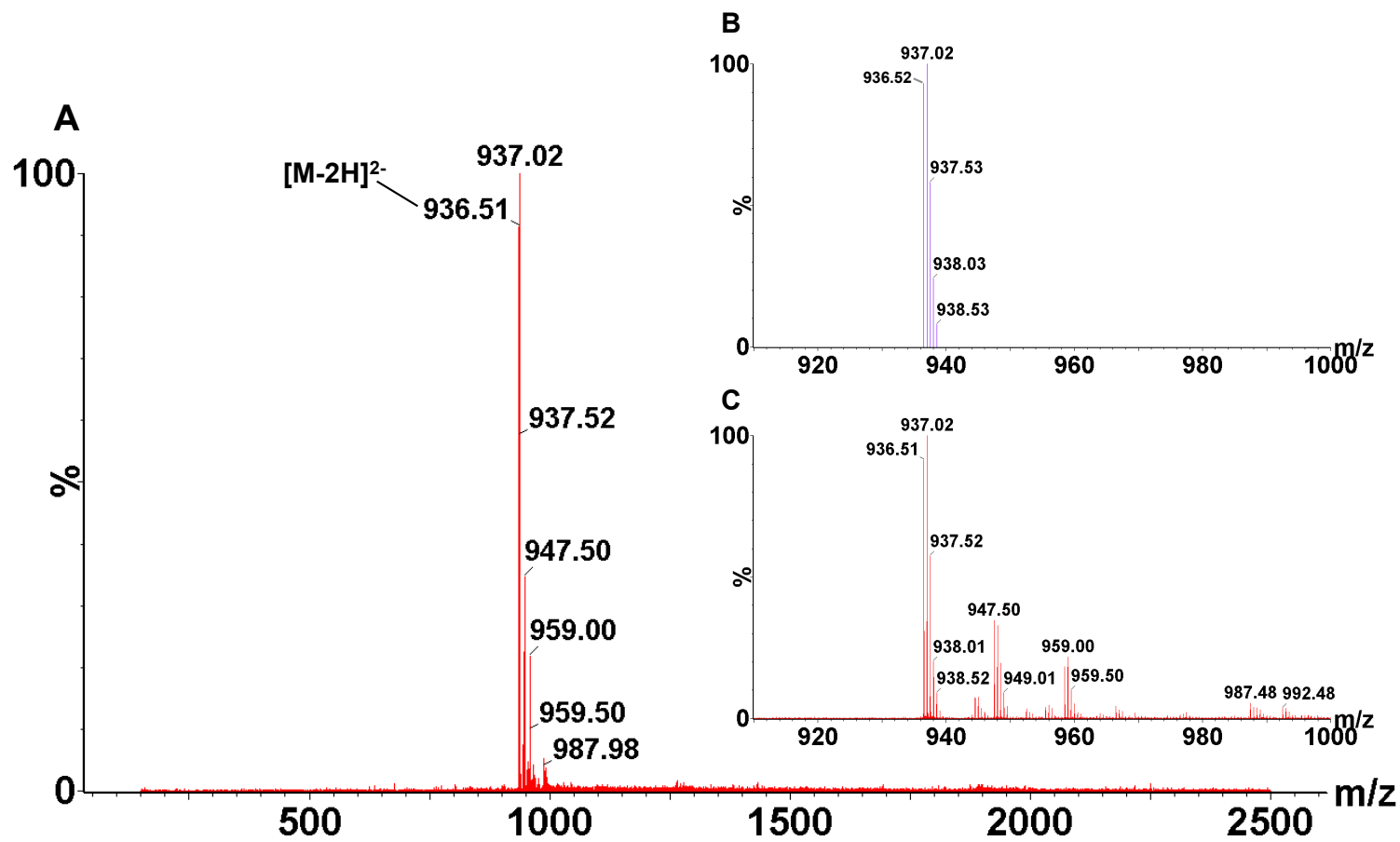
Figure A6.1: Negative ion mass spectra of Lipid II (Glu). A: Mass spectra with [M-2H]²⁻ indicated (observed 936.51, expected 936.52). B: Predicted isotope distribution based on the empirical formula of Lipid II (Glu). C: Observed isotope distribution (zoomed in view of [M-2H]²⁻ from A).

Figure A6.2: Negative ion mass spectra of Lipid II (Gln). A: Mass spectra with [M-2H]$^{2-}$ indicated (observed 936.02, expected 936.03). B: Predicted isotope distribution based on the empirical formula of Lipid II (Gln). C: Observed isotope distribution (zoomed in view of [M-2H]$^{2-}$ from A).
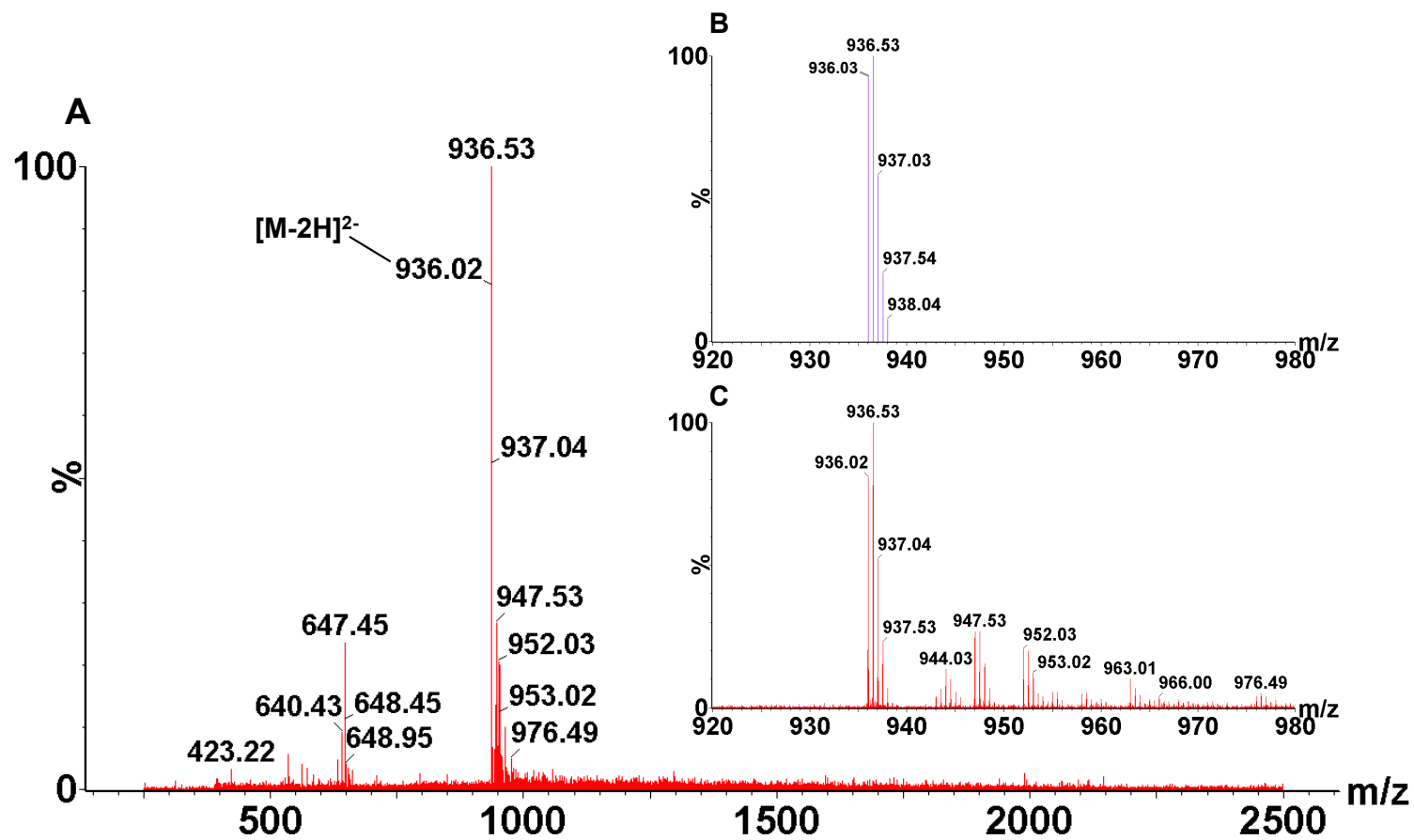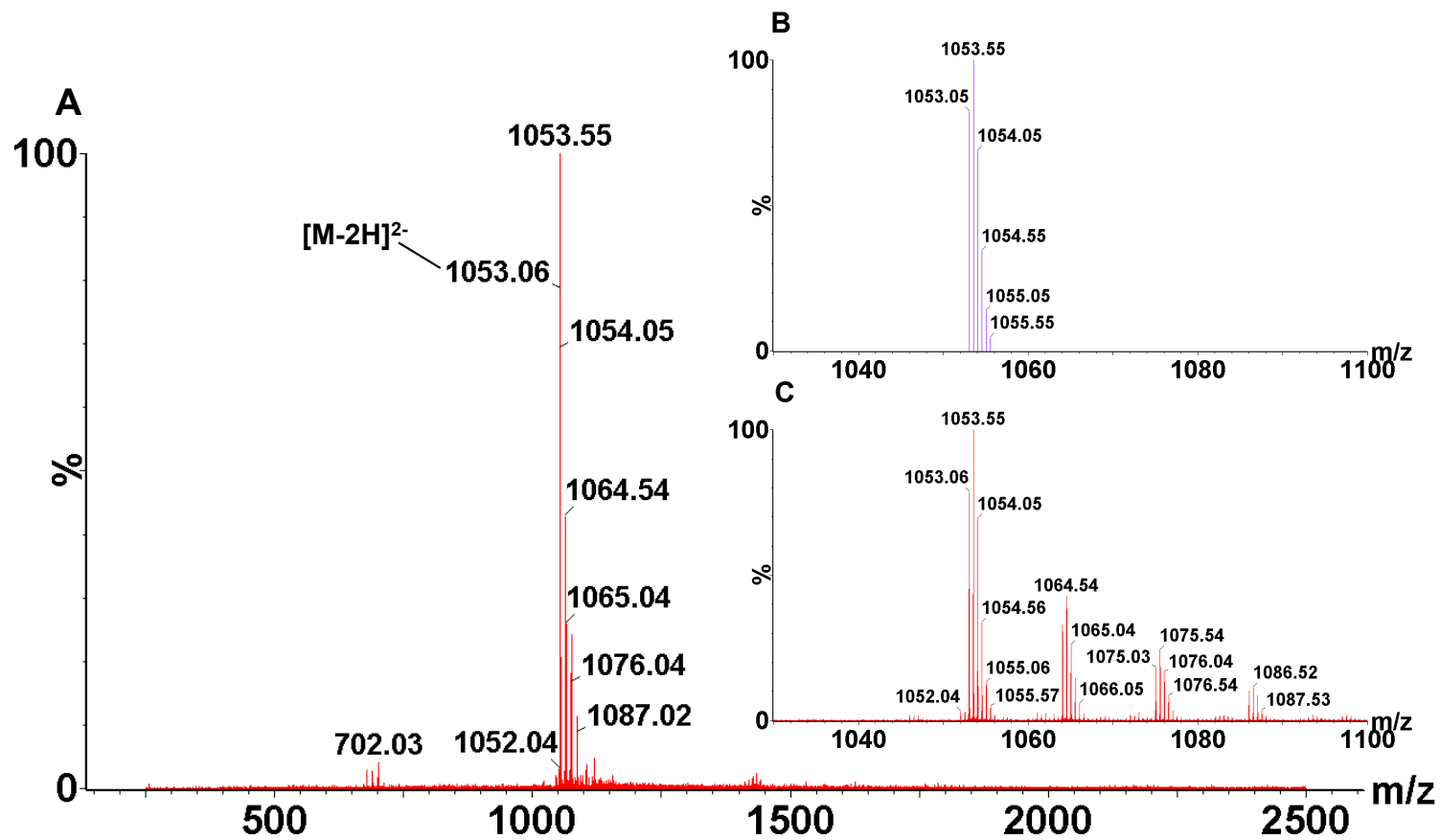
Figure A6.3: Negative ion mass spectra of Lipid II (Glu, Dans). A: Mass spectra with [M-2H]$^{2-}$ indicated (observed 1053.06, expected 1053.05). B: Predicted isotope distribution based on the empirical formula of Lipid II (Glu, Dans). C: Observed isotope distribution (zoomed in view of [M-2H]$^{2-}$ from A).

Figure A6.4: Negative ion mass spectra of Lipid II (Gln, Dans). A: Mass spectra with [M-2H]$^{2-}$ indicated (observed 1052.54, expected 1052.56). B: Predicted isotope distribution based on the empirical formula of Lipid II (Gln, Dans). C: Observed isotope distribution (zoomed in view of [M-2H]$^{2-}$ from A).
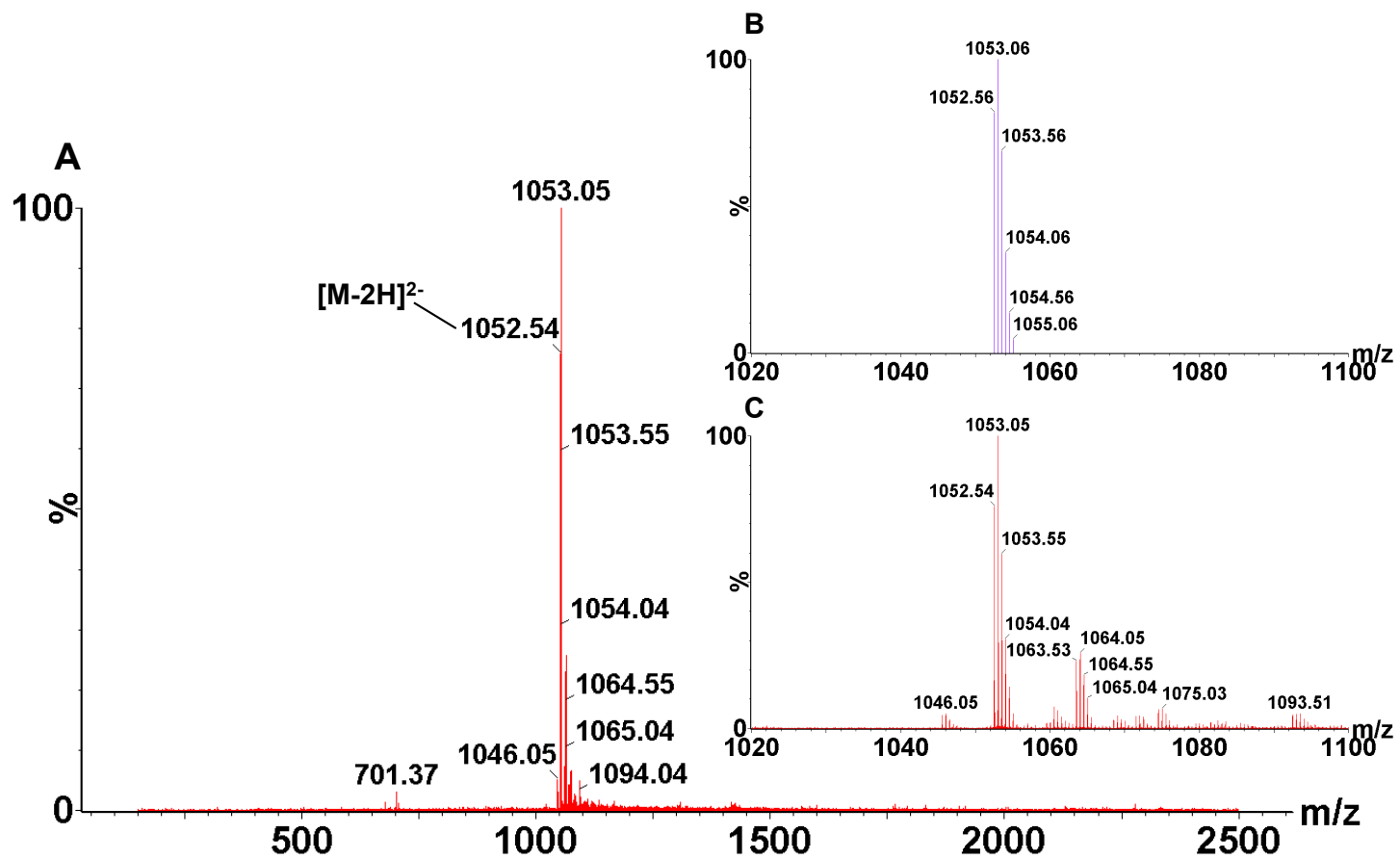
Appendix 7

Liquid chromatography positive ion mass spectrometry of Amplex Red assay cuvette contents

Amplex Red assay cuvette contents were prepared for liquid chromatography mass spectrometry (LC-MS) as described in Section 6.4.6. LC-MS in positive mode and subsequent data analysis was performed by Dr A. Lloyd.

Figure A7.1 shows the total ion chromatogram and separate chromatogram of ions eluting with an m/z value consistent with the anomeric structure of the product of lipid II Lys transpeptidation (2 peaks). Both the α- and β- anomer are present due to failure of the $NaBH_4$ treatment (these are structurally shown in Figure A7.1 (C)). Figure A7.2 shows the positive ion mass spectra of each of the two peaks, and spectra from the corresponding liquid chromatography elution time in the minus Lipid II control. The positive ion mass spectra of the singly and doubly charged product of both the 15.2 min and 15.5 min peaks are also shown in Chapter 6 (Figures 6.14 and 6.15), along with the collision induced fragmentation pattern confirming the species as the product of transpeptidation (Figure 6.17).

Masses corresponding to the PBP1a D,D carboxypeptidase tetrapeptide product and dissacharide-pentapeptide of lipid II or its transglycosylation product were also identified and are shown in Figure A7.3 and A7.4 respectively.
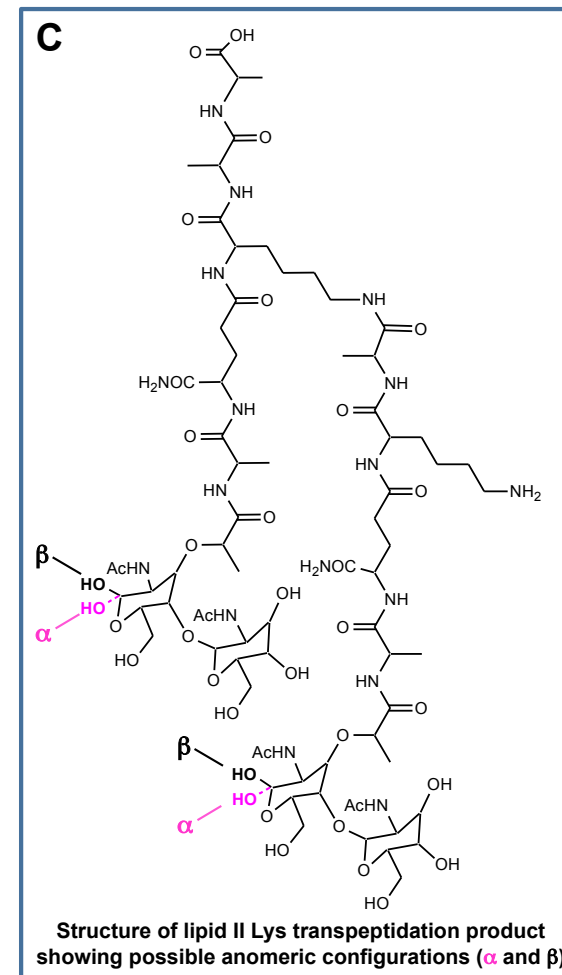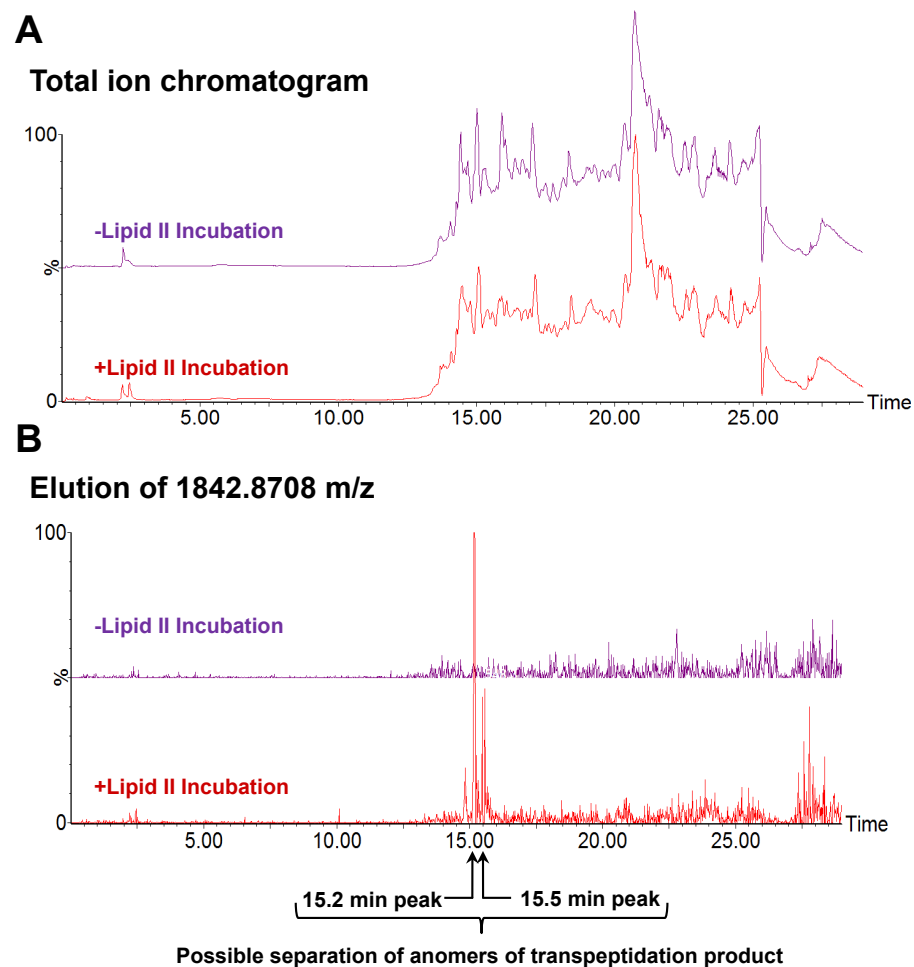
Figure A7.1: LC-MS (positive ion) chromatogram of ions eluting with an m/z value consistent with the anomeric structure of the product of lipid II Lys transpeptidation. A: Total ion chromatogram of +Lipid II and – Lipid II reactions. B: Elution of two peaks containing ions with m/z values consistent with the anomeric structure of the product of transpeptidation ($[m+H^+]$ 1842.87) in + Lipid II sample (absent in – Lipid II sample). C: Structure of the Lipid II (Gln) transpeptidation product highlighting the difference between the α and β anomeric forms. Figure generated by Dr A. Lloyd.
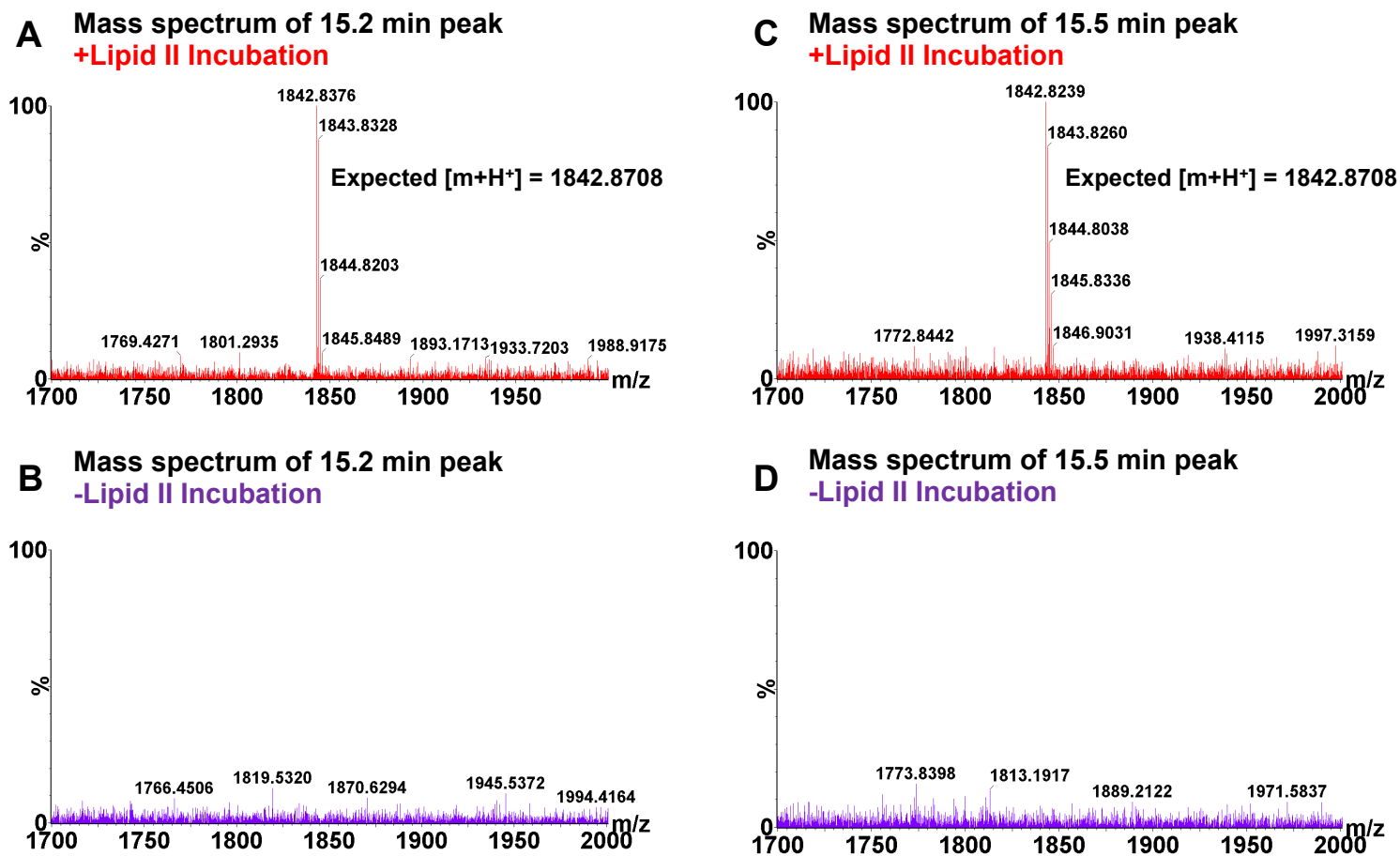
326

Figure A7.2: Mass spectrum of putative PBP1a transpeptidation product ([m+H$^+$) expected: 1842.8708) formed from Lipid II (Gln) in the 15.2 (A) and (B) and 15.5 (C) and (D) min LC-MS peaks containing ions with m/z values consistent with predicted structure. A: Positive ion mass spectrum of 15.2 min peak of +Lipid II incubation showing the m/z value consistent with the product ([m+H$^+$] expected 1842.8707, observed 1842.8239) B. Positive ion mass spectrum of 15.2 min min elution of –Lipid II incubation. C: Positive ion mass spectrum of 15.5 min peak of +Lipid II incubation showing the m/z value consistent with the product ([m+H$^+$] expected 1842.8707, observed 1842.8376). D: Positive ion mass spectrum of 15.5 min elution of –Lipid II incubation. Figure generated by Dr A. Lloyd.
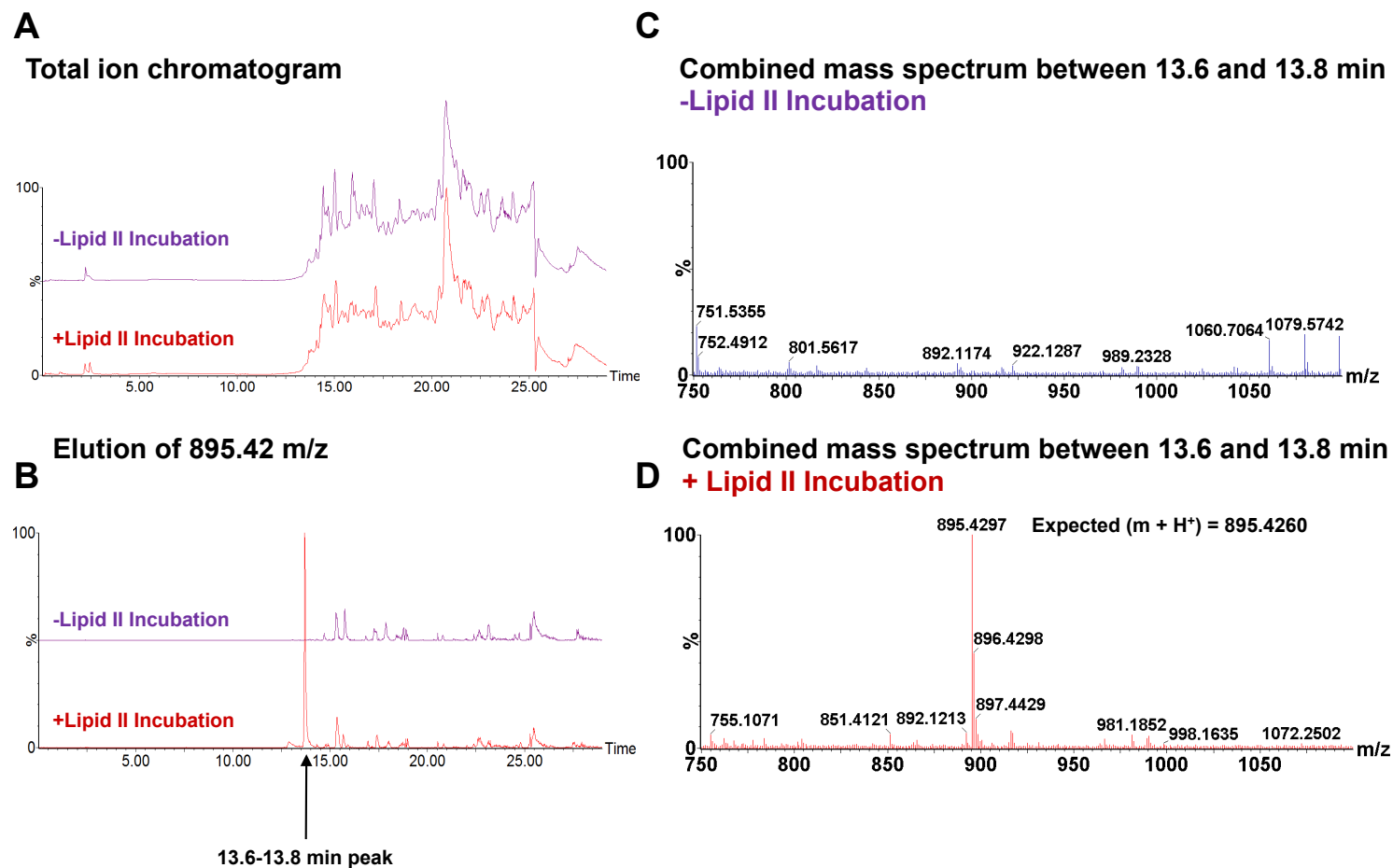
A

Total ion chromatogram

C

Combined mass spectrum between 13.6 and 13.8 min
-Lipid II Incubation

Elution of 895.42 m/z

B

D

Combined mass spectrum between 13.6 and 13.8 min
+ Lipid II Incubation

Figure A7.3: LC-MS (positive ion) detection of disaccharide-tetrapeptide (PBP1a D,D carboxypeptidase) A: Total ion chromatogram of +Lipid II and – Lipid II reactions. B: Elution of single peak containing ions with m/z consistent with disaccharide-tetrapeptide ([m+H$^+$] 895.42) in + Lipid II sample (absent in – Lipid II sample). C: Positive ion mass spectrum of elution between 13.6 and 13.8 min of –Lipid II incubation. D: Positive ion mass spectrum of elution between 13.6 and 13.8 min of +Lipid II incubation showing the m/z value consistent with the product ([m+H$^+$] expected 895.4260, observed 895.4297). Figure generated by Dr A. Lloyd.

Figure A7.4: LC-MS (positive ion) detection of disaccharide-pentapeptide (from Lipid II or its transglycosylation product) A: Total ion chromatogram of +Lipid II and – Lipid II reactions. B: Elution of two peaks containing ions with m/z consistent with disaccharide-pentapeptide ([m+H^{+}] expected 966.46) in + Lipid II sample (only one in – Lipid II sample). C: Positive ion mass spectrum of elution at 13.9 min of –Lipid II incubation. D: Positive ion mass spectrum of elution at 13.9 min of +Lipid II incubation showing the m/z value consistent with the product ([m+H^{+}] expected 966.46316, observed 966.4741). Figure generated by Dr A. Lloyd.
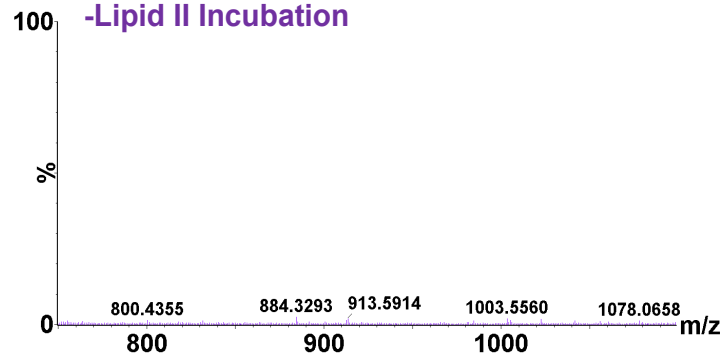
329

Appendix 8

Publications

This section contains the following publications (in the order listed):

Review Article

- Galley, N. F., O'Reilly, A. M., and Roper. D. I., Prospects for novel inhibitors of peptidoglycan transglycosylases. *Bioorganic Chemistry* **2014** 55**:** 16-26.

Primary Literature

- Paulin, S, Jamshad, M., Dafforn, T. R., Garcia-Lara, J., Foster, S. J., Galley, N. F., Roper, D. I., Rosado, H., Taylor, P. W., Surfactant-free purification of membrane protein complexes from bacteria: application to the staphylococcal penicillin-binding protein complex PBP2/PBP2a. *Nanotechnology* **2014**, 25, 285101-285108

- Zuegg, J., Muldoon, C., Adamson, G., McKeveney, D., Le Thanh, G., Premraj, R., Becker, B., Cheng, M., Elliot, A. G., Huang, J. X., Butler, M. S., Bajaj, M., Seifert, J., Sing, L., Galley, N. F., Roper, D. I., Lloyd, A. J., Dowson, C. G., Cheng, TJ., Cheng, WC., Demon, D., Meyer, E., Meutermans, W., Cooper, M. A., Carbohydrate scaffolds as glycosyltransferase inhibitors with *in vivo* antibacterial activity. *Nature Communications* **2015** 6, 7719-7730

Prospects for novel inhibitors of peptidoglycan transglycosylases

Nicola F. Galley [1], Amy M. O'Reilly [1], David I. Roper *

School of Life Sciences, University of Warwick, Coventry CV4 7AL, UK

ABSTRACT

The lack of novel antimicrobial drugs under development coupled with the increasing occurrence of resistance to existing antibiotics by community and hospital acquired infections is of grave concern. The targeting of biosynthesis of the peptidoglycan component of the bacterial cell wall has proven to be clinically valuable but relatively little therapeutic development has been directed towards the transglycosylase step of this process. Advances towards the isolation of new antimicrobials that target transglycosylase activity will rely on the development of the enzymological tools required to identify and characterise novel inhibitors of these enzymes. Therefore, in this article, we review the assay methods developed for transglycosylases and review recent novel chemical inhibitors discovered in relation to both the lipidic substrates and natural product inhibitors of the transglycosylase step.

© 2014 Published by Elsevier Inc. This is an open access article under the CC BY license (http://creativecommons.org/licenses/by/3.0/).

1. Introduction

In the search for new treatments of bacterial infections and to combat the increasing threat of resistance to existing antimicrobials, there is renewed interest in the exploitation of existing validated targets with novel approaches. With respect to bacterial cell wall biosynthesis, the validity of the peptidoglycan biosynthetic apparatus is well established, particularly in consideration of the fact that many of these antimicrobial targets exist at or beyond the extra-cytoplasmic surface of the cell membrane and are well conserved across all bacterial species [1,2]. The biosynthetic pathway leading to peptidoglycan precursor lipid II and the generalised scheme for its polymerisation into the peptidoglycan layer is well documented. Briefly, uridine 5′-pyrophosphoryl-N-acetyl muramyl-L-alanyl-γ-D-glutamyl-meso-diaminopimelyl-D-alanyl-D-alanine (UDP-Mur*N*Ac-L-Ala-D-Glu-L-(Lys/meso-DAP)-D-Ala-D-Ala) or its L-lysine derivative (UDP-Mur*N*Ac-L-Ala-D-Glu-L-(Lys)-D-Ala-D-Ala) is produced in the cytoplasmic pathway before linkage at the cytoplasmic membrane surface to an undecaprenyl (C55) carrier lipid, prior to the addition of Glc*N*Ac, forming lipid II [3]. This peptidoglycan precursor is then transferred to the outer surface of the cytoplasmic membrane where

it is polymerised by monofunctional transglycosylases and class A bifunctional Penicillin Binding Proteins (PBPs) into long glycan chains [4] (Fig. 1). The transpeptidase activity of Class A and B PBPs then produce inter-strand peptide cross-links from pentapeptides emanating from adjacent glycan chains. The resulting polymer has the mechanical strength and rigidity required to resist cytoplasmic osmotic stress and forms a scaffold for a number of extracellular structures and functions.

Both academic and industrial effort over many decades has been directed towards the transpeptidase function of the penicillin binding proteins (PBPs) in this context, with the development of many generations of β-lactam-based antibiotics [5]. However, there has been relatively little development directed towards the essential transglycosylase function required to provide the polymeric transpeptidase substrate, which can also be the product of the same bifunctional peptidoglycan biosynthetic enzyme [6]. Dual inhibition of both transglycosylase and transpeptidase functions would be a powerful antimicrobial strategy providing therapeutic options in a variety of scenarios, including those currently untreatable. Since the active site of the transglycosylase enzymes exist at the membrane surface where peptidoglycan intermediates are presented to the enzymes, this has been viewed as a difficult interface to target [7]. In addition, consideration of the catalytic function of the enzymes leads to the conclusion that the transglycosylase enzymes have long extended active sites, which traditionally have been viewed as more difficult to target [8]. Nevertheless, nature has already provided an exemplar solution to this issue in the form of the moenomycin group of antimicrobials, which appear to mimic the polymerised form of
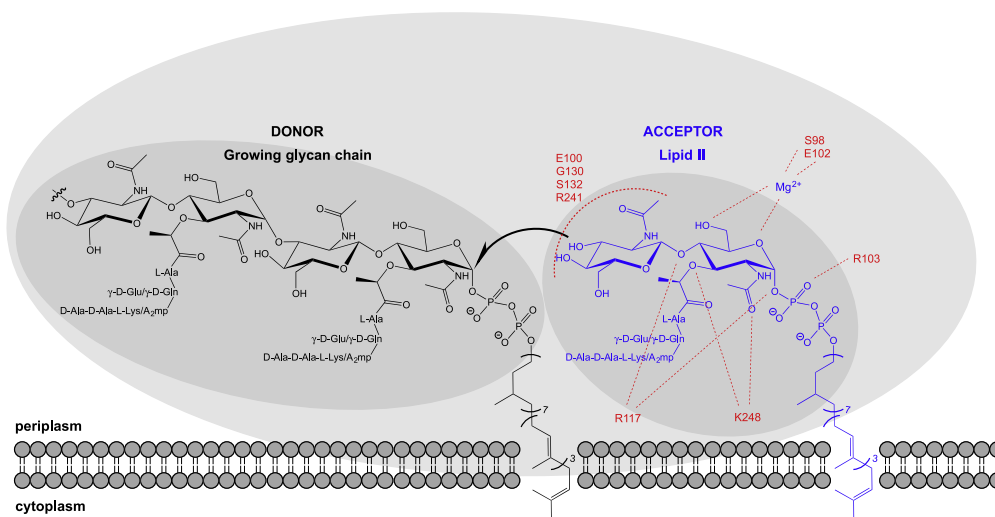
Fig. 1. Schematic diagram of the transglycoylase active site showing doner and acceptor sites. Residue numbers in the acceptor sites refer to those determined for *S. aureus* monofunctional transglycosylase in relation to lipid II analogue as described by Huang et al. [28].

the substrate within the transglycosylase active site. Poor pharmacokinetics prohibits the use of moenomycins in humans, yet this group of antibiotics has been used for decades in agriculture, principally in animal husbandry applications [9]. Remarkably, there is almost no incidence of resistance to these compounds, which implies that the transglycosylase activity may have significant attraction for future targeting.

Understanding the active site architecture of the transglycosylase through X-ray crystallographic analysis along with advances in biochemical study through the provision of native substrate and chemically defined probes, and the development of assay technologies that can support industry standard screening techniques, provide a new prospect for inhibitor discovery for new generation chemotherapy (Fig. 1). In this review article we provide a perspective of the assay technologies available and compounds recently discovered, that are pertinent in that context.

2. Assays for transglycosylase activity

Bacterial transglycosylases have been studied for over 50 years [10]. The discovery and development of novel transglycosylase inhibitors has been highly dependent on appropriate activity assays. However, progress has been hampered by the lack of quantitative and high throughput approaches capable of fast, accurate enzyme activity measurement. In addition, such efforts have been affected by the relative chemical complexity and lack of availability of the transglycosylase substrate, lipid II. Chemical and chemi-enzymatic approaches to overcome this hurdle have been reported by several groups, [11–22]. In addition, lipid II and other peptidoglycan intermediates have become available from the UK Bacterial Cell Wall Biosynthesis Network (UK-BaC-WAN). Since both the transglycosylase enzymes and substrate are within a lipid membrane environment, assay conditions and design needs to factor in these chemical properties and physical limitations. The solution of several X-ray crystal structures of mono-functional and bifunctional enzymes has enhanced structure based drug design efforts [7,23–28], an advance which has depended upon the design and implementation of reliable and accurate high-throughput assays. The following sections discuss the main assay types currently available, whilst Fig. 2 and Table 1 provide concise summaries.

2.1. Paper and thin layer chromatography

Paper chromatography was first used to study the full polymerisation of peptidoglycan using particulate enzyme preparations isolated from *Staphylococcus aureus* with radiolabelled UDP-*N*-acetylmuramyl-pentapeptide and UDP-*N*-acetylglucosamine as substrates [29]. The assay was adapted to use [^{14}C]-labelled lipid II with membrane protein preparations [22]. The use of penicillin to inhibit transpeptidase and carboxypeptidase activities of bifunctional PBPs facilitated analysis of the transglycosylation reaction, and the assay has been used for several studies [30–34]. Whilst scintillation counting allows collection of quantitative data in a stopped assay format, paper chromatography remains a cumbersome technique that is low throughput and lacks the ability to rapidly characterise the product post reaction.

Thin layer chromatography has also been used to study polymerisation, using fluorescent lipid II for detection [35]. With the fluorescent substrate, a dansyl reporting group was linked to the ε-amino group of the lysine side chain of the pentapeptide via a sulfonamide linkage to generate fluorescent dansyl lipid II. Transglycosylase kinetic parameters have been shown to be unaffected by the presence of this group (see Section 2.6 for further discussion).

The presence of a dansyl group prevents transpeptidation from occurring on this molecule, which results in a transglycosylation-specific assay when used as the sole substrate in a stopped assay format. Paper and thin layer chromatography are both highly sensitive techniques, allowing very small amounts of material to be detected. However, the assay remained inherently low throughput and qualitative.

2.2. Polyacrylamide gel based techniques

Transglycosylase activity can also be studied using a polyacrylamide gel based assay developed from a technique initially used in the late 1980s. Tricine–SDS–PAGE [36,37] is a variation on the more commonly used glycine SDS-PAGE that has been optimised for low molecular weight proteins. Glycan products made of repeating disaccharide units have a net negative charge, allowing their separation by electrophoresis, and shorter chain lengths in particular are within the optimum separation size range. The system was modified to separate the polymeric products of isolated transglycosylase domains using [^{14}C]-lipid II and lipid IV as
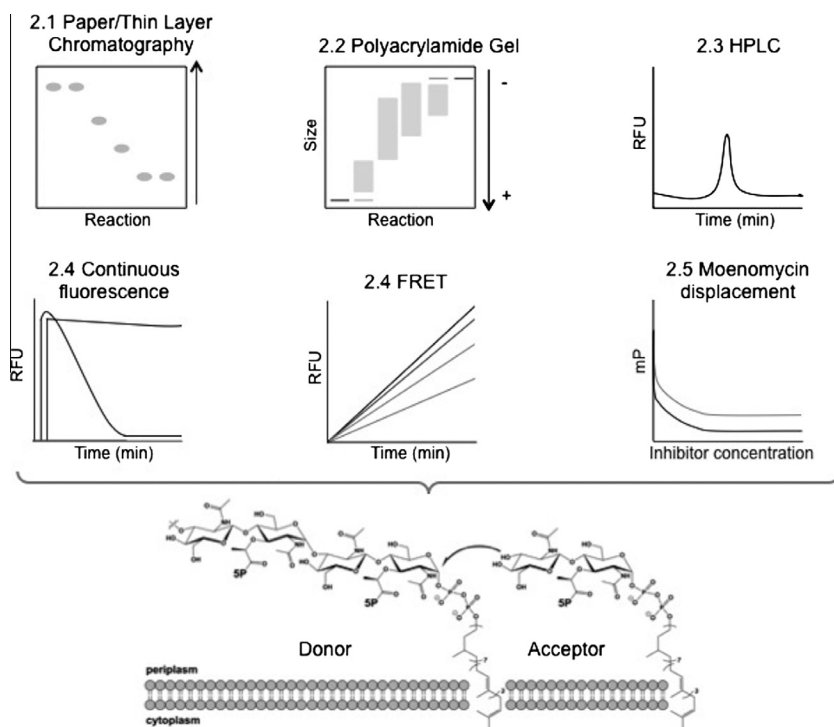
Fig. 2. Schematic of the main techniques currently available to assay transglycosylase activity allowing inhibitor discovery as discussed in Section 2. A cartoon representation of a typical reaction trace is shown for each technique and section numbers corresponding to the text are included.

substrates on a 9% acrylamide gel [38]. In additional experiments, full-length PBPs were used along with penicillin G to inhibit transpeptidase activity. These assays were able to detect the presence of polymeric products, and also allowed visualisation of a range of glycan chain lengths for the first time. Fluorescently labelled lipid II, as discussed above, can also be used as a substrate in gel-based assays [39].

The main strength of this technique is the unique ability to visualise discrete lengths of polymerised material. However this is only possible for shorter chain lengths, with longer polymerised material forming an unresolved smear or high molecular weight product, which does not enter the resolving gel phase [38,39], thus the techniques is not particularly sensitive. The main limitation with this approach is the lack of quantitative data in a continuous assay format. Unpolymerised and polymerised products can be quantified using densitometry for both fluorescent and radioactive material, and rates can be crudely estimated using time-course experiments. Nonetheless, gel-based assays are useful for studying the processivity of enzymes, and they allow simple comparison between different enzymes, which other systems cannot do at present. It has been reported that separation of glycan chains using this approach is not affected by other proteins, salts or additives in reaction buffers [38].

2.3. High-pressure liquid chromatography

High-pressure liquid chromatography (HPLC) has been used to separate native muropeptides extracted from bacteria [40] and adapted to identify the products of *in vitro* transglycosylase activity using suitably labelled fluorescent lipid II intermediates created either pre or post reaction [18,41] In the method described by Schwartz et al. 2001, reactions were in the presence of Penicillin G and products are labelled post reaction with fluorescamine via the ε-amino of lysine in the lipid II pentapeptide side chain before being separated by anion exchange [18]. Size exclusion chromatography has been used to separate mixtures of unlabelled

and Alexa 647-fluor labelled lipid II substrates and polymerised products [26]. In these cases the reaction products were applied directly to the column with no requirement for sample preparation, although *N*-acetylmuramidase digestion could also be used prior to separation [28]. When the lipid II substrate is radiolabelled, this technique can be adapted to monitor both transglycosylase and transpeptidase products of the reaction by appropriate post reaction enzymatic treatment of the resulting polymer [42,43] since the ε-group of lysine or DAP at position 3 of the pentapeptide stem is free to participate in transpeptidation. HPLC assays in this context are reasonably sensitive, allowing low levels of material to be detected, although sensitivity is dependent on the exact equipment being used and its capabilities.

2.4. Fluorometric continuous assays

The first continuous, coupled assay of transglycosylase activity reported was based upon the increased quantum yield of fluorescence signal from a dansyl fluorophore when in a hydrophobic micellar environment [41]. Under the assay conditions used, dansyl lipid II (see Section 2.1) is presented to the transglycosylase in detergent micelles, and can be polymerised into glycan chains. Whilst *N*-acetylmuramidase digestion of the glycan chains generates aqueous soluble labelled monomers, resulting in a reduction in fluorescence as the environment of the fluorophore changes from hydrophobic micellar environment to the soluble phase. The initial rate of this decreased fluorescence was attributed to incorporation of lipid II into glycan chains and was used to determine kinetic parameters for *Escherichia coli* PBP1b transglycosylase activity [41]. The presence of the dansyl group in the third position of the lipid II pentapeptide, prevented subsequent transpeptidation by bifunctional enzymes, allowing measurement of transglycosylation alone. This assay [41] has been converted to a multi-well format, which enables the rapid parallel screening of a range of reaction conditions [44]. This can allow, therefore, the screening and determination of optimal conditions for multiple

Table 1
Summary of transglycosylase activity assays as discussed in the text.

Assay type	Section number	Stopped or continuous	Sensitivity	Inhibitor screens
Paper/thin layer chromatography	2.1	Stopped	High	No
Polyacrylamide gel	2.2	Stopped	Low	No
HPLC	2.3	Stopped	Medium	No
Fluorometric: continuous fluorescence	2.4	Continuous	High	Yes
Fluorometric: FRET	2.4	Continuous	High	Yes
Moenomycin displacement	2.5	Continuous	High	Yes

transglycosylases from a range of microorganisms, essential in the study of these membrane proteins. In addition, this demonstrated the basis for utility of this assay in library screening of compounds to identify potential novel inhibitors, as did a second study [45].

Whilst measuring changes in fluorescence serve well for efficient enzyme and inhibitor characterisation, they are not always suitable for high throughput, pharmaceutical industry standard, compound screening. Thus, the development of time resolved Förster Resonance Energy Transfer (FRET) assays is of interest to address these requirements since it is possible to avoid contaminating fluorescence signals from compounds within the libraries screened. Huang et al. utilised a FRET-Based Lipid II Analogue (FBLA), with a Coumarin fluorophore in the third position of the peptide stem and a dimethylamino-azobenzenesulfonyl quencher in the lipid chain of the same substrate molecule [46]. Prior to polymerisation of the FBLA, the coumarin fluorescence is quenched, but once polymerised into glycan chains, the quencher is lost as the polyprenyl lipid tail is released from the transglycosylase-substrate complex, and the polymerised glycan product is fluorescent. Inclusion of N-acetylmuramidase to digest the glycan product into smaller and more soluble intermediates enhanced the fluorescence changes observed. When adapted to a 1536-well format, a very high throughput approach was achieved, and a library of 120,000 compounds was screened. A number of previously characterised inhibitors including moenomycin were identified in screens utilising a variety of Class A PBPs (including *Acinetobacter baumannii* PBP1b, *Clostridium difficile* PBP, *E. coli* PBP1b, *Klebsiella pneumoniae* PBP1b, and *Mycobacterium tuberculosis* PonA1). This was the first application of FRET in the study of transglycosylation, and represents a new sensitive method for continuously following transglycosylation activity.

The high throughput nature of these assays is a clear advantage, and the ability to continuously monitor enzyme activity and accurately determine kinetic parameters for a wide range of conditions and enzymes makes this a powerful approach. Both types of fluorometric assay described here measure overall transglycosylation rates, and are capable of identifying inhibitors which interfere with substrate availability as well as those that directly inhibit enzyme activity, which may increase the range of possible lead compounds identified. However, both assays use a modified lipid II substrate that differs from the native substrate by addition of large fluorescent groups, and this will be discussed further in Section 2.6.

2.5. High throughput screening based on moenomycin displacement

A different approach to high throughput assay design has been taken by a number of groups, based upon chemically modified derivatives of moenomycin, which binds to the transglycosylase active site with high affinity.

Following a surface plasmon resonance (SPR) study of various immobilised Class A PBPs binding to moenomycin, Cheng et al. designed a highly sensitive fluorescence anisotropy based assay utilising a fluorescein labelled moenomycin (F-Moe) [47]. When bound to the transglycosylase active site F-Moe displayed fluorescence anisotropy properties which decreased when the

F-Moe was displaced by compounds binding competitively to the active site at comparable or greater affinity. Of all class A PBP homologs tested, it was found that a combination of *Helicobacter pylori* PBP1a with F-Moe had a Kd of 25 (±14) nM and anisotropy reaching 0.2 upon binding of the ligand. This high throughput assay was used to screen 57,000 compounds with a Z′ value of 0.895, which proved valuable as a robust initial screen and identified a number of moenomycin derivatives and small molecules, with 3 small molecule hits showing both antibacterial and transglycosylase inhibitory action (HTS6-8) (Table 2). The major limitation of this approach is the inability of compounds with relatively low affinity to displace high affinity moenomycin, precluding for example fragment based drug design or delineation of structure activity relationships of transglycosylase inhibitors.

Gampe et al. described a fluorescence polarisation, displacement assay based upon the binding of a fluorescently labelled, truncated analogue of moenomycin that displayed weaker binding than moenomycin A [48]. This fluorescent probe represented a minimal pharmacophore to specifically identify low micromolar inhibitor binding to the transglycosylase active site and was designed from a consideration of the X-ray crystal structures of moenomycin in complex with transglycosylase active sites. This probe was used in 1536-well plate format using non-essential *S. aureus* monofunctional transglycosylase enzyme SgtB [49], against 110,000 compounds in the Harvard Medical School screen, resulting in a Z′ value of 0.78 and initially identifying 186 hits [48]. After dose response studies and the elimination of fluorescent compounds from the initial hits, a number of leads were identified including one (Compound 10) with inhibition constants ranging from 2.6 mM to 95 nM against transglycosylase enzymes from *S. aureus*, *Enterococcus faecalis*, and *E. coli* (Table 2).

Both the assays described by Cheng et al. [47] and Gampe et al. [48] utilise the properties of existing drug-enzyme interaction for the basis of detection, eliminating the need for lipid II substrates in the primary screen and the detection of the reaction products. Both are also sensitive methods, which can detect low levels of displacement. However these assays rely on chemical modification of the pharmacophore for detection in a fluorescence mode and the ability of library compounds to displace existing interactions between enzyme and that pharmacophore.

2.6. Prospects for assay development in transglycosylase inhibitor discovery

The transglycosylase activity of purified, recombinant PBPs is highly sensitive to the conditions *in vitro*. In particular: temperature, DMSO, detergents and divalent cations can have significant effects [41,44,50,51]. Also, despite recent advances in membrane protein biochemistry, the level of understanding of the separate functions of Class A PBPs and MGTs and more importantly, their coordinated activity with other cell wall biosynthetic proteins as well as cell division is still somewhat lacking. Additionally, studies have shown that the transmembrane portion of the PBPs may be highly involved in substrate binding as well as in transglycosylase activity [27,28,39]. In fact, enzyme activities of full-length enzymes

Table 2
Reference and chemical structure of transglycosylase inhibitors discussed.
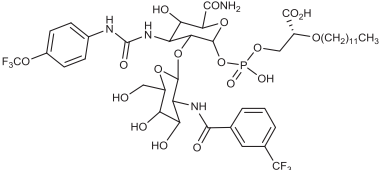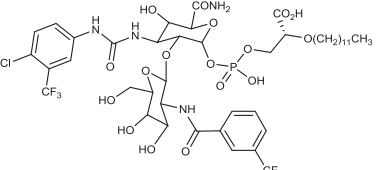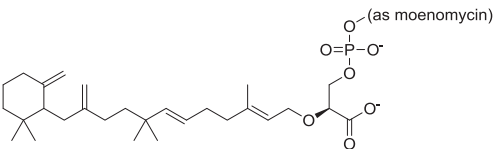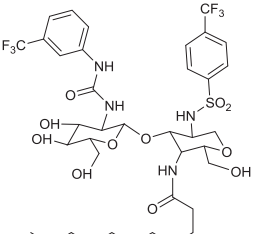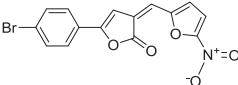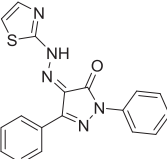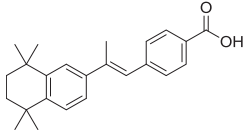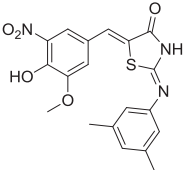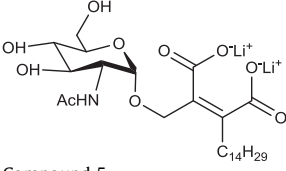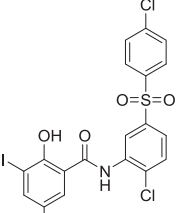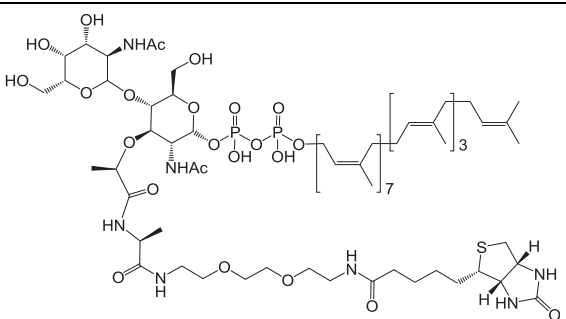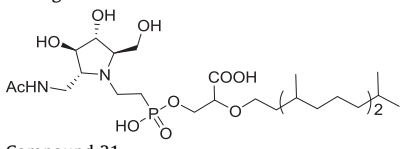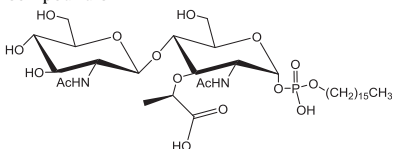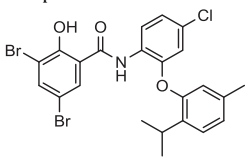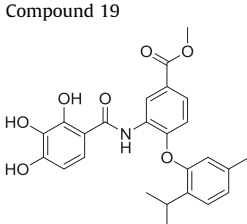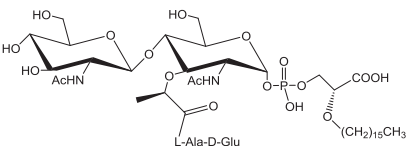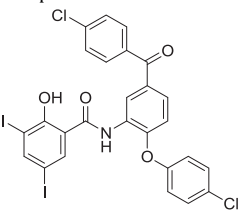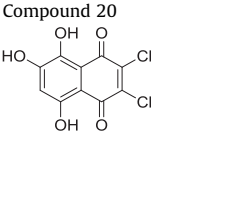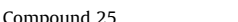
Reference	Compound name/features	Year
Sofia et al. [68]	TS30153 TS30663 TS30888	1999
He et al. [72]	AC326-α	2000
Halliday et al. [6]	ACL 19273	2006
Cheng et al. [47]	HTS-6 HTS-7 HTS-8	2008
Gampe et al. [48]	Compound 10	2013
Garneau et al. [76]	Compound 5	2004
Cheng et al. [80]	Compound 24	2010

Table 2 (continued)

Reference	Compound name/features	Year
Huang et al. [28]	 Analogue 3	2012
Huang et al. [28]	 Compound 31	2012
Dumbre et al. [78]	 Compound 21 Compound 62	2012
Huang et al. [46]	 Compound 19 Compound 20	2013
	 Compound 24 Compound 25	

are often higher than the truncated forms, which supports this hypothesis. Assaying full-length enzymes in a membrane environment and in the presence of a full complement of cell wall proteins may be a highly significant factor in future inhibitor discovery, and this is undoubtedly highly challenging.

It has been demonstrated that transglycosylase kinetic parameters are largely unaffected by addition of side groups on the third position lysine or DAP of the lipid II pentapeptide [16,41]. The effects of fluorophores on the lipid and peptide chains were compared, and those on the lipid chain appear less likely to interfere with enzyme-substrate recognition [52]. Even taking this into consideration, the kinetic parameters measured still appear too low to meet the demands of growing and dividing cells. In order to support growth, an *E. coli* cell would require 300 transglycosylase reactions/minute/molecule, but published data on *E. coli* PBP1a (as a representative example) *in vitro* gave only 0.8 transglycosylase reactions/minute/molecule [53]. Thus, there is a significant gap between observed *in vitro* behaviour and that required to support life *in vivo*, leading to the hypothesis that other regulatory and coordinating factors are necessary for a more accurate reflection of transglycosylase activity during *in vitro* analysis [54].

Taking all of the above into account, it may be desirable to measure alternative product release, rather than polymerised product, to follow transglycosylase reactions [13]. Despite this approach being unsuccessful to date, the concept could pave the way for new ideas on how to assay these biologically and pathophysiologically important enzymes. Eventually it may be advantageous to move away from utilisation of highly modified substrates for enzyme characterisation, and minimise the differences from the physiological substrates. Furthermore, it is apparent that PBPs function in a coordinated manner, and it may be intuitive to include multiple enzymes in assays. Several groups have developed high throughput assays of the coupled transglycosylase-transpeptidase activities of peptidoglycan synthesis using membranes as a source of PBPs [50,55,56], in which the transglycosylases can make many of the interactions they would make *in vivo*, and are thus being studied in a more physiologically relevant environment.

3. Known inhibitors of peptidoglycan transglycosylase enzymes

As previous eluded to, peptidoglycan transglycosylases are under-exploited as antimicrobial drug targets, despite their key

and clear role in an area of bacterial metabolism that is a validated target for a number of existing antibiotics. Moreover, since most pathogens have at least two transglycosylase enzymes required for peptidoglycan biosynthesis which utilise the same mechanism, resistance to novel compounds would require simultaneous and multiple compensatory mutations. Additionally, the fact that the natural product moenomycin has been used for several decades in agriculture without reports for resistance [57], suggests promise in the search for novel inhibitors targeting the same mechanism, but requiring more acceptable pharmacokinetic properties for human use. The structure, biosynthesis and chemical properties of moenomycin have been reviewed extensively in the recent past [9] and will not form part of this discussion except for reference to the binding site within the transglycosylase active site. The transglycosylases are processive enzymes utilising a donor site in which the growing glycan chain resides anchored to the membrane by the undecaprenyl chain of the previously appended lipid II, and an adjacent acceptor site for the incoming lipid II monomer. As a result, the enzyme active site is comparatively long and extended and must accommodate at least four sugar binding sites. Similar active site architecture is seen in lysozyme which also binds alternating N-acetylglucosamine and N-acetylmuramic acid repeat units [8]. In the following section, we summarise the latest advancements in inhibitors of transglycosylation, including those based on moenomycin and its analogues, as well as analogues of lipid II.

3.1. Moenomycin: The 'blueprint' transglycosylase inhibitor

The moenomycins are a family of glycolipid antibiotics naturally produced as a complex of related compounds by Streptomyces ghananensis with moenomycin A representing the major component with antimicrobial activity [9,58]. Moenomycin consists of a pentasaccharide of units B, C, D, E and F with a chromophore (unit A) and a C25 lipid chain connected to the F saccharide via a phosphoglycerate linker (see Fig. 3). The C25 chain is required for antimicrobial action and in essence the moenomycin structure resembles that of the lipid IV product formed within the transglycosylase active site [59].

Moenomycin has amphiphilic properties due to the hydrophilic nature of the A to F carbohydrate units, the phosphate group of the phosphorglycerate linker and the folded hydrophobic domain formed by the lipid chain. Structure-activity relationships have been carried out on the moenomycin A molecule through selective degradation of its structure and the synthesis of di- and trisaccharide analogues, resulting in an understanding of the minimal pharmacophore [9,60,61]. The degradation of moenomycin to chemical entities that retain the carbohydrate units C, E and F, can be performed with retention of transglycosylase inhibition and antibacterial activity [62,63]. Degradation to retain only the E and F carbohydrate units, still yields transglycosylase inhibition but with the loss of antibacterial activity [64]. The C25 lipid chain is required to achieve full anti-bacterial activity of moenomycin, but is also the origin of its long half-life and contributes to its poor bioavailability and incompatibility for human consumption [9]. Decreasing the length of the lipid chain slowly reduces the inhibitory ability of moenomycin [63], most likely due to loss of ability to anchor itself into the cytoplasmic membrane. Modifying or truncating the lipid chain improves pharmacokinetic properties but the loss of activity needs to be compensated by maintaining essential polar active-site contacts or by utilisation of other hydrophobic chemophores with acceptable properties.

3.2. The binding of moenomycin and lipid II to transglycosylase

The two natural molecules known to bind to the transglycosylase domain of PBPs are moenomycin and lipid II. The structural

differences between the two must be responsible for inhibition (Fig. 1), as lipid II is the natural substrate for transglycosylation and moenomycin is the most potent inhibitor. Understanding how these two molecules interact and bind to the transglycosylase domain is fundamental in pursuing structural analogues for inhibition.

Moenomycin A binds with high affinity to the transglycosylase domain of several Class A PBPs and is the most potent inhibitor of the transglycosylase function of PBPs with MICs in the region of 0.01–0.1 μg/mL [58]. The mode of inhibition of moenomycin is such that it directly (and reversibly) binds to the active site of the transglycosylase domain, preventing lipid II polymerisation. It first binds to the cytoplasmic membrane via its lipid chain, followed by selective binding of the sugar moiety to the donor site of the transglycosylase.

The transglycosylase domain contains five motifs representative of the GT_{51} fold-family [65] and which are conserved among both mono- and bi-functional PBPs. Six residues in the transglycosylase domain have been identified as important in the interaction with moenomycin in Aquifex aeolicus PBP1A [24,25], and are conserved across other species. These 6 interactions bind to the F-ring and the phosphoglycerate portion of the drug. The transglycosylase active site is buried in the membrane in order to access the lipid II substrate, explaining the need for a lipid chain on moenomycin A for its inhibitory potency. It is thought that the C25 chain of moenomycin interacts with the transmembrane (TM) segment of E. coli PBP1B [47], increasing the binding affinity 5-fold of moenomycin to the transglycosylase domain, highlighting the importance of the TM domain for activity. The regions of moenomycin that make essential contacts with the transglycosylase domain include the C2 on the E ring, C3 on the F ring, the phosphoglycerate moiety and possibly the C10 region of the moenocinol lipid tail. The phosphoryl group and the carboxylate moiety form interactions with conserved active site residues of the transglycosylase domain [66]. The A unit chromophore is not essential for the interaction but may provide higher binding affinity [9].

At the time of writing, the only structural information available for the interaction of lipid II with the transglycosylase domain is that derived from the X-ray crystal structure of S. aureus non-functional glycosyltransferase with an analogue of Lipid II [28]. The lipid II analogue used in this study has an undecaprenyl lipid tail, biotinylated ethylene glycol diethyl amine in place of the pentapeptide stem and GalNAc in place of GlcNAc in the disaccharide moiety and has a Kd of 12.9 μM. Despite the clear importance of the undecaprenyl lipid tail of lipid II for location of the substrate in relation to the enzyme active site, only a discrete section of the disaccharide-pyrophosphate moiety of the lipid II is represented in the electron density at 2.3 Å resolution. The presence of GalNAc within the lipid II analogue precludes its elongation in the normal transglycosylation reaction, since the position 4 hydroxyl on the sugar ring is in the opposite orientation compared to GlcNAc. but is proposed to bind more tightly to the active site as the distance between that hydroxyl and main-chain carbonyl of G130 is reduced [28].

In consideration of lipid II binding to both the donor and acceptor sites of transglycosylase, lipid II is thought to bind at a lower affinity for the donor site compared to that of lipid IV [14] and this is consistent with the observation of a lag phase in catalysis, seen with many transglycosylase enzymes in the presence of lipid II substrate only. Many inhibitors that bind to transglycosylases occupy the donor site, mimicking the elongating chain of polymerised lipid II [7]. Lovering and co-workers have proposed that moenomycin structurally mimics lipid IV [7,23], a supposition further supported in that lipid IV and moenomycin are suggested to bind to the same site on the transglycosylase domain [67] and that lipid IV may bind to E. coli PBP1B with a higher affinity than lipid II [14].
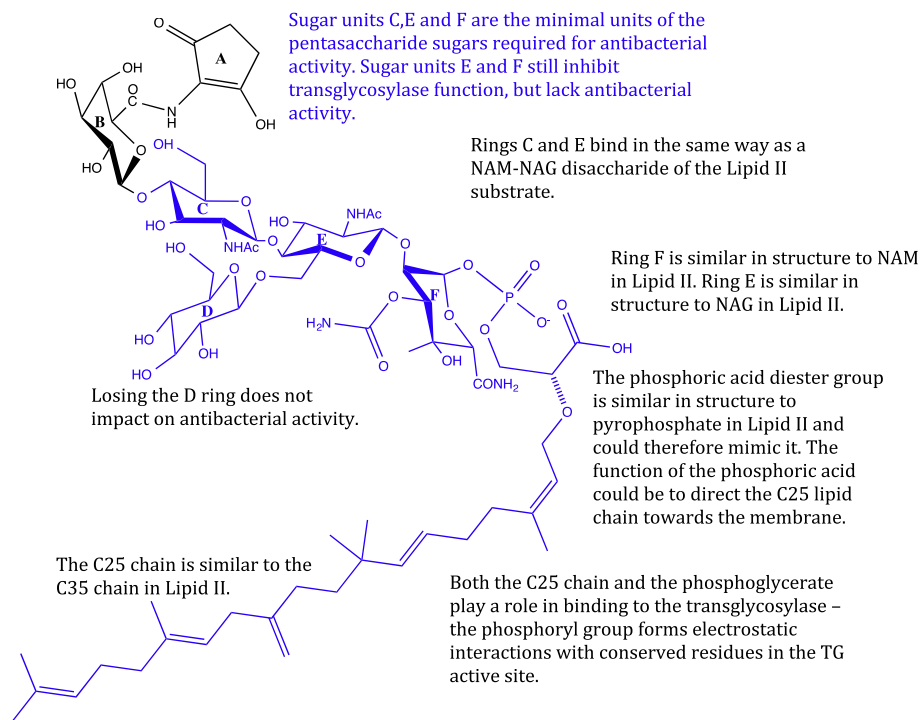
Fig. 3. The structure of Moenomycin A, the only known potent inhibitor for bacterial transglycosylases. The region highlighted in blue is the minimal inhibitory pharmacophore, which is often used as a scaffold for the design of new potential inhibitors (discussed in Section 3.1).

3.3. Moenomycin analogues

Finding that the moenomycin degradation products exhibit inhibitory activity against transglycosylases prompted a study in 1999 by Sofia et al., to develop a combinatorial library of 1300 analogues of the moenomycin disaccharide core [68]. These analogues explored modifications at C2 of the E ring and C3 of the F ring (the critical interaction points with the transglycosylase domain). Modifications included aromatic groups attached to the E and F rings and a lipid tail of 12 rather than 25 carbons. Three compounds showed particular promise (Table 2: TS30663, TS30153 and TS30888, with some being more active than the EF disaccharide. These compounds were orders of magnitude less potent than the parent molecule moenomycin, but had IC_{50} values in the range of 10–15 µM [69]. These putative inhibitors also exhibited activity against Gram-positive strains including *Enterococcus faecium* which have tolerance to moenomycin, highlighting that simple degradation compounds show potency against clinically relevant pathogens. The IC_{50} values obtained are within a similar range to other cell wall inhibitors such as bacitracin, vancomycin and ramoplanin. These compounds showed differing activities against transglycosylases in different species, suggesting that they may target different subsets of the transglycosylases [70] as is also seen for β-lactams [71]. A new member of the moenomycin group AC326-α was introduced by He et al. (2000) which has a cyclic moenocinol chain, giving a diumycinol chain [72]. Branched chain lipids show more potent antibacterial activity than linear chained lipids. Putative inhibitors could be designed to mimic moenomycin and could exhibit antibacterial activity to cyclic lipid chains.

Halliday et al. [6] presented a class of compounds from Alchemia, based on the disaccharide scaffold of Sofia et al. [68] with a focus on maintaining the important transglycosylase binding regions. The hits had MIC values of 1–4 µg/mL, against a broad range of Gram-positive organisms [6,68]. One example compound from this class: ACL 19273, showed direct binding and inhibition of the transglycosylase domain, potentially binding to either the acceptor or donor site of the enzyme [6]. Inhibitors that bind to the transglycosylase acceptor site, which may be the case for these small disaccharides, are binding to the contrary site to where moenomycin binds. Determining whether inhibitors bind to the donor or acceptor site of the transglycosylase is important is elucidating their mode of action.

3.4. Lipid II analogues

In the early 1990s, efforts were focused on synthesizing transglycosylase inhibitors based on monosaccharide and disaccharide analogues of lipid II, but most were not very active [73–75]. A combination of mono- and disaccharide analogues of lipid II and moenomycin were synthesised by Garneau et al. based on the active part of moenomycin and combining with structural features of lipid II [76]. A lipid II monosaccharide analogue, Compound 5, was designed to mimic the pyrophosphate of lipid II with a dicarboxylate group. Modest activity with just monosaccharide analogues was exhibited, with 28% inhibition of transglycosylases at 100 µM [76]. Clearly the potency of such compounds is weak and it may be that monosaccharide analogues do not have comparable complexity to moenomycin, to sufficiently inhibit transglycosylases [77].

Lipid I and lipid II substrate analogues (both mono- and disaccharides) were synthesised by Terrak and co-workers [77–79] to test the consequences of variations in the lipid chain length, the pyrophosphate and the length of the peptide stem. The disaccharide analogues were 2-fold greater inhibitors than their cognate monosaccharides and as the length of the peptide stem increased from no peptide to l-Ala-d-Glu, to l-Ala-d-Glu- l-Lys, inhibition decreased. This was attributed to the presence of a peptide preventing high affinity binding between the GlcNAc and the transglycosylase. Analogues were tested to highlight important moieties for the future design of substrate-based inhibitors with two hits: C16-phosphoglycerate-MurNAc-GlcNAc (Compound 21) and C16-phosphoglycerate-MurNAc-(l-Ala-d-Glu)-GlcNAc (Compound 62).

The latter was most active, exhibiting inhibitory activity against the transglycosylase as well as antibacterial ability.

The continuous and quantitative FRET-based assay by Huang and co-workers (as described in Section 2.4) was used to screen a 120,000 compound library containing a variety of bioactive and synthetic molecules, including lipid II analogues [46]. Initially, 25 primary hits were revealed which were subjected to secondary screening. Dose-dependent studies using HPLC and other FRET-based assays identified 7 compounds as transglycosylase inhibitors. The antibacterial activities and MICs were acquired, which showed activity against *S. aureus* and *M. smegmatis*, but not Gram-negative bacteria tested (*E. coli, Pseudomonas aeruginosa* and *A. baumannii*). Compounds 19 and 20 were competitive inhibitors of transglycosylase and compounds 24 and 25 were active small molecule inhibitors, with 24 being a previously identified hit [80] with a salicylanilide core structure.

Huang et al. solved the crystal structure of *S. aureus* MGT (SaMGT) in complex with a lipid II substrate analogue, Analogue 3, designed with an inverted 4-OH group on the GlcNAc, which can bind more tightly to the lipid II binding pocket [28]. The compound was used as a donor substrate only, and bound to the SaMGT acceptor site. The purpose of this analogue was primarily as a means to understand binding interactions with the transglycosylase domain, rather than as an inhibitor *per se*.

The role of the pentapeptide moiety in lipid II and its mode of interaction with the transglycosylase has been explored [81]. Lipid II analogues with an assortment of peptide stems were synthesised to analyse their capabilities as transglycosylase substrates. Modifications include incorporating a fluorescent NBD label into position 3 of the peptide or a d-lactyl group at the hydroxyl group of MurNAc. Surface Plasmon Resonance binding studies were conducted to determine the binding affinity of these analogues to transglycosylase. The three main conclusions from this work were (a) the terminal d-Ala-d-Ala is *not* essential for substrate binding and does not significantly interact with the transglycosylase domain, (b) the fluorescent probe NBD on the ε-amino group of the 3rd position lysine does not affect binding affinity to transglycosylase and (c) the minimum structural requirement for the peptide moiety in lipid II as a transglycosylase is d-lactyl-l-Ala. Further research has shown that only the d-lactyl of the MurNAc is required for the substrate binding to transglycosylase [78].

3.5. Vancomycin derivatives bind to transglycosylase

The natural product antibiotic vancomycin normally inhibits peptidoglycan polymerisation by binding to the terminal d-Ala-d-Ala moiety on the lipid II pentapeptide stem, inhibiting transpeptidation. Controversially, hydrophobic vancomycin derivatives have been shown to inhibit peptidoglycan polymerisation through preventing transglycosylation, most likely through binding the transglycosylase domain of PBPs and in the absence of dipeptide and depsi-peptide binding [34,82–84]. Common examples of vancomycin derivatives have lipid moieties at the aglycone or on the carbohydrates. One is produced from alkylating vancomycin on the vancosamine sugar with chlorobiphenyl, giving chlorobiphenyl-vancomycin (CBP-V) [85] (Fig. 4). CBP-V showed antibacterial activity against vancomycin-resistant strains, e.g. vancomycin-resistant *Enterococci* (VRE), where the di-peptide moiety in lipid II is substituted for d-Ala-d-lactate.

When the vancomycin N-terminal methyl leucine required for binding d-Ala-d-Ala, was removed from chlorobiphenyl vancomycin (yielding chlorobiphenyl desleucyl-vancomycin), the derivative retained antibacterial activity for both sensitive and resistant bacteria, despite no longer being able to bind its di-peptide ligand [85]. In contrast, when the N-terminal methyl-leucine was removed from full-length vancomycin, it could no longer bind to

the d-Ala- d-Ala of lipid II and so was no longer active. The mechanism of action of chlorobiphenyl desleucyl-vancomycin on vancomycin sensitive strains is through either binding the d-Ala-d-Ala of lipid II, or by preventing transglycosylation. Chlorobiphenyl desleucyl vancomycin is missing an important portion of the di-peptide binding pocket [85]. Activity of the vancomycin derivatives decreases when the peptide-binding pockets are damaged [34], suggesting that inhibition is through a mechanism not involving di-peptide binding [84].

4. Prospects for new transglycosylase inhibitors

Developing new drugs with antibacterial properties through inhibition of peptidoglycan transglycosylation is of current interest to both academia and the pharmaceutical industry. Currently, most compounds discovered, summarised in Table 2 have greater potency against Gram-positive bacteria than Gram-negative presumably due to accessibility, as is the case with many other targeted compounds. Progress on the development of transglycosylase inhibitors has been slow historically due to complexity of the active site of the enzymes, lack of suitable assays for high throughput screening, provision of suitable substrates for such assays and the difficulties surrounding the reconstitution of activity of these membrane proteins. The availability of lipid II substrate from chemi-enzymatic and total chemical synthesis domains allows transglycosylases from various species to be studied along with a growing literature detailing molecular architecture interactions within the active site. Further understanding of substrate specificity will aid the design of future substrate analogues, common features of which are becoming apparent.

The development of glycolipids and glycopeptides as putative transglycosylase inhibitors has shown that there are new prospects for the combinatorial biosynthesis of phosphoglycolipid antibiotics [86] and there are new generation glycopeptides currently in clinical development that inhibit the transglycosylation process [87].
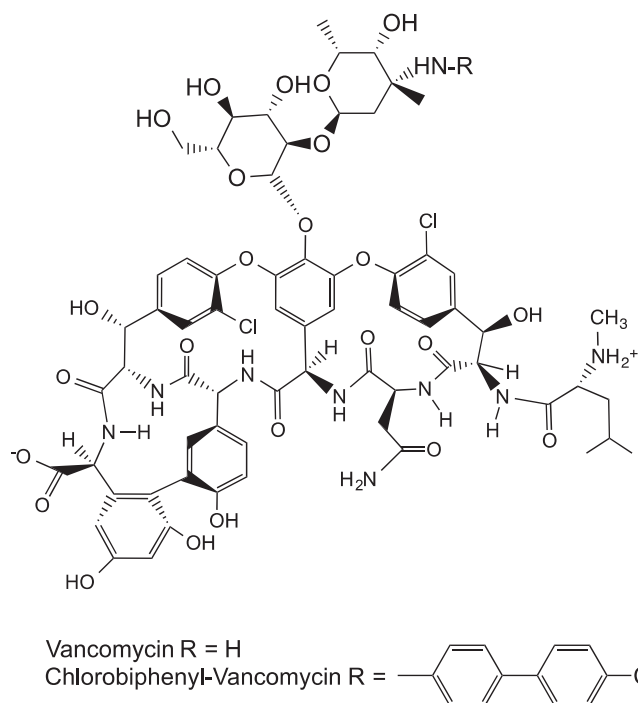

Fig. 4. The structure of vancomycin and its derivative chlorobiphenyl vancomycin (CBP-V), which showed antibacterial activity against vancomycin-resistant *Enterococci* (VRE) [85] (discussed in Section 3.5).

In addition, research is on-going to determine the exact inhibitory mechanism of moenomycin on transglycosylases, with a drive towards finding novel inhibitory compounds with distinct structural features. Total synthesis of moenomycin A has been achieved [88] and the biosynthetic pathway variants can be theoretically generated which could help in the quest to design new compounds with better pharmacokinetics [89].

We now have the ability to synthesise structurally diverse substrates and to combine synthetic and biological compounds by either enzymatic modification of synthetic analogues or by chemical modification of biosynthetic intermediates. These capabilities enable better comprehension of the role of lipid II in binding to the transglycosylase domain and help to optimise structures for the transglycosylase donor and acceptor sites. These sites have different requirements for lipid chain length, which is important for the processivity of the transglycosylase, with the donor site requiring a C20 lipid chain and the acceptor site tolerating shorter lipids, so there is a compromise between lipid chain length and antibiotic activity [90]. Walker and co-workers have predicted that lipid II with four successive *cis* isoprene units in a 35-carbon chain is the best transglycosylase substrate [21]. Investigating the optimal substrate for transglycosylases such as lipid IV or longer as potential substrate inhibitors may be a worthwhile focus and could be fruitful in generating moenomycin mimics, without the poor pharmacokinetics [14]. Despite the evolution of structurally diverse substrates, there is still more room to understand transglycosylase-substrate mimics.

The structures of transglycosylase domains resemble more closely the structures of glycosidases such as lysozyme, rather than other glycosyl-transferases. Therefore, glycosidases may be better representatives for inhibitor design and lessons may be learned from several decades of experience with the great glycosyl-transferase families [65]. Although there are now in the region of ten structures of transglycosylase enzymes in the protein data-bank, only a small subset are below 2.5 Å resolution and thus reliable for structure based drug design efforts. This does include however the *S. aureus* monofunctional enzyme in apo (2.5 Å) and lipid II analogue (2.3 Å) forms [28] and the 2.2 Å *E. coli* PBPIb structure in complex with moenomycin [27]. Curiously, the latter structure is monomeric whereas the enzyme in solution has been shown to dimerise at a Kd well below that achieved in both crystallisation and presumable *in-crystallo* [42]. The recent crystal structures of transglycosylase domains in complex with moenomycin have highlighted essential interactions but their significance in structure based drug design efforts must be viewed in the context of the overall processive transglycosylase mechanism.

In the recent past, a number of robust high throughput assays for screening have emerged that provide new prospects for inhibitor discovery. As with all such efforts, the quality and suitability of such libraries must be carefully considered to maximise the potential outputs. The development of a fluorescence polarisation based assay utilising a weaker binding derivative of moenomycin in a displacement assay scenario is particularly encouraging in this respect [48]. Cell based screening assays are also worthy of discussion in this context since they preselect those compounds with the required properties to gain entry to the target cell and are selected on bacteriostatic or bactericidal effects. A set of compounds with a non-carbohydrate, salicylanilide core were identified by Cheng et al. and showed modest inhibitory action against transglycosylases, providing an alternative starting point for medicinal chemical approaches [80].

Further knowledge of the catalytic mechanism and *in vivo* regulation of transglycosylation activity may provide further insight into the chemistry of potential novel lead compounds required for effective chemotherapeutic intervention. Given the renaissance of interest in antimicrobials, the growing concern by public and policy makers regarding antibiotic resistance, the development of new approaches and collaborative efforts between academia and pharma, progress in inhibitor design against transglycosylase may be on the horizon.

Acknowledgments

References

[1] T.D. Bugg, D. Braddick, C.G. Dowson, D.I. Roper, Trends Biotechnol. 29 (2011) 167–173.
[2] L.L. Silver, Clin. Microbiol. Rev. 24 (2011) 71–109.
[3] H. Barreteau, A. Kovac, A. Boniface, M. Sova, S. Gobec, D. Blanot, FEMS Microbiol. Rev. 32 (2008) 168–207.
[4] P.J. Mattei, D. Neves, A. Dessen, Curr. Opin. Struct. Biol. 20 (2010) 749–755.
[5] M.P. Page, Beta-lactam antibiotics, in: T.J. Dougherty, M.J. Pucci (Eds.), Antibiotic Discovery and Development, Springer, US, 2012, pp. 79–117.
[6] J. Halliday, D. McKeveney, C. Muldoon, P. Rajaratnam, W. Meutermans, Biochem. Pharmacol. 71 (2006) 957–967.
[7] A.L. Lovering, M. Gretes, N.C. Strynadka, Curr. Opin. Struct. Biol. 18 (2008) 534–543.
[8] A.L. Lovering, S.S. Safadi, N.C. Strynadka, Annu. Rev. Biochem. 81 (2012) 451–478.
[9] B. Ostash, S. Walker, Nat. Prod. Rep. 27 (2010) 1594–1617.
[10] J.S. Anderson, M. Matsuhashi, M.A. Haskin, J.L. Strominger, Proc. Natl. Acad. Sci. USA 53 (1965) 881–889.
[11] C. Fraipont, F. Sapunaric, A. Zervosen, G. Auger, B. Devreese, T. Lioux, D. Blanot, D. Mengin-Lecreulx, P. Herdewijn, J. Van Beeumen, J.M. Frere, M. Nguyen-Disteche, Biochemistry 45 (2006) 4007–4013.
[12] H.W. Shih, K.T. Chen, S.K. Chen, C.Y. Huang, T.J. Cheng, C. Ma, C.H. Wong, W.C. Cheng, Org. Biomol. Chem. 8 (2010) 2586–2593.
[13] H. Liu, C.H. Wong, Bioorg. Med. Chem. 14 (2006) 7187–7195.
[14] H.W. Shih, K.T. Chen, T.J. Cheng, C.H. Wong, W.C. Cheng, Org. Lett. 13 (2011) 4600–4603.
[15] C.M. Gampe, H. Tsukamoto, T.S. Wang, S. Walker, D. Kahne, Tetrahedron 67 (2011) 9771–9778.
[16] Y. Zhang, E.J. Fechter, T.S. Wang, D. Barrett, S. Walker, D.E. Kahne, J. Am. Chem. Soc. 129 (2007) 3080–3081.
[17] E. Breukink, H.E. van Heusden, P.J. Vollmerhaus, E. Swiezewska, L. Brunner, S. Walker, A.J. Heck, B. de Kruijff, J. Biol. Chem. 278 (2003) 19898–19903.
[18] B. Schwartz, J.A. Markwalder, Y. Wang, J. Am. Chem. Soc. 123 (2001) 11638–11643.
[19] M.S. VanNieuwenhze, S.C. Mauldin, M. Zia-Ebrahimi, J.A. Aikins, L.C. Blaszczak, J. Am. Chem. Soc. 123 (2001) 6983–6988.
[20] M.S. VanNieuwenhze, S.C. Mauldin, M. Zia-Ebrahimi, B.E. Winger, W.J. Hornback, S.L. Saha, J.A. Aikins, L.C. Blaszczak, J. Am. Chem. Soc. 124 (2002) 3656–3660.
[21] X.Y. Ye, M.C. Lo, L. Brunner, D. Walker, D. Kahne, S. Walker, J. Am. Chem. Soc. 123 (2001) 3155–3156.
[22] Y. Van Heijenoort, M. Derrien, J. Van Heijenoort, FEBS Lett. 89 (1978) 141–144.
[23] A.L. Lovering, L.H. de Castro, D. Lim, N.C. Strynadka, Science 315 (2007) 1402–1405.
[24] Y. Yuan, D. Barrett, Y. Zhang, D. Kahne, P. Sliz, S. Walker, Proc. Natl. Acad. Sci. USA 104 (2007) 5348–5353.
[25] Y. Yuan, S. Fuse, B. Ostash, P. Sliz, D. Kahne, S. Walker, ACS Chem. Biol. 3 (2008) 429–436.
[26] H. Heaslet, B. Shaw, A. Mistry, A.A. Miller, J. Struct. Biol. 167 (2009) 129–135.
[27] M.T. Sung, Y.T. Lai, C.Y. Huang, L.Y. Chou, H.W. Shih, W.C. Cheng, C.H. Wong, C. Ma, Proc. Natl. Acad. Sci. USA 106 (2009) 8824–8829.
[28] C.Y. Huang, H.W. Shih, L.Y. Lin, Y.W. Tien, T.J. Cheng, W.C. Cheng, C.H. Wong, C. Ma, Proc. Natl. Acad. Sci. USA 109 (2012) 6496–6501.
[29] P.M. Meadow, J.S. Anderson, J.L. Strominger, Biochem. Biophys. Res. Commun. 14 (1964) 382–387.
[30] H. Hara, H. Suzuki, FEBS Lett. 168 (1984) 155–160.
[31] M. Terrak, T.K. Ghosh, J. van Heijenoort, J. Van Beeumen, M. Lampilas, J. Aszodi, J.A. Ayala, J.M. Ghuysen, M. Nguyen-Disteche, Mol. Microbiol. 34 (1999) 350–364.
[32] Y. van Heijenoort, M. Gomez, M. Derrien, J. Ayala, J. van Heijenoort, J. Bacteriol. 174 (1992) 3549–3557.
[33] M. Terrak, M. Nguyen-Disteche, J. Bacteriol. 188 (2006) 2528–2532.
[34] L. Chen, D. Walker, B. Sun, Y. Hu, S. Walker, D. Kahne, Proc. Natl. Acad. Sci. USA 100 (2003) 5658–5663.
[35] A.M. Di Guilmi, A. Dessen, O. Dideberg, T. Vernet, J. Bacteriol. 185 (2003) 4418–4423.
[36] H. Schagger, G. von Jagow, Anal. Biochem. 166 (1987) 368–379.
[37] A.J. Lesse, A.A. Campagnari, W.E. Bittner, M.A. Apicella, J. Immunol. Methods 126 (1990) 109–117.

[38] D. Barrett, T.S. Wang, Y. Yuan, Y. Zhang, D. Kahne, S. Walker, J. Biol. Chem. 282 (2007) 31964–31971.
[39] N. Helassa, W. Vollmer, E. Breukink, T. Vernet, A. Zapun, FEBS J. 279 (2012) 2071–2081.
[40] B. Glauner, Anal. Biochem. 172 (1988) 451–464.
[41] B. Schwartz, J.A. Markwalder, S.P. Seitz, Y. Wang, R.L. Stein, Biochemistry 41 (2002) 12552–12561.
[42] U. Bertsche, E. Breukink, T. Kast, W. Vollmer, J. Biol. Chem. 280 (2005) 38096–38101.
[43] J. Biboy, N.K. Bui, W. Vollmer, Methods Mol. Biol. 966 (2013) 273–288.
[44] J. Offant, M. Terrak, A. Derouaux, E. Breukink, M. Nguyen-Disteche, A. Zapun, T. Vernet, FEBS J. 277 (2010) 4290–4298.
[45] A. Derouaux, S. Turk, N.K. Olrichs, S. Gobec, E. Breukink, A. Amoroso, J. Offant, J. Bostock, K. Mariner, I. Chopra, T. Vernet, A. Zervosen, B. Joris, J.M. Frere, M. Nguyen-Disteche, M. Terrak, Biochem. Pharmacol. 81 (2011) 1098–1105.
[46] S.H. Huang, W.S. Wu, L.Y. Huang, W.F. Huang, W.C. Fu, P.T. Chen, J.M. Fang, W.C. Cheng, T.J. Cheng, C.H. Wong, J. Am. Chem. Soc. 135 (2013) 17078–17089.
[47] T.J. Cheng, M.T. Sung, H.Y. Liao, Y.F. Chang, C.W. Chen, C.Y. Huang, L.Y. Chou, Y.D. Wu, Y.H. Chen, Y.S. Cheng, C.H. Wong, C. Ma, W.C. Cheng, Proc. Natl. Acad. Sci. USA 105 (2008) 431–436.
[48] C.M. Gampe, H. Tsukamoto, E.H. Doud, S. Walker, D. Kahne, J. Am. Chem. Soc. 135 (2013) 3776–3779.
[49] P. Reed, H. Veiga, A.M. Jorge, M. Terrak, M.G. Pinho, J. Bacteriol. 193 (2011) 2549–2556.
[50] B. Chandrakala, R.K. Shandil, U. Mehra, S. Ravishankar, P. Kaur, V. Usha, B. Joe, S.M. deSousa, Antimicrob. Agents Chemother. 48 (2004) 30–40.
[51] D.S. Barrett, L. Chen, N.K. Litterman, S. Walker, Biochemistry 43 (2004) 12375–12381.
[52] C.Y. Liu, C.W. Guo, Y.F. Chang, J.T. Wang, H.W. Shih, Y.F. Hsu, C.W. Chen, S.K. Chen, Y.C. Wang, T.J. Cheng, C. Ma, C.H. Wong, J.M. Fang, W.C. Cheng, Org. Lett. 12 (2010) 1608–1611.
[53] W. Vollmer, J.V. Holtje, J. Bacteriol. 186 (2004) 5978–5987.
[54] A.H. Williams, I.G. Boneca, L.L. Burrows, T.D. Bugg, Res. Microbiol. 165 (2014) 60–67.
[55] V. Ramachandran, B. Chandrakala, V.P. Kumar, V. Usha, S.M. Solapure, S.M. de Sousa, Antimicrob. Agents Chemother. 50 (2006) 1425–1432.
[56] B. Chandrakala, B.C. Elias, U. Mehra, N.S. Umapathy, P. Dwarakanath, T.S. Balganesh, S.M. deSousa, Antimicrob. Agents Chemother. 45 (2001) 768–775.
[57] P. Butaye, L.A. Devriese, F. Haesebrouck, Clin. Microbiol. Rev. 16 (2003) 175–188.
[58] P. Welzel, Chem. Rev. 105 (2005) 4610–4660.
[59] M. Adachi, Y. Zhang, C. Leimkuhler, B. Sun, J.V. LaTour, D.E. Kahne, J. Am. Chem. Soc. 128 (2006) 14012–14013.
[60] P. Welzel, F. Kunisch, F. Kruggel, H. Stein, J. Scherkenbeck, A. Hiltmann, H. Duddeck, D. Muller, J.E. Maggio, H.W. Fehlhaber, G. Seibert, Y. Vanheijenoort, J. Vanheijenoort, Tetrahedron 43 (1987) 585–598.
[61] G. Yang, L. Hennig, M. Findeisen, R. Oehme, S. Giesa, P. Welzel, Helvetica Chim. Acta 87 (2004) 1794–1806.
[62] U. Moller, K. Hobert, A. Donnerstag, P. Wagner, D. Muller, H.W. Fehlhaber, A. Markus, P. Welzel, Tetrahedron 49 (1993) 1635–1648.
[63] N. El-Abadla, M. Lampilas, L. Hennig, M. Findeisen, P. Welzel, D. Muller, A. Markus, J. van Heijenoort, Tetrahedron 55 (1999) 699–722.
[64] P. Welzel, F. Kunisch, F. Kruggel, H. Stein, J. Scherkenbeck, A. Hiltmann, H. Duddeck, D. Muller, J.E. Maggio, H.W. Fehlhaber, G. Seibert, Y. Vanheijenoort, J. Vanheijenoort, Tetrahedron 43 (1987) 585–598.
[65] L.L. Lairson, B. Henrissat, G.J. Davies, S.G. Withers, Annu. Rev. Biochem. 77 (2008) 521–555.
[66] S. Fuse, H. Tsukamoto, Y. Yuan, T.S. Wang, Y. Zhang, M. Bolla, S. Walker, P. Sliz, D. Kahne, ACS Chem. Biol. 5 (2010) 701–711.
[67] C.M. Gampe, H. Tsukamoto, T.S. Wang, S. Walker, D. Kahne, Tetrahedron 67 (2011) 9771–9778.
[68] M.J. Sofia, N. Allanson, N.T. Hatzenbuhler, R. Jain, R. Kakarla, N. Kogan, R. Liang, D. Liu, D.J. Silva, H. Wang, D. Gange, J. Anderson, A. Chen, F. Chi, R. Dulina, B. Huang, M. Kamau, C. Wang, E. Baizman, A. Branstrom, N. Bristol, R. Goldman, K. Han, C. Longley, H.R. Axelrod, et al., J. Med. Chem. 42 (1999) 3193–3198.
[69] R.C. Goldman, D. Gange, Curr. Med. Chem. 7 (2000) 801–820.
[70] B. Ostash, S. Walker, Curr. Opin. Chem. Biol. 9 (2005) 459–466.
[71] C. Miller, L.E. Thomsen, C. Gaggero, R. Mosseri, H. Ingmer, S.N. Cohen, Science 305 (2004) 1629–1631.
[72] H. He, B. Shen, J. Korshalla, M.M. Siegel, G.T. Carter, J. Antibiot. (Tokyo) 53 (2000) 191–195.
[73] G. Brooks, P.D. Edwards, J.D.I. Hatto, T.C. Smale, R. Southgate, Tetrahedron 51 (1995) 7999–8014.
[74] S.J. Hecker, M.L. Minich, K. Lackey, J. Org. Chem. 55 (1990) 4904–4911.
[75] L. Qiao, J.C. Vederas, J. Org. Chem. 58 (1993) 3480–3482.
[76] S. Garneau, L. Qiao, L. Chen, S. Walker, J.C. Vederas, Bioorg. Med. Chem. 12 (2004) 6473–6494.
[77] A. Derouaux, E. Sauvage, M. Terrak, Front Immunol. 4 (2013) 78.
[78] S. Dumbre, A. Derouaux, E. Lescrinier, A. Piette, B. Joris, M. Terrak, P. Herdewijn, J. Am. Chem. Soc. 134 (2012) 9343–9351.
[79] M. Terrak, Anti-Infective Agents Med. Chem. 7 (2008) 180–192.
[80] T.J. Cheng, Y.T. Wu, S.T. Yang, K.H. Lo, S.K. Chen, Y.H. Chen, W.I. Huang, C.H. Yuan, C.W. Guo, L.Y. Huang, K.T. Chen, H.W. Shih, Y.S. Cheng, W.C. Cheng, C.H. Wong, Bioorg. Med. Chem. 18 (2010) 8512–8529.
[81] H.W. Shih, Y.F. Chang, W.J. Li, F.C. Meng, C.Y. Huang, C. Ma, T.J. Cheng, C.H. Wong, W.C. Cheng, Angew. Chem. Int. Ed. Engl. 51 (2012) 10123–10126.
[82] R. Sinha Roy, P. Yang, S. Kodali, Y. Xiong, R.M. Kim, P.R. Griffin, H.R. Onishi, J. Kohler, L.L. Silver, K. Chapman, Chem. Biol. 8 (2001) 1095–1106.
[83] C. Leimkuhler, L. Chen, D. Barrett, G. Panzone, B. Sun, B. Falcone, M. Oberthur, S. Donadio, S. Walker, D. Kahne, J. Am. Chem. Soc. 127 (2005) 3250–3251.
[84] M. Ge, Z. Chen, H.R. Onishi, J. Kohler, L.L. Silver, R. Kerns, S. Fukuzawa, C. Thompson, D. Kahne, Science 284 (1999) 507–511.
[85] R.C. Goldman, E.R. Baizman, C.B. Longley, A.A. Branstrom, FEMS Microbiol. Lett. 183 (2000) 209–214.
[86] B. Ostash, J. Campbell, A. Luzhetskyy, S. Walker, Mol. Microbiol. 90 (2013) 1324–1338.
[87] G. Yim, M.N. Thaker, K. Koteva, G. Wright, J. Antibiot. (Tokyo) 67 (2014) 31–41.
[88] J.G. Taylor, X. Li, M. Oberthur, W. Zhu, D.E. Kahne, J. Am. Chem. Soc. 128 (2006) 15084–15085.
[89] B. Ostash, A. Saghatelian, S. Walker, Chem. Biol. 14 (2007) 257–267.
[90] D.L. Perlstein, T.S. Wang, E.H. Doud, D. Kahne, S. Walker, J. Am. Chem. Soc. 132 (2010) 48–49.

Surfactant-free purification of membrane protein complexes from bacteria: application to the staphylococcal penicillin-binding protein complex PBP2/PBP2a

Sarah Paulin[1], Mohammed Jamshad[2], Timothy R Dafforn[2], Jorge Garcia-Lara[3], Simon J Foster[3], Nicola F Galley[4], David I Roper[4], Helena Rosado[1] and Peter W Taylor[1]

[1] School of Pharmacy, University College London, 29-39 Brunswick Square, London WC1N 1AX, UK
[2] School of Biosciences, University of Birmingham, Edgbaston, Birmingham B15 2TT, UK
[3] Krebs Institute, University of Sheffield, Firth Court, Western Bank, Sheffield S10 2TN, UK
[4] School of Life Sciences, University of Warwick, Gibbet Hill Campus, Coventry CV4 7AL, UK

E-mail: peter.taylor@ucl.ac.uk

Abstract

Surfactant-mediated removal of proteins from biomembranes invariably results in partial or complete loss of function and disassembly of multi-protein complexes. We determined the capacity of styrene-co-maleic acid (SMA) co-polymer to remove components of the cell division machinery from the membrane of drug-resistant staphylococcal cells. SMA-lipid nanoparticles solubilized FtsZ-PBP2-PBP2a complexes from intact cells, demonstrating the close physical proximity of these proteins within the lipid bilayer. Exposure of bacteria to (-)-epicatechin gallate, a polyphenolic agent that abolishes β-lactam resistance in staphylococci, disrupted the association between PBP2 and PBP2a. Thus, SMA purification provides a means to remove native integral membrane protein assemblages with minimal physical disruption and shows promise as a tool for the interrogation of molecular aspects of bacterial membrane protein structure and function.

S Online supplementary data available from stacks.iop.org/NANO/25/285101/mmedia

(Some figures may appear in colour only in the online journal)

1. Introduction

Integral membrane proteins participate in a variety of activities essential for survival, homeostasis and division. Many function only within dynamic multi-protein assemblages embedded in specialized lipid microdomains of the bacterial cytoplasmic membrane (CM). Thus, the bacterial cell division machinery is localized at mid-cell within a divisome of more than 20 proteins [1]; their dynamic and amphipathic nature makes them difficult to study in their native state, as their removal by surfactants leads to decreased structural integrity, complex disassembly and loss of activity. Advances in membrane solubilization have enabled surfactant-free extraction and purification of functionally active membrane proteins [2, 3]. Amphipathic poly(styrene-co-maleic acid) (SMA), soluble at neutral and alkaline pH and insoluble at

lower pH, auto-assembles at neutral or alkaline pH into membranes to form discoidal nanostructures around membrane proteins and associated lipids. Preservation of the native lipid environment of embedded proteins yields correctly folded, functionally active protein. The technique has been used to remove and purify functionally active proteins from liposomes [2–4] and over-expressed proteins from isolated membranes of eukaryotes and prokaryotes. SMA-lipid particles (SMALPs) have also been employed to remove respiratory enzyme complexes from mitochondrial membranes [5], suggesting that SMALP encapsulation provides a tool to identify and characterize protein complexes in which monomeric components are in close physical proximity.

Staphylococcus aureus rapidly acquires genes encoding antibiotic resistance; strains resistant to *β*-lactam agents, typified by methicillin-resistant *S. aureus* (MRSA), are usually insensitive to other antibiotic classes and there are few treatment options [6]. MRSA is resistant to *β*-lactam drugs due to acquisition of the *mecA* gene encoding penicillin-binding protein (PBP) 2a, an enzyme that takes over the transpeptidase function of PBP2 following *β*-lactam inactivation of the PBP2 transpeptidase, to ensure continued synthesis of cell wall peptidoglycan [7]. PBPs are embedded in the CM, which is comprised of an asymmetric array of lipids with differing charge characteristics, in the main phosphatidylglycerol (PG), lysyl-PG and cardiolipin [8]. It has proven difficult to determine the spatial proximity of PBP2 and PBP2a in the CM, even though they form part of the cell division machinery at the division septum; divisome assembly is regulated by polymerization of the tubulin homologue FtsZ to a ring-like structure that acts as a scaffold for recruitment of other proteins, including PBPs [1, 9]. Membrane-intercalating agents that abrogate *β*-lactam resistance disperse PBP2 from the septum [8] and conversion to drug susceptibility may be due to disruption of functional and spatial associations between these proteins. We used the SMALP technique to determine that PBP2/PBP2a complexes can be captured together in nanoparticles from normally dividing MRSA cells and to demonstrate that the drug resistance modifier (-)-epicatechin gallate (ECg) alters the spatial relationship between the two proteins.

2. Experimental details

Epidemic MRSA isolate EMRSA-16 was from a clinical sample obtained at the Royal Free Hospital (London, UK). Methicillin-susceptible *S. aureus* SH1000 was obtained from Alex O'Neill (University of Leeds, UK). Bacteria were grown in Mueller-Hinton broth (Oxoid) to mid-logarithmic phase at 35 °C with constant agitation and aeration; PBP2a was induced with sub-inhibitory concentrations (125 μg l^{-1}) of oxacillin. Lysostaphin, a glycine–glycine endopeptidase, and the protease and phosphatase inhibitor mixture HALT were purchased from Sigma-Aldrich. Anti-PBP2 antiserum was produced in rabbits with recombinant his$_6$-tagged PBP2; mouse anti-PBP2a antibody was purchased from My Biosource and 1,2-dimyristoyl-sn-glycero-3-phosphocholine

(DMPC) from Avanti Polar Lipids. Rabbit anti-FtsZ antiserum was a gift from Jeff Errington (Newcastle University, UK). SMA was composed of styrene and maleic acid residues in a ratio of 2:1 and was synthesized in-house; 5% stock solutions of SMA were prepared in 1.0 M NaCl and refluxed for 2 h followed by overnight dialysis at 4 °C in 50 mM Tris-HCl (pH 8.0). The composition of the lyophilized product was confirmed by FTIR. ECg was a gift from Mitsui Norin, Tokyo, Japan and was used at a concentration of 12.5 mg l^{-1}.

Proteins were separated by sodium dodecyl sulfate-polyacrylamide gel electrophoresis (SDS-PAGE) on a 10% acrylamide/ bis-acrylamide gel matrix and visualized with Coomassie brilliant blue (Sigma-Aldrich) with a limit of detection of 0.2 μg. N-(2-hydroxy-1,1-bis(hydroxymethyl) ethyl) glycine (tricine) modification of SDS-PAGE was also used to avoid aggregation of membrane proteins in the gel, essentially as described by Schägger [10]. Protein-containing samples were concentrated in Vivaspin columns (<10 000 kDa) to approximately 20 mg ml^{-1} protein. For Western blotting, proteins were transferred by electrophoresis to Millipore polyvinylidene membranes and probed with antibodies to proteins of interest. Binding was detected with monoclonal secondary antibody conjugated to horseradish peroxidase (HRP) followed by peroxide substrate and Supersignal West Pico Chemiluminescent Substrate (Thermo Scientific), an enhanced chemiluminescence HRP substrate. Different secondary antibodies were used for detection of PBP2 (anti-rabbit) and PBP2a (anti-mouse). For transmission electron microscopy (TEM), suspensions were dropped on a grid, washed twice with 50 mM Tris buffer, stained with uranyl acetate [2] and viewed and photographed using a Philips 201 microscope.

Protein content of nanoparticles was determined by absorbance at 280 nm using a Nanodrop 2000 spectrophotometer. The hydrodynamic particle size distribution of SMALPs was measured by dynamic light scattering (DLS) using a Zetasizer Nano ZS. Samples (1 ml) were placed in a semi-micro PS disposable polystyrene cuvette (Fischer Scientific) and equilibrated at 25 °C for 5 min to ensure temperature homogeneity prior to taking 16 measurements for each sample, repeated three times. Data was analyzed using Zetasizer software (V. 6.20). SMALPs were further characterized with respect to their capacity to induce forward light scatter (FSC; reflecting predominantly size, but also refractive index and shape) and side scatter (SSC; indicative of geometry and internal structure, or 'granularity') using flow cytometry in tandem with fluorescein isothiocyanate (FITC)-coupled second antibodies and excitation at 488 nm, adapted for the analysis of nanoparticles by van der Vlist *et al* [11]. SMALPs (500 μl aliquots) in buffer pH 7.6 were labeled with 60 μM Nile Red (Invitrogen) for 30 min in the dark and detected using a Miltenyi MACSQuant Analyzer with voltage set between 300 V and 500 V, gated for fluorescence (trigger 3.0) and subsequently back gated for SSC and FSC. Twenty thousand events were collected for each sample and data analyzed with Miltenyi MACS Quantify Software. Fluorescence was used as the parameter for setting the acquisition trigger and the trigger level was adjusted to minimize

electronic noise. All assays were performed three times on separate days.

To determine if PBP2 and PBP2a were present in close proximity within nanoparticles and membrane preparations, proteins were cross-linked with 3,3′Dithiobis (sulfosuccinimidylpropionate) (DTSSP) linked by a spacer arm of 12 Å (Thermo Scientific). DTTSP was dissolved to a final concentration of 10 mM in 300 μl of SMALP solution (25 mg ml^{-1} protein) and incubated at 4 °C for 30 min. The cross-linking reaction was quenched by the addition of 2.5 μl of 1 M Tris-HCl, pH 7.5 and incubated for 15 min [12]. Cross-links were cleaved by addition of 5% 2-mercaptoethanol (Sigma) in tricine sample buffer. For immunoaffinity chromatography (IAC), protein G HP spintrap columns (GE Healthcare Life Sciences) were equilibrated in Tris-buffered saline (TBS; 50 mM Tris-HCl, 150 mM NaCl; pH 7.5), antibody bound to the column (0.5–1.0 mg ml^{-1} in 200 μl TBS) and excess removed by washing. SMALPs (maximum volume 500 μl) were added to the column, maintained with shaking at 4 °C for 60 min, washed extensively with TBS and centrifuged at 150 g for 1 min at 4 °C. Bound material was eluted from the column with 100 μl 0.1 M glycine pH 2.5 and centrifuged for 1 min at 1000 g; pH was neutralized with 1 M Tris-HCl pH 8.0. For co-immunoprecipitation (Co-IP), paramagnetic beads coated with protein G (Dynal) and complexed with either anti-PBP2 or anti-PBP2a antibodies were used to purify PBP2/PBP2a-containing nanoparticles; SMALPs (200–400 μl protein) were mixed with the Dynabeads and the mixture incubated at 4 °C for 2 h with constant agitation. The complex was eluted following manufacturer's instructions and captured proteins analyzed by SDS-PAGE and Western blotting.

3. Results and discussion

Initially, attempts were made to solubilize PBP2/PBP2a complexes from EMRSA-16 membranes with Triton X-100. Cells from 1 l cultures were suspended in 1–4 ml of ice-cold distilled water and disrupted using a FastPrep FP120 Homogenizer (Thermo Scientific). Cell wall debris was removed by centrifugation (5000 g; 10 min; 4 °C), CMs collected (130 000 g; 1 h; 4 °C) and the pellet suspended in ~200 μl of 10 mM Tris-HCl (pH 7.0) containing 2% Triton X-100 [8]. Exposure of solubilized proteins to DTSSP followed by Co-IP with anti-PBP2 antibody failed to elicit cross-linked PBP2/PBP2a; only PBP2 could be detected in Western blots of Co-IP eluents separated by SDS-PAGE (figure S1; in the supplementary file, available at stacks.iop.org/NANO/25/285101/mmedia). We also attempted unsuccessfully (data not shown) to cross-link the two proteins after solubilization with 1% formaldehyde (95 °C; 5 min). We conclude that any PBP2/PBP2a complexes are disrupted by detergent extraction; this accords with published reports demonstrating recovery of PBPs by non-ionic detergents in exclusively monomeric form [13, 14]. Consequently, we examined the potential of SMA co-polymer solubilization to reveal the presence of closely associated PBP2/PBP2a.

As the composition of the staphylococcal CM is unusual, we determined if SMA was able to solubilize proteins from purified EMRSA-16 membranes. Cells were suspended in 3 ml 20% sucrose, 0.05 M Tris-HCl, 0.145 M NaCl (pH 7.6) and the cell wall digested with 80 μg lysostaphin (with 25 μg DNase I and protease inhibitors) for 10 min at 37 °C. SMA was added to final concentration of 2.5% and the mixture (6 ml) incubated for 1 h at 37 °C; membranes were collected by centrifugation (100 000 g; 1 h; 4 °C). Proteins were separated by tricine-SDS-PAGE. Western blotting revealed the presence of both PBP2 and PBP2a in SMALPs. As the preparation of bacterial membranes may lead to redistribution of bilayer protein and lipid, we modified this procedure to enable solubilization of PBPs from intact cells; the lysostaphin digestion components were added to 3 ml bacterial suspension from 2 l culture and incubated for 10 min at 37 °C prior to addition of SMA. Omission of this cell wall digestion step resulted in failure to extract membrane proteins; lysostaphin, which disrupts the pentaglycine cross-bridges of peptidoglycan [15], breached the integrity of the cell wall as determined by TEM (figure 1(B)). After addition of SMA and further 50 min incubation, SMALPs were recovered from the supernatant (100 000 g; 1 h; 4 °C). TEM showed that partial digestion of the cell wall was necessary to allow ingress of SMA and egress of SMALPs (figure 1(C)). Initial experiments included sonication of bacteria and 16 h incubation at 37 °C prior to centrifugation, as these steps were considered essential to obtain homogeneous preparations of SMA liposomal extracts [2, 3], but neither were found to be necessary for membrane protein extraction and were omitted from our optimized protocol, as sonication is likely to disrupt physical associations between membrane proteins. The amount of membrane protein extracted from EMRSA-16 by SMA was comparable to that extracted by 2% Triton X-100 (figure S2).

TEM images of material solubilized by SMA from DMPC vesicles, *S. aureus* SH1000 and EMRSA-16 revealed monodispersed, homogeneous suspensions (figure 2) with mean diameters of 12 ± 2 nm (±1SD) for particles from protein-free DMPC vesicles and 18 ± 3 nm and 24 ± 5 nm (all n = 75) for those from SH1000 and EMRSA-16, indicating that incorporation of proteins results in SMALPs of increased size. Nanoparticle size distribution and dispersion were investigated by DLS and flow cytometry (figure 3). DLS confirmed the monodispersed nature of SH1000 and EMRSA-16 preparations and indicated that hydrodynamic diameters of SMALPs were 17.4 ± 2.23 nm and 24.5 ± 2.64 nm, in good agreement with measurements from TEM. Although these nanoparticles are close to the lower limits of detection, they were readily quantified and analyzed by flow cytometry, employing fluorescence threshold triggering to discriminate fluorescently labelled SMALPs from non-fluorescent noise [11]. Figure 3(A) shows the forward- (influenced by size, refractive index, shape) and side-scatter distribution (geometry, internal structure) of nanoparticles from EMRSA-16, visualizing both Nile Red-labeled SMALPs and noise events. SMALPs labeled with the lipophilic dye Nile Red could be discriminated from non-fluorescent noise (figure 3(B)); raising the fluorescence threshold
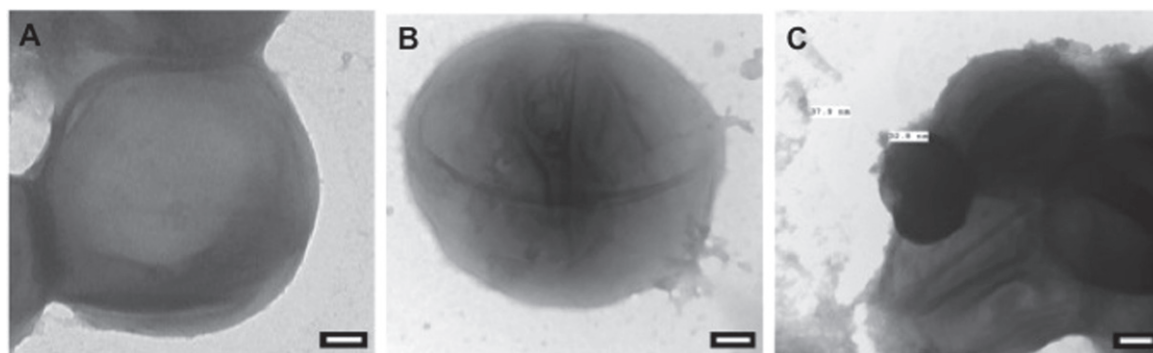
Figure 1. TEM of (A) EMRSA-16 cell, (B) after 10 min exposure to lysostaphin (26.7 mg l^{-1}), (C) after 10 min lysostaphin digestion followed by 2.5% SMA and incubation for 50 min. Two SMALPs of diameter 37.9 nm and 32.8 nm can be seen. Scale bar = 100 nm.
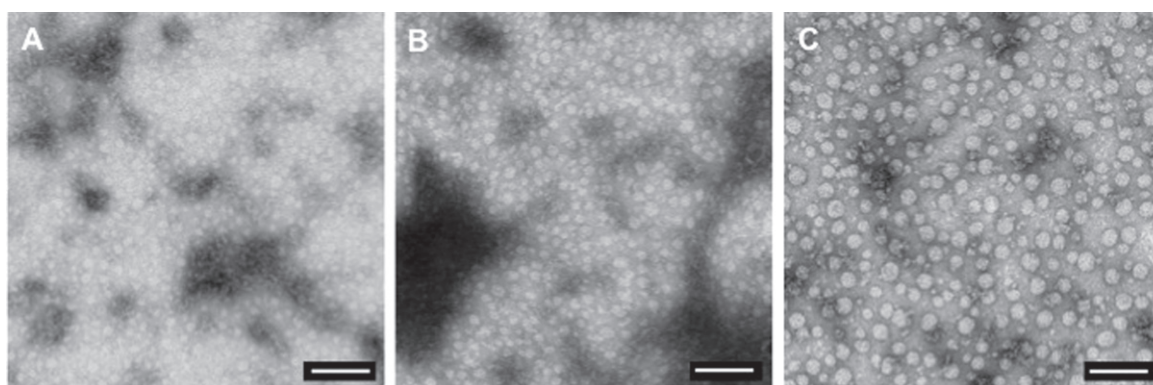

Figure 2. TEM of (A) DMPC, (B) SH1000 membranes and (C) EMRSA-16 membranes incorporated into SMALPs. Bacterial membranes were solubilized directly from viable bacteria with no intermediate membrane purification step. Scale bar = 100 nm.

to eliminate noise (figure 3(C)) showed that the majority of particles formed a homogeneous population with respect to forward- and side-scatter but with a short tail of small fluorescent particles (figures 3(C) and (D)). When particles were stained with Nile Red (for lipid) and Bocillin FL (for PBPs) and examined by fluorescence microscopy, the two stains co-localized, indicating successful protein extraction. PBP2 and PBP2a were detected in unfractioned SMALPs from EMRSA-16 by Western blotting.

Protein-containing SMALPs were enriched by IAC or Co-IP; prior to enrichment, proteins separated by 12 Å or less were cross-linked with DTSSP. IAC was employed to determine if PBP2 or PBP2a could be detected in protein complexes recovered using antibodies raised against FtsZ. Western blotting of proteins from EMRSA-16 SMALPs reacting with anti-FtsZ antibodies contained PBP2, PBP2a and FtsZ (figure 4), indicating that these proteins exist on or within the CM in close spatial proximity. IAC and Co-IP with both anti-PBP2 and anti-PBP2a antibodies yielded nanoparticles in which PBP2 and PBP2a, but not FtsZ, could be detected in Western blots with the appropriate antibodies, but the bands were less prominent in comparison to blots of anti-FtsZ-recovered nanoparticles, almost certainly reflecting the low number of copies of PBPs in each *S. aureus* cell [16].

ECg completely abolishes β-lactam resistance in clinical MRSA isolates; it reduces the minimum inhibitory concentration of oxacillin required to prevent growth of EMRSA-

16 from 512 to <1 mg l^{-1}, due to its capacity to intercalate deep within the CM, fundamentally altering the biophysical characteristics of the bilayer and forcing the bacteria to respond by reconfiguration of CM architecture [8, 17]. The polyphenol induces partial delocalization of PBP2 from the septal divisome [8], indicating that reversible sensitization to β-lactam antibiotics may be due to dissipation of the PBP2/PBP2a-facilitiated resistance machinery. In this study, it is clear that 12.5 mg l^{-1} ECg alters the spatial relationship between these two proteins, as PBP2a can no longer be recovered by SMA extraction and capture with anti-FtsZ antibodies (figure 4), providing support for this supposition.

Eluents from Co-IP were also investigated by analytical flow cytometry. SMALPs were enriched with anti-PBP2 antibodies, lipid labeled with Nile Red and probed with anti-PBP2a antiserum and FITC-conjugated second antibody. Conversely, nanoparticles enriched with anti-PBP2a were probed for the presence of PBP2. In both cases, the partner protein was readily detected, with 8260 of 20 000 reacting with anti-PBP2a antibodies after enrichment with anti-PBP2 antibodies and 7260 of 20 000 with anti-PBP2 antibodies after enrichment with anti-PBP2a antibodies (figure 5). These data provide strong evidence that PBP2 and PBP2a are in close spatial proximity following recruitment by FtsZ and are recovered from the CM in ~40% of SMALPs. It is likely that this reflects the proportion of PBP2/PBP2a complexes actively involved in cell division, with the remainder
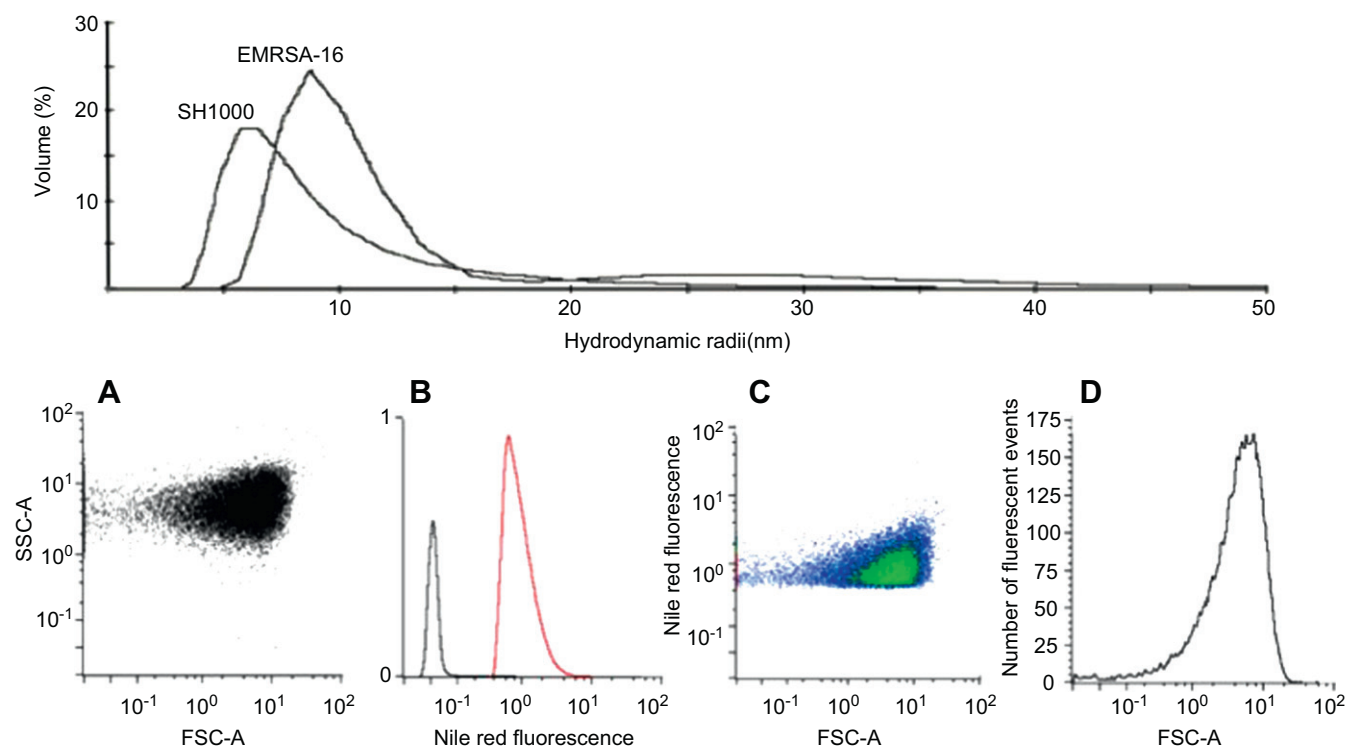
Figure 3. Size determination of SMALPs from EMRSA-16 membranes. Upper panel: distribution of hydrodynamic radii determined by DLS. Lower panel: flow cytometry of SMALPs labeled with 60 μM Nile Red by (A) size (forward scatter; FSC-A) and granularity (side scatter; SSC-A), no discrimination between fluorescent and non-fluorescent nanoparticles, all arbitrary units; (B) fluorescence intensity of Nile Red within SMALPs (red) and non-fluorescent SMALPs (black); (C) separation of SMALPs labeled with Nile Red by fluorescence sorting; number of particles in the scatter plot follow the transition from blue (low) through green to red (high); (D) size distribution (FSC-A) of Nile Red-labeled SMALPs.
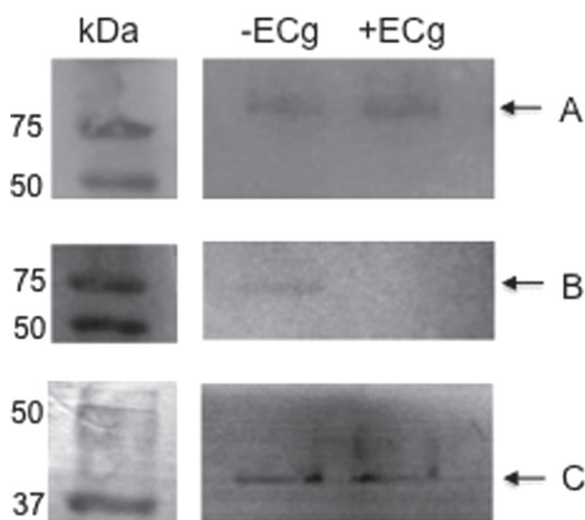

Figure 4. Western blots of EMRSA-16 SMALP proteins recovered by anti-FtsZ IAC. Bacteria were grown in the absence (−ECg) or presence (+ECg) of the drug resistance modifier ECg (12.5 mg l^{-1}) and proteins probed with anti-PBP2 (A), anti-PBP2a (B) and anti-FtsZ (C) antibodies. Arrows indicate the target protein in each blot.

complexes. Co-IP of SMALPs from control and ECg-exposed cells was undertaken with anti-PBP2 and anti-PBP2a antibodies and PBP2 and PBP2a quantified with the appropriate antibody combinations. With anti-PBP2 Co-IP pull down, there was a 1.76-fold reduction in the PBP2/PBP2a ratio following ECg exposure, reflecting a reduction in PBP2a FITC fluorescence (normalized against PBP2 Nile Red fluorescence) from 231.6 arbitrary fluorescence units (AFU) to 131.6 AFU. With anti-PBP2a Co-IP, a 1.43-fold reduction was observed, corresponding to a reduction in normalized PBP2a fluorescence from 53.7 AFU to 37.6 AFU. Flow cytometry scatter plots from these experiments are shown in figure S3. Flow cytometry was used as it is a highly sensitive, quantitative method with a much lower limit of detection compared to semi-quantitative Western blotting. In this context, we were unable to detect a band corresponding to PBP2a by Western blotting of SMA-extracted proteins from ECg-exposed EMRSA-16 cells; flow cytometry clearly indicated residual PBP2a, in agreement with a study showing partial, rather than complete, disruption of the complex [8]. Also of note was our ability to obtain fluorescence data by flow cytometry from nanoparticles of 20–25 nm diameter, using methods [11] designed for detection and analysis of vesicles of ~100 nm.

We show for the first time that SMA trapping of membrane domains can be used to extract native membrane-embedded protein complexes directly from intact bacteria.

recovered from regions of the membrane other than those accommodating divisome complexes. Flow cytometry provided further evidence that exposure of EMRSA-16 to 12.5 mg l^{-1} ECg caused partial dissociation of PBP2/PBP2a
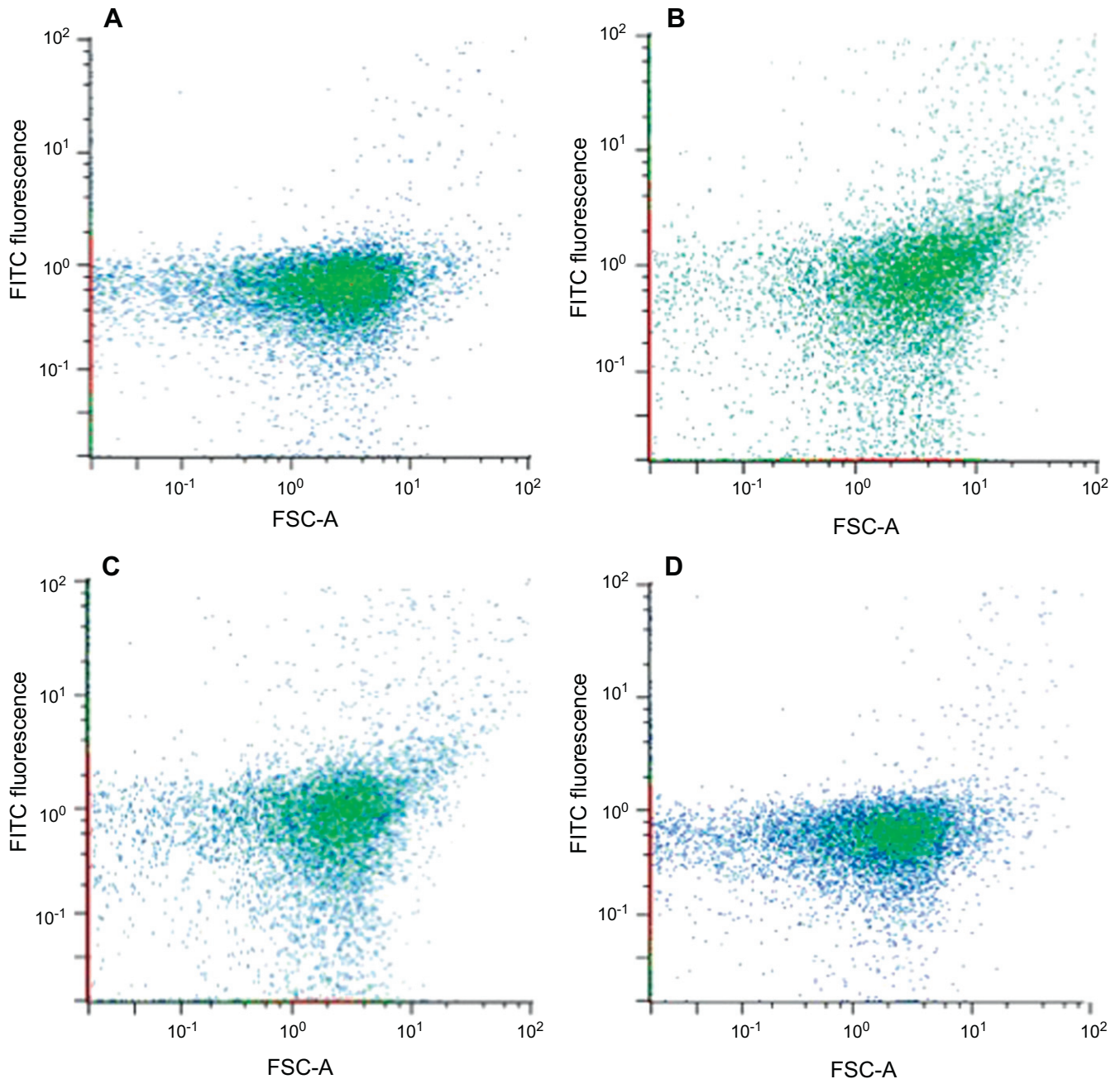
Figure 5. Flow cytometry of EMRSA-16 SMALPs enriched for PBP2 and PBP2a by Co-IP. Nanoparticles were labeled with Nile Red and size (forward scatter; FSC-A) and granularity (side scatter; SSC-A) determined after pull down with (A), (B) anti-PBP2 and (C), (D) anti-PBP2a antibodies. Nanoparticles from A were labeled with murine anti-PBP2a antibodies followed by FITC-conjugated anti-mouse IgG secondary antibody (B) and those from B with rabbit anti-PBP2 antibodies and FITC-conjugated anti-rabbit IgG second antibody (D). In each experiment, 20 000 Nile Red-labeled nanoparticles; 8260 reacted with anti-PBP2a antibodies when enriched with anti-PBP2 antibodies (B) and 7260 with anti-PBP2 antibodies when enriched with anti-PBP2 antibodies (D).

Other studies [2–4] have effected removal of single proteins within model lipid bilayers or over-expressed proteins from protoplasts of viable bacteria. The latter approach would not be suitable for SMALP enrichment of divisome proteins as key components remain at the septum due to interactions with D-alanyl-D-alanine termini on nascent peptidoglycan chains [18]; removal of the cell wall will destroy this anchor and delocalize proteins. It was necessary to minimally digest the cell wall whilst retaining overall architecture and we established that 10 min lysostaphin digestion of whole cells led to

optimal cell wall perturbation compatible with protein extraction. SMA solubilized substantial amounts of protein from the membrane but native PBP2 and PBP2a copy numbers are low and this restricted our capacity to purify enough protein using PBP-specific antisera for analysis by Western blotting, but not by the more sensitive flow cytometry technique. In contrast, there are many more copies of FtsZ, the major cytoskeletal protein, within the membrane bilayer [19]. The presence of FtsZ within PBP2/PBP2a-containing nanoparticles could only be demonstrated when anti-FtsZ

antiserum was used for purification by IAC. SMALP capture of FtsZ, PBP2 and PBP2a with antiFtsZ antiserum shows that the procedure can remove large protein complexes. The *S. aureus* division machinery is comprised of many membrane-located and cytosolic proteins that interact with the FtsZ scaffold: removal of functionally active components of the divisome in a spatially relevant manner will provide a new tool for elucidation of their complex interactions.

Acknowledgements

References

[1] Egan A J F and Vollmer W 2013 The physiology of bacterial cell division *Ann. New York Acad. Sci.* **1277** 8–28

[2] Knowles T J, Finka R, Smith C, Lin Y P, Dafforn T and Overduin M 2009 Membrane proteins solubilized intact in lipid containing nanoparticles bounded by styrene maleic acid copolymer *J. Am. Chem. Soc.* **131** 7484–5

[3] Jamshad M *et al* 2011 Surfactant-free purification of membrane proteins with intact native membrane environment *Biochem. Soc. Trans.* **39** 813–8

[4] Orwick-Rydmark M, Lovett J E, Graziadei A, Lindholm L, Hicks M R and Watts A 2012 Detergent-free incorporation of a seven-transmembrane receptor protein into nanosized bilayer lipodisq particles for functional and biophysical studies *Nano Lett.* **12** 4687–92

[5] Long A R, Malhotra K, Schwall C T, Albert A D, Watts A and Alder N N 2013 A detergent-free strategy for the reconstitution of active enzyme complexes from native biological membranes into nanoscale discs *BMC Biotechnol.* **13** 41

[6] Johnson A P, Davies A, Guy R, Abernathy J, Sheridan E, Pearson A and Duckworth G 2012 Mandatory surveillance of methicillin-resistant *Staphylococcus aureus* (MRSA) bacteraemia in England: the first 10 years *J. Antimicrob. Chemother.* **67** 802–9

[7] Fuda C C S, Fisher J F and Mobashery S 2005 *β*-lactam resistance in *Staphylococcus aureus*: the adaptive resistance of a plastic genome *Cell. Mol. Life Sci.* **62** 2617–33

[8] Bernal P, Lemaire S, Pinho M G, Mobashery S, Hinds J and Taylor P W 2010 Insertion of epicatechin gallate into the cytoplasmic membrane of methicillin-resistant *Staphylococcus aureus* disrupts penicillin-binding protein (PBP) 2a-mediated beta-lactam resistance by delocalizing PBP2 *J. Biol. Chem.* **285** 24055–65

[9] Adams D W and Errington J 2009 Bacterial cell division: assembly, maintenance and disassembly of the Z ring *Nat. Rev. Microbiol.* **7** 642–53

[10] Schägger H 2006 Tricine-SDS-PAGE *Nat. Protocols* **1** 16–22

[11] van der Vlist E J, Nolte-'t Hoen E S M, Stoorvogel W, Arkesteijn G J A and Wauben M H M 2012 Fluorescent labeling of nano-sized vesicles released by cells and subsequent quantitative and qualitative analysis by high-resolution flow cytometry *Nat. Protocols* **7** 1311–26

[12] Bennett K L, Kussmann M, Björk P, Godzwon M, Mikkelsen M, Sørensen P and Roepstorff P 2000 Chemical cross-linking with thiol-cleavable reagents combined with differential mass spectrometric peptide mapping–a novel approach to assess intermolecular protein contacts *Protein Sci.* **9** 1503–18

[13] Chase H A 1980 Purification of four penicillin-binding proteins from *Bacillus megaterium J. Gen. Microbiol.* **117** 211–24

[14] Di Guilmi A M, Mouz N, Andrieu J P, Hoskins J, Jaskunas S R, Gagnon J, Dideberg O and Vernet T 1998 Identification, purification, and characterization of transpeptidase and glycosyltransferase domains of *Streptococcus pneumoniae* penicillin-binding protein 1a *J. Bacteriol.* **180** 5652–9

[15] Schindler C and Schuhardt V 1964 Lysostaphin: a new bacteriolytic agent for the staphylococcus *Proc. Natl. Acad. Sci. USA* **51** 414–21

[16] Pucci M J and Dougherty T J 2002 Direct quantitation of the numbers of individual penicillin-binding proteins per cell in *Staphylococcus aureus J. Bacteriol.* **184** 588–91

[17] Palacios L, Rosado H, Micol V, Rosato A, Bernal P, Arroyo R, Grounds H, Anderson J C, Stabler R A and Taylor P W 2014 Staphylococcal phenotypes induced by naturally occurring and synthetic membrane-interactive polyphenolic *β*-lactam resistance modifiers *PLoS One* **9** e93830

[18] Pinho M G and Errington J 2003 Dispersed mode of *Staphylococcus aureus* cell wall synthesis in the absence of the division machinery *Mol. Microbiol.* **50** 871–81

[19] Erickson H P, Anderson D E and Osawa M 2010 FtsZ in bacterial cytokinesis: cytoskeleton and force generator all in one *Microbiol. Mol. Biol. Rev.* **74** 504–28

ARTICLE

Carbohydrate scaffolds as glycosyltransferase inhibitors with *in vivo* antibacterial activity

Johannes Zuegg[1,2], Craig Muldoon[2], George Adamson[2], Declan McKeveney[2], Giang Le Thanh[2], Rajaratnam Premraj[2], Bernd Becker[2], Mu Cheng[1], Alysha G. Elliott[1], Johnny X. Huang[1], Mark S. Butler[1], Megha Bajaj[1], Joachim Seifert[2], Latika Singh[2], Nicola F. Galley[3], David I. Roper[3], Adrian J. Lloyd[3], Christopher G. Dowson[3], Ting-Jen Cheng[4], Wei-Chieh Cheng[4], Dieter Demon[5], Evelyne Meyer[5], Wim Meutermans[2] & Matthew A. Cooper[1]

The rapid rise of multi-drug-resistant bacteria is a global healthcare crisis, and new antibiotics are urgently required, especially those with modes of action that have low-resistance potential. One promising lead is the liposaccharide antibiotic moenomycin that inhibits bacterial glycosyltransferases, which are essential for peptidoglycan polymerization, while displaying a low rate of resistance. Unfortunately, the lipophilicity of moenomycin leads to unfavourable pharmacokinetic properties that render it unsuitable for systemic administration. In this study, we show that using moenomycin and other glycosyltransferase inhibitors as templates, we were able to synthesize compound libraries based on novel pyranose scaffold chemistry, with moenomycin-like activity, but with improved drug-like properties. The novel compounds exhibit *in vitro* inhibition comparable to moenomycin, with low toxicity and good efficacy in several *in vivo* models of infection. This approach based on non-planar carbohydrate scaffolds provides a new opportunity to develop new antibiotics with low propensity for resistance induction.

[1] Institute for Molecular Bioscience, The University of Queensland, St Lucia, Queensland 4072, Australia. [2] Alchemia Ltd, PO Box 4851, Eight Mile Plains, Brisbane, Queensland 4113, Australia. [3] School of Life Science, University of Warwick, Gibbet Hill Road, Coventry CV4 7AL, UK. [4] Genomics Research Center, Academia Sinica, 128 Academia Road, Section 2, Taipei 115, Taiwan. [5] Faculty of Veterinary Medicine, Laboratory of Biochemistry, Ghent University, Salisburylaan 133, 9820 Merelbeke, Belgium. Correspondence and requests for materials should be addressed to W.M. (email: wmeutermans@optusnet.com.au) or to M.A.C. (email: m.cooper@uq.edu.au).

Peptidoglycan glycosyltransferases (GT) and transpeptidases (TP) are two key enzymes in the final steps of peptidoglycan (PG) biosynthesis essential for bacterial cell wall integrity and stability. GTs catalyse the polymerization of lipid II disaccharide units, forming a long chain of alternating β-1,4-linked N-acetylglucosamines and N-acetylmuramic acid, leading to a linear glycan chain and the release of undecaprenyl-pyrophosphate carrier[1–3]. These carbohydrate chains are further crosslinked by TP enzymes, forming linkages between the peptide chain and the D-alanine of a neighboring unit (Fig. 1). GT and TP enzymes are unique to bacteria and are expressed either as individual domains, monofunctional GT (MGT) and penicillin-binding proteins (PBP), respectively or as bifunctional proteins that possess both GT and TP domains (class A PBP)[4,5].

Inhibition of extracellular bacterial cell wall synthesis has been a very successful strategy in the development of many important antibacterial agents, with teixobactin[6], one of the most recently reported. The β-lactam class, which includes cephalosporins, monobactams and carbapenems, inhibit PG crosslinking by covalently binding to the TP enzyme, while glycopeptides such as vancomycin bind directly to the lipid II unit and sterically inhibit further polymerization and crosslinking of PG. Bacteria developed resistance to cell wall inhibitors via β-lactamases, thickened cell walls and modification of the lipid II unit, with extended-spectrum β-lactamases such as NDM-1 and vancomycin-resistant enterococci representing a significant health threat[7]. Glycolipopeptides (for example, ramoplanin), cyclic peptides (for example, AC98-6446) and lantibiotics (for example, nisin or NVB302) also bind to lipid II of Gram-positive bacteria[8]. Only nisin has reached the market, and then only as a food preservative[9].

Antibacterial compounds that bind directly to GT have never been developed for human use. Of the few examples reported in the literature, moenomycin is by far the best described[10]. Moenomycin is produced by various streptomyces species and has a broad-spectrum activity against a range of Gram-positive bacteria. The poor pharmacokinetic properties of moenomycin have prevented further clinical development[10,11], and it has been commercialized only as a 'growth promoter' within animal feed stocks (Flavomycin and Flavophospholipol). Despite evidence that regular application of antibiotics as growth promoters in animals in general leads to increased antibiotic resistance[12,13], remarkably no moenomycin-resistant bacteria in animals have been reported to date[14,15]. In vitro resistance induction experiments showed extremely slow development of resistance with low-resistant frequencies[16], as well as no transferable resistance between organisms[17,18], no cross-resistance to other antimicrobials or co-selection of resistant strains[19]. Intrinsic resistance in moenomycin-producing organisms is not associated with the biosynthesis cluster, but is likely to arise from the presence of GT's with low affinity for moenomycin, or some peculiarities of their cell wall organization[10]. Further, moenomycin is primarily accumulated inside of the cells, while its target is located on the cell surface[20,21]. In vitro-induced resistance with S. aureus showed mutations in the binding site of PBP2 with reduced affinity for moenomycin as well as its ligand, resulting in strains with shorter PG polymers and major cell division defects[16]. The lack of a specific resistance mechanism and the paucity of antibiotics that specifically mimic the carbohydrate portion of bacterial lipid II suggest that direct GT inhibition remains an attractive strategy for the development of novel antibacterial agents with low potential for resistance development.

Moenomycin A is a highly functionalized pentasaccharide attached via a phosphoglycerate linkage to a polyprenyl chain[22] (Fig. 1) that binds competitively to GT enzymes by mimicking the disaccharide–pyrophosphate–prenol linkage of the donor lipid
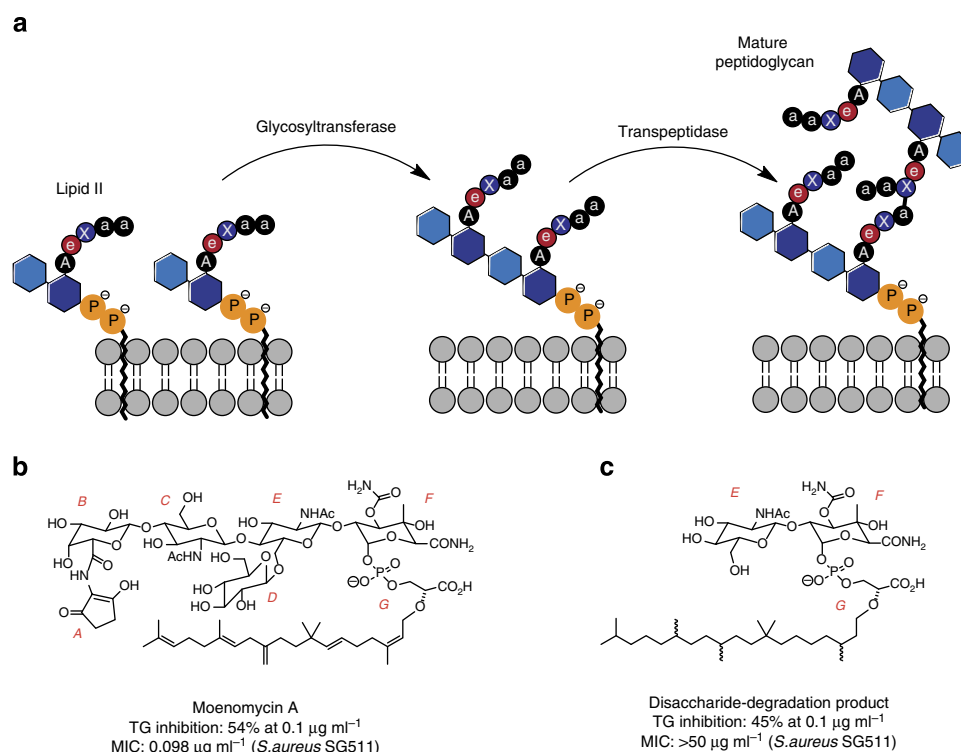
Figure 1 | Overview of PG cell wall synthesis and inhibitors. (**a**) PG synthesis in bacteria from lipid II with subsequent GT and TP catalysis, with A: L-Ala, a: D-Ala, e: D-iGln, X: either D-Lys(Ala₅) in case of *Staphylococcus*, or mDap in case of *Bacillus*. (**b**) Structure and *in vitro* activity of moenomycin A, indicating the different moieties with A to G. (**c**) Structure and *in vitro* activity of moenomycin's disaccharide degradation product.

Moenomycin A
TG inhibition: 54% at 0.1 µg ml⁻¹
MIC: 0.098 µg ml⁻¹ (*S.aureus* SG511)

Disaccharide-degradation product
TG inhibition: 45% at 0.1 µg ml⁻¹
MIC: >50 µg ml⁻¹ (*S.aureus* SG511)

II[10,23,24]. Although the E and F rings and the phosphoglycerate (G) portion of moenomycin A are important for GT inhibitory activity, analogues of this pharmacophore subunit did not maintain whole cell antibacterial activity[25,26]. Attempts to mimic the EFG structural fragment with disaccharide derivatives[27–30] resulted in compounds (such as TS30153 (ref. 17)) with cell-based activity, that is, minimum inhibitory concentration (MIC) of 3.12 and 12.5 μg ml^{-1} against staphylococci and enterococci, but with no *in vivo* activity. Compound TS30153 (ref. 17) has three hydrophobic binding elements that mimic the acyl and alkyloxy moieties of moenomycin A (Fig. 2b). Attempts to mimic directly lipid II[31], or the ring F of moenomycin[32], with monosaccharide scaffolds gave compounds with only low to medium activity (MIC = 60 μM against *Bacillus cereus*[31]). More recently, *de novo* inhibitors for GT discovered using high-throughput screening[33–35] or *in silico* methods[36], were shown to have improved *in vitro* activity (MIC = 0.25 μM against MRSA[33]), but no *in vivo* activity.

In this study, we explore novel chemistry based on a monosaccharide scaffold[37] to mimic the essential structure features of moenomycin and to improve the drug-like properties, in particular reduced molecular weight and hydrophobicity. Compared with other scaffolds, the monosaccharide scaffold approach provides structural diversity using up to five chiral attachment points within a small volume[38]. This allows for more efficient pharmacophore optimization, while still enabling the generation of a broad structural diversity to scope and improve activity and physicochemical properties. Here we use the approach to produce moenomycin-focused libraries and select compounds with *in vitro* antibacterial activity and *in silico* potential to inhibit the GT enzyme. We demonstrate the strength of this strategy with two of the most promising candidates showing inhibition of GT and PG synthesis in *in vitro* assays, as well as *in vivo* efficacy in eliminating *S. aureus* infection from a mouse mammary gland.

Results

Design and synthesis. We synthesized a small library of compounds by replacing the phosphoglycerate/phosphate moieties (G, Fig. 1) with simpler lipophilic substituents (that is, phenyl, biphenyl or naphthyl groups linked via a urea) and

changing the orientation and nature of ring F. This approach yielded compounds like ACL19378 (Fig. 2a, Supplementary Figs 1–8) and ACL19333 (Supplementary Fig. 1), with MICs against Gram-positive bacteria in the range of 2 μg ml^{-1}, but with limited activity in the presence of 50% serum. In the second stage, we used the disaccharide structure–activity relationship information to design more synthetically feasible and smaller monosaccharide molecules. A versatile solid-phase method was developed to rapidly synthesize the representatives of three different core chemotypes M1 to M3, starting from a single monosaccharide building block, that is, 1,5-anhydro-galactitol (see Fig. 3). Chemotype M1 explored the option of using only two of the hydrophobic elements, whereas the other two, M2 and M3, used a benzimidazole moiety as the third hydrophobic group (Fig. 3).

Five hundred compounds were thus synthesized combinatorially on solid-phase resin, purified using high-performance liquid chromatography, and tested for their MIC activity against two Gram-positive staphylococcal strains (methicillin-sensitive (MSSA) and methicillin-resistant *S. aureus* (MRSA)), three enterococcal strains and *Escherichia coli* as a Gram-negative control. Although most compounds were inactive against *E. coli*, many compounds displayed activity against the Gram-positive strains. The derivatives with Gram-positive antibacterial activity generally contained a lipophilic substituent such as an alkyl moiety (minimum length of 10 carbon atoms) or a biaryl, and one or two electron-deficient aryl groups. All active compounds were then tested for haemolytic activity and, after filtering out the haemolytic compounds, a series of compounds of chemotype M3 containing substituted amino-benzimidazoles were selected for further study (Supplementary Table 1). Two compounds (Fig. 4), ACL20215 (Supplementary Figs 10–15) and ACL20964 (Supplementary Figs 16–20), showed broad activity against a range of drug resistant *S. aureus* strains, including MRSA, GISA (glycopeptide-intermediate *S. aureus*), VRSA (vancomycin-resistant *S. aureus*) and DRSA (daptomycin-resistant *S. aureus*) and multi-drug-resistant *S. pneumoniae*, with low haemolytic activity against human red blood cells (Table 1). ACL20215 was assayed for resistance potential and showed a spontaneous mutation frequency against *S. aureus* (ATCC 13709; Smith strain) of less than 2.5×10^{-10} at four times its MIC value.
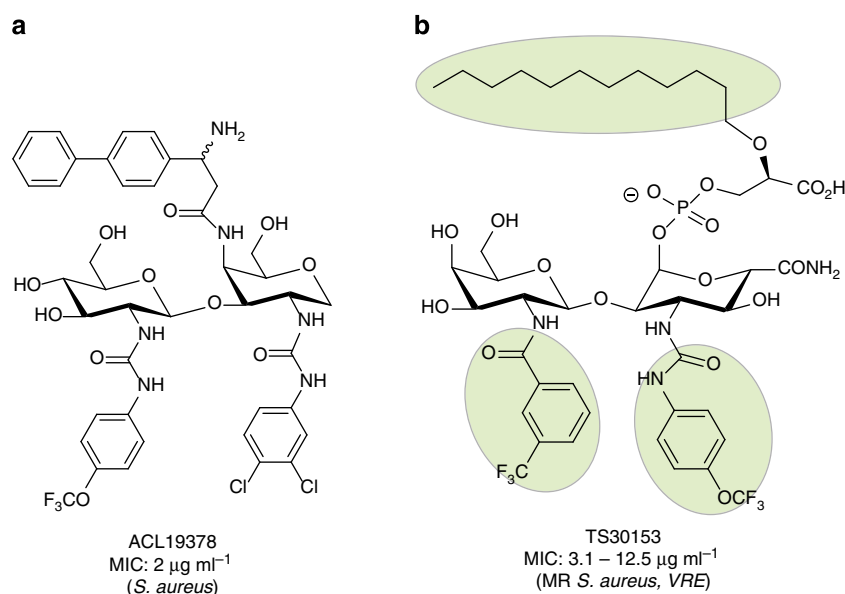

Figure 2 | Disaccharide templates for design of monosaccharides. (**a**) ACL19378, representative compounds from disaccharide library. (**b**) TS30153 (ref. 27) highlighting the three binding elements required for GT inhibition in green.

ACL19378
MIC: 2 μg ml^{-1}
(*S. aureus*)

TS30153
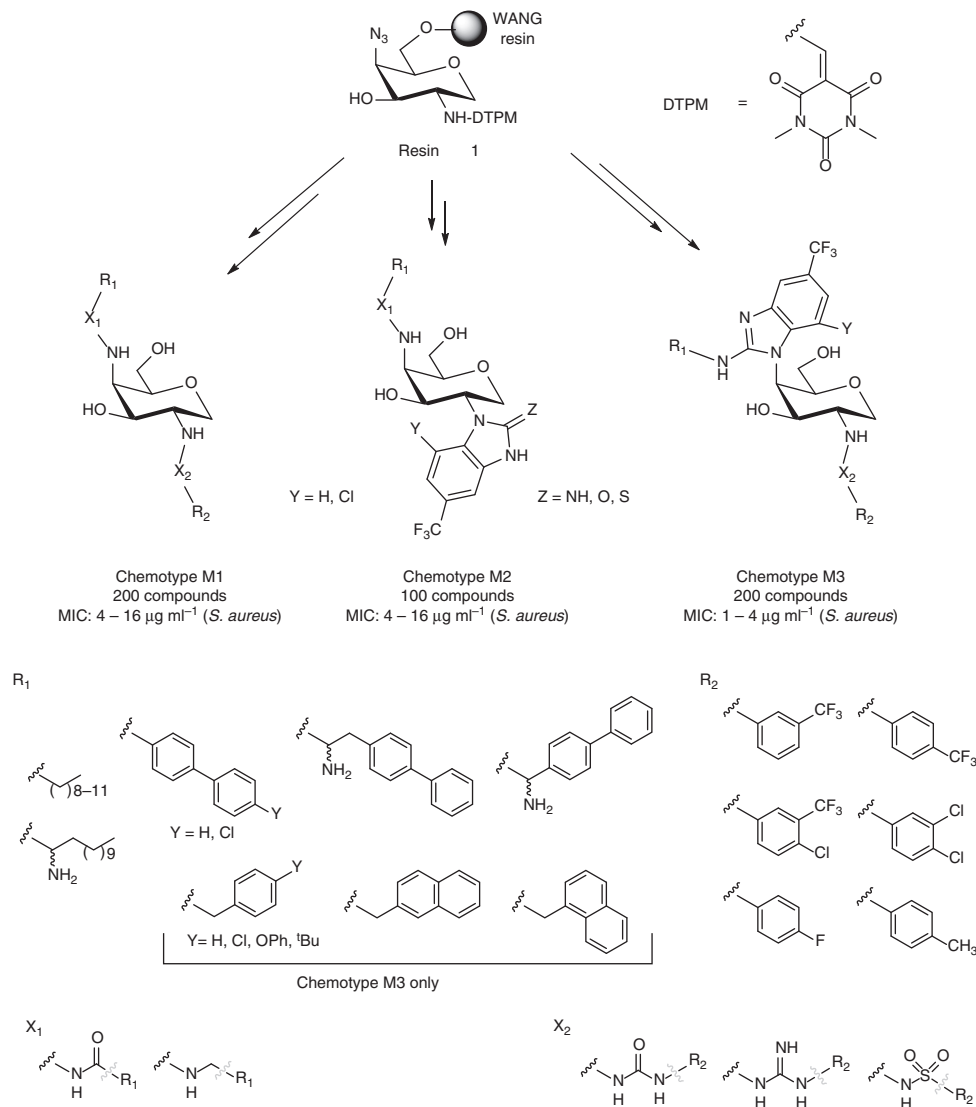MIC: 3.1 – 12.5 μg ml^{-1}
(MR *S. aureus*, VRE)

Figure 3 | Design of monosaccharide libraries. The figure illustrates the common starting building block, the three different chemotypes (M1, M2 and M3) and corresponding diversification at each substitution point.
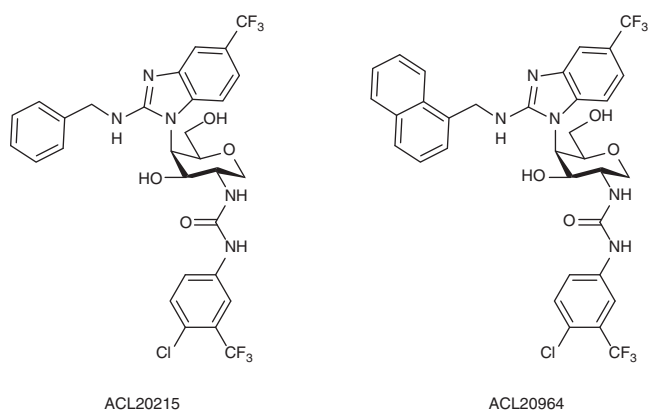

ACL20964 in an *in vitro* assay for bacterial PG biosynthesis, using crude *Bacillus megaterium* membrane preparations. This assay monitors [14C]UDP-GlcNAc incorporation into lipid II and mature PG, in the presence of different concentrations of antibiotics[39,40]. Owing to the sequential nature of the glycosyltransfer and transpeptidation, it is not possible to determine at which step PG biosynthesis is blocked in this assay. The low concentration of lipid II can be detected by thin-layer chromatography (TLC) separation and subsequent phosphorimaging of pre-solubilized membranes, which was incubated with the cytoplasmic PG precursors UDP-MurNAc-pentapeptide and UDP-[14C]GlcNAc[41,42]. As shown in Fig. 5 (and Supplementary Table 2 and Fig. 21), both ACL20215 and ACL20964 caused an inhibition of mature PG production at a concentration of $200 \, \mu g \, ml^{-1}$, to a similar extent as the controls, vancomycin and moenomycin A. Both inhibitors also caused an accumulation of lipid II, although to a lesser extent compared with vancomycin or moenomycin A.

Membrane-disruption experiments were performed using *S. aureus* (ATCC 25923) in combination with membrane potential-sensitive cyanine dye diSC$_3$5 (ref. 43). Neither compounds showed membrane disruption (Supplementary

Figure 4 | Structures of ACL20215 and ACL20965. ACL20215 and ACL20965 are two of the most active monosaccharide compounds.

Evaluation of mode of action. To elucidate the mode of action of the inhibitors, we conducted various GT enzyme inhibition assays. We first examined the inhibitory effect of the compounds in a bacterial membrane environment, comparing ACL20215 and

Table 1 | *In vitro* activity data of ACL20215 and ACL20964.

Organism	Strain/type	Vancomycin	Moenomycin A	ACL20215	ACL20964
MIC ($\mu g\,ml^{-1}$)					
S. aureus	MSSA, ATCC 25923	1		4	4
	MRSA, ATCC 43300	1	4	4	8
	Newbould 305			2	1
	NRS 17—GISA	8	16–32	8	32
	NRS 1—GISA	4	1	4	16
	VRS 1	>64	8	4	8
	mMRSA, DRSA, ci	4	16	4	8
E. faecium	ATCC 35667			16	2
	VanA, ATCC 51559	>64	32	8	>64
E. faecalis	ATCC 29212			4	8
	VanA, ci	>64	>64	8	64
S. pneumoniae	MDR, ATCC 700677	2	8–16	4	8–16
E. coli	ATCC 25922	>64	>64	>64	>64
Mutation frequency					
S. aureus (at 4 × MIC)	ATCC 13709			2.5×10^{-10}	
HC$_{50}$ ($\mu g\,ml^{-1}$)					
Human	RBC			74	>100
IC$_{50}$ ($\mu g\,ml^{-1}$)					
S. aureus	MGT			17.1	11.1

ci, clinical isolate; DRSA, daptomycin-resistant *S. aureus*; GISA, glycopeptide-intermediate *S. aureus*; HC$_{50}$, half maximal haemolytic concentration; IC$_{50}$, half maximal inhibitory concentration; MDR, multi-drug-resistant; MGT, monofunctional glycosyltranferease; MIC, minimum inhibitory concentration; mMRSA, multi-drug-resistant methicillin-resistant *S. aureus*; Moenomycin A (Sigma, 32404); MRSA, methicillin-resistant *S. aureus*; MSSA, methicillin-sensitive *S. aureus*; RBC, red blood cells; Vancomycin (Sigma, 861987); VRS, vancomycin-resistant *S. aureus*.
All values are $\mu g\,ml^{-1}$.

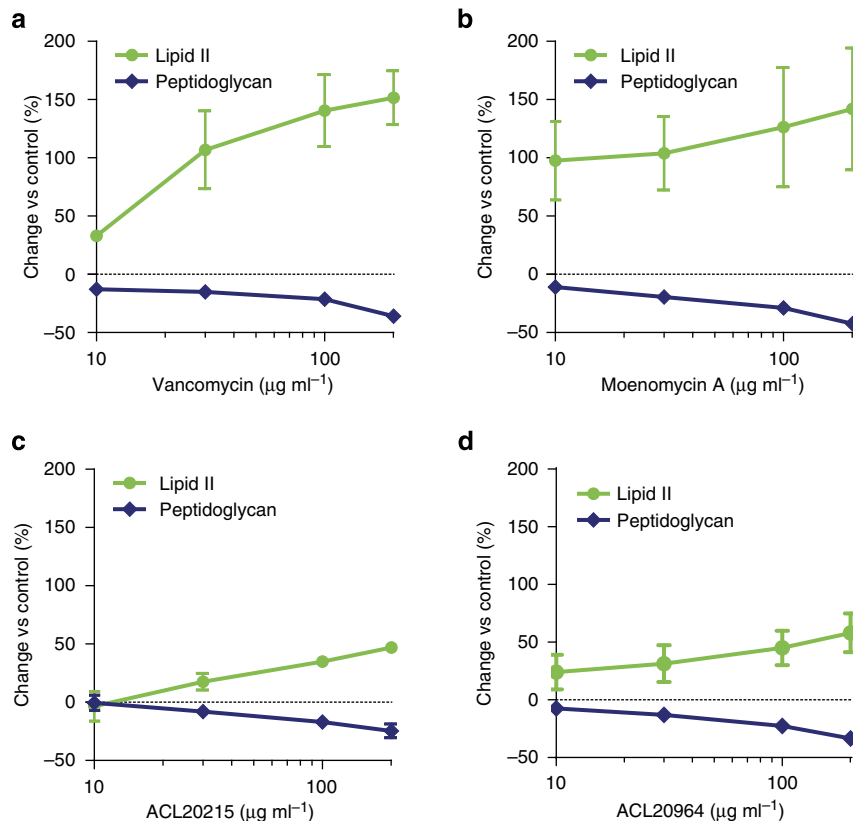**Figure 5 | Inhibition of PG synthesis.** The inhibitory effect in bacterial PG biosynthesis within a crude *B. megaterium* membrane is shown for (**a**) vancomycin, (**b**) moenomycin A, (**c**) ACL20215 and (**d**) ACL20964, showing the relative change of lipid II and PG isolated from the crude membrane by TLC, after 3 h, compared with non-antibiotic treatment. Error bars show s.d. for $n = 3$.
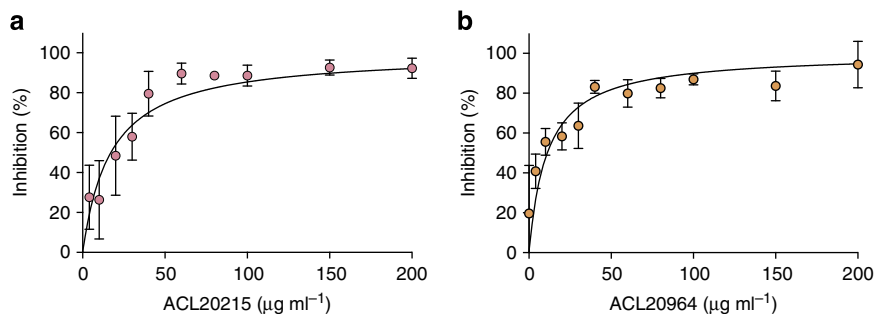
Figure 6 | Inhibition of glycosyltransferase. The inhibition of MGT from *S. aureus* is shown for ACL20215 (**a**) and ACL20964 (**b**), by measuring the transformation rate of fluorescent lipid II analogue and comparing it with the maximum inhibitory effect of moenomycin A at 50 µM or 79.2 µg ml^{-1}. Error bars show s.d. for $n = 4$.

Fig. 22) compared with a positive control Citropin 1.1 (refs 44–46), which suggested that the GT inhibitors disrupt PG biosynthesis without disrupting the cell membrane.

We then monitored the transformation of fluorescent NBD-lipid II by two different GT enzymes, PBP1 from *Clostridium difficile* and MGT from *S. aureus*. The single concentration test at 200 µg ml^{-1} revealed that both inhibitors showed an inhibitory effect against MGT *S. aureus*, while showing only moderate effect against PBP1 *C. difficile* (Supplementary Fig. 23). Confirmative dose–response assays were subsequently conducted with continuous fluorescent activity assay using a dansyl-labelled, lysine-lipid II substrate[47]. The assay revealed that both ACL20215 and ACL20964 were able to inhibit MGT from *S. aureus* with an IC$_{50}$ of 17 and 11 µg ml^{-1}, respectively (Fig. 6). In the same assay, moenomycin A was used as positive control showing an IC$_{50}$ of 5 µM or 8 µg ml^{-1}.

Virtual docking. Several crystal structures of GT domains have been reported for Gram-positive (MGT[48,49] and PBP2 (refs 50,51) from *S. aureus*) and Gram-negative bacteria (PBP1 (ref. 52) from *E. coli* and PGT[11,53] from *Aquifex aeolicus*), showing a high structural similarity between the difference species. One main feature of the structures is a binding site loop (MGT *S. aureus* Phe$_{120}$–Gly$_{130}$; PBP2 *S. aureus* Gly$_{134}$–Gly$_{145}$)[54] located between the donor-binding site, occupied by moenomycin, and the acceptor binding site occupied by the incoming lipid II molecule. This binding site loop is highly flexibly and partly disordered in most of the crystal structures (see Supplementary Table 3). Even when the loop is resolved, it can occupy different conformations, either separating the donor from the acceptor sites or opening a groove between the sites (see Supplementary Fig. 24 and Supplementary Note 1). We have carried out *in silico* virtual docking with the monosaccharides ACL20215 and ACL20964, choosing the receptor model (and loop conformation), which best reproduced the binding orientation of moenomycin. A receptor model based on the crystal structure of MGT from *S. aureus* with a loop conformation blocking the access to the acceptor site, 3HZS[48], was thereby selected (see Supplementary Fig. 25). As shown in Fig. 7, the benzimidazole group of both inhibitors was located similarly to portion G of moenomycin, with one of the other hydrophobic groups located in the donor-binding site (similar to ring E of moenomycin), and the other was located towards the acceptor site not occupied by moenomycin. While the virtual docking experiments were able to reproduce the binding orientation of moenomycin, a degree of uncertainty remained due to the flexibility of the binding site loop (Fig. 7), and its ability to adopt different conformations depending on the ligand[49]. However, the docking experiments clearly indicated the
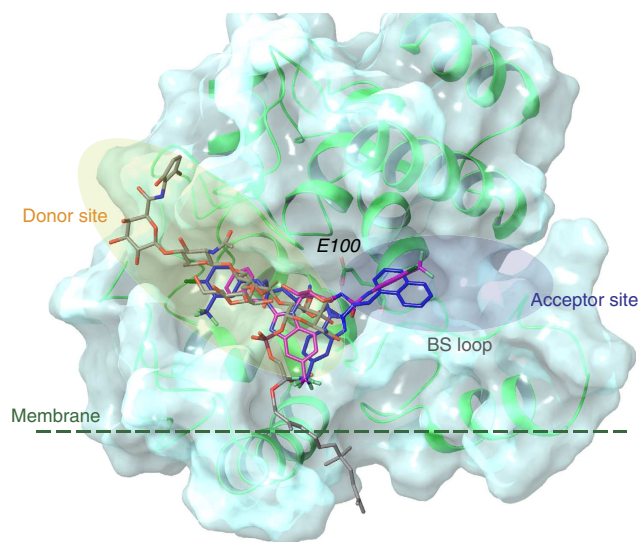

Figure 7 | Virtual docking studies of ACL20215 and ACL20215. The virtual docking poses are shown for ACL20215 (pink) and ACL20964 (blue) within the GT domain of MGT *S. aureus* (pdb: 3HZS[48]) shown as ribbon (green) and surface representation. Binding orientation of moenomycin is shown as found in the corresponding crystal structure (grey). The structure illustrates that both inhibitors are able to occupy the donor, as well as part of the acceptor sites. The dotted line is illustrating the suggested membrane interface[49,50]. BS loop marks the region of the binding site loop with high conformational variation or disorder in the different crystal structure, while E100 marks the active site residue Glu$_{100}$.

potential of the inhibitors to extend to the acceptor binding site not occupied by moenomycin.

***In vivo* studies.** ACL20215 testing with *in vitro* metabolic stability assays showed no degradation of the compound using both human and mouse liver microsomes. The *in vivo* pharmacokinetic properties of ACL20215 and ACL20964 were investigated using intravenous (i.v.) administration at 3.5 mg kg^{-1} to male rats (Table 2 and Supplementary Table 4). Both compounds had a high apparent half-life ($t_{1/2}$) of 27.2 and 33.8 h, respectively. They also showed a very high volume of distribution (V_D) and a high clearance (Cl$_{total}$). No urinary excretion was detected for either compound, and no metabolites were observed in plasma. The maximum tolerated dose for both compounds (see Supplementary methods) was determined following intraperitoneal (i.p.) administration of the compounds to mice, and showed good tolerance up to 60 mg kg^{-1}, with no mortality up to 100 mg kg^{-1}. Both compounds induced some minor changes to central/

Table 2 | Pharmacokinetic properties and *in vivo* efficacy of ACL20215 and ACL20964.

	ACL20215	ACL20964
Pharmacokinetic properties		
Metabolic stability (*in vitro*)	No degradation	ND
Rat (i.v.)		
Dose (mg kg^{-1})	3.5	3.5
$t_{1/2}$ (h)	27.2	33.8
Plasma Cl$_{total}$ (ml min^{-1} kg^{-1})	42.1	17.9
Blood Cl$_{total}$ (ml min^{-1} kg^{-1})	48.9	21.5
V_Z (l kg^{-1})	97.2	53.0
Mice (i.p.)		
MTD (mg kg^{-1})	100	100
In vivo efficacy		
Mouse (i.p.)		
Survival 7 days (%)	100	100
Mouse (i.v.)		
Survival 7 days (%)	10	10
Mouse (mastitis)		
ED$_{2logc.f.u.}$ (µg per gland)	730	510
ED$_{4logc.f.u.}$ (µg per gland)	1,400	770
PD$_{50}$ (µg per gland)	>1,000	800–1,000
PD$_{100}$ (µg per gland)	>1,000	>1,000

Cl, clearance; ED$_{2logc.f.u.}$, effective dose to reduce bacterial load by 2 × log(c.f.u.); ED$_{4logc.f.u.}$, effective dose to reduce bacterial load by 4 × log(c.f.u.); i.p., intraperitoneal injection; i.v., intravenous injection; MTD, maximal tolerated dose; ND, not determined; PD$_{50}$, 50% protective dose; PD$_{100}$, 100% protective dose; $t_{1/2}$, half-life; V_Z, volume of distribution.

autonomic responses at the higher dose of 100 mg kg^{-1}. No adverse effects were observed in a single-dose study (4 mg kg^{-1}) following i.v. administration.

ACL20215 and ACL20964 were subsequently tested in a mouse model of septicemia, using 10 male CD-1 (*Crl.*)-derived mice, inoculated i.p. with a LD$_{90-100}$ of *S. aureus* (Smith; 3.7 × 10^5 c.f.u. per mouse). Both compounds administered i.p. 10 min after inoculation at 50 mg kg^{-1} resulted in 100% survival rate after 7 days. However, same studies with i.v. administration of the compounds (4 mg kg^{-1}, 10 min after inoculation) showed no antibacterial effect, resulting only in a 10% survival rate, compared with 90% for ampicillin (0.1 mg kg^{-1}). The lack of efficacy following i.v. administration is most likely due to a lower dose (4 mg kg^{-1}, limited by solubility) combined with the high volume of distribution and serum-binding properties of the compounds, which effectively lowers the free drug concentration at the site of infection. When a higher dose (50 mg kg^{-1} as a suspension) was administered i.p. at the site of infection, the high local concentration of the drug ensures effective clearance of the bacterial infection. Further optimization of compound properties, dose or formulation is required for parenteral administration.

Additional *in vivo* studies were conducted with ACL20215 and ACL20964 using a mouse mammary gland infection (mastitis) model with intraductal inoculation of *S. aureus* (Newbould 305, ATCC 29740). Each compound was instilled at different doses into the teat canal of both contralateral glands from the fourth mammary gland pair of lactating mice at 4 h after bacterial inoculation. Mice were killed at 14 h post infection and both glands were analyzed for c.f.u. counts (Fig. 8, Table 2 and Supplementary Tables 5 and 6). The effective dose to reduce the bacterial load by 2 × log(c.f.u.) (ED$_{2log}$) were 730 and 510 µg per gland, for ACL20215 and ACL20964, respectively, indicating that both compounds cleared 99% of the staphylococci from the infected mammary gland at a moderate dose. Similarly, the protective doses to clear all bacteria in 50% (PD$_{50}$) and 100% (PD$_{100}$) of the glands, respectively, indicated that a high dose of ACL20964 very efficiently cleared *S. aureus* from the infected glands (Table 2). In contrast, no PD values could be determined for ACL20215 as the latter compound was unable to eradicate all

bacteria in 50 or 100% of the glands in the analyzed doses to at least the detection limit of the assay.

Discussion

Using moenomycin A and previously reported GT inhibitors[27,28], we designed and synthesized a small library of disaccharide-based compounds with a smaller, more drug-like, hydrophobic tail[29]. These compounds (such as ACL19378) showed good *in vitro* antibacterial activity but had unfavourable physicochemical properties that limited their *in vivo* application. Nevertheless, this set of active compounds gave valuable structure–activity relationship information, which was used to design libraries of compounds based on a smaller monosaccharide scaffold[37]. This strategy also reduced compound hydrophobicity and chemical complexity, enabling the synthesis of the first reported direct GT inhibitors with *in vivo* efficacy against bacteria.

A reductionist approach, moving from disaccharide mimics of the moenomycin EFG fragment to a smaller monosaccharide scaffold, maintains the key pyranose scaffold and the substitution pattern derived from the disaccharide actives. Chemical chirality inherent in the pyranose scaffold ensures a rigid three-dimensional positioning of substituents that is maintained in the series. Second, the solid-phase synthetic method allowed us to make substantial libraries of chemotypes designed to mimic the disaccharide series. In this way, we identified a series of compounds, corresponding to the amino-benzimidazole chemotype, which showed clear antibacterial activity against a range of drug-resistant Gram-positive bacteria. While the cell-based activity suggests a preference for more hydrophobic substituents, some structural variations are not reflected in their activity, such as the difference in activity between a 2- and 1-naphthyl group and the lack of activity of the corresponding biphenyl compound.

The two most promising compounds from this monosaccharide library, that is, ACL20215 and ACL20964, showed good *in vitro* antibacterial activity against a range of Gram-positive bacteria, including those resistant to common antibiotics, that is, MRSA, GISA and VanA enterococci. PG biosynthesis assay data, taken together, suggests that both compounds trigger an accumulation of lipid II and a decrease of mature PG, as is the
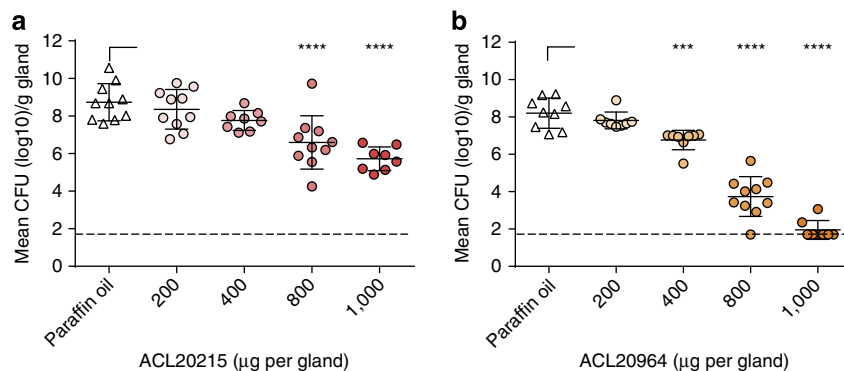
Figure 8 | *In vivo* efficacy in mastitis mouse model. *S. aureus* c.f.u. counts (c.f.u. g^{-1} gland) at 14 h post treatment in infected mouse mammary glands treated with increasing doses of ACL20215 (**a**) and ACL20964 (**b**). Significance compared with control (paraffin oil) are given as $P < 0.001$ (***) and $P < 0.0001$ (****), calculated by one-way analysis of variance followed by Holm–Sidak *post hoc* test. Dashed line represents the detection limit at 1.7 log$_{10}$c.f.u. Data values are given in Supplementary Table 5.

case for moenomycin A. Compounds can inhibit the function of GT with IC$_{50}$ values similar to that determined for moenomycin. The virtual docking experiment suggest that the compounds are able to bind in the catalytic site of the GT by occupying part of the donor lipid II-binding site (similar to moenomycin A) as well as part of the acceptor lipid II-binding site (not occupied by moenomycin A).

Both hit compounds can be tolerated in mice up to a dose of 100 mg kg^{-1}, while showing good metabolic stability in rats. Even though the library design aimed to reduce the lipophilicity, it is apparent that GT inhibitory compounds require a certain degree of hydrophobicity to be active *in vitro* and *in vivo*. The monosaccharide scaffold is an excellent scaffold for drug design, as it is able to present various substituents or binding elements (in this case, three hydrophobic elements) in diverse spatial orientation using up to five chiral attachment points[38]. The scaffold is also able to present those substituents in a conformational rigid form, indicated by the fact that both monosaccharide compounds, ACL20215 and ACL20964, existed as two atropisomers[55,56] (see Supplementary Fig. 1 and Supplementary Note 1), conformational restricted isomers or rotamers, which would not occur if the carbohydrate scaffold itself was flexible. Virtual docking experiments show both atropisomers among the top ranked poses. It is reasonable to assume that one isomer will be the preferred binding partner for the GT active site, but our *in silico* and *in vitro* experiments were unable to distinguish them.

The membrane-associated nature of the GT enzyme and the hydrophobicity of its natural substrate lipid II necessitates a certain degree of lipophilicity for a compound with an inhibitory effect. While serum binding could not be eliminated in this pilot series, ACL20215 and ACL20964 showed *in vivo* efficacy without toxicity. GT inhibition hence remains a very attractive drug discovery target[3], as the current inhibitor moenomycin shows extremely low induction of antibiotic resistance[14,15], and also inhibits the conjugative transfer of resistance plasmids[19,57]; significant advantages given the current background of increased antimicrobial resistance.

Methods

Solid-phase synthesis. All monosaccharide compounds were synthesized on solid-phase using an orthogonally protected galactitol-building block attached to WANG resin. The synthesis of ACL20215 and ACL20964 is given in Supplementary Fig. 9 and below as a representative example.

DTPM removal: the resin was treated with a solution of 5% hydrazine hydrate in dimethylformamide (DMF; 10 ml g^{-1} of resin), shaken (1 h, RT), drained and washed (3× DMF, 3× DCM, 3× DMF). Urea formation: the resin was treated with a solution of 4-chloro-3-trifluoromethyl-phenyl isocyanate (0.15 M) in DMF

(10 ml g^{-1} of resin), shaken (O/N, RT), drained and washed (3× DMF, 3× DCM). The resin was taken up in a solution of sodium methoxide (0.15 M) in MeOH (5 ml g^{-1} of resin) and tetrahydrofuran (20 ml g^{-1} of resin), shaken (3 h, RT), drained and washed (3× tetrahydrofuran, 3× MeOH, 3× DCM, 3× DMF). Azide reduction: the resin was treated with a solution of lithium *tert*-butoxide (0.2 M) and DL-dithiothreitol (DTT, 0.2 M) in DMF (15 ml g^{-1} of resin), shaken (O/N, RT), drained and washed (3× DMF, 3× MeOH, 3× DCM, 3× DMF).

Formation of the substituted benzimidazoles: the resin was treated with a solution of 4-fluoro-3-nitro-benzotrifluoride (0.36 M) and DIPEA (0.36 M) in DMF (10 ml g^{-1} of resin), and heated at 50 °C. The resin was drained and washed with (3× DMF, 3× DCM, 3× DMF). Reduction the nitro group: the resin was treated with a solution of SnCl$_2$.2H$_2$O in DMF (2.0 M, 10 ml g^{-1} of resin), shaken (O/N, RT), drained and washed (3× DMF, 3× DMF/MeOH 1:1, 3× DCM, 3× DMF, 3× DMF/MeOH 1:1, 3× DCM).

To form the benzimidazole, the resin was treated with DIPEA (0.5 M) in DCM (10 ml g^{-1} of resin), shaken (1 h, RT), drained and washed (3× DCM), followed by a solution of cyanogen bromide (1.0 M, 10 ml g^{-1} of resin), shaken (O/N, RT), drained and washed (3× DCM, 3× MeOH, 3× DCM). To alkylate the 2-amine, the resin was treated with a solution of benzyl bromide or 1-(bromomethyl) naphthalene (0.4 M) and DIPEA (0.8 M) in DMF (10 ml g^{-1} of resin), shaken (O/N, RT), drained and washed (3× DCM, 3× MeOH, 3× DCM).

Cleavage and purification: each resin was treated with 10% TFA, 20% triethylsilane in dry DCM (1.5 ml), allowed to stand at RT for 3 h, drained into a test tube and washed (3× DCM). The concentrated samples were treated with a solution of saturated ammonia in methanol (1.0 ml) and left to stand at RT for 2 h, and concentrated by vacuum. Crude samples were purified using preparative high-performance liquid chromatography on a C-18 column (water/acetonitrile gradient).

Analytical data for ACL20215. The analytical data for ACL20125 are given as ^{1}H-NMR, temperature dependent ^{1}H-NMR, ^{13}C-NMR, COSY, edCOSY and HMBC NMR spectra in Supplementary Figs. 10–15, respectively. The structure of ACL20215 exists as two distinctive rotamers or conformational isomers that can be detected in NMR experiments. Transition between the two isomers, or atropisomers, can be achieved by heating the sample to 45 °C (see Supplementary Fig. 11). *In silico* analysis of the structure and conformation of ACL20125 indicate restricted torsional rotation of the C^4–N^{Benzimidazole} bond, due to size of the benzimidazole group. Energy barrier calculation indicate an upper range of 25 kcal/mol for this rotational barrier (see Supplementary Fig. 3), which, in relation to other known atropisomers, corresponds to an interconversion rate from a few hours to a few days[56].

^{1}H-NMR (600 MHz, dimethylsulphoxide (DMSO)-d6): major rotamer δ 9.20 (br s, 1H, 7-NH), 8.10 (d, $J = 8.0$ Hz, 1H, H-20), 8.02 (d, $J = 2.2$ Hz, 1H, H-9), 7.50 (d, $J = 8.9$ Hz, 1H, H-13), 7.48 (dd, $J = 2.2$, 8.9 Hz, 1H, H-12), 7.42 (s, 1H, H-17), 7.39 (d, $J = 7.3$ Hz, 2H, H-25, H-29), 7.27 (dd, $J = 7.3$, 7.3 Hz, 2H, H-26, H-28), 7.22 (d, $J = 8.0$ Hz, 1H, H-19), 7.19 (dd, $J = 7.3$, 7.3 Hz, 1H, H-27), 7.14 (t, $J = 5.8$ Hz, 1H, 15-NH), 6.34 (d, $J = 6.0$ Hz, 1H, 2-NH), 5.41 (d, $J = 5.8$ Hz, 1H, 3-OH), 4.91 (m, 1H, H-4), 4.91 (t, $J = 5.1$ Hz, 1H, 6-OH), 4.63 (m, 2H, H-23), 4.27 (dd, $J = 5.2$, 11.2 Hz, 1H, H-1β), 4.00 (m, 2H, H-3, 5), 3.87 (dddd, $J = 5.2$, 5.8, 11.2, 11.2 Hz, 1H, H-2), 3.40 (m, 1H, H-6a), 3.39 (m, 1H, H-1α), 3.18 (dd, $J = 5.8$, 5.8, 11.2 Hz, 1H, H-6b); minor rotamer δ 9.25 (br s, 1H, 7-NH), 8.10 (d, $J = 2.2$ Hz, 1H, H-9), 7.78 (t, $J = 5.2$ Hz, 1H, 15-NH), 7.54 (m, 2H, H-12, H-13), 7.54 (d, $J = 7.3$ Hz, 2H, H-25, H-29), 7.45 (s, 1H, H-17), 7.36 (d, $J = 8.0$ Hz, 1H, H-20), 7.35 (dd, $J = 7.3$, 7.3 Hz, 2H, H-26, H-28), 7.27 (dd, $J = 7.3$, 7.3 Hz, 1H, H-27), 7.21 (d, $J = 8.0$ Hz, 1H, H-19), 6.36 (d, $J = 6.0$ Hz, 1H, 2-NH), 5.29 (d, $J = 6.1$ Hz, 1H, 3-OH), 5.00 (m, 1H, H-4), 4.96 (t, $J = 5.2$ Hz, 1H, 6-OH), 4.65 (m, 1H, H-23a), 4.63 (m, 1H, H-23b), 4.24 (dddd, $J = 5.2$, 5.8, 11.2, 11.2 Hz, 1H, H-2), 4.16 (dd, $J = 5.2$, 11.2 Hz, 1H, H-1β), 4.07 (m, 2H, H-3, 5), 3.48 (ddd, $J = 5.2$, 5.2, 11.2 Hz, 1H, H-6a), 3.39

(m, 1H, H-1α), 3.27 (dd, $J = 5.8, 5.8, 11.2$ Hz, 1H, H-6b); ^{13}C-NMR (150 MHz, DMSO-d6): major rotamer δ 158.9 (C-15), 154.9 (C-7), 143.0 (C-16), 140.1 (C-24), 139.9 (C-8), 137.4 (C-21), 131.8 (C-12), 128.0 (C-26, C-28), 126.8 (C-25, C-29), 126.4 (C-27), 125.5 (q, 1JCF = 271 Hz, C-22), 122.9 (q, 1JCF = 273 Hz, C-14), 122.6 (q, 2JCF = 31 Hz, C-10), 122.3 (C-13), 121.5 (C-11), 121.0 (q, 2JCF = 31 Hz, C-18), 116.1 (C-9), 115.0 (C-19), 112.1 (C-20), 111.4 (C-17), 77.7 (C-5), 70.7 (C-3), 68.8 (C-1), 60.3 (C-6), 55.2 (C-4), 48.8 (C-2), 46.0 (C-23); minor rotamer δ 155.8 (C-15), 155.0 (C-7), 142.1 (C-16), 140.9 (C-21), 139.9 (C-8), 139.0 (C-24), 131.9 (C-12), 128.4 (C-26, C-28), 127.5 (C-25, C-29), 127.0 (C-27), 125.5 (q, 1JCF = 271 Hz, C-22), 122.9 (q, 1JCF = 273 Hz, C-14), 122.6 (q, 2JCF = 31 Hz, C-10), 122.3 (C-13), 121.5 (C-11), 121.0 (q, 2JCF = 31 Hz, C-18), 116.1 (C-9), 115.0 (C-19), 109.4 (C-20), 111.1 (C-17), 77.9 (C-5), 70.8 (C-3), 69.0 (C-1), 59.9 (C-6), 56.4 (C-4), 48.5 (C-2), 46.8 (C-23); HRESIMS (m/z): [M + H] + calcd. for $C_{29}H_{27}Cl_1F_6N_5O_4$, 658.1650; found, 658.1659.

Analytical data for ACL20964. The analytical data for ACL20964 are given as ^{1}H-NMR, ^{13}C-NMR, COSY, edCOSY and HMBC NMR spectra in Supplementary Figs 16–20, respectively. Similar to ACL20215, ACL20964 exists as two conformational isomer, due to rotational restriction of the C^4–N^{Benzimidazole} bond, caused by the large benzimidazole group.

^{1}H-NMR (600 MHz, DMSO-d6): major rotamer δ 9.26 (br s, 1H, 7-NH), 8.14 (d, $J = 8.2$ Hz, 1H, H-32), 8.13 (d, $J = 8.2$ Hz, 1H, H-20), 8.04 (s, 1H, H-9), 7.94 (d, $J = 8.2$ Hz, 1H, H-29), 7.81 (d, $J = 8.2$ Hz, 1H, H-27), 7.63 (d, $J = 8.2$ Hz, 1H, H-25), 7.54 (m, 2H, H-12, H-13), 7.42 (s, 1H, H-17), 7.39 (dd, $J = 8.2, 8.2$ Hz, 1H, H-26), 7.22 (d, $J = 8.2$ Hz, 1H, H-19), 7.19 (t, $J = 5.7$ Hz, 1H, 15-NH), 6.34 (br s, 1H, 2-NH), 5.47 (br s, 1H, 3-OH), 5.09 (m, 2H, H-23), 4.97 (m, 1H, H-4), 4.95 (br s, 1H, 6-OH), 4.28 (dd, $J = 4.8, 11.2$ Hz, 1H, H-1β), 4.01 (m, 2H, H-3, H-5), 3.92 (m, 1H, H-2), 3.45 (m, 1H, H-6a), 3.39 (m, 1H, H-1α), 3.23 (m, 1H, H-6b); minor rotamer δ 9.26 (br s, 1H, 7-NH), 8.21 (d, $J = 8.2$ Hz, 1H, H-32), 8.10 (s, 1H, H-9), 7.96 (d, $J = 8.2$ Hz, 1H, H-29), 7.87 (d, $J = 8.2$ Hz, 1H, H-27), 7.78 (t, $J = 5.1$ Hz, 1H, 15-NH), 7.73 (d, $J = 8.2$ Hz, 1H, H-25), 7.60 (dd, $J = 8.2, 8.2$ Hz, 1H, H-31), 7.55 (m, 2H, H-12, H-13), 7.54 (m, 1H, H-30), 7.47 (s, 1H, H-17), 7.50 (m, 1H, H-26), 7.37 (d, $J = 8.2$ Hz, 1H, H-20), 7.22 (d, $J = 8.2$ Hz, 1H, H-19), 6.36 (br s, 1H, 2-NH), 5.31 (br s, 1H, 3-OH), 5.16 (dd, $J = 5.6, 15.3$ Hz, 1H, H-23a), 5.11 (dd, $J = 4.8, 15.3$ Hz, 1H, H-23b), 5.01 (m, 1H, H-4), 4.95 (br s, 1H, 6-OH), 4.24 (m, 1H, H-2), 4.16 (dd, $J = 5.2, 11.2$ Hz, 1H, H-1β), 4.05 (m, 1H, H-3), 4.01 (m, 1H, H-5),3.48 (m, 1H, H-6a), 3.39 (m, 1H, H-1α), 3.27 (m, 1H, H-6b); ^{13}C-NMR (150 MHz, DMSO-d6): major rotamer δ 158.7 (C-15), 154.9 (C-7), 143.1 (C-16), 140.0 (C-8), 137.5 (C-21), 134.9 (C-33), 134.2 (C-28), 131.9 (C-12), 130.9 (C-24), 128.5 (C-29), 127.0 (C-27), 126.6 (q, 2JCF = 31 Hz, C-10), 126.1 (C-31), 125.6 (C-30), 125.5 (C-26), 125.4 (q, 1JCF = 271 Hz, C-22), 124.6 (C-25), 123.4 (C-32), 122.8 (q, 1JCF = 273 Hz, C-14), 122.3 (C-13), 121.5 (C-11), 121.0 (q, 2JCF = 31 Hz, C-18), 116.1 (C-9), 115.0 (C-19), 112.1 (C-20), 111.4 (C-17), 77.6 (C-5), 70.7 (C-3), 68.8 (C-1), 60.3 (C-6), 55.1 (C-4), 49.0 (C-2), 44.3 (C-23); minor rotamer δ 155.8 (C-15), 154.9 (C-7), 142.1 (C-16), 140.9 (C-21), 140.0 (C-8), 134.2 (C-33), 133.2 (C-28), 131.8 (C-12), 130.9 (C-24), 128.6 (C-29), 127.7 (C-27), 126.6 (q, 2JCF = 31 Hz, C-10), 126.5 (C-31), 125.8 (C-30), 125.6 (C-26), 125.4 (q, 1JCF = 271 Hz, C-22), 125.4 (C-25), 123.4 (C-32), 122.8 (q, 1JCF = 273 Hz, C-14), 122.3 (C-13), 121.5 (C-11), 121.0 (q, 2JCF = 31 Hz, C-18), 116.1 (C-9), 115.0 (C-19), 111.1 (C-17), 109.5 (C-20), 77.8 (C-5), 70.9 (C-3), 68.5 (C-1), 59.8 (C-6), 56.4 (C-4), 48.5 (C-2), 44.7 (C-23); HRESIMS (m/z): [M + H] + calcd. for $C_{33}H_{29}Cl_1F_6N_5O_4$, 708.1807; found, 708.1797.

Virtual docking. The virtual docking of inhibitor and moenomycin structures into the binding site of MGT from *S. aureus* were done using the software Glide (version 6.5, Schrödinger, LLC, New York, 2014 (ref. 58)) and using several different crystal structures with different binding site loop conformations. In addition, the induced fit protocol in the Schrödinger software package (Induced Fit Docking protocol 2014-4, Glide version 6.5, Prime version 3.7, Schrödinger, LLC[59,60]) was used to allow conformational flexibility of the GT domain. The docking experiments were all done using the standard precision (SP) in Glide and defining a binding site with 13 Å around the crystal structure of moenomycin, large enough to include also the acceptor site which is not occupied by moenomycin. For the structure of moenomycin, a truncated version was used, without the fatty acid chain and only a lactic acid attached to the phosphate group. Models for inhibitors were built in four different conformations, $^4C_1$ and $_1C^4$ chair conformation for the galactose moiety, and two different orientations for the benzimidazole moiety compared with the galactose ring. All inhibitor structure models were built using Maestro (version 10.0, Schrödinger, LLC, New York, 2014).

The different approaches, that is, crystal structures and protocols, were validated and the best one selected by comparing the docking orientation of moenomycin with the one found in the crystal structures, by visual inspection. The following models for MGT from *S aureus* have been used for the docking experiments: 3HZSm–3HZS[48] changing to wild type, by mutating Asn100 to Asp, 3VMRm–3VMR[49] modelling the missing loop residues (2 residues) with loop search, 3NB6sa-Homology model of MGT *S. aureus* sequence using 3NB6 (ref. 11) (PGT from *A. aeolicus*) with complete loop as template, 3VMSm–3VMS[49] modelling missing loop (7 residues) using the loop in 3NB6 (ref. 11) as template.

From these receptor models, 3HZSm was able to reproduce the binding orientation of moenomycin A as found in the crystal structure (see Supplementary

Fig. 25; a, green: crystal structure; grey; docked structure). The 3VMRm model produced similar orientations for moenomycin but with different orientation of the D ring. In 3NB6sa model, moenomycin was binding in the same binding pocket but its orientation was always different, with phosphoglycerate (G) portion of the molecule facing either to the solvent, the donor or acceptor binding site. In the 3VMSm model, which has the most open groove between the donor and acceptor site, moenomycin was actually oriented partly across the acceptor binding site. Induced fit protocol on those models did not produce better moenomycin binding orientations compared with the standard docking protocol.

In vitro PG biosynthesis. The cell-free particulate fraction of *B. megaterium* KM (ATCC13632), capable of catalysing the polymerization of PG from UPD-linked precursors was performed as described previously[61]. *B. megaterium* was grown in standard medium, harvested and washed with Tris-buffer by centrifugation. Resuspended bacteria were subjected to three freeze/thaw cycles (5 min dry ice, followed by 10 min at RT), homogenized by the glass homogenizer and centrifuged all at 4 °C, leaving most of the cell wall in the pellet. Resuspended pellet was combined with UDP-*N*-acetylmuramyl-pentapeptide, [^{14}C]UDP-*N*-acetylglucosamine and individual compounds or antibiotics (that is, vancomycin hydrochloride or moenomycin A), and incubated at for 3 h at RT, placed in a boiling water bath for 3 min to inactivate enzymes and to prevent any further lipid II transformation, and analysed by TLC on silica gel plates. After separation, plates were dried, exposed to phosphorimaging screen (1 week), scanned by Typhoon 8600 calculating the integrated density value of each band on silica gel. Changes of PG or lipid II were calculated as a percentage from negative control (for more details see Supplementary Methods).

Inhibition of glycosyltransferase. Inhibition of glycosyltransferase was measured using a fluorescence detection method[62] by adding 1 µM *S. aureus* MGT to 1.45 µM fluorescent dansyl-Lys Lipid II and different concentration of inhibitors, all in a buffer of 50 mM Tris pH 8 containing 10 mM MnCl$_2$, 0.08% (v/v) decyl PEG, 10% (v/v) DMSO, 100 µg ml^{-1} hen egg-white lysozyme, in 96-well microtiter plates. Initial rates were measured as a decrease in fluorescence (ex/em: 340/521 nm) and calculated as a percentage compared with no inhibitor as negative control (0% of rate inhibition) and moenomycin A (Sigma, Cat. no.: 32404) as positive control (100% of rate inhibition). The data were fitted to a simple saturation model of inhibitor binding to a single site, from which IC$_{50}$ values were extracted. Moenomycin A showed an IC$_{50}$ of 5 µM in this assay.

Minimal inhibitory concentration (MIC) determination. The compounds along with standard antibiotics were serially diluted twofold across the wells of 96-well standard polystyrene non-treated plates (Corning 3370). Compounds and standard antibiotic controls ranged from 1.28 mg ml^{-1} to 0.06 µg ml^{-1} with final volumes of 50 µl per well. Bacteria were cultured in Brain–Heart Infusion (Bacto laboratories, Cat. no. CM1135B) at 37 °C overnight. A sample of each culture was then diluted 40-fold in fresh brain–heart infusion broth and incubated at 37 °C for 2–3 h. The resultant mid-log phase cultures were diluted to 5×10^5 c.f.u. ml^{-1} then 50 µl was added to each well of the compound-containing 96-well plates giving a final compound concentration range of 64 µg ml^{-1} to 0.03 µg ml^{-1} in 2.5×10^5 c.f.u. ml^{-1}. All the plates were covered and incubated at 37 °C for 24 h. MICs were determined visually as the lowest concentration showing no visible growth.

Antibiotic control compound vancomycin (Sigma, Cat. no.: 861987) was prepared as water solution, while moenomycin A (Sigma, Cat. no.: 32404) was dissolved in DMSO and 20 mM ammonium acetate, due to solubility issues. The average MIC for moenomycin for *S. aureus* was, however, within the range of recent literature[35].

In vivo mouse mammary gland infection model. For the infection of the mice, *S. aureus* Newbould 305 (ATCC 29740) isolated from a clinical mastitis cases[63] was used and prepared. The procedure for mouse mammary gland infection has been recently described[64]. CD-1 lactating mice were utilized 12–14 days after giving birth, with pups weaned 1–2 h before bacterial inoculation of the mammary glands. Inoculation of both left (L4) and right (R4) glands of the fourth abdominal mammary gland pair of anesthetized mice with 150 c.f.u. of *S. aureus*, was done using 32-gauge syringes (blunt needle). The antimicrobial formulation was instilled into the mammary gland of anesthetized mice at 4 h after bacterial inoculation, followed by i.p. administration of postoperative analgesic Buprecare. Mice were killed 14 h post treatment, mammary glands (two per mouse) were harvested, weighed and homogenized. Bacterial c.f.u. counts were obtained after quantification of serial logarithmic dilutions of mammary gland homogenates on TSA. The detection limit (DL) was 1.7 log$_{10}$ c.f.u. g^{-1} gland weight (for more details see Supplementary Methods). The animal experiments were approved by the Ethical Committee of the Faculty of Veterinary Medicine, Ghent University (EC2009/133).

References

1. Derouaux, A., Sauvage, E. & Terrak, M. Peptidoglycan glycosyltransferase substrate mimics as templates for the design of new antibacterial drugs. *Front. Immunol.* **4,** 78 (2013).

2. Bouhss, A., Trunkfield, A. E., Bugg, T. D. & Mengin-Lecreulx, D. The biosynthesis of peptidoglycan lipid-linked intermediates. *FEMS Microbiol. Rev.* **32,** 208–233 (2008).

3. Galley, N. F., O'Reilly, A. M. & Roper, D. I. Prospects for novel inhibitors of peptidoglycan transglycosylases. *Bioorg. Chem.* **55,** 16–26 (2014).

4. Goffin, C. & Ghuysen, J. M. Multimodular penicillin-binding proteins: an enigmatic family of orthologs and paralogs. *Microbiol. Mol. Biol. Rev.* **62,** 1079–1093 (1998).

5. Coutinho, P. M., Deleury, E., Davies, G. J. & Henrissat, B. An evolving hierarchical family classification for glycosyltransferases. *J. Mol. Biol.* **328,** 307–317 (2003).

6. Ling, L. L. *et al.* A new antibiotic kills pathogens without detectable resistance. *Nature* **517,** 455–459 (2015).

7. Arias, C. A. & Murray, B. E. The rise of the *Enterococcus*: beyond vancomycin resistance. *Nat. Rev. Microbiol.* **10,** 266–278 (2012).

8. Gualerzi, C. O., Brandi, L., Fabbretti, A. & Pon, C. L. *Antibiotics: Targets, mechanisms and resistance* (John Wiley & Sons, 2013).

9. Gharsallaoui, A., Oulahal, N., Joly, C. & Degraeve, P. Nisin as a food preservative: part 1: physicochemical properties, antimicrobial activity, and main uses. *Crit. Rev. Food Sci. Nutr.* http://www.tandfonline.com/doi/abs/10.1080/10408398.2013.763766 (2015).

10. Ostash, B. & Walker, S. Moenomycin family antibiotics: chemical synthesis, biosynthesis, and biological activity. *Nat. Prod. Rep.* **27,** 1594–1617 (2010).

11. Fuse, S. *et al.* Functional and structural analysis of a key region of the cell wall inhibitor moenomycin. *ACS Chem. Biol.* **5,** 701–711 (2010).

12. O'Brien, T. F. *et al.* Facts about antibiotics in animals and their impact on resistance. *Clin. Infect. Dis.* **34,** S71–S144 (2002).

13. Silbergeld, E. K., Graham, J. & Price, L. B. Industrial food animal production, antimicrobial resistance, and human health. *Annu. Rev. Public Health* **29,** 151–169 (2008).

14. Butaye, P., Devriese, L. A. & Haesebrouck, F. Differences in antibiotic resistance patterns of *Enterococcus faecalis* and *Enterococcus faecium* strains isolated from farm and pet animals. *Antimicrob. Agents Chemother.* **45,** 1374–1378 (2001).

15. Hentschel, S., Kusch, D. & Sinell, H. J. *Staphylococcus aureus* in poultry—biochemical characteristics, antibiotic resistance and phage pattern. *Zentralbl. Bakteriol. [B]* **168,** 546–561 (1979).

16. Rebets, Y. *et al.* Moenomycin resistance mutations in *Staphylococcus aureus* reduce peptidoglycan chain length and cause aberrant cell division. *ACS Chem. Biol.* **9,** 459–467 (2014).

17. Huber, G. Mechanism of action of antibacterial agents. Moenomycin and related phosphorus-containing antibiotics. *Antibiotics* **5,** 135–153 (1979).

18. Butaye, P., Devriese, L. A. & Haesebrouck, F. Antimicrobial growth promoters used in animal feed: effects of less well known antibiotics on gram-positive bacteria. *Clin. Microbiol. Rev.* **16,** 175–188 (2003).

19. Pfaller, M. A. Flavophospholipol use in animals: positive implications for antimicrobial resistance based on its microbiologic properties. *Diagn. Microbiol. Infect. Dis.* **56,** 115–121 (2006).

20. Makitrynskyy, R. *et al.* Genetic factors that influence moenomycin production in streptomycetes. *J. Ind. Microbiol. Biotechnol.* **37,** 559–566 (2010).

21. Ostash, B. *et al.* Complete characterization of the seventeen step moenomycin biosynthetic pathway. *Biochemistry* **48,** 8830–8841 (2009).

22. Ostash, B., Doud, E. & Fedorenko, V. The molecular biology of moenomycins: towards novel antibiotics based on inhibition of bacterial peptidoglycan glycosyltransferases. *Biol. Chem.* **391,** 499–504 (2010).

23. Van Heijenoort, J. Formation of the glycan chains in the synthesis of bacterial peptidoglycan. *Glycobiology* **11,** 25R–36R (2001).

24. Schneider, T. & Sahl, H. G. An oldie but a goodie - cell wall biosynthesis as antibiotic target pathway. *Int. J. Med. Microbiol.* **300,** 161–169 (2010).

25. Welzel, P. *et al.* Moenomycin A: minimum structural requirements for biological activity. *Tetrahedron* **43,** 585–598 (1987).

26. El-Abadla, N. *et al.* Moenomycin A: the role of the methyl group in the moenuronamide unit and a general discussion of structure-activity relationships. *Tetrahedron* **55,** 699–722 (1999).

27. Sofia, M. J. *et al.* Discovery of novel disaccharide antibacterial agents using a combinatorial library approach. *J. Med. Chem.* **42,** 3193–3198 (1999).

28. Baizman, E. R. *et al.* Antibacterial activity of synthetic analogs based on the disaccharide structure of moenomycin, an inhibitor of bacterial transglycosylase. *Microbiology* **146,** 3129–3140 (2000).

29. Halliday, J., McKeveney, D., Muldoon, C., Rajaratnam, P. & Meutermans, W. Targeting the forgotten transglycosylases. *Biochem. Pharmacol.* **71,** 957–967 (2006).

30. Shih, H. W. *et al.* Effect of the peptide moiety of lipid II on bacterial transglycosylase. *Angew. Chem. Int. Ed.* **51,** 10123–10126 (2012).

31. Kuhn, H. *et al.* Anti-bacterial glycosyl triazoles - Identification of an N-acetylglucosamine derivative with bacteriostatic activity against *Bacillus. Med. Chem. Commun.* **5,** 1213–1217 (2014).

32. Dumbre, S. *et al.* Synthesis of modified peptidoglycan precursor analogues for the inhibition of glycosyltransferase. *J. Am. Chem. Soc.* **134,** 9343–9351 (2012).

33. Cheng, T.-J. R. *et al.* High-throughput identification of antibacterials against methicillin-resistant *Staphylococcus aureus* (MRSA) and the transglycosylase. *Bioorg. Med. Chem.* **18,** 8512–8529 (2010).

34. Huang, S. H. *et al.* New continuous fluorometric assay for bacterial transglycosylase using Forster resonance energy transfer. *J. Am. Chem. Soc.* **135,** 17078–17089 (2013).

35. Gampe, C. M., Tsukamoto, H., Doud, E. H., Walker, S. & Kahne, D. E. Tuning the moenomycin pharmacophore to enable discovery of bacterial cell wall synthesis inhibitors. *J. Am. Chem. Soc.* **135,** 3776–3779 (2013).

36. Wang, Y. *et al.* Structure-based design, synthesis, and biological evaluation of isatin derivatives as potential glycosyltransferase inhibitors. *Chem. Biol. Drug Des.* **84,** 685–696 (2014).

37. Abbenante, G. *et al.* Biological diversity from a structurally diverse library: systematically scanning conformational space using a pyranose scaffold. *J. Med. Chem.* **53,** 5576–5586 (2010).

38. Le, G. T. *et al.* Molecular diversity through sugar scaffolds. *Drug Discov. Today* **8,** 701–709 (2003).

39. Ge, M. *et al.* Vancomycin derivatives that inhibit peptidoglycan biosynthesis without binding D-Ala-D-Ala. *Science* **284,** 507–511 (1999).

40. Lugtenberg, E. J. J., Van Schijndel-Van Dam, A. & Van Bellegem, T. H. M. *In vivo* and *in vitro* action of new antibiotics interfering with the utilization of N-acetylglucosamine-N-acetylmuramyl-pentapeptide. *J. Bacteriol.* **108,** 20–29 (1971).

41. Somner, E. A. & Reynolds, P. E. Inhibition of peptidoglycan biosynthesis by ramoplanin. *Antimicrob. Agents Chemother.* **34,** 413–419 (1990).

42. Ruzin, A. *et al.* Further evidence that a cell wall precursor [C(55)-MurNAc-(peptide)-GlcNAc] serves as an acceptor in a sorting reaction. *J. Bacteriol.* **184,** 2141–2147 (2002).

43. Wu, M., Maier, E., Benz, R. & Hancock, R. E. Mechanism of interaction of different classes of cationic antimicrobial peptides with planar bilayers and with the cytoplasmic membrane of *Escherichia coli*. *Biochemistry* **38,** 7235–7242 (1999).

44. Chia, C. S., Gong, Y., Bowie, J. H., Zuegg, J. & Cooper, M. A. Membrane binding and perturbation studies of the antimicrobial peptides caerin, citropin, and maculatin. *Biopolymers* **96,** 147–157 (2011).

45. Giacometti, A. *et al. In vitro* activity and killing effect of citropin 1.1 against Gram-positive pathogens causing skin and soft tissue infections. *Antimicrob. Agents Chemother.* **49,** 2507–2509 (2005).

46. Wegener, K. L. *et al.* Host defence peptides from the skin glands of the Australian blue mountains tree-frog *Litoria citropa*. Solution structure of the antibacterial peptide citropin 1.1. *Eur. J. Biochem.* **265,** 627–637 (1999).

47. Lloyd, A. J. *et al.* Characterization of tRNA-dependent peptide bond formation by MurM in the synthesis of *Streptococcus pneumoniae* peptidoglycan. *J. Biol. Chem.* **283,** 6402–6417 (2008).

48. Heaslet, H., Shaw, B., Mistry, A. & Miller, A. A. Characterization of the active site of *S. aureus* monofunctional glycosyltransferase (Mtg) by site-directed mutation and structural analysis of the protein complexed with moenomycin. *J. Struct. Biol.* **167,** 129–135 (2009).

49. Huang, C.-Y. *et al.* Crystal structure of *Staphylococcus aureus* transglycosylase in complex with a lipid II analog and elucidation of peptidoglycan synthesis mechanism. *Proc. Natl Acad. Sci* **109,** 6496–6501 (2012).

50. Lovering, A. L., de Castro, L. H., Lim, D. & Strynadka, N. C. J. Structural insight into the transglycosylation step of bacterial cell-wall biosynthesis. *Science* **315,** 1402–1405 (2007).

51. Lovering, A. L., De Castro, L. & Strynadka, N. C. Identification of dynamic structural motifs involved in peptidoglycan glycosyltransfer. *J. Mol. Biol.* **383,** 167–177 (2008).

52. Sung, M.-T. *et al.* Crystal structure of the membrane-bound bifunctional transglycosylase PBP1b from *Escherichia coli*. *Proc. Natl Acad. Sci. USA* **106,** 8824–8829 (2009).

53. Yuan, Y. *et al.* Crystal structure of a peptidoglycan glycosyltransferase suggests a model for processive glycan chain synthesis. *Proc. Natl Acad. Sci. USA* **104,** 5348–5353 (2007).

54. Zuegg, J. & Meutermans, W. Crystal structures of the PBP2 glycosyltransferase domain: new opportunities for antibacterial drug design. *ChemMedChem* **2,** 1403–1404 (2007).

55. Oki, M. in *Top. Stereochem.* (eds Allinger, N. L., Eliel, N. L. & Wilen, S. H.) Vol. 14, 1–81 (John Wiley & Sons, 1983).

56. Laplante, S. R. *et al.* Assessing atropisomer axial chirality in drug discovery and development. *J. Med. Chem.* **54,** 7005–7022 (2011).

57. Riedl, S., Ohlsen, K., Werner, G., Witte, W. & Hacker, J. Impact of flavophospholipol and vancomycin on conjugational transfer of vancomycin resistance plasmids. *Antimicrob. Agents Chemother.* **44,** 3189–3192 (2000).

58. Friesner, R. A. *et al.* Glide: a new approach for rapid, accurate docking and scoring. 1. Method and assessment of docking accuracy. *J. Med. Chem.* **47,** 1739–1749 (2004).

59. Sherman, W., Beard, H. S. & Farid, R. Use of an induced fit receptor structure in virtual screening. *Chem. Biol. Drug Des.* **67,** 83–84 (2006).

60. Sherman, W., Day, T., Jacobson, M. P., Friesner, R. A. & Farid, R. Novel procedure for modeling ligand/receptor induced fit effects. *J. Med. Chem.* **49,** 534–553 (2006).

61. Reynolds, P. E. Peptidoglycan synthesis in bacilli. I. Effect of temperature on the in vitro system from *Bacillus megaterium* and *Bacillus stearothermophilus*. *Biochim. Biophys. Acta* **237,** 239–254 (1971).

62. Schwartz, B., Markwalder, J. A., Seitz, S. P., Wang, Y. & Stein, R. L. A kinetic characterization of the glycosyltransferase activity of *Escherichia coli* PBP1b and development of a continuous fluorescence assay. *Biochemistry* **41,** 12552–12561 (2002).

63. Prasad, L. B. & Newbould, F. H. Inoculation of the bovine teat duct with *Staphylococcus aureus*: the relationship of teat duct length, milk yield and milking rate to development of intramammary infection. *Can. Vet. J.* **9,** 107–115 (1968).

64. Demon, D. *et al.* The intramammary efficacy of first generation cephalosporins against *Staphylococcus aureus* mastitis in mice. *Vet. Microbiol.* **160,** 141–150 (2012).

Acknowledgements

Author contributions

C.M., G.A., D.M., G.L.T., R.P., B.B., L.S. and J.S. developed the chemistry and performed the synthesis, with J.Z. contributing to the design of the library. M.C., A.G.E., J.X.H., M.S.B., T.-J.C., W.-C.C., N.F.G., D.I.R., A.J.L. and C.G.D. developed, performed or supervised the various biochemical assays including analytical methods. D.D. and E.M. performed the *in vivo* assays. J.Z. and M.B. performed the *in silico* experiments. J.Z., C.M. and M.S.B. contributed to the writing of the manuscript. W.M. and M.A.C. supervised the studies, with W.M. establishing the project.

Additional information